EVALUATION OF THE ENVIRONMENTAL PERFORMANCE OF CCPS IN ROADWAY APPLICATIONS

by

Principal Investigator: Tuncer B. Edil
Co-Principal Investigator: Craig H. Benson
Graduate Assistants: Jonathan B. O'Donnell and Kanokwan Komonweeraket

2010

This report consists of two thesis prepared at the University of Wisconsin-Madison.

The two theses are:
1. LEACHING OF TRACE ELEMENTS FROM ROADWAY MATERIALS STABILIZED WITH FLY ASH by Jonathan O'Donnell (2009) MS Thesis
2. LEACHING FROM SOIL STABILIZED WITH FLY ASH: BEHAVIOR AND MECHANISMS by Kanokwan Komonweeraket (2010) PhD Thesis

LEACHING OF TRACE ELEMENTS FROM ROADWAY MATERIALS STABILIZED WITH FLY ASH

by

JONATHAN B. O'DONNELL

A thesis submitted in partial fulfillment of

the requirements for the degree of

MASTER OF SCIENCE

(GEOLOGICAL ENGINEERING)

at the

UNIVERSITY OF WISCONSIN-MADISON

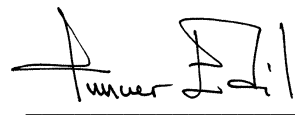**2009**

LEACHING OF TRACE ELEMENTS FROM ROADWAY MATERIALS STABILIZED WITH FLY ASH

Approved:

_____ 12-17-09

signature   date

Craig H. Benson, Distinguished Professor

_____ 12-17-09

signature   date

Tuncer B. Edil, Professor

ABSTRACT
LEACHING OF TRACE ELEMENTS FROM ROADWAY MATERIALS
STABILIZED WITH FLY ASH

Jonathan B. O'Donnell
Under the Supervision of Professors Craig H. Benson and Tuncer B. Edil
at the University of Wisconsin Madison

This study evaluated the leaching of trace elements from roadway materials physically stabilized with fly ash from coal combustion. Five field sites with stabilized materials and three sites with control materials used as base course or subgrade were constructed with pan lysimeters to collect leachate discharging from the bottom of the roadway layers. Pore volumes of flow from the layers was calculated from the volume of leachate collected, pH and Eh of the leachate was measured, and samples were collected for chemical analysis. Laboratory column leach tests (CLTs) and water leach tests (WLTs) were also conducted on specimens of some fly ash and base course/subgrade materials collected in the field. The type, concentration, and pattern of elemental leaching from field and laboratory specimens were determined, and concentrations were compared to those from control materials and relevant groundwater maximum contaminant levels (MCLs). The laboratory tests were compared for their utility in predicting field leaching behavior. The elements As, Cd, Cr, Mo, Ni, Pb, Se, and V exceeded MCLs and were elevated relative to control concentrations, with B, Mo, and V concentrations the most elevated from the controls, and exceeding the MCL for the longest time. Both CLTs and WLTs were similar in their utility for estimating peak field concentrations, especially when peak field concentrations were >500 µg/L.

ACKNOWLEDGEMENTS

TABLE of CONTENTS

LIST OF FIGURES

LIST OF TABLES

SECTION 1

1. INTRODUCTION

Cementitious fly ash is mixed with soils or granular materials in roadway construction to increase strength and stiffness (Edil *et al.* 2002; Bin-Shafique *et al.* 2004; Li *et al.* 2007; Hatipoglu *et al.* 2008; Li *et al.* 2009), as well as to reduce the swelling of expansive soils (Cokca, 2001; Buhler and Cerato 2007). Use of fly ash as a stabilizer in road construction has also been found to reduce construction costs and energy use (Kumar and Patil 2006; US EPA 2008) depending on the scale of the project and the local availability of fly ash and other construction materials (Kumar and Patil 2006).

Fly ash is a coal combustion product (CCP) captured from hot flu gases. Most fly ashes contain trace elements that were present in the coal, including As, B, Ba, Be, Cd, Cr, Co, Cu, Pb, Mn, Ni, Se, Sr, Tl, V, and Zn (NRC, 2006; US EPA 2008). A primary limitation to greater use of fly ash in road construction is concern about environmental impacts to soil and groundwater from trace elements leaching from the ash. This report describes field and laboratory experiments conducted. Particularly of interest were the type, concentration, and pattern of elemental leaching. The paper also evaluates the utility of laboratory water leach tests and column leach tests to predict field leaching of elements from fly ash stabilized materials. A discussion and summary of current state policies in the United States concerning use of fly ash in road construction is presented in Appendix D.

SECTION 2

2. FIELD SITES

Data from five field sites employing fly-ash-stabilized base course or subgrade were evaluated in this study. Additionally, some roadway materials and fly ash from the field sites were used for laboratory leaching tests for comparison with the field data. The field sites were Wisconsin State Highway 60 (STH60) in Lodi, WI; US Highway 12 (US12) in Fort Atkinson, WI; the Scenic Edge subdivision (Scenic Edge) in Cross Plains; WI, 7th Avenue in Waseca, MN; and the Minnesota Department of Transportation MnROAD highway testing laboratory (MnROAD) in Albertville, MN. During construction of the stabilized roadway sections, at least one pan lysimeter was installed directly beneath the stabilized materials to collect leachate discharging from the bottom of the layer. Control lysimeters were also installed beneath unstabilized materials at STH60, US12, and MnROAD.

2.1. State Highway 60 Site

During reconstruction of STH60 between Lodi and Prairie du Sac, WI in August 2000, a 0.1-km section located 8.2-km west of Lodi, WI (Fig. 2.1) was reconstructed using fly ash to stabilize the subgrade soil. STH60 is a two lane highway carrying approximately 3500 vehicles per day (WISDOT 2003). The upper 300 mm of the subgrade was mixed with 18% fly ash by weight using a road reclaimer and then compacted using tamping foot, steel drum, and rubber tire compactors.

The stabilized subgrade was overlain with 140-mm of recycled paving material (RPM) subbase followed by 115-mm of crushed limestone base course and 125 mm of hot mix asphalt (HMA). Details of stabilized materials for all sites can be found in Table 2.1. The construction of STH60 is described in Edil *et al.* (2002) and Bin Shafique *et al.*

(2004). A profile of the roadway layers for all field sites is included in Figures 2.2 and 2.3.

Two pan lysimeters were installed during construction directly beneath the stabilized subgrade to collect leachate discharged from the stabilized layer. One is located beneath the centerline, and the other is located near the shoulder (half is beneath the HMA and half beneath the shoulder) (Fig. 2.4). Two identical lysimeters were installed beneath a control section composed of a 840-mm crushed dolostone sub-base in place of the fly ash stabilized subgrade, with identical overlying layers. A cross-section of typical lysimeter construction is shown in Figure 2.5. Construction methods for all lysimeters are described in Section 3.3, and lysimeter details are included in Table 2.1. Leachate from STH60 has been monitored since September 2000.

2.2.   US Highway 12 Site

A 15.1-km section of US US12 between Fort Atkinson and Cambridge, WI was reconstructed between April 2004 and January 2005 (Fig. 2.1). US12 is one of the primary truck routes in Dane and Jefferson Counties in Wisconsin, and carries approximately 7400 vehicles per day (WISDOT 2006). A 0.6-km section of this project employed fly ash to stabilize the soft subgrade.

The upper 300-mm of subgrade was mixed with 12% fly ash by weight using a road reclaimer and then compacted using tamping foot and vibratory steel drum compactors. The stabilized subgrade was cured for 7-d and then overlain with 254 mm of base course (mixed recycled paving material (RPM) and gravel) and 203 mm of Portland cement concrete riding surface.

Two pan lysimeters were installed during construction beneath the stabilized subgrade to collect leachate discharged from the stabilized layer. One is located at the eastern end of the stabilized subsection and the other at the western end. A third

identical control lysimeter was installed beneath unstabilized subgrade soils near the western stabilized soil lysimeter. Additional information on the US12 lysimeters can be found in Li *et al.* (2009). Leachate from US12 has been monitored since November 2005.

2.3. Scenic Edge Site

During the 2000 construction of a 200-m section of a residential street in the Scenic Edge subdivision in Cross Plains, WI (Fig. 2.1), the existing subgrade soil was stabilized with fly ash. Subgrade was mixed with 12% fly ash by weight to a depth of 300 mm. The mixture was compacted using tamping foot, steel drum, and rubber tire compactors. The stabilized subgrade was overlain with a 175-mm thick crushed stone base course, and 100 mm of hot-mix asphalt (HMA). Details of the Scenic Edge site construction can be found in Bin Shafique *et al.* (2004). One pan lysimeter was installed beneath the stabilized subgrade during construction. Leachate from Scenic Edge has been monitored since February 2006.

2.4. Waseca Site

During Summer 2004 road construction, fly ash was used to stabilize RPM base course near the intersection of 7th St. and 7th Ave. in Waseca, Minnesota, located 125 km south of Minneapolis (Fig. 2.3). The RPM was reclaimed on-site by pulverizing the existing asphalt pavement and base course materials using a road reclaimer. The *in situ* water content of the RPM was approximately 4% dry of standard Proctor optimum water content based on standard compaction effort (ASTM D 698).

The RPM was spread to form a 225 mm base course and then fly ash (10% by dry weight) was spread and mixed using a road reclaimer with water added during mixing using a water truck. The mixture was compacted by tamping foot and vibratory steel drum compactors, and then cured for 7 d and overlain with 75 mm of HMA.

One lysimeter was installed below the stabilized base course. Photographs showing the road and lysimeter construction are in Appendix A-1. Leachate from Waseca was monitored from September 2004 to September 2008.

2.5. MnROAD Site

The Minnesota Department of Transportation (MNDOT) MnROAD Facility is a full scale highway testing laboratory located in east-central Minnesota adjacent to Interstate 94 between Albertville and Monticello, Minnesota (Fig. 2.1). The facility contains a low traffic volume road loop that simulates traffic on rural roads as well as a high volume freeway section that carries live traffic from Interstate 94 when active. Test sections at MnROAD contain sensors that measure load response and environmental data (MNDOT 2009).

Three test sections were constructed in 2007 on the low volume loop at MnROAD to evaluate fly-ash-stabilized RPM as base course. One test section contains stabilized RPM base course, a control section contains unstabilized RPM, and a second control section contains crushed stone (Class 5, as classified by MNDOT) as the base course. The RPM was reclaimed from to a depth of 305 mm from a HMA wearing course and MNDOT Class 4 aggregate base course at the MnROAD facility. The RPM was stockpiled before use.

The base courses were initially constructed in early August 2007. Each is 203 mm thick and was compacted with a steel-drum vibratory roller. The stabilized RPM base course was mixed with 14% fly ash, compacted and then covered with plastic sheets and allowed to cure for one week. The RPM and crushed stone aggregate base courses had to be reconstructed due to heavy rainfall. Both were excavated, air dried, and recompacted. The RPM and crushed stone aggregate sections were compacted in

early October 2007, and all three sections were then paved with a 102 mm HMA wearing course was paved.

One pan lysimeter was installed in each of the three sections during construction directly beneath the base course layer to collect leachate discharged from the layers above. The lysimeters are located beneath the HMA wearing course and base course, off set to one side, approximately 600-mm from the shoulder along the closest side of the lysimeter. Photographs of lysimeter construction at MnROAD are included in Appendix A-2. Leachate from MnROAD has been monitored since October 2007.

SECTION 3

3. METHODS AND MATERIALS

3.1. FLY ASH

Fly ash is classified based on chemical composition by ASTM C 618 as either Class C or Class F. Fly ash that does not meet the requirements of Class C or F is often referred to as "off-specification". The composition within a class can vary significantly The majority of the fly ash that is recycled in the United States is Class C or F (US EPA, 2008).

Fly ash is in a highly oxidized state and chemically reacts and cements in the presence of water and lime (CaO and CaOH). Lime may already be present in the ash, constituting a self-cementitious fly ash, or lime may be added to produce cementitious ash. The field sites in this study employed three cementitious fly ashes for stabilization of base course or subgrade: Columbia, Riverside 7, and Riverside 8. Chemical and physical properties of the fly ashes are presented as Table 3.1. Columbia fly ash is from Alliant Energy's Columbia Power Station in Portage, WI, whereas the Riverside 7 and Riverside 8 fly ashes are from Xcel Energy's Riverside Power Plant in Minneapolis, MN. Columbia ash was used at the STH60, Scenic Edge, and US12 sites. The Riverside ashes were used at the MnROAD and Waseca sites. Columbia fly ash and both Riverside fly ashes were captured using electrostatic precipitators.

Columbia ash contains 98% fines, and classifies as Class C in ASTM C 618 and AASHTO M 295 (Table 3.1). Riverside 7 classifies as Class C in ASTM C 618 and AASHTO M 295, whereas Riverside 8 is an off-specification ash due to its high carbon content (>5%) (Table 3.1). Elemental composition of the Columbia and Riverside 8 ashes is presented in Table 3.2. The major components of the fly ashes (in descending

order) are Ca, Al, V, Mg, Fe, Na, P, K, Ba, and Sn. All other elements comprised less than 0.1% of the fly ash mass (Table 3.2).

3.2.   BASES AND SUBGRADES

Particle size distributions of the soils and RPMs that were stabilized with fly ash are presented in Figure 3.1. The subgrades at STH60 and Scenic Edge both classify as low plasticity clay (CL) in the USCS system and A-6 in AASHTO. At US12 the subgrade ranges in properties across the site from low plasticity clay (CL) in the USCS system and A-7-6 in AASHTO (east lysimeter) to clayey sand (SC) in the USCS system and A-6 in AASHTO (west and control lysimeters) (Fig. 3.1). The RPMs used at MnROAD and Waseca both classify as well graded silty gravel (GW-GM) in the USCS system and A-1-a in AASHTO. The stone sub-base at STH60 and the stone base course at MnROAD both classify as poorly graded sand (SP) in the USCS system and A-1-b in AASHTO (Fig. 3.1).

3.3.   FIELD LEACHATE MONITORING

Pan lysimeters were employed in this study to monitor leachate transmitted from the overlying pavement layers. A profile of a typical pan lysimeter is shown in Fig. 2.5. A depression was excavated to the size of the desired lysimeter and the depression bottom was graded for drainage to a single point. A 120-L HDPE leachate collection tank was installed along the road shoulder, buried approx. 2 m deep. The tanks were connected to the lysimeter through a trench using PVC pipe with adequate drainage gradient from the pan to the tank, and were connected vertically to the surface for leachate collection. The depression was lined with 1.5 mm thick LDPE geomembrane which was connected and heat-sealed to the PVC drainage pipe. A drainage layer consisting of geonet between two layers of geotextile was installed in the lysimeter. The

stabilized layers were then compacted above the lysimeter. Photographs of lysimeter construction at Waseca and MnROAD are located in Appendix A.

Leachate in the 120-L tanks was pumped and sampled periodically. Volume of leachate discharged from the layer was recorded and pore volumes of flow (PVF) was calculated from the porosity of the stabilized layer. Volumetric fluxes from the layers were compared to local precipitation data. A daily precipitation rate was averaged for each month of the study (mm/day), and flux from the layer (mm/day) was calculated from the volume of leachate collected, the time between tank pumping events, and the area of the lysimeter. Long-term average fluxes were calculated from the total volume collected, lysimeter area, and total days of lysimeter operation.

Aqueous samples were collected for chemical analysis during pumping events. All samples were collected in HDPE sample bottles with zero head space. Within 24 hr of sampling, pH and oxidation-reduction potential (Eh) were measured in the laboratory. The equipment used to test pH and Eh varied over the course of the study. The leachate was then filtered with a 0.2-μm micropore filter and preserved to pH<2 using trace-metal-grade HNO_3.

3.4. LABORATORY LEACH TESTS

3.4.1. Column Leach Tests (CLTs)

Column leach tests (CLT) were conducted on materials obtained from three of the field sites. These were the stabilized subgrade from STH60, the stabilized RPM from Waseca, and the three base course materials from MnROAD. The column testing conditions are summarized in Table 3.3. The CLTs were used to evaluate leaching under saturated steady-flow conditions.

Specimens were prepared from each material by compaction to field dry unit weight and water content. Material was mixed to field water content using deionized

water in a spray bottle, and compacted by mallet and tamp in three lifts. Columns were either compacted in molds, and extruded and tested in flexible wall permeameters (STH60 and Waseca), or compacted directly in rigid wall permeameters (MnROAD) (Table 3.3). After compaction, the stabilized specimens were cured for one week at constant temperature and 100% humidity.

All specimens were permeated from bottom to top with 0.1 M LiBr solution using gravity with constant-head (STH60 and Waseca) or peristaltic pumps with constnt flow rate (MnROAD). This solution was chosen to simulate percolate in regions where salt is used to manage ice and snow (Bin-Shafique *et al.* 2006). Neither lithium nor bromide have drinking water maximum contaminant levels (MCLs), and therefore would not be chemicals of interest in the leachate analysis. Effluent was collected in sealed Teflon bags to minimize chemical interaction with the atmosphere. Volume of leachate was measured by weighing the bag, PVF was calculated using weight-volume computations based on layer compaction and material properties. A sample was collected for chemical analysis and filtered with 0.2-μm mircopore filters and preserved with trace-metal-grade nitric acid to pH < 2. The Teflon bags were rinsed with deionized water between sampling events.

3.4.2. Water Leach Tests (WLTs)

Water leach tests (WLTs) were conducted on the stabilized subgrade from STH60 and the three materials from MnROAD according to ASTM D3987-85. The unstabilized materials were passed through a US No. 4 sieve and dried as in Bin-Shafique *et al.* (2006). The stabilized materials were compacted to average field dry unit weight and water content, and then were cured for 7 d at constant temperature and 100% humidity. After curing, the stabilized materials were crushed by hand until the gradation appeared similar to the unstabilized RPM.

WLTs were conducted on all the materials using a 20:1 liquid:solid (L:S) ratio (by mass) with deionized water as the eluent as described in the ASTM D3987-85. The MnROAD materials were also tested with deionized water at 3:1, 5:1, and 10:1 L:S ratios. Only the 20:1 ratio is described in the standard.

Leaching was conducted in 2-L HDPE bottles rotated for eighteen hours. Afterwards the solids were allowed to settle 5 min., and then a sample was collected from the supernatant using a wide mouth syringe. The sample was filtered with 0.2-μm micropore filters, and preserved to < pH of 2 using trace-metal-grade HNO_3. Pictures of the MnROAD WLTs are in Appendix A-2.

3.5. LEACHATE ANALYSIS

3.5.1. Chemical Indicator Parameters

The pH and oxidation-reduction potential (Eh) of all field and laboratory leachate samples were measured in the laboratory within 24 hours of sampling. The water quality instruments used for leachate testing varied between sites and over the years of testing.

3.5.2. Major and Minor Elements

Numerous methods for chemical analysis have been used over the course of this project due to the availability of equipment and changing requirements for certain analytes. The methods used were atomic adsorption (AA), inductively coupled plasma (ICP), and cold vapor atomic fluorescence spectrometry (CVAFS). These methods with the dates of use, chemicals analyzed for, and minimum detection limits are summarized in Table 3.4.

All chemical analyses of field and laboratory leachates prior to Fall 2005 were performed by atomic adsorption (AA) according to EPA Standard Methods 213.2, 218.2, 270.2, and 272.2. Due to the complexity of the AA method, only four elements were

considered; cadmium (Cd), chromium (Cr), selenium (Se), and silver (Ag). The only active site during this period was STH60.

After Fall 2005, AA analysis was discontinued and chemical analyses of field and laboratory leachates were conducted by inductively coupled plasma - mass spectrometry (ICP-MS) according to USEPA Method 200.8. Seventeen elements were analyzed by ICP-MS for the STH60, Scenic Edge, and US12 sites. These analytes along with minimum detection limits (MDLs) are presented in Table 3.4. A suite of calibration standards containing the seventeen elements was prepared spanning a range of concentrations appropriate for trace elements and based on expected concentrations of each element. The analytes tested using ICP-MS are presented with MDLs in Table 3.4.

After June 2007, field and laboratory leachates for the STH60, US12, Scenic Edge, and MnROAD sites were analyzed by inductively coupled plasma - optical emission spectrometry (ICP-OES) using a Varian Vista-MPX CCD Simultaneous ICP-OES instrument. All Waseca site leachate was analyzed using ICP-MS including samples from prior to June 2007. The number of chemical analytes increased in June 2007 to 23 for the STH60, US12, Scenic Edge sites. All leachates from the MnROAD, and Waseca sites were analyzed for these 23 elements. The analytes tested for using ICP-OES are presented with MDLs in Table 3.4.

Beginning in 2008 leachate from field lysimeters at the STH60, US12, Scenic edge, and MnROAD sites was periodically sampled and analyzed for mercury (Hg) using USEPA Method 1631, Revision E: Mercury in Water by Oxidation, Purge and Trap, and Cold Vapor Atomic Fluorescence Spectrometry (CVASF). All sampling equipment that contacted the leachate samples was acid cleaned, dried, and double bagged in cleaned and sealed bags. Samples were collected using two people following the procedure in USEPA Method 1669. In this method, one person only touched the sample bottle and the inner of the two bags containing the bottle. Handling of the outer of the two bags

containing the sample bottle and all other equipment and was conducted by the other person. A field blank and duplicate sample were collected for every 10 to 15 lysimeters sampled. Samples were collected in LDPE bottles with zero head space. All Samples were maintained at 4° C, and were preserved and analyzed according to USEPA Method 1631.

Minimum detection limits (MDLs) for AA, ICP-MS, ICP-OES, and CVAFS were determined for each instrument and set of calibration solutions according to US Code of Federal Regulations Title 40, Appendix B to Part 136. The method and analytes tested for during each time period are presented with MDLs in Table 3.4.

SECTION 4

4. RESULTS AND DISCUSSION

4.1. FIELD LEACHING BEHAVIOR

4.1.1. Precipitation Patterns and Lysimeter Drainage

The flux of leachate from the bottom of the stabilized and control layers was compared to the local precipitation rate for each site. Short-term leachate fluxes and precipitation rates from stabilized subgrade are shown in Figs. 4.1 and stabilized RPM in Fig. 4.2. Peak fluxes from the layers tend to occur in the spring months when heavy rains and snow melt occur, and again in late summer and early fall (Figs. 4.1 and 4.2). The peak flux occurs one to two months after the peak monthly precipitation. The minimum flux tends to occur in the winter when precipitation and pore water are often frozen, and in July or August when evaporation tends to exceed precipitation in the upper Midwest (Figs. 4.1 and 4.2). Occasionally the flux from the stabilized layers approaches 15% of precipitation for a period of several months (Fig. 4.2.b). However, as shown subsequently, the long-term average is never more than 7.8% of precipitation for stabilized RPM or 2.4% for stabilized subgrade (Fig. 4.3). Short-term fluxes were calculated from the volume of leachate collected during each pumping event, the surface area of the lysimeter pan, and the time between pumping events. The daily precipitation corresponds to the average precipitation per day occurring during each month (Figs. 4.1 and 4.2) (NOAA 2009).

Long-term fluxes from the pavement layers and precipitation rates averaged over the entire time of the study are shown in Fig. 4.3. Long-term flux of leachate discharged from the fly-ash-stabilized layers was less than 8% of the local precipitation, and often only 1-3% of precipitation. Greater discharge of leachate (relative to precipitation) occurs in the fly-ash-stabilized RPM base courses (2.1 to 7.8% of precipitation) compared to the stabilized soil

subgrades (1.8 to 2.4% of precipitation). The control base courses also had greater flux relative to precipitation than the control subgrades. Flux from the MnROAD RPM control base course was 6.1% of precipitation and flux from the stone aggregate control base course was 14% of precipitation. The STH60 stone subgrade control layer had a leachate flux that was 2.9% of precipitation, and the US12 soil subgrade control had 1.6% of precipitation (Fig. 4.3).

The regional average percentage of precipitation recharging the groundwater is estimated to range from 19% to 24% for the Minnesota sites and from 20% to 21% for the Wisconsin sites (USGS 2007). The asphalt or Portland cement concrete wearing courses on the roadways likely have lower hydraulic conductivity than adjacent road shoulder and native soils. Therefore recharge rates in the areas adjacent to a stabilized roadway may be significantly higher than the percentage of precipitation that leaches from the stabilized layers, which may affect the transport of leachate in the subsurface.

According to the US National Weather Service (May 2009), the annual precipitation in the region that includes Waseca and MnROAD ranges from approximately 500 mm to 900 mm, with an average of 750 mm. The annual precipitation in the region that includes STH60, US12, and Scenic Edge ranges from approximately 500 mm to 1200 mm, with an average of 930 mm (US NWS 2009). Based on the leachate volumes that were collected, total annual flux from a stabilized base course in eastern-central Minnesota should range from 11 to 70 mm/year, and total annual flux from a stabilized fine-grained soil subgrade in south-central Wisconsin should range from 9 to 30 mm/year.

Long-term fluxes from the layers were calculated from the total volume of leachate collected, the surface area of the lysimeter pan, and the total time of leachate collection, and are shown in Fig. 4.3 with long-term average precipitation rates for each site during the testing periods (NOAA 2009). The long-term average precipitation was calculated as the total

precipitation during the study divided by the total time of the study. Leachate volume from each pair of lysimeters at the STH60 site (Fig. 2.2) from each pumping event were compared using a paired t-test to determine if statistically significant differences existed between fluxes measured beneath the pavement and beneath the shoulder. A two-tailed P-value of 0.05 was obtained by the t-test, indicating that the fluxes were not statistically different, although the outcome was marginal. Therefore each lysimeter pair at STH60 is treated as one data set.

4.1.2. Chemical Indicator Parameters

The pH and Eh of the leachates collected in the lysimeters are presented in Fig. 4.4. The pH in the field leachate ranged from 6 to 9, with most of the data near neutral (Fig. 4.4a) for both stabilized and control materials. Only the east stabilized lysimeter at the US12 site regularly had pH greater than 8, and no lysimeters had pH regularly less than 6. Ganglof *et al.* (1997) also found near neutral pH in leachate collected from fly ash amended sandy soil using ceramic-cup pore-water lysimeters in an agricultural field.

The leachate Eh generally ranged from +300 to -150 mV, with most data predominantly oxidizing (Eh > 0) and occasional samples in a reducing state (Eh < 0) (Fig. 4.4b). Only the east lysimeter at the US12 site had Eh less than -150 mV on a regular basis (Fig. 4.4b). The US12 east lysimeter regularly had leachate that was grey in color and had a strong odor, possibly indicating anaerobic conditions. All other field leachates were generally clear to yellow and had no noticeable odor. The differences in color and odor are likely associated with the differences in pH and Eh between leachate from US12 east and the other field leachates.

4.1.3. Elements Released and Magnitude of Concentrations

Of the twenty-four trace elements considered in the analysis (Ag, Al, As, B, Ba, Be, Cd, Co, Cr, Cu, Fe, Hg, Mn, Mo, Ni, Pb, Sb, Se, Sn, Sr, Ti, Tl, V, and Zn), all except Be were present in detectable quantities in leachate from the fly-ash-stabilized layers. The elements detected in the leachate are presented in Table 4.1 with the peak concentration and average peak concentration (average of the three highest concentrations). The following elements are presented in order of descending peak concentration observed in leachate from the fly-ash-stabilized materials (Table 4.1): Mo (maximum peak concentration of 18,176 µg/L); Sr, Al, Fe, B, and Mn (maximum peak concentration between 10,000 and 1,000 µg/L); Sn, Ba, V, Se, Zn, As, Cu, Tl, and Ni (maximum peak concentration between 1,000 and 100 µg/L); and Pb, Cr, Sb, Ti, Co, Cd, and Ag (maximum peak concentration between 100 and 10 µg/L). Peak concentrations of both Hg and Be were less than 1 µg/L.

The relationship between peak aqueous concentration in the leachate and solid-phase concentration in the fly ash is shown in Fig. 4.5. Linear regression of the base 10 logarithms of the peak aqueous concentration and the solid-phase concentration in the fly ash for all sites and elements indicates a statistically significant, but weak correlation between peak aqueous concentration and solid phase concentration (R^2 = 0.30, F-test p value = 2.8 x 10^{-12}). Fly ash particles contain multiple solid forms (crystalline, glass, and oxide crusts) with different solubilities. Elements such as Cd and Ni may be concentrated in the least soluble crystal phase, and other elements may be preferentially occluded in the glass phase, which is more soluble than the crystalline phase, but less soluble that than metal oxides in the outer crust of the particles (Huett *et al.* 1980)

4.1.4. Elution Patterns

Concentrations of each element recorded in each lysimeter are reported as a function of PVF in Appendix B. Not all elements were tested during the early years of some sites (Table 3.4). Therefore initial leaching patterns could not be observed in these cases. Among elements that were tested during the entire operation of each site and that were detected at the site, 61% of elements had the peak concentration occur during the first two PVF (Table 4.2). The elements most commonly with early peak concentrations are Cd, Co, Cr, Ni, and Se. As an example, the leaching pattern of Cd and Cr is shown in Fig. 4.6. All other elements except Be, Hg, and Ti were observed to have peak concentration occur during the first two PVF for at least one site (Table 4.2).

4.2. POTENTIAL ENVIRONMENTAL IMPACTS

4.2.1. Field Concentrations Compared to Control Sections

An analysis was conducted to determine if element concentrations in leachate from stabilized materials were elevated relative to concentrations in leachate from adjacent control sections. The average peak concentration and the geometric mean of all observed concentrations for each site and element were compared. The determination of concentration elevation was conducted using Equation 4-1,

$$(C^*_c + 2\sigma) \geq (C^*_s - 2\sigma) \text{ OR } (C^*_c + 2\sigma) \leq (C^*_s - 2\sigma) \qquad \textbf{Eq. 4-1}$$

where C^*_s is the average peak or geometric mean concentration from stabilized materials, C^*_c is the average peak or geometric mean concentration from control materials, and σ is the

standard deviation. If $(C^*_c + 2\sigma) \leq (C^*_s - 2\sigma)$ was true, then the concentration from stabilized material was considered significantly elevated relative to concentration from control material. The standard deviation, σ, was obtained as the product of the average peak or geometric mean concentration and the coefficient of variation (COV). The COV for each element was determined from 7 replicate tests on the ICP-OES at 20 µg/L.

For the three sites with control lysimeters (STH60, US12, and MnROAD), 19 of the 24 elements were elevated in concentration relative to the control. The following six elements had elevated concentrations at all 3 sites (in order of descending magnitude of concentration elevation): Mo, B, Cu, Cr, Cd, and Zn (Table 4.3). Eleven elements were elevated at two of the three sites (Sr, Al, Ba, Ti, Co, Fe, Sn, As, V, Ni, and Mn). Both Pb and Ag were elevated at one of the sites. Concentrations of five elements in stabilized leachate (Hg, Be, Se, Tl, and Sb) were not elevated relative to control leachate concentrations at any of the sites with control sections (Table 4.3). Adriano *et al.* (2002) found elevated As, B, Be, Ba, Mo, and Se in pore water in fly ash amended soil, but found all these elements were below detection limits in groundwater collected from a depth of 3.6-m below the amended soil.

4.2.2. Elements Exceeding Regulatory Maximum Contaminant Levels

Concentrations of all elements observed in lysimeter leachates were compared to the maximum contaminant levels (MCLs) for groundwater or drinking water promulgated by the States of Minnesota and Wisconsin (Minnesota - MN MDH IC 141-0791, Wisconsin - WI NR 140.10). The US government also has MCLs for groundwater (US CFR Title 40 Chapter 141.62), but the State MCLs are equal to or lower than those promulgated by the US government (Table 4.4).

Concentrations of the following eleven elements in lysimeter leachate from fly-ash stabilized materials exceeded MCLs at least once: As, B, Cd, Cr, Mo, Ni, Pb, Sb, Se, Tl, and V. The other thirteen elements never exceeded an applicable MCL in leachate from stabilized materials. Concentrations observed in the lysimeters are only representative of leachate as it exits the bottom of the stabilized or control layer, and do not represent concentrations as leachate drains downward from the pavement through the unsaturated zone and then merges with local groundwater flow.

Concentrations of As and Tl exceeded the MCL most frequently. Leachate from all five stabilized materials and all four control materials had average peak concentrations of As and Tl exceeding MCLs. The geometric mean concentration of Tl also exceeded the MCL at all stabilized and control sites, and As had geometric mean concentration exceed the MCL at two stabilized sites and two control sites (Table 4.5). Concentrations of all elements in field leachate from stabilized and control materials during the course of the study are shown with MCLs in Appendix B.

Average peak concentrations of B, Pb, Sb, and V exceeded the MCL in four of the five stabilized sections, and in none (B), two (V), three (Pb), or all four (Sb) of the control materials. The average peak concentrations of Cd, Mo, Ni, and Se exceeded the MCL in one (Ni), two (Cd and Mo) or three (Se) of the stabilized sections, and in none (Se and Ni) or one (Cd and Mo) of the control sections. (Table 4.5).

Geometric mean concentrations of V exceeded the MCL at three stabilized sites and two control sites. Both Pb and Sb had geometric mean concentration exceed the MCL at one stabilized site and two control sites. Geometric mean concentrations of Cd, Cr, Mo and Ni exceeded the MCL in one of the five stabilized sections, and in none of the control sections.

Geometric mean concentrations of elements that have MCLs are presented with the relevant MCL in Figures 4.7 and 4.8.

4.2.2.1. Concentrations Exceeding MCL and Elevated at All Sites

Concentrations of B, Mo, Cr, and Cd in leachate from fly-ash-stabilized materials exceeded MCLs and were elevated relative to the adjacent control sections at all sites with control sections (Figs. 4.9 to 4.12) (Table 4.3). At sites where B and Mo exceeded the MCL, concentrations of both elements exceed the MCL for many PVF (the stabilized RPM at MnROAD is an exception) (Figs. 4.9 and 4.10). Concentrations of Cd and Cr only exceeded MCLs in the first sample collected (total PVF < 0.25), and then remain well below the MCL in all subsequent leachate (Figs. 4.11 and 4.12).

4.2.2.2. Concentrations Exceeding MCL and Elevated at Some Sites

Concentrations of V, Ni, As, and Pb exceeded MCLs and were elevated in leachate from stabilized materials relative to control materials at only one or two of the three sites (Figs. 4.13 to 4.16) (Table 4.3). Vanadium (V) persists at concentrations above the MCL when the MCL is exceeded (Fig 4.13). Nickel (Ni) only exceeded the MCL and was elevated relative to the control at the US12 site which has higher pH and more reducing conditions than the other sites.

Both As and Pb have concentrations that remain very close to the MCL for many PVF, and were observed to periodically exceed the MCL. The concentrations of As and Pb from stabilized materials were only slightly elevated relative to the concentrations from the control materials (Figs. 4.15 and 4.16) (Table 4.3).

4.2.2.3. Elements in Exceedance of MCL but Not Elevated Compared to Controls

Concentrations of Se, Tl, and Sb in leachate from the fly ash stabilized materials exceeded MCLs, but were not elevated relative to the controls (Figs. 4.17 to 4.19). Both Tl and Sb concentrations tended to be below detection limits with occasional concentrations above the MCL. Concentrations of Se were consistently below the MCL except for the US12 (West) site and the earliest sample taken from the stabilized section at the MnROAD site.

4.2.3. Effects of pH and Eh on Element Mobility

Chemical speciation of elements in the roadway pore water can affect mobility and concentrations. Elements that exist as anions, oxy-anions, or non-ionic soluble molecules at the range of pH and Eh in the field leachate are less likely to be sorbed to solids, and therefore will have greater mobility than elements that form cations (which are likely to sorb on mineral surfaces) or elements that precipitate out as a solid (Jury and Horton 2004). For the elements that exceeded MCLs, the most probable speciation was estimated by pH-Eh speciation diagrams produced by the Geologic Survey of Japan (2005). All probable species over the range of pH and Eh observed in the field leachates were included (Table 4.6). Speciation was not determined in the laboratory.

Six of the eleven elements that exceeded MCLs are likely to form anions, oxy-anions, or non-ionic soluble molecules at the observed pH-Eh conditions (As, B, Mo, Sb, Se, and V). Five of the elements primarily form cations (Cd, Cr, Ni, Pb, and Tl) (Geologic Survey of Japan 2005) (Table 4.6).

Of the three elements with concentrations exceeding MCLs in early PVF and then having concentrations fall below the MCL (Cd, Cr, and Se), two (Cd and Cr) primarily form cations at field pH-Eh conditions. Se is likely to be present as an anion or oxy-anion. Five of the eight elements with concentrations that persistently exceed MCLs for at least several PVF (As,

B, Mo, Sb, and V) form anions, oxy-anions, or non-ionic soluble molecules at field pH-Eh conditions (Table 4.6). The other three elements with concentrations that persistently exceed the MCL (Ni, Pb, and Tl) primarily form cations at the observed field pH-Eh conditions.

4.3.   LABORATORY TESTS

Two laboratory leaching methods were employed on specimens of fly-ash-stabilized and control materials prepared in the laboratory using materials obtained from the field sites: column leach tests (CLTs) and water leach tests (WLTs). Specimens were prepared using field conditions whenever possible. Chemical properties of the laboratory leachates were compared to those of the field lysimeter leachates to determine the effectiveness of the tests in predicting field leachate qualities. CLTs were conducted on stabilized materials from STH60, Waseca, and MnROAD, as well as the MnROAD control materials. WLTs were conducted on stabilized materials from STH60 and MnROAD as well as the MnROAD control materials.

4.3.1. Chemical Indicator Parameters

The pH of the CLT and field leachates are presented in Fig. 4.20. The pH of leachate from the fly-ash-stabilized CLTs is higher than from the same materials in the field (3 to 4 pH units higher for MnROAD,1 to 2 pH units for STH60) (Fig. 4.20). All field leachate from stabilized materials (except at the US12 site) had pH near neutral (Fig. 4.4a). The CLT leachate from the control materials also tended to be near neutral. In contrast, the pH of leachate from stabilized CLTs (from MnROAD) remained elevated relative to the field pH for over 45 pore volumes of flow, which is longer than the life-cycle flow for most of the field lysimeters.

The lower pH in the field compared to WLTs and CLTs on stabilized material may be due to unsaturated conditions in the field. Microbial respiration in the field can enhance soil pore

gas CO_2 (Zwick *et al.*, 1984). Diffusion of CO_2 from the atmosphere or microbial respiration into pore water may form weak carbonic acid and may reduce the pH. In contrast, the CLTs are saturated and therefore have no opportunity for CO_2 to reduce the pH. The pH of WLT leachate from MnROAD materials was also 3 to 4 pH units higher than field leachate. Bin-Shafique *et al.* (2006) also found similar pH in leachate from CLT and WLT on stabilized soils and sand. The WLT data is in Appendix C.

The Eh of the CLT and field leachates are presented in Fig. 4.21. Leachate from stabilized RPM at the MnROAD field site consistently had positive oxidation-reduction potential (Eh), of approximately +150 mV, indicating oxidizing conditions (Fig. 4.21). The stabilized RPM CLT leachate had lower Eh than the field, ranging generally from -5 mV to +40 mV. Leachate from control CLTs had similar Eh to the field leachates from stabilized and control materials.

The differences in leachate Eh between field and CLT concentrations are likely associated with the differences in pH between field and CLT concentrations. For MnROAD field and CLT leachates (the only site with CLT, pH, and EH results), leachate Eh and pH are linearly related (and statistically signinificant) (R^2 = 0.80, F-test p = 5.7 x 10^{-20}) (Fig. 4.22). Altering the CLT method used in this study to obtain pH near neutral in CLT leachate may cause the Eh of CLT leachate to more closely match the observed field Eh.

4.3.2. Column Leach Tests

4.3.2.1. Prediction of Field Leaching Concentrations

Average peak concentrations of 23 elements (calculated from the mean of the three highest concentrations) in leachate from the field lysimeters and CLTs on the same materials are compared in Fig. 4.22. The data are for the MnROAD, Waseca, and STH60 sites (the only sites with CLTs performed. Average peak concentrations from the CLTs are within one order of

magnitude of the average peak field concentration for 77% of elements (Fig. 4.23). Graphs of all field concentrations as a function of PVF are included in Appendix B and all CLT concentrations as a function of PVF are included in Appendix C.

Of the eight elements in field leachate with concentrations elevated relative to the control section and exceeding MCLs (As, B, Cd, Cr, Mo, Ni, Pb, and V), four also exceeded the MCL and were elevated in the CLT leachate relative to the controls (B, Cr, Mo, and V) (Fig. 4.24) (Tables 4.7 and 4.8). Concentrations of these four elements were among the most elevated relative to the control concentrations in both the field and lab. In addition, concentrations of B, Mo, and V may remain higher than MCL for many pore volumes of flow in both the field and CLTs. Field and laboratory concentrations of all elements for the entire monitoring period are presented in Appendices B and C.

The CLT provided measurable concentrations of all 23 elements analyzed, and was most successful at estimating the average peak field concentrations for the three elements most likely to leach at concentrations above MCL for long periods of time (B, Mo, and V) (Figs. 4.9, 4.10, and 4.13). The CLT concentrations of Bo, Mo, and V were greater (1.2, 1.1, and 3.5 times, respectively) than the average peak field concentrations.(Table 4.3).

Concentrations of As, Cd, Ni, and Pb exceeded the MCL and were elevated relative to control concentrations in the field, but not in CLTs. Concentrations of these elements were either only slightly elevated in the field but not in the CLT (As, Cd, and Pb), or were elevated in both the field and CLT (Ni) but only exceeded the MCL at US12 where pH and Eh conditions were different than the other sites and CLTs were not conducted (Fig. 4.25). Of these elements, only As had a peak field concentration greater than 20 μg/L.

Average peak field concentrations of As, Cd, and Ni may be significantly underestimated by the CLT procedure used in this study. The CLT concentrations of As, Cd, and Ni tend to be

below or near the detection limit and well below the MCL. In contrast, peak field concentrations for these elements may exceed the MCL. For example, the average peak field concentration of As was 26 times the average peak from the CLT, Cd was 15 times the peak from the CLT, and peak Ni concentration was 2.5 times greater in the field. Detection limits for Pb differed significantly for the field and CLT leachates. All field Pb concentrations were below the detection limit (above the MCL) and most CLT concentrations were below a lower detection limit (below the MCL). Because of these differences the ability of CLTs to predict field leaching of Pb can not be adequately assessed from this study.

All three elements that exceeded MCLs in the field but were not elevated relative to control materials (Sb, Se, and Tl) also exceeded the MCL in CLTs. However, Sb and Se concentrations were elevated relative to controls concentrations from the CLTs. These differences are possibly due to differences in pH and Eh between the field and CLT leachates.

4.3.2.2.   Comparison of Leaching Patterns

Under saturated constant-flow conditions in the CLTs, concentrations of thirteen of the 24 elements displayed a first-flush elution pattern, with the peak concentration occurring during the first or second PVF (Ag, B, Be, Cd, Cr, Cu, Mo, Mn, Sb, Se, Sr, V, and Zn). All of these elements also had first-flush elution pattern for at least one field site. Examples of observable first-flush behavior in CLT concentrations are presented in Figure 4.26.

Concentrations of the thirteen elements with a first-flush elution pattern peaked at an average of 1.5 PVF, with the latest peak at 6 PVF for Zn. The remaining 11 elements either had very low initial CLT concentrations (As, Co, Hg, Ni, Pb, Sn, Ti, and Tl) and long-term concentrations just above or below the MDL, or had distinctly different leaching patterns (Al, Ba,

and Fe). Elements that exceeded the MCL in field leachates and did not have a first-flush pattern in the CLTs were As, Ni, Pb, and Tl.

Flow through the MnROAD CLT columns was halted after approximately 46 pore volumes of flow. The columns were left saturated with no flow for 54 days, and then restarted. Concentrations of 11 elements increased when flow was restarted (As, B, Be, Cd, Cu, Mo, Sb, Se, Sr, V, and Zn). This spike in concentrations suggests that under the constant flow conditions in the CLT equilibrium conditions do not exist between the liquid and solid phases. Following the spike, concentrations decreased to those observed just before the flow was stopped (Figs. 4.26.b, 4.26.d, and 4.26.f).

Three elements had the concentration rise back to original peak (Sb), or higher (1.5 to 2.9 times) after the columns were restarted (As and Cd), although As and Cd had very low initial CLT concentrations. Low initial concentrations with subsequent fluctuations at or above initial concentrations were observed for As in the field. For the other seven elements the initial peak concentration was significantly higher then the secondary peak concentration caused by the stoppage and restarting (1.5 to 14 times higher than the secondary peak).

4.3.3. Water Leach Tests

Peak concentrations from the field lysimeters at STH60 and MnROAD are compared with concentrations from WLTs on the same materials in Figure 4.27a. WLTs were not performed on the materials from the other sites. Four liquid-to-solid mass ratios were tested (3:1, 5:1, 10:1, and 20:1). Figure 4.27a shows that concentrations from the 3:1 WLT most closely estimated the peak field concentrations. For elements that were detectable in the 3:1 WLT, the concentrations were within one order of magnitude of the peak field concentration for 91% of tests (Fig. 4.27b). All further discussion of the WLTs will refer to the 3:1 WLT.

Of twenty elements that were detected in field leachate at the MnROAD site, eight elements (Ag, Cd, Co, Fe, Mn, Se, Sn, and Tl) were not detected in 3:1 WLTs on the MnROAD materials (Fig. 4.28). Of these elements, three (Cd, Se, and Tl) had concentrations that exceeded the MCL in field leachate from stabilized materials, but only Cd was found to be elevated relative to the control sections.

The WLT was most useful in predicting field concentrations of elements when the peak field concentration was greater than 200 µg/L. Seven of the eight elements that were not detected in WLT leachate had peak field concentrations of 170 µg/L or less. All elements with peak field concentrations of 500 µg/L or greater were detected in the WLT (Fig. 4.27b).

4.3.4. Comparison of CLT and WLT Prediction Of Field Leaching

Detection limits for the WLT samples were generally higher than those for the CLT samples (Table 3.4). Figure 4.28a compares peak concentrations from the CLT and WLT concentrations to field peak concentrations, with two sets of detection limits for the two laboratory tests. When the CLT has lower detection limits than the WLT, the CLT detects all elements, and is better at predicting the field concentrations of elements that have lower (<500 µg/L) peak field concentrations. If the higher WLT detection limits are applied to the CLT data, the WLT and CLT become very similar in their ability to predict peak field concentrations of elements that exceeded MCLs in the field (Fig. 4.28b). The WLT may have been more successful at predicting elements with lower peak field values if the WLT samples were analyzed with lower detection limits similar to those for the CLT leachates (Table 3.4)

When the higher WLT detection limits are applied to both the WLT and CLT, 45% of elements detected in the field, 36% of elements that exceeded MCLs in the field (Cd, Sb, Se, and Tl), and 13% of elements that exceeded MCL and were elevated relative to the control in

the field (Cd) were not detected in the WLT leachate. When the higher WLT detection limits are applied, 25% of elements detected in the field, 27% of elements that exceeded MCLs in the field (Cd, Ni, and Pb), and 38% of elements that exceeded MCL and were elevated relative to the control in the field (Cd, Ni, and Pb) were not detected in the CLT leachate.

SECTION 5

5. CONCLUSIONS

5.1. Conclusions from Field Lysimeters

- Peak concentration of elements observed in leachate from the fly-ash-stabilized materials are, in descending order, Mo (maximum peak concentration of 18,176 µg/L); Sr, Al, Fe, B, and Mn (maximum peak concentration between 10,000 and 1,000 µg/L); Sn, Ba, V, Se, Zn, As, Cu, Tl, and Ni (maximum peak concentration between 1,000 and 100 µg/L); and Pb, Cr, Sb, Ti, Co, Cd, and Ag (maximum peak concentration between 100 and 10 µg/L). Peak concentrations of both Hg and Be were less than 1 µg/L.

- Among elements that were tested during the entire operation of each site and that were detected at the site, 61% of elements had the peak concentration occur during the first two PVF. Cd, Co, Cr, Ni, and Se are the most common elements with early peak concentrations.

- Elements that exceeded MCLs in field leachate from stabilized materials were As, B, Cd, Cr, Mo, Ni, Pb, Sb, Se, Tl, and V. Of these 11 elements, As, B, Cd, Cr, Mo, Ni, Pb, and V had concentrations of were elevated relative to concentrations from control materials at the same site.

    o B, Mo, and V concentrations in leachate from the fly-ash-stabilized materials were elevated relative to concentrations from control sections, and were above the MCL at most sites. B, Mo, and V concentrations exceeded the MCL for at least 6 PVF and 9 years at the STH60 site.

    o Ni concentrations only exceeded the MCL, and were elevated relative to concentrations from control sections, at the US12 site. Leachate at this site had

higher pH and more reducing conditions than the other sites. These conditions are not common, but illustrate how pH and Eh influence leaching behavior.

- o Concentrations of As and Pb in field leachate remained near the MCL and periodically exceed the MCL, over many PVF. Concentrations of As and Pb were elevated only slightly relative to control concentrations.

- o At sites where Cd and Cr exceeded the MCL, the MCL was only exceeded during the first sampling event (PVF at Peak ≤ 0.25). Concentrations were below the MCL in all subsequent PVF.

- All sites except for US12 East had pH near 7 and predominantly oxidizing conditions (Eh of approximately +150 to +300 mV). US12 East had higher pH (up to 9) and reducing conditions (Eh of approximately -370 to +250 mV). The US12 East leachate was grey in color, and a strong odor. All other field leachates were generally clear to yellow and had no noticeable odor. Differences in pH and Eh between sites may influence solubility and leaching of trace elements.

- Long-term average flux discharged from the stabilized roadway layers is 1% to 3% of precipitation for stabilized subgrade and 2% to 8% of precipitation for stabilized RPM base course. Flux discharged from the stabilized roadway materials is less than average regional recharge rates (approximately 20% of precipitation). The difference between flux discharged from the stabilized materials and recharge in areas adjacent to the road will affect the fate in the subsurface of elements in the leachate, and may reduce the impact to groundwater.

- Peak volumetric fluxes from the layers occur in the spring months when heavy rains and snow melt occur, and in the late summer and early fall. Minimum fluxes occur in the winter, and in July or August. Occasionally the flux from the stabilized materials approaches 15% of

precipitation for a period of several months, but the long-term average is never more than 7.8% of precipitation.

- There is a statistically significant, but weak correlation between peak concentration in the field leachate and the solid-phase concentration in the fly ash (R^2 = 0.30).

5.2.   Conclusions from Laboratory Leaching Tests

- When using laboratory tests to predict field leaching concentrations, an analytical method with minimum detection limits equal to or less than the lowest MCL should be used. Without sufficiently low MDLs in the laboratory tests, elements that are not detected in the laboratory tests may be present in field leachate, and may exceed the MCL in the field. 45% of elements detected in the field, 36% of elements that exceeded MCLs in the field (Cd, Sb, Se, and Tl), and 13% of elements that exceeded MCL and were elevated relative to the control in the field (Cd) were not detected in the WLT leachate. When the higher WLT MDLs were applied to the CLT data, 25% of elements detected in the field, 27% of elements that exceeded MCLs in the field (Cd, Ni, and Pb), and 38% of elements that exceeded MCL and were elevated relative to the control in the field (Cd, Ni, and Pb) were not detected in the CLT leachate The method detection limits should be determined before testing of samples begins.

- The pH of leachate from CLT and WLT on stabilized materials (generally 10 to 11) is higher than from the same materials in the field (6 to 8). Eh of leachate from CLT and WLT on stabilized materials is lower (-5 to +40 mV) than from the same materials in the field (mostly between +150 to +300 mV), where leachate is generally oxidizing. The differences in pH and Eh between stabilized materials in the field and in a CLT may be caused by the difference in saturation (saturated flow in CLTs and unsaturated flow in the field). This may

affect element speciation, solubility, and mobility, and therefore affect the prediction of field concentrations using the CLT and WLT methods described in this study.

- Average peak concentrations from the CLT were within one order of magnitude of the average peak field concentration in 77% of cases. Both the CLT and field leachates had concentrations that were above the MCL, elevated relative to the control, and 1.1 to 3.5 times higher than the field average peak) for the elements consistently elevated relative to the control concentrations and MCLs (B, Mo, and V), as well as for Cr (CLT average peak 8.6 times higher than the field average peak).

- As, Cd, Ni, and Pb had concentrations exceeding the MCL in the field, but not in the CLTs. Concentrations of these elements were either slightly elevated in the field but not in the CLT (As, Cd, and Pb), or elevated in both the field and CLT (Ni).

- Sb, Se, and Tl concentrations exceeded MCLs in the field but were not elevated relative to concentrations from control materials. Concentrations of these elements also exceeded the MCL in CLTs. However, Sb and Se were elevated relative to controls in the CLT.

- First-flush leaching patterns were more commonly observed in CLTs compared to field leaching patterns, First-flush leaching patterns were observed in CLTs for 13 elements, all of which had first-flush leaching pattern in leachate from at least on field site with stabilized materials. B, Cd, Cr, Mo, Sb, Se, and V exceeded MCLs in field leachate and had first-flush leaching patterns in CLTs. As, Ni, Pb, and Tl exceeded the MCL in the field and did not have a first-flush CLT patterns.

- Stopping and restarting the CLTs caused concentrations of 11 of the elements to spike (As, B, Be, Cd, Cu, Mo, Sb, Se, Sr, V, and Zn), suggesting that local equilibrium between liquid and solid phases may not exist in CLT tests with steady saturated flow. Following the spike, concentrations decreased to those observed just before the flow was stopped.

- Of the four liquid-to-solid (L:S) ratios used in the WLTs, the 3:1 L:S ratio provided concentrations closest to field peak concentrations. Of twenty elements that were detected in field leachate at the MnROAD site, eight of these were not detected WLTs conducted with 3:1 L:S ratio on the materials. Seven of the eight elements that were not detected in WLT leachate had peak field concentrations of 170 µg/L or less. All elements with peak field concentrations of 500 µg/L or greater were detected in the WLT. If the WLT leachates were analyzed with lower detection limits, the WLT with 3:1 L:S ratio may have detected more or all of the elements detected in the field.

- When CLT and WLT concentrations are compared using the same detection limits, concentrations from both tests are similar in the ability to predict peak field concentrations within one order of magnitude.

REFERENCES

Adriano, D C., Weber, J., Bolan, N.S., Paramasivam, S., Koo, B.J., and Sajwan, K.S. (2002) "Effects of high rates of fly ash on soil, turfgrass, and groundwater quality." *Water, Air, and Soil Pollution.* 139, 365-385.

Bin-Shafique, S, Edil, T B., Benson, C H., and Senol, A. (2004) "Incorporating a fly-ash stabilised layer into pavement design," *Geotechnical Engineering*, 157, 239-259.

Bin-Shafique, S, Edil, T B., Benson, C H., and Hwang, K. (2006) "Concentrations from Water Leach and Column Leach Tests on Fly Ash Stabilized Soils," *Environmental Engineering Science.* 23 (1). 53-67.

Buhler, R L. and Cerato, A B. (2007) "Stabilization of Oklahoma Expansive Soils using Lime and Class C Fly Ash," *ASCE – GeoDenver 2007: New Peaks in Geotechnics.* GSP 162. 1-10.

Cokca, E. (2001) "Use of Class C Fly Ash for the Stabilization of an Expansive Soil," *Journal of Geotechnical and Geoenvironmental Engineering.* July, 568-573.

Edil, T B., Benson, C H., Bin-Shafique, S, Tanyu, B F., Kim, W, and Senol, A. (2002) "Field Evaluation of Construction Alternatives for Roadways over Soft Subgrade," *Transportation Research Record* 1786, 36-48.

Ganglof, W J, Ghodrati, M, Sims, J T, and Vasilas, B L. (1997) "Field Study: Influence of Fly Ash on Leachate Composition in an Excessively Drained Soil." *Journal of Environmental Quality.* 26. 714-23.

Geologic Survey of Japan (2005). "Atlas of Eh-pH Diagrams-Intercomparison of thermodynamic databases." National Institute of Advanced Industrial Science and Technology, Research Center for Deep Geologic Environments. Open File Report No. 419.

Hatipoglu, B, Edil, T B., and Benson, C H. (2008) "Evaluation of Base Prepared from Road Surface Gravel Stabilized with Fly Ash," *ASCE - GeoCongress 2008: Geotechnics of Waste Management and Remediation.* 288-295.

Hulett, L D, Weinberger, A J, Northcutt, K J, and Ferguson, M. (1980) "Chemical Species in Fly Ash from Coal-Burning Power Plants." *Science.* 210 (4476), 1356-1358.

Jury, W A. and Horton, R. (2004). <u>Soil Physics</u>. Jon Wiley & Sons. Hoboken, NJ.

Kumar, S, and Patil, C B. (2006) "Estimation of resource savings due to fly ash utilization in road construction," *Resources, Conservation and Recycling.* 48. 125-140.

Li, L, Edil, T B., and Benson, C H., Hatipoglu, B, and Tastan, O. (2007) "Evaluation of Recycled Asphalt Paving Layer Stabilized with Fly Ash," *ASCE – GeoDenver 2007: New Peaks in Geotechnics.* GSP 169. 1-10.

Li, L, Tastan, O, Benson, C H, and Edil, T B. (2009) "Field Evaluation of Fly Ash Stabilized Subgrade in US 12 Highway," *ASCE - 2009 International Foundation Congress and Equipment Expo, Ground Modification, Problem Soils, and Geo Support.* 385-392.

Minnesota Department of Transportation. (2009) "MnROAD - Minnesota's Cold Weather Road Research Facility." http://www.dot.state.mn.us/mnroad. Viewed on May 15, 2009

National Oceanic and Atmospheric Administration. (2009) "NNDC Climate Data Online". http://cdo.ncdc.noaa.gov/cgi-bin/cdo/cdostnsearch.pl. Viewed on June 23, 2009

National Research Council, Committee on Mine Placement of Coal Combustion Wastes (2006), Managing Coal Combustion Residues in Mines. National Academies Press. Washington, DC.

United States Department of Energy - National Energy Technology Laboratory, (2009) "Current Regulations Governing Coal Combustion By-Products". http://www.netl.doe.gov/technologies/coalpower/ewr/coal_utilization_byproducts/states/select_state.html. Website viewed July 15, 2009.

United States Environmental Protection Agency. (2008) "Waste and Materials-Flow Benchmark Sector Report: Beneficial Use of Secondary Materials - Coal Combustion Products". 530-R-08-003.

United States Geological Survey. (2007) "Ground-Water Recharge in Humid Areas of the United States - A Summary of Ground-Water Resources Program Studies, 2003-2006". USGS FS-2007-3007.

United States National Weather Service, Forecast Office. http://www5.ncdc.noaa.gov /climatenormals/clim60/states/Clim_MN_01.pdf. Data retrieved on 2009-05-03.

Wisconsin Department of Transportation. (2009) "Traffic count maps by county." http://www.dot.wisconsin.gov/travel/counts/maps.htm. Viewed on July 22, 2009.

Zwick, T C., Van, V P., Tolle, D A, Arthur, M F. (1984) "Effects of Fly Ash on Microbial CO_2 Evolution from an Agricultural Soil." *Water Air & Soil Pollution.* 22 (2), 209.

FIGURES

FIGURES
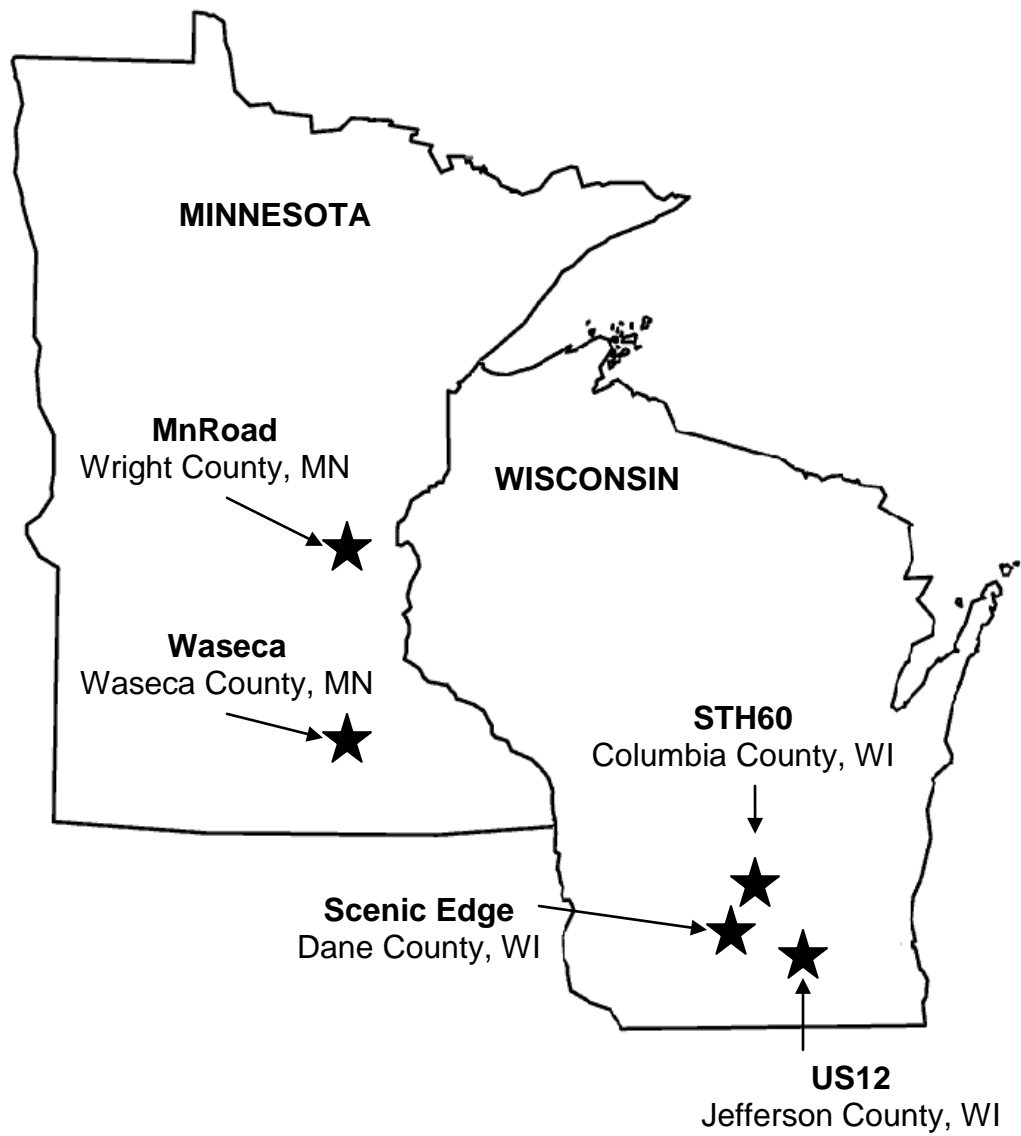
Fig. 2.1.   Location of field sites in Wisconsin and Minnesota.

STH60   **US12**   **Scenic Edge**   **MnROAD**   **Waseca**

STH60
- 125-mm HMA
- 115-mm crushed limestone base
- 140-mm RPM
- 300-mm subgrade with 10% Columbia fly ash by weight
- Lysimeter
- subgrade

US12
- 203-mm PCC
- 254-mm RPM and gravel base
- 300-mm subgrade with 12% Columbia fly ash by weight
- Lysimeter
- subgrade

Scenic Edge
- 100-mm HMA
- 115-mm crushed stone base
- 300-mm subgrade with 12% Columbia fly ash by weight
- Lysimeter
- subgrade

MnROAD
- 102-mm HMA
- 203-mm RPM with 14% Riverside 8 fly ash or RPM
- Lysimeter
- subgrade

Waseca
- 75-mm HMA
- 150-mm RPM with 10% Riverside 8 fly ash
- 75-mm RPM
- Lysimeter
- subgrade

PCC = Portland cement concrete

HMA = Hot Mix Asphalt

RPM = Recycled Pavement Material

Fig. 2.2.   Profiles of Fly-Ash Stabilized Roadway Sections Being Evaluated at the Field Sites.
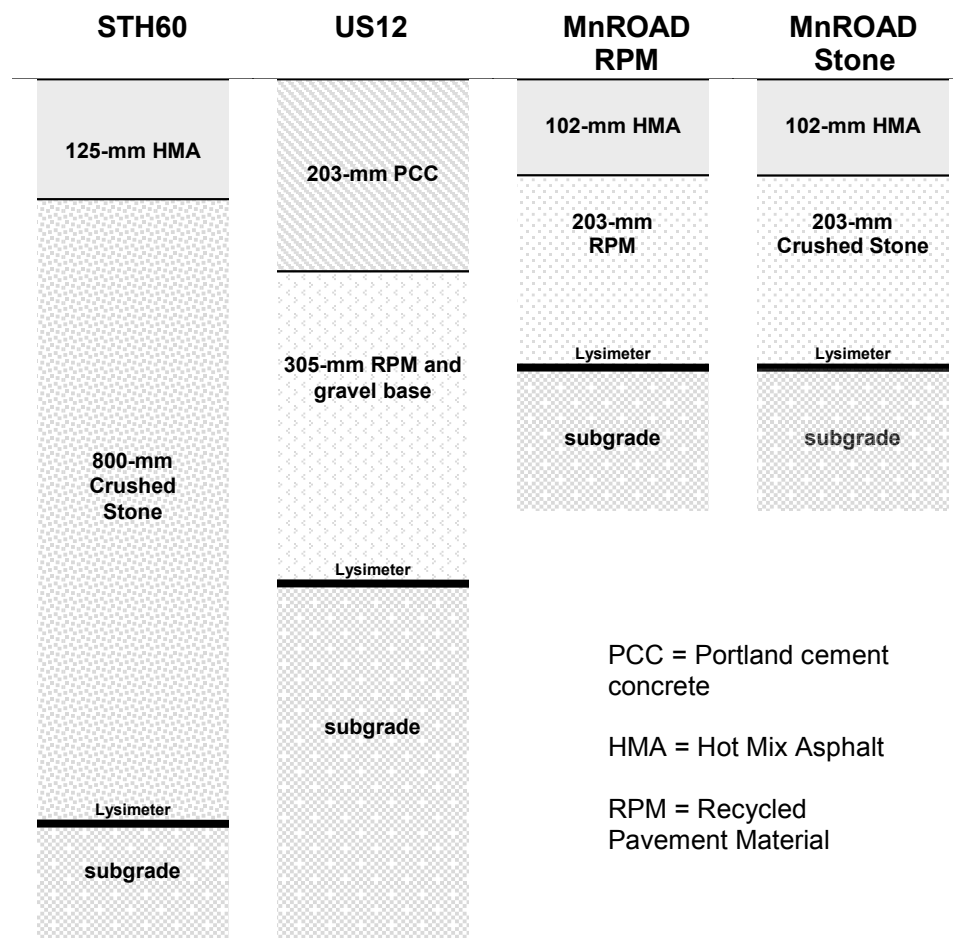
Fig. 2.3.   Profiles of Control Roadway Sections Being Evaluated at the Field Sites.
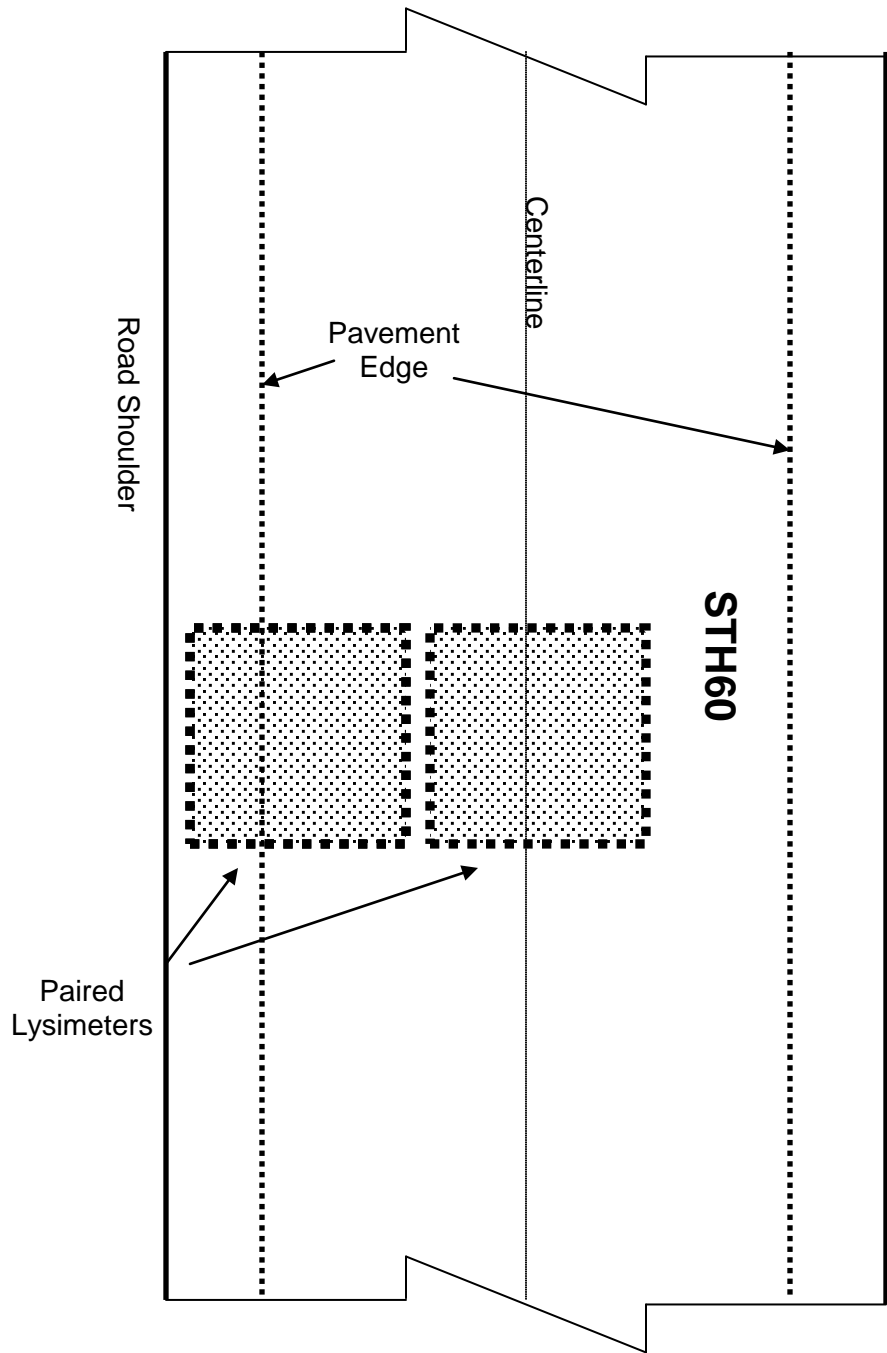
Fig. 2.4.   Schematic of lysimeter pairs at STH60.
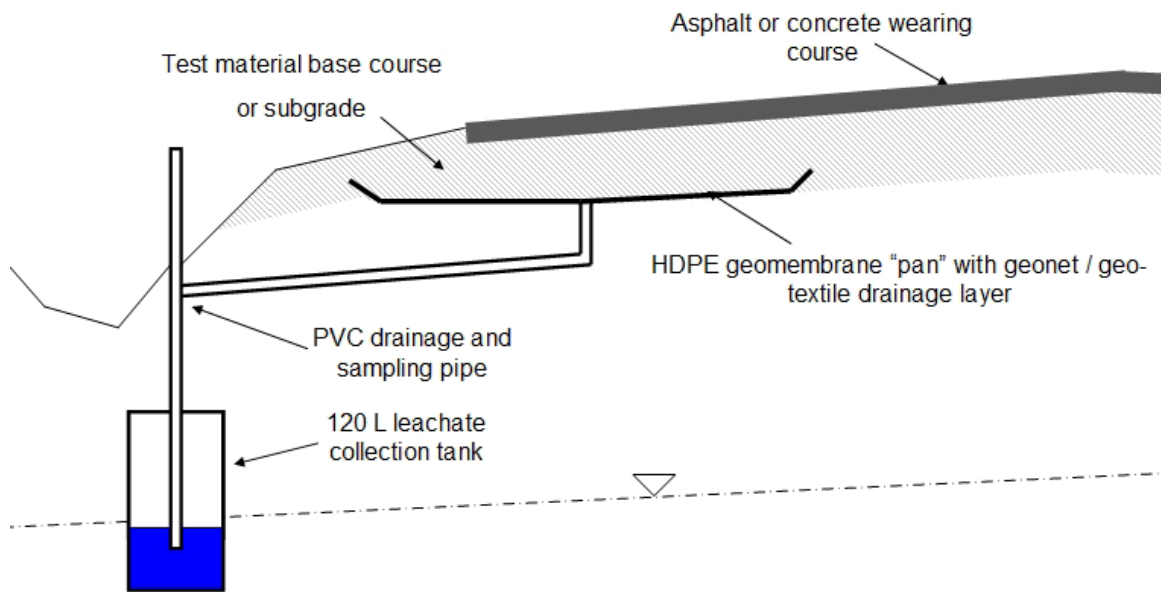
Fig. 2.5.   Cross-section of typical pan lysimeter in roadway.
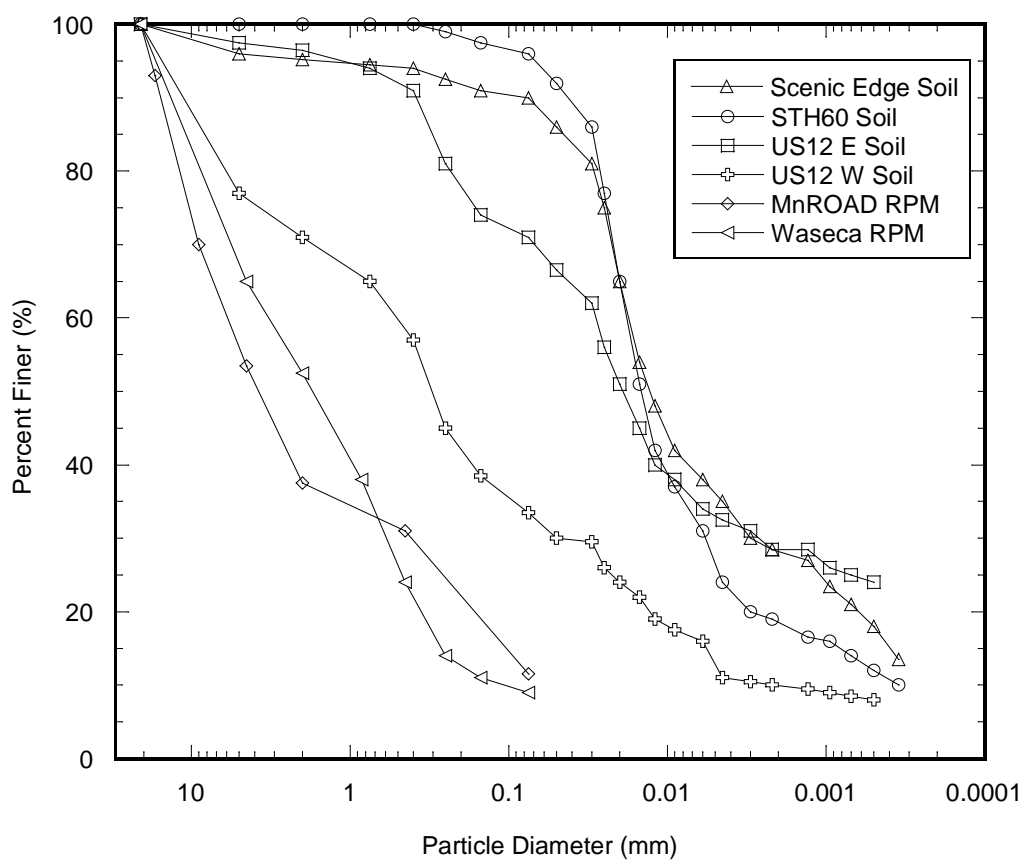
Fig. 3.1.   Particle Size Distribution of Subgrade Soils and RPMs
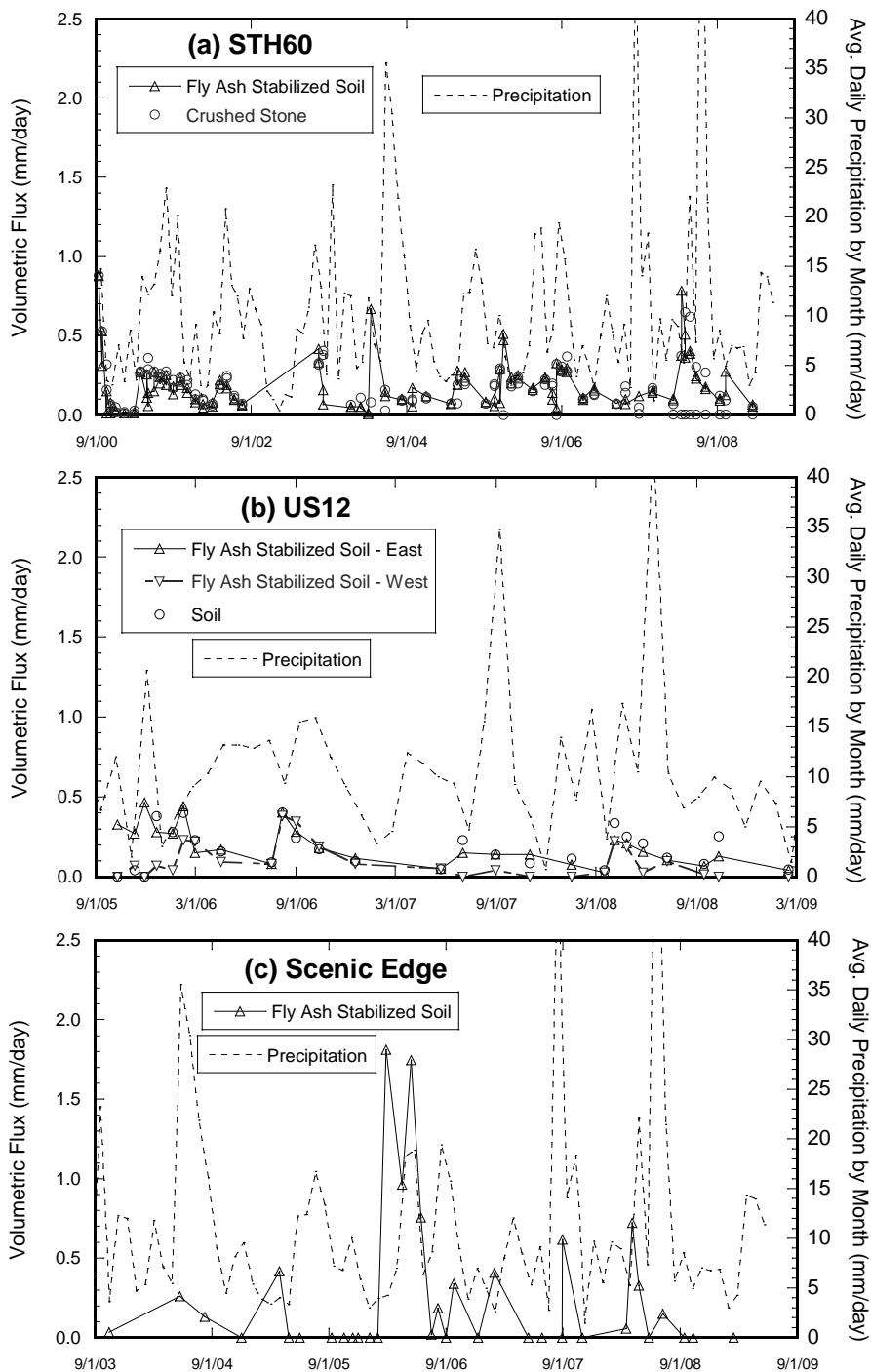
Fig. 4.1.   Volumetric flux from stabilized subgrade and control layers with local average daily precipitation rates from the (a) STH60, (b) US12, and (c) Scenic Edge sites.
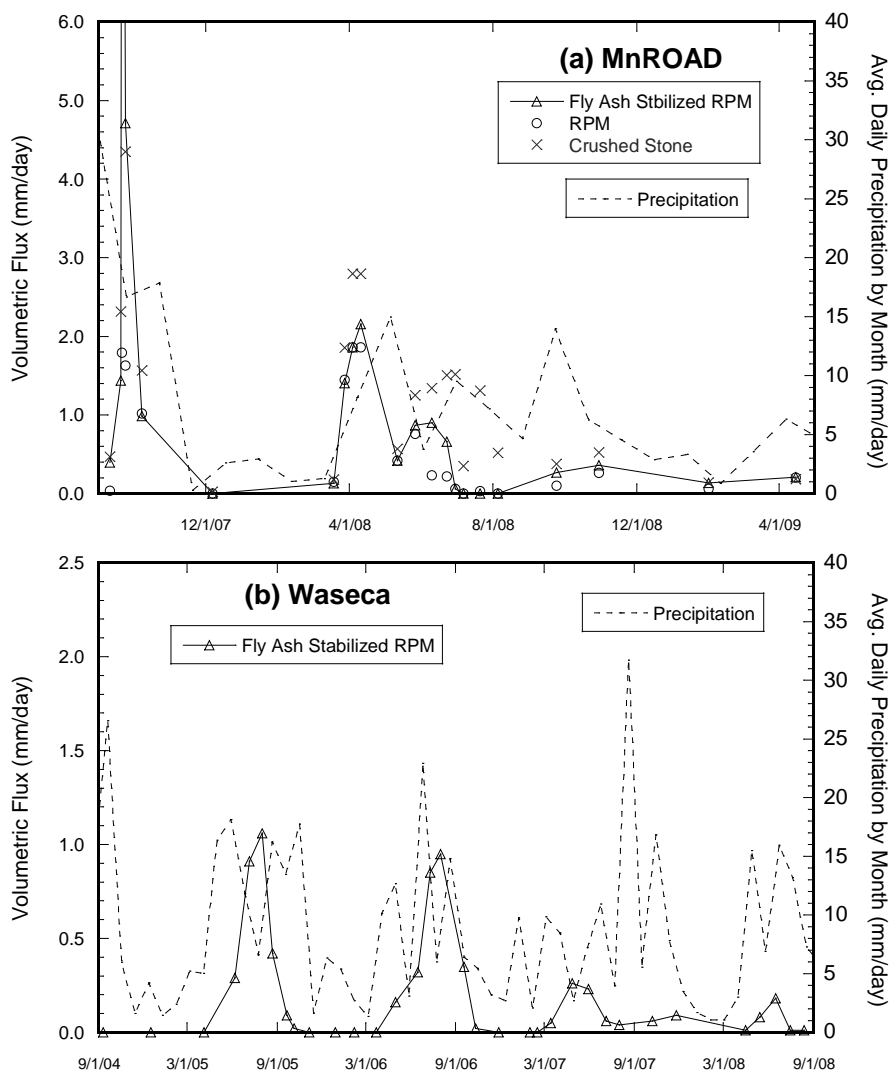
Fig. 4.2.   Volumetric flux from the stabilized RPM base courses and control layers with local average daily precipitation rates from the (a) MnROAD and (b) Waseca sites.
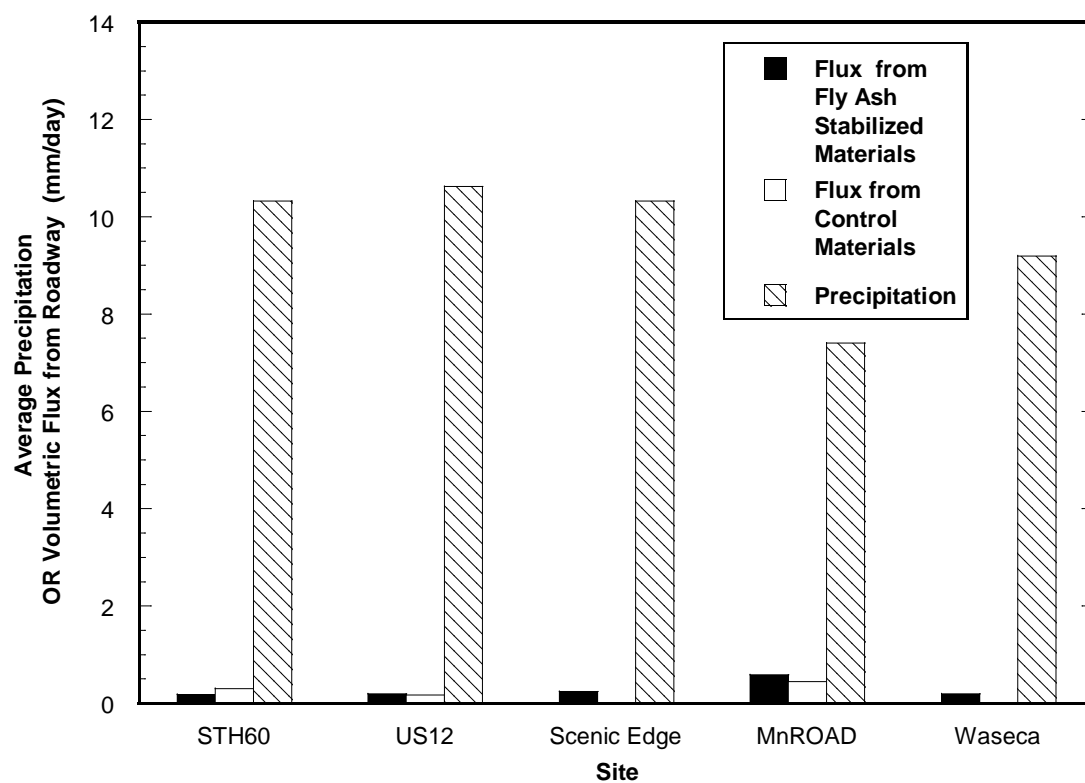
Fig. 4.3.   Comparison of Long-term Volumetric Flux from the Road Layers Relative to Average Daily Precipitation.
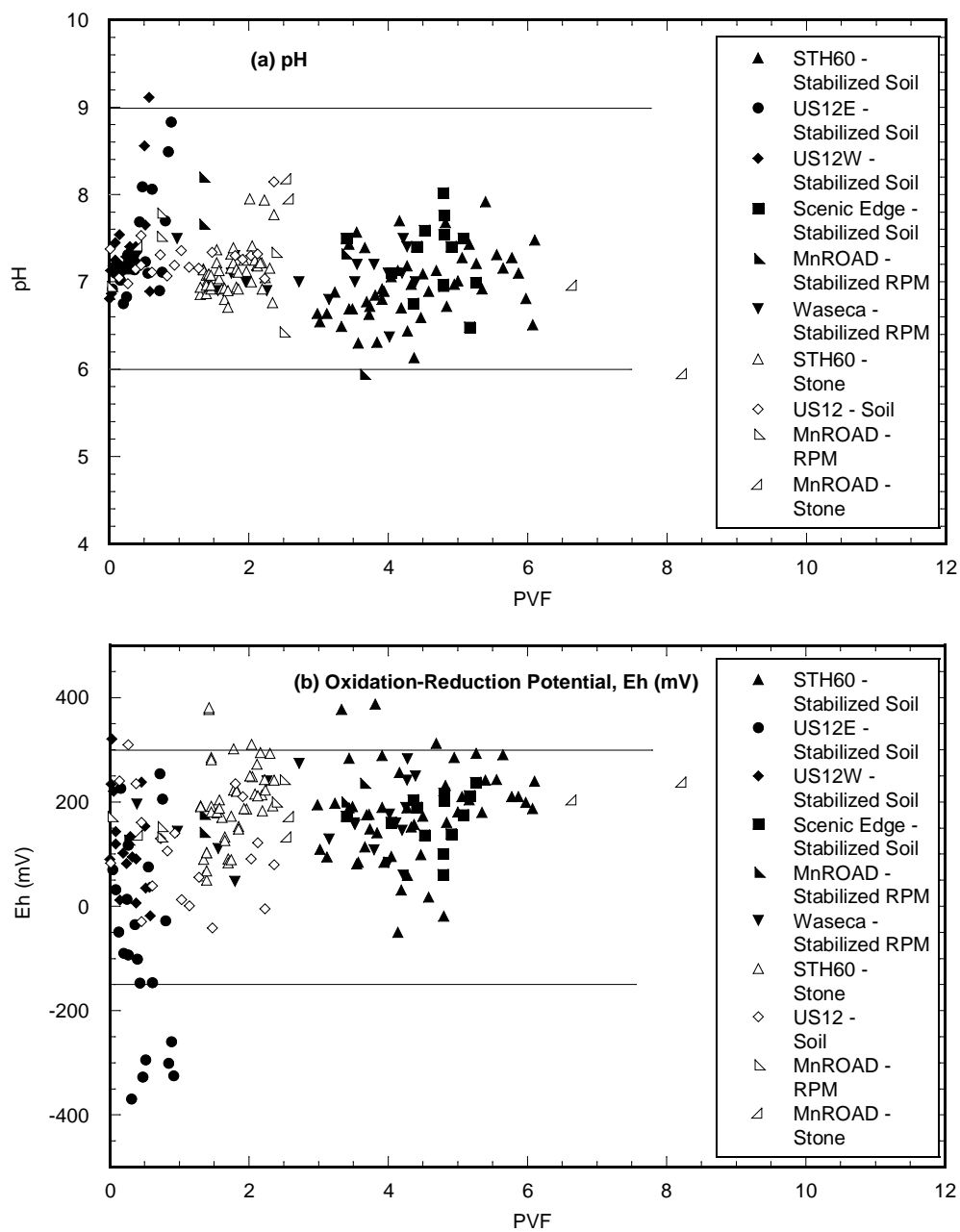
Fig. 4.4.   (a) pH and (b) Eh of Leachate from Field Lysimeters for Fly-ash-stabilized and
Control Materials.
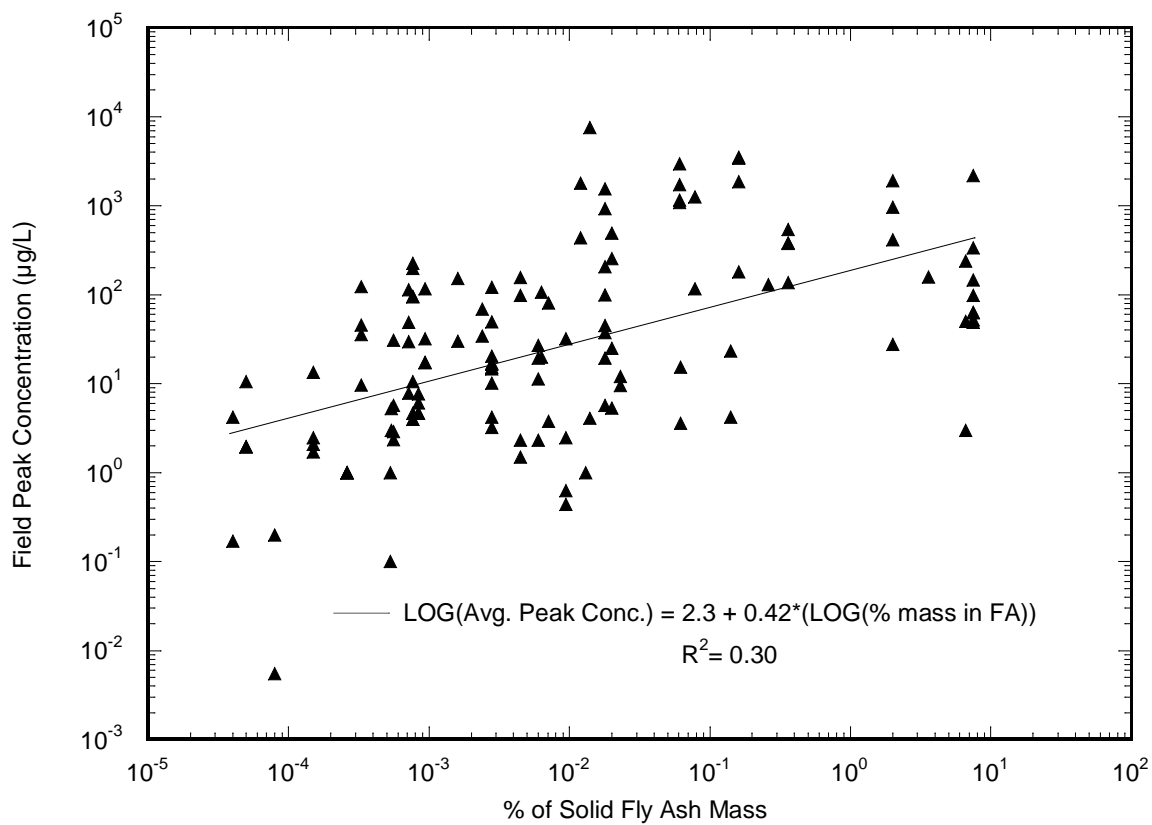
Fig. 4.5. Average Peak Concentrations from Field Relative to Percentage of Each Element in Solid Fly Ash Mass.
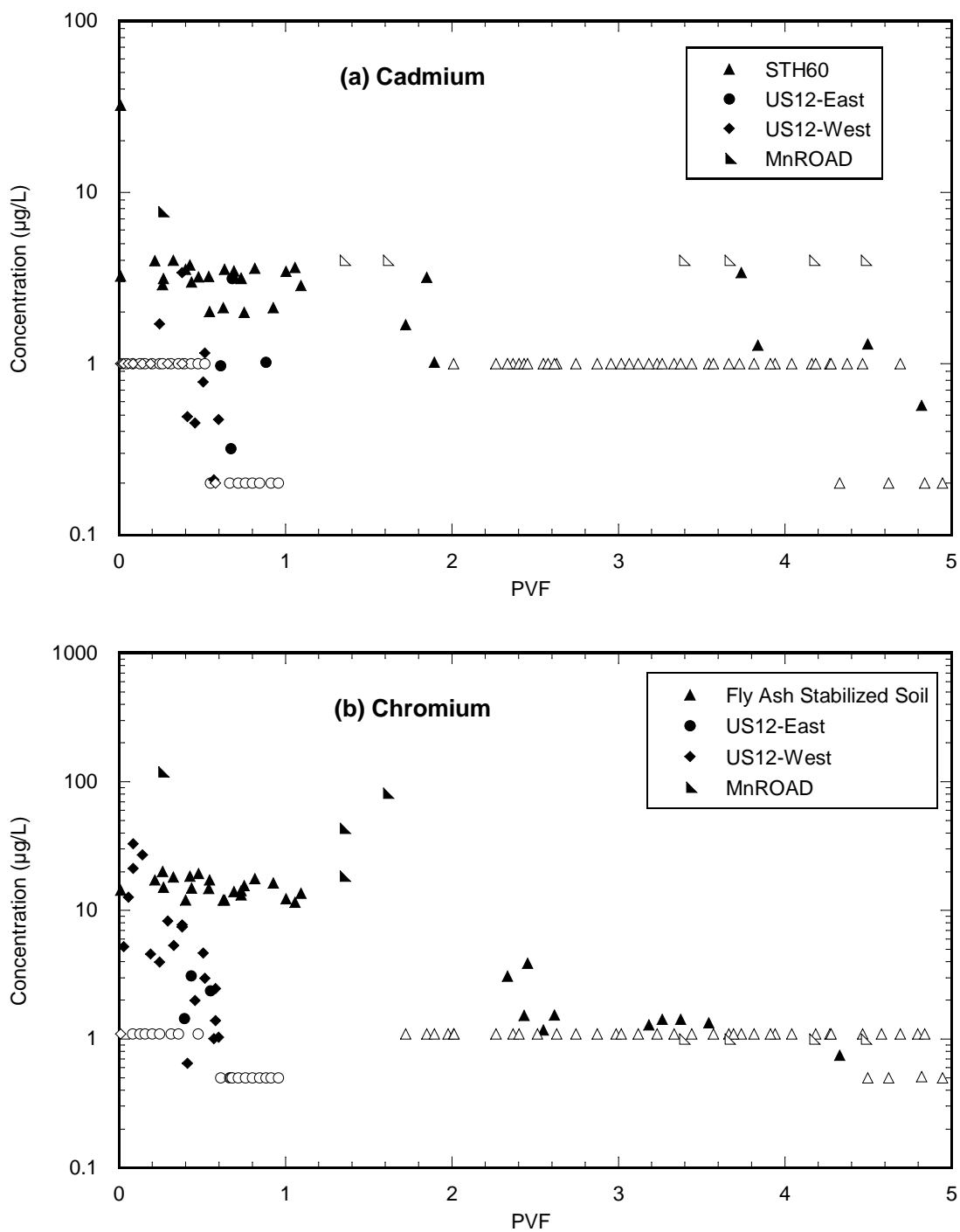
Fig. 4.6. Peak Concentrations occurring during first two PVF for (a) cadmium and (b) chromium.
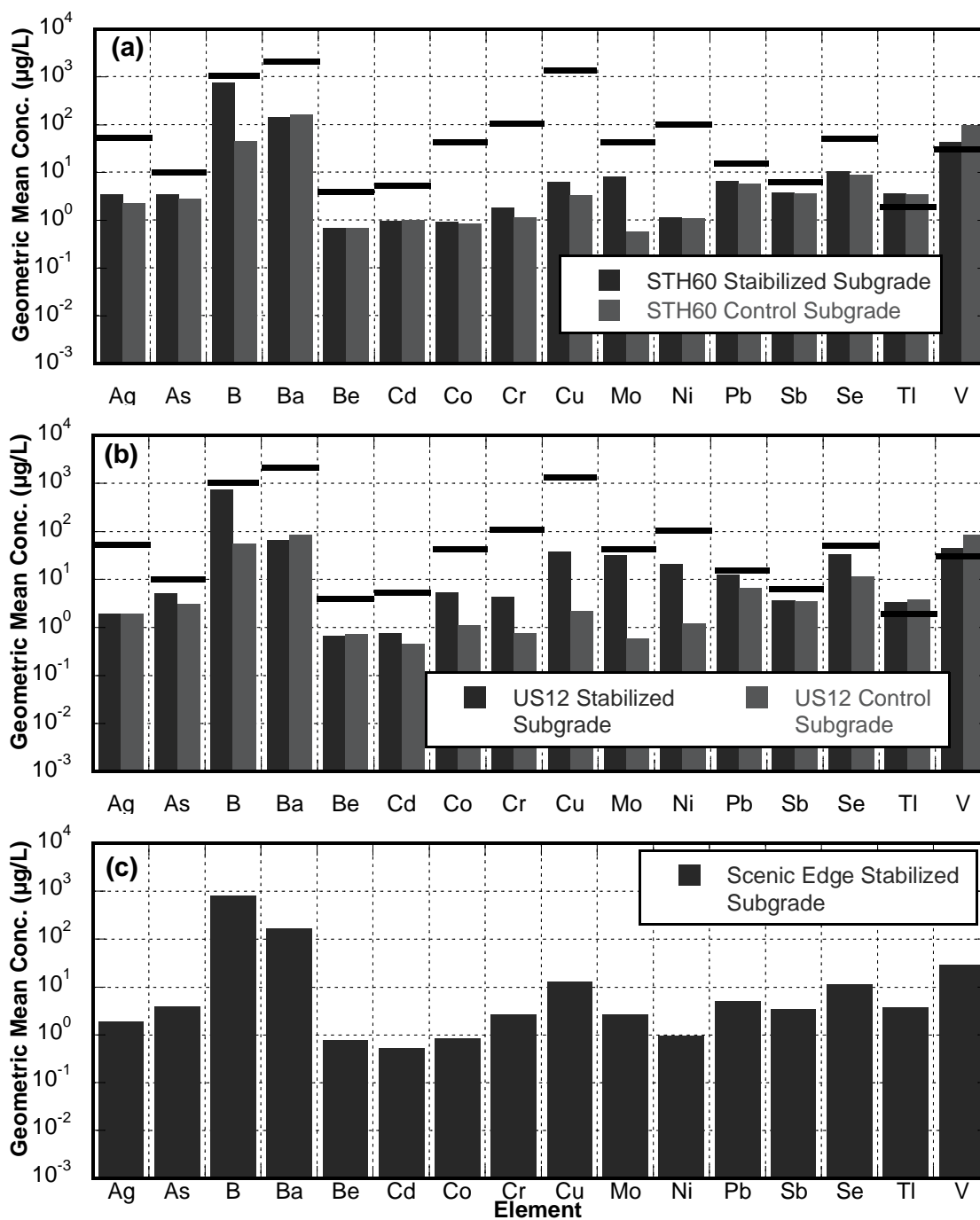
Fig. 4.7.   Geometric mean concentrations over the entire study compared to MCLs (indicated by thick black bars) for the (a) STH60, (b) US12, and (c) Scenic Edge sites.
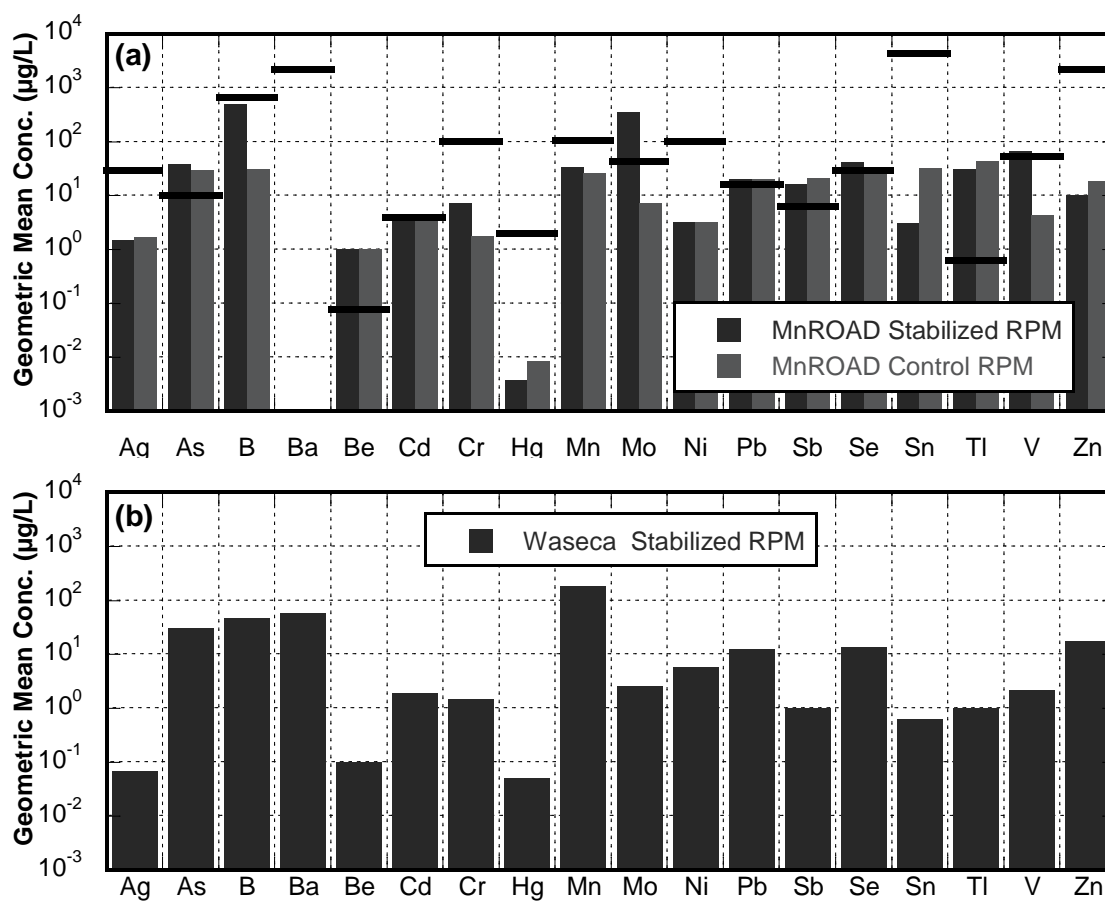
Fig. 4.8. Geometric mean concentrations over the entire study compared to MCLs (indicated by thick black bars) for the (a) MnROAD, and (b) Waseca sites.
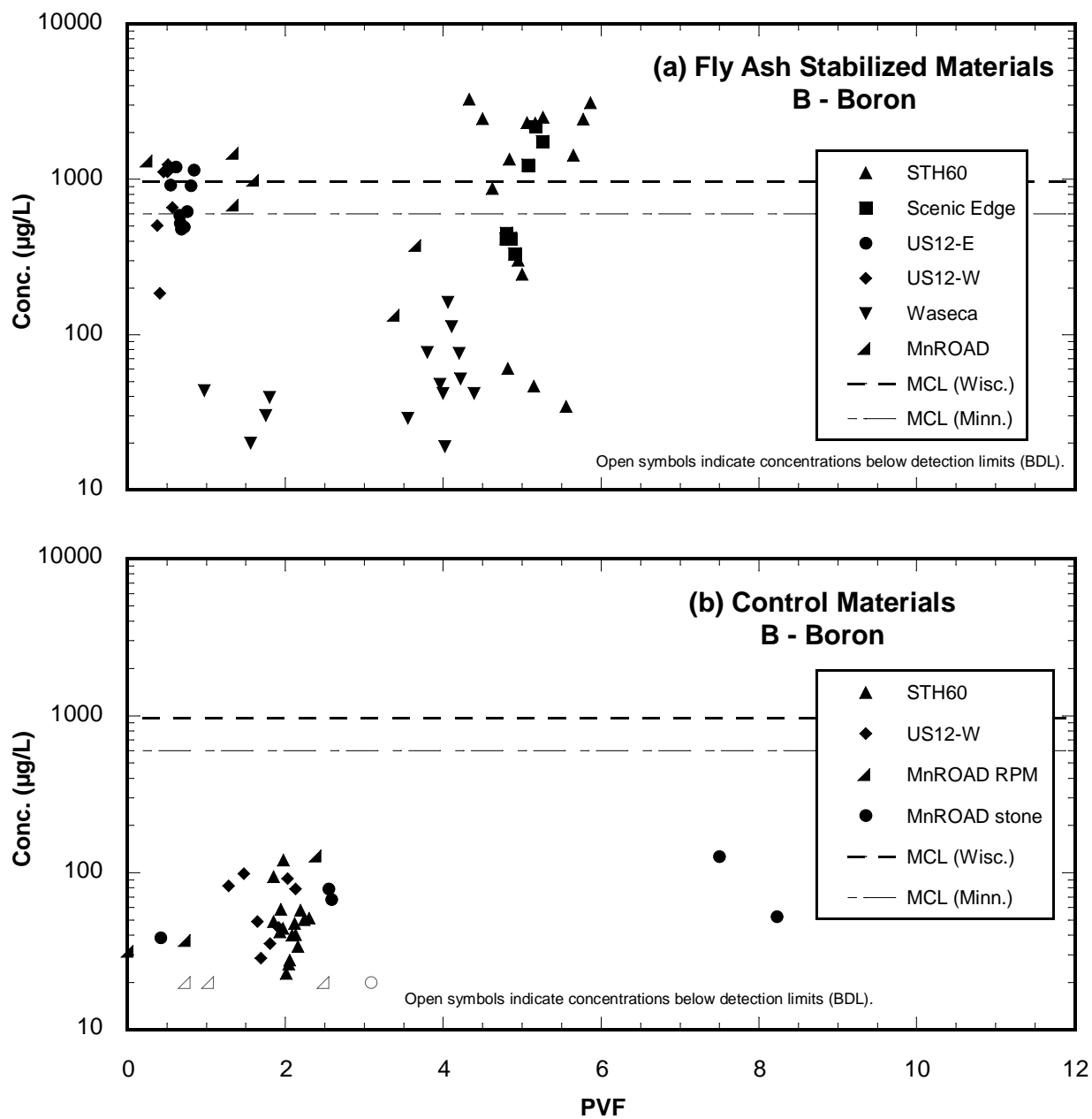
Fig. 4.9.   Boron (B) concentrations in leachate from field road layers composed of (a) fly-ash-stabilized materials, and (b) control materials.
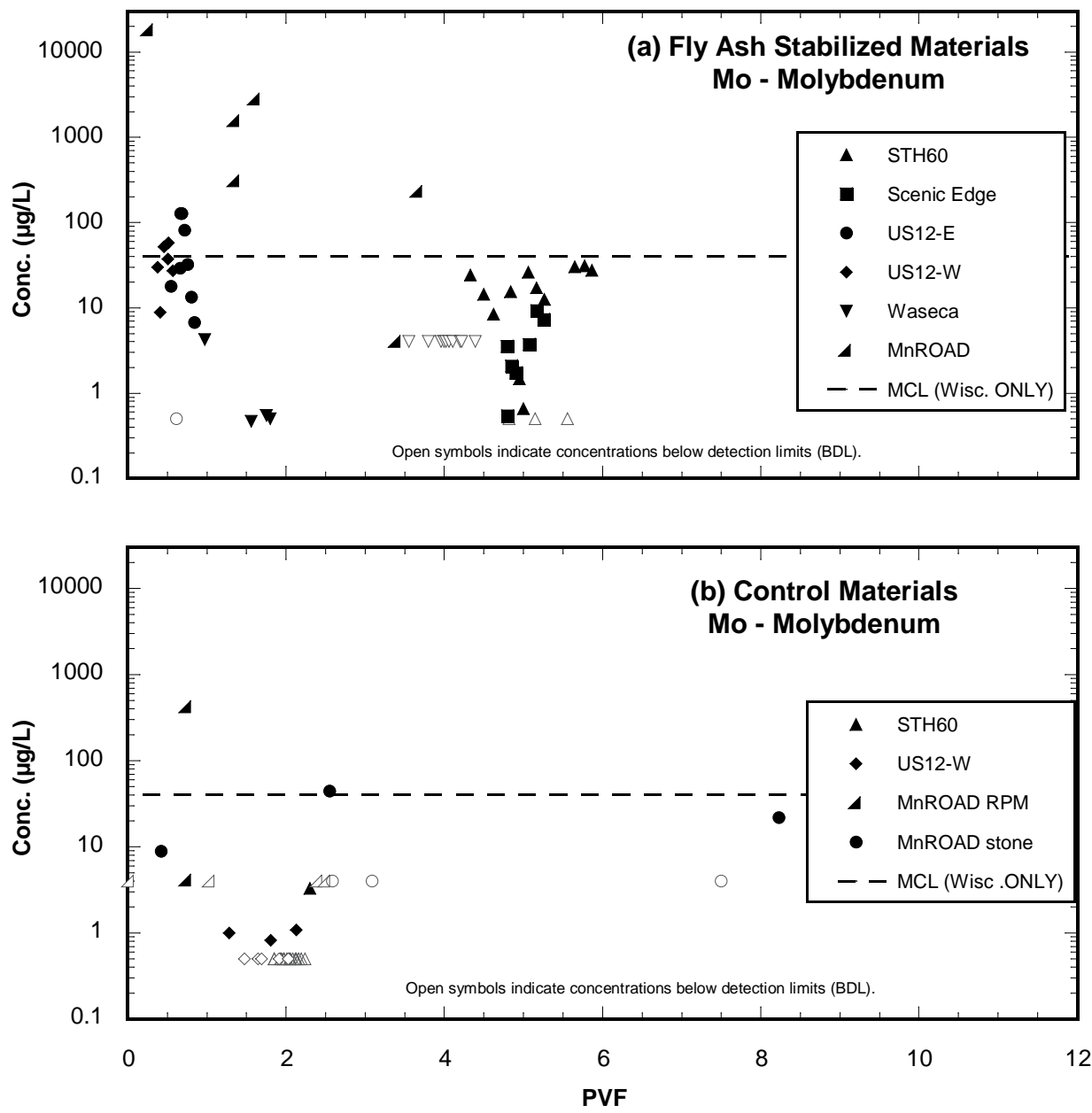
Fig. 4.10.   Molybdenum (Mo) concentrations in leachate from field road layers composed of (a) fly-ash-stabilized materials, and (b) control materials.
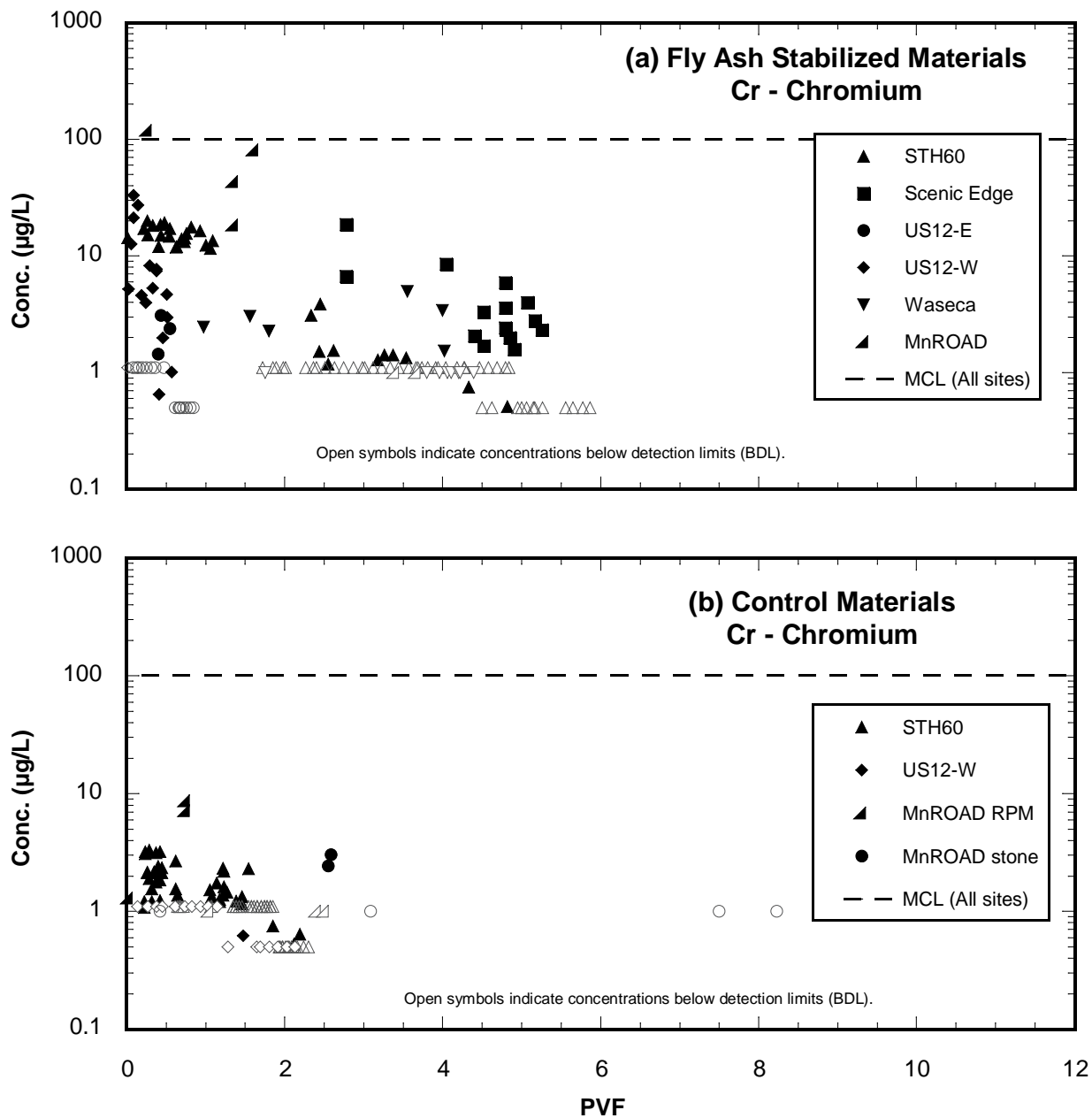
Fig. 4.11. Chromium (Cr) concentrations in leachate from field road layers composed of (a) fly-ash-stabilized materials, and (b) control materials.
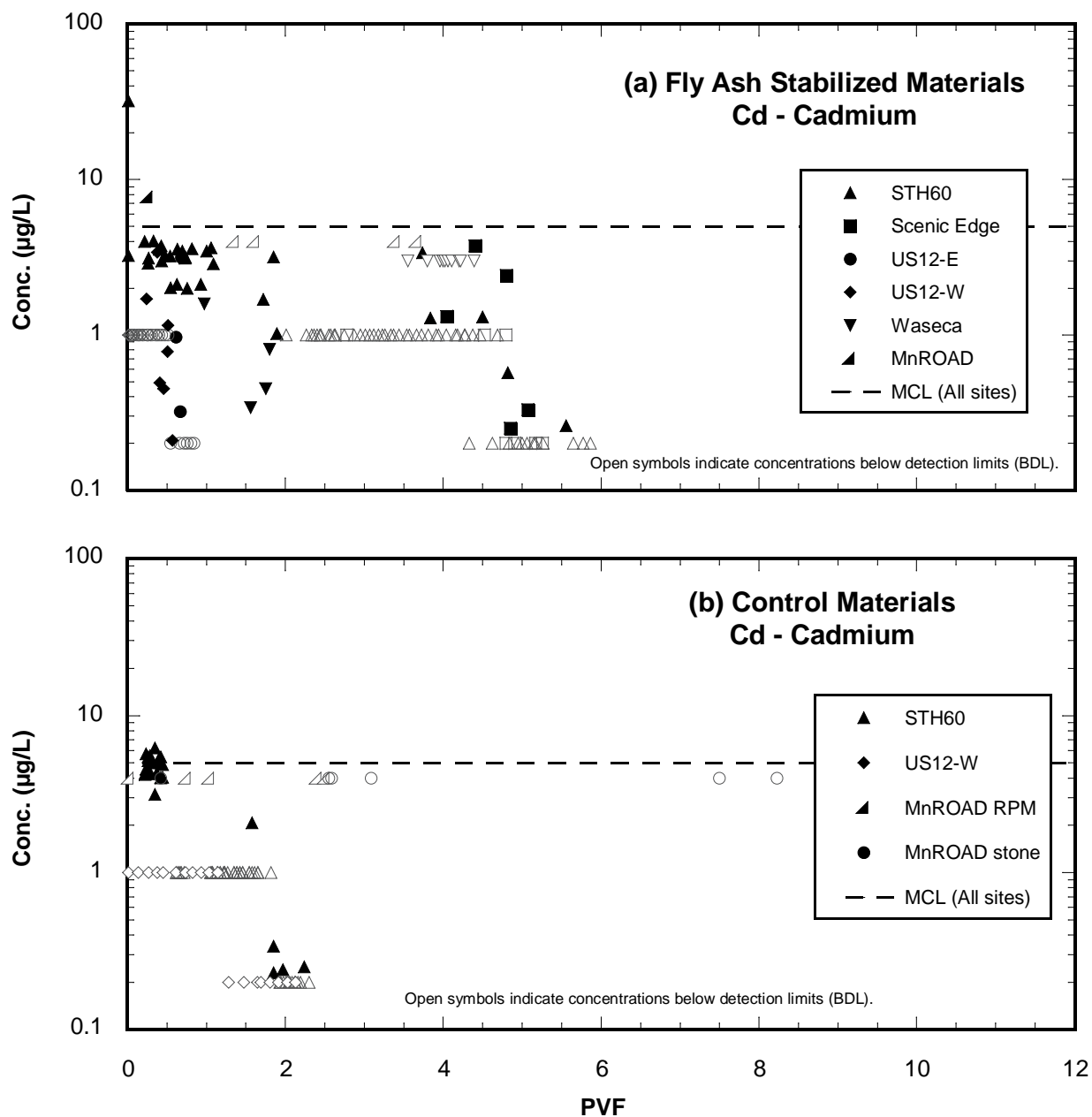
Fig. 4.12. Cadmium (Cd) concentrations in leachate from field road layers composed of (a) fly-ash-stabilized materials, and (b) control materials.
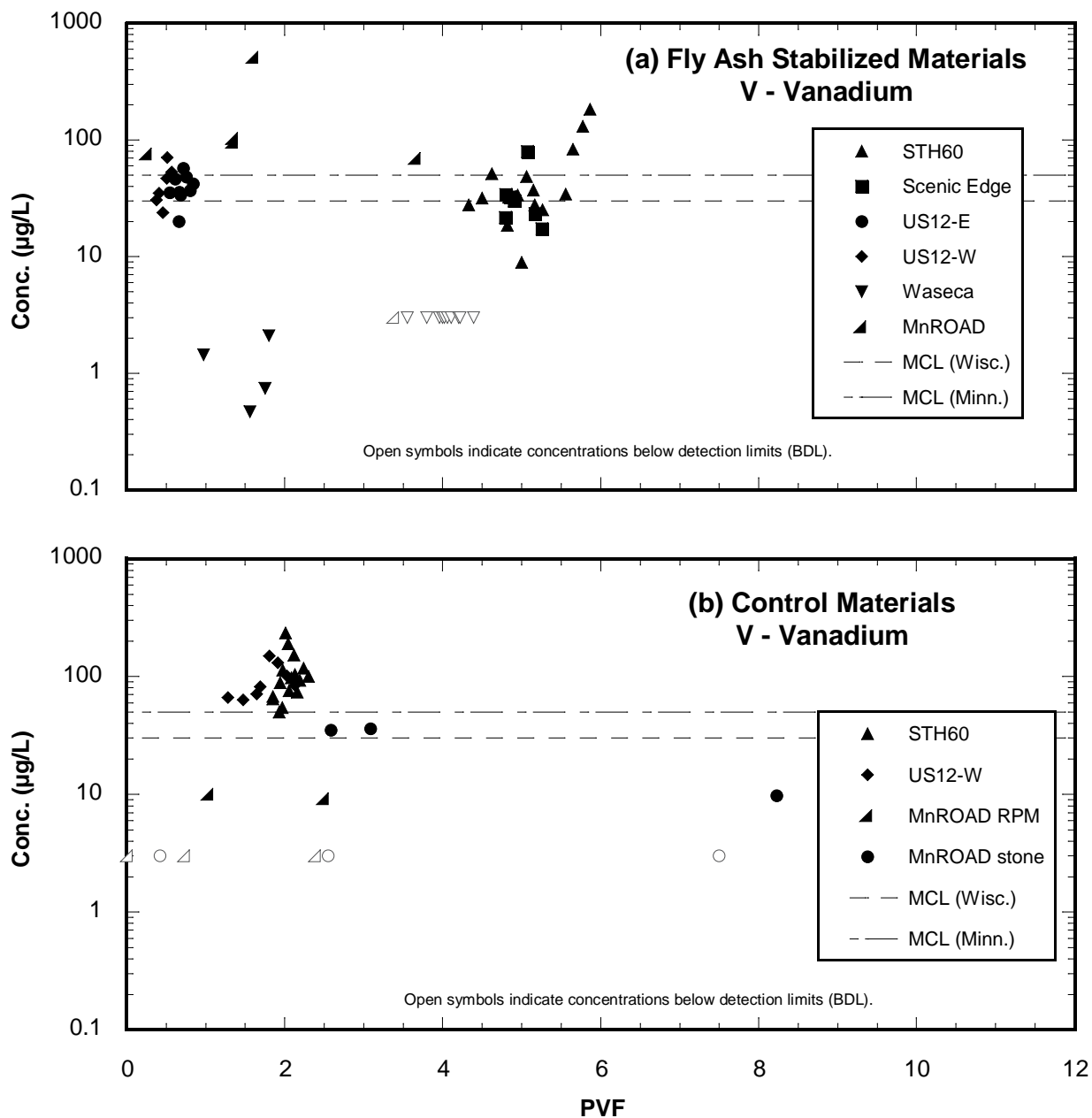
Fig. 4.13. Vanadium (V) concentrations in leachate from field road layers composed of (a) fly-ash-stabilized materials, and (b) control materials.
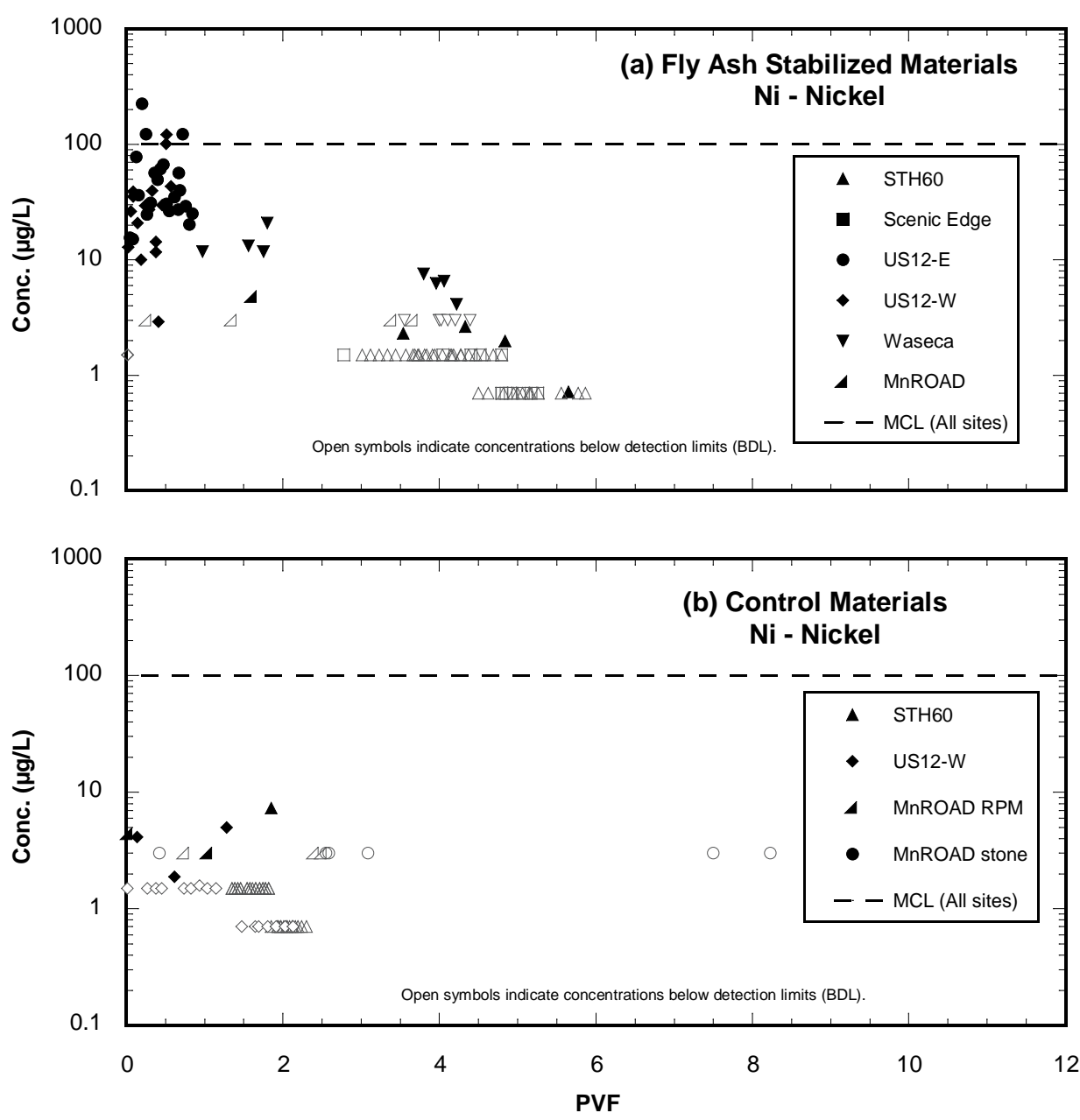
Fig. 4.14. Nickel (Ni) concentrations in leachate from field road layers composed of (a) fly-ash-stabilized materials, and (b) control materials.
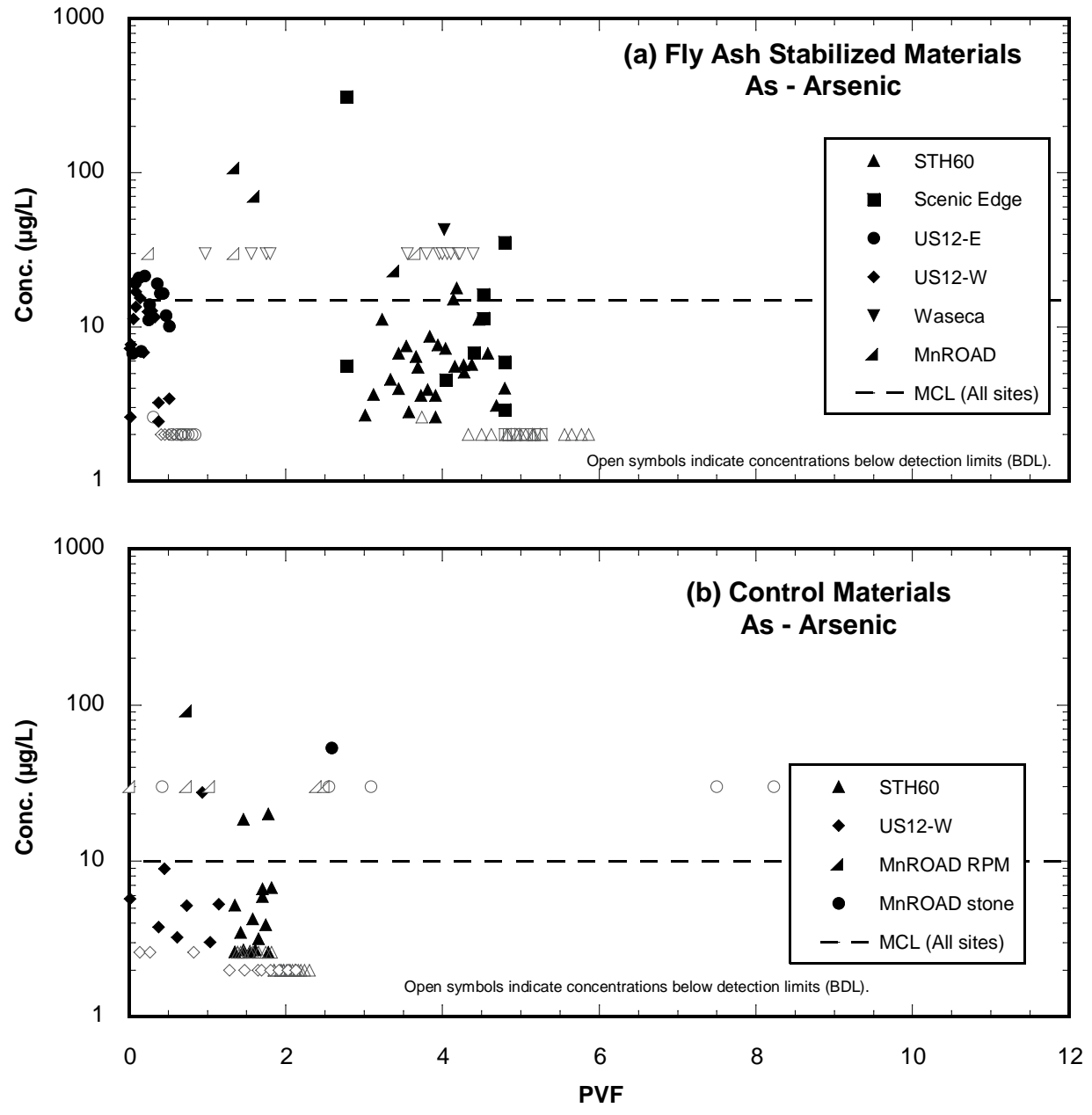
Fig. 4.15.   Arsenic (As) concentrations in leachate from field road layers composed of (a) fly-ash-stabilized materials, and (b) control materials.
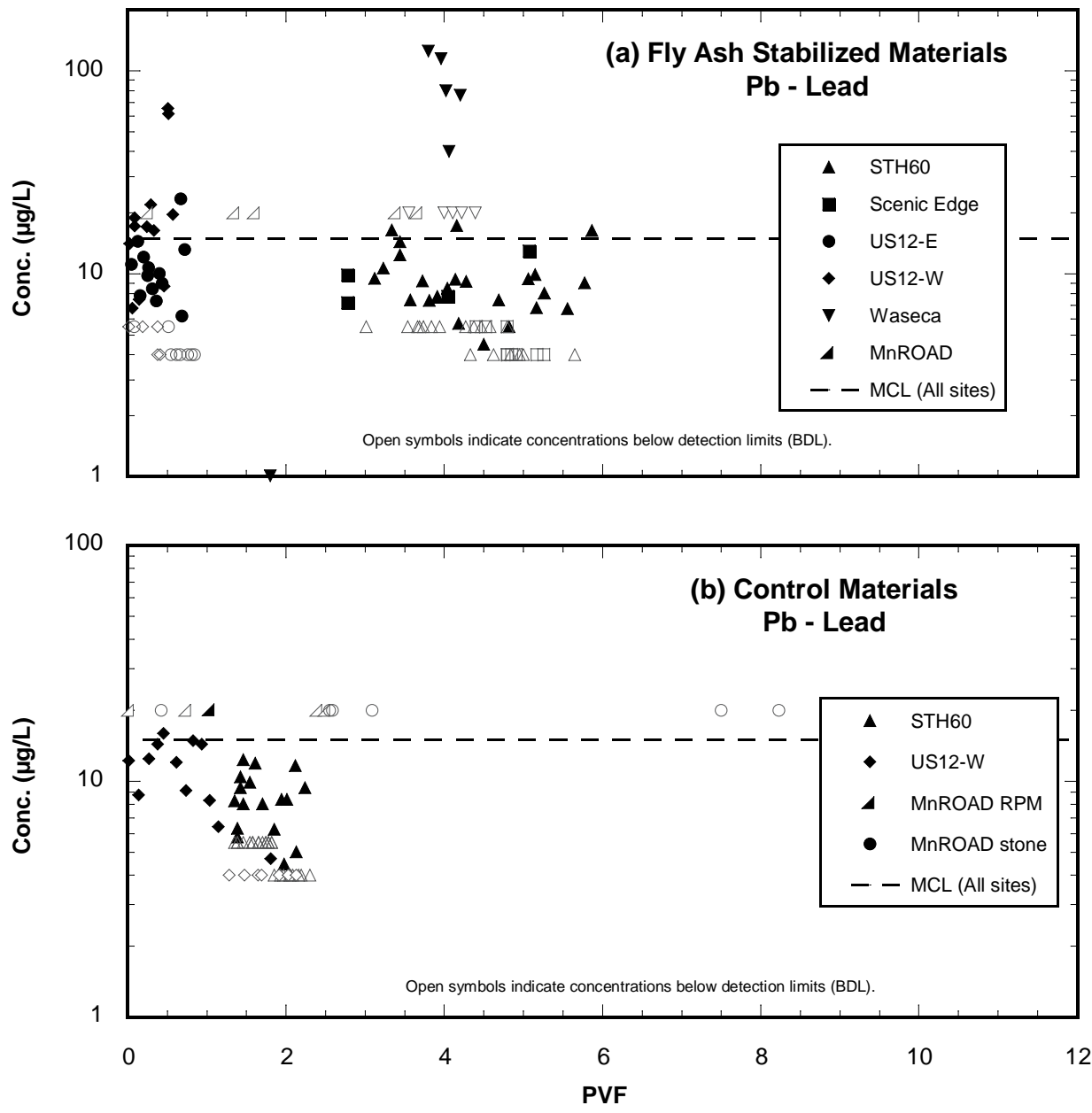
Fig. 4.16. Lead (Pb) concentrations in leachate from field road layers composed of (a) fly-ash-stabilized materials, and (b) control materials.
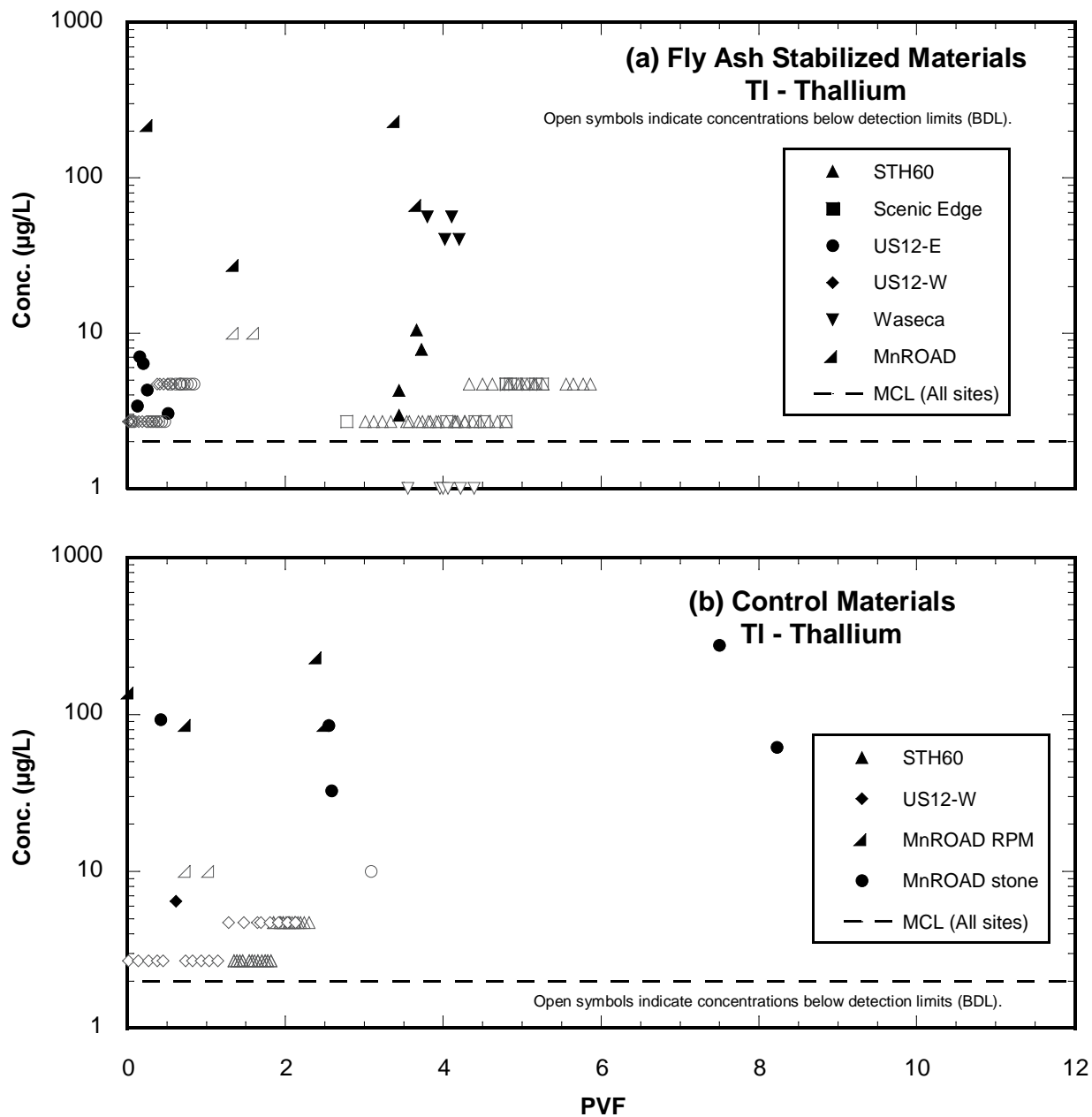
Fig. 4.17. Thallium (Tl) concentrations in leachate from field road layers composed of (a) fly-ash-stabilized materials, and (b) control materials.
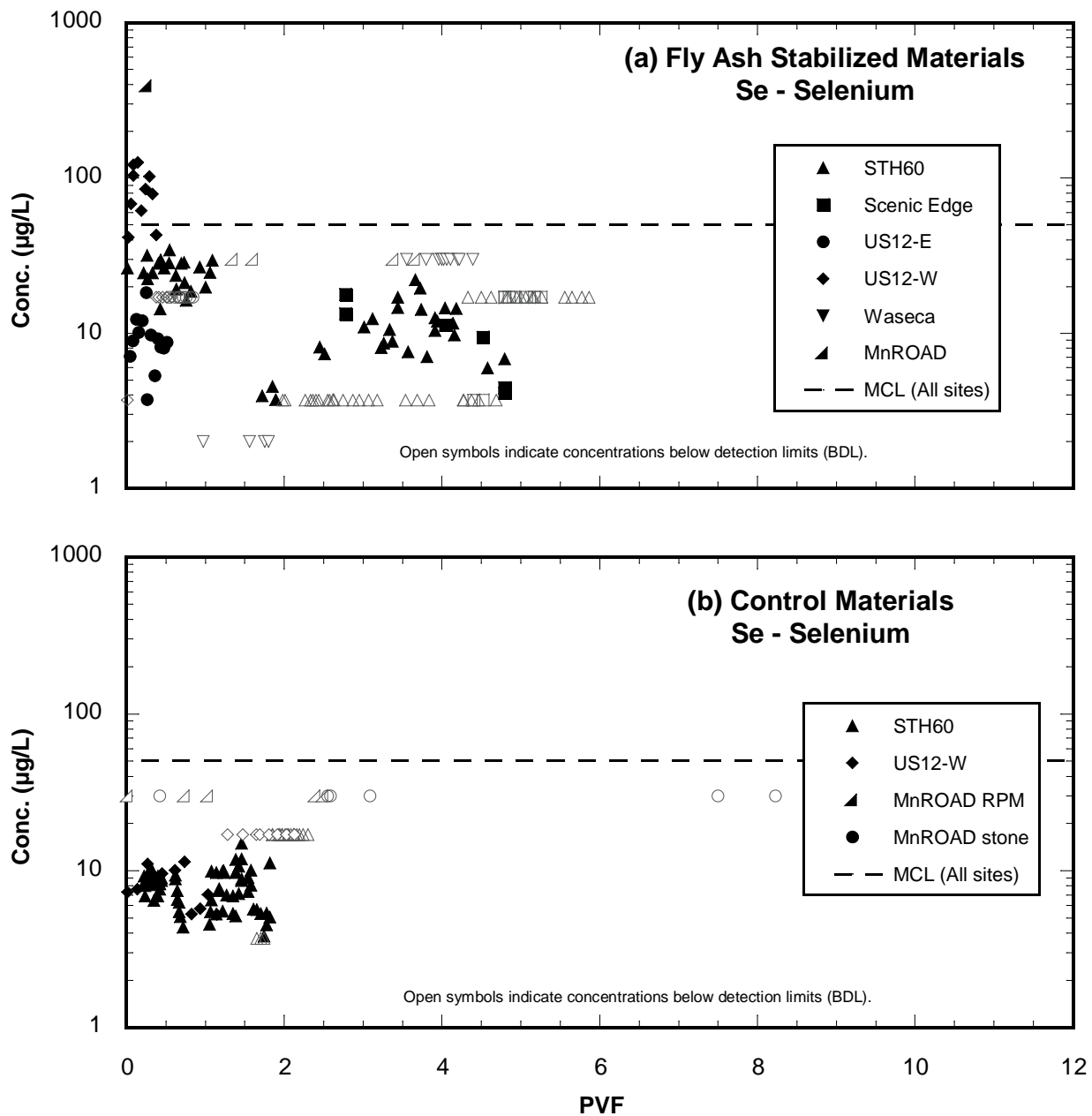
Fig. 4.18. Selenium (Se) concentrations in leachate from field road layers composed of (a) fly-ash-stabilized materials, and (b) control materials.
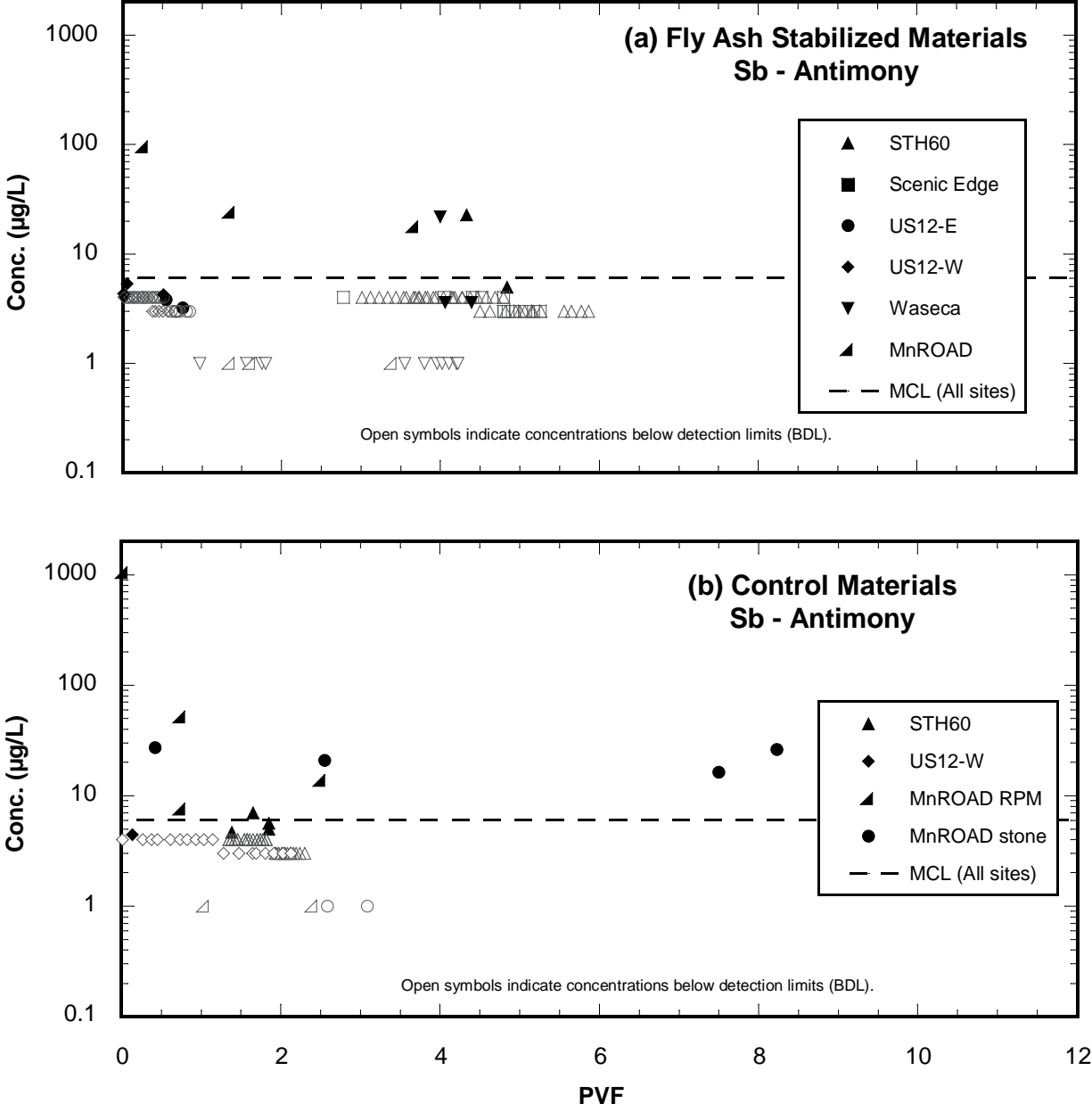
Fig. 4.19. Antimony (Sb) concentrations in leachate from field road layers composed of (a) fly-ash-stabilized materials, and (b) control materials.
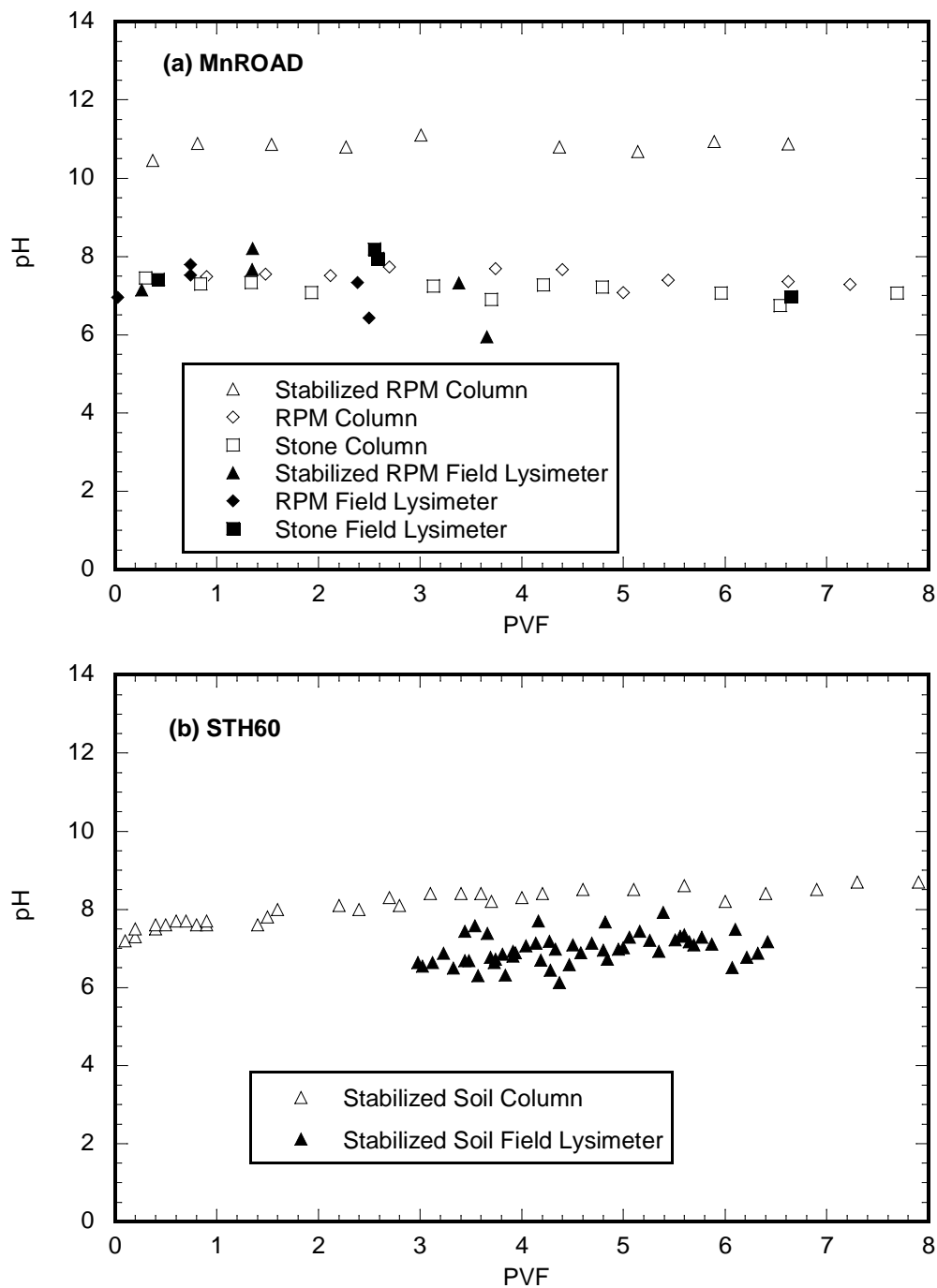
Fig. 4.20.   Comparison of leachate pH from Field Lysimeters and CLTs for the (a) MnROAD and (b) STH60 sites.
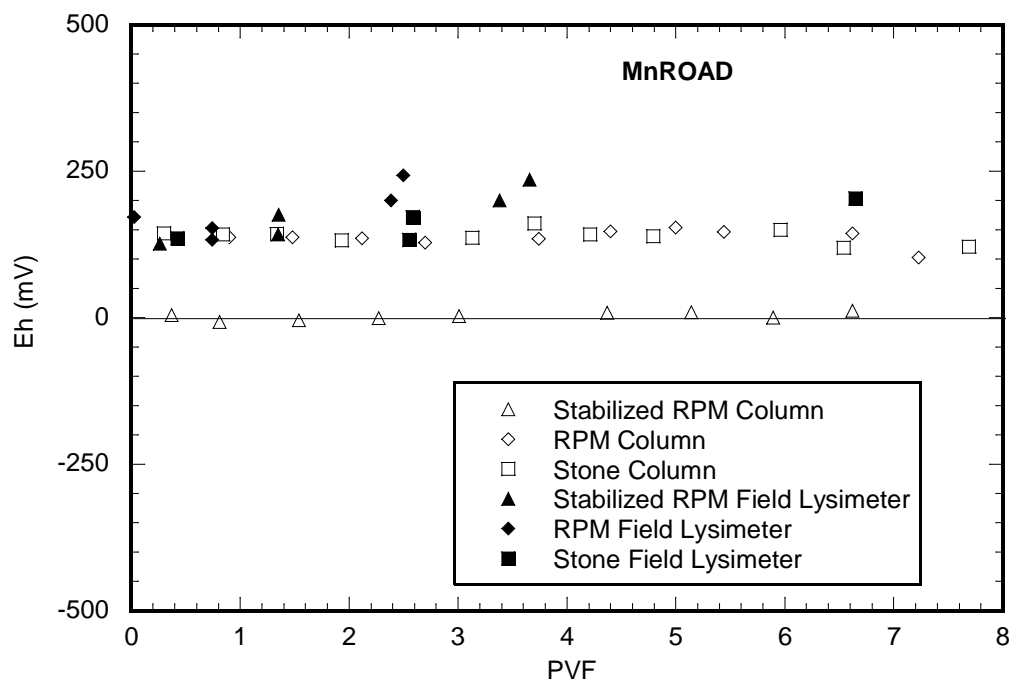
Fig. 4.21. Comparison of leachate Eh from Field Lysimeters and CLTs for the MnROAD site
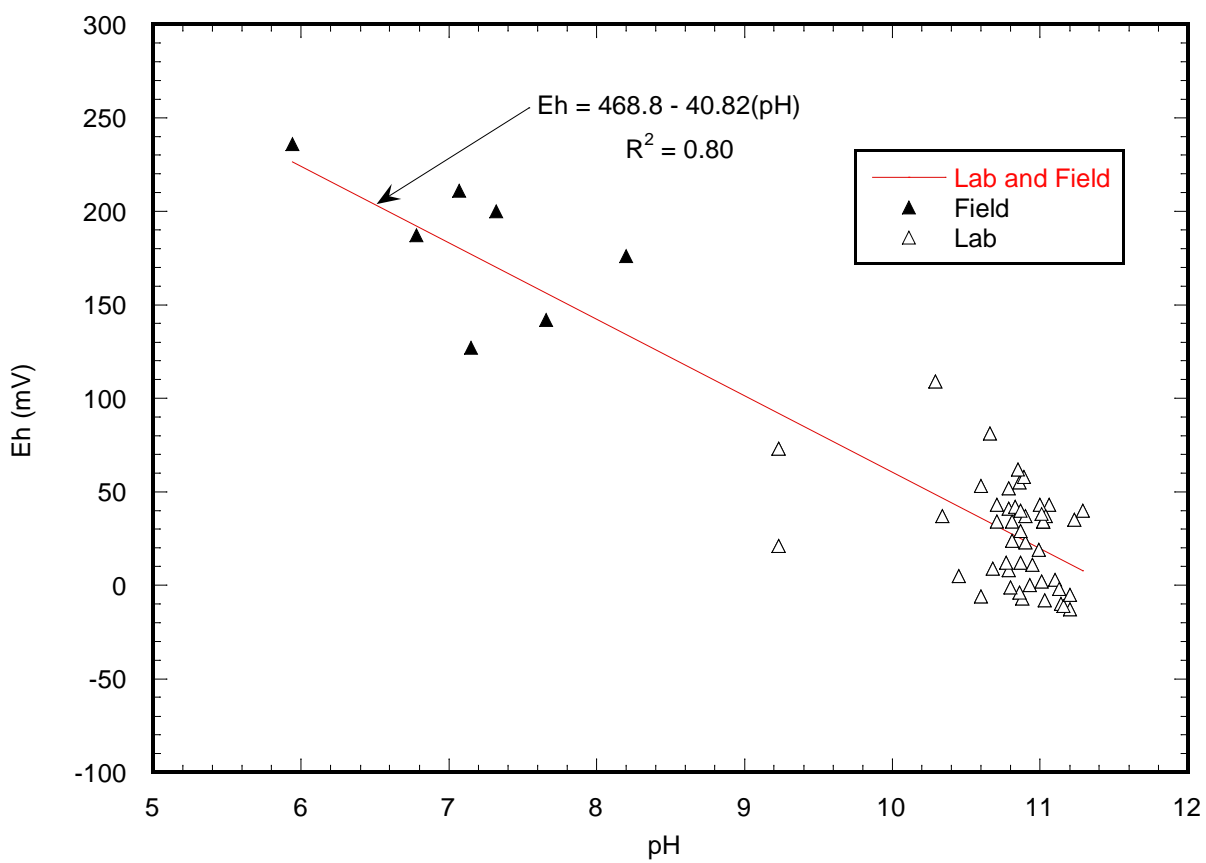
Fig. 4.22.   Eh and pH relationship for MnROAD field and CLT leachate
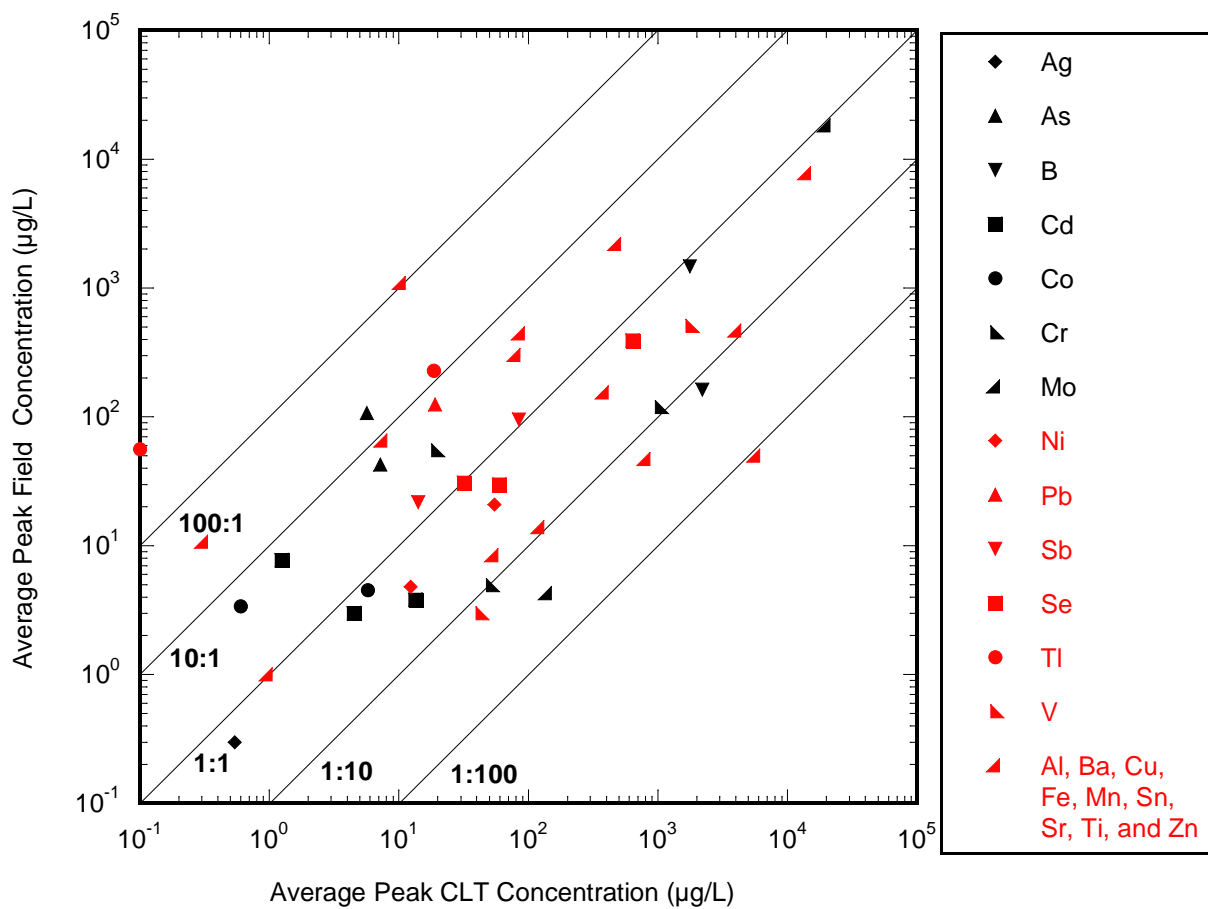
Fig. 4.23. Comparison of average peak concentrations in field lysimeters and column leach tests at STH60, MnRoad, and Waseca.
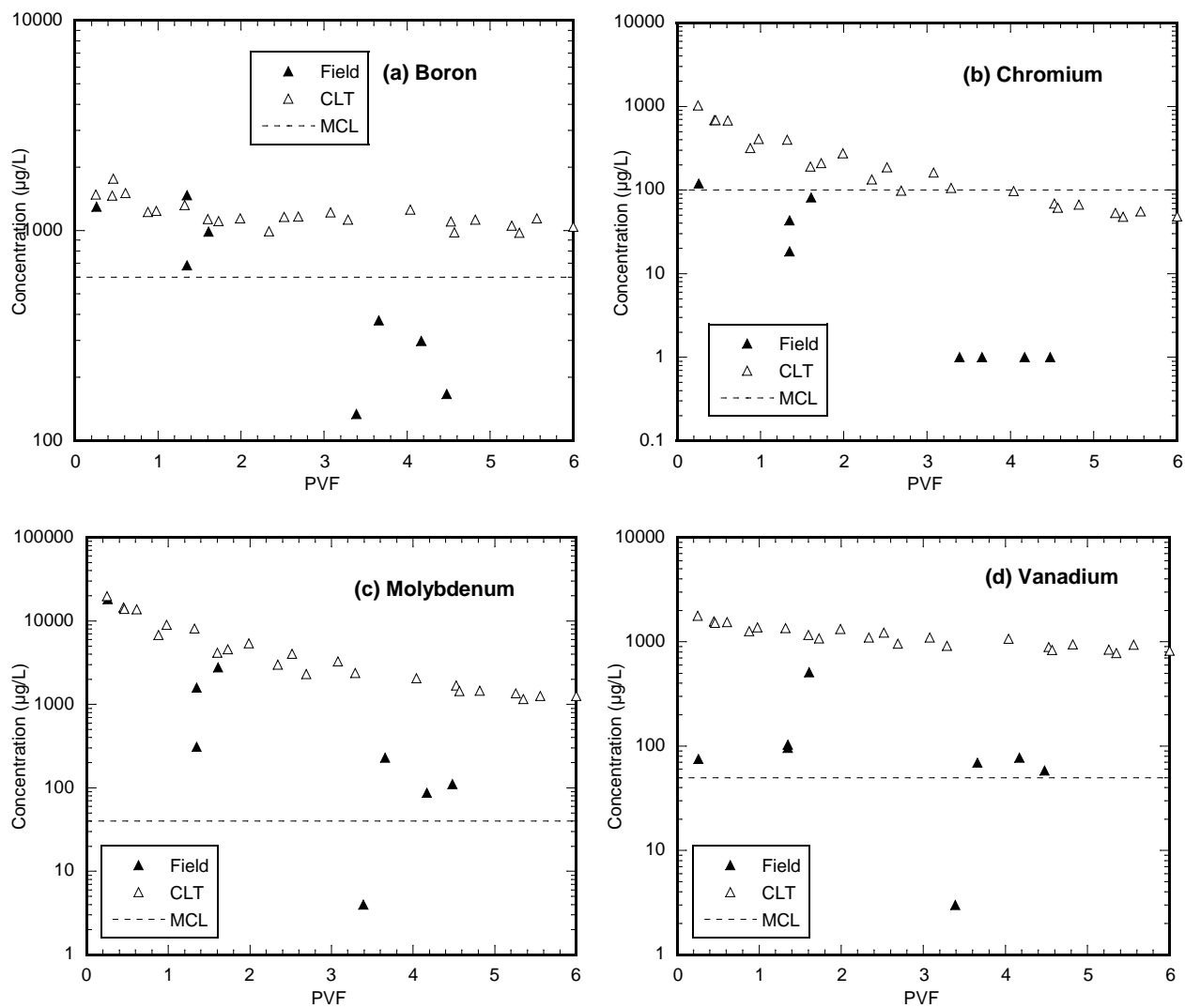
Fig. 4.24. Elements in both field and CLT Leachate that were elevated relative to the control and exceeded the MCL at the MnROAD site. Inverted triangles indicate concentrations that are BDL.
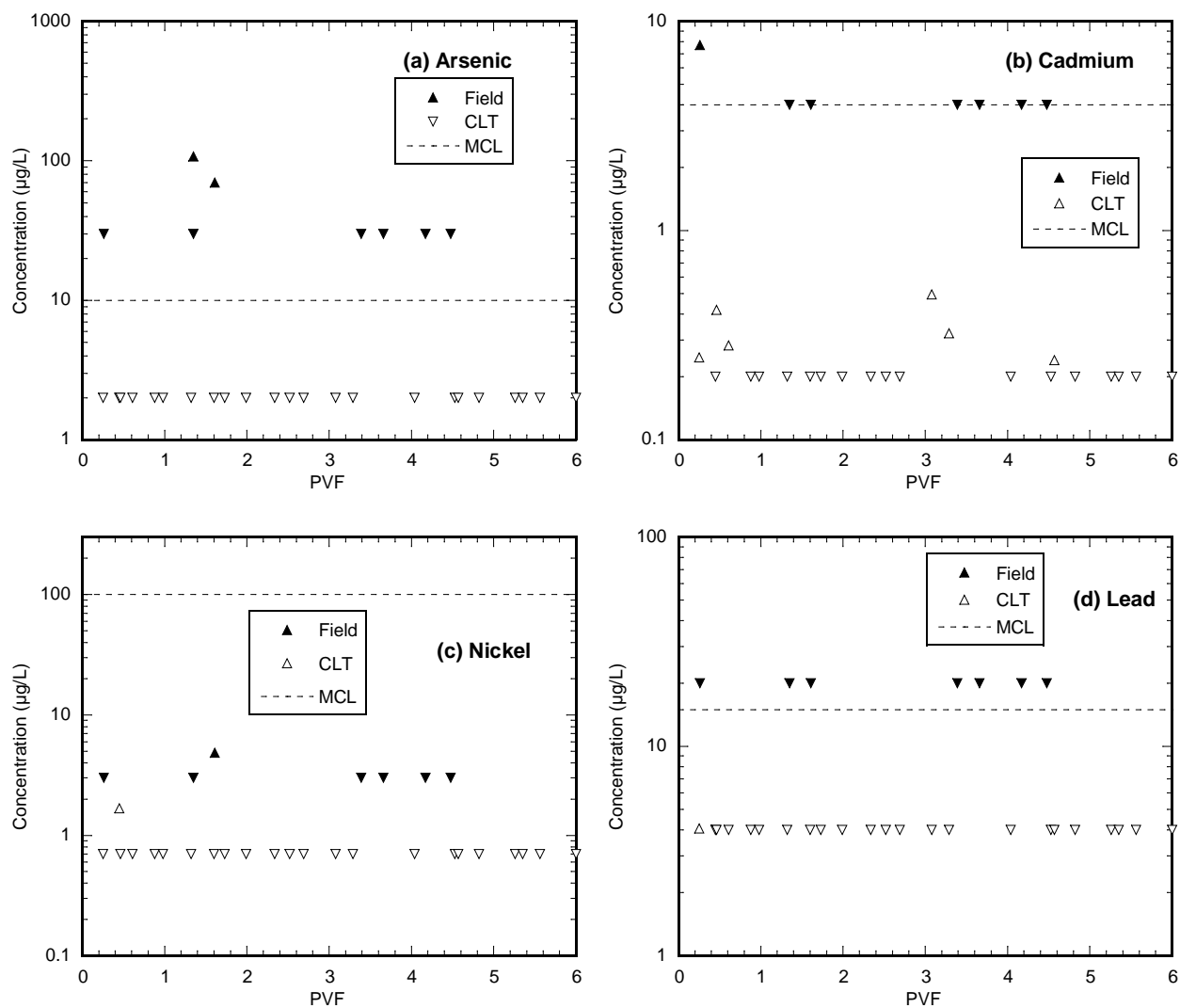
Fig. 4.25. Elements that were elevated relative to the control and exceeded the MCL in the field but not in CLT leachate at the MnROAD site. Inverted triangles indicate concentrations that are BDL.
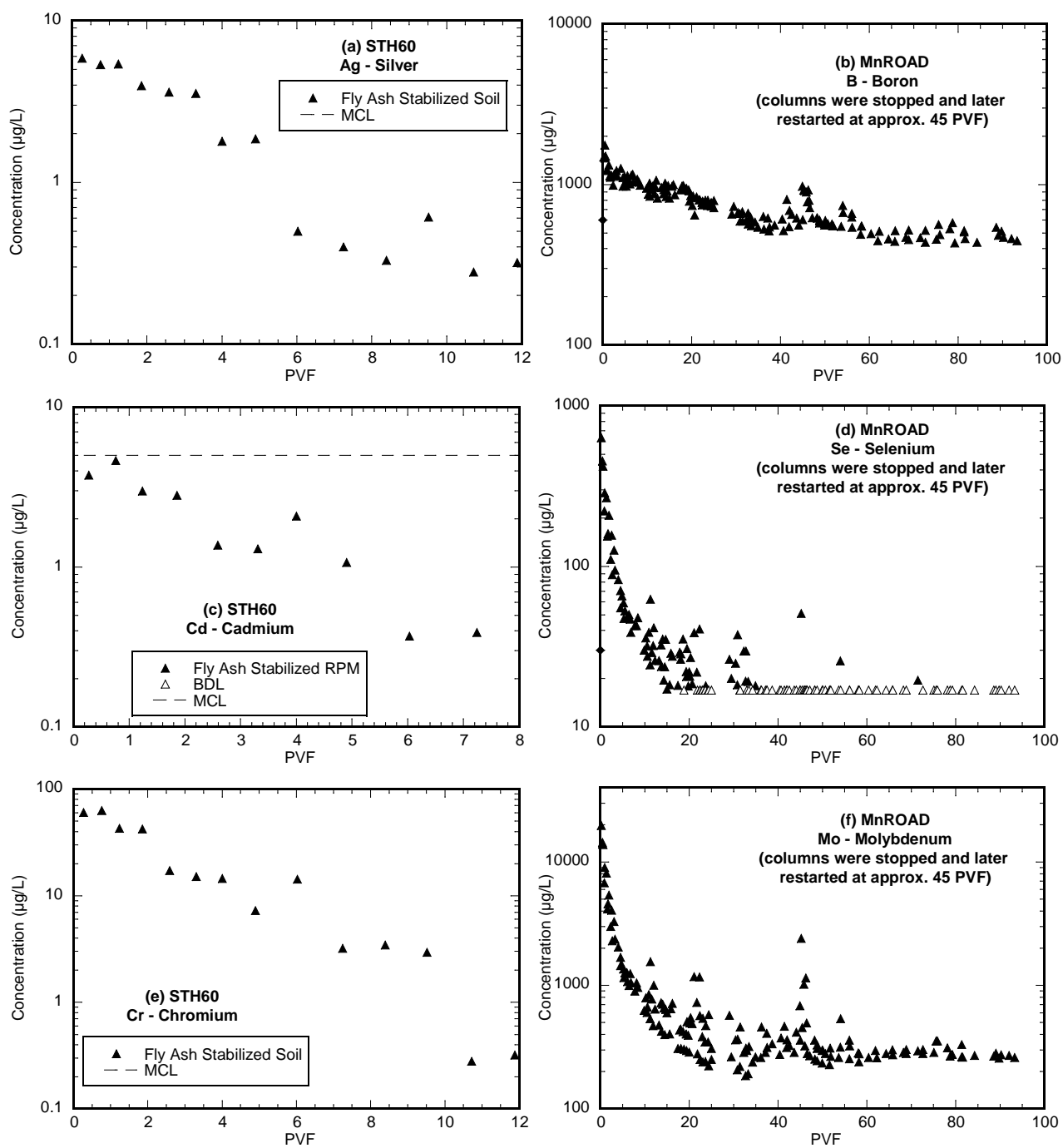
Fig. 4.26. Typical first-flush leaching patterns from CLTs for (a) Ag at STH60, (b) B at MnROAD, (c) Cd at STH60, (d) Se at MnROAD, (e) Cr at STH60, and (f) Mo at MnROAD, and increase in concentrations after MnROAD columns were left saturated with no flow (b, d, and f)
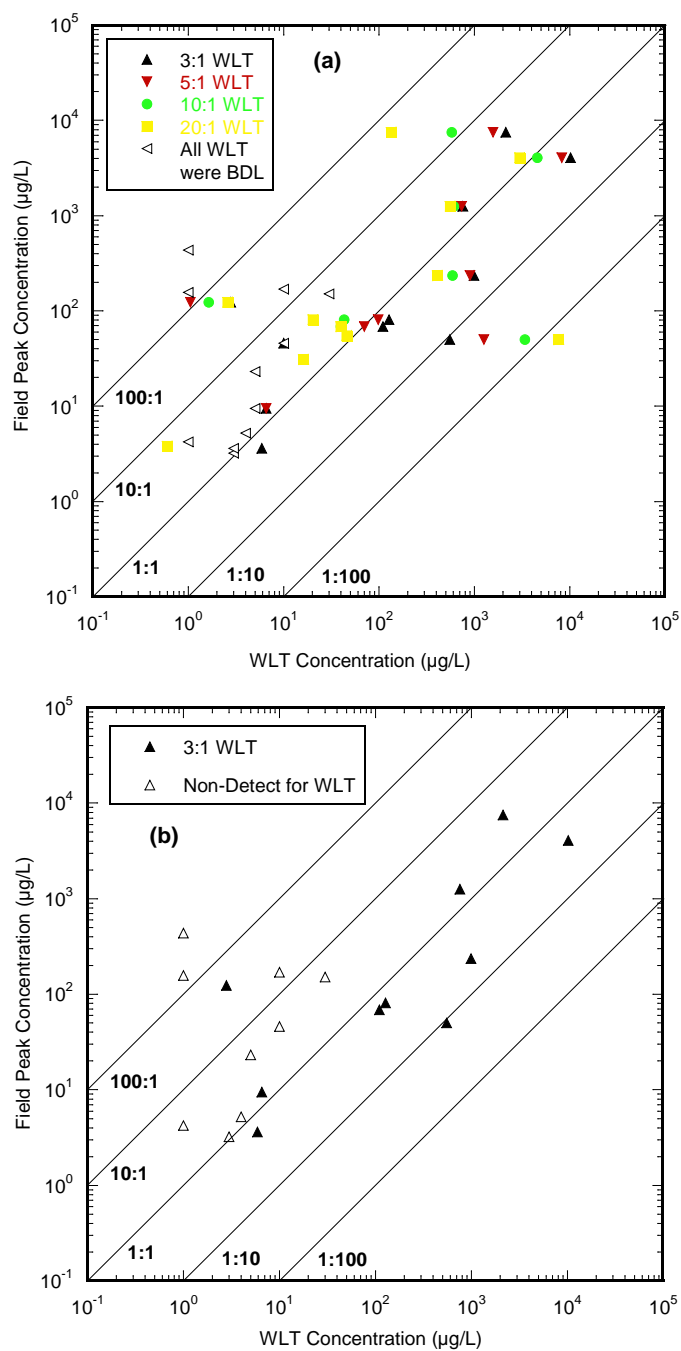
Fig. 4.27. Comparison of average peak field concentrations and WLT concentration at STH60 and MnROAD for (a) all WLT liquid:solid ratios, and (b) only the 3:1 WLT. Only elements detected in the field are shown. Open Symbols indicate WLT below detection limit.
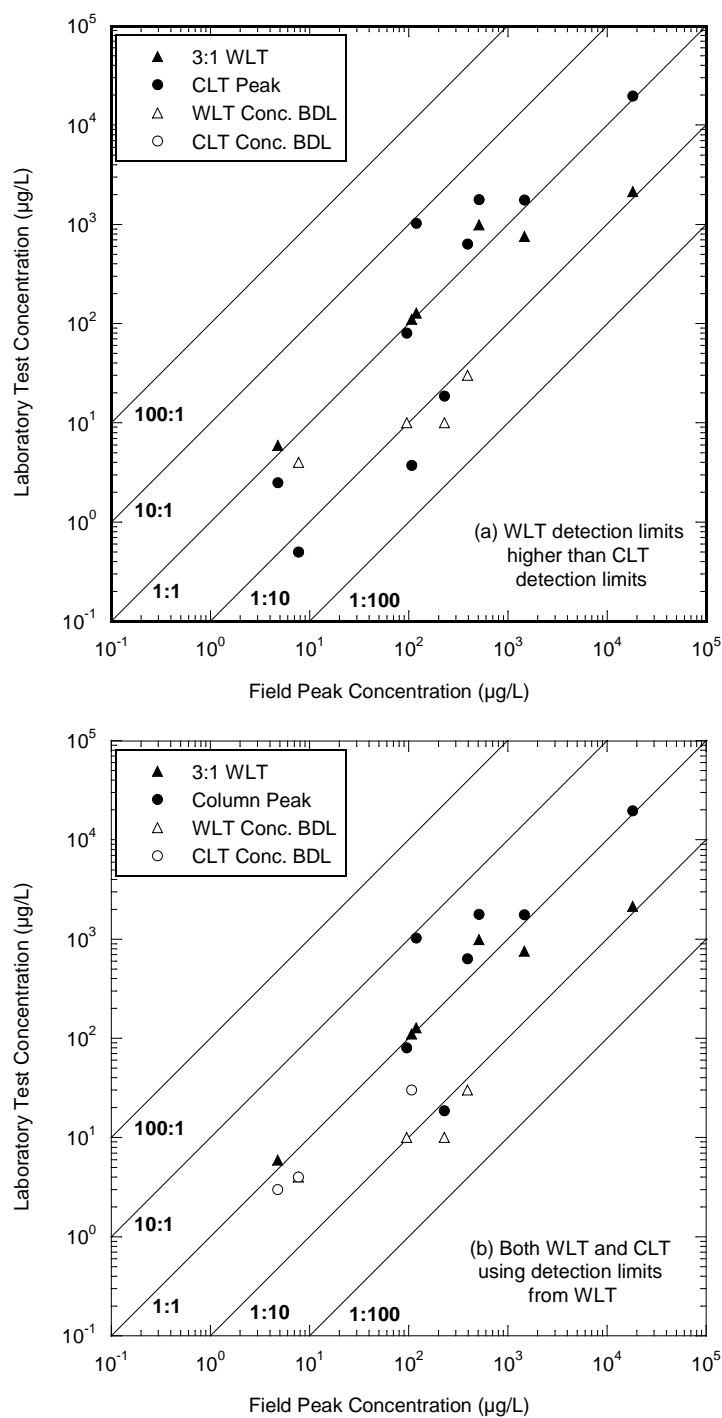
Fig. 4.28. Comparison of ability of CLT and WLT to predict peak field concentration of elements that exceeded MCLs in field leachate when (a) detection limits were lower for the CLT, and (b) when both tests use the WLT detection limits.

TABLES

Table 2.1. Properties of stabilized layers and lysimeters.

Site	STH60	US12	Scenic Edge	MnROAD	Waseca
Layer Stabilized	Subgrade	Subgrade	Subgrade	Base Course	Base Course
Material Stabilized	Fine Grained Soil	Fine Grained Soil	Fine Grained Soil	Recycled Paving Material	Recycled Paving Material
USCS and AASHTO Class.	CL, A-6	CL or SC, A-6	CL, A-7-6	GW-GM, A-1-a	GW-GM, A-1-a
Fly Ash Type	Columbia	Columbia	Columbia	Riverside 8	Riverside 7
Percent Fly Ash by Mass (%)	18	12	12	14	10
Compacted Dry Unit Weight of Stabilized Layer (kN/m^3)	15.4	18.9 - 20.0	15.9	19.6	15.9
Porosity	0.41	0.23 - 0.27	0.39	0.25	0.39
Water Content at Compaction Relative to Optimum Standard Proctor (w_{opt})	1% wet of w_{opt}	2% dry of w_{opt}	7% wet of w_{opt}	1% wet of w_{opt}	4% dry of w_{opt}
Stabilized Layer Thickness (mm)	300	300	300	203	150
Lysimeter Dimensions (m)	3.75 x 4.75	3.00 x 3.00	3.75 x 4.75	3.00 x 3.00	4.00 x 4.00

Table 3.1.   Classification of fly ashes.

Parameter	Percent of Composition			Specifications	
	Riverside 7	Riverside 8	Columbia	ASTM C 618	AASHTO M 295
				Class C	Class C
SiO_2 (silicon dioxide) (%)	32	19	Not Tested		
Al_2O_3 (aluminum oxide) (%)	19	14	Not Tested		
Fe_2O_3 (iron oxide) (%)	6	6	Not Tested		
$SiO_2 + Al_2O_3 + Fe_2O_3$ (%)	57	39	56	50 Min	50 Min
CaO (calcium oxide) (%)	24	22	23		
MgO (magnesium oxide) (%)	6	5.5	Not Tested		
SO_3 (sulfur trioxide) (%)	2	5.4	3.7	5 Max	5 Max
CaO/SiO_2	0.75	1.18	Not Tested		
$CaO/(SiO_2+Al_2O_3)$	0.47	0.68	Not Tested		
Loss on Ignition (%)	0.9	16.4	0.7	6 Max	5 Max
Moisture Content (%)	0.17	0.32	0.09	3 Max	3 Max
Specific Gravity	2.71	2.65	2.7		
Fineness, amount retained on #325 sieve (%)	12.4	15.5	<34	34 Max	34 Max
Classification	C	Off-Spec.	C		

Table 3.2.   Total elemental analysis of Riverside 8 and Columbia fly ashes.

Description	Riverside 8 Ash		Columbia Ash	
	(mg/kg)	% of Total Mass	(mg/kg)	% of Total Mass
Ag	0.40	0.000040	0.50	0.000050
Al	66000	6.6	75000	7.5
As	24	0.0024	28	0.0028
B	780	0.078	610	0.061
Ba	2600	0.26	3600	0.36
Be	5.3	0.00053	2.6	0.00026
Ca	120000	12	240000	24
Cd	5.4	0.00054	1.5	0.00015
Co	28	0.0028	5.6	0.00056
Cr	71	0.0071	60	0.0060
Cu	230	0.023	180	0.018
Fe	36000	3.6	20000	2.0
Hg	0.80	0.000080	Not Tested	-
K	2600	0.26	3000	0.30
Mg	29000	2.9	25000	2.5
Mn	120	0.012	180	0.018
Mo	140	0.014	7.2	0.00072
Na	15000	1.5	8700	0.87
Ni	620	0.062	45	0.0045
P	4800	0.48	3400	0.34
Pb	63	0.0063	28	0.0028
S	1.1	0.00011	ND	-
Sb	3.3	0.00033	7.7	0.00077
Se	16	0.0016	9.4	0.00094
Sn	1400	0.14	200	0.020
Sr	ND		1600	0.16
Ti	130	0.013	94	0.0094
Tl	ND	-	8.4	0.00084
V	66000	6.6	75000	7.5
Zn	3.3	0.00033	7.7	0.00077

Table 3.3. Column leach testing construction and testing details.

Site	MnROAD	MnROAD	MnROAD	STH60	Waseca	CR53
Material	RPM	Class 5 crushed stone	Stabilized RPM	Stabilized Soil	Stabilized RPM	Stabilized RSG
Rigid or Flexible Wall Permeameter	Rigid	Rigid	Rigid	Flexible	Flexible	Flexible
Specimen Diameter (mm)	202	202	202	102	102	102
Specimen Length (mm)	102	102	102	114	116	116
Specimen Volume (mL)	3269	3269	3269	932	948	948
Effective Confining Pressure (kPa)	0	0	0	15	15	15
Porosity	0.25	0.21	0.25	0.41	0.26	0.26
Dry Unit Weight (kN/m3)	19.4	20.5	19.6	15.4	19.1	19.3
Approx. Darcy Flux (mm/day)	16	16	16	9 for first 1.5 PVF, 2 after 1.5 PVF	2	2

Table 3.4. Minimum detection limits of chemical analytical methods used throughout the monitoring program. All MDLs are in µg/L. Hyphens indicate elements that were not tested with the method indicated.

Site	STH60				US12 & Scenic Edge			Waseca	CR53	MnROAD	
Element	2000-2005	2005-2007	2007-2009	2008-2009	2005-2007	2007-2009	2008-2009	2004-2008	2004-2006	2007-2009	2008-2009
	AA	ICP-MS	ICP-OES	OPT-CVAFS	ICP-MS	ICP-OES	OPT-CVAFS	ICP-MS	ICP-MS	ICP-OES	OPT-CVAFS
Ag	0.2	1.9	-	-	1.9		-	0.02	0.02		-
Al	-	3.0	2.5	-	3.0	2.5	-	-	-	2.5	-
As		2.6	2.0	-	2.6	2.0	-	30	30	2.0	-
B		-	4.0	-	-	4.0	-	3.0	3.0	4.0	-
Ba	-	1.2	0.04	-	1.2	0.04	-	0.08	0.08	0.04	-
Be	-	0.5	1.0	-	0.5	1.0	-	0.1	0.1	1.0	-
Cd	0.1	1.0	0.2	-	1.0	0.2	-	3.0	3.0	0.2	-
Co		1.0	0.6	-	1.0	0.6	-	4.0	4.0	0.6	-
Cr	2.0	1.1	0.5	-	1.1	0.5	-	1.0	1.0	0.5	-
Cu	-	2.0	0.7	-	2.0	0.7	-	1.0	1.0	0.7	-
Hg	-	-	-	0.001	-		0.001	0.02	0.02		0.001
Fe	-	1.5	3.2	-	1.5	3.2	-	-	-	3.2	-
Mn	-	0.8	0.05	-	0.8	0.05	-	0.5	0.5	0.05	-
Mo	-	-	0.5	-		0.5	-	4.0	4.0	0.5	-
Ni	-	1.5	0.7	-	1.5	0.7	-	3.0	3.0	0.7	-
Pb	-	5.5	4.0	-	5.5	4.0	-	20	20	4.0	-
Sb	-	4.0	3.0	-	4.0	3.0	-	1.0	1.0	3.0	-
Se	2.0	3.7	17	-	3.7	17	-	30	30	17	-
Sn	-	-	5.0	-	-	5.0	-	1.0	1.0	5.0	-
Sr	-	-	0.3	-	-	0.3	-	1.0	1.0	0.3	-
Ti	-	-	0.4	-	-	0.4	-	- -		0.4	-
Tl	-	2.7	4.7	-	2.7	4.7	-	1.0	1.0	4.7	-
V	-	-	0.1	-	-	0.1	-	3.0	3.0	0.1	-
Zn	-	0.8	0.1	-	0.8	0.1	-	1.0	1.0	0.1	-

Table 4.1. Magnitude of peak concentrations and the average of three highest concentrations in field leachate.

Element	STH60 - Stabilized Soil		US12 East - Stabilized Soil		US12 West - Stabilized Soil		Scenic Edge - Stabilized Soil		MnROAD - Stabilized RPM		Waseca - Stabilized RPM	
	Peak Conc. (µg/L)	Average Peak Conc. (µg/L)	Peak Conc. (µg/L)	Average Peak Conc. (µg/L)	Peak Conc. (µg/L)	Average Peak Conc. (µg/L)	Peak Conc. (µg/L)	Average Peak Conc. (µg/L)	Peak Conc. (µg/L)	Average Peak Conc. (µg/L)	Peak Conc. (µg/L)	Average Peak Conc. (µg/L)
Mo #	31.12	29.69	128.71	112.97	58.16	49.17	9.23	7.78	@ 18176	7511.14	4.28	4.09
Sr #	4687.56	3406.28	3913.35	3486.59	280.45	180.68	3450.61	1867.11	7770.00	4057.37	468.00	320.33
Al ^	164.47	98.44	418.44	334.93	4243.35	2182.92	77.85	62.67	All BDL	All BDL	NT	NT
Fe ^	712.00	413.19	1560.83	968.78	3314.73	1926.45	38.14	27.80	442.81	157.75	NT	NT
B #	3267.55	2959.54	1195.96	1085.05	1243.07	1156.21	2181.14	1731.36	1470.55	1252.82	162.00	117.33
Mn ^	1204.54	929.27	2103.38	1538.82	127.83	100.31	26.26	19.35	1094.57	438.17	2200.00	1785.23
Sn #	41.71	24.95	414.29	253.16	891.06	491.03	6.02	5.34	65.50	23.17	10.70	4.23
Ba ^	604.05	540.87	406.24	376.36	185.31	137.40	396.21	381.92	NT	NT	155.00	129.00
V #	183.03	146.77	57.17	52.13	70.56	63.46	79.74	48.72	510.00	236.48	All BDL	All BDL
Se *	34.21	31.89	18.34	17.45	126.11	116.99	17.83	17.28	392.84	150.95	All BDL	All BDL
Zn ^	285.04	198.04	110.59	95.32	378.74	225.58	154.01	94.54	301.58	123.82	47.01	35.55
As ^	17.94	14.75	21.35	20.53	16.92	15.25	311.76	121.09	107.46	69.15	42.81	34.27
Cu ^	44.14	37.72	9.91	5.71	309.61	206.58	52.75	45.01	8.44	9.47	14.00	12.00
Tl ^	10.50	7.68	7.02	6.03	All BDL	All BDL	All BDL	All BDL	228.80	170.40	55.90	50.67
Ni ^	2.65	2.32	225.72	157.19	121.62	98.56	All BDL	All BDL	4.84	3.61	20.81	15.28
Pb ^	17.23	16.68	23.40	17.00	65.44	49.63	12.96	10.19	All BDL	All BDL	125.00	106.67
Cr *	20.15	19.34	3.11	2.31	32.96	27.09	18.59	11.24	119.18	81.25	4.94	3.78
Sb ^	22.75	10.58	All BDL	All BDL	5.32	4.64	All BDL	All BDL	95.20	45.73	21.80	9.67
Ti #	1.09	0.63	3.11	2.46	44.41	31.96	0.52	0.44	1.00	1.00	NT	NT
Co ^	3.54	2.90	11.57	5.70	32.43	30.62	3.09	2.34	3.44	3.22	4.53	4.18
Cd *	32.10	13.37	3.14	1.72	3.40	2.09	3.74	2.49	7.69	5.23	3.00	3.00
Ag *	11.30	10.65	All BDL	All BDL	All BDL	All BDL	All BDL	All BDL	2.80	4.23	0.30	0.17
Hg $	NT	NT	NT	NT	NT	NT	NT	NT	0.01	0.01	0.20	0.20
Be ^	All BDL	All BDL	All BDL	All BDL	All BDL	All BDL	All BDL	All BDL	All BDL	All BDL	All BDL	All BDL

BDL - below detection limit

NT - element not tested for at site

* - Element NT for at Scenic Edge for first 65 months of study

^ - Element NT for at Scenic Edge for first 65 months of study, or at STH60 for first 60 months of study

- Element NT for at Scenic Edge and STH60 for first 80 months of study, or at US12 for first 18 months of study

$ - Long term monitoring of Hg only at MnROAD and Waseca sites

@ - concentration is out of method calibration range, and is estimated from linear extrapolation

Table 4.2. Elements with peak concentrations occurring
during or after the first 2 PVF.

Element	Site				
	STH60	US12	Scenic Edge	MnROAD	Waseca
Ag	▼	ND	NT	▼	X
Al	NT	▼	NT	ND	NT
As	NT	▼	NT	▼	X
B	NT	NT	NT	▼	X
Ba	NT	▼	NT	NT	X
Be	NT	ND	NT	ND	ND
Cd	▼	▼	NT	▼	ND
Co	NT	▼	NT	▼	▼
Cr	▼	▼	NT	▼	X
Cu	NT	▼	NT	▼	X
Fe	NT	X	NT	X	X
Hg	NT	NT	NT	NT	ND
Mn	NT	X	NT	X	X
Mo	NT	NT	NT	▼	▼
Ni	NT	▼	NT	▼	▼
Pb	NT	▼	NT	ND	X
Sb	NT	▼	NT	▼	X
Se	▼	▼	NT	▼	ND
Sn	NT	NT	NT	X	X
Sr	NT	NT	NT	▼	X
Ti	NT	NT	NT	ND	NT
Tl	NT	▼	NT	X	X
V	NT	NT	NT	▼	ND
Zn	NT	▼	NT	X	X

▼ - Peak Concentration occurred during the first 2 PVF

X - Peak Concentration occurred after the first 2 PVF

NT - Element was not tested for at the beginning of site operation

ND - All concentrations were below detection limit

Table 4.3. Comparison of field concentrations from fly ash stabilized sections
and control sections to determine if element is statistically elevated in
the stabilized material leachate.

Element	Avg. Magnitude of elevated concentration (μg/L)	
	Average Peak Concentration	Geometric Mean of Concentrations
Sr	-12187.36	-4512.66
Mo	-15021.91	-629.6
Al	-4828.99	-2721.92
V	-1473.99	-764.32
B	-1168.34	-667.87
Cr	-790.71	-16.48
Ba	-325.89	-168.48
Cu	-37.78	-0.41
Sb	-31.39	3.57
Ni	-3.36	0.07
Be	-3.24	0.05
Ti	-0.1	0.01
Co	0.03	0.03
Cd	0.67	0.02
As	2.13	0.51
Sn	2.89	1.9
Pb	2.88	2.07
Zn	23.46	0.81
Se	-4.66	29.71
Tl	25.02	10.77
Fe	64.04	3.12
Mn	980.51	14.42

* - more negative number indicates concentration from
   stabilized materials is more elevated relative to the
   concentrations from control materials

Table 4.4. USEPA, Minnesota, and
Wisconsin maximum contaminant
limits (MCLs) for groundwater and
drinking water.

Element	MN MCL (µg/L)	USEPA MCL (µg/L)	WI MCL (µg/L)
Ag	-	30	50
As	10	-	10
B	600	-	960
Ba	2000	2000	2000
Be	4	0.08	4
Cd	4	5	5
Co	-	-	40
Cr	100	100	100
Cu	-	-	1300
Hg	2	-	2
Mo*	-	-	40
Ni	100	-	100
Pb	15	-	15
Sb	6	6	6
Se	30	50	50
Sn	4000	-	-
Tl	0.6	2	2
V	50	-	30
Zn	-	2000	-

* - Minnesota does not have a MCL for Mo, the Wisconsin MCL was used to compare Mo
   concentrations from Minnesota sites.

Table 4.5.   Ratio of average peak concentration or geometric mean of all concentrations to MCLs in field leachate.

Average Peak Concentrations										
Fly-Ash-Stabilized Materials										
Site	**As**	**B**	**Cd**	**Cr**	**Mo**	**Ni**	**Pb**	**Sb**	**Se**	**Tl**	**V**
STH60	1.8	5.4	6.4	-	□	□	1.1	5.7	1.1	18	3.7
US12	1.7	2.1	-	-	1.5	1.2	4.4	1.3	4.2	7.8	1.4
Scenic Edge	31	3.6	□	□	□	□	□	□	□	7.8	1.6
MnROAD	11	2.5	1.5	1.2	450*	-	1.3	24	13	380	10
Waseca	4.3	-	-	-	-	-	8.3	5.5	-	93	-
Control Materials										
Site	**As**	**B**	**Cd**	**Cr**	**Mo**	**Ni**	**Pb**	**Sb**	**Se**	**Tl**	**V**
STH60 Stone	2	□	1.2	-	□	□	□	1.7	-	7.8	4.7
US12 Soil	2.7	□	-	-	-	-	1.1	1.1	-	11	3
MnROAD RPM	9.1	-	-	-	11*	-	1.3	260	-	380	-
MnROAD Stone	5.3	-	-	-	-	-	1.3	6.8	-	460	-

Geometric Mean of Concentrations										
Fly-Ash-Stabilized Materials										
Site	**As**	**B**	**Cd**	**Cr**	**Mo**	**Ni**	**Pb**	**Sb**	**Se**	**Tl**	**V**
STH60	□	□	□	□	□	□	□	□	□	1.8	1.4
US12	-	□	-	-	□	-	-	-	-	2.0	1.5
Scenic Edge	□	□	□	□	□	□	□	□	□	1.8	□
MnROAD	3.8	-	1.1	-	8.7	-	1.3	2.7	-	52.0	1.3
Waseca	3.1	-	-	-	-	-	-	-	-	1.7	-
Control Materials										
Site	**As**	**B**	**Cd**	**Cr**	**Mo**	**Ni**	**Pb**	**Sb**	**Se**	**Tl**	**V**
STH60 Stone	□	□	□	□	□	□	□	□	□	1.7	3.2
US12 Soil	-	□	-	-	□	-	-	-	-	1.9	2.8
MnROAD RPM	2.9	-	-	-	-	-	1.3	3.6	-	73.9	-
MnROAD Stone	3.2	-	-	-	-	-	1.3	2.5	-	87.2	-

□ - Was not tested for during the early operation of the site.
    May have exceeded the MCL prior to testing began.
* - Minnesota has no MCL for Mo, but the concentration exceeded the
Hyphen indicates element did not exceed MCL

Table 4.6. Speciation of select trace elements under Eh-pH Conditions.

Element	pH	Species Eh (mV) -150	0	150	+300
As	6			$H_2AsO_4^{[-]}$	$H_2AsO_4^{[-]}$
	7	$HAsO_2^{(aq)}$	$HAsO_2^{(aq)}$	$HAsO_4^{[2-]}$	$HAsO_4^{[2-]}$
	8	$HAsO_2^{(aq)}$	$HAsO_4^{[2-]}$	$HAsO_4^{[2-]}$	$HAsO_4^{[2-]}$
	9	$HAsO_4^{[2-]}$	$HAsO_4^{[2-]}$	$HAsO_4^{[2-]}$	$HAsO_4^{[2-]}$
B	6			$H_3BO_3^{(aq)}$	
	7				
	8				
	9				
Cd	6			$Cd^{[2+]}$	
	7				
	8				
	9				
Cr	6			$CrOH^{[2+]}$	
	7				
	8			$Cr_2O_3^{(s)}$	
	9				$CrO_4^{[2-]}$
Mo	6			$MoO_4^{[2-]}$	
	7				
	8				
	9				
Ni	6			$Ni^{[2+]}$	
	7				
	8				
	9				
Pb	6			$Pb^{[2+]}$	
	7				
	8			$PbOH^{[+]}$	
	9				
Sb	6			$HSbO_2^{(aq)}$	
	7				$SbO4^{(s)}$
	8				
	9				
Se	6			$HSeO_3^{[-]}$	$HSeO_3^{[-]}$
	7	$HSe^{[-]}$	$HSe^{[-]}$		
	8		$SeO_3^{[2-]}$	$SeO_3^{[2-]}$	$SeO_3^{[2-]}$
	9				
Tl	6			$Tl^{[+]}$	
	7				
	8				
	9				
V	6	$VO^{[2+]}$	$VO^{[2+]}$		
	7			$VO_3^{[-]}$	
	8				
	9			$HVO_4^{[2-]}$	

Table 4.7. Concentrations of elements elevated in the CLT stabilized leachate relative to the control leachate.

Element	Avg. Magnitude of elevated concentration (µg/L) (more negative indicates a greater difference between stabilized and control concentrations	
	Average Peak Concentration	Geometric Mean Concentration
Ag	Not Tested in CLT	Not Tested in CLT
Al	-4828.99	-2721.92
As	2.13	0.51
B	-1168.34	-667.87
Ba	-325.89	-168.48
Be	-3.24	0.05
Cd	0.67	0.02
Co	0.03	0.03
Cr	-790.71	-16.48
Cu	-37.78	-0.41
Fe	64.04	3.12
Hg	Not Tested in CLT	Not Tested in CLT
Mn	980.51	14.42
Mo	-15021.91	-629.6
Ni	-3.36	0.07
Pb	2.88	2.07
Sb	-31.39	3.57
Se	-4.66	29.71
Sn	2.89	1.9
Sr	-12187.36	-4512.66
Ti	-0.1	0.01
Tl	25.02	10.77
V	-1473.99	-764.32
Zn	23.46	0.81

85

Table 4.8. Comparison of field and CLT leachate concentrations exceeding MCL and concentrations relative to control materials.

All Elements	Elevated in the field	Exceeded MCL in Field	**Exceeded MCL and Elevated**	Exceeded MCL but the same or less than Controls (Field)	Elevated in Columns	Exceeded MCL in Columns	**Exceeded MCL and Elevated in Columns**	Exceeded MCL but the same or less than Controls (Columns)
Ag	Ag				Ag			
Al	Al				Al			
As	As	As	**As**					
B	B	B	**B**		B	B	**B**	
Ba	Ba				Ba			
Be								
Cd	Cd	Cd	**Cd**					
Co	Co							
Cr	Cr	Cr	**Cr**		Cr	Cr	**Cr**	
Cu	Cu				Cu			
Fe	Fe							
Hg								
Mn	Mn							
Mo	Mo	Mo	**Mo**		Mo	Mo	**Mo**	
Ni	Ni	Ni	**Ni**		Ni			
Pb	Pb	Pb	**Pb**					
Sb		Sb		Sb	Sb	Sb	**Sb**	
Se		Se		Se	Se	Se	**Se**	
Sn	Sn							
Sr	Sr				Sr			
Ti	Ti				Ti			
Tl		Tl		Tl		Tl		Tl
V	V	V	**V**		V	V	**V**	
Zn	Zn							

Note; Bold indicates elements that were both elevated and exceeding the MCL

APPENDIX A - PHOTOGRAPHS

A-1.   WASECA CONSTRUCTION PHOTOGRAPHS

Fig. A1-1. RPM before placement of fly ash.

Fig. A1-2. Lay-down truck placing fly ash on RPM.

Fig. A1-3. Water truck and road-reclaimer blending fly ash, water, and RPM.

Fig. A1-4. Surface of fly ash and RPM after compaction.

Fig. A1-5. Mid-section of road-reclaimer showing tines used to blend fly ash, water, and RPM.

Fig. A1-6. Measuring water content and unit weight of stabilized RPM after compaction.

Fig. A1-7. Installing geomembrane for lysimeter.

Fig. A1-8. Installing collection tank for lysimeter.

A-2.   MnROAD CONSTRUCTION, SAMPLING, AND LABORATORY   PHOTOGRAPHS

Fig. A2-1. Preparing indentation in sub-base for lysimeter geomembrane.

Fig. A2-2.   Preparing drainage pipe from lysimeter to collection tank.

Fig. A2-3.   Installing geomembrane for lysimeter.

Fig. A2-4. Welding geomembrane to lysimeter drainage pipe assembly.

Fig. A2-5. Preparing hole for leachate collection tank and trench for drainage pipe.

Fig. A2-6. Assembling leachate collection tank.

Fig. A2-7. Installing leachate collection tank.

Fig. A2-8. Installing leachate collection tank.

Fig. A2-9. Collecting lysimeter leachate using submersible pump.
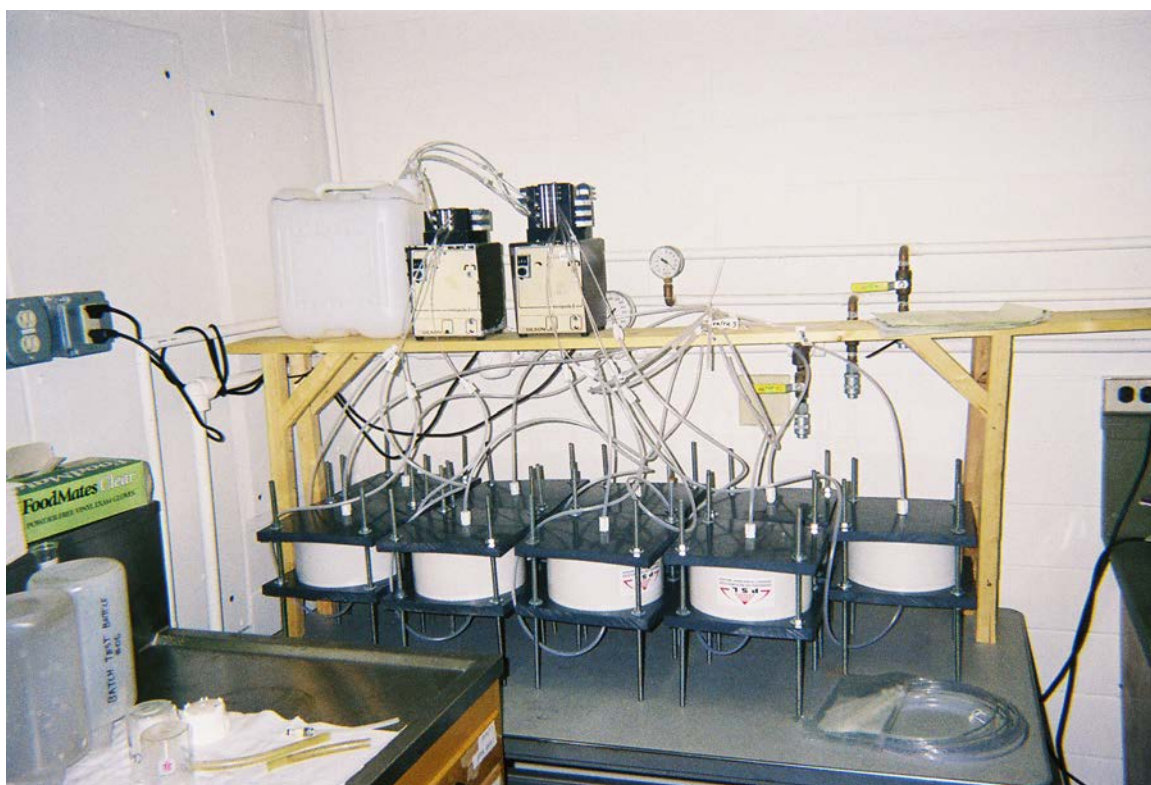
Fig. A2-10.   Column leach test on MnROAD materials.

Fig. A2-11.   Water leach test rotator.

Fig. A2-12.   MnROAD water leach test samples immediately after rotation.

APPENDIX B – LYSIMETER LEACHATE CHEMICAL CONCENTRATIONS

108
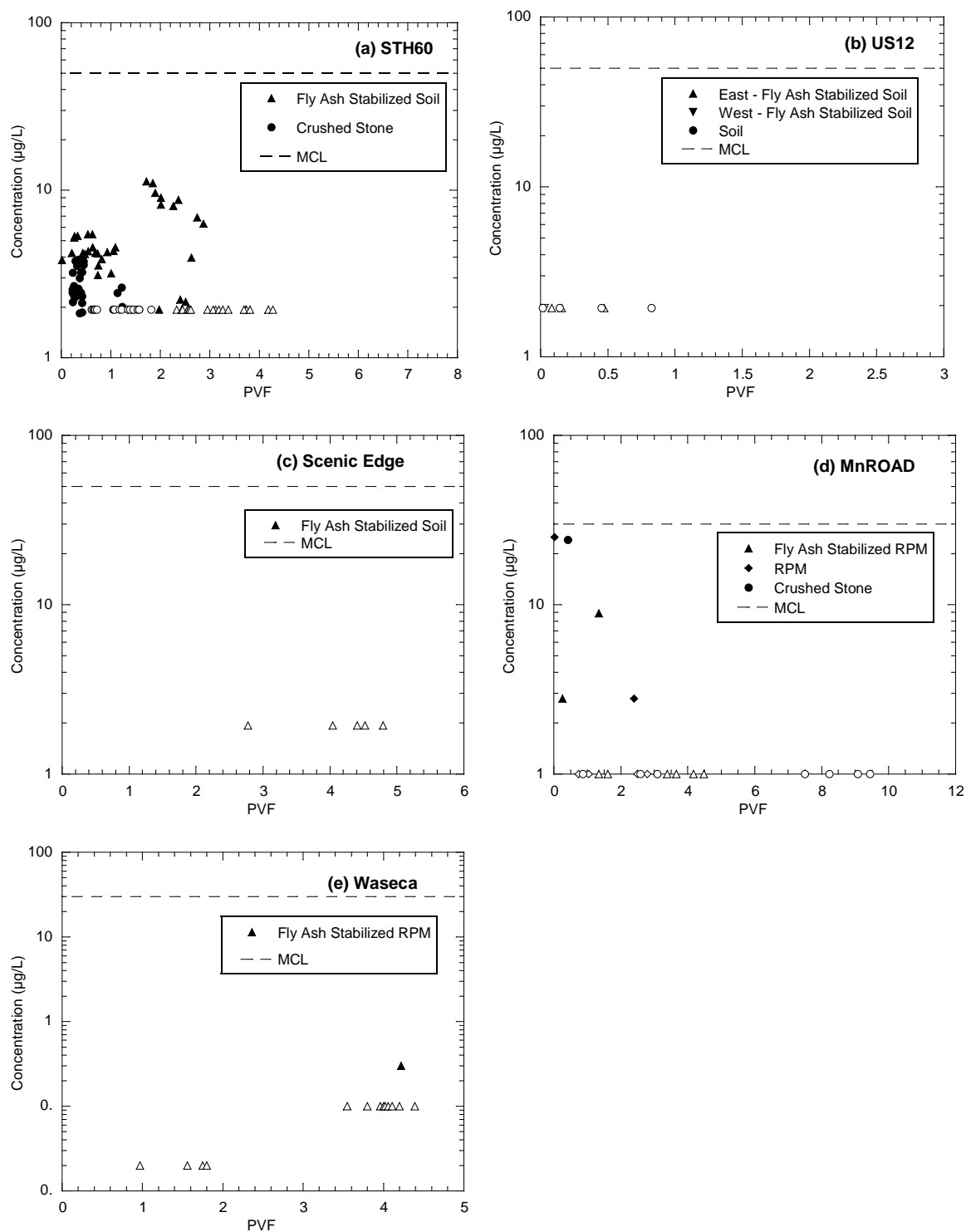
Fig. B-1.   Silver (Ag) concentrations in leachate from field lysimeters.
Concentrations below minimum detection limits are plotted at the
limit, and represented with an open symbol.
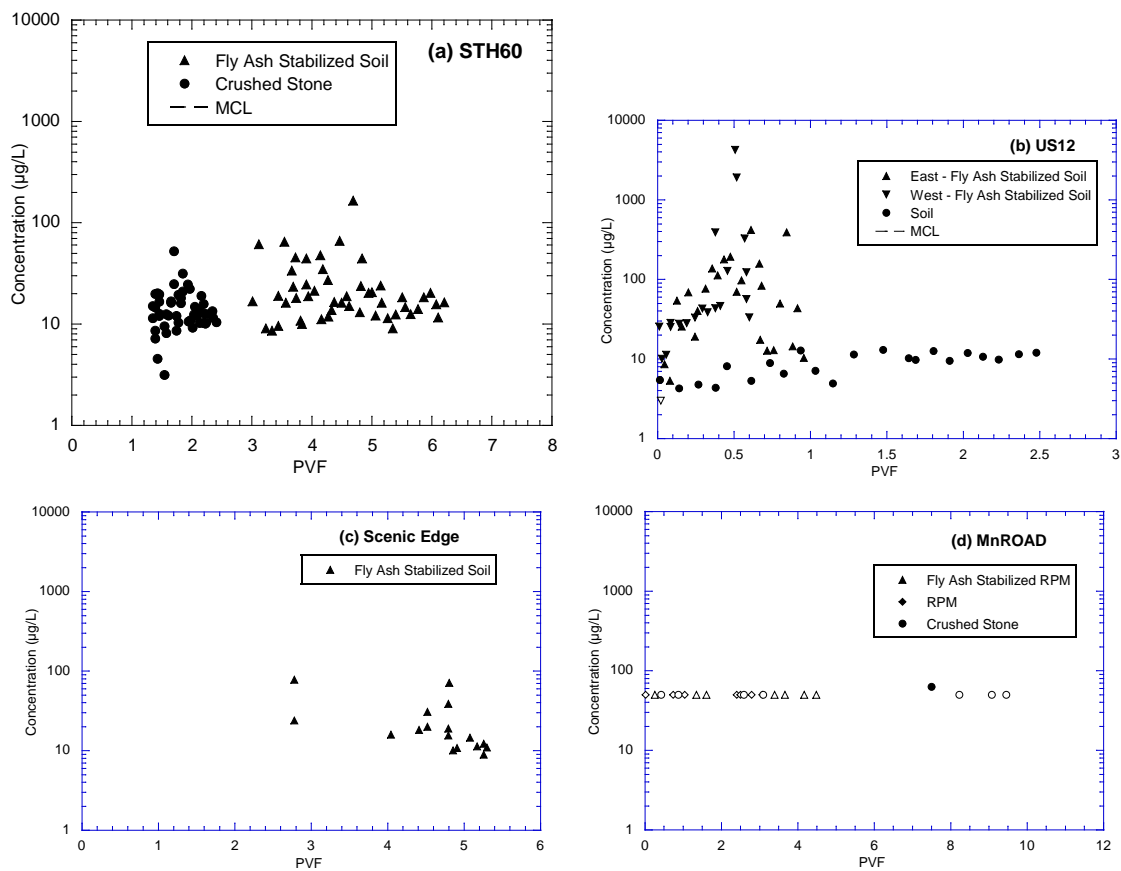
Fig. B-2. Aluminum (Al) concentrations in leachate from field lysimeters.
Concentrations below minimum detection limits are plotted at the
limit, and represented with an open symbol.
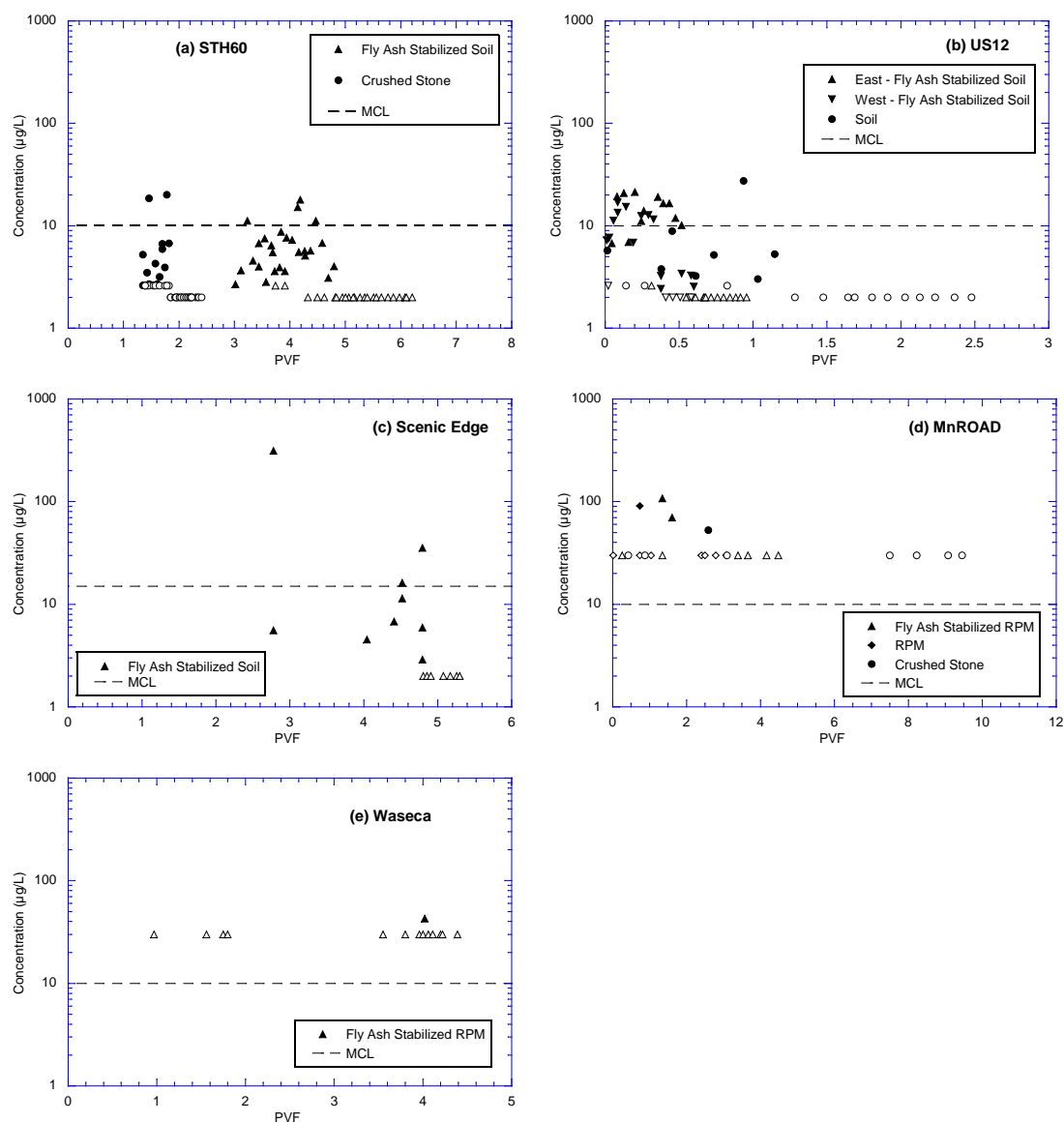
Fig. B-3.   Arsenic (As) concentrations in leachate from field lysimeters.
Concentrations below minimum detection limits are plotted at the limit,
and represented with an open symbol.
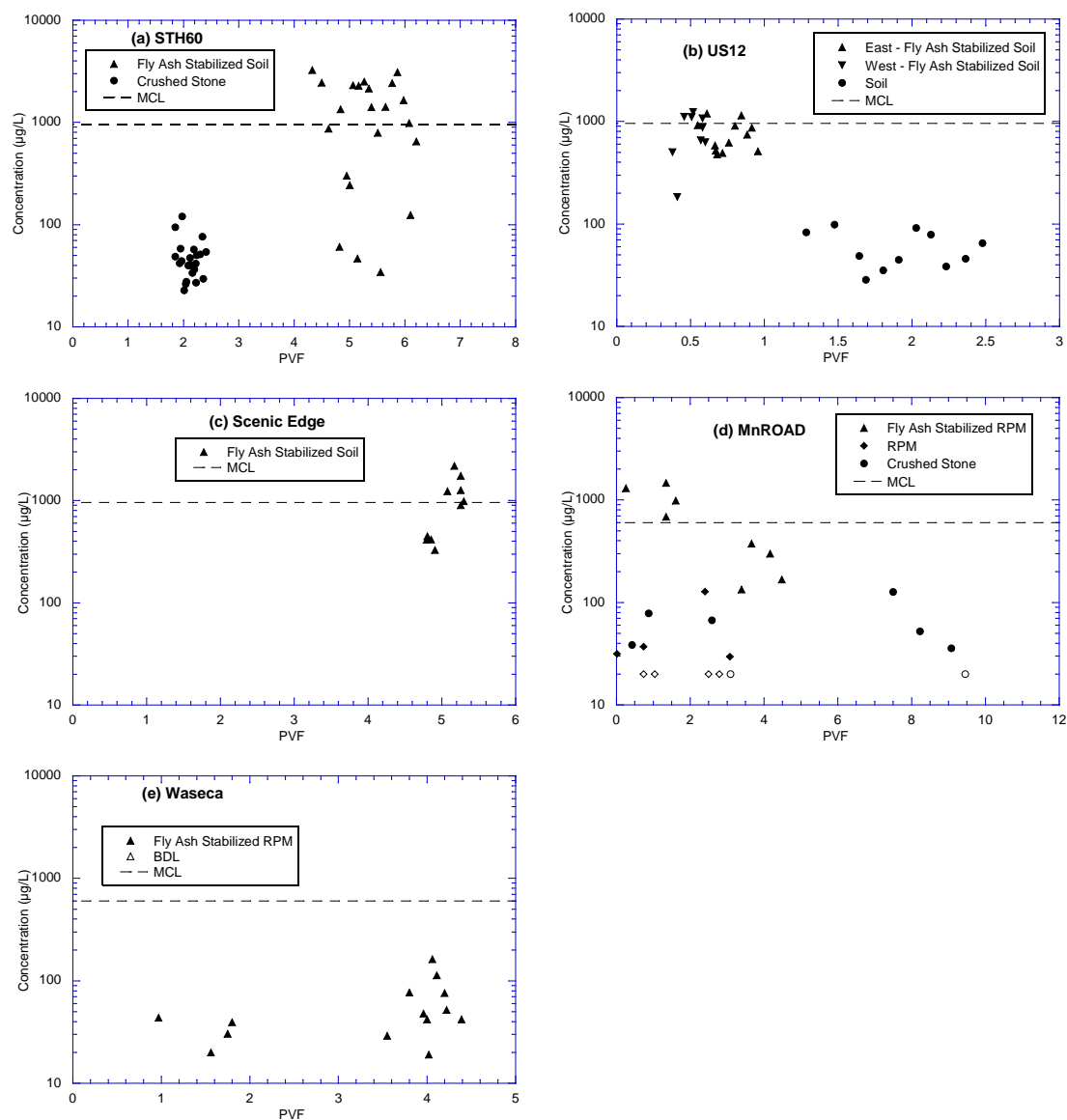
Fig. B-4.   Boron (B) concentrations in leachate from field lysimeters. Concentrations below minimum detection limits are plotted at the limit, and represented with an open symbol.
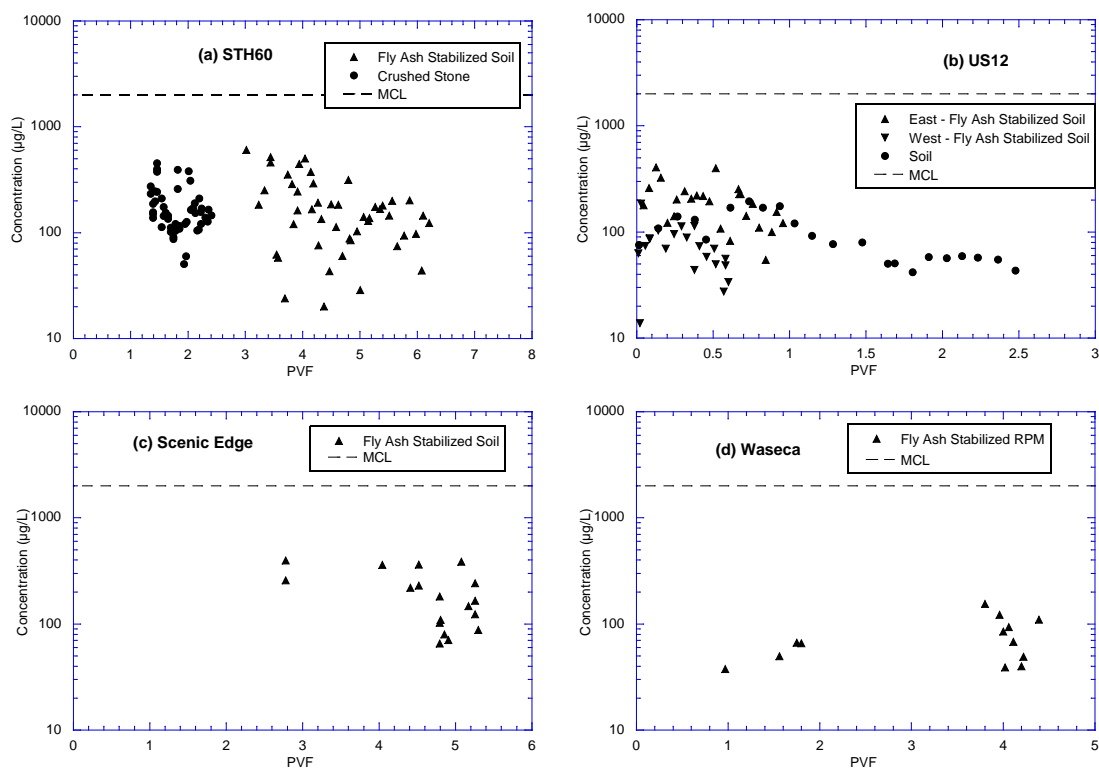
Fig. B-5.   Barium (Ba) concentrations in leachate from field lysimeters.
Concentrations below minimum detection limits are plotted at the limit,
and represented with an open symbol.
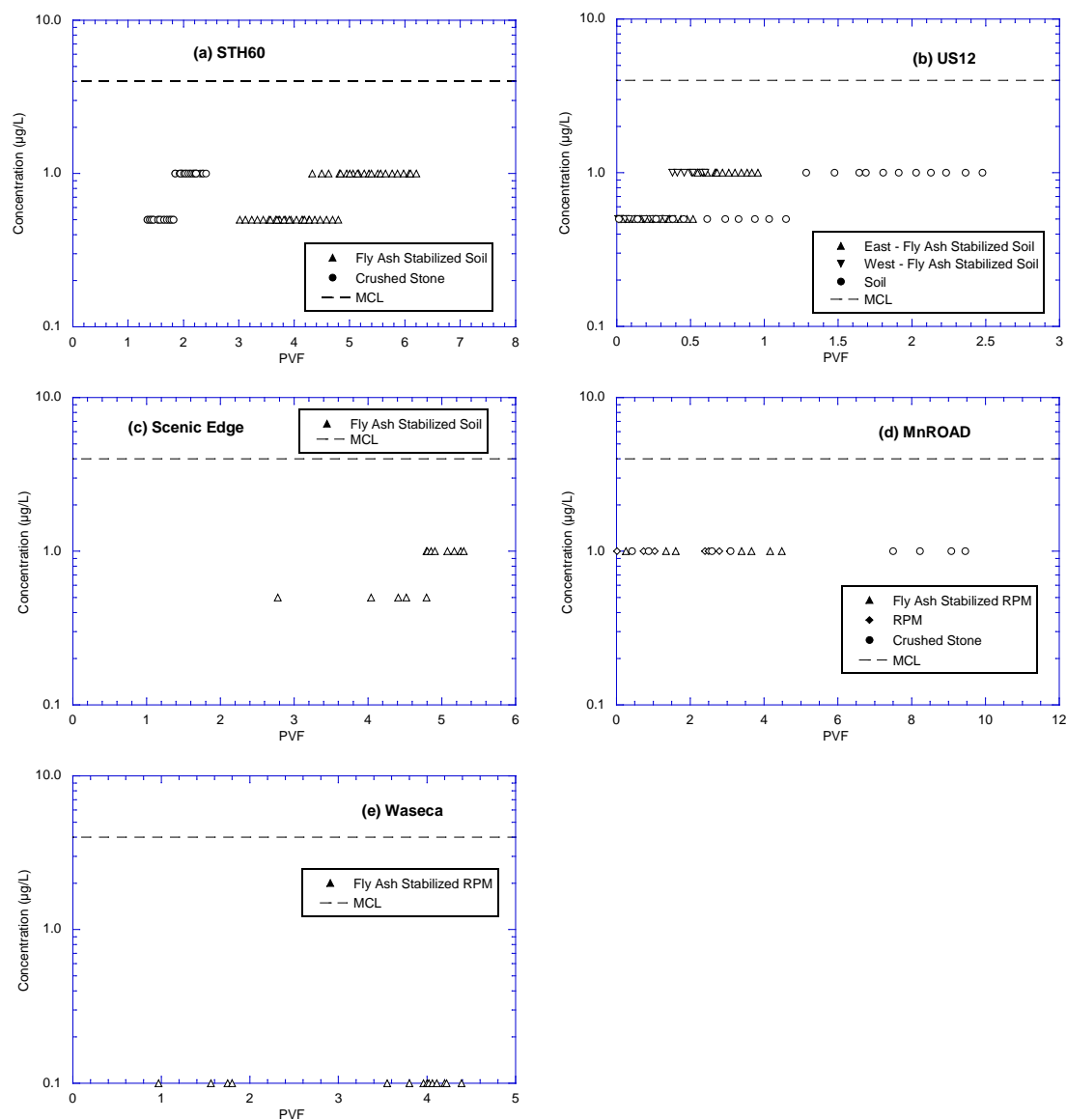
Fig. B-6.   Beryllium (Be) concentrations in leachate from field lysimeters.
Concentrations below minimum detection limits are plotted at the limit,
and represented with an open symbol.
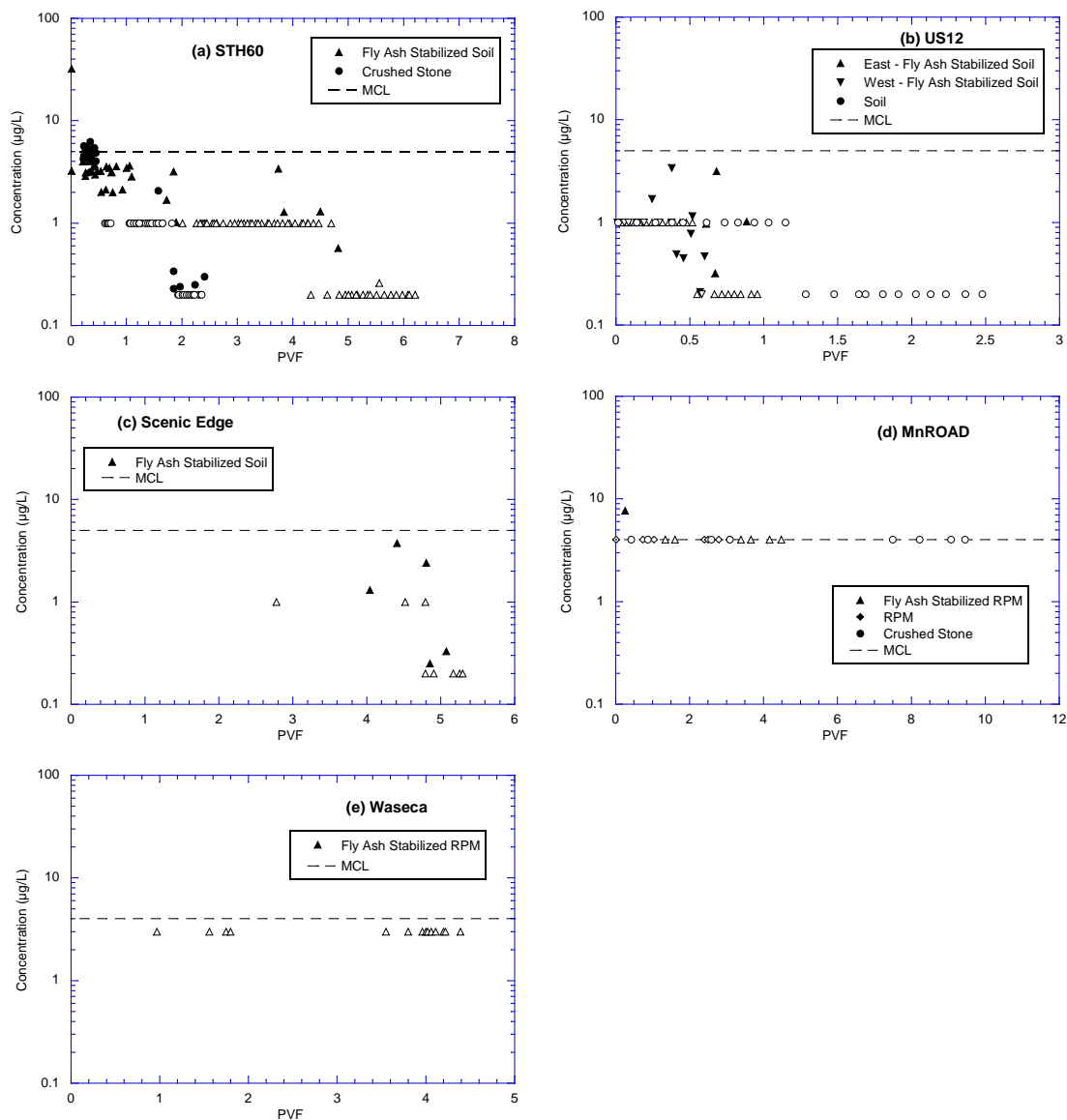
Fig. B-7.   Cadmium (Cd) concentrations in leachate from field lysimeters.
Concentrations below minimum detection limits are plotted at the limit,
and represented with an open symbol.
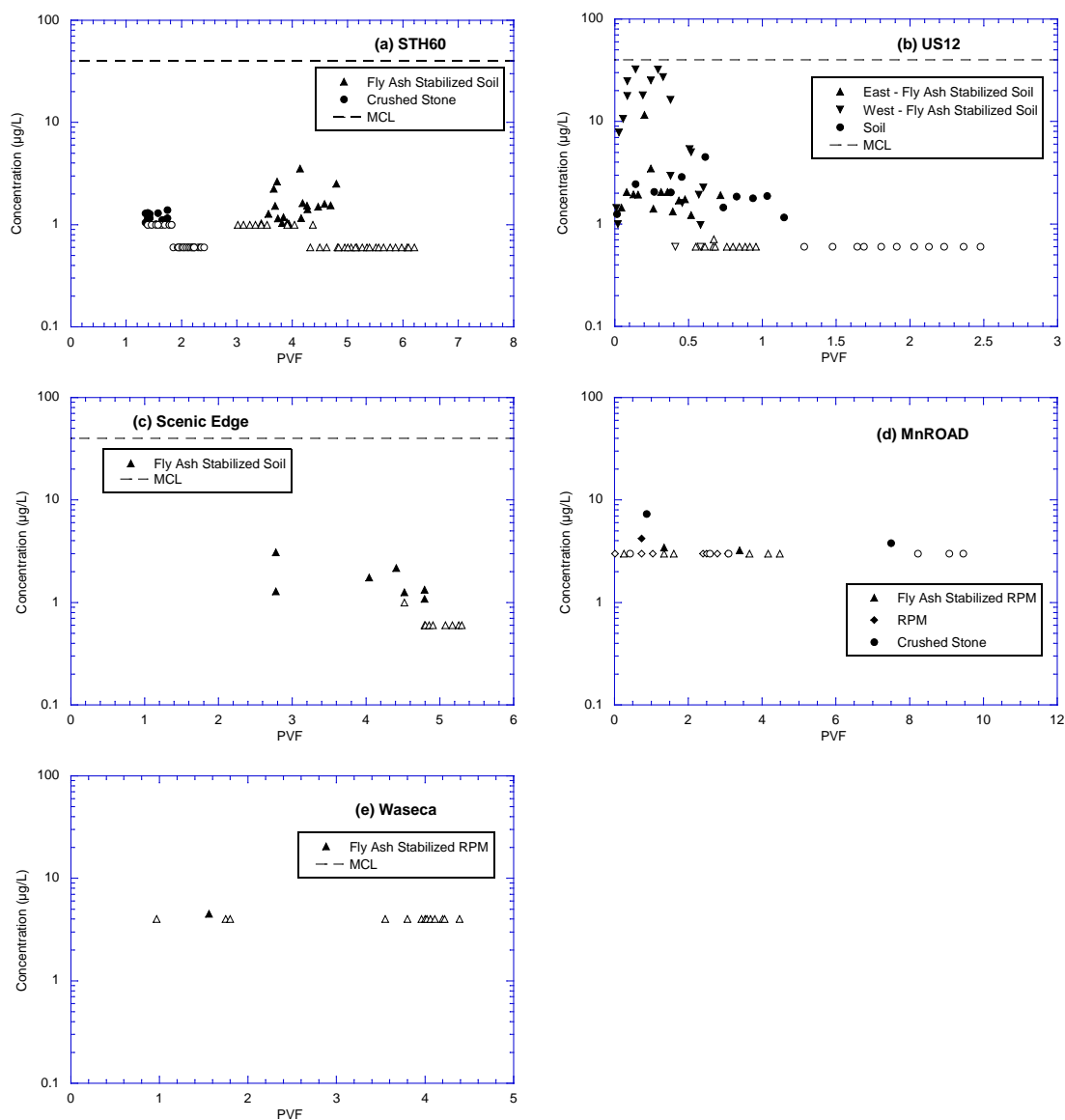
Fig. B-8.   Cobalt (Co) concentrations in leachate from field lysimeters.
Concentrations below minimum detection limits are plotted at the limit,
and represented with an open symbol.
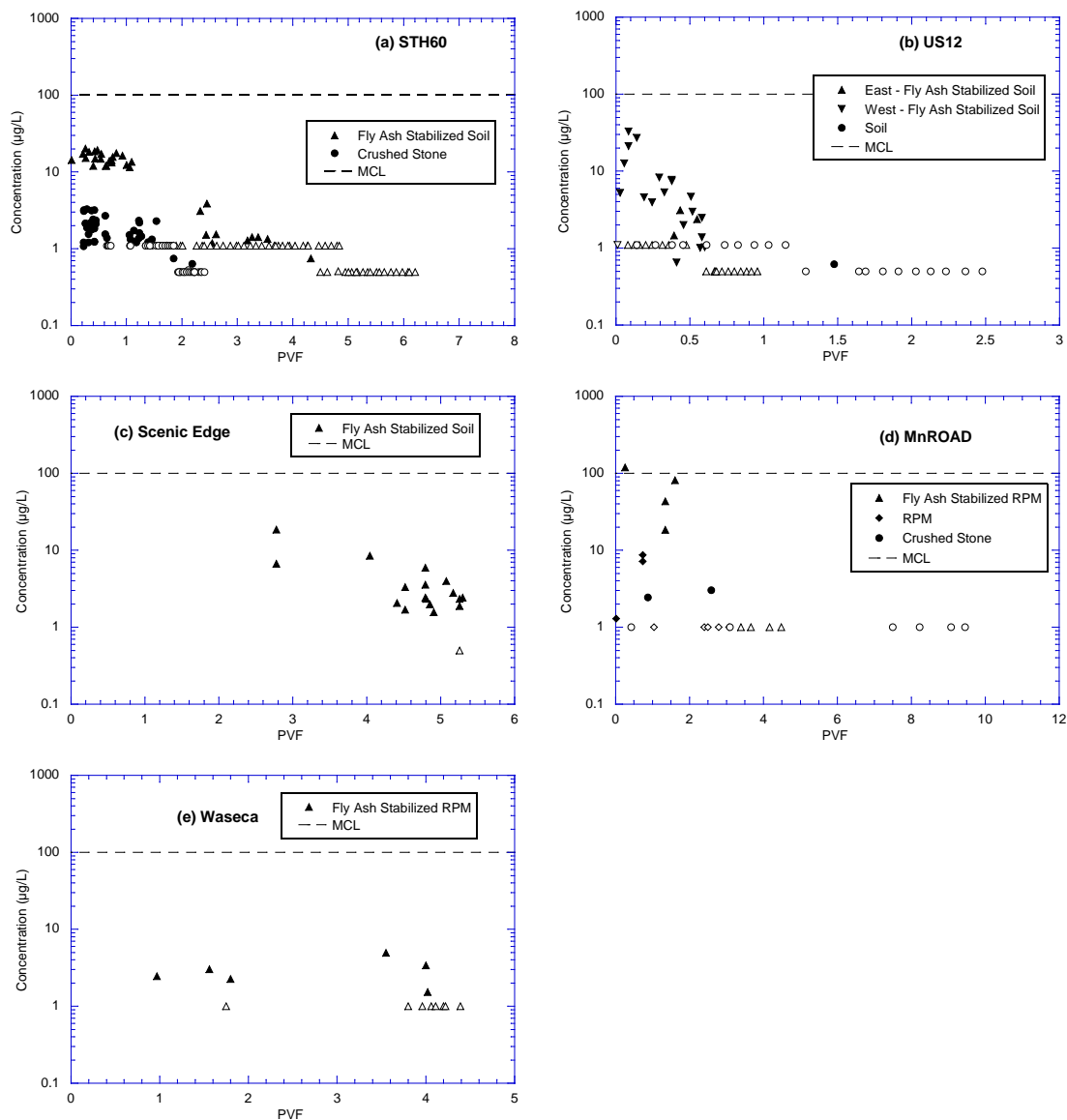
Fig. B-9.   Chromium (Cr) concentrations in leachate from field lysimeters.
Concentrations below minimum detection limits are plotted at the limit,
and represented with an open symbol.
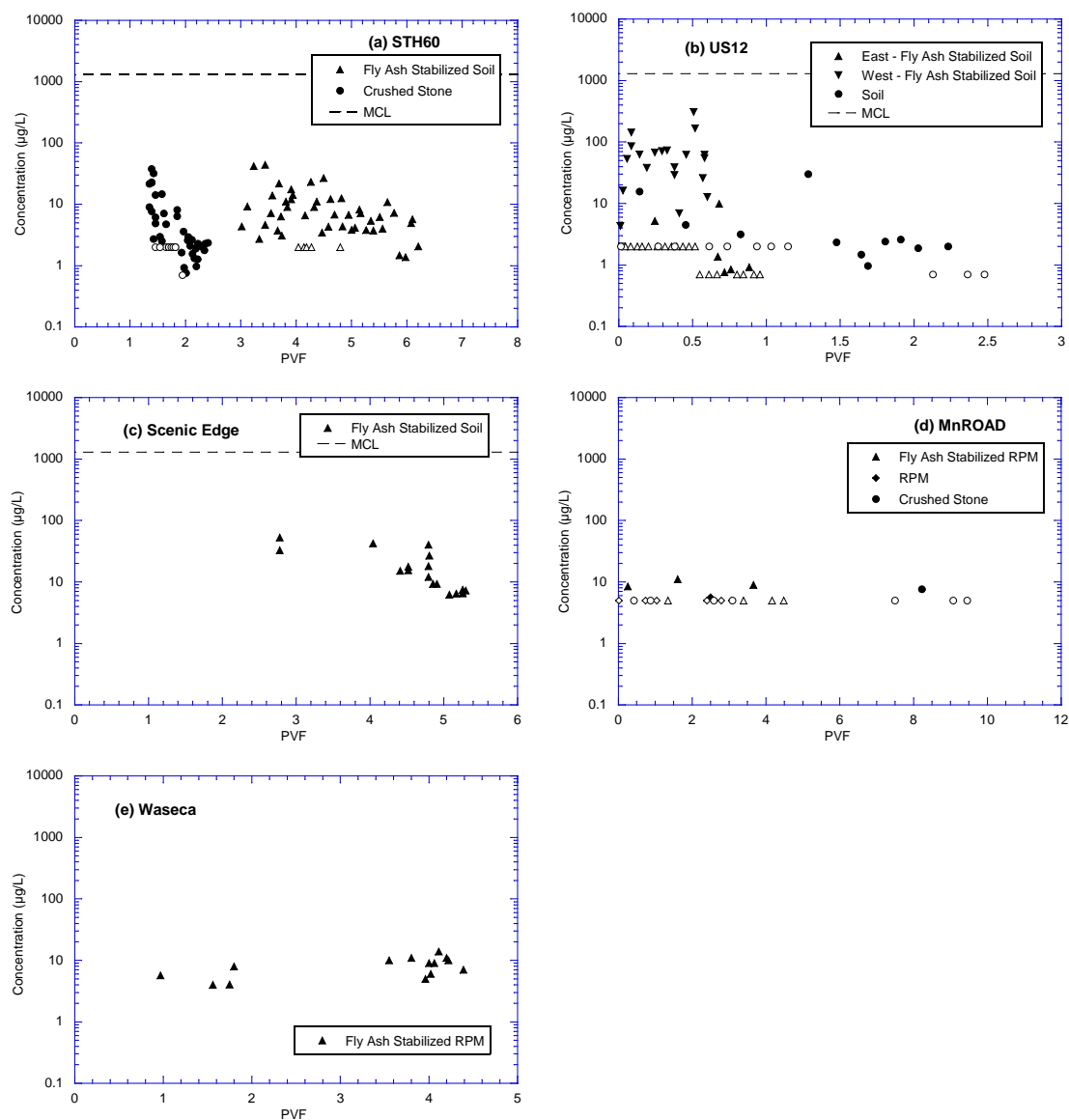
Fig. B-10. Copper (Cu) concentrations in leachate from field lysimeters. Concentrations below minimum detection limits are plotted at the limit, and represented with an open symbol.
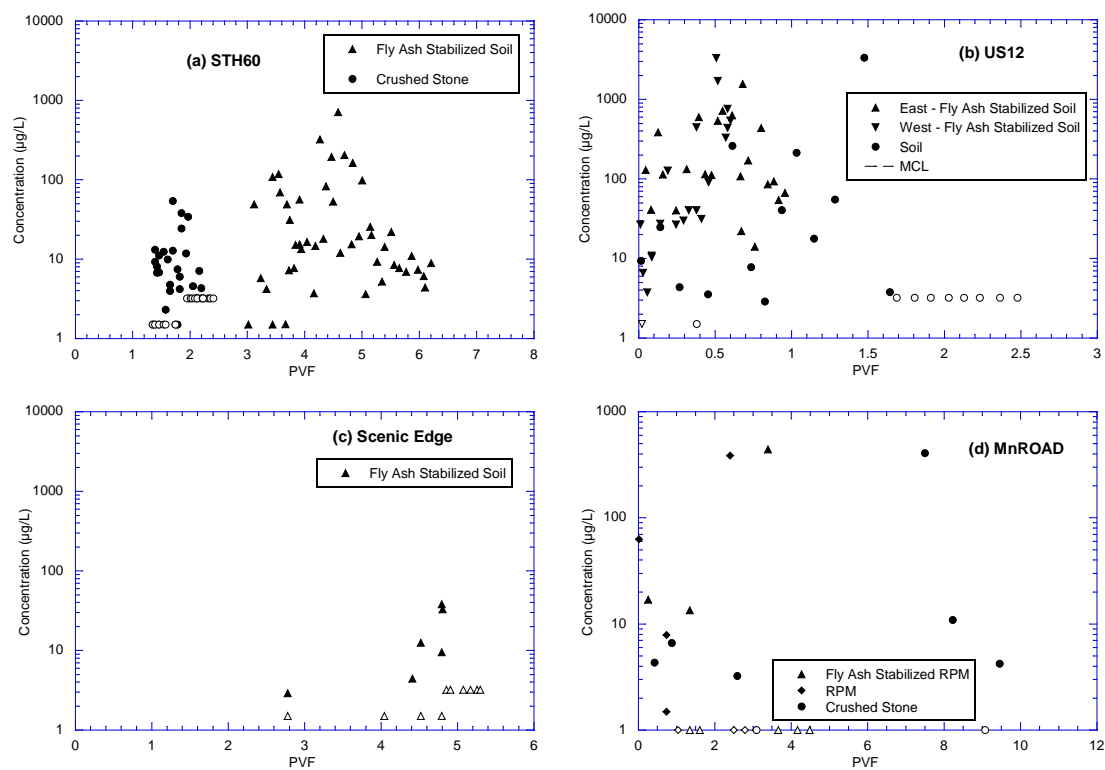
Fig. B-11.   Iron (Fe) concentrations in leachate from field lysimeters. Concentrations
below minimum detection limits are plotted at the limit, and represented
with an open symbol.
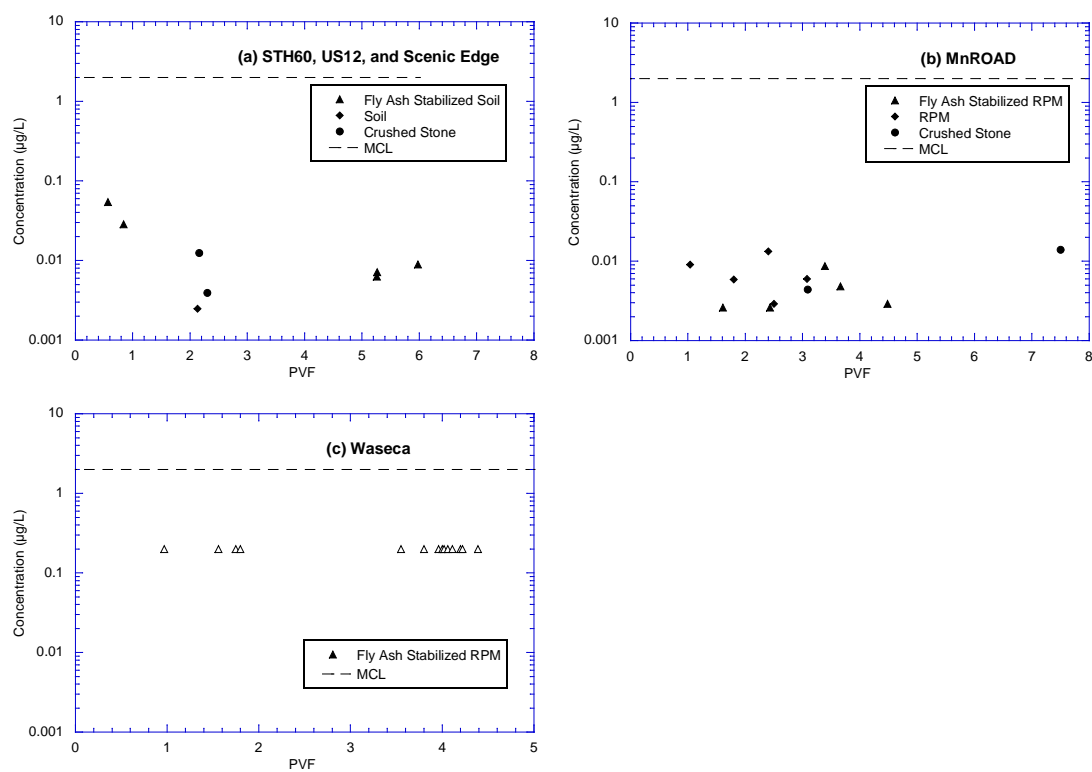
Fig. B-12.   Mercury (Hg) concentrations in leachate from field lysimeters. Concentrations below minimum detection limits are plotted at the limit, and represented with an open symbol.
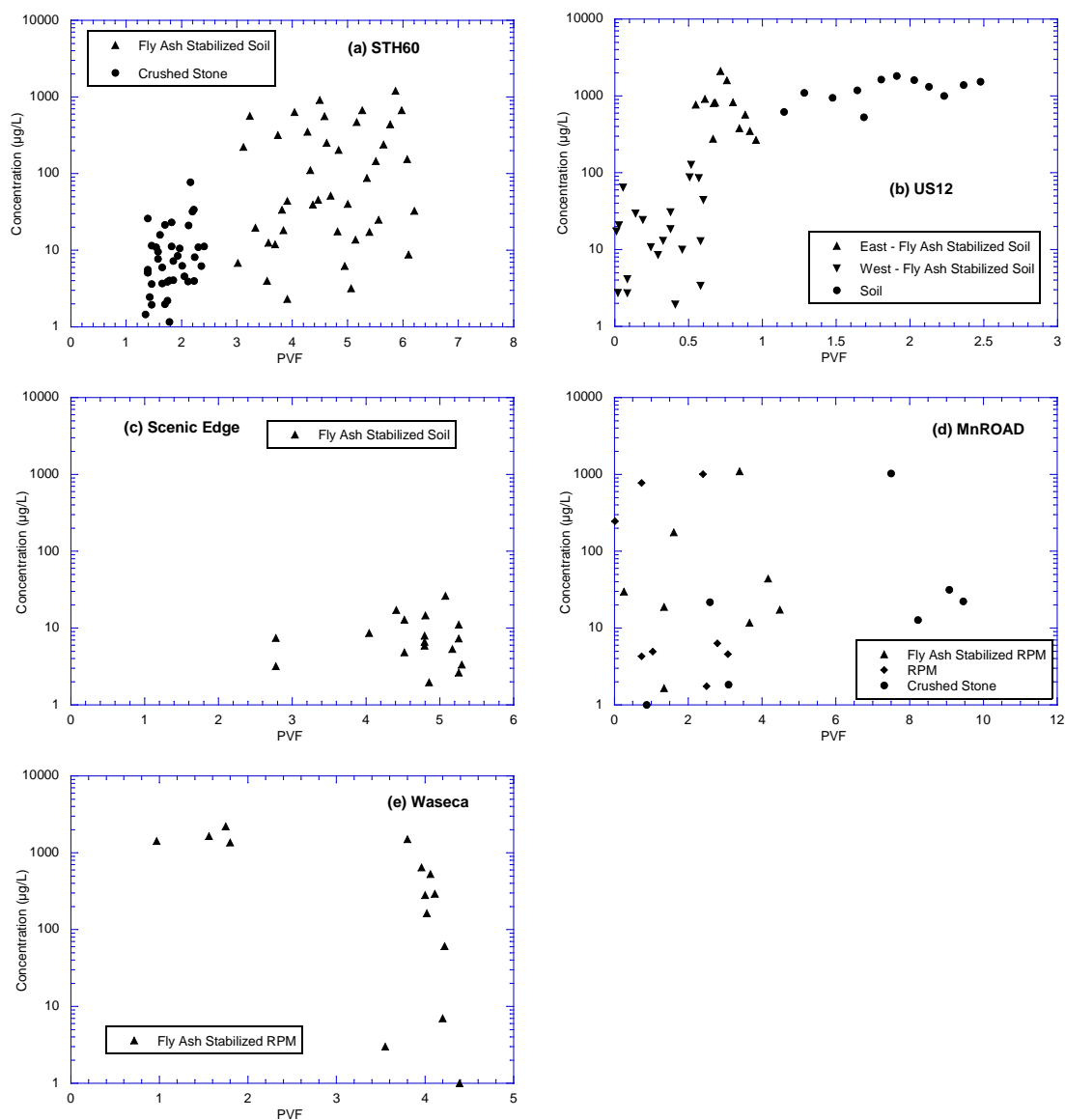
Fig. B-13.   Manganese (Mn) concentrations in leachate from field lysimeters.
Concentrations below minimum detection limits are plotted at the limit,
and represented with an open symbol.
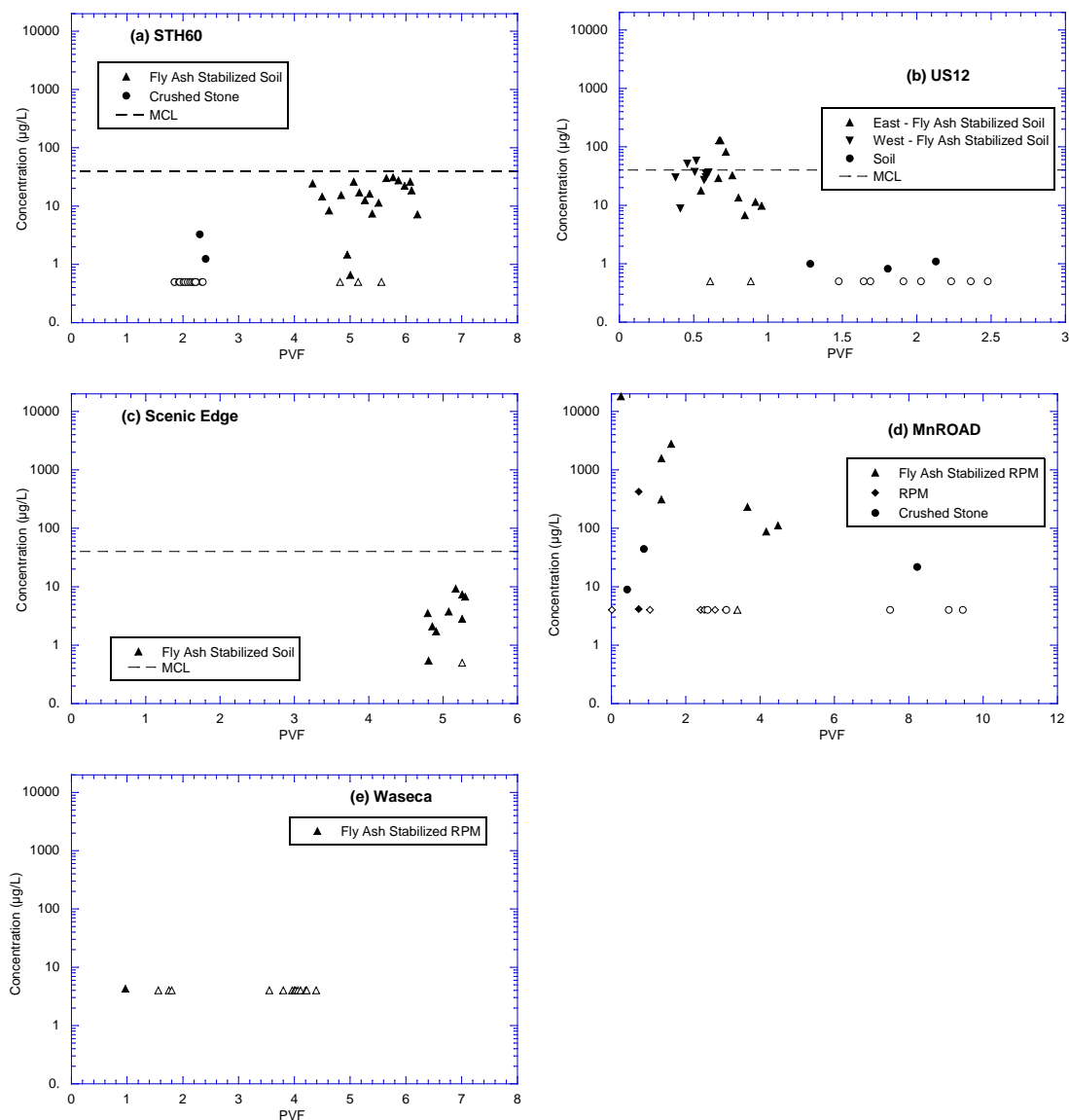
Fig. B-14.   Molybdenum (Mo) concentrations in leachate from field lysimeters.
Concentrations below minimum detection limits are plotted at the limit,
and represented with an open symbol.
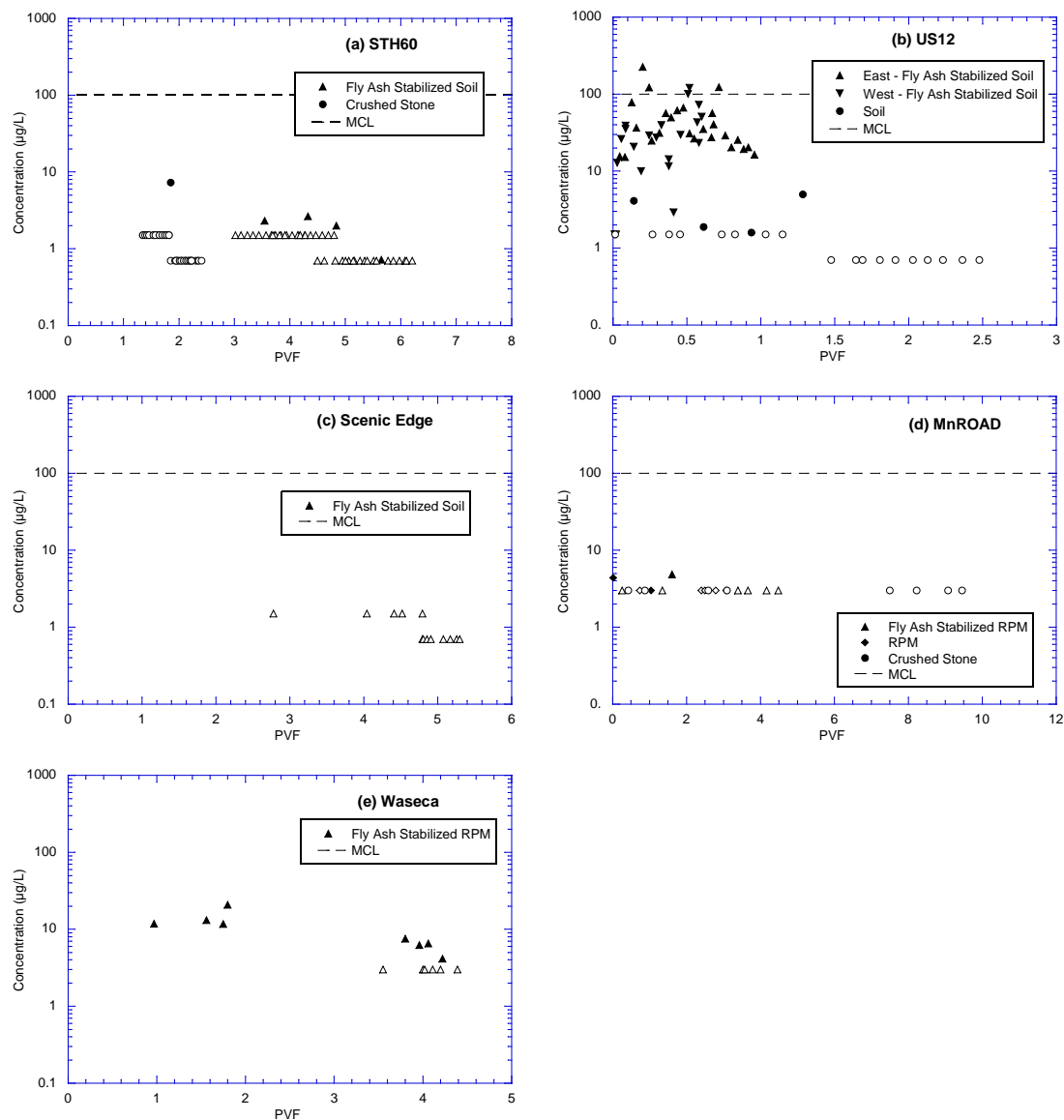
Fig. B-15.   Nickel (Ni) concentrations in leachate from field lysimeters.
Concentrations below minimum detection limits are plotted at the limit,
and represented with an open symbol.

Fig. B-16.   Lead (Pb) concentrations in leachate from field lysimeters.
Concentrations below minimum detection limits are plotted at the limit,
and represented with an open symbol.
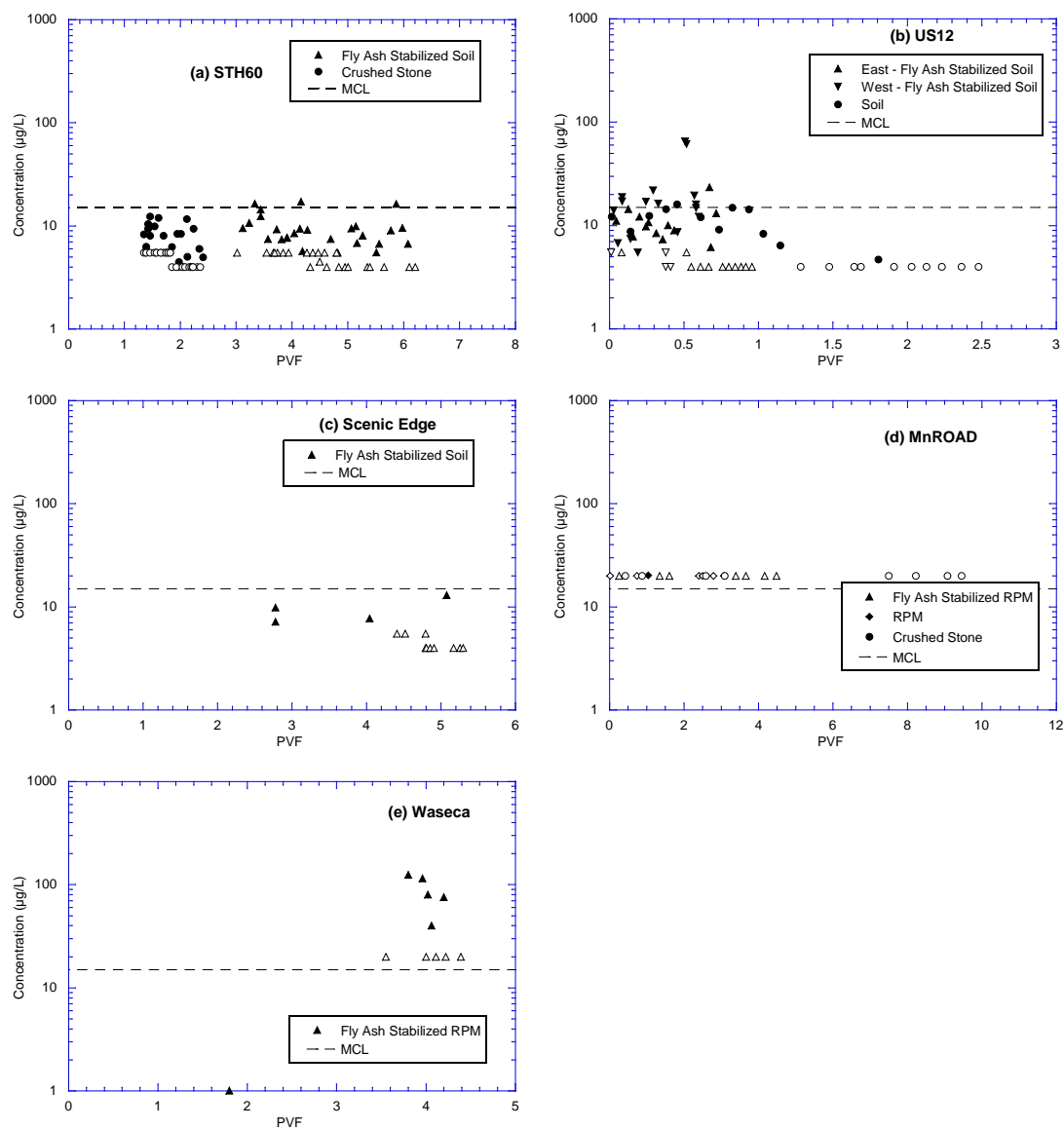
Fig. B-17.   Antimony (Sb) concentrations in leachate from field lysimeters.
Concentrations below minimum detection limits are plotted at the limit,
and represented with an open symbol.
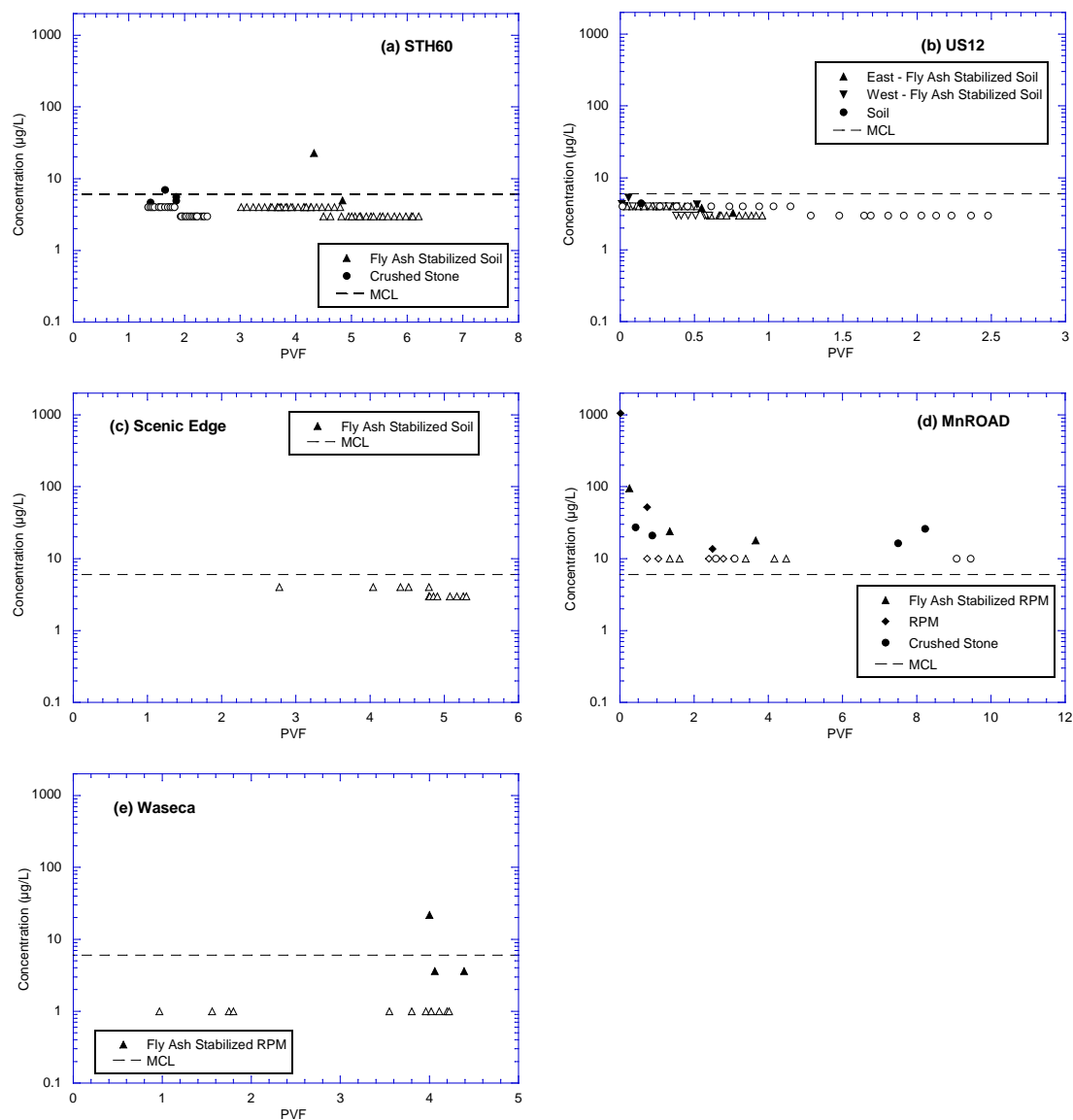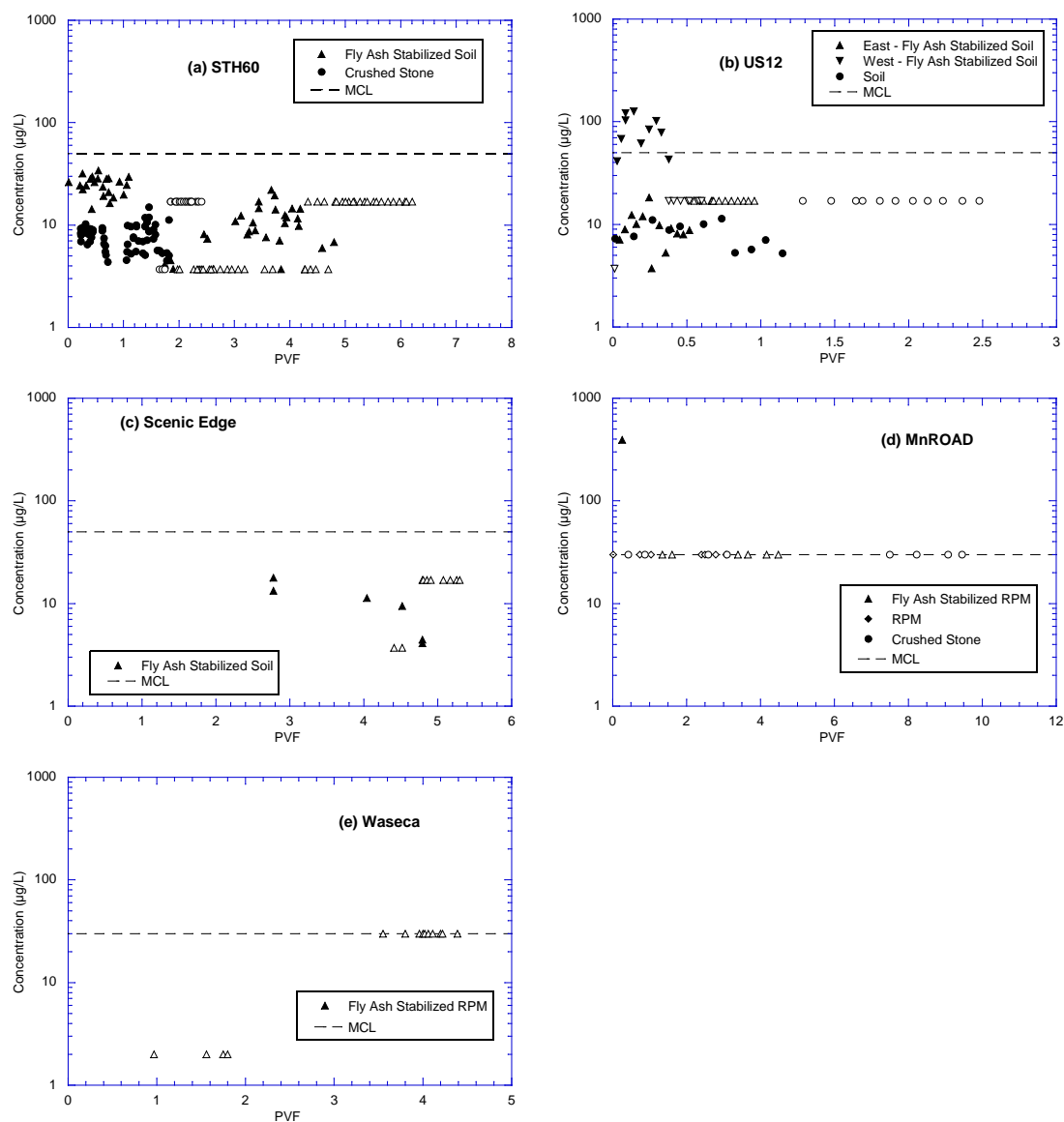
Fig. B-18.   Selenium (Se) concentrations in leachate from field lysimeters.
Concentrations below minimum detection limits are plotted at the limit,
and represented with an open symbol.
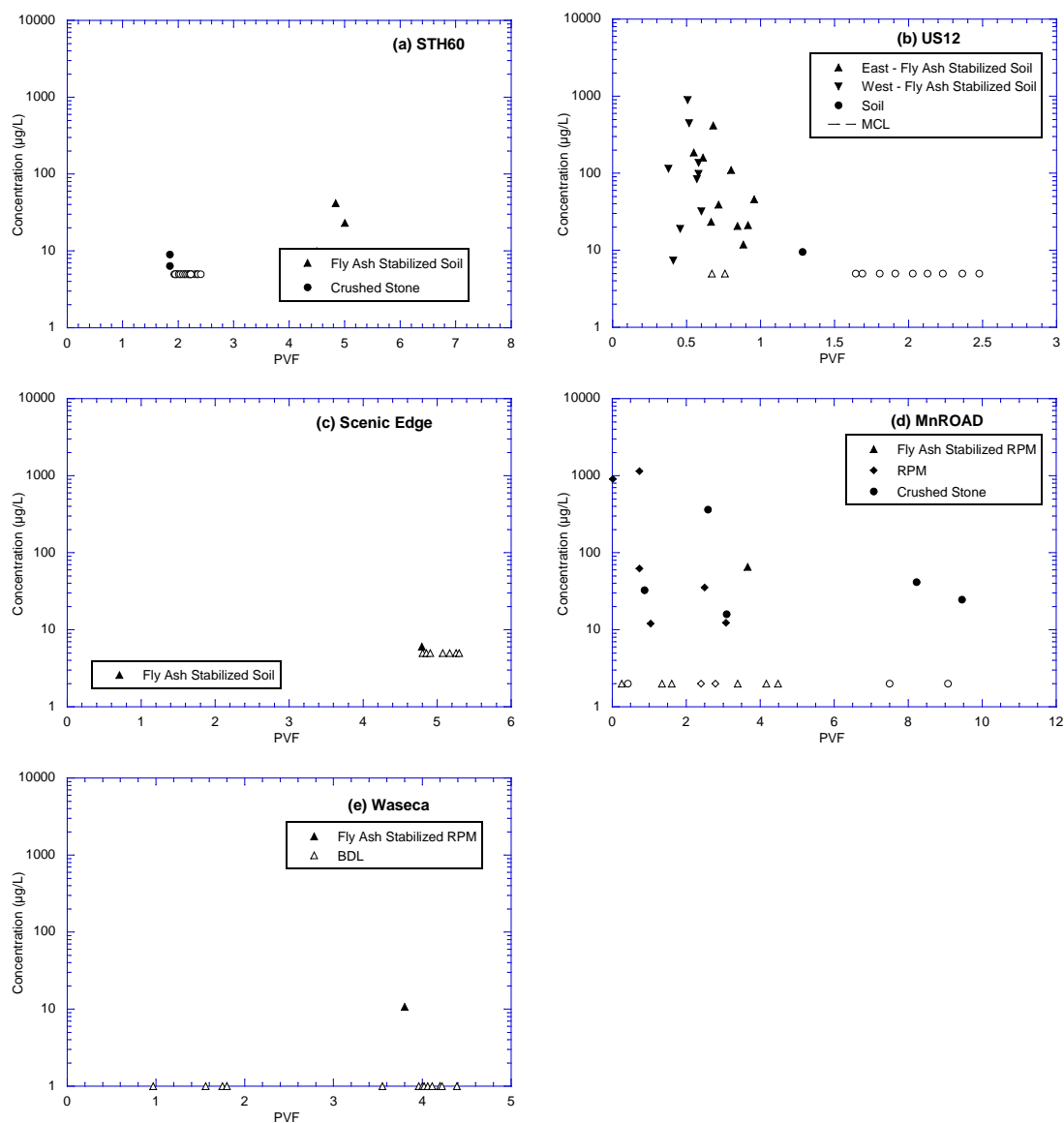
Fig. B-19.   Tin (Sn) concentrations in leachate from field lysimeters. Concentrations below minimum detection limits are plotted at the limit, and represented with an open symbol.
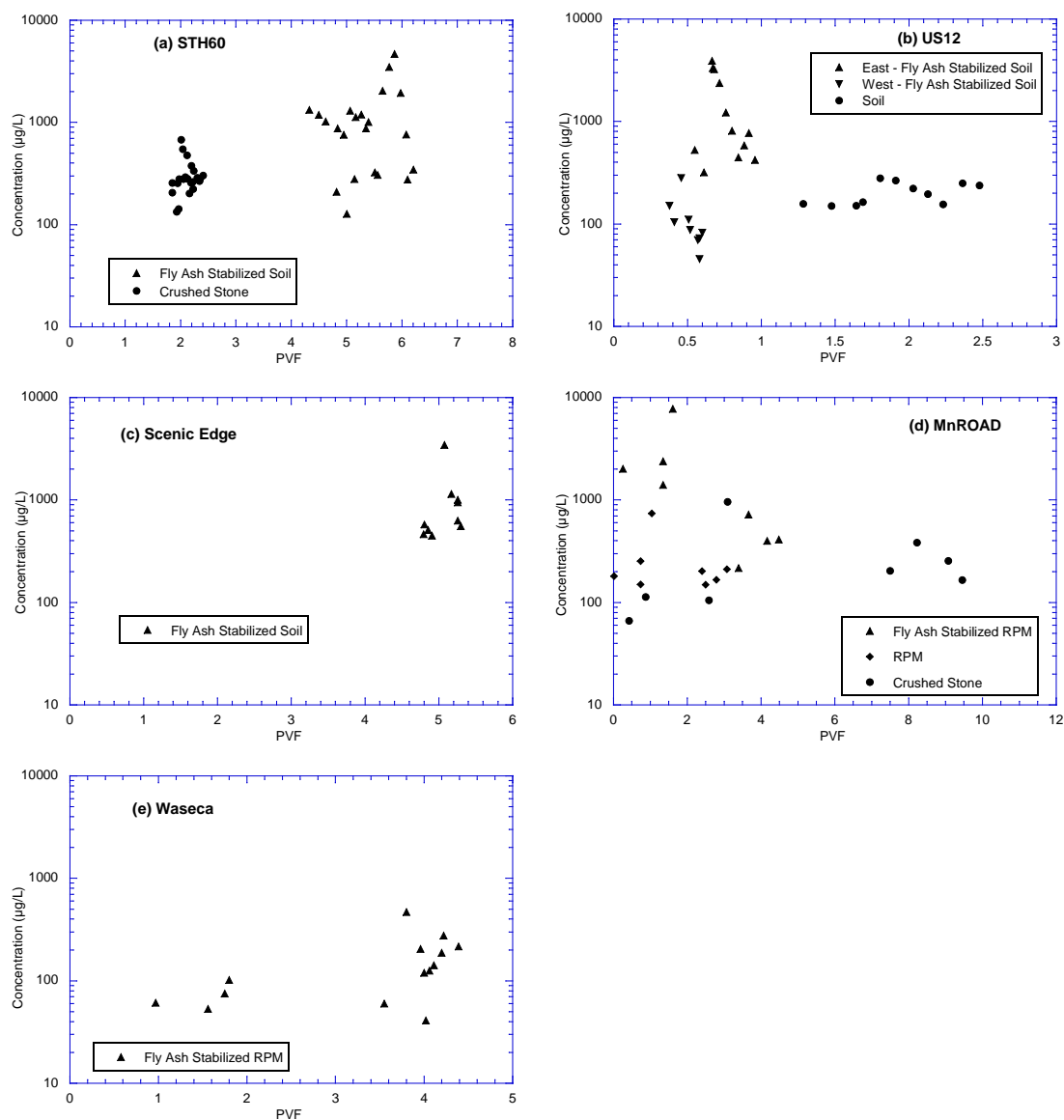
Fig. B-20.   Strontium (Sr) concentrations in leachate from field lysimeters.
Concentrations below minimum detection limits are plotted at the limit,
and represented with an open symbol.

Fig. B-21.   Titanium (Ti) concentrations in leachate from field lysimeters. Concentrations below minimum detection limits are plotted at the limit, and represented with an open symbol.
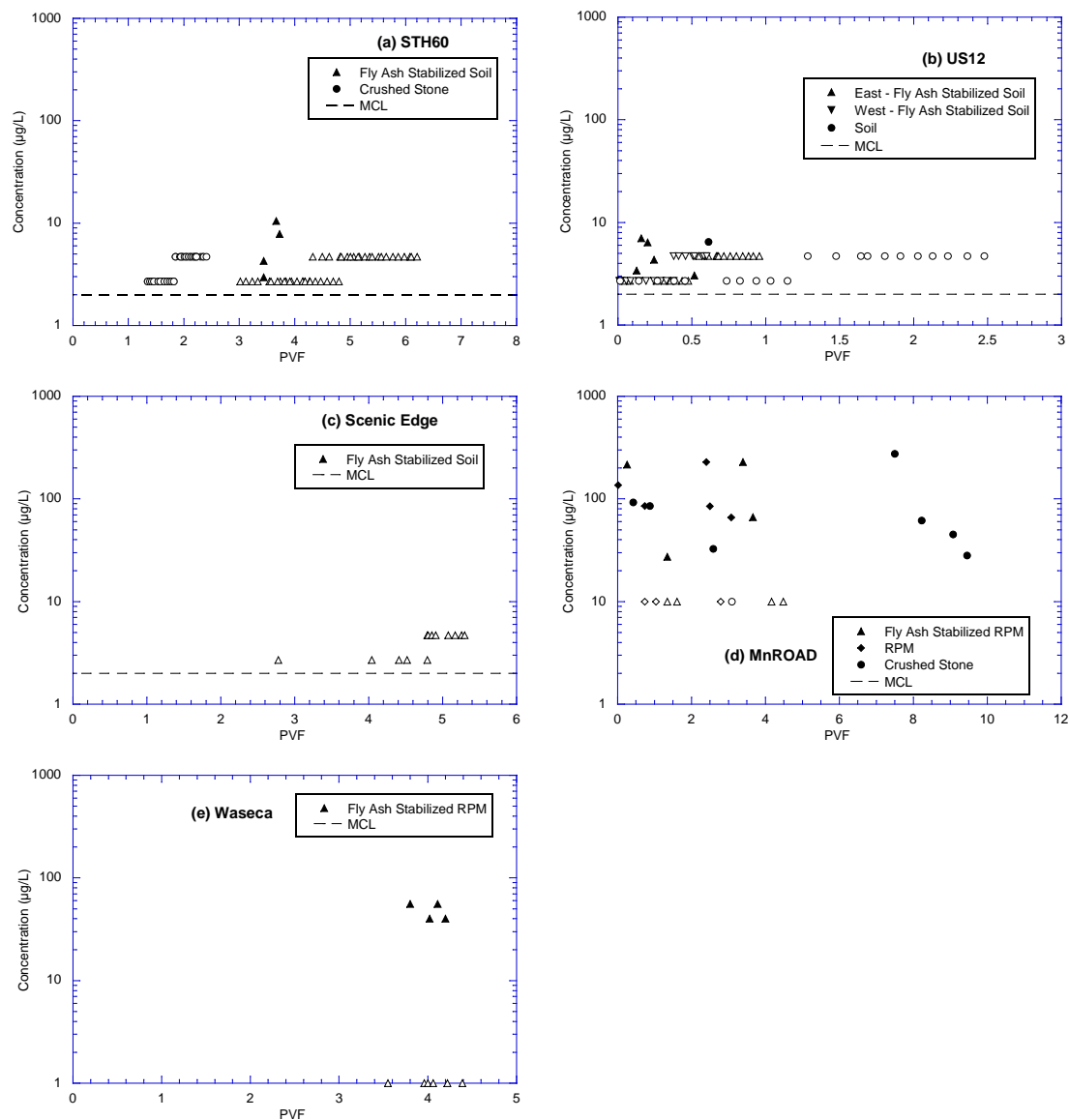
Fig. B-22.   Thallium (Tl) concentrations in leachate from field lysimeters. Concentrations below minimum detection limits are plotted at the limit, and represented with an open symbol.
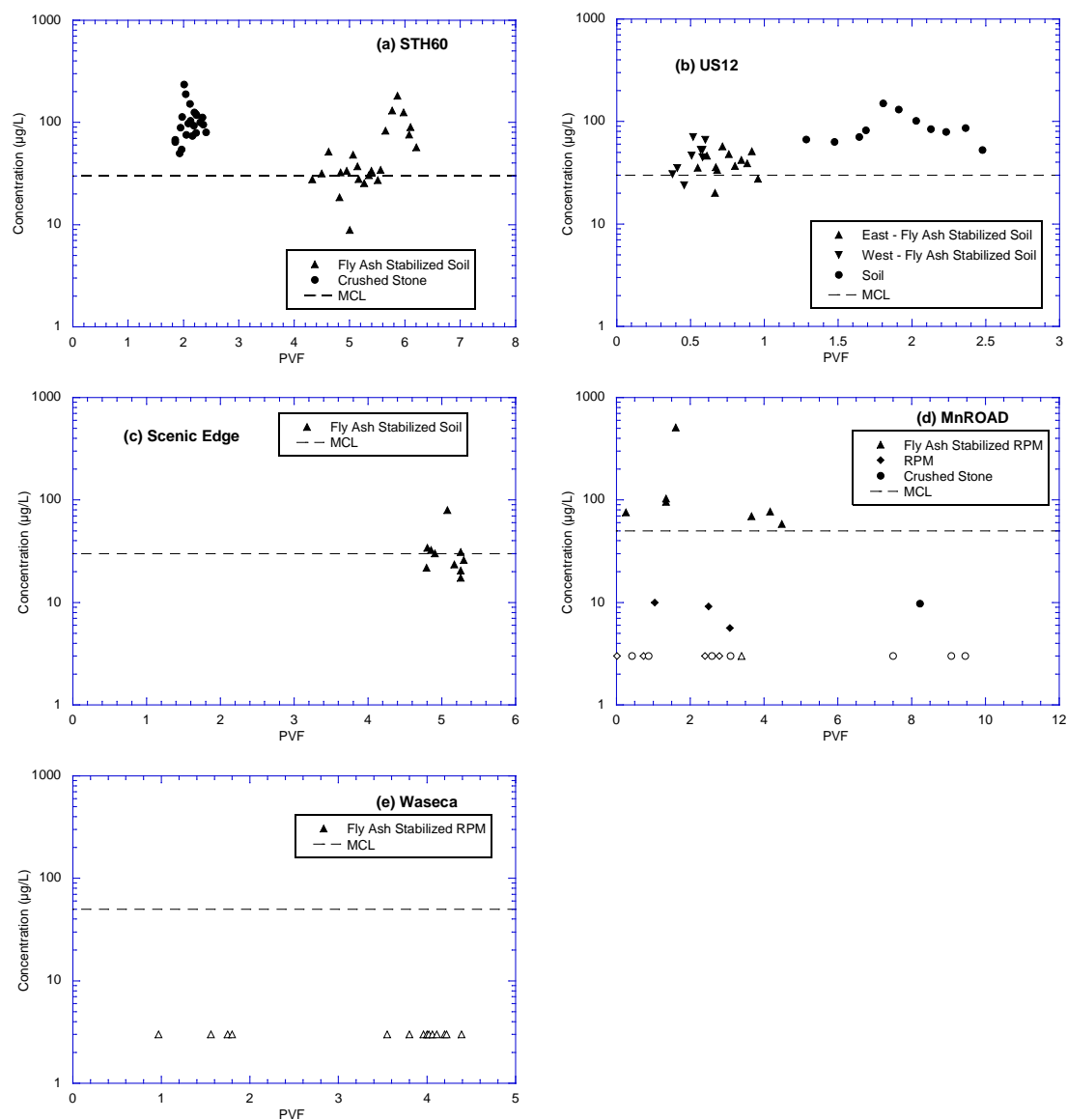
Fig. B-23.   Vanadium (V) concentrations in leachate from field lysimeters.
Concentrations below minimum detection limits are plotted at the limit,
and represented with an open symbol.
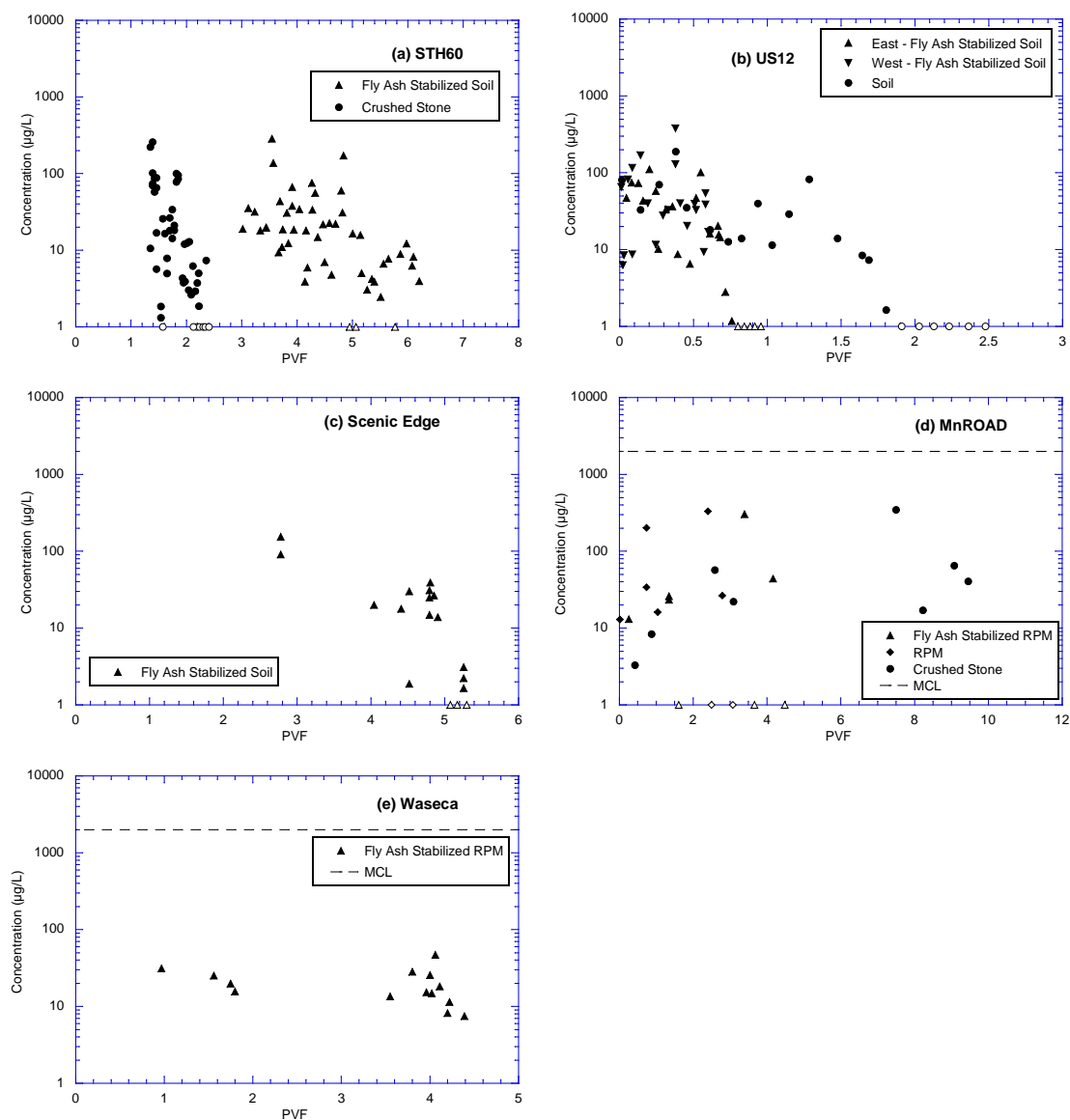
Fig. B-24.   Zinc (Zn) concentrations in leachate from field lysimeters. Concentrations below minimum detection limits are plotted at the limit, and represented with an open symbol.

APPENDIX C – LABORATORY CHEMICAL CONCENTRATIONS
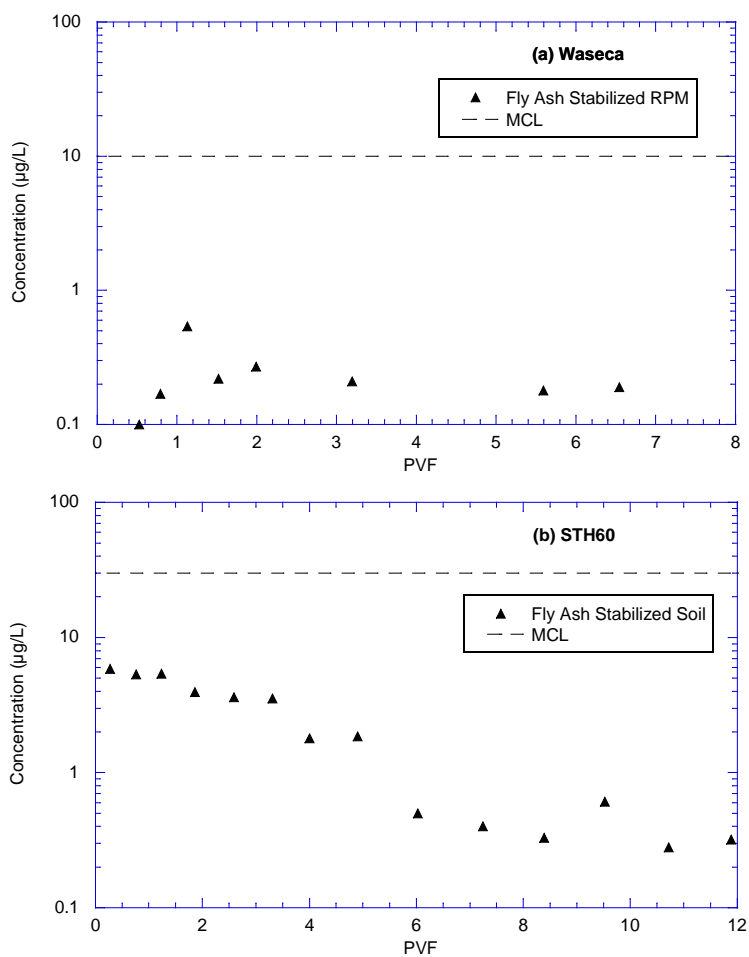
Fig. C-1.   Silver (Ag) concentrations in leachate from column leach tests (CLTs).
           Concentrations below minimum detection limits are plotted at the limit,
           and represented with an open symbol.
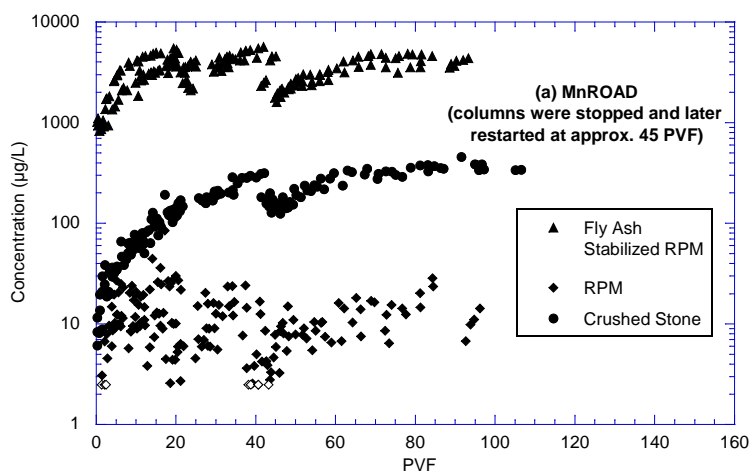
Fig. C-2.   Aluminum (Al) concentrations in leachate from column leach tests (CLTs).
         Concentrations below minimum detection limits are plotted at the limit,
         and represented with an open symbol.
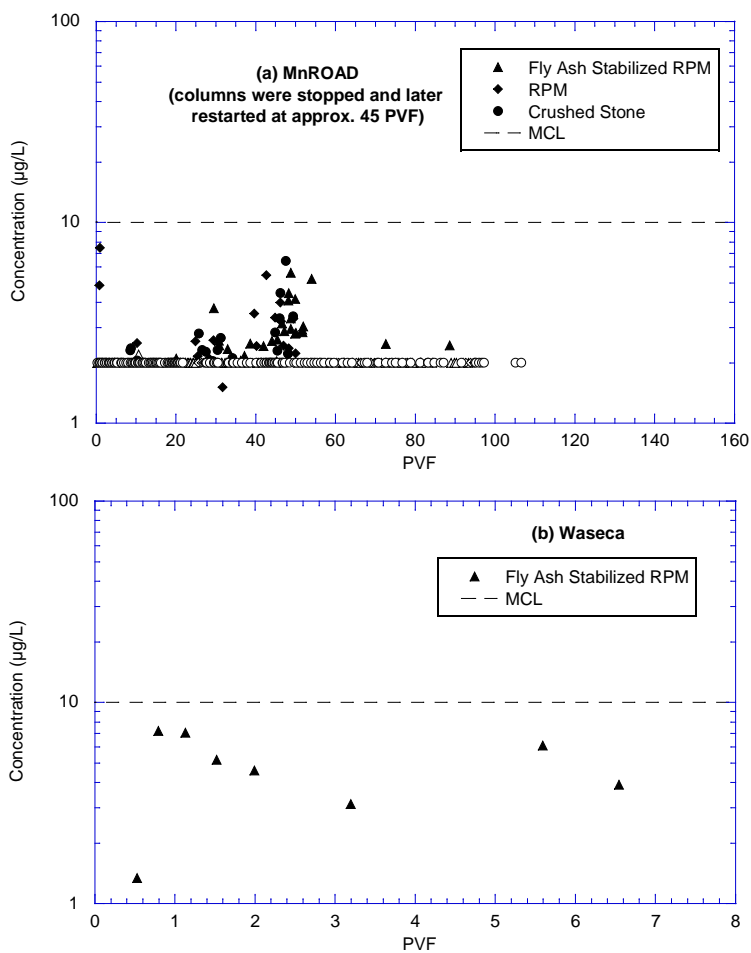
Fig. C-3.   Arsenic (As) concentrations in leachate from column leach tests (CLTs).
Concentrations below minimum detection limits are plotted at the limit,
and represented with an open symbol.
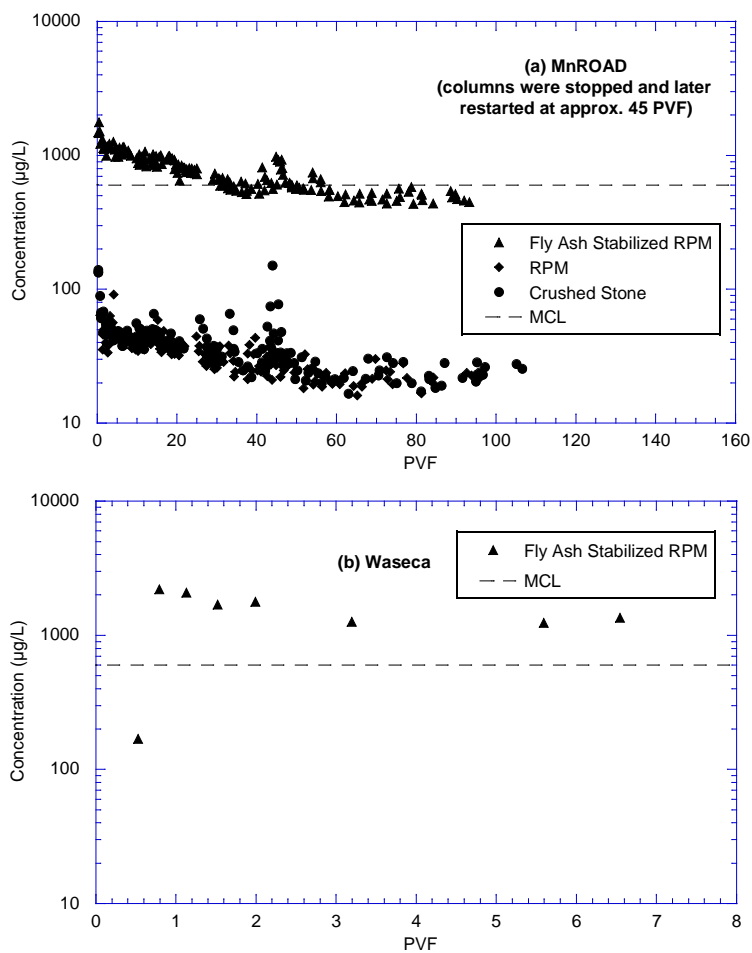
Fig. C-4. Boron (B) concentrations in leachate from column leach tests (CLTs). Concentrations below minimum detection limits are plotted at the limit, and represented with an open symbol.
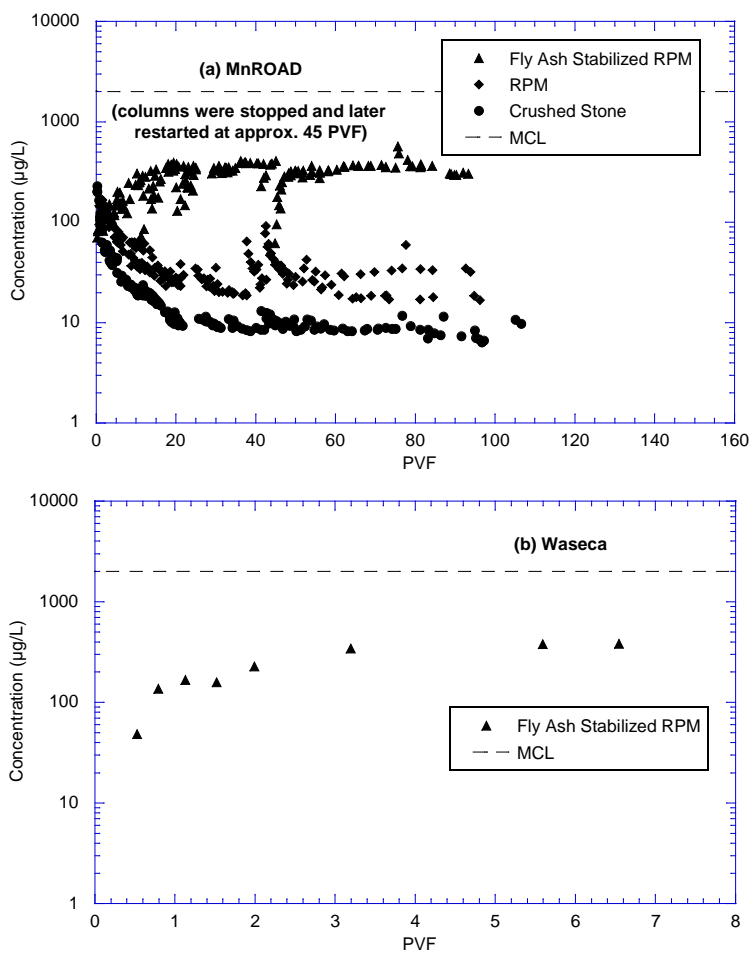
Fig. C-5.   Barium (Ba) concentrations in leachate from column leach tests (CLTs). Concentrations below minimum detection limits are plotted at the limit, and represented with an open symbol.
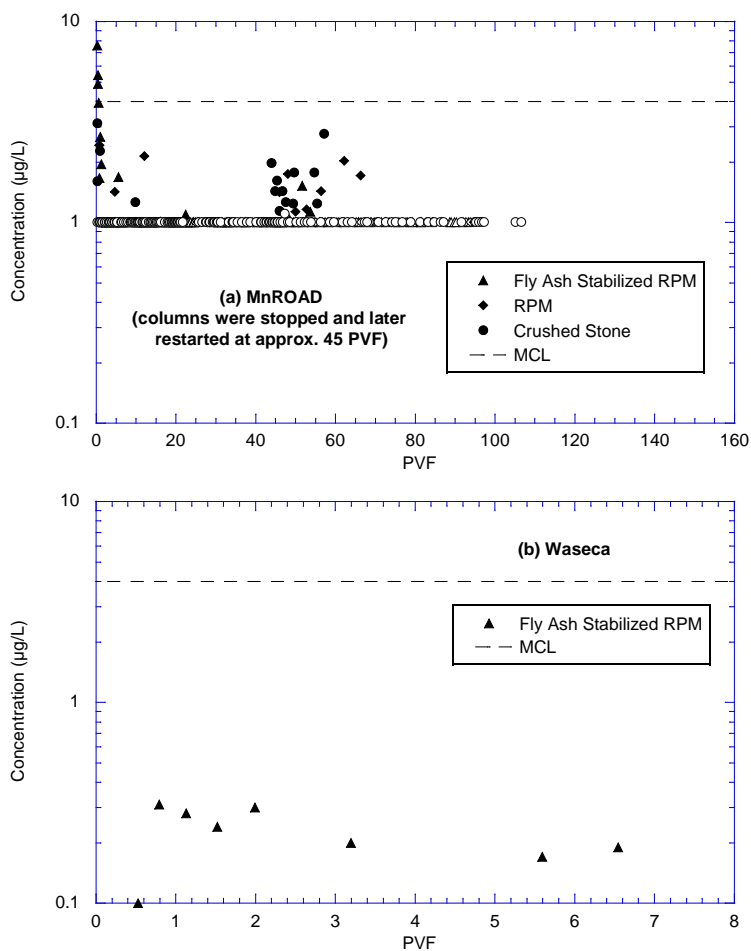
Fig. C-6.   Beryllium (Be) concentrations in leachate from column leach tests (CLTs).
Concentrations below minimum detection limits are plotted at the limit,
and represented with an open symbol.
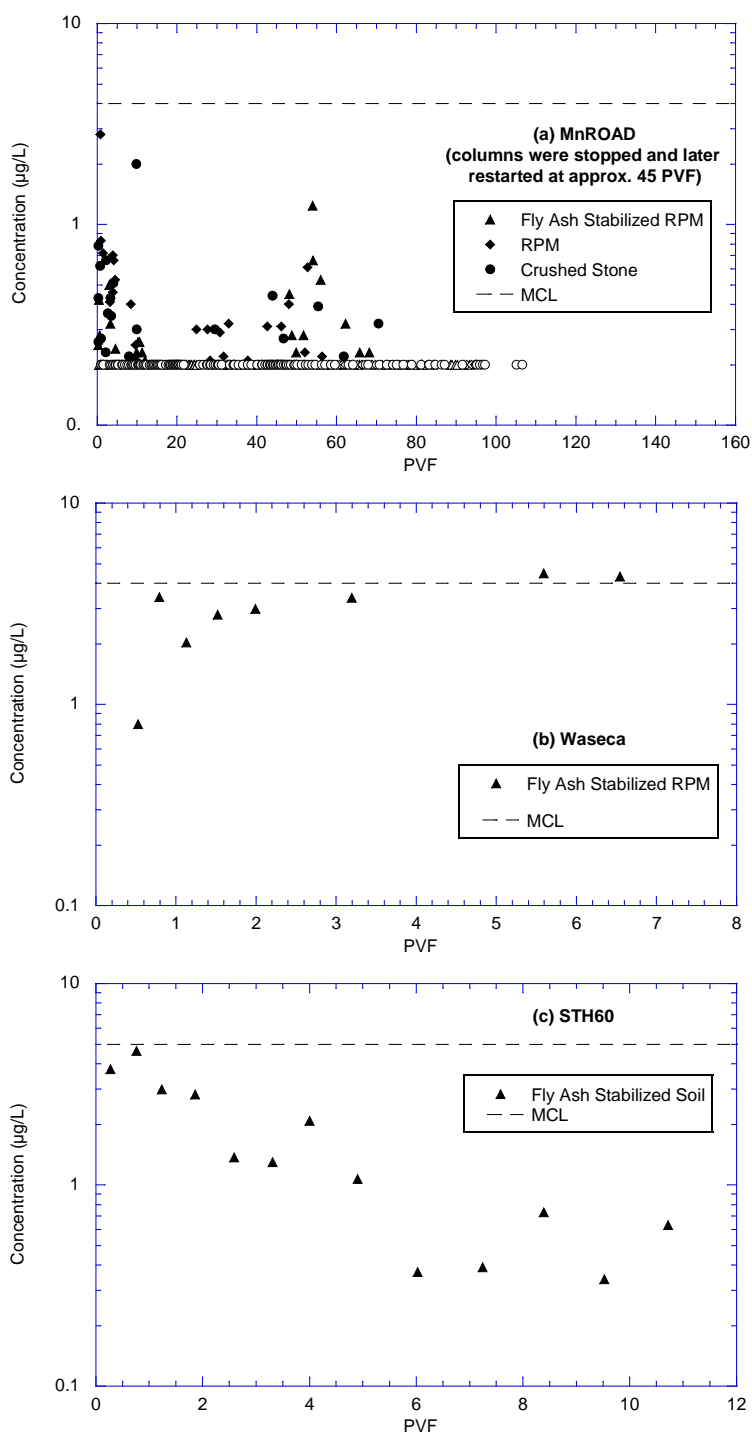
Fig. C-7.   Cadmium (Cd) concentrations in leachate from column leach tests (CLTs). Concentrations below minimum detection limits are plotted at the limit, and represented with an open symbol.
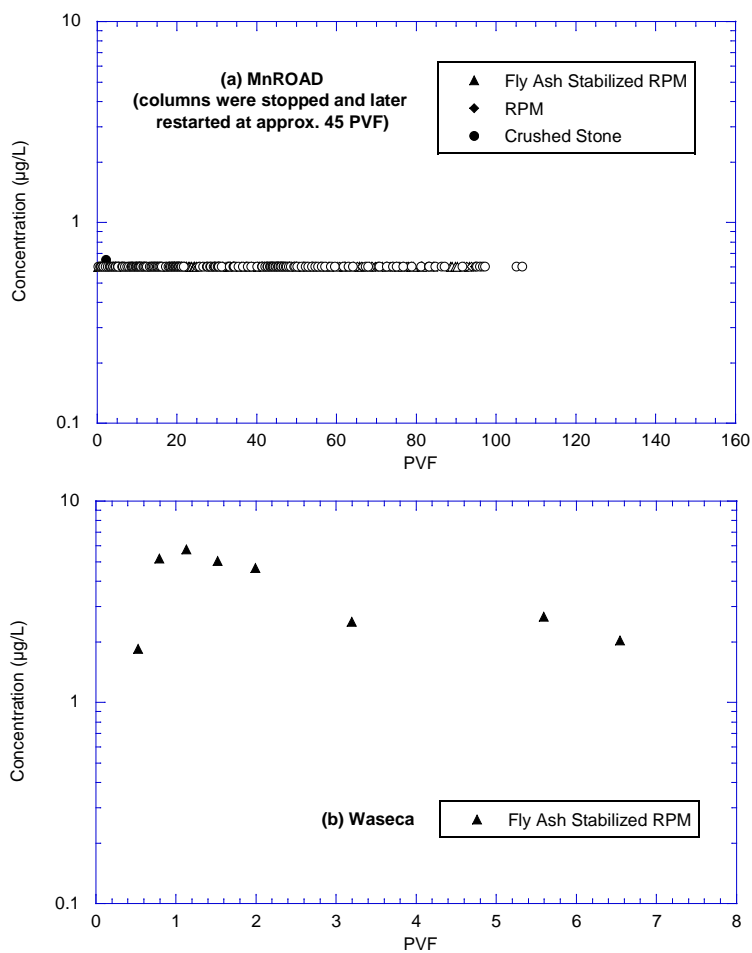
Fig. C-8.   Cobalt (Co) concentrations in leachate from column leach tests (CLTs).
Concentrations below minimum detection limits are plotted at the limit,
and represented with an open symbol.
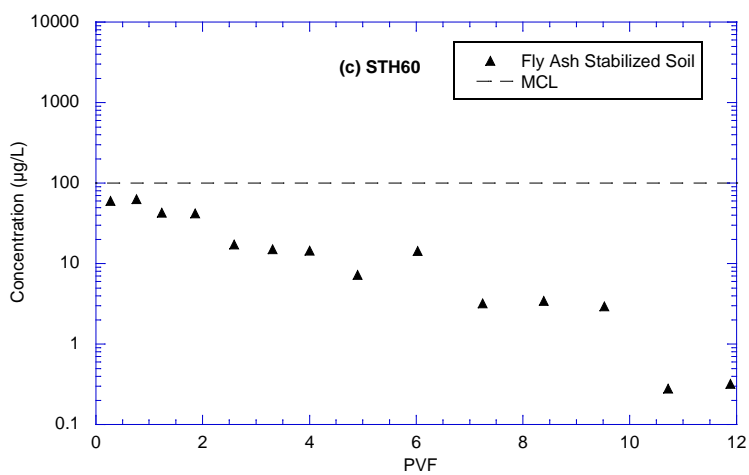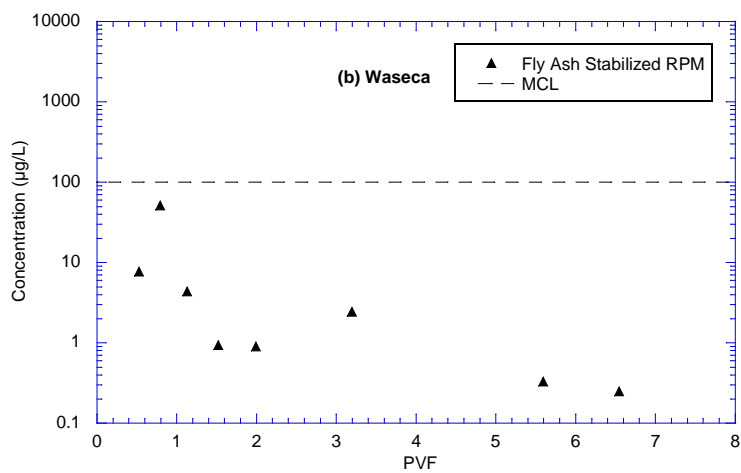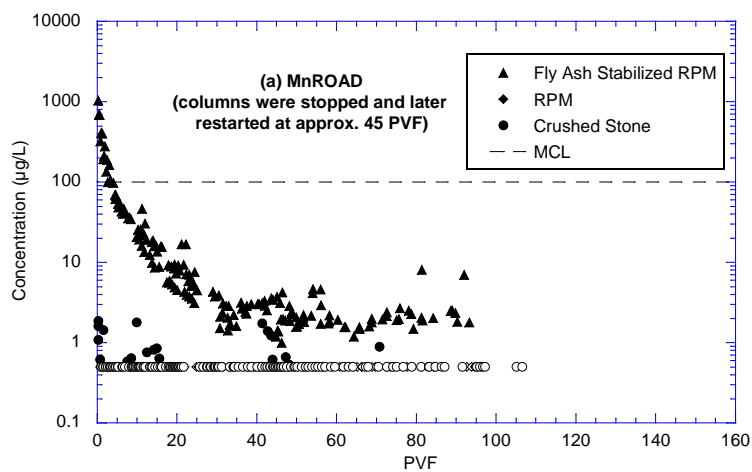
Fig. C-9.   Chromium (Cr) concentrations in leachate from column leach tests
(CLTs). Concentrations below minimum detection limits are plotted at the
limit, and represented with an open symbol.
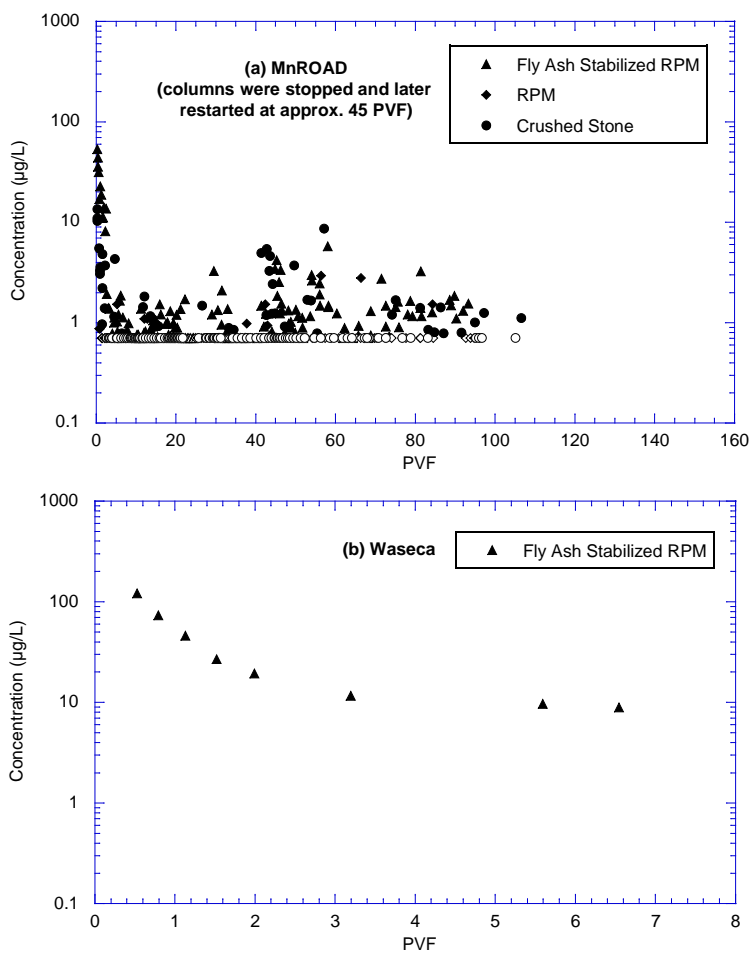
Fig. C-10.   Copper (Cu) concentrations in leachate from column leach tests (CLTs).
Concentrations below minimum detection limits are plotted at the limit,
and represented with an open symbol.
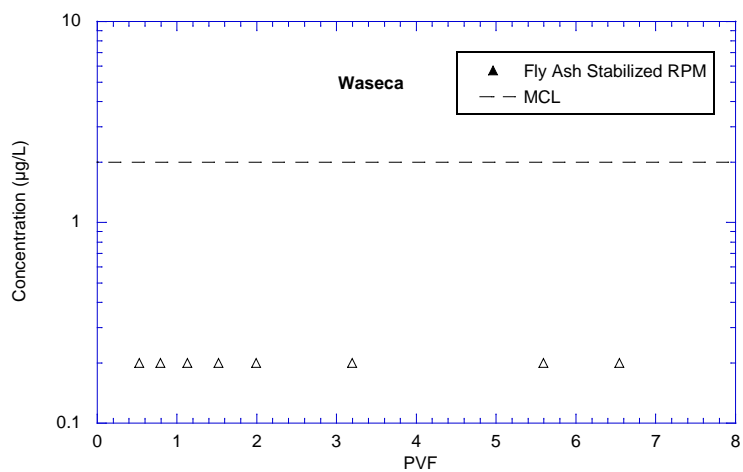
Fig. C-11.   Mercury (Hg) concentrations in leachate from column leach tests (CLTs). Concentrations below minimum detection limits are plotted at the limit, and represented with an open symbol.
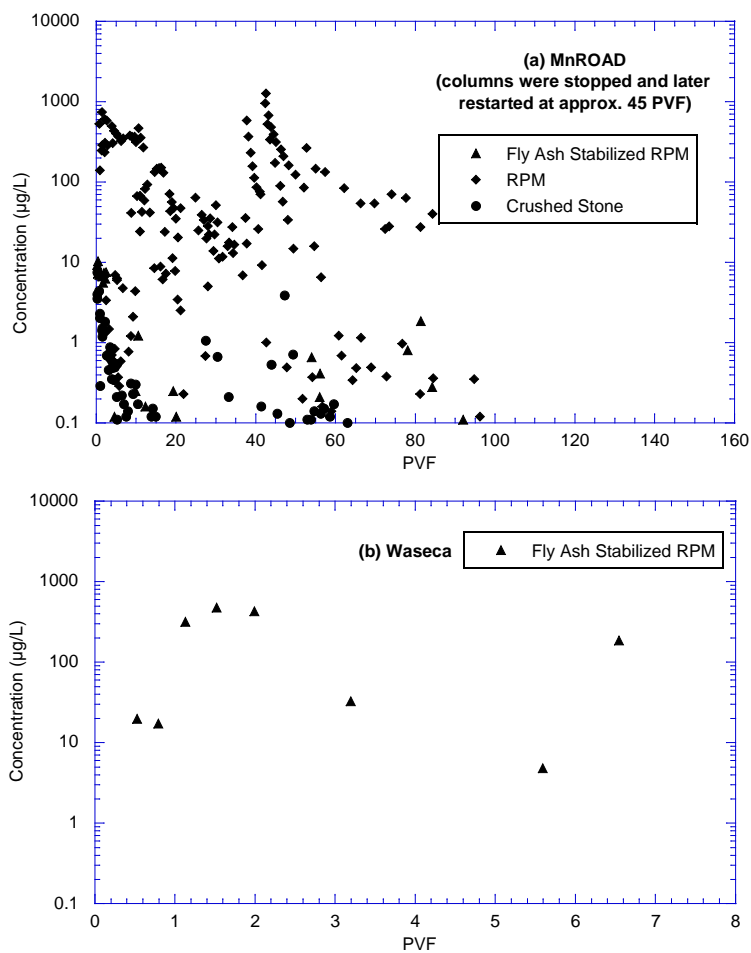
Fig. C-12.   Manganese (Mn) concentrations in leachate from column leach tests
          (CLTs). Concentrations below minimum detection limits are plotted at the
          limit, and represented with an open symbol.
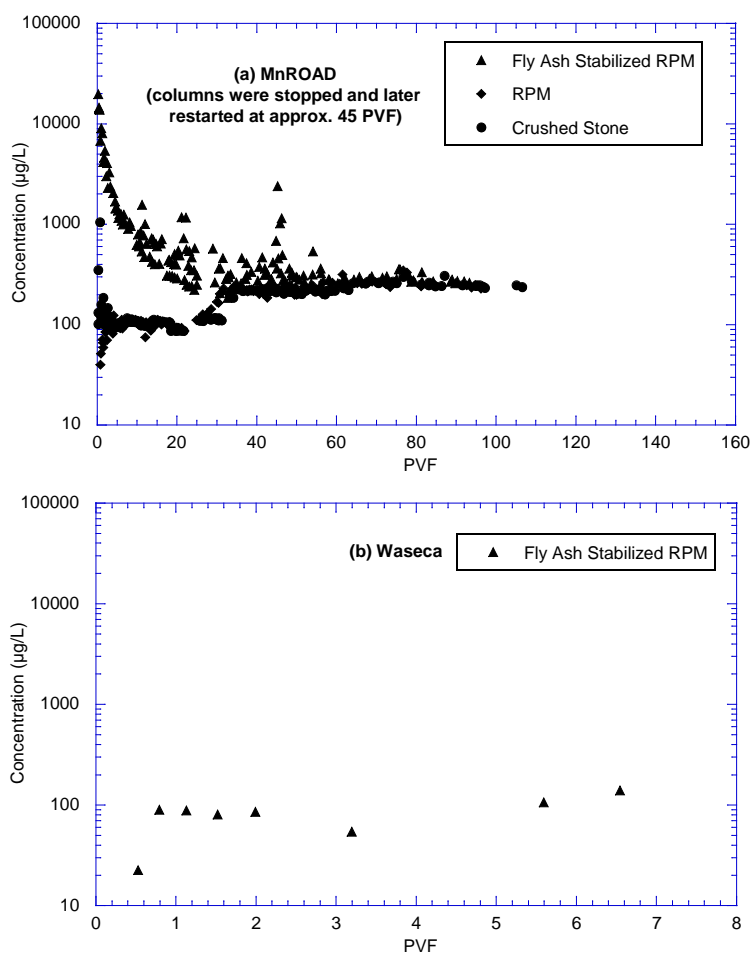
Fig. C-13.   Molybdenum (Mo) concentrations in leachate from column leach tests
              (CLTs). Concentrations below minimum detection limits are plotted at the
              limit, and represented with an open symbol.
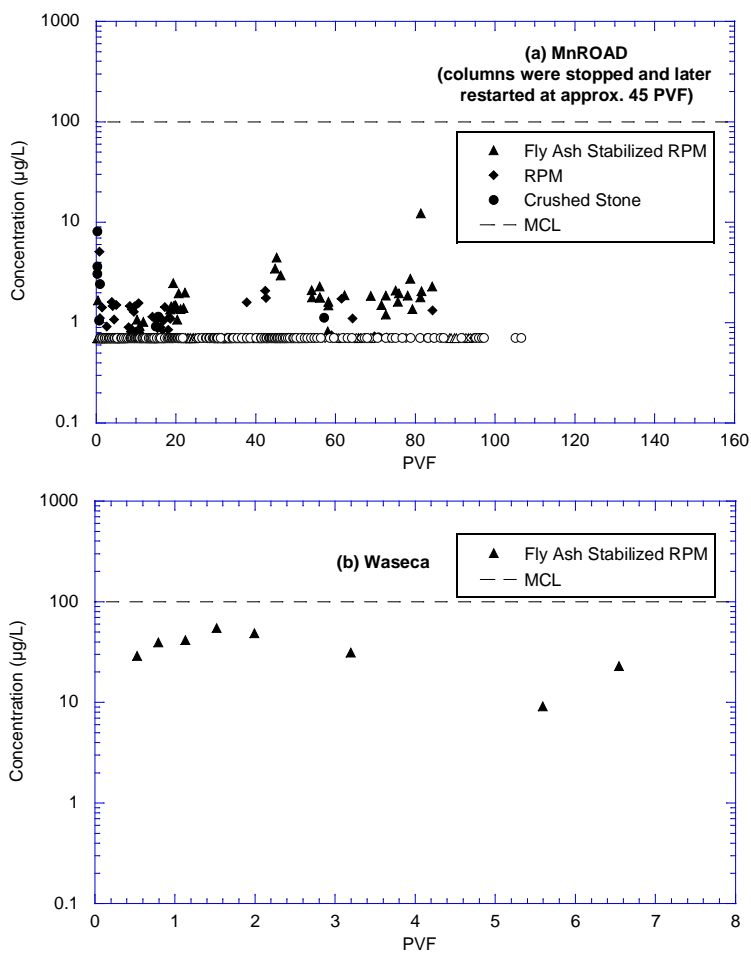
Fig. C-14.   Nickel (Ni) concentrations in leachate from column leach tests (CLTs).
Concentrations below minimum detection limits are plotted at the limit,
and represented with an open symbol.
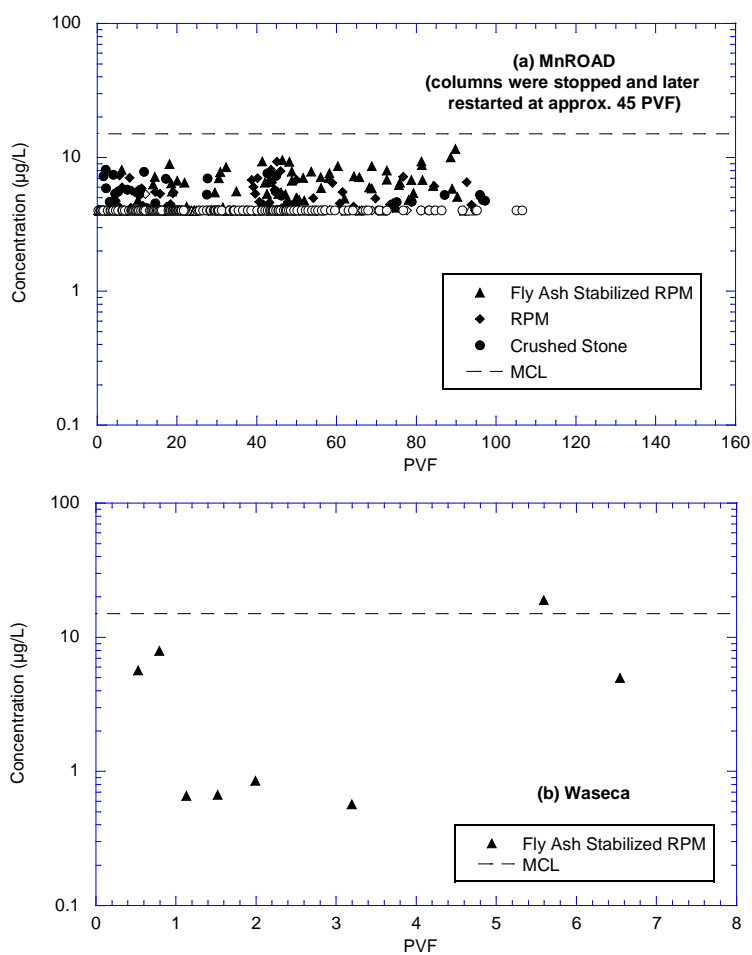
Fig. C-15.   Lead (Pb) concentrations in leachate from column leach tests (CLTs).
Concentrations below minimum detection limits are plotted at the limit,
and represented with an open symbol.
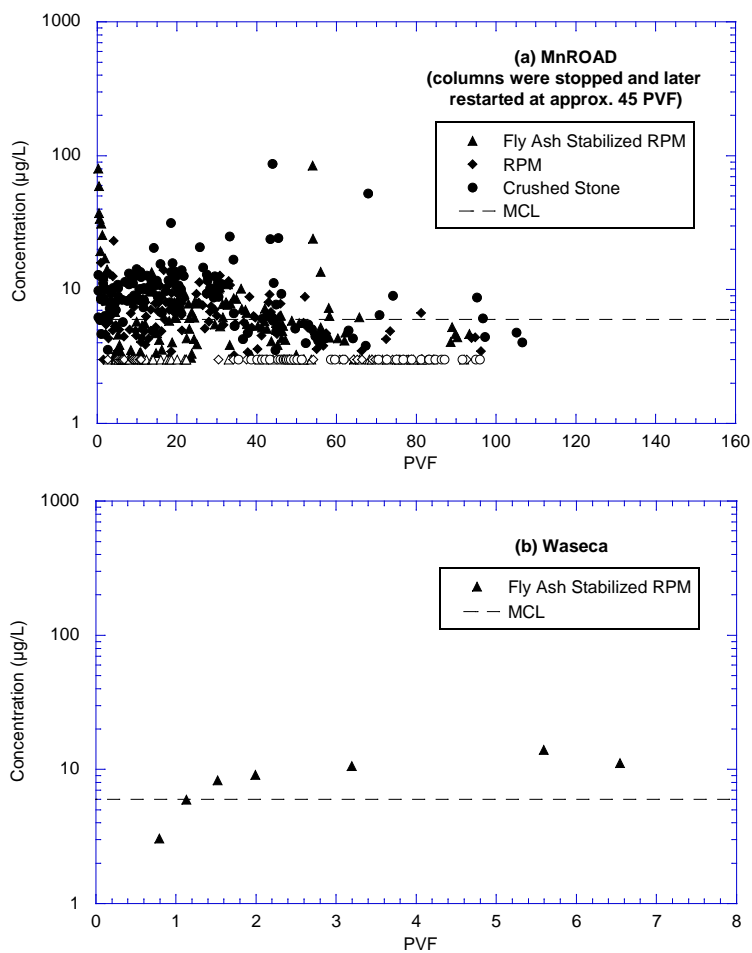
Fig. C-16.   Antimony (Sb) concentrations in leachate from column leach tests (CLTs).
Concentrations below minimum detection limits are plotted at the limit,
and represented with an open symbol.

151
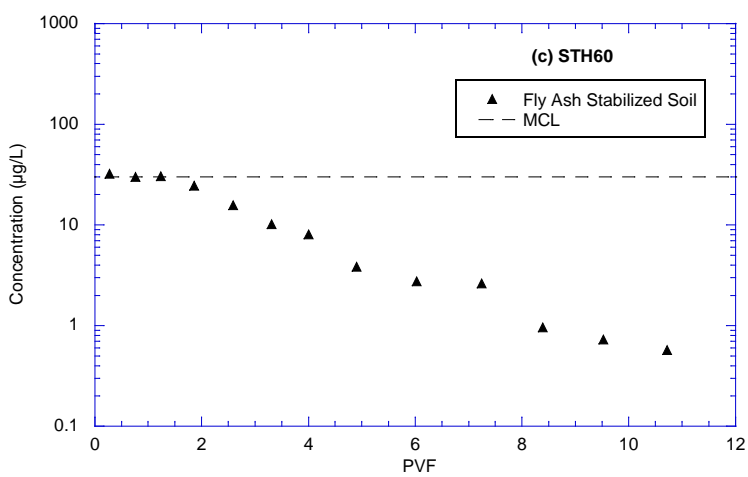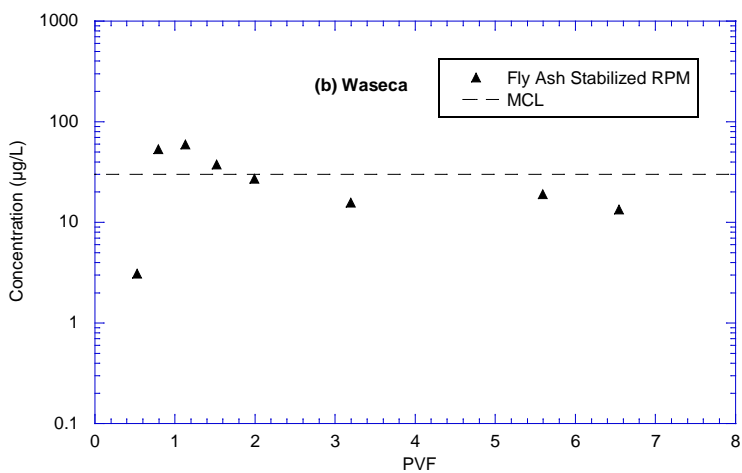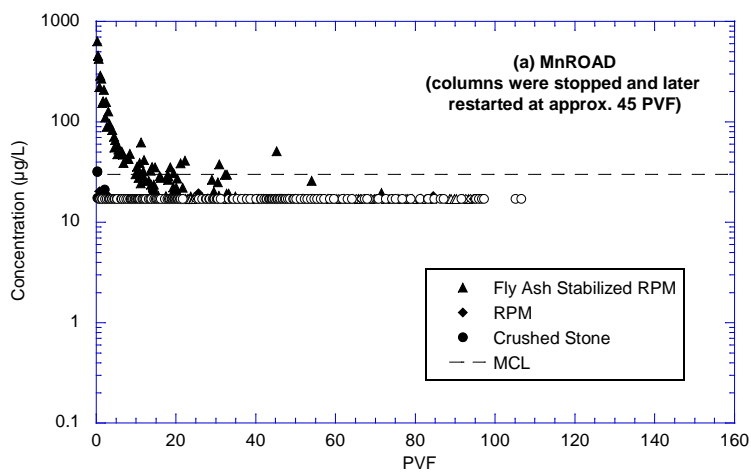
Fig. C-17.   Selenium (Se) concentrations in leachate from column leach tests (CLTs). Concentrations below minimum detection limits are plotted at the limit, and represented with an open symbol.
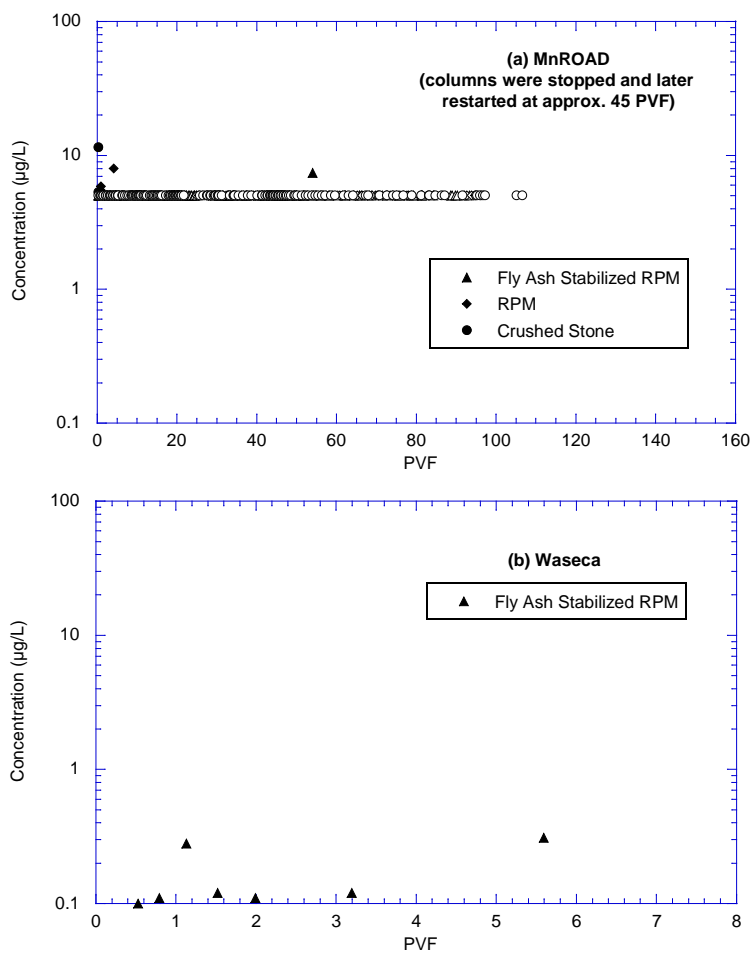
Fig. C-18.   Tin (Sn) concentrations in leachate from column leach tests (CLTs).
          Concentrations below minimum detection limits are plotted at the limit,
          and represented with an open symbol.

153
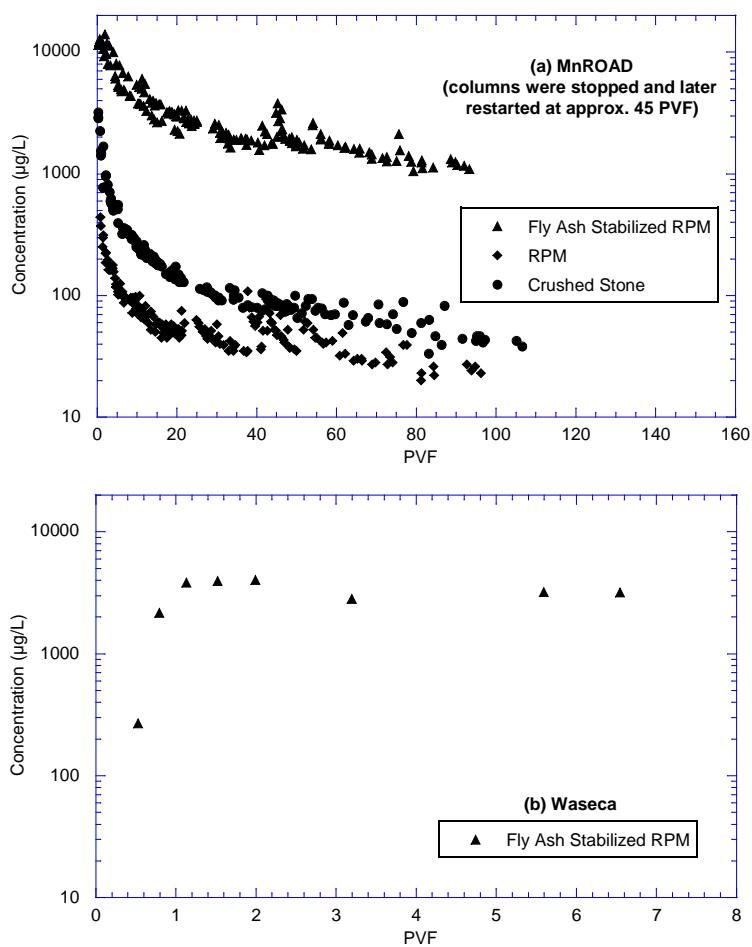
Fig. C-19.   Strontium (Sr) concentrations in leachate from column leach tests (CLTs).
Concentrations below minimum detection limits are plotted at the limit,
and represented with an open symbol.
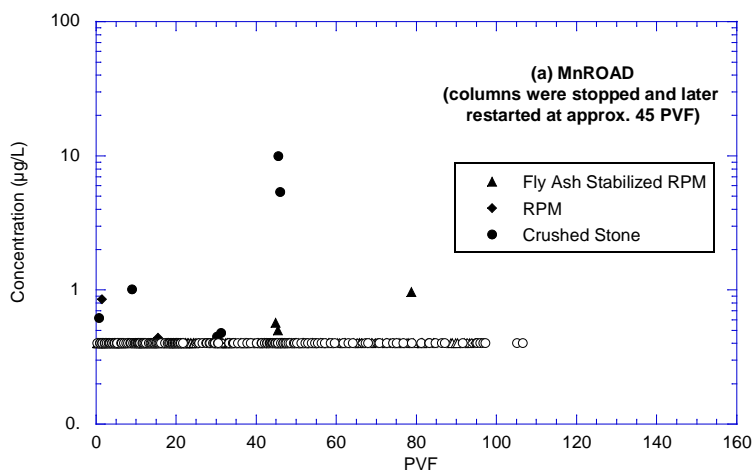
Fig. C-20.   Titanium (Ti) concentrations in leachate from column leach tests (CLTs).
        Concentrations below minimum detection limits are plotted at the limit,
        and represented with an open symbol.
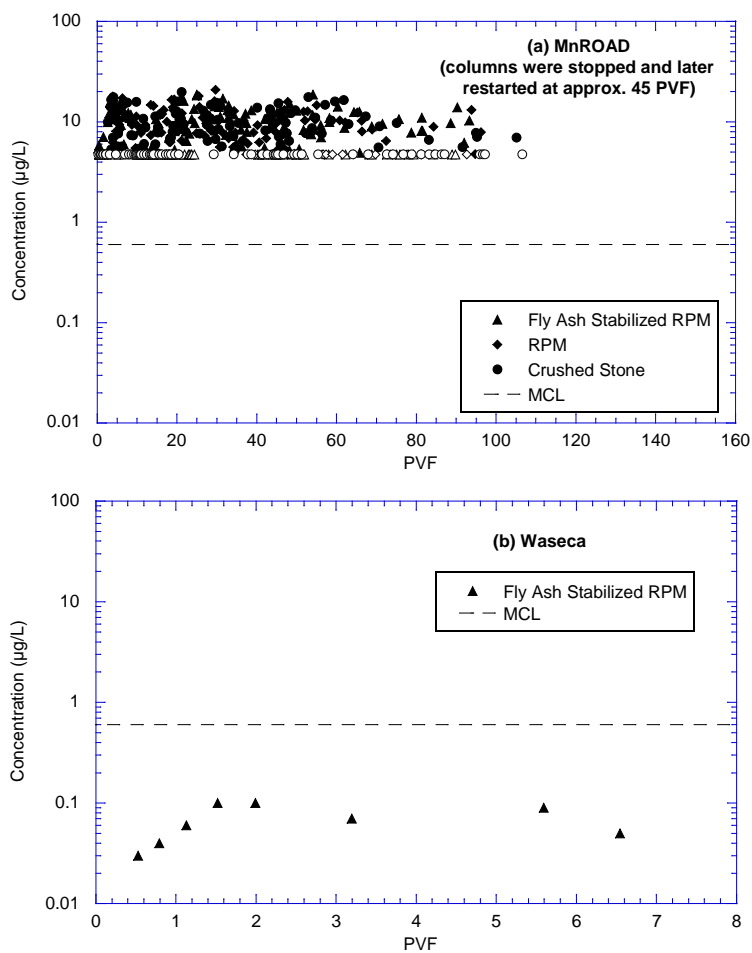
Fig. C-21. Thallium (Tl) concentrations in leachate from column leach tests (CLTs).
Concentrations below minimum detection limits are plotted at the limit,
and represented with an open symbol.
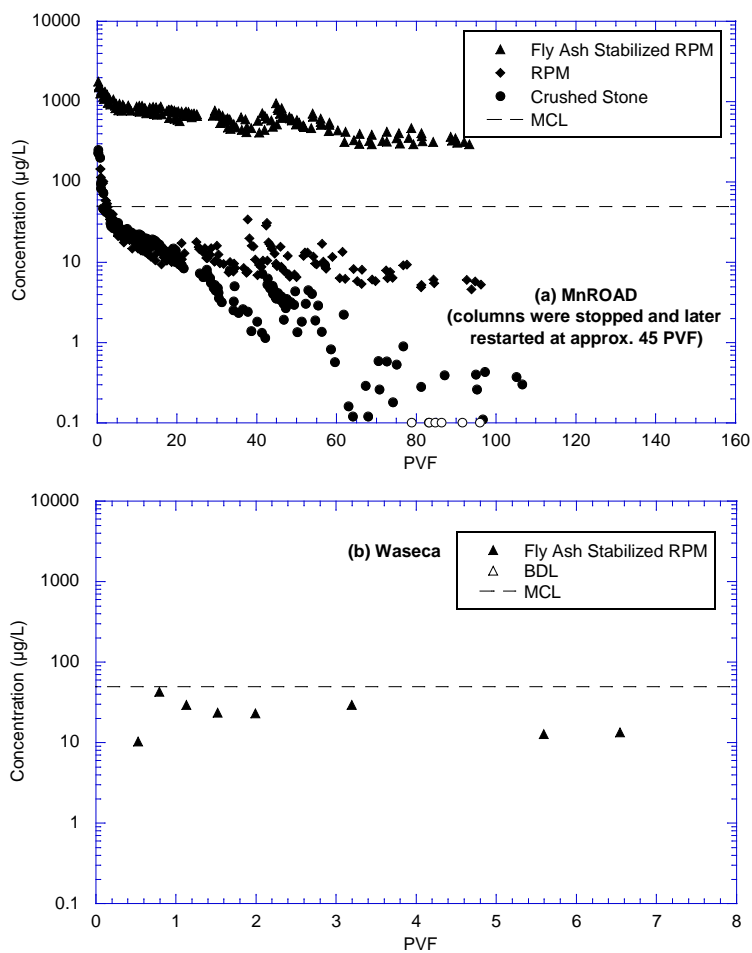
Fig. C-22.   Vanadium (V) concentrations in leachate from column leach tests (CLTs).
Concentrations below minimum detection limits are plotted at the limit,
and represented with an open symbol.
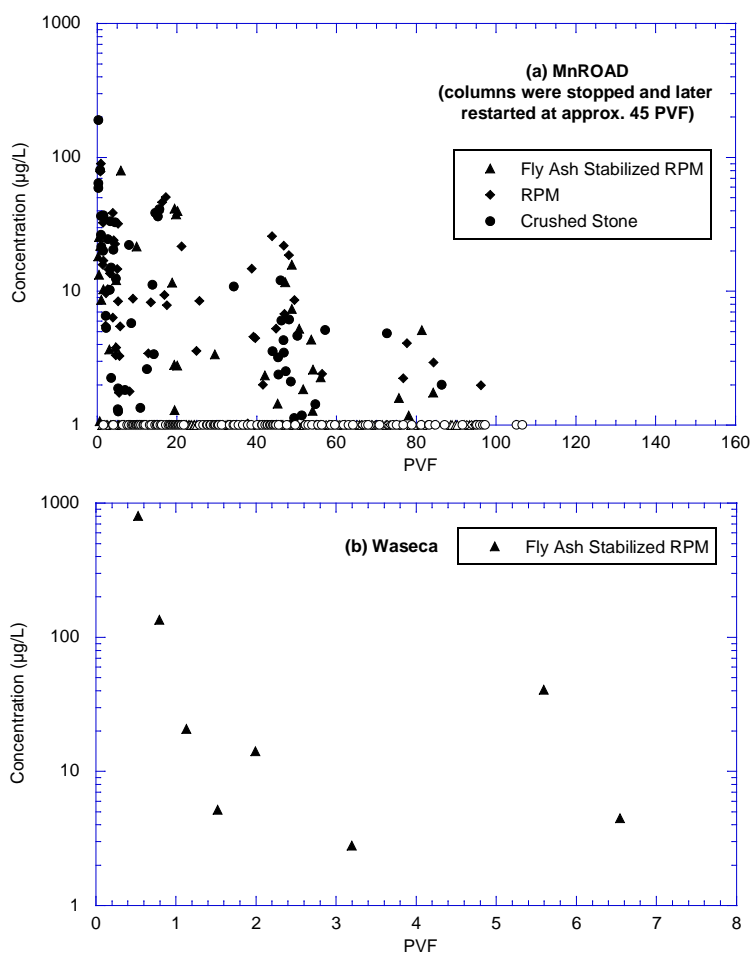
Fig. C-23.   Zinc (Zn) concentrations in leachate from column leach tests (CLTs).
Concentrations below minimum detection limits are plotted at the limit,
and represented with an open symbol.

Table C-1.   MnROAD Water Leach Test Results

Sample	Ag	Al	As	B	Be	Cd	Co	Cr	Cu	F
Material and L:S Ratio	ppb	ppb	ppb	ppb	ppb	ppb	ppb	ppb	ppb	pp
Crushed Stone - 3:1	3	56.6	<30	<20	<1	<4	<3	<1	<5	23
Crushed Stone - 5:1	<1	128.4	<30	<20	<1	<4	<3	1.1	<5	20
Crushed Stone - 10:1	3	167.2	<30	<20	<1	<4	<3	<1	<5	5
Crushed Stone - 20:1	<1	61.9	<30	<20	<1	<4	<3	<1	<5	
RPM - 3:1	<1	<50	<30	<20	<1	<4	<3	<1	<5	
RPM - 5:1	<1	<50	50	<20	<1	<4	<3	1.9	<5	
RPM - 10:1	<1	<50	<30	<20	<1	<4	<3	<1	<5	
RPM - 20:1	<1	<50	<30	<20	<1	<4	<3	<1	<5	1
Fly-ash-stabilized RPM - 3:1	<1	554.9	110	755.7	<1	<4	<3	127.0	6.6	
Fly-ash-stabilized RPM - 5:1	<1	1263.6	70	739.8	<1	<4	<3	98.4	6.6	
Fly-ash-stabilized RPM - 10:1	<1	3395.1	40	608.1	<1	<4	<3	42.9	<5	
Fly-ash-stabilized RPM - 20:1	<1	7667.8	40	557.8	<1	<4	<3	20.5	<5	

Sample	Ni	Pb	Sb	Se	Sn	Sr	Ti	Tl	V	Z
ID	ppb	ppb	ppb	ppb	ppb	ppb	ppb	ppb	ppb	pp
Crushed Stone - 3:1	<3	<20	<10	<30	<5	24	<1	<10	<3	
Crushed Stone - 5:1	<3	24.4	<10	<30	<5	24	<1	<10	<3	
Crushed Stone - 10:1	<3	<20	<10	<30	26	24	<1	<10	<3	
Crushed Stone - 20:1	<3	<20	<10	<30	<5	21	<1	<10	<3	
RPM - 3:1	<3	<20	<10	<30	<5	41	<1	<10	<3	
RPM - 5:1	<3	<20	<10	<30	14	31	<1	<10	<3	
RPM - 10:1	<3	<20	<10	<30	<5	22	<1	<10	<3	1
RPM - 20:1	<3	<20	<10	<30	<5	15	<1	<10	<3	4
Fly-ash-stabilized RPM - 3:1	5.9	<20	<10	<30	<5	10258	<1	<10	990	
Fly-ash-stabilized RPM - 5:1	<3	37.8	<10	<30	<5	8293	<1	<10	900	
Fly-ash-stabilized RPM - 10:1	<3	<20	<10	<30	<5	4566	<1	<10	590	
Fly-ash-stabilized RPM - 20:1	<3	<20	<10	<30	<5	2978	<1	<10	410	

Table C-2.   STH60 Water Leach Test Results

Material	WLT pH and Concentration (µg/L)				
	Cd	Cr	Se	Ag	pH
Fly-Ash-Stabilized Soil	0.6	46	16.2	1.8	11
Fly Ash Alone	0.7	95	26	2.2	11.8

APPENDIX D – STATE REGULATIONS REGARDING FLY ASH USE

Limitations placed by states on the use of fly ash focus on the potential toxicity of the ash (US DOE NETL 2009). Twenty four states in the US have formal regulatory policy regarding the use of fly ash in the production of concrete which then may be used as a road construction material. Twenty states in the US have formal regulatory policy regarding the use of fly ash as a stabilizing additive in construction of roadway layers under certain conditions. Fly Ash usage requirements among states that allow use vary from no requirements, to a requirement to prove non-toxicity by Toxicity Characteristic Leaching Procedure (TCLP), metals analysis, elemental analysis, Water Leach Tests (WLT), or other leaching test results. Thirteen states do not have any formal policy regarding use of fly ash in road construction, but permit use of fly ash on a case by case basis, and seventeen states do not permit fly ash to be used in road construction (US DOE NETL 2009).

Table D-1.   Fly ash regulatory status in US states

State	Haz. Waste Status	Status	Use in PCC Specifically Authorized	Road/Soil STable Use Specifically Authorized	If No, Use Possible on case by case basis?
Alabama	Exempt	Special Waste	No	No	Yes
Alaska	Exempt	Indust. Solid or Inert	No	No	Yes, with TCLP and metals, meet requirements
Arizona	Exempt	None	No	No	No
Arkansas	Exempt	Recovered Materials	No	No	Yes, if not "disposal"
California	NOT Exempt	Haz. Waste unless proven not by TCLP	No	No	No
Colorado	Exempt	None	No	No	No
Connecticut	Exempt	Special or Regulated	No	No	Yes
Delaware	Exempt	Nonhaz. Indust.	No	No	Yes, TCLP required

State	Haz. Waste Status	Status	Use in PCC Specifically Authorized	Road/Soil STable Use Specifically Authorized	If No, Use Possible on case by case basis?
Florida	Exempt	Solid or Indust. Byproduct	Yes	No	Yes
Georgia	Exempt	Indust. Solid	No	No	No
Hawaii	Exempt	None	No	No	Yes, with metals
Idaho	Exempt	Indust. Solid	No	No	No
Illinois	Exempt	CCW or CCB	Yes	Yes	-
Indiana	Exempt	Indust. Solid	Yes	Yes	-
Iowa	Exempt	None	Yes	Yes	-
Kansas	Exempt	Indust. Solid	No	No	No
Kentucky	Exempt	Special	Yes	Yes	-
Louisiana	Exempt	Indust. Solid	No	No	Yes
Maine	Exempt	Haz. Waste unless proven not	Yes	No	No
Maryland	Exempt	Pozzolan	No	Yes	-
Massachusetts	Exempt	Solid unless beneficial reuse	Yes	Yes	-
Michigan	Exempt	Low Hazard Indust.	Yes	Yes	-
Minnesota	Exempt	None	No	No	Yes
Mississippi	Exempt	Indust. Solid	No	No	Yes
Missouri	Exempt	None	Yes	No	Yes
Montana	Exempt	Indust. Solid	Yes	No	Yes
Nebraska	Exempt	Special	Yes	Yes	-
Nevada	Exempt	None	No	No	No
New Hampshire	Exempt	waste derived product	Yes	Yes	-
New Jersey	Exempt	Solid unless beneficial reuse	Yes	Yes	-
New Mexico	Exempt	Indust. Solid	No	No	Yes
New York	Exempt	None	Yes	Yes	-
North Carolina	Exempt	None	Yes	Yes	-
North Dakota	Exempt	None	No	No	Yes
Ohio	Exempt	None	Yes	Yes	-
Oklahoma	Exempt	None	Yes	Yes	-
Oregon	Exempt	None	No	No	No
Pennsylvania	Exempt	None	Yes	Yes	-

State	Haz. Waste Status	Status	Use in PCC Specifically Authorized	Road/Soil STable Use Specifically Authorized	If No, Use Possible on case by case basis?
Rhode Island	NOT Exempt	Haz. Waste unless proven not by TCLP	No	No	No
South Carolina	Exempt	Indust. Solid	No	No	Yes
South Dakota	Exempt	Solid or Indust. Byproduct	No	No	Yes
Tennessee	NOT Exempt	Haz. Waste unless proven not by TCLP	Yes	No	No
Texas	Exempt	Indust. Solid	Yes	Yes	-
Utah	Exempt	None	Yes	Yes	-
Vermont	Exempt	None	No	No	No
Virginia	Exempt	None	Yes	Yes	-
Washington	NOT Exempt	Haz. Waste unless proven not by TCLP	No	No	No
West Virginia	Exempt	None	Yes	Yes	-
Wisconsin	Exempt	Indust. Byproduct	Yes	Yes	-
Wyoming	Exempt	Indust. Solid	No	No	No

From US DOE (2009)

LEACHING FROM SOIL STABILIZED WITH FLY ASH:

BEHAVIOR AND MECHANISMS

by

Kanokwan Komonweeraket

A dissertation submitted in partial fulfillment of

the requirements for the degree of

Doctor of Philosophy

(Civil and Environmental Engineering)

at the

UNIVERSITY OF WISCONSIN - MADISON

2010

ABSTRACT

LEACHING FROM SOIL STABILIZED WITH FLY ASH:

BEHAVIOR AND MECHANISMS

Kanokwan Komonweeraket

Under the supervision of Professor Craig H. Benson and Professor Tuncer B. Edil
at the University of Wisconsin-Madison

In situ stabilizing soil with fly ash has become a practical and economical solution for construction on soft ground. However, leaching of trace elements from stabilized soil can be a concern. Understanding the pH-dependent leaching behavior and mechanisms controlling release of elements from soil-fly ash mixture is important for assessing the environmental impacts associated with using fly ash in soil stabilization. In this study, pH-dependent leaching tests were conducted to investigate the leaching behavior of soil-fly ash mixtures used in roadway construction. The soils included organic clay, silt, clay, and sand. The fly ashes included Class C and off-specification high-carbon fly ashes.

Four leaching patterns as a function of pH were observed: (i) leaching of Ca, Cd, Mg, and Sr follows a cationic pattern; (ii) leaching of Al, Fe, Cr, Cu, and Zn follows an amphoteric pattern; (iii) leaching of As and Se follows an oxyanionic pattern for some mixtures and anomalous leaching patterns for other mixtures; and (iv) leaching of Ba presents amphoteric-like pattern but less pH-dependent.

Consistency in leaching behavior for many elements was observed between fly ash and soil-fly ash mixtures. Some constituents in soil or fly ash can enhance or diminish leaching, e.g. the high concentration of dissolved organic carbon in leachate is likely responsible for the increased leaching of Cu from the mixtures with soil having high

organic matter. Class C and high-carbon fly ashes show different abilities in immobilizing trace elements to some extent.

Modeling results from MINTEQA2 indicated that release of the elements, except As and Se are solubility-controlled. For a given element, the solubility-controlling solids were found to be very consistent. Oxide and hydroxide minerals control leaching of Al, Fe, Cr, and Zn, whereas carbonate minerals control leaching of Mg and Cd. Leaching of Cu is controlled by oxide and/or carbonate minerals. Both carbonate and sulfate minerals are controlling solids for Ca, Ba, and Sr depending on pH of the leachate. The difference and inconsistency between the release behavior for As and Se and the other elements are probably due to different controlling mechanisms, such as sorption, or solid-solution formation.

ACKNOWLEDGEMENTS

This dissertation would not have been possible without help and support from a great number of people whose contribution in assorted ways to its completion. It is a pleasure to convey my gratitude to them all in my humble acknowledgement.

My deepest gratitude is to my advisors, Professor Craig Benson and Professor Tuncer Edil, for their supervision, mentorship, thoughtfulness, and support throughout my doctoral study. I have been fortunate to have advisors who gave me the opportunity to develop my own individuality and self-sufficiency by allowing me to work independently. Their continuous practical guidance, insightful comments, and constructive discussion in every states of my research helped me thoroughly understand and accomplish this research project.

I gratefully and sincerely thank to Professor William Bleam who devoted his precious time for numerous discussions and lectures that helped me broaden my knowledge and sort out the technical and scientific details of my modeling study and soil science. I am grateful to him for his crucial contribution, mentorship, and friendship. I would like to extend my sincere thanks to Professor David Armstrong and Professor Nita Sahai for serving as thesis committee members and for their helpful advice, supervision in chemistry, valuable time to review this thesis, and insight comments about it.

I am indebted to Jackie Cooper, environmental lab manager, who helped tutor me in running many analytical instruments and gave me technical advice for years. I gratefully acknowledge Xiaodong Wang, geo engineering lab manager, for his friendship, assistance in soil testing, and exceptional skills in experimental equipment handling and repair.

I am very grateful to Assistant Professor Kumthorn Thirakhupt, a former secretary of Inter-Department of Environmental Science, Chulalongkorn University, Dr. Supichai Tangjaitrong, my Master's advisor at Chulalongkorn University, Associate Professor

Thavivongse Sriburi, Director of Environmental Research Institute, Chulalongkorn University, Dr Saovapak Suktrakoolvait, Faculty of Science and Technology Rajamangala Institute of Technology. Their assistance and guidance enrich my growth as a student, a researcher, and a scientist want to be. Without their support and encouragement in a number of ways, my ambition to study abroad can hardly be realized.

Special thanks to my colleagues in the Environmental Engineering program, Geo Engineering group, Jennifer Stibitz and friends at Periodical Room, Memorial Library, life-long friends at Ratchawinit Bang Kaeo School, friends at Chulalongkorn University, Thairat-Thammarat Lee, Luksana Chaisawing, and Chatchai Choopanich, who have helped me stay sane through these difficult years. Their support and care helped me overcome setbacks and stay focused on my doctoral study. I greatly value their friendship and I deeply appreciate their belief in me.

Most importantly, my deepest thanks go to my beloved families for their unconditional love, patience, endless support, and encouragement throughout my life. Thank you for giving me strength, having faith in me, allowing me to be as ambitious as I wanted during this endeavor. I would not have come to this far without them. I am heartily thankful to my husband, Nuntapol Khonkhayun. His support, encouragement, quiet patience, and unwavering love have been undeniably wonderful and grateful for over sixteen years. I also cordially appreciate the generosity, encouragement and support of my husband's families. I also would like to dedicate this dissertation to the memory of my dearly loved grandmother who passed away in the last year of my study.

TABLE OF CONTENTS

LIST OF FIGURES

LIST OF TABLES

SECTION 1

INTRODUCTION

Coal fly ash is a coal combustion product that is produced annually in substantial quantities by coal-fired power plants (ACAA 2008b). The pozzolanic properties of fly ash make it an attractive material for civil engineering applications, such as concrete production, road base and subgrade stabilization, embankments, and flowable fill (USEPA 2005, ACAA 2008a). However, only approximately 40-45% of fly ash is currently used. The remainder is disposed in landfills or in ponds (ACAA 2008a). Utilization of fly ash in construction reduced the cost and environmental impact associated with producing conventional construction materials, and also significantly reduces the amount of fly ash to be disposed. Thus, there is considerable interest in increasing the amount of fly ash being used.

In areas where soft soils exist, they generally are removed and replaced with stronger material or stabilized using physical or chemical methods to form a strong platform to support construction (Hampton and Edil 1998, Edil et al. 2000). Research has shown that coal fly ashes can be effective in stabilizing inorganic and organic clays, providing significantly improved strength, durability, and stiffness (Turner 1997, Acosta et al. 2003). Accordingly, *in situ* soil stabilization with fly ash has become a practical and economical solution, especially in highway construction where removal and replacement of local soils requires substantial construction cost and time. However, because fly ash contains trace elements of environmental concern, use of fly ash in construction presents a potential risk to the environment (Theis and Richter 1979, Adriano et al. 1980, Fruchter et al. 1990, Garavaglia and Caramuscio 1994, Georgakopoulos et al. 2002).

The leaching behavior of trace elements from soil-fly ash mixtures has been studied by Edil et al. (1992), Heebink and Hassett (2001), Bin-Shafique et al. (2002), Sauer et al. (2005), and Goswami and Mahanta (2007). However, none of these studies has investigated how the leaching behavior of soil-fly ash mixtures varies with pH, even though pH is a master variable governing the release of constituents from the solid phase into solution. Knowledge of the leaching behavior from soil-fly ash mixtures as a function of pH will help elucidate the mobility of trace elements in different types of soil and fly ash used in roadway construction.

Several leaching studies have identified two key mechanisms controlling the release of constituents from coal combustion residues such as fly ash: solubility control and sorption control (Fruchter et al. 1990, Kosson et al. 1996, Dijkstra et al. 2002, Mudd et al. 2004, van der Sloot and Dijkstra 2004, Wang et al. 2004). However, mechanisms controlling leaching of trace elements from soil-fly ash mixtures have not yet been investigated. Understanding these mechanisms is a key step in predicting the release of trace elements and quantifying the potential risks associated with using fly ash in soil stabilization.

The objectives of this study are to (1) examine leachate characteristics and leaching behavior from soil-fly ash mixtures as a function of pH compared to fly ash alone, (2) identify mechanism controlling the release of major and trace elements from soil-fly ash mixtures; and (3) determine how the type of soil and fly ash used in a stabilization application affects the leaching mechanism and leaching behavior. The experimental program consisted of the following tasks:

(1) Conducting pH-dependent leaching tests on fly ashes and soil-fly ash mixtures using a range of fly ashes and soils encountered in roadway construction;

(2) Examining leachate chemical properties and determining chemical composition, including major and trace elements, sulfate, and dissolved organic carbon (DOC) in leachate from fly ash and soil-fly ash mixtures;

(3) Identifying predominant chemical species of elements of interest in leachates from fly ashes and soil-fly ash mixtures, and identifying potential solubility-controlling solids using the geochemical modeling code MINTEQA2

This report consists of five sections as follows: Section 2 contains background information on fly ash, soil-fly ash stabilization, leaching from fly ash, mechanisms controlling leaching, and factors controlling leaching. Section 3 describes leachate characteristics and leaching behavior from soil stabilized with fly ash, Section 4 presents information on mechanisms controlling release based on data obtained from pH-dependent leaching test and MINTEQA2 simulations, Section 5 is summary and conclusions, and Section 6 is references.

SECTION 2

BACKGROUND

2.1   Fly Ash

Coal fly ash is a siliceous or alumino-siliceous pozzolanic material that can form cementitious compounds in the presence of water. Fly ash is a byproduct generated from burning pulverized coal in coal combustion facilities, such as power plants or industrial boilers.

Typically, pulverized coal particles are injected with air into the combustion chamber and immediately ignited to generate heat. The molten residue hardens and forms ash as heat is extracted from the boiler and the flue gas cools. Coarse ash particles falling to the bottom of the combustion chamber are known as bottom ash, whereas the lighter fine ash particles that remain suspended in the flue gas are referred to as fly ash. Fly ash is removed from flue gas by particulate emission control devices, such as electrostatic precipitators, fabric filters, or mechanical collection devices, such as cyclones (ACAA 2003).

The physical, chemical and mineralogical properties of fly ash are significantly influenced by coal source, type of feed coal, type of combustion process, type of pollution control facilities, and handling method. Therefore, the composition and properties of fly ash vary greatly from one facility to another (Reardon et al. 1995, Tsiridis et al. 2004).

2.1.1   Physical Properties

Fly ash is a heterogeneous material consisting of fine and glassy particles that are spherical in shape. The particle size of fly ash is normally in the range of 0.01 -100

micron (Theis and Wirth 1977a), and the mean diameter of fly ash particles generally is one or two orders of magnitude smaller than that of bottom ash particles. Fly ash particles are comparable in size to silt and sand, while bottom ash particles are comparable to sand and gravel sizes (ACAA 2003).

Fly ash particles typically have three morphologies (1) cenospheres; (2) plerospheres; and (3) magnetite spheres (Figure 2.1). In the finer fractions of fly ashes, the cenospheres (hollow) and pherospheres (filled with microspheres) are the dominate forms and constitute 67% to 95% of the mass (Fisher and Natusch 1979). The occurrence of fly ash morphologies is believed to be associated with the chemical and physical reactions that occur during coal combustion, and the presence of some constituents in feed coal (Mattigod et al. 1990).

The color of fly ash can vary from gray to black depending on its chemical and mineral composition. Tan and light colors are generally associated with high lime content, whereas a dark gray to black color is typically due to high unburned carbon content (ACAA 2003). Nagataki et al. (1995) studied 27 pulverized fuel ash samples produced from Australian and Japanese coals. They found that the surface area varied from 0.7 to 37 m^2/g, specific gravity varied from 2.01 to 2.31, and the maximum bulk density was between 0.7 and 1.4 g/cm^3 (Nagataki et al. 1995).

2.1.2   Phase Minerals

During combustion, the mineral in coal can become fluid or volatile, and may oxidize or go through other gas phase reactions. Some minerals, such as silicates, clay and sand, and especially those with high melting points, may remain chemically unchanged in the combustion zone (Kim and Kazonich 2004). The transformation of deposited minerals in coals to those found in fly ash is related to the combustion temperature and the rate of cooling of the molten minerals (Kim 2002). Table 2.1

presents the thermal transformation compounds in fly ash and related parent minerals in source coal. Quartz, glass, and mullite ($Al_6Si_2O_{13}$) are most frequently reported as key constituents in the majority of fly ashes. Hematite (Fe_2O_3) and magnetite (Fe_3O_4) are the principal Fe-bearing compounds. The main Ca compounds are anhydrite ($CaSO_4$) and lime (CaO), whereas key Mg compounds are periclase (MgO) (Mattigod et al. 1990).

Vassilev et al. (2003) studied fly ashes derived from the combustion of six feed coals in four Spanish electric power stations. They report that the fly ashes consist of aluminosilicate glass as an ash-forming phase, to a lesser extent of mineral matter, and moderate char content. The major minerals and phases are mullite, quartz, char, kaolinite-metakaolinite, and hematite, whereas the minor minerals include cristobalite, plagioclase, K-feldspar, melilite, anhydrite, wollastonite, magnetite, and corundum. Additional minor and accessory minerals were also identified, inluding oxide-hydroxide, to a lesser extent from silicate and sulfate, and rarely from carbonate, phosphate and chloride mineral classes

2.1.3 Chemical Composition

All natural existing elements found in soil can be found in fly ash but may occur in a greater concentration (Adriano et al. 1980, Kim 2002). Many different metal oxides containing in coal become concentrated on the ash particle and form a surface coating during combustion process. The composition of this coating is greatly variable from one ash to another and influence on the solution condition when the ash come into contact with water (Theis and Wirth 1977a). Fly ash enriched in certain major and trace elements can have potential adverse effects on ground water and surface water quality if releases into the environment in sufficient quantity (Garavaglia and Caramuscio 1994).

The compounds containing major elements in fly ashes are mostly the products of thermal transformation of minerals presenting in feed coals (Mattigod et al. 1990).

Approximately 95% of the ash is composed of inert mineral oxides, such as oxide of Si, Al, Fe, and Ca (ACAA 2003). A lesser amount of other constituents, such as S, Na, Mg, Mn, K, Sr, Ti also present as minor elements (Kim and Kazonich 2004).

Trace elements in fly ash include As, B, Ba, Be, Cd, Cu, Hg, Mo, Ni, Pb, Sb, Se, V and Zn (Kim and Kazonich 2004). The distribution of trace elements varies greatly in coal from different areas and even in a single coal seam (Kim 2002). Rousseau et al. (1997) identified three mechanisms involved in the distribution of trace elements in fly ash particles: (1) trace elements that remain associated with unaltered mineral phases; (2) minerals containing trace elements that were dissolved in larger particles; and (3) volatile trace elements reacted with molten fly ash particles. Trace elements, though found in a relatively small quantity in fly ash, are of important interest for the environmental and health concerns due to their toxicity, potential accumulation, and persistence when released into the environment (Fytianos et al. 1998).

The detection of all trace elements as well as the evaluation of environmental emissions is complicated by the large number of compounds contained in ashes and the various chemical forms of the elements (Tsiridis et al. 2004). The potential impact for health and the environment of heavy metals in ash depends on the concentration as well as the chemical properties (solubility, toxicity and volatility), which are a function of speciation in the ash (Kim 2002).

2.1.4   Fly Ash Classification

According to ASTM C 618, fly ashes are classified into two classes, Class C and Class F, based on the chemical composition and physical properties of the fly ash. Table 2.2 describes the chemical requirements specified for Class C and Class F. Class C is produced from burning lignite and sub-bituminous coals that contain a high quantity of calcium carbonate ($CaCO_3$), resulting in an abundance of calcium ash (Table 2.3). The

calcium in the ash, reported as lime (CaO), reacts with water and yields cementitious products similar to those produced from the hydration of Portland cement. Consequently, Class C ash is considered to be a self-cementing fly ash.

Class F ash is derived from burning bituminous and anthracite coals that contain lower concentration of calcium compounds. The hydration products produced from Class F fly ash possess little or no self-cementing characteristics. When Class F is used in civil engineering applications, activators, such as lime, must be added to produce cementitious products.

Fly ashes that do not meet the criteria for Class C or Class F are referred to as "off-specification" fly ashes. High unburned-carbon fly ash is one kind of off-specification ash produced from power plants that employ low-NOx burners and selective catalytic and noncatalytic reduction systems in the coal combustion furnaces. The unburned carbon in the fly ash renders it unsuitable as a Portland cement admixture and affects construction-related applications. Therefore, the majority of high carbon fly ash is disposal in landfill (ACAA 2003).

Studies of the unburned carbon in fly ash have been conducted to gain more understanding about this byproduct and search for the potential utilization of high-unburned-carbon fly ash. Zhang et al.(2003) report that the composition and loss of ignition (LOI) vary from one sample to another ranging from of 32% to 86% by weight. The fly ash they studied consisted primarily of carbon and trace amounts of hydrogen, nitrogen, sulfur and oxygen. Three types of carbon were found in the fly ash, including inertinite, isotropic coke, and anisotropic coke. The anisotropic coke is a dominant carbon component in unburned fly ash (Baltrus et al. 2001), whereas isotropic coke is typically found in precursors for activated carbon.

2.2   Soil Stabilized with Fly Ash

Soil stabilization is defined as the changing of any physical or chemical properties of soil to improve engineering performance. Stabilization is usually done by mechanical, hydraulic, electrical, thermal, or chemical methods (Arman and Munfakh 1970). Using fly ash in soil stabilization for highway construction is a chemical method that involves mixing fly ash and soil with water to improve the engineering properties of materials. The engineering properties that determine the performance properties of highway materials are strength, durability, stiffness, compressibility, and hydraulic conductivity (Turner 1997).

Several chemical reactions occur when soil is stabilized with fly ash. Calcium oxide (CaO) in the fly ash undergoes pozzolanic reactions with silica and alumina to form calcium silicate gels and calcium aluminate gels, both of which are cementitious compounds (Turner 1997). These compounds bind the mineral solids together (Senol et al. 2002), which provides the long-term strength gain of stabilized mixtures (Turner 1997, Dermatas and Meng 2003). The strength and durability are directly related to the quantity of cementitious compounds formed by this pozzolanic reaction (Terrel et al. 1979).

The pozzolanic reaction of soil stabilized with fly ash occur in the manner similar to the hydration of Portland cement, but can occur more slowly and may require more time for hydration (Arman and Munfakh 1970). The simplified representation of pozzolanic reactions is demonstrated as follows:

$$CaO + H_2O \rightarrow Ca(OH)_2 \hspace{4cm} (2.1)$$

$$Ca(OH)_2 \rightarrow Ca^{2+} + 2[OH]^- \hspace{3.5cm} (2.2)$$

$$Ca^{2+} + 2[OH]^- + SiO_2(\text{clay silica}) \rightarrow CSH \hspace{2cm} (2.3)$$
$$\text{(silica)} \hspace{2cm} \text{(gel)}$$

$$Ca^{2+} + 2[OH]^- + Al_2O_3 \text{ (clay alumina)} \rightarrow CAH \qquad (2.4)$$
$$\qquad\qquad \text{(alumina)} \qquad\qquad \text{(gel)}$$
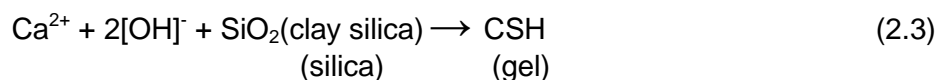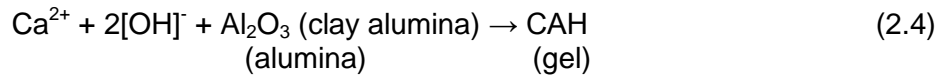
where C = CaO, S = SiO$_2$, A = Al$_2$O$_3$, and H = H$_2$O. When Class F fly ash is used, addition of lime is required to provide CaO for the reaction to proceed.

In addition to the primary reaction of CaO with alumina and silica compounds from the fly ash, CaO may also react with the fines in the material being stabilized. The reactions include cation exchange, flocculation-agglomeration, and soil-lime pozzolanic reaction (Terrel et al. 1979). In cation exchange reaction, divalent calcium (Ca^{2+}) ions from the fly ash or lime compete and replace univalent ions on clay particle, such as sodium (Na$^+$), potassium (K$^+$), and hydrogen (H$^+$), providing a stronger attraction between clay particles. Soil particles then form clumps and become a larger aggregate through a flocculation-agglomeration reaction. Cation exchange and flocculation-agglomeration reactions occur rapidly when soil and fly ash are initially mixed, which contribute to the initial strength gain and a reduction in the plasticity of the soil. The reduction of plasticity improves workability (Terrel et al. 1979).

Additional cementation occurs through soil-lime pozzolanic reactions when CaO reacts with silica and alumina in soils. Possible sources of silica and alumina in typical fine-grained soils are clay minerals, quartz, feldspars, micas, and other similar silicate or alumino-silicate materials. The extent of soil-lime pozzolanic reactions is greatly influenced by, and sometimes is inhibited by certain soil properties and characteristics, such as soil pH, organic carbon, clay mineralogy, silica-alumina ratio, etc (Terrel et al. 1979).

2.3 Leaching of Elements from Fly Ash

Because fly ash contains toxic trace elements, the reuse or disposal of fly ash can be a potential risk to the environment (Theis and Richter 1979, Adriano et al. 1980,

Fruchter et al. 1990, Garavaglia and Caramuscio 1994, Georgakopoulos et al. 2002). Understanding the leaching behavior and mechanisms for fly ash is important for proper assessment of reuse applications.

2.3.1 Controlling Release Mechanisms

Leaching is the process by which the constituents in the solid phase are released into the water phase (van der Sloot et al. 2003). The controlling release mechanisms can be described as either equilibrium control or kinetic (mass-transfer rate) control (Reardon et al. 1995, van der Sloot et al. 1996, Kosson et al. 2002). Distinguishing these two mechanisms is important when defining potential controlling mechanisms occurring in the conditions under consideration (Kosson et al. 2002) and for the proper impact assessment from leaching (van der Sloot et al. 1996).

Equilibrium-controlled release occurs when percolation through the waste occurs slowly enough so that an equilibrium condition can exist between the solid phase and the water phase. Kinetic-controlled release occurs if the flow is predominantly at the exterior boundary of waste materials or the flow rate is high relative to the rate at which mass is released to the percolating water (Kosson et al. 2002). Equilibrium-controlled release is typically associated with chemical processes, such as dissolution of minerals, and adsorption, whereas kinetic-controlled release is associated with physical transport processes including advection, diffusion, and surface wash-off (van der Sloot and Dijkstra 2004).

Several leaching studies have identified two key mechanisms controlling the release of constituents from combustion residues and leachate composition: solubility control and sorption control (Fruchter et al. 1990, Kosson et al. 1996, Dijkstra et al. 2002, Mudd et al. 2004, van der Sloot and Dijkstra 2004, Wang et al. 2004). However, physical transport processes have to take into account besides the chemical processes when

assess the distribution of contaminants in field situation (Dijkstra et al. 2002). Typically, the liquid-solid partitioning equilibrium is governed by the aqueous solubility as a function of pH for many major elements, whereas sorption processes dominates for minor and trace elements (Kosson et al. 2002).

2.3.1.1 Solubility Control

Solubility control occurs when the solution in contact with the solid is saturated with regard to the constituent species of interest (Kosson et al. 1996) and is generally associated with the dissolution of metal oxides present in the solid, such as aluminum oxide, iron oxide, and zinc oxide (Iyer et al. 1999, van der Sloot and Dijkstra 2004). These mineral and glass phases are unstable when water is added to fly ash. They dissolve and become more stable hydrous alumiosilicate phases (Reardon et al. 1995). The dissolution of mineral phases can occur partially or completely depending on the solubility of each phase and factors, such as pH, redox condition, and ionic strength (Kirby and Rimstidt 1994, Fleming et al. 1996, Mudd et al. 2004).

Compounds in fly ash that have relatively low solubility, rapid dissolution/precipitation kinetics, and are present in large quantities control the concentrations of their released constituents in leachates (Murarka et al. 1992). Generally, the major constituents in fly ash leachate are predominantly controlled by the dissolution and/or precipitation of the minerals containing these elements (Langmuir 1997). The dissolution of abundant elements can successively affects the release behavior of trace metals because the leaching of trace element is greatly influenced by the impact of geochemically abundant elements on the leachate chemistry (Kirby and Rimstidt 1994).

Solubility has been reported as a leaching controlling process for many elements. Roy (1984) indicates that concentrations of major elements (Al, Ca, Fe and Si) in fly ash

leachates are controlled by the solubility of anhydrite, mullite, aluminum and iron hydroxides. Fruchter (1990) studied leaching in the field using a large-scale fly ash lysimeter and reported that the release of Al, Ba, Ca, Cr, Cu, Fe, S, Si and Sr was solubility-controlled. Garavaglia and Caramuscio (1994) also report solubility-controlled leaching for both major and trace elements (Al, Ba, Ca, Cr, Cu, Fe, Mg, Mn, Ni, Pb, S, Si, Sr and Zn) in a lysimeter study. Kirby and Rimstidt (1994) indicate that relatively soluble gypsum ($CaSO_4.2H_2O$), anhydrite ($CaSO_4$), and calcite ($CaCO_3$) are the major sources of Ca^{2+} in solution and contribute to the majority of the observed electrical conductivity. Reardon et al. (1995) report solubility control for Ca, Sr, SO_4^{2-}, Al, Si, As(V), and Se in fly ash leachates.

2.3.1.2 Sorption control

Sorption processes control the release of elements that exhibit sorptive affinity to the active sites on the solid surface. Trace metals are likely controlled by sorption processes on sorption site surfaces, such as oxides, oxyhydroxides, organic matter, and clay (McBride 1994). Positively charged ions (such as Cu^{2+}) that are not controlled by the dissolution of minerals are often controlled by the adsorption onto the sorption sites available on the solid surface, such as metal oxides and organic matter (van der Sloot and Dijkstra 2004). Oxides are abundant in fly ashes, and about 30-40% of the oxide content in fly ash consists of aluminum and iron oxides (Fan et al. 2005). Many trace metals in fly ash are associated with either iron aluminum or manganese oxide on the fly ash (Theis and Wirth 1977a), which have a high affinity for trace metals (Jenne 1968).

Unburned carbon in fly ash is also an important factor affecting sorption of heavy metals by fly ash. The high specific surface area of carbon provides sorption sites for some trace metals, such as Cu (II) (Lin and Chang 2001) and Hg (Hwang et al. 2002). The trace metals sorbed by carbon have been found in higher amount than those in

mineral phases (Lin and Chang 2001, Hwang et al. 2002). Under certain conditions, unburned carbon has proven to have a sorption capacity for Hg equal or better than commercial activated carbon (Hwang et al. 2002).

The adsorption of ions onto active sites can be either non-specific adsorption, specific adsorption, or both. Non-specific adsorption involves electrostatic attraction where ions are adsorbed to positively or negatively charged-sites by Coulombic forces (attraction or repulsion). Specific adsorption occurs when short-range interactions between ions and the interphase become important. Ions penetrate into the inner layer and may come into contact with the surface. Specific adsorption can occur through the exchange of an electron, such as ligand exchange reaction (Xu et al. 2001).

The arsenate ion ($H_2AsO_4^-$) leached from coal fly ash is an example of an ion that can be specifically and/or non-specifically adsorbed onto Al_2O_3 and/or Fe_2O_3. In addition to solid phase adsorption, dissolved arsenate ion can also be adsorbed by the dissolved metal hydroxide in the aqueous phase. Leaching of elements associated with both dissolution/precipitation of metal oxides, such as Fe_2O_3 and Al_2O_3, and adsoption/desorption of dissolved arsenate ions onto the relevant metal oxides and hydroxides in the leaching system (Xu et al. 2001).

2.3.2 Factors Affecting Leaching

The rate and extent at which constituents are released from solids is influenced by chemical and physical properties of the material under consideration, characteristics of environment where leaching takes place, and the chemistry of the constituents of interest (Kida et al. 1996, van der Sloot et al. 2003, van der Sloot and Dijkstra 2004). In addition, the concurrent release or the presence of other constituents, such as other ions and dissolved organic carbon, can affect leaching by modifying the composition and

characteristics of the solution as well as the liquid-solid partitioning equilibrium (Kosson et al. 2002).

2.3.2.1 pH

The pH of the material and the pH of the environment are key factors affecting the release of many constituents for various kinds of materials, especially for those whose release are solubility controlled or sorption controlled. pH has a strong influence because dissolution and sorption processes are pH dependent (van der Sloot and Dijkstra 2004).

The pH at which leaching occurs is affected by the pH of the material, the pH of the environment, and the acid-base neutralization capacity of the material. The acid-base neutralization capacity determines how the pH changes over time under influence of environment factors (van der Sloot and Dijkstra 2004).

Leachate pH generally increases as the fly ash content increases (Bin-Shafique et al. 2002, Sauer et al. 2005) due to dissolution of CaO (Elseewi et al. 1980, de Groot et al. 1989, Fytianos et al. 1998, Ugurlu 2004). Thus CaO content is a key factor determining the acid-base characteristic of fly ash (de Groot et al. 1989). However, Theis and Wirth (1977a) found that the leachant pH may become either basic or acidic when the fly ash content in the soil-fly ash mixture is increased. Factors that are believed to be responsible for this alteration are amorphous iron that is associated with the acid content, and soluble calcium that represents the alkaline component of fly ash.

The change in pH affects the release of heavy metals from fly ash by (1) increasing of dissolution and/or desorption of metal-bearing mineral phases under acidic conditions (Edil et al. 1992, Fleming et al. 1996, Sauer et al. 2005); or (2) diminishing leaching due to precipitation and/or an increasing of partitioning into a solid phase at

higher pH or under alkaline conditions (Theis and Richter 1979, Brunori et al. 1999, Sauve et al. 2000, Bin-Shafique et al. 2002, Wang et al. 2004).

(1) Effect of pH on solubility

Low pH generally favors the leaching of many metals from fly ashes (Fleming et al. 1996, Rao et al. 2002). Leachability of metals (such as Cd, Cr, Zn, Pb, Hg and Ag) were also enhanced at the lower pH when an intensity of acid increased (Kirby and Rimstidt 1994, Fleming et al. 1996). However, the alkaline nature of the ashes can diminish the release of metals from many coal fly ashes (Drakonaki et al. 1998).

The release of metals due to dissolution of metal-bearing mineral phases under acidic conditions is attributed to the attack of hydrogen ion on the bonds of mineral oxides and other phases. The rate and concentration of leached metals are a function of the original abundance of metal-bearing mineral oxides, the oxide mineralogy of the ash, the spatial distribution of the oxides within ash particles, and the physical properties of ash particles (e.g. porosity) (Fleming et al. 1996).

When a solid oxide and hydroxide is in equilibrium with free ions in solution, the solubility is decreased linearly with increasing pH represented by decreasing in free metal-ion concentration $[Me^{z+}]$ in solution (Figure 2.2). However, this $\log[Me^{z+}]$-pH diagram assumes that only uncomplexed species of metal ions and hydroxide ions are present. The occurrence of hydroxo-metal complexes in equilibrium with solid has to take into account for evaluation of complete solubility (Stumm and Morgan 1996).

In addition, the change in solution pH highly affects which solid phases control the release of elements. For instance, Al^{3+} activities in leachate from fly ash and flue gas desulfurization sludge are controlled by the solubility of $AlOHSO_4$ at low pH, by amorphous $Al(OH)_3$ at midrange pH (~6-9), and by gibbsite at higher pH (Mattigod et al. 1990).

Under alkaline conditions, the leachability of many metals decrease as a result of increasing precipitation and/or adsorption (Theis and Richter 1979, Mizutani et al. 1996). Divalent cations can react with hydroxide ion (OH^-) and precipitate as metal hydroxides at high pH (Mizutani et al. 1996). Precipitation at high pH can completely remove Cu(II), Ni(II), Zn(II) and Pb(II) (Ricou et al. 1999). In contrast, amphoteric metals, such as Pb, Cr, Zn and Cu, can readily dissolve in leachate under both acidic and extremely alkaline conditions (Lim et al. 2004) and form complex ions and solutes (Mizutani et al. 1996). For example, the leaching test conducted by Lim et al. (2004) on clay-amended with combustion fly ash showed that amphoteric metals were least mobile at pH between 9 and 10 and their concentration increased significantly when the pH was outside this range.

(2) Effect of pH on sorption

Adsorption-desorption mechanisms play a significant role in the release of heavy metals from fly ashes when the equilibrium concentration of metals is far below the saturation concentration. Key factors affecting metal partitioning in fly ash include pH and surface physical-chemical characteristics of fly ash, including surface site densities, acidity constants, surface electrical characteristics, specific surface area, metal binding capacities, and metal binding strength (Wang et al. 2004).

Solution pH affects sorption on metal oxides by influencing the solid-phase surface and the speciation of the adsorbate in solution (Riemsdijk and Hiemstra 1993). Metal oxide or hydroxide surfaces exhibit an amphoteric behavior of which the surface can be either positively charged or negatively charged depending on pH of the system. A change in the surface charge of the reactive solid phases results in a change in electrostatic repulsion or attraction that affects metal adsorption. The pH at which the

mineral surface is neutral or uncharged is called the *point of zero charge* (*ZPC*) (Riemsdijk and Hiemstra 1993).

Surface charge of oxides, hydroxides, phosphates, and carbonates is established mainly by ionization of surface groups. Typically, the surface of minerals is positively charged at low pH and negatively charged at high pH (Figure 2.3). In case proton is only cation in the system, the positively charged is attributed to protonation, whereas the negatively charges is due to deprotonation. An example of the pH-dependent surface charge of a silicate with increasing of pH can be described as $SiOH_2^+$, $SiOH$, and SiO^- (Langmuir 1997).

For fly ash, Wang et al. (2004) found that the surface of fly ash is positively charged when the solution pH is less than pH_{zpc} and negatively charged when the solution pH is higher than pH_{zpc} (Figure 2.4). Sorption of metals (Cd, Cr, Cu, Ni and Pb) increased with an increase in pH as (Figure 2.5). All metals they studied were almost completely removed from solution for pH greater than 8 (Wang et al. 2004).

2.3.2.2 Reduction/Oxidation

The chemical form is important affecting leaching behavior. Metals may be present in an oxidized or reduced form depending on the redox state of the metal and the environment. For instance, chromium may be present as CrO_4^{2-} or Cr^{3+} (van der Sloot and Dijkstra 2004).

The redox condition of a solution is often reported in term of the redox potential (Eh), which indicates the tendency of a chemical species to accept or transfer electrons (Stumm and Morgan 1996). Reducing conditions, indicated by low or negative Eh, have been reported for leachate from alkaline fly ash (Garavaglia and Caramuscio 1994). However, the redox potential in coal waste field disposal sites have been reported vary widely from very reduced condition for flue gas desulfurization (FGD) disposal site (EPRI

1989), to very oxidized condition in a fly ash field lysimeter containing chrome (Fruchter et al. 1990).

Electrochemical processes influence metal speciation and redox behavior by modifying the nature of the metal itself, or by conversion of other species within the environment (Pohland et al. 1993). Many elements (e.g. As, Cr, Cu, Fe, Hg, Mn, Mo, Se, U, V and the actinide elements) may exist in more than one oxidation state (Davis et al. 1993), and oxidation state can dramatically affect solubility, toxicity, reactivity, and mobility (Fish 1993). For example, leachability and mobility can differ orders of magnitude under oxidizing conditions and reducing conditions (Davis et al. 1993, van der Sloot et al. 1994).

The effect of redox condition on leachability varies depending on the chemical species. Leaching of some metals (e.g. As, V, Fe, and Pb) increases significantly under reducing conditions, whereas leaching of other metals (e.g. Cr) increases under oxidizing conditions (Dusing et al. 1992). Other metals (e.g. Mo) are hardly affected under reducing environment (van der Sloot 1991).

2.3.2.3 Ionic Strength

Ionic strength of a solution influences both dissolution (van der Sloot and Dijkstra 2004) and sorption of heavy metals (Impellitteri et al. 2001). The interaction of charged particles in solution deviates particles from ideal behavior and affects the "effective concentration" or "activities" of particles for the reaction (Stumm and Morgan 1996, Langmuir 1997). The intensity of the interactions of the charged particles in solution depends on the charges of the ions and the total concentrations of ions in solution. These effects are embodied and expressed as ionic strength (Langmuir 1997). Since the solubility equilibrium is calculated from the "effective concentration" of each species in solution, the solubility equilibrium is strongly influenced by ionic strength (Stumm and

Morgan 1996). Generally, higher ionic strength promotes leaching of contaminants (van der Sloot and Dijkstra 2004).

In contrast, an increasing in ionic strength decreases sorption of cations in soil systems, which is attributed to a decreasing in thickness of the reactive layer for cation sorption (Impellitteri et al. 2001). As reported by Egozy (1980), Co distribution coefficients in soil decreased as ionic strength increased.

2.3.2.4 Presence of Other Chemical Species

The release of contaminants from materials can be influenced by the presence of other chemical species, such as inorganic compounds, organic compounds, and humic substances (van der Sloot 1996). Most trace metal and many major elements are charged species which may react with inorganic or organic ligands to form various soluble complexes (Riemsdijk and Hiemstra 1993, Stumm and Morgan 1996).

Ligands are anions or molecules with which cations form a complex compound. Some common ligands found in natural water include anions (HCO_3^-, CO_3^{2-}, Cl^-, SO_4^{2-}, F^-, $HS-/S^{2-}$), organic acids, and particle surface groups (Stumm and Morgan 1996). Complexation can increase the solubility of a mineral, which results in a higher total concentration of the species of interest in solution than would occur without complexation (Langmuir 1997). For example, total calcium concentration that is controlled by calcite solubility, an example of complexation effect, can include the complexes $CaSO_4^o$ and $CaHCO_3^+$ besides Ca^{2+} if sulfate and bicarbonate are present in a significant amount (Langmuir 1997).

Adsorption of cations or anions can be either enhanced or diminished when ions are present in complex forms rather than as free ions (Langmuir 1997). According to Riemsdijk (1993) the presence of a soluble metal complex frequently reduces metal

adsorption because metal complexes have much lower affinity for reactive surfaces on solids relative to free metal ions.

Organic matter can have a significant impact on total metal concentration and metal mobility (Kinniburgh et al. 1999, Zhou and Wong 2003). Soil organic matter is generally referred to as humus (Stevenson 1994), which consists mainly (70%) of humic substances (humic acids and fulvic acids) (Bohn et al. 2001). Humic substances extracted from soil are frequently more hydrophobic and higher in molecular weight than those of aquatic humic substances. These high molecular weight substances are less soluble and strongly adsorbed to mineral surfaces and therefore are expected to be less mobile in the environment compared to hydrophilic and low molecular weight humic substances (Kretzschmar and Christ 2001).

The major metal binding sites in humic and fulvic acids are carboxylic (COOH) and phenolic groups (OH). Other lesser abundant functional groups, such as N- and S-containing groups, may also be important for metal binding (Kinniburgh et al. 1999). Hydrogen ions dissociate from these reactive groups when humic substances are dissolved in water, which contributes to negatively charged sites for metal-binding (Stevenson 1982, Bohn et al. 2001). The magnitude of dissociation depends on the pH (Kinniburgh et al. 1999, Bohn et al. 2001) and electrolyte concentration (Kinniburgh et al. 1999).

Formation of complexes with organic matter and monovalent cations (e.g. Na^+, K^+) is a cation exchange reaction that forms salts (Stevenson 1982) and the bonding is primarily coulombic or electrostatic (Bohn et al. 2001). In contrast, multivalent cations (e.g. Cu^{2+}, Zn^{2+}, Mn^{2+}, Co^{2+}) form coordinate linkages with organic molecules with strong covalent bonds (Stevenson 1982).

Two different effects have been identified regarding the solubility and mobility of metals in the presence of organic matter: (1) increased metal solubility through binding

with water-soluble organic matter (Stevenson 1982, McCarthy and Zachara 1989, Kinniburgh et al. 1999, Bohn et al. 2001), (2) immobilization through the formation of insoluble complexes (Stevenson 1982) or through sorption (Stevenson 1982, Kinniburgh et al. 1999, Zhou and Wong 2003).

Humic and fulvic acids form both soluble and insoluble complexes with multivalent cations depending on the degree of saturation and the properties of organic compounds. (Stevenson 1982). Divalent and polyvalent cations (e.g. Fe^{2+}, Cu^{2+}, Zn^{2+}) form soluble complexes with various low molecular weight and water-soluble components of organic matter, such as fulvic acids. The complexation shields the cations from hydrolysis and precipitation reactions, which results greater water solubility (Bohn et al. 2001). In contrast, the insoluble salts of divalent and trivalent cations can form when cations bind with high molecular weight and hydrophobic humic acids (Bohn et al. 2001). Immobilization of metals by sorption process can occur through direct exchange at the clay-organic interface. Soluble complexes can become associated with mineral surfaces through adsorption as well (Stevenson 1982).

Several studies have reported that leaching of metals is facilitated by the presence of dissolved organic matter for many cations [Cu (Jackson et al. 1999, Meima and Comans 1999, Meima et al. 1999, Ashworth and Alloway 2004), Ni (Ashworth and Alloway 2004), Cr (Jackson et al. 1999), Zn (Boyd and Sommers 1990)], and some oxyanions [Mo, Se, As (Jackson et al. 1999)].

The liming effect associated with fly ash, which causes an increasing in pH, has been shown to reduce the availability of trace metals in fly ash-sewage sludge mixtures (Li and Shuman, 1997) and soil-fly ash mixtures (Bin-Shafique et al. 2002). Solubility of metals is diminished at high pH due to adsorption and precipitation reactions. However, complexation with soluble organic matter may maintain cationic species in the solution (Jackson et al. 1999, van der Sloot et al. 2003). Different organic compounds derived

from different waste can affect the metal solubility. The metal solubility can be enhanced when fly ash is mixed with organic waste containing more soluble organic matter, such as poultry litter, in comparison to sewage sludge (Jackson et al. 1999).

Table 2.1.   Thermal transformation of major inorganic compounds in fly ash.

Mineral in coal*	Transformation products in fly ashes
Phyllosilicates	Glass, Mullite ($Al_6Si_2O_{13}$), Quartz (SiO_2)
Quartz	Glass, Quartz (SiO_2)
Pyrite (FeS_2), Siderite ($FeCO_3$), Iron sulfates	Hematite (Fe_2O_3), Magnetite (Fe_3O_4)
Calcite ($CaCO_3$)	Lime (CaO)
Dolomite [$CaMg(CaO_3)_2$]	Lime (CaO), Periclase (MgO)
Gypsum ($CaSO_4.2H_2O$)	Anhydrite ($CaSO_4$)
Ankerite [$CaMg_xFe_{(1-x)}(CO_3)_2$]	Calcium ferrite ($CaFe_2O_4$), Periclase (MgO)

*Iron oxides, feldspars, and anhydrite do not undergo phase changes during combustion (Mattigod et al. 1990).

Table 2.2.   Chemical Requirements for Class F and Class C Fly Ash in ASTM C618.

Chemical Requirements	ASTM Requirements	
	Class F	Class C
SiO_2 + Al_2O_3 + Fe_2O_3, min (%)	70	50
SO_3, max (%)	5	5
Moisture Content, max (%)	3	3
Loss on Ignition, max (%)	6	6

Table 2.3.   Typical Chemical Composition of Fly Ash (ACAA 2003).

Compounds	Fly Ash Class F	Fly Ash Class C
SiO_2	55	40
Al_2O_3	26	17
Fe_2O_3	7	6
CaO (lime)	9	24
MgO	2	5
SO_3	1	3
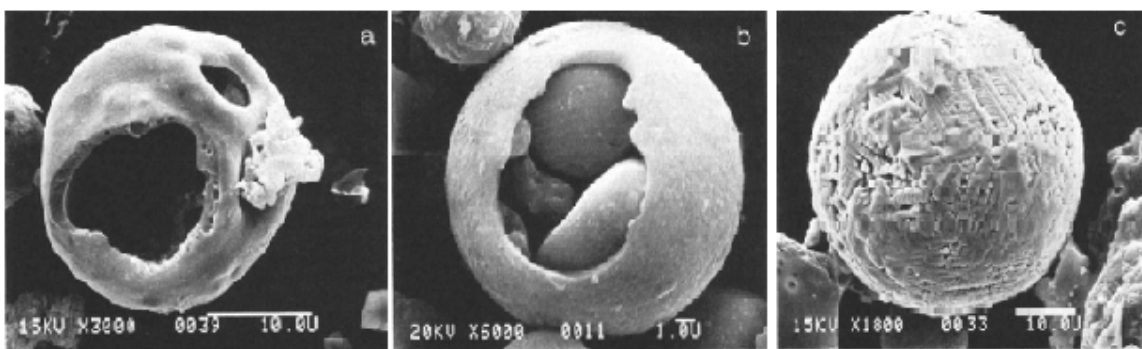
Figure 2.1.   Typical morphology of fly ash particles (a) cenospheres; (b) plerospheres; and (c) magnetite spheres (Mattigod et al. 1990).
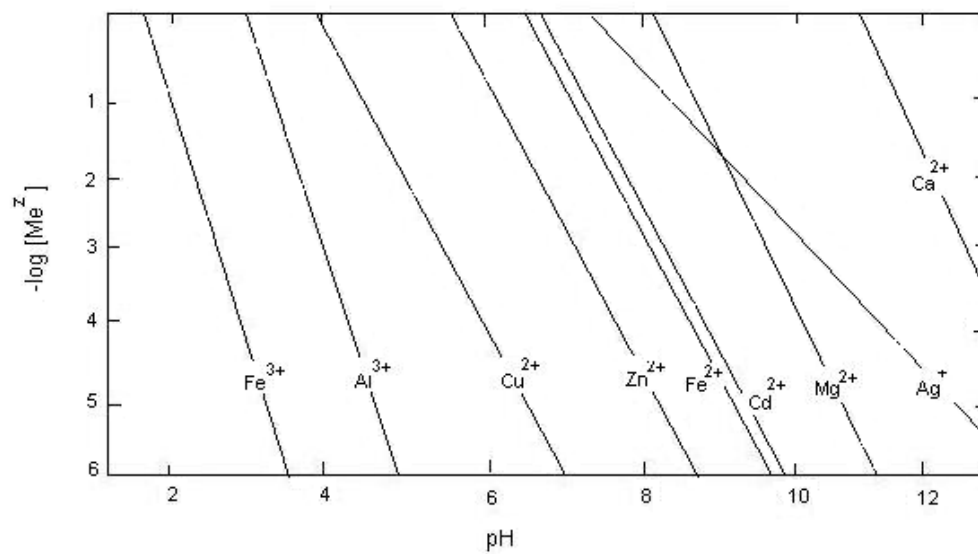
Figure 2.2.   Free metal-ion concentration as a function of pH (Stumm and Morgan 1996).

29
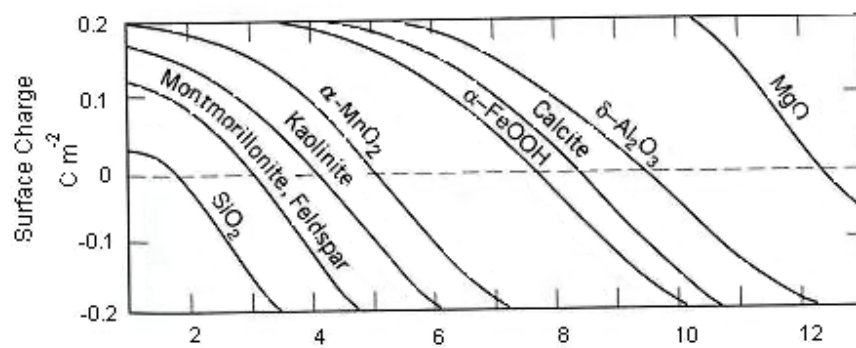
Figure 2.3. Surface charge of some minerals as a function of pH (Stumm and Morgan 1996).
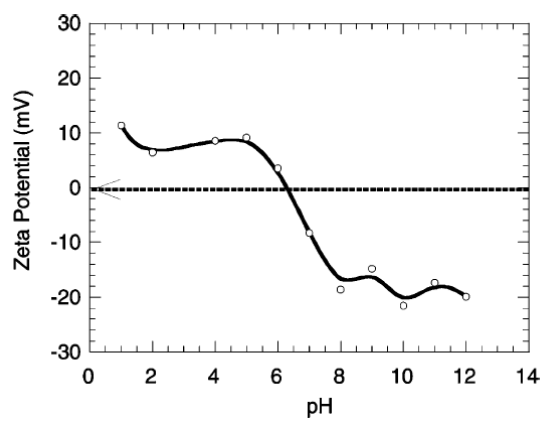
Figure 2.4.   Zeta potential of fly ash as a function of pH for ionic strength = 0.01 M (NaCl)
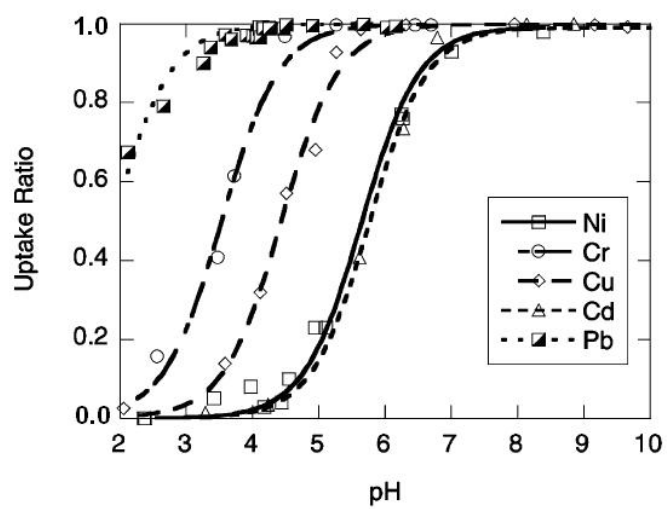
Figure 2.5.   Uptake ratio (percentage) of metals adsorption onto fly ash as a function of pH (Wang et al. 2004).

SECTION 3

LEACHATE CHARACTERISCTICS AND LEACHING BEHAVIOR OF SOILS

STABILIZED WITH FLY ASH

Soft fine-grained soils, especially silts and clays with high organic content, are generally unsuitable for supporting civil works, such as roads or buildings. In areas where organic soils exist, they generally are removed and replaced with a stronger material or stabilized in situ using physical or chemical methods to form a strong platform to support construction (Hampton and Edil 1998, Edil et al. 2002). Research has shown that coal fly ashes can be effective in stabilizing inorganic and organic clays, providing significantly improved strength, durability, and stiffness (Turner 1997, Acosta et al. 2003). Accordingly, in situ soil stabilization with fly ash has become a practical and economical solution for soil stabilization, especially in highway construction where evacuation and replacement of soft subgrades incurs substantial construction cost and time. However, because fly ash contains toxic trace elements, the use of fly ash in roadway construction presents a potential risk to the environment (Theis and Richter 1979, Adriano et al. 1980, Fruchter et al. 1990, Garavaglia and Caramuscio 1994, Georgakopoulos et al. 2002).

The leaching behavior of trace elements from soil-fly ash mixtures has received more attention in recent years (Creek and Shackelford 1992, Edil et al. 1992, Heebink and Hassett 2001, Bin-Shafique et al. 2002, Sauer et al. 2005, Goswami and Mahanta 2007). However, none of the past studies has investigated how the leaching characteristics and behavior of different soil-fly ash mixtures varies with pH, even though pH is one of the most crucial parameters governing the leaching of constituents from the solid phase into solution. Understanding the pH-dependent leaching behavior and

mechanisms controlling leaching of major and trace elements from soil-fly ash mixture is important for assessing the environment impacts associated with using fly ash in soil stabilization.

pH-dependent leaching tests have been used to investigate leaching of major and trace elements from various solids, including fly ash (Talbot et al. 1978, Garavaglia and Caramuscio 1994, Kosson et al. 1996), stabilized waste, construction materials, and soils (van der Sloot et al. 1996), steel slag (Apul et al. 2005), municipal solid waste incineration (MSWI) ash, and bottom ash (Kosson et al. 1996, Dijkstra et al. 2002, 2006). The test provides information on leaching characteristics and leaching behavior that is needed for geochemical modeling to identify mechanisms controlling leaching of trace elements and to predict aqueous concentrations in leachate (Dijkstra et al. 2002, Dijkstra et al. 2004, Apul et al. 2005, van der Sloot et al. 2005).

In this study, a pH-dependent leaching test was used to investigate the leaching behavior of soil-fly ash mixtures. The study focused on Al, As, Ba, Ca, Cd, Cu, Cr, Fe, Mg, Se, Sr, and Zn. Tests were conducted on a range of soils and fly ashes used for soil stabilization in roadway construction projects in Wisconsin and Minnesota. The soils included organic clay, clay, silt, and sand, whereas the fly ashes included Class C and off-specification high-carbon fly ashes.

3.1 Materials

3.1.1 Fly Ashes

Three fly ashes were used in this study: Dewey, Presque Isle, and Columbia fly ash. These fly ashes were selected to represent differences in composition and properties. Dewey fly ash is produced from the combustion of sub-bituminous coal by Alliant Energy in Cassville, WI, Presque Isle (PI) fly ash is a byproduct from burning a

bituminous coal by WE Energy in Marquette, MI, and Columbia fly ash is derived from burning sub-bituminous coal by Alliant Energy at Columbia Power Station in Portage, WI. Table 3.1 presents information on each fly ash, including type of coal and source, collection method, and type of storage and boiler used at the power plants.

Dewey and Presque Isle fly ashes are referred to as 'off-specification' fly ashes because their composition and properties do not meet the criteria for Class C or Class F ash in ASTM C 618 (Table 3.2 and Table 3.3). Dewey has a granular texture and dark grey color, whereas Presque Isle is finer and has a black color. A dark grey to black color is typically associated with elevated unburned carbon represented by a high loss on ignition (LOI) (ACAA 2003). Both Dewey and Presque Isle fly ash have high LOI (49.1% for Dewey; 32.4% for Presque Isle), whereas the LOI of Columbia fly ash is much lower (0.98%). The high LOIs of Dewey and Presque Isle fly ash exceed maxima for Class C and F, rendering both fly ashes as "off-specification" quality. Dewey and Presque Isle fly ashes are alkali materials possessing a pH of 10.41 and 11.68, respectively.

The chemical composition of Columbia fly ash meets the Class C criteria. The powdery Columbia fly ash has a light yellow color, which is attributed to the high CaO content of the ash (ACAA 2003). The high CaO content also provides Columbia fly ash with strong cementing characteristics. Columbia fly ash contains the lowest loss on ignition of the ashes that were tested (less than 1%), and is highly alkaline (pH 12.55).

3.1.2 Soils

Four fine-grained soils and one sand were used in this study: Lawson, Kamm, Red Wing, MnRoad, and Portage sand. The soil sampling locations are illustrated in Figure 3.1. Lawson is a highly plastic organic clay encountered during highway construction near Hwy 11 in Green County, WI (Sauer 2006). Kamm clay is light brown

moderately plastic clay that was obtained from McFarland, WI. Red Wing silt is from the city of Red Wing in southeastern Minnesota. MnRoad clay is from the MnDOT experimental facilities north of Minneapolis, Minnesota on Interstate 94. Red Wing silt and MnRoad clay have low plasticity. Portage sand is uniformly graded silica sand from Portage, WI. Classifications and general properties of the soils are shown in Table 3.4.

Organic matter contents in soils were determined using ASTM D 2974. As shown in Table 3.4, Lawson soil has the highest organic matter (6.3%), which is consistent with its classification as organic soil. Kamm clay (2.0%), Red Wing silt (1.2%), and MnRoad clay (1.5%) have three to four times lower organic matter content than Lawson soil. The sand (control material) has no measurable organic matter.

Cation exchange capacity (CEC) of the fine-grained soils was determined using the ammonium acetate buffer method (Lavkulich 1981). A 10.0-g sample of soil was tumbled in 40 mL of neutral (pH 7) 1 M of NH_4OAc solution at 30 rpm for 5 min. After mixing, the slurry was allowed to equilibrate for 24 h in NH_4OAc solution and then tumbled again at 30 rpm for 15 min. The slurry was then vacuum filtered through Whatman No. 42 filter paper. Residual ammonium was removed by rinsing the soil with three 40-mL portions of isopropanol. The ammonium (NH_4^+) was then extracted with four 50-mL portions of 1 M KCl. Concentration of NH_4^+ in the extract was determined using HACH Method 10031 (salicylate method) with a Spectronic 20 Genysys spectrophotometer. CEC was calculated using the concentration of NH_4^+ in the extract.

CEC of the four fine-grained soils and the sand are in Table 3.4. The CEC is highest for the highly plastic Lawson soil (45 $cmol_c$/kg), intermediate for the moderate to low plasticity Kamm clay (25 $cmol_c$/kg) and MnRoad clay (19 $cmol_c$/kg), and lowest for the Red Wing silt (8 $cmol_c$/kg). The CEC for some sorbing minerals in soils are strongly pH dependent (McBride 1994, Langmuir 1997). However, the majority constituent in all

soils investigated is montmorillonite, which is less or independent of pH (Langmuir 1997).

Total elemental analysis of each soil and fly ash was determined by digestion using US EPA Method 3050B. The method does not ensure total digestion, but does dissolve almost all elements that are environmentally available except those bound in the silicate structure (USEPA 1996). Dry soil or ash was refluxed with 70% HNO_3 at 95 $^{o}C \pm 5$ until the reaction was complete. After digestion, the digestate was filtered with Whatman No. 41 filter paper and analyzed using a Varian Vista-MPX inductively coupled plasma-optical emission spectrometer (ICP-OES) following US EPA Method 6010B. The Vista-MPX employs a megapixel charge coupled device (CCD) array and provides wavelength coverage between 175-785 nm. Calibration curves for the ICP were generated using multi-element standard solutions.

Quality control (QC) was conducted following measures described in Chapter 1 of US EPA SW-846 and the QC procedures outlined in US EPA Method 6010B. Continuing calibration verifications (CCV) and continuing calibration blanks (CCB) were analyzed immediately following calibration, after every 10 samples, and at the end of each sample run. A matrix-spike and sample duplicate were analyzed every 20 samples. Method blanks were also analyzed for each set of batch tests performed. CCVs were within 15% of expected values, CCBs were below detection limits, matrix-spikes had a recovery of 75-125% of the non-spiked matrix, and concentrations of sample duplicate were within 20% of the concentration in the original sample. The method detection limit (MDL) was determined for each analyte following the procedure in Appendix B of 40 CFR 136. The MDLs are reported in Appendix A.

The elemental composition of each fly ash is summarized in Table 3.5. The soils and fly ashes contain considerable amounts of major elements, including Al, Ca, Fe, K, Mg, Na, and P. The Red Wing and MnRoad soils contain greater amounts of Ca and Mg

than the Lawson and Kamm soils, which is likely associated with dolomite [Mg,Ca(CO$_3$)] and calcite (CaCO$_3$) in these soils (Table 3.6). Columbia fly ash, a Class C fly ash, has the highest amount of Ca, which is consistent with the results obtained from X-ray fluorescence spectrometry (XRF) (Table 3.3). Trace elements (As, Cd, Co, Cr, Sb, and Zn) in the soils vary from non-detect to contents comparable to those in the fly ashes. Among the three fly ashes, Presque Isle fly ash contains the least As, Cd, Co, Cr, Cu, Mn, Mo, Sr, and Zn.

3.2 Methods

3.2.1 Sample Preparation

All fine-grained soils were prepared by air-drying followed by crushing until the soil passed the No. 10 sieve (2 mm opening). The air-dried fine-grained soils were then ground again using a mortar and pestle to reduce the particle size into a fine powder. The sand was air dried, but was not sieved or crushed. Soil-fly ash mixtures were prepared by mixing the air-dried and crushed soil with 20% by weight fly ash and deionized (DI) water to achieve a target gravimetric water content of 25%. A study by Taştan (2005) found that the highest level of stabilization (strength and stiffness) of organic soil can be achieved when 20% fly ash is used. Each mixture was thoroughly blended, stored in sealed plastic bags, and allowed to cure in a 100% humidity room for 7 d prior to testing.

3.2.2 Acid-Base Neutralization Capacity (ANC)

An acid-base titration was used to estimate the acid or base needed to obtain the endpoint solution pH for each material. The test was conducted on slurries prepared with 8 g of dry solid and DI water at a liquid to solid (LS) ratio of 100. Aliquots of 2 M nitric

acid (HNO$_3$) or 1 M potassium hydroxide (KOH) were added to the slurry to adjust the pH in the range of 3 to 12. For each acid or base addition, the solution pH was measured after 15-20 min of stirring using a magnetic stirrer. The cumulative acid or base addition and the corresponding pH were recorded and a titration curve was created.

Kinetic batch experiments were conducted using the acid-base equivalences derived from the titration tests to determine whether the desired endpoint pH was obtained. The slurries were prepared with 40 g of dry material having a particle size < 2 mm at a LS ratio of 100. DI water was added into the bottle in combination with acid or base to obtain each desired endpoint pH from 3 to 12. After acid or base addition, the samples were thoroughly mixed in tumbler at 28 ± 2 rpm, with the solution pH being monitored hourly during the first 6 h and every 12 h afterwards until equilibrium was reached (indicated by pH change less than 0.5 pH units over 24 h).

Acid neutralization capacity (ANC) curves for the fly ashes from the titration tests and the kinetic batch tests are shown in Figure 3.2. ANC curves for other samples are in Appendix B. The acid-base addition derived from the titration test was insufficient to obtain the target endpoint pH in the batch test for any of the materials. Furthermore, the contact time to achieve equilibrium for the kinetic batch test is much longer than in the titration test. This observation is consistent with Hodgson et al. (1981), which reports that acid neutralization occurs slowly for fly ash. In the kinetic batch test, the solution pH changes over time, with more rapid changes occurring within the first 6 h as demonstrated in Figure 3.3. Similar trends were observed for all other materials (see Appendix C). Equilibrium was achieved in approximately 72 h for the soils and fly ashes and 48 h for the soil-fly ash mixtures. The soil-fly ash mixtures attained equilibrium faster than the fly ashes because of their lesser amount of fly ash (20% fly ash in the mixture) to neutralize.

These results indicate that the titration test can be used only as a preliminary guide to estimate the acid/base neutralization properties of soils and fly ashes. The contact time to achieve equilibrium at 72 hr and the quantities of acid-base addition obtained from the kinetic batch test were used for further leaching study as a function of pH.

Neutralization curves obtained from the batch test are illustrated in Figure 3.4 for the fly ashes and soils and Fig 3.5 for the soil-fly ash mixtures. Dewey and Presque Isle fly ash have a similar neutralization behavior, in which the solution pH decreases considerably as acid is added. However, Dewey has a slightly higher neutralization capacity than Presque Isle, which is consistent with its higher CaO and MgO contents (Table 3.3). In the pH range from 10 to 4, approximately 0.5 meq of acid was required to change 1 pH unit for 1 g of Dewey, but only 0.1 meq of acid was needed for Presque Isle. Among the three fly ashes, Columbia fly ash has the highest neutralization capacity due to its high CaO and MgO content.

All soils have narrow neutralization capacities of approximately 0.1 to 0.2 meq of acid/g solid to change up to 4 pH units in the pH range of 4-11 (Figure 3.4 b). However, Red Wing and MnRoad have a large buffer region under slightly acidic conditions (pH 5-6). They contain significant amounts of dolomite and calcite (Table 3.6) that can react with acid. Qualitative gas analysis obtained via gas chromatography (GC) showed that CO_2 was produced when acid was added into the slurry of the Red Wing and MnRoad soils in DI water. Alkalinity contributed by carbonate species is most likely responsible for pH buffering in this pH range.

The neutralization behavior of the soil-fly ash mixtures is influenced by the soil and the fly ash (Figure 3.5). The acid required to neutralize the alkalinity of the soil-fly ash mixtures falls between the acid required for neutralization of soils and fly ashes. A

range of 0.1-0.5 meq acid/g solid was needed to reduced pH from very alkaline (pH 11) to neutral (pH 7) for the soil-fly ash mixtures.

Some soils and fly ashes and soil-fly ash mixtures used in this study show an increase in neutralization capacity at pH < 6 (Figure 3.5), particularly, the mixtures with soil and fly ash having high neutralization capacity, including calcareous soils (Red Wing silt and MnRoad clay) and class C Columbia fly ash. Therefore, resistance to pH change at low pH region would be anticipated for acidic conditions.

3.2.3 Leaching as a Function of pH

Leaching tests were performed to investigate the release of major and trace elements for pH 3 to 13. This pH range represents exposure conditions for soil stabilization, such as acidic rain (slightly acid to neutral), natural soils (neutral to slightly alkaline), and soil stabilized with fly ash (alkaline to highly alkaline).

All tests were conducted in HDPE bottles with 40 g of dry crushed material having a particle size < 2 mm at a LS of 10. Deionized (DI) water was added to the bottle in combination with HNO_3 or KOH to obtain the desired endpoint pH (3 to 13). Another 40 g of sample in 400 mL of deionized water (DI) without HNO_3 or KOH addition was also included in the tests to examine natural leachate pH for each material. All samples were rotated end-over-end at 28 ± 2 rpm for 72 hr.

After rotation, the suspension was allowed to settle and the supernatant was withdrawn and filtered through a 0.45-μm membrane filter. An aliquot of unpreserved filtrate from each extraction was collected for measurement of pH and oxidation-reduction (redox) potential (Eh). Another non-acidified aliquot of filtrate was collected for dissolved organic carbon (DOC) and sulfate analysis. The remaining filtrate was stored in an acid-washed bottle and acidified with concentrated nitric acid to pH < 2 to preserve

the sample for elemental analysis (major and minor elements). All samples were refrigerated at $4\,^{o}C$.

DOC was analyzed on a Shimadzu TOC-5000 analyzer with ASI-5000 autosampler and Balston 78-30 high purity TOC gas generator. Organic carbon was converted to CO_2 by high-temperature combustion $(690\,^{o}C)$ and quantified by a non-dispersive infrared detector. Potassium hydrogen phthalate was used to generate the calibration curves. Millique (MQ) water was run as a check blank before and after each group of 8 samples. The instrument was re-calibrated after every 10 samples.

Sulfate concentration was determined by high-performance liquid chromatography (HPLC) using a Shimadzu Liquid Chromatography Model LC-10ATvp equipped with system controller, degasser, auto-injector, column oven, and conductivity detector. Sulfate was separated from other anions on an Alltech Allsep anion column (51207 – 100 x 4.6 mm) using 4-mM p-hydroxybenzoic acid adjusted to pH 7.5 with lithium hydroxide as a mobile phase for elution. The column temperature was set at 35 ^{o}C and the flow rate was 1.0 mL/min.

Elemental analysis was conducted with a Varian Vista-MPX ICP-OES. Prior to ICP analysis, all samples were prepared and digested following Standard Methods 3010 and 3030 (Clesceri et al. 1999). Digestion was conducted beforehand to reduce interference from organic matter and to convert metals associated with particulates to free metal forms. Nitric acid was used for digestion as recommended in Clescerl et al. (1999). The digestion was conducted using 10 mL of well-mixed sample and 0.5 mL of concentrated nitric acid in a polypropylene tube placed in a block heater at 105 ^{o}C for 12 h. The digested samples were allowed to cool, adjusted to original 10-mL volume with DI water, and analyzed by ICP-OES using US EPA Method 6010B. Calibration curves for the ICP were generated using multi-element standard solutions. Quality control was

performed following the procedures aforementioned in Section 3.3.1 and satisfactorily maintained throughout the analysis.

3.3   Results and Discussion

3.3.1   Leachate pH

Solution pH of leachates from the soils, fly ashes, and the soil-fly ash mixtures in DI water measured at the end of the leaching test are summarized in Table 3.7. Leachates from the soils are neutral to slightly alkaline with pH varying from 7.05 to 8.80. Leachates from fly ash, on the other hand, are very alkaline with pH >9. Columbia fly ash has the highest pH (pH 12.55) relative to other two fly ashes (Dewey-10.41; Presque Isle-11.68).

Solution pH of fly ash leachates is controlled by two opposing processes associated with dissolution and hydrolysis reactions of chemical constituents in fly ash particles contacted with water. Dissolution and hydrolysis of oxide components, such as CaO and MgO, contribute to an increase in solution pH, whereas dissolution of soluble acids, such as B_2O_3 and salts containing hydrolysable constituents (e.g. $Fe_2(SO_4)_3$ and $Al_2(SO_4)_3$) offset the increase in pH from dissolution oxides (Gitari et al. 2008). Thus, the relative quantities of soluble bases (oxides) and soluble acids and hydrolysable constituents in fly ash control the final solution pH. The alkaline leachate from fly ash generally is associated with dissolution of alkali and alkaline earth oxides upon exposure to water (Adriano et al. 1980).

Dewey fly ash has the highest dissolved Ca (Table 3.8), representing base-forming component in the leachate at natural pH. However, the concentration of dissolved Al as acid-forming component in Dewey is much higher than Columbia and Presque Isle fly ash (~10 fold higher than Columbia and 13 fold higher than Presque

Isle). Acid from the high concentration of Al counterbalances the base from the high concentration of Ca, which results in Dewey fly ash having the lowest solution pH. Columbia and Presque Isle fly ashes have comparable concentrations of acid- and base-forming component (Ca, Mg, Al, and Fe), except B. The high alkalinity of leachate from Columbia is probably due to the lower concentration of B as an acid-forming component in leachate compared to Presque Isle and also Dewey fly ash. Neither chemical composition in the solid phase, nor dissolution of single component alone directly dictates final pH of the leachate. The final pH is a combined result of dissolution and hydrolysis reactions of all soluble acid and base components.

Leachate pH from soil-fly ash mixtures varies from slightly alkaline to extremely alkaline (pH 8.85-12.28). Leachates from mixtures prepared with Columbia fly ash have the highest pH, whereas leachates from mixtures with Presque Isle fly ash have the lowest pH. The alkaline leachates obtained from the soil-fly ash mixtures indicates that leachate pH is greatly influenced by the high alkalinity of the fly ashes, even though the mixtures contain only 20% of fly ash, as previously reported by Bin-Shafique et al. (2002) and Sauer (2006).

In the field, neutralization of alkaline leachate can occur by acid rain infiltration, uptake of atmospheric $CO_{2(g)}$, or by microbiological processes (van der Sloot 1996), all of which can occur in roadways constructed with soil-fly ash mixtures. Neutralization via atmospheric carbonation may occur rapidly in alkaline leachates or alkaline materials exposed to the atmosphere (van der Sloot et al. 2007), and may be responsible for the neutral pH of leachates collected in lysimeters beneath roadways in Wisconsin and Minnesota where base and subgrades were stabilized with alkaline fly ashes (O'Donnell 2009). Therefore, leachate pH in the field is established by the pH of the material and the pH of the environment. Environmental conditions may result in considerable changes in pH and should be accounted for when assessing impacts from leaching.

In addition, the neutralization capacity of the material plays a significant role in resistance to changes in pH in the short term and long term. The decrease in pH of alkaline leachate, especially leachates from the mixtures with Columbia fly ash (high neutralization capacity, Figure 3.4), are anticipated to take more time than leachates from the mixtures with Dewey and Presque Isle fly ash (lower neutralization capacity, Figure 3.4).

3.3.2 Redox Properties

Besides leachate pH, the reduction-oxidation condition is one of the most important factors affecting leaching of major and trace elements. The relationship between redox potential (E_h) and pH for the fly ashes and soil-fly ash mixtures is shown in Figure 3.6. Under acidic conditions, E_h is high, indicating oxidizing conditions. The E_h decreases linearly with increasing pH and is negative under very alkaline pH.

Based solely on the measured redox potential, elements in the leachates should exist in an oxidized form. However, the redox potential measured by a platinum (Pt) electrode can differ significantly from values computed from thermodynamic data. In natural water, the redox potential measured by a Pt electrode in the presence of atmospheric oxygen lies nearly 0.4-0.5 volts lower than the upper limit of water stability on E_h-pH diagram (Langmuir 1997). This means that the measured E_h may not be thermodynamically accurate and may be underestimated that could lead to an inaccurate interpretation (reducing conditions).

Due to a headspace of the bottle used in the leaching test and an exposure of the leachates to the atmosphere, oxidizing conditions are more likely than reducing conditions. The conditions in the leaching system also discourage reducing conditions because of the absence of biological activity or material-specific constituents (e.g,

degrading organic matter, or sulfide). Therefore, the predominant species were assumed to be in oxidized form for all elements studied throughout the pH range investigated.

3.3.3 Leaching Behaviors

Four broad leaching behaviors as a function of pH were observed from the soils, the fly ashes and the soil-fly ash mixtures: (i) leaching of Ca, Cd, Mg, and Sr follows a cationic pattern where the concentration decreases monotonically as pH increases; (ii) leaching of Al, Fe, Cr, Cu, and Zn follows an amphoteric pattern where the concentration increases at acidic and alkaline pH; (iii) leaching of As and Se shows both the behaviors following oxyanionic pattern where concentration increases at acidic and alkaline pH and those not following a cationic, an amphoteric, or oxyanionic behavior; and (iv) leaching of Ba presents amphoteric-like pattern but less pH-dependent. A conceptual illustration of leaching behavior of element as a function of pH is shown in Figure 3.7.

3.3.3.1 Leaching of Ca, Cd, Mg, and Sr

Leaching behavior as a function of pH for Ca (Figure 3.8), Cd (Figure 3.9), Mg (Figure 3.10), and Sr (Figure 3.11) follows a cationic pattern where the concentration decreases monotonically as pH increases. For elements controlled by solubility or sorption, cationic pattern involves increasing dissolution and/or desorption of metal-bearing mineral phases as the pH decreases and diminishing leaching due to precipitation and/or increasing sorption as the pH increases (Theis and Wirth 1977a, Theis and Richter 1979, Mattigod et al. 1990, Edil et al. 1992, Fleming et al. 1996, Brunori et al. 1999, Sauve et al. 2000, Bin-Shafique et al. 2002, Wang et al. 2004, Sauer et al. 2005).

Increasing dissolutions of mineral phases and decreasing sorption of dissolved cationic ions most likely contribute to high concentrations of Ca, Cd, Mg, and Cd in the

leachates at acidic pH. Increasing leaching extent as pH decreases is due to increasing attacking on the metal-bearing mineral phases as acid strength increases (Kirby and Rimstidt 1994, Fleming et al. 1996, Rao et al. 2002, Tiruta-Barna et al. 2004). Modeling study using MINTEQA2 (Section 4) found that Ca, Cd, Mg and Sr are solubility-controlled. Sulfate and carbonate minerals were identified as controlling solids for these elements depending on the leachate pH.

Sorption process is less likely to be the mechanism controlling for Ca, Cd, Mg, and Sr, but might affect the dissolved species of these elements in the leachate in some extent. Sorption of dissolved Ca^{2+}, Cd^{2+}, Mg^{2+}, and Sr^{2+}, as dominant species in slightly acidic pH range (pH 5-6) determined by MINTEQA2 (Section 4), are less favorable on fly ash and soil particles at acidic pH. Class C and Class F fly ashes (including Columbia fly ash) typically have pH at the point of zero charge (pH_{pzc}) varying in the range of 6.2-7.6 (Talbot et al. 1978, Bayat 2002, Wang et al. 2004, Wang et al. 2007), whereas the $pH_{(pzc)}$ of SiO_2(quartz) and montmorillonite as a major component of soils used in this study (Table 3.6) varies in the pH less than 3 (Langmuir 1997). Under acidic conditions (i.e., pH 3-6) fly ashes are positively charged (pH < pH_{pzc}), but soils are negatively charged (pH > pH_{pzc}). However, the increasing H^+ ion concentrations as pH decreased compete more effectively with fixed metal cation concentrations for adsorption sites on the clay resulting in decreasing metal adsorption on the clay with decreasing pH (Langmuir 1997). Therefore, sorption of cationic ions on soil and fly ash particles, if involve, tend to decrease with decreasing pH due to competition with H^+ ion and repulsive effect.

Precipitation with carbonate as pH increased diminishes the leaching of these elements. At alkaline pH and in contact with atmospheric $CO_{2(g)}$, carbonate (CO_3^{2-}) is predominant (Stumm and Morgan 1996) and many divalent cations form insoluble carbonate precipitates (Langmuir 1997). Geochemical modeling study (Section 4) identified that only carbonate minerals are important controlling solid for Ca, Cd, Mg, and

Sr at alkaline pH. pH (i.e., calcite [$CaCO_3$] and/or aragonite [$CaCO_3$] for Ca, strontianite [$SrCO_3$] for Sr, dolomite [$Mg,Ca(CO_3)_2$] and magnesite [$MgCO_3$] for Mg, and otavite [$CdCO_{3(s)}$] for Cd).

3.3.3.2 Leaching of Al, Fe, Cr, Cu, and Zn

Leaching of Al (Figure 3.12), Fe (Figure 3.13), Cr (Figure 3.14), Cu (Figure 3.15), and Zn (Figure 3.16) as a function of pH demonstrates a U-shaped curve. The leaching behavior is consistent with an amphoteric pattern reflecting increased leaching at acidic and alkaline pH with a minimum leaching at neutral pH (Eighmy et al. 1995, Langmuir 1997, Kenkel 2003). Amphoteric elements can behave both as an acid and a base that readily dissolve under acidic and alkaline conditions (Eighmy et al. 1995, Lim et al. 2004), but are relatively insoluble at neutral pH (Garrabrants et al. 2004). Amphoteric behavior of these elements in waste leachates, including leachates from fly ash, has been reported by Eighmy et al. (1995), Garrabrants et al. (2004), Lim et al. (2004), Camacho and Munson-McGee (2006), Malviya and Chaudhary (2006), and Fernandez-Olmo et al. (2007).

Solubility of amphoteric elements is associated with the solubility of oxide/hydroxide minerals. The geochemical modeling results in Section 4 show that Al, Fe, Cr, Cu, and Zn are controlled by dissolution-precipitation oxide and hydroxide minerals. Garrabrants et al. (2004) also report that leaching behavior amphoteric elements is consistent with the solubility of oxides and hydroxides of that element. Hydroxo complexes have been reported as the dominant species for amphoteric elements for the pH ranging from acid to alkaline (Rai et al. 1987b, Malviya and Chaudhary 2006). However, the geochemical modeling study (Section 4) shows that Al, Fe, Cr, Cu, and Zn in the leachates in this study are primarily present in hydroxo-, sulfato, and carbonato-complexes and as dissolved single ions depending on pH and

element. The presence of sulfato- and carbonato-complexes is because of the abundant of SO_4^{2-} in the leachates and the influence of atmospheric $CO_{2(g)}$.

The amphoteric oxides/hydroxides are relatively insoluble at neutral pH, which is likely attributed to significant drop in concentrations of these elements. At the isoelectric point, pH_{IEP}, (also known as pH_{pzc}) of 7.5-7.6, Talbot et al. (1978) report that essentially 100% of Al and Fe is associated with various solid phases on fly ash particles and their hydrous-oxide phases are most thermodynamically stable. The observation is in good agreement with other leaching studies where amphoteric elements have their theoretical lowest solubility at approximately neutral pH (Talbot et al. 1978, Rai and Szelmeczka 1990, Eighmy et al. 1995, Lim et al. 2004, Camacho and Munson-McGee 2006, Malviya and Chaudhary 2006).

3.3.3.3 Leaching of As and Se

Oxyanionic pattern was evident for As in the leachates from soils, Dewey fly ash, Dewey-soil mixtures (Figure 3.17a), and some Presque Isle-soil mixtures (Figure 3.17b). For Se, only leachates from Dewey and Dewey-Lawson mixture show weakly oxyanionic patterns. Oxyanionic pattern reflects sorption of anions on mineral surfaces exhibiting an increase of concentration in leachate as pH increases. As and Se are the only two among elements investigated that exist as oxyanions throughout the pH range of 5-13 (Section 4).

The change in concentration as a function of pH can be explained by the species in the leachate and pH-dependent surface charge of soil and fly ash. Negatively charged oxyanionic As and Se (e.g., AsO_4^{3-}, SeO_3^{2-} or SeO_4^{2-}) precludes adsorption onto the negatively charged surface of the fly ash and soil contributing to high As and Se concentrations at alkaline pH. Geochemical modeling (Section 4) indicates that As and Se predominantly exist as $CaAsO_4^-$, AsO_4^{3-}, SeO_3^{2-} [or SeO_4^{2-} in case of Se(VI)] when pH

> 7.5. At this pH and higher, fly ash and soils are negatively charged (i.e. pH > pH_{pzc} of 6.2-7.6 for fly ashes, and pH_{pzc} of 3.0 for soils) (Talbot et al. 1978, Langmuir 1997, Bayat 2002, Wang et al. 2004, Wang et al. 2007). Therefore, sorption of negatively charged As and Se onto negatively fly ash and soil surfaces are unfavorable because of repulsive effect. The increased concentrations of As and Se at alkaline pH has been observed in other leaching studies from coal fly ash and various stabilized wastes (Tiruta-Barna et al. 2006, van der Sloot et al. 2007, Wang et al. 2007).

The leaching of As and Se also exhibits a similar U-shaped pattern to amphoteric Al (Figure 3.12) and Fe (Figure 3.13), which is believed to be influenced by sorption of As and Se onto amphoteric Fe and Al solids (Anderson et al. 1976, Anderson and Malotky 1979). Amorphous Fe (hydr)oxides and amorphous Al (hydr)oxides are known to have strong affinity for surface complexation with As and Se (Pierce and Moore 1982, Crecelius et al. 1986, Frankenberger 2002, Gimenez et al. 2006, Peak 2006, Cornelis et al. 2008a). Sorption of As and Se on to Al and Fe oxides/hydroxides is likely to occur (Turner 1981, Crecelius et al. 1986, van der Hoek et al. 1994, Frankenberger 2002, Wang et al. 2007) because Al and Fe oxides are abundant in fly ash used in this study (Table 3.3) and many other alkaline wastes (Warren and Dudas 1985, van der Hoek et al. 1994, Meima and Comans 1997). Amphoteric behavior of Al and Fe possibly dominate the leaching pattern of As and Se, especially at acidic pH.

Negatively charged As and Se are likely protonated with decreasing pH. The increased As and Se concentrations at acidic pH is probably due to low affinity of As and Se species for sorption at pH < 5. Dijkstra et al. (2002) concluded that increasing concentrations of oxyanions at low pH is due to increased protonation of oxyanionic species, resulting in a lower affinity for the surface.

Significant drops in As and Se concentration observed at pH 6 to 7.5 (Figure 3.17a and 3.18a) are probably as a result of maximum adsorption on soil and fly ash.

Gupta and Chen (1978) report that negatively charged As are removed effectively onto the slightly positive or neutral charge surfaces of activated alumina and bauxite. Electrostatic interaction and specific adsorption (e.g., ligand exchange) seem to be mechanisms controlling As at pK_a for As(V) (an acid dissociation constant) values (pK_1~pH 7). This corresponds well to a number of studies reporting that significant sorption of arsenate on minerals, such as goethite, alumina oxides, and iron oxides, occur at near neutral pH (Gupta and Chen 1978, Lumsdon et al. 1984, Merrill et al. 1986). Other studies also report that As is least mobile in soil (Goldberg et al. 2005) and fly ash (Theis and Wirth 1977a, Warren and Dudas 1986) around neutral pH. The maximum adsorption of selenite onto hydrous iron oxide was also observed in pH between 4 and 6, which is shifted from pK_1 (~pH 2.75) (Hingston et al. 1972). However, the maximum adsorption should occur at pH near the pK_a since the energy required to dissociate a proton from molecule is at a minimum, and the energy for adsorption may be sufficiently enough to induce the reaction. Shifting of optimum adsorption from pK_1 (~pH 2.75) is probably because the soil and fly ash not reaching their capacity for maximum adsorption (Hingston et al. 1972). Other studies have also reported the maximum adsorption of selenite on soils occurring in a range from slightly acidic to slightly alkaline pH (Goldberg and Glaubig 1988, Hyun et al. 2006).

Although As and Se are present as oxyanions in all leachates, an oxyanionic pattern is unable to explain the leaching behavior of As and Se in many leachates (Figure 3.17b, 3.17c, and 3.18a-c). The variation in leaching behavior for As and Se is probably due to several factors, including different controlling mechanism, a variation of dominant species of As and Se existing in the leachates for a given pH range, and effects from the presence of other dissolved ions in the leachates.

Geochemical modeling (Section 4) shows that the dissolved concentrations of As and Se are far below As-, and Se-mineral phase solubility. In addition, no solubility-

controlling solids were found for As and Se. Thus, mechanisms controlling the As and Se concentration in the leachates is other than solubility control. Solid-solution formation with other common minerals (Cornelis et al. 2008a) or sorption may be occurring; both mechanisms can reduce concentrations of As and Se below saturation levels with respect to As-, and Se-mineral solubility.

Different As and Se species have different affinity for surface interaction (for adsorption) or ion incorporation (for solid solution formation), and consequently favoring the occurring of one reaction over the other. Adsorption can be either specific (e.g., ligand exchange) or non-specific (e.g., electrostatic attraction or repulsion), but solid solution formation is always specific depending on such parameters as ion size, charge, and geometry. Significant immobilization of oxyanions occurs through specific interactions only (Cornelis et al. 2008a). The great variation in leaching pattern is anticipated because the dominant species of As and Se in the leachates highly vary between fly ashes and soil-fly ash mixtures (Section 4). In the pH 5-12, As was present from uncharged (i.e., $AlAsO_4$ and $CaHAsO_4$) to negatively charged (i.e., $CaAsO_4^-$ and AsO_4^{3-}), whereas the selenite [Se(IV)] species ranged from $HSeO_3^-$, $CaSeO_3$, and SeO_3^{2-} [in case of selenate Se(VI): SeO_4^{2-}, $CaSeO_4$, and $MgSeO_4$] (Section 4). Additionally, adsorption and solid-solution formation of trace oxyanions can also be diminished by the presence of other ubiquitous anions in leachate, such as SO_4^{2-}, CO_3^{2-}, NO_3^-, Cl^-, and silicate, which can compete with oxyanions for sorption sites (Cornelis et al. 2008a).

Immobilization of As and Se in cementitious compounds produced from self-cementing Class C Columbia fly ash is likely to be responsible for reducing As concentration to below detection limit in the leachates from the mixtures of Columbia fly ash with soil throughout the pH range from 4 to 12 (Figure 3.17c) and Se at pH > 11 (Figure 3.18c). Columbia fly ash is enriched with CaO, a key precursor for pozzolanic reactions with silica and alumina to form cementitious compounds, such as calcium

silicate gels and calcium aluminate gels (Turner 1997), therefore, Columbia fly ash is more likely to induce the pozzolanic reactions than Dewey and Presque Isle fly ash having much lower CaO (Table 3.3). In this study, chemical inclusion of As in binder hydration products (e.g. calcium silicate hydrates) is likely to be mechanism for As immobilization in stabilized soils rather than the formation of insoluble Ca-As precipitates or physical encapsulation. Formation of insoluble Ca-As precipitates is unlikely because all the leachates were undersaturated with respect to Ca-As solids/minerals (Section 4). Physical encapsulation is also unlikely because the aggregates were crushed into fine particles (~2 mm) for the leaching test.

Significant drop of Se in leachates from Columbia fly ash and their soil-fly ash mixtures at extremely alkaline pH (pH > 11.5) (Figure 3.18c) is probably due to a solid solution formation with ettringite ($3CaO.Al_2O_3.3CaSO_4.32H_2O$), a hydrated phase crystallizing from the hydration reaction of alkaline fly ash at highly alkaline pH (Hesbach et al. 2005). Oxyanions, including AsO_4^{3-}, SeO_3^{2-}, and SeO_4^{2-}, can be immobilized by incorporating in ettringite by partial or full replacement of SO_4^{2-} (Kumarathasan et al. 1990, Myneni et al. 1997, Baur and Johnson 2003, Zhang and Reardon 2003). The formation of ettringite occur only when sufficient lime (CaO) is available (Hassett et al. 2003) and when pH > 10.7 (Gabrisova et al. 1991). Sulfate is another important precursor for a formation of ettringite (White et al. 2005). The decreased leaching of SO_4^{2-} at pH > 11 seen in Columbia fly ash and its soil-fly ash mixtures (Figure 3.20) implies a formation of insoluble ettringite at highly alkaline pH (van der Sloot 2002). Accordingly, Columbia fly ash and its soil-fly ash mixtures have more potential to favor the formation of ettringite compared to Dewey and Presque Isle fly ash due to the high alkalinity and abundant in CaO (Table 3.3).

3.3.3.4 Leaching of Ba

Barium shows a leaching pattern that is similar to amphoteric pattern (Figure 3.19), although its oxides and hydroxides are not amphoteric like those of Al, Fe, Cr, Cu, and Zn. The leaching of Ba from Dewey and Columbia fly ash is relatively independent of pH at mildly acid to alkaline pH and then slightly elevated at highly alkaline pH.

The geochemical modeling (Section 4) shows that Ba in leachates from fly ash and soil-fly ash mixtures is controlled by dissolution-precipitation of barite [$BaSO_4$] at pH 5-10 and witherite [$BaCO_3$] at pH > 10. Ba-Sr sulfate co-precipitates [barite-celestite or $(Ba,Sr)SO_4$] may also affect Ba concentrations (Eary et al. 1990, Fruchter et al. 1990, Mudd et al. 2004). The distinctive pattern of Ba identified in the modeling study showing an order of magnitude oversaturated with respect to barite and an order of magnitude undersaturated with respect to celestite is an evidence suggesting the formation of a solid-solution of Ba-Sr sulfate (Ainsworth and Rai 1987, Eary et al. 1990, Fruchter et al. 1990, Mudd et al. 2004). The Ba leaching pattern similar to those found in this study was also observed in the leachate from MSWI air-pollution-control residues (Astrup et al. 2006) and in steel slag (Fallman 2000), which is believed to be associated with solubility of barite [$BaSO_4$] and $Ba(S,Cr)O_4$ solid solutions (Fallman 2000, Astrup et al. 2006). Therefore, the concentration of Ba maybe controlled by dissolution-precipitation of barite and celestite, and/or $(Ba,Sr)SO_4$ solid solutions and/or $Ba(S,Cr)O_4$ solid solutions. Different controlling mechanisms might be responsible for different leaching behavior, especially the leachates from Presque Isle fly ash and its soil-fly ash mixtures.

3.3.4   Effects of Soil and Fly Ash on Leaching Behavior and Leaching Extent

3.3.4.1 Similarities in Leaching Pattern of Fly Ash vs. Soil-Fly Ash Mixture

The leaching behavior for a given element, except As and Se, from soil-fly ash mixtures are similar to those observed in corresponding fly ashes alone. Similar

controlling mechanisms and similar controlling factors (i.e., pH and redox conditions) are believed to be responsible for the similarities in leaching behavior in both fly ashes and soil-fly ash mixtures.

The geochemical modeling (Section 4) indicates that dissolution-precipitation reactions control the leaching of most of the major and trace elements studied (i.e. Al, Ca, Cd, Cu, Cr, Fe, Mg, Sr, Zn, and maybe Ba) from fly ash and soil-fly ash leachates. Sorption may also affect the dissolved elements in the leachate. Dissolution-precipitation reactions and sorption are strongly dependent on solution pH and redox conditions (Theis and Wirth 1977b, Davis et al. 1993, Fish 1993, van der Sloot et al. 1994, van der Sloot and Dijkstra 2004).

van der Sloot (1996, 2007) and van der Sloot et al. (van der Sloot 1990, van der Sloot 1991, van der Sloot et al. 2001) concluded that similar controlling mechanisms (e.g. solubility control) and controlling factors (e.g. pH, redox conditions) result in the consistency in leaching behaviors observed in various types of waste (such as coal fly ash, MSWI fly ash, MSWI bottom ash, sewage sludge), stabilized wastes (such as cement-stabilized MSWI fly ash, stabilized waste construction materials), and soils.

In addition, the leaching pattern of fly ash appears to dominate that of soil in soil-fly ash mixtures, which can be seen in the leaching of Ba (Figure 3.19) and Cd (Figure 3.9). The controlling mechanism in fly ash prevailing over that in soil in soil-fly ash mixture might be associated with higher concentrations of Ba and Cd present in fly ash compared to those in soils (Table 3.5). For example, Cd in fly ashes is approximately 2-3 times higher than in soil. Cd leached from fly ashes and soil-fly ash mixtures exhibits cationic pattern, whereas Cd leached from soils shows amphoteric pattern. Similar finding has been reported by Goswami and Mahanta (2007) where higher concentrations of Al and Zn in soils relative to fly ash seem to dominate the leaching pattern of Al and Zn in the leachate from soil stabilized with fly ash and lime.

3.3.4.2 Sources of Trace Elements in Leachate from Soil-Fly Ash Mixture

The concentrations of most of elements in the leachate from soil-fly ash mixtures are comparable to those from fly ash alone. Both soil and fly ash in the mixtures appear to be significant sources contributing to the concentrations in leachate. High concentrations in leachate from soil-fly ash mixture were noticed for Ba, Cr, and Cu in most of the mixtures (Figure 3.23, 3.24, and 3.25).

Fly ashes used in this study contain significant quantity of trace elements, including Ba, Cr (Columbia fly ash), Cu (Dewey and Columbia fly ash), Se, and Sr (Table 3.5). Even though only 20% of fly ash is used in the soil-fly ash mixture, fly ash can be a significant source releasing these trace elements into leachate. Although soils are uncontaminated, soils (except sand) also contain relatively high concentrations of As, Cd, Cr, Cu, and Zn (Table 3.5), which are comparable to those found in the three fly ashes. Soil is the major component (80% by weight) of the soil-fly ash mixture. Soil enriched with trace elements can also be a potential source that significantly contributes to the concentration in leachate from soil-fly ash mixture besides fly ash.

The amount of element released from soil and fly ash establishing the concentration in leachates from soil-fly ash mixtures was not investigated in this study. However, the tendency on element to be released from soil and fly ash can be speculated by the change in pH of the soil-fly ash mixture relative to those of soil and fly ash alone. Mixing soil with fly ash may have two different effects on leaching of trace elements as a result of the change of intrinsic material pH: increasing leaching of element in fly ash and decreasing leaching of element in soil. Soil-fly ash mixtures generated leachate pH falling between those of corresponding soils and fly ashes alone, i.e. leachates from the mixtures are more alkaline than those from soil alone, whereas they are less alkaline than those from fly ash alone (Table 3.7). Release of elements from soils in the soil-fly ash mixtures is likely decreased relative to soil alone due to an

increase in sorption or precipitation when alkalinity increases. Conversely, blending fly ash with soil should increase release because of the rising in solubility due to a decrease in alkalinity.

The effect of pH change on release of element in soil-fly ash mixture has been reported in the previous leaching study in soil stabilized fly ash by Bin-Shafique et al. (2002). The study concluded that adding fly ash to the fine-grained soils results in the decreased leaching of Cd and Ag from soil in the soil-fly ash mixture due to increasing leachate pH, and therefore a greater adsorption of metals on the solid surface.

Goswami and Mahanta (2007) also report similar pH effects on leaching lateritic soils stabilized with fly ash and lime. Adding 20% fly ash to the soil reduces the concentrations of Cd, Hg, Mn, Ni, Zn, and Mg compared to those from soil alone. The reduction in concentrations is due to the decrease in mobility with increasing pH. Conversely, the concentrations of Zn and Mn from fly ash in the soil-fly ash mixture tend to increase compared to fly ash alone with increasing in fly ash content. The increased concentration is due to a rise in solubility as pH of fly ash in the mixture decrease relative to fly ash alone.

3.3.4.3 Effect of DOC on Leaching from Soil-Fly Ash Mixture

Dissolved organic carbon (DOC) appears to enhance the leaching Cu, especially at alkaline pH. Cu is known to have a very high affinity for organic ligands, especially DOC, which can lead to a significant enhanced leaching (Dijkstra et al. 2002). Approximately 95-100% of dissolved Cu is complexed with DOC (Lim et al. 2004).

Elevated DOC concentrations from the mixtures of fly ash with Lawson organic clay at alkaline pH (Figure 3.21) is likely due to the dissolution of high molecular weight humic acids, which are insoluble at acidic pH but dissolve at alkaline pH (Langmuir

1997). Sorption of organic matter to mineral surfaces also decreases with increasing pH (Dijkstra et al. 2002), which contributes to the increase of DOC with increasing pH.

The increased Cu concentration in leachates from the mixtures of three fly ashes with Lawson clay (Figure 3.15) coincides with the increased DOC concentrations from these mixtures under alkaline pH (Figure 3.21). The relationship between Cu and DOC concentrations in these leachates at pH > 8 (Figure 3.22) shows that leaching of Cu is highly dependent with leaching of DOC. Cu concentrations increased significantly with increasing DOC concentration.

3.3.4.4 Effect of CEC on Leaching from Soil-Fly Ash Mixture

Soils contain many constituent that provide sorption sites for elements, such as clay, oxide minerals, and organic matter (Table 3.4 and 3.6) reflecting by the CEC values (Lim et al. 2004). Lawson clay has the highest CEC (45 cmol/kg), which is most likely due to high organic matter and clay. Kamm clay (25 cmol/kg) and MnRoad clay (19 cmol/kg) have comparable CEC, whereas Red Wing silt has the lowest CEC (8 $cmol_c$/kg) (Table 3.4). Silica sand as a control material has no CEC. Theoretically, the capacity of soil to adsorb or exchange cations should be: Lawson > Kamm > MnRoad > Red Wing > sand. The higher the CEC, the greater sorption capacity the soil is to hold cations against leaching, and the lower the concentration is in the leachate.

However, only few mixtures of Columbia fly ash with soils follow this inverse relationship between the CEC and the concentrations in leachate, which can be seen in Cu at pH 5-7 (Figure 3.23 c), Cr at pH 7-9 (Figure 3.24c), and Ba at pH > 9 (Figure 3.25c). Furthermore, the concentration for a given element in most of the leachates highly varies from one leachate to another. No conclusive relationship was found between the CEC of soil and the concentration of element in leachate.

The concentration of element in leachate is greatly affected by several factors, such as mechanism controlling the release, the presence of other chemical species in the leachates (e.g. competed ions for the reaction, sorption sites on the solid phase), and leaching conditions (e.g. pH and redox conditions). Therefore, only the CEC of soil is insufficient to predict the tendency of leaching concentration from soil-fly ash mixture.

Bin-Shafique et al. (2002) report that the concentration of Cr from soil stabilized with Columbia fly ash follows this inverse relationship but this is not the case for the leaching of Se from soil stabilized with different fly ash (i.e., King fly ash). Leachate pH is believed to be a factor affecting the leaching of the element and the role of CEC of soil to retain ions.

3.3.4.5 Effect of Fly Ash on Leaching from Soil-Fly Ash Mixture

In spite of enrichment with trace elements, fly ash seems to play an important role in element immobilization in soil-fly ash mixture indicated by significant reduction in concentrations of several elements in leachates from soil-fly ash mixtures relative to those from fly ash alone. These elements include Cd (3.9a, b, and c), Sr (Figure 3.11b), Cr (Figure 3.14a), Cu (Figure 3.15a, and b), Zn (Figure 3.16c), As (Figure 3.17c), and Se (Figure 3.18b, and c). The reduction in concentrations of these elements might be associated with material-specific constituent in fly ash, such as unburned carbon, mineral oxides, and CaO.

Unburned carbon in off-specification Dewey and Presque Isle fly ashes are believed to be responsible for the reduction in the concentrations of Cd, Cr, Sr, and Se in leachates from the mixtures of soil with Dewey and Presque Isle fly ashes. Studies have reported the sorption ability of carbon in fly ash for Cu(II) (Hwang et al. 2002) and Hg (Lin and Chang 2001). Unburned carbon showed sorption ability comparable to the commercial activated carbon, which is probably because unburned carbon has a porous

structure similar to the activated carbon (Hwang et al. 2002). In addition, the surface area of fly ash is found to be increased with increasing carbon content in fly ash (Lin and Chang 2001).

Dewey and Presque Isle fly ashes show somewhat different sorption abilities for trace metals in leachates. Although Presque Isle fly ash has lower LOI (32.4%) than Dewey fly ash (49.1%), Presque Isle fly ash can remove more number of elements than Dewey fly ash. The better sorption ability of Presque Isle fly ash in soil-fly ash mixture might be associated with higher amount of mineral oxides, such as Al_2O_3 and Fe_2O_3, and higher percent fineness (reflecting the surface area) (Table 3.3) that provides more sorption capacity for element (Gorman et al. 2000) relative to Dewey fly ash. Leachates from the mixtures of soil with Presque Isle fly ash have significantly lower concentrations of Cd (Figure 3.9b), Sr (Figure 3.11b), and Se (Figure 3.18b) than those in fly ash alone, whereas leachates from the mixtures of soil with Dewey fly ash have remarkably lower concentrations of Cr (Figure 3.14a) compared to those in fly ash alone.

Incorporation of As and Se in cement hydration products produced from self-cementing Columbia fly ash is likely to be responsible for a significant reduction of As (Figure 3.17c), Se (Figure 3.18c) in leachates from the mixtures of soil with Columbia fly ash compared to leachates from Columbia fly ash alone and the mixtures of soil with Dewey and Presque Isle fly ash. Columbia fly ash is abundant in CaO, which is a key precursor for pozzolanic reactions with silica and alumina to form cementitious compounds. Chemical inclusion is most likely a mechanism for As immobilization in the mixtures of soil with Columbia fly ash resulting in a substantial decrease in As concentrations to below detection limit when pH > 5.5. Significant drop of Se in leachates from Columbia fly ash and their soil-fly ash mixtures at extremely alkaline pH (pH > 11.5) (Figure 3.18c) is probably due to solid-solution formation with ettringite, a

hydrated phase crystallizing from the hydration reaction of alkaline fly ash at highly alkaline pH (Hesbach et al. 2005).

3.4   Conclusions

Leaching test as a function of pH was performed on soils, fly ashes, and soil-fly ash mixtures. Four broad leaching behaviors as a function of pH were observed: (i) leaching of Ca, Cd, Mg, and Sr follows a cationic pattern where the concentration decreases monotonically as pH increases; (ii) leaching of Al, Fe, Cr, Cu, and Zn follows an amphoteric pattern where the concentration increases at acidic and alkaline pH; (iii) leaching of As and Se shows both the behaviors following oxyanionic pattern where concentration increases at acidic and alkaline pH and those not following a cationic, an amphoteric, or oxyanionic behavior; and (iv) leaching of Ba presents amphoteric-like pattern but less pH-dependent.

In spite of different types and composition of soil and fly ash investigated, the study reveals the similarity in leaching behavior as a function of pH for a given element from soil, fly ash, and soil-fly ash mixtures. The similarity is most likely due to similar controlling mechanisms (e.g., solubility, sorption, and solid-solution formation) and similar controlling factors (e.g., leachate pH and redox conditions). This offers the opportunity to transfer knowledge of fly ash that has been extensively characterized and studied to soil stabilized with fly ash.

Both soil and fly ash enriched with trace elements can be a potential source releasing trace element into leachate from soil-fly ash mixture. In addition, some material-specific constituent in soil and fly ash can also have significant enhancing or diminishing effect on leaching of trace element. The leaching of Cu is significantly increased with the leaching of DOC. Conversely, unburned carbon in off-specification fly ashes may provide sorption sites for Cd, Cr, and Cu resulting in a reduction in

concentration of these elements in leachate from soil-fly ash mixture. Class C fly ash provides sufficient CaO to initiate the pozzolanic reaction yielding hydrated cement products that oxyanions, including As and Se, can be incorporated into.

These factors should be taken into consideration when selecting soil and fly ash used in stabilization, especially organic soil and soil or fly ash abundant in trace elements of concern. However, different fly ash types show different abilities in immobilizing trace elements to some extent. The abilities of fly ash to retain trace element should promote the beneficial use of fly ash in soil stabilization, especially off-specification fly ash.

Table 3.1.   Coal source, fly ash collection method, storage type, and boiler type of the power plants producing Dewey, Presque Isle, and Columbia fly ashes.

Information	Dewey[1]	Presque Isle[1]	Columbia[2]
Company	Alliant Energy	WE Energy	Columbia Power Station (Unit 2)
Location	Cassville, WI	Marquette, MI	Portage, WI
Type of Coal and Source	Sub-Bituminous	Bituminous	Sub-Bituminous
	80% Montana Coal with Colorado or Petroleum Coke	100% Colorado Bituminous	Wyoming Power River Basin coal with Colorado or Petroleum Coke
Collection Method	Electrostatic	Fabric Filter	Electrostatic
Storage Type	Dry Silo	Dry Silo	Dry Silo
Type of Boiler	Cyclone	Front Wall/Tangential	Pulverized
Combustion Temperature (°F)	2000[3]	3000-3200[4]	2450[3]

Source: [1]Sauer (2006); and [2]Acosta (2003), [3]Alliant Energy, and [4]WE Energy.

Table 3.2.   Properties of Dewey, Presque Isle, and Columbia fly ashes along with chemical and physical criteria for Class C and Class F fly ashes stated in ASTM C 618.

Chemical Requirements	ASTM Requirements		Dewey	Presque Isle	Columbia
	Class F	Class C			
$SiO_2 + Al_2O_3 + Fe_2O_3$ (%)	≥ 70	≥ 50	19.04[1]	59.65[1]	58.88[1]
SO_3 (%)	≤ 5	≤ 5	-	-	3.7[3]
Moisture Content (%)	≤ 3	≤ 3	0.44	0.18	0.06
Loss on Ignition (%)	≤ 6	≤ 6	49.1[1]	32.4[1]	0.98[1]
Physical Requirements	ASTM Requirements		Dewey[2]	Presque Isle[2]	Columbia[4]
	Class F	Class C			
Fineness (%)	≤ 34	≤ 34	12.7	39.2	14.4
Strength Activity @ 7 d (%)	≥ 75	≥ 75	82.7	48.5	95.8

Source: [1]X-ray fluorescence (XRF) spectrometry; [2]Sauer (2006); [3]Bin-Shafique et al. (2002); and [4]Acosta et al. (2003).

Table 3.3.   Chemical composition of Dewey, Presque Isle, and Columbia fly ashes along with the composition of typical Class C and Class F fly ashes.

Chemical Species	Percent of Composition				
	Typical Class F[1]	Typical Class C[1]	Dewey[2]	Presque Isle[2]	Columbia[2]
CaO	9	24	9.43	2.99	26.86
SiO_2	55	40	9.43	36.07	33.77
Al_2O_3	26	17	7.43	19.94	19.34
Fe_2O_3	7	6	2.18	3.64	5.77
MgO	2	5	2.16	1.06	5.64
Na_2O	-	-	5.44	1.02	2.05
K_2O	-	-	0.36	0.73	0.35
Cr_2O_3	-	-	0.02	0.01	0.01
TiO_2	-	-	0.56	0.59	1.55
MnO	-	-	0.02	0.01	0.04
P_2O_5	-	-	0.156	0.56	0.814
SrO	-	-	0.38	0.19	0.38
BaO	-	-	0.7	0.23	0.68

Source: [1]ACAA(2003); and [2]X-ray fluorescence (XRF) spectrometry.

Table 3.4.   Sampling locations and properties of soils used in study.

| Sample | Sampling Location | USCS[1] Soil Classification | | Properties | | | | | |
		Group Symbol	Group Name	Liquid Limit	Plastic Limit	Percent Fines (%)	Percent Clay (%)	Organic Matter Content (%)	CEC (cmol$_c$/kg)
Lawson	Hwy 11 Green County, WI	OL-OH[2]	Organic clay[2]	50[2]	19[2]	97[2]	54[2]	6.3	45
Kamm	McFarland, Dane County, WI	CL-CH[3]	Lean clay/fat clay	48[4]	30[4]	91[4]	38[4]	2.0	25
Red Wing	Red Wing, Goodhue County, Mn	ML[5]	Silt[5]	28[5]	11[5]	88[5]	6[5]	1.2	8
MnRoad	I-94 Wright County, WI	CL[5]	Lean clay[5]	26[5]	9[5]	60[5]	15[5]	1.5	19
Sand	Portage County, WI	SP[6]	Poorly graded sand[6]	Non-plastic	Non-plastic	Non-plastic	0	0.0	0

Note: [1] Unified Soil Classification System; [2] Tastan (2005); [3] Department of Natural Resources, WI; [4] Park (2007); [5] Gupta et. al. (2006); [6] Lee and Benson (2004).

Table 3.5.   Solid-phase concentration (mg/kg) from total elemental analysis of soils and fly ashes.

Element	Solid phase concentration (mg/kg)							
	Soil					Fly Ash		
	Lawson	Kamm	Red Wing	MnRoad	Sand	Dewey	Presque Isle	Columbia
Ag	0.06	0.05	<0.00048*	0.03	<0.00048*	0.50	0.19	0.55
Al	24,770	17,510	8577	11,770	25.74	28,280	19,610	75,230
As	13.51	13.06	8.49	8.55	4.16	79.63	11.91	28.11
B	55.04	44.51	31.53	35.82	9.22	509	600	610
Ba	244	168	93.38	151	<0.00003*	575	1279	3621
Be	0.88	0.69	0.31	0.46	<0.00001*	1.70	1.91	2.64
Ca	6641	5180	43,760	28,790	135	49,740	17,770	246,300
Cd	0.89	0.36	0.37	0.41	0.01	1.26	0.61	1.51
Co	<0.00016*	<0.00016*	<0.00016*	1.01	<0.00016*	4.99	<0.00016*	5.60
Cr	33.35	26.90	16.56	21.89	0.25	34.05	12.45	60.44
Cu	20.89	21.52	11.44	12.97	0.99	145	26.20	179
Fe	19,920	18,820	11,750	13,010	144	12,790	13,240	20,270
K	3,022	1869	1788	2259	9.12	4572	1074	3111
Li	16.73	11.18	7.75	11.43	<0.00029*	28.30	27.16	29.80
Mg	5394	5375	16,840	9992	80.52	10,010	3290	24,650
Mn	929	760	401	551	1.32	150	39.27	176
Mo	0.60	<0.00052*	<0.00052*	<0.00052*	<0.00052*	177	28.65	7.22
Na	99.17	78.62	696	424	143	25,561	1,162	8,692
Ni	24.39	23.03	13.51	18.49	0.20	1001	157	44.96
P	1087	531	589	395	<0.00313*	649	2325	3357
Pb	51.35	14.08	8.03	7.39	<0.00085*	20.46	20.79	27.91
Sb	5.27	3.44	1.64	2.24	<0.00344*	<0.00344*	1.93	7.65
Se	<0.00118*	<0.00118*	<0.00118*	<0.00118*	<0.00118*	2.11	4.31	9.43
Sn	3.17	1.45	2.85	1.60	7.87	34.17	13.20	8.45
Sr	20.75	23.40	41.34	36.30	0.85	1385	968	1622
Tl	<0.00404*	<0.00404*	<0.00404*	<0.00404*	<0.00404*	<0.00404*	<0.00404*	<0.00404*
V	55.62	51.89	32.46	50.41	<0.00024*	1514	406	198
Zn	252.20	74.70	46.64	61.34	29.84	97.27	34.54	94.11

Note: *concentration below method detection limit.

Table 3.6.   Mineral constituents of soils determined by X-ray diffraction (XRD).

Mineral Constituents	Chemical Formula	Weight Percent (%)			
		Lawson	Kamm	Red Wing	MnRoad
Quartz	SiO_2	52	48	46	44
Plagioclase	$(Na,Ca)AlSi_3O_8$	16	15	8	9
K-Feldspar	$KAlSi_3O_8$	7	8	5	4
Calcite	$CaCO_3$	NA	NA	2	2
Dolomite	$(Ca,Mg)CO_3$	3	2	9	6
Kaolinite	$Al_2Si_2O_5(OH)_4$	2	2	2	2
Chlorite	$(Mg,Al)_6(Si,Al)_4O_{10}(OH)_8$	0.2	0.2	1	1
Illite/Mica	$KAl_2(Si_3AlO_{10})(OH)_2$	6	6	2	3
Montmorillonite	$Na_{0.3}(Al,Mg)_2Si_4O_{10}(OH)_2.xH_2O$	15*	19*	25	29

Note: *randomly ordered mixed-layer illite/smectite with 90% smectite layer, NA = not applicable.

Table 3.7.   Leachate pH for soils, fly ashes, and mixtures of soil-fly ash.

Sample		pH
Soil	Lawson	7.05
	Kamm	6.94
	Red Wing	8.00
	Mn Road	8.27
	Sand	8.80
Fly ash	Dewey	10.41
	Presque Isle	11.68
	Columbia	12.55
Soil-Fly ash Mixtures	Dewey-Lawson	9.14
	Dewey-Kamm	9.55
	Dewey-Red Wing	10.37
	Dewey-Mn Road	10.30
	Dewey-Sand	10.32
	PI-Lawson	8.85
	PI-Kamm	9.40
	PI-Red Wing	9.90
	PI-Mn Road	9.22
	PI-Sand	9.98
	Columbia-Lawson	10.54
	Columbia-Kamm	10.77
	Columbia-Red Wing	12.28
	Columbia-Mn Road	11.00
	Columbia-Sand	11.11

Table 3.8.   Concentration of elements representing acid- and base-forming components obtained from the leaching test as a function of pH.

Fly ash	Solution pH	Dissolved concentration (mg/L)				
		Ca	Mg	Al	B	Fe
Dewey	10.41	271	0.16	80.8	11.0	0.01
Presque Isle	11.68	128	0.01	5.60	16.3	0.01
Columbia	12.55	134	0.01	7.95	1.96	0.04

Figure 3.1.   Locations where soils were obtained.
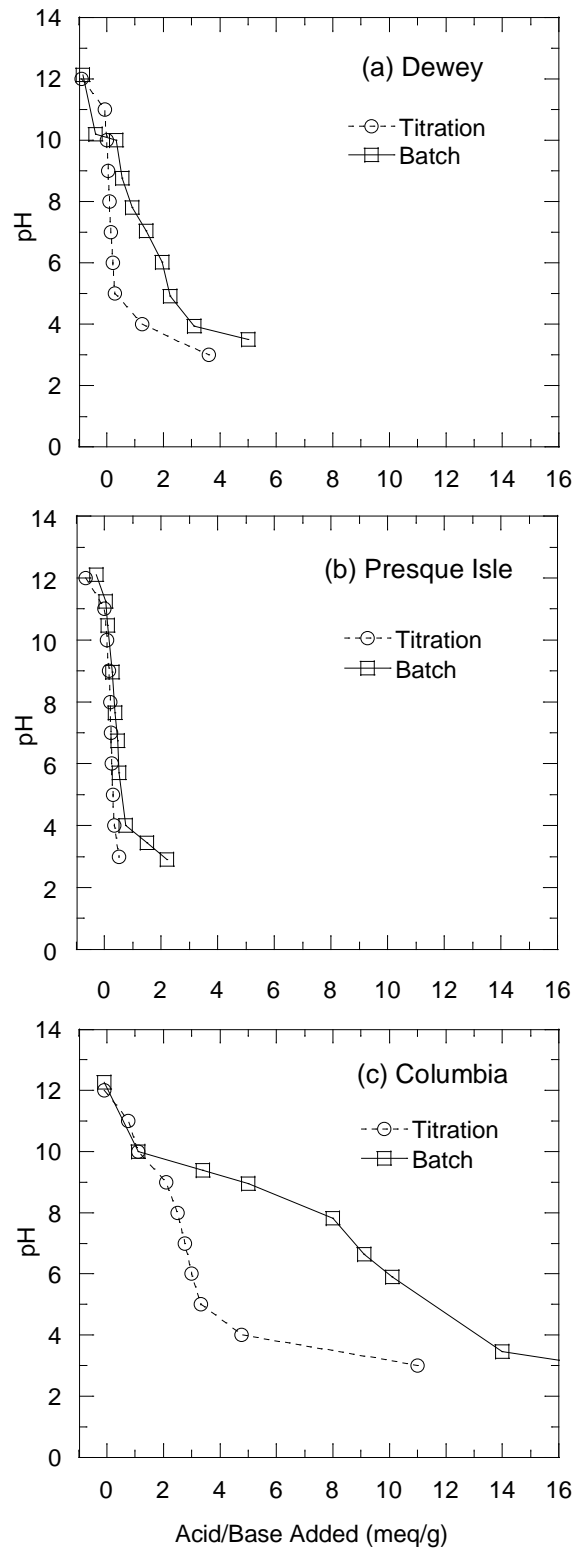
Figure 3.2. ANC curves from titration and batch tests on (a) Dewey, (b) Presque Isle, and (c) Columbia fly ash.
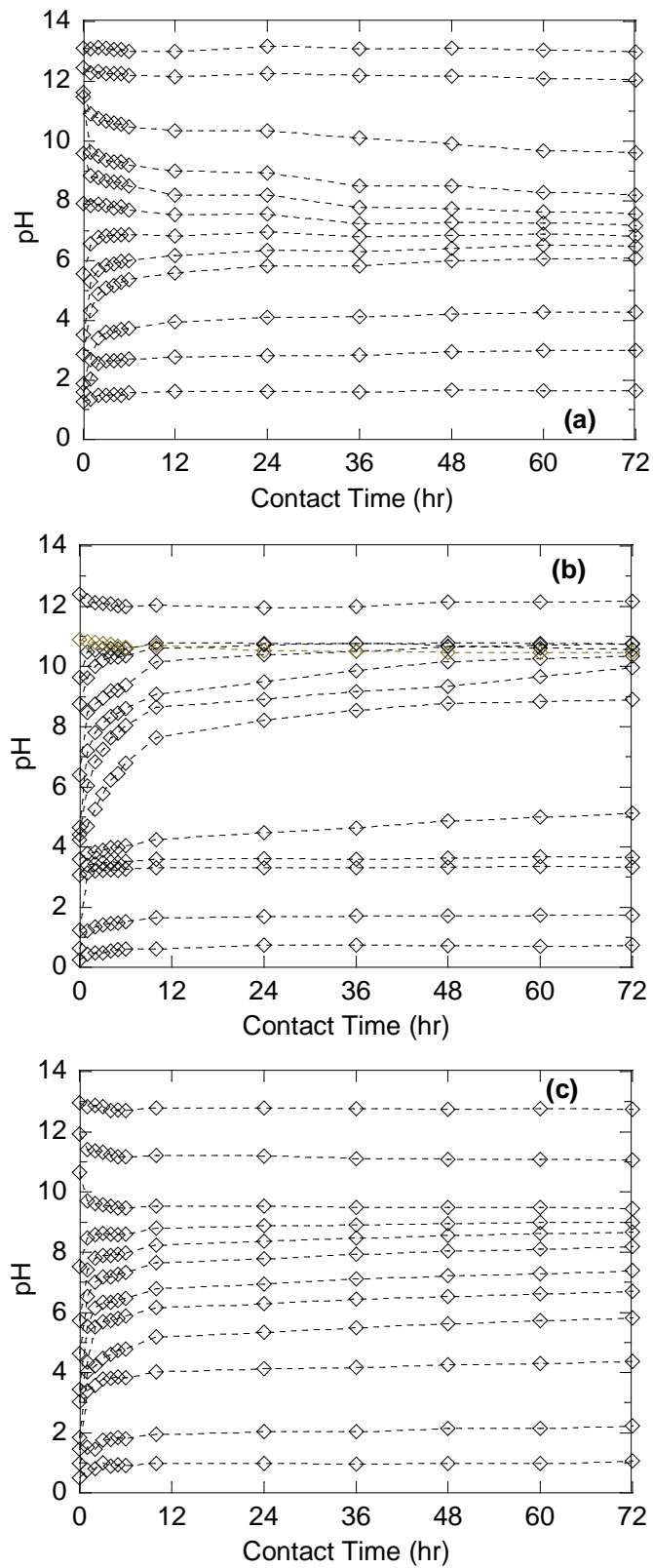
Figure 3.3.   pH vs. time from kinetic batch tests on (a) Lawson soil, (b) Dewey fly ash, and a mixture of Lawson soil and Dewey fly ash (20%).
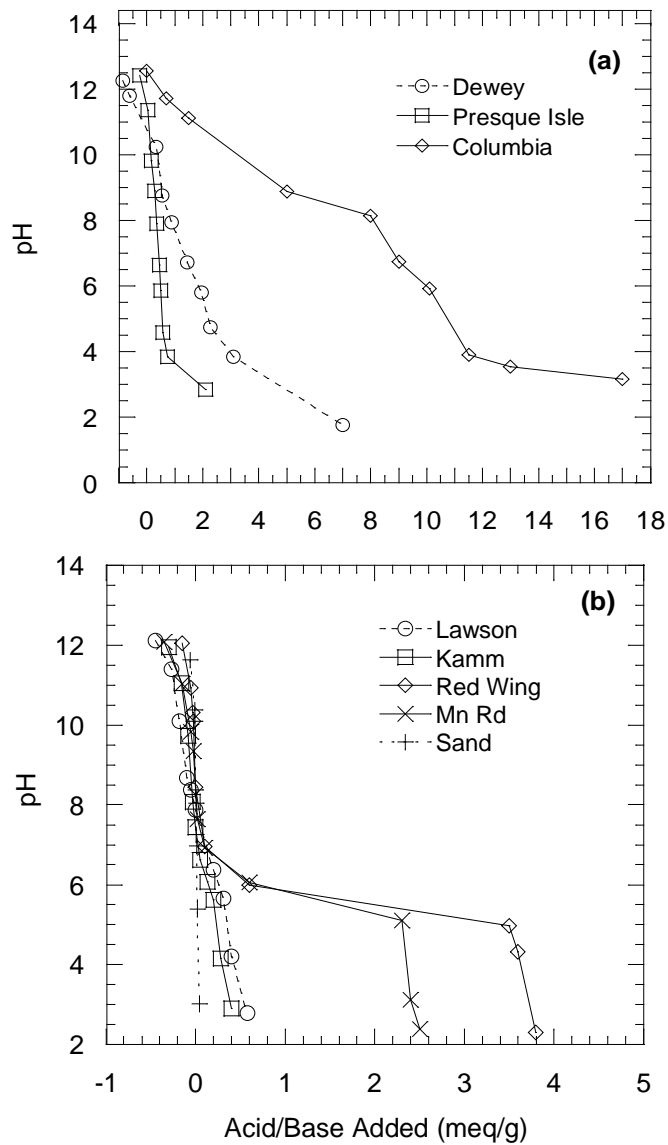
Figure 3.4. ANC curves obtained from batch test: (a) Dewey, Presque Isle, and Columbia fly ash and (b) Lawson soil, Kamm clay, Red Wing silt, MnRoad clay, and sand.
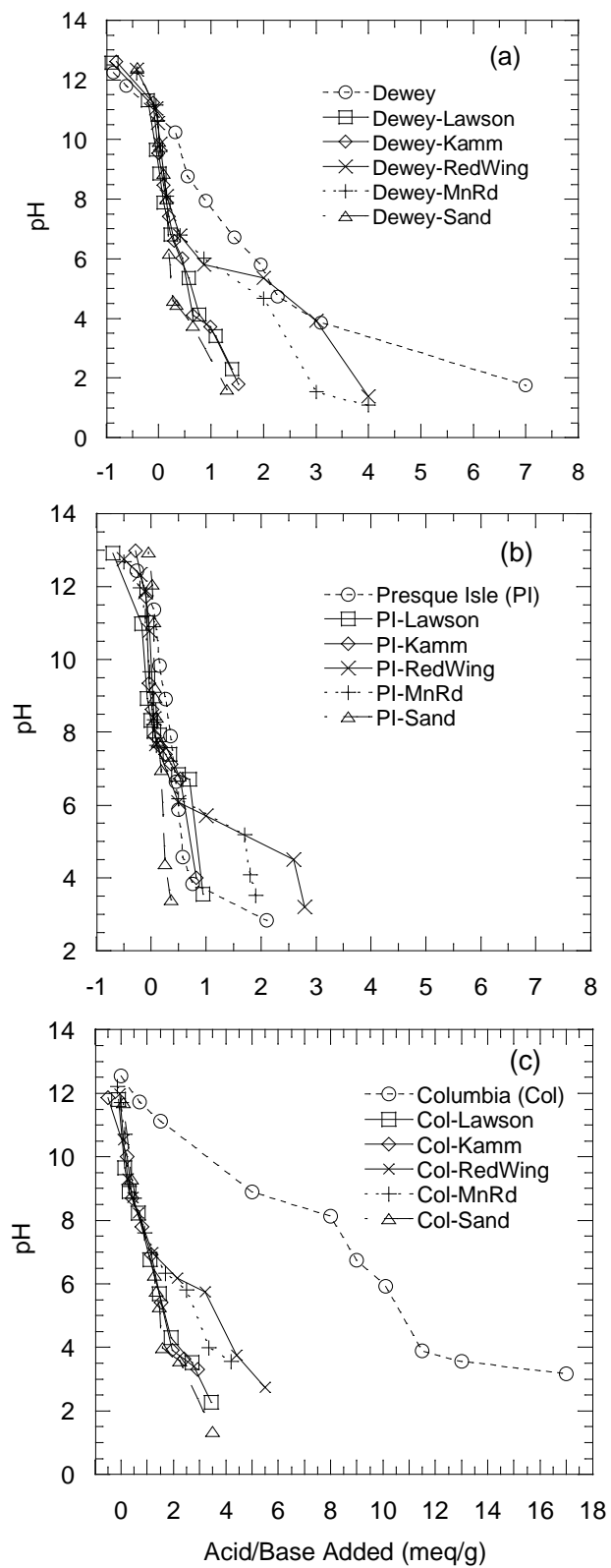
Figure 3.5.   ANC curves obtained from batch test for soil-fly ash mixtures: (a) mixtures of Dewey and soil, (b) mixtures of Presque Isle and soil, and (c) mixtures of Columbia and soil.
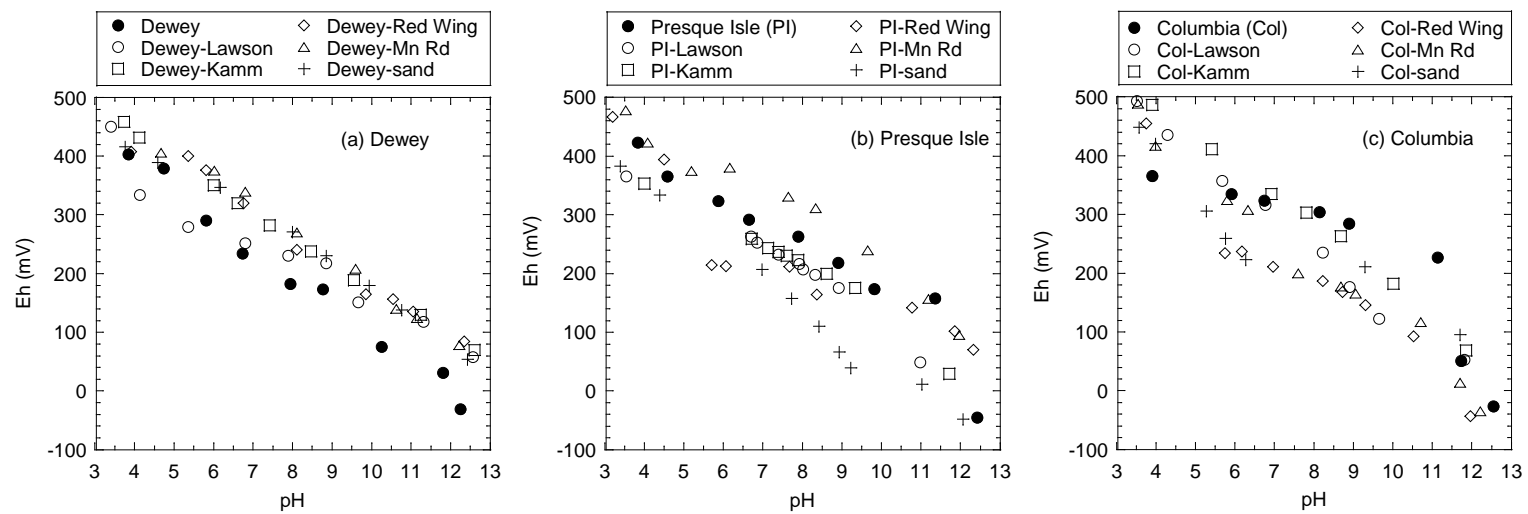
Figure 3.6.   Redox potential as a function of pH for leachates from fly ashes and soil-fly ash mixtures: (a) Dewey fly ash, (b) Presque Isle fly ash, and (c) Columbia fly ash.
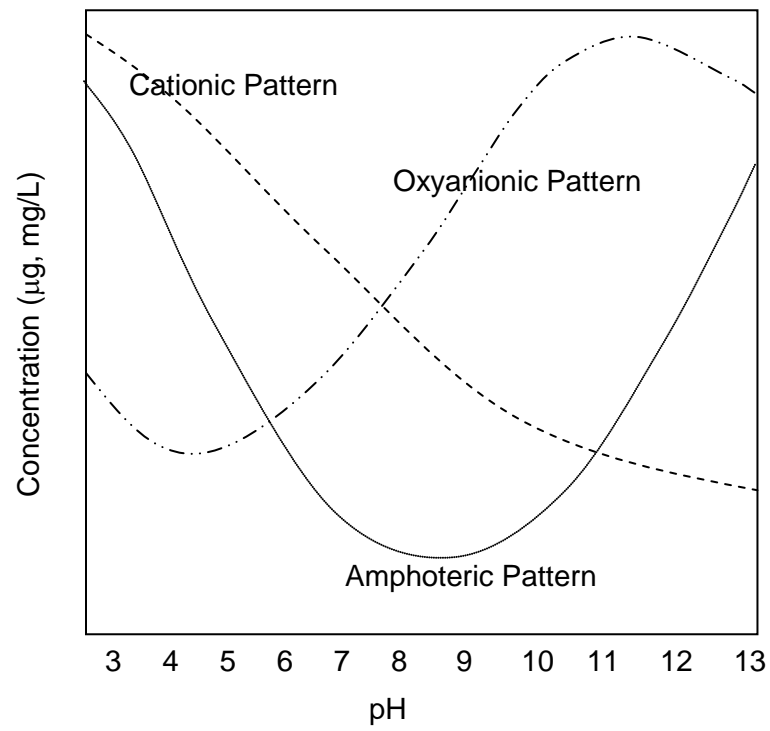
Figure 3.7. Conceptual illustration of leaching patterns as a function of pH. Modified after Kosson et al. (1996).
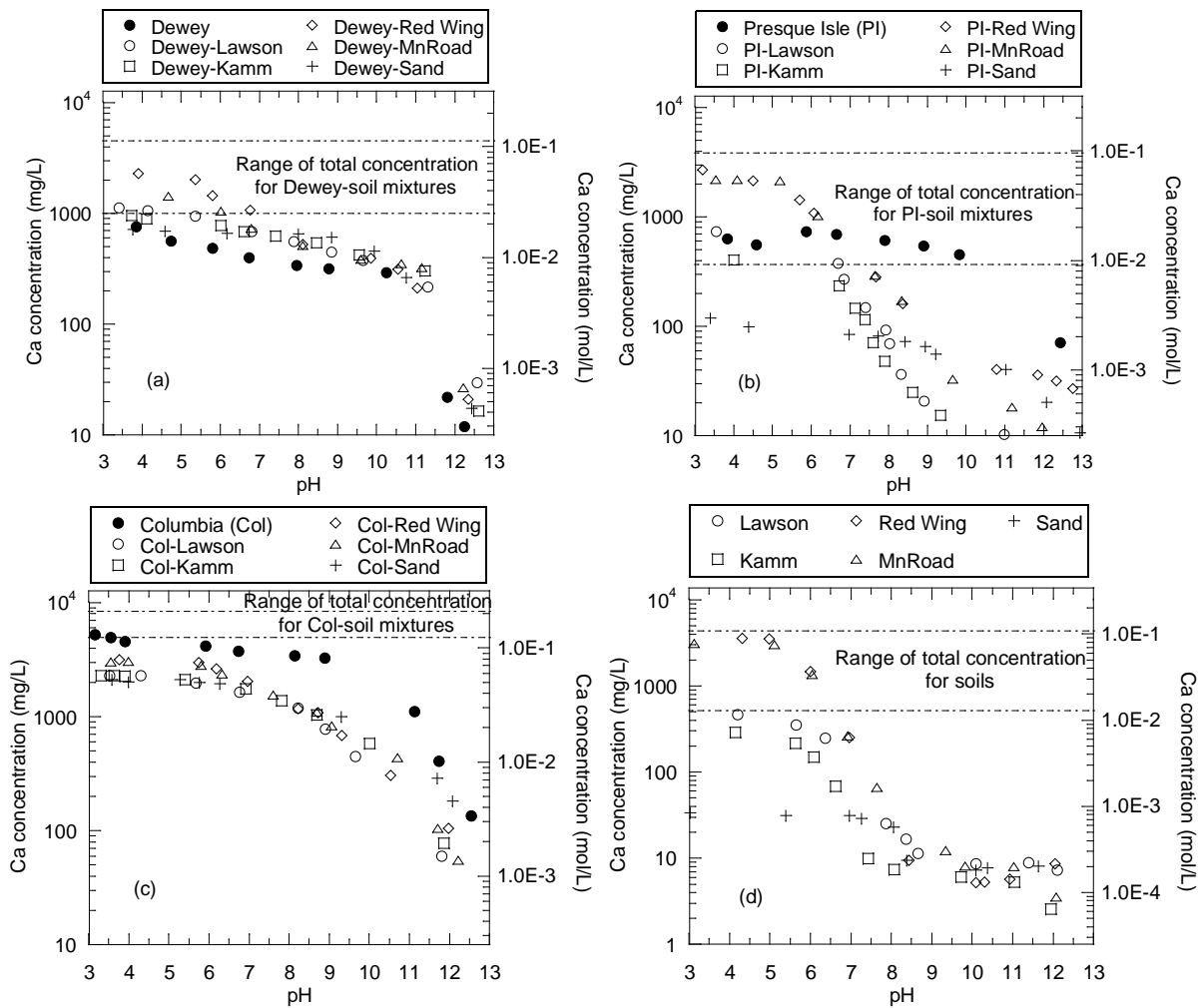
Figure 3.8. Concentrations of Ca as a function of pH in leachates from fly ashes, soil-fly ash mixtures, and soils: (a) Dewey fly ash, (b) Presque Isle fly ash, (c) Columbia fly ash, and (d) soils.
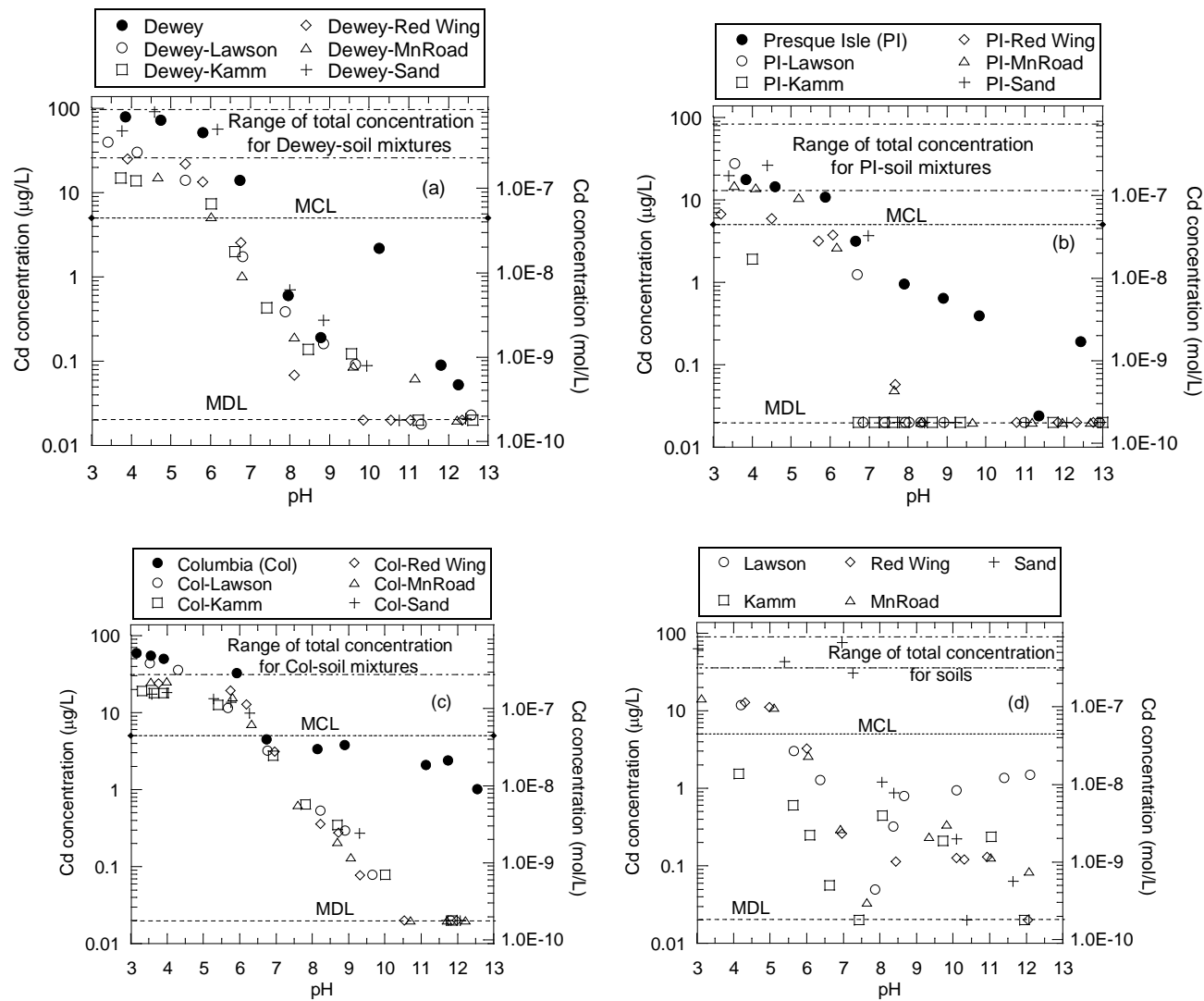
Figure 3.9. Concentrations of Cd as a function of pH in leachates from fly ashes, soil-fly ash mixtures, and soils: (a) Dewey fly ash, (b) Presque Isle fly ash, (c) Columbia fly ash, (d) soils. Note: MDL = method detection limit, MCL = maximum contaminant level.
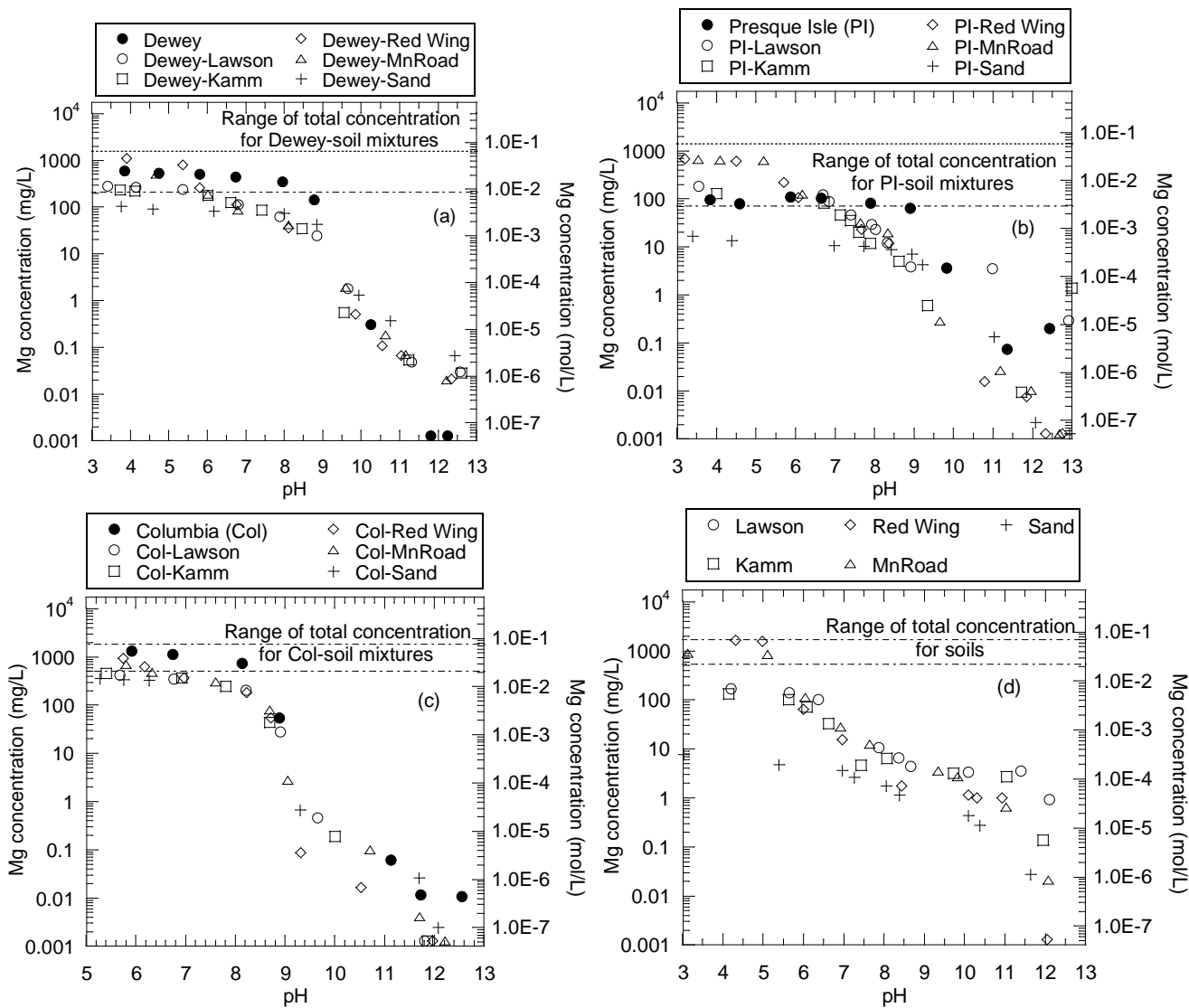
Figure 3.10. Concentrations of Mg as a function of pH in leachates from fly ashes, soil-fly ash mixtures, and soils: (a) Dewey fly ash, (b) Presque Isle fly ash, (c) Columbia fly ash, and (d) soils.
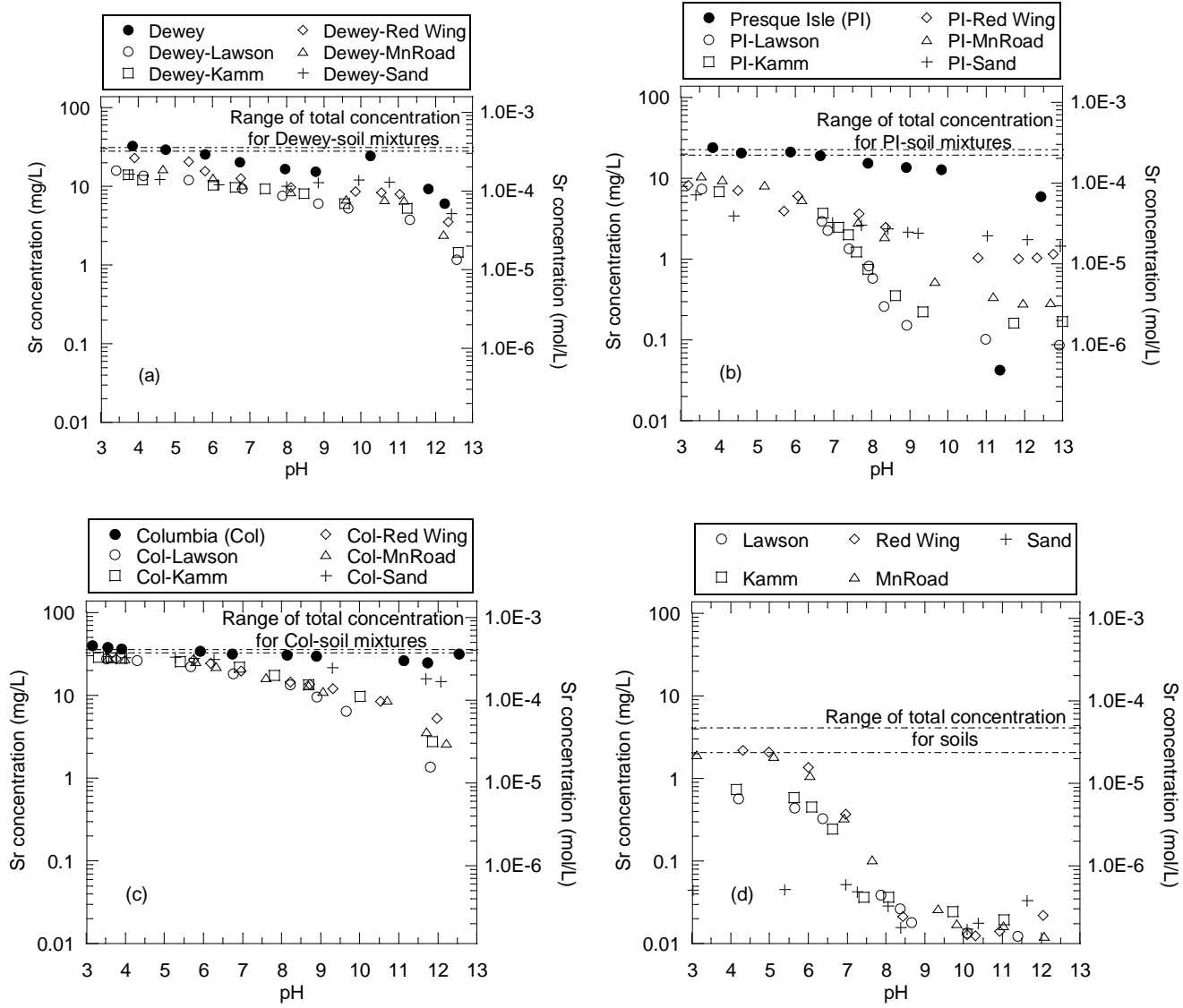
Figure 3.11. Concentrations of Sr as a function of pH in leachates from fly ashes, soil-fly ash mixtures, and soils: (a) Dewey fly ash, (b) Presque Isle fly ash, (c) Columbia fly ash, and (d) soils.
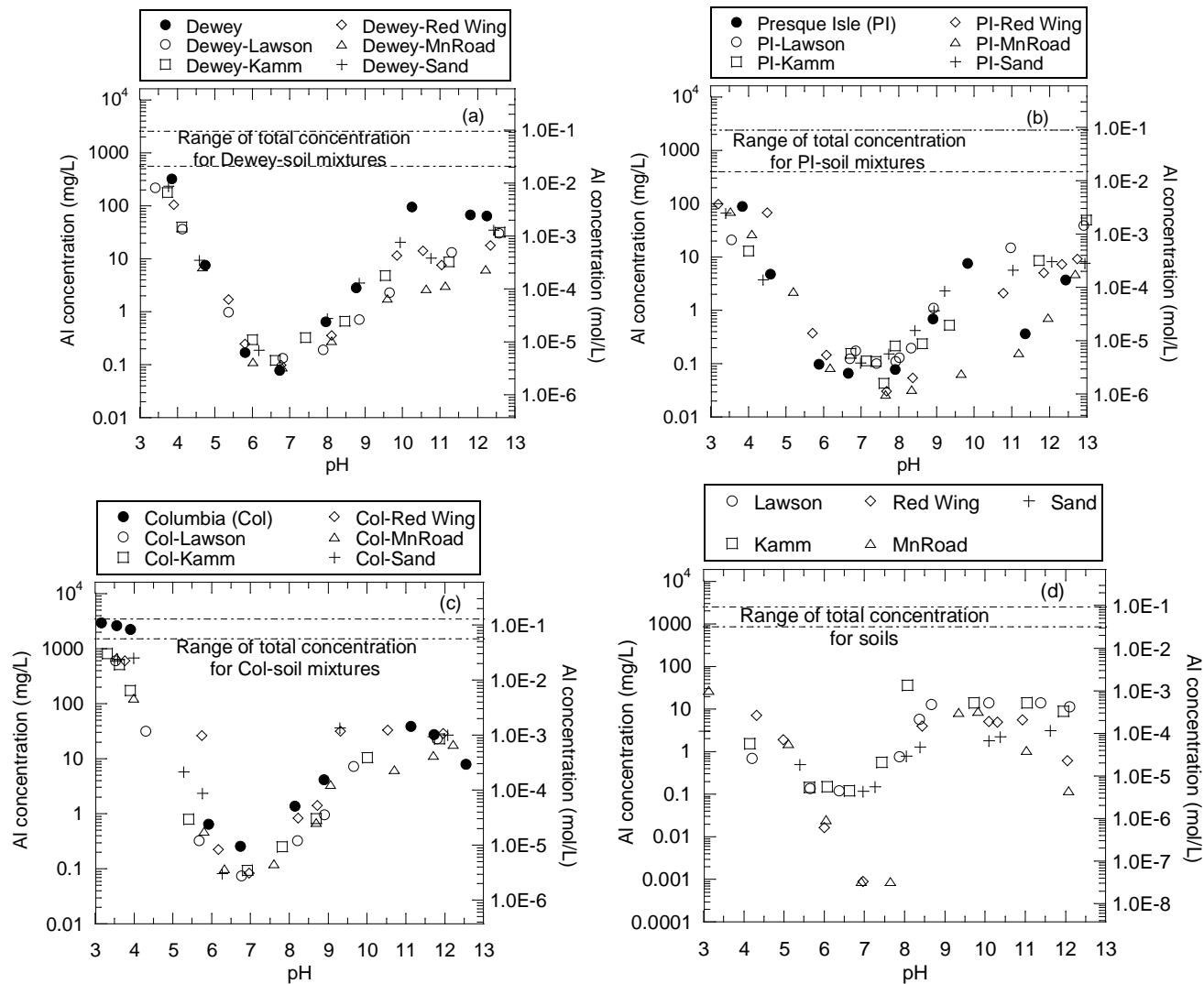
Figure 3.12. Concentrations of Al as a function of pH in leachates from fly ashes, soil-fly ash mixtures, and soils: (a) Dewey fly ash, (b) Presque Isle fly ash, (c) Columbia fly ash, and (d) soils.
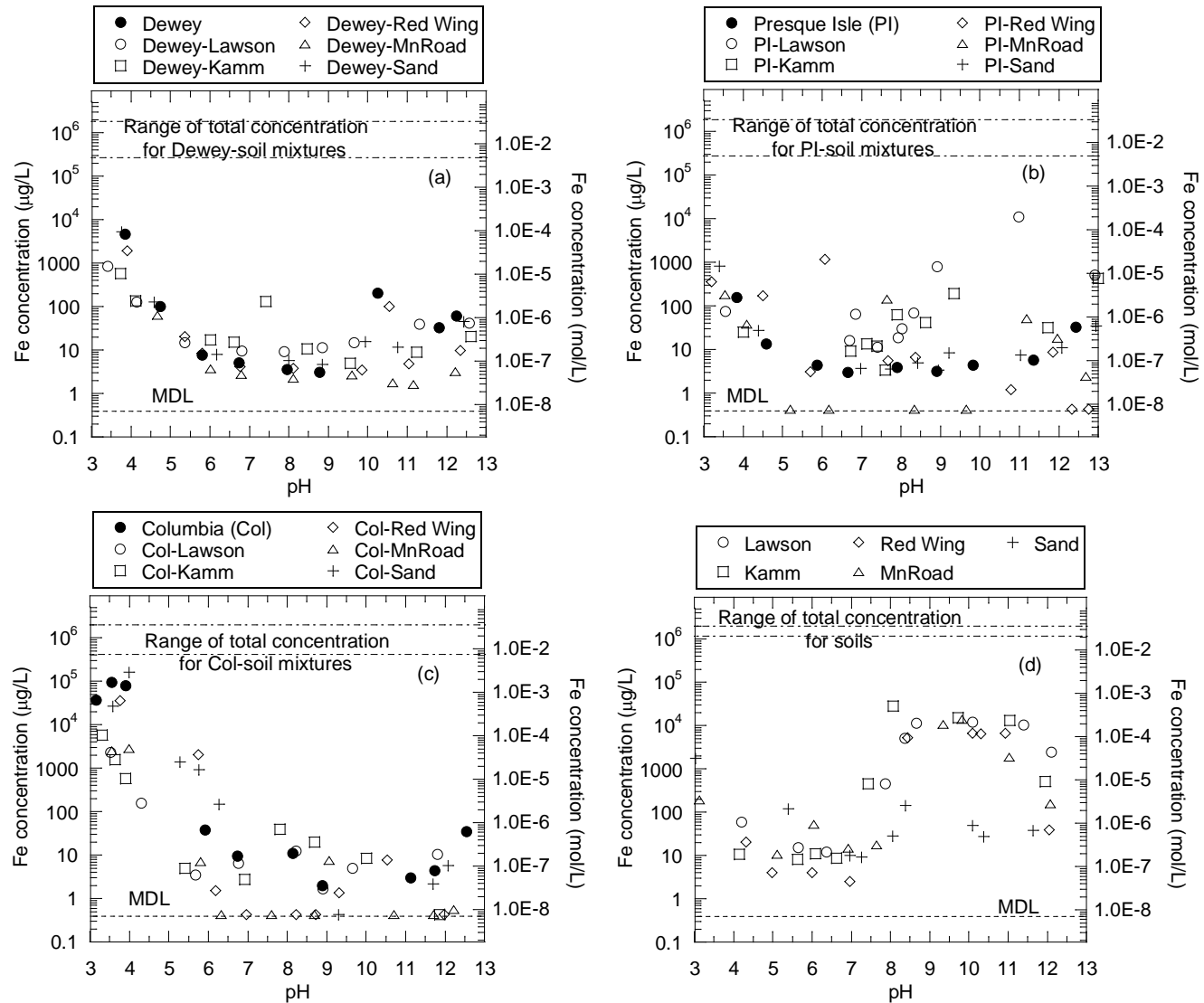
Figure 3.13. Concentrations of Fe as a function of pH in leachates from fly ashes, soil-fly ash mixtures, and soils: (a) Dewey fly ash, (b) Presque Isle fly ash, (c) Columbia fly ash, and (d) soils. Note: MDL = method detection limit.
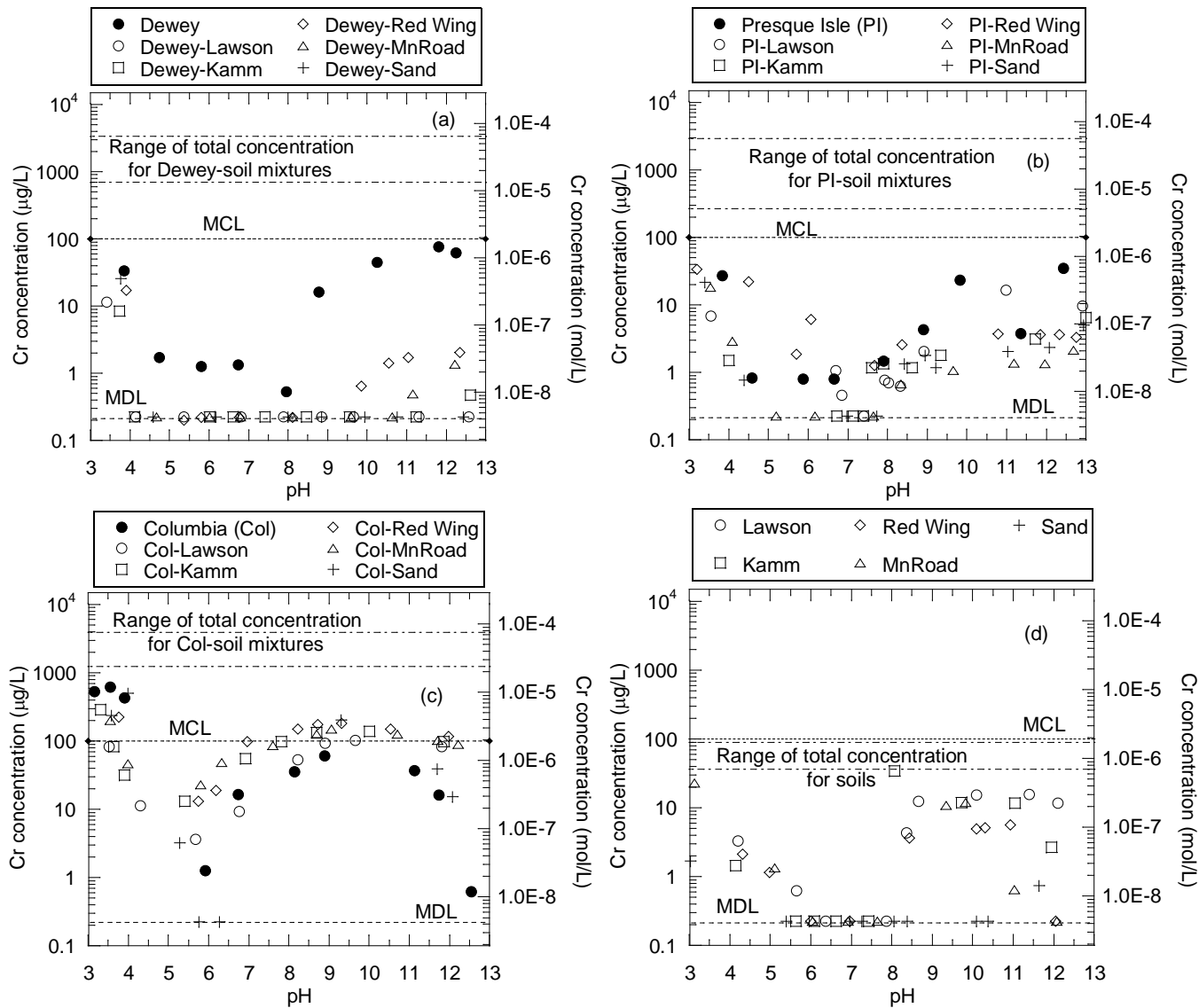
Figure 3.14. Concentrations of Cr as a function of pH in leachates from fly ashes, soil-fly ash mixtures, and soils: (a) Dewey fly ash, (b) Presque Isle fly ash, (c) Columbia fly ash, and (d) soils. Note: MDL = method detection limit, MCL = maximum contaminant level.
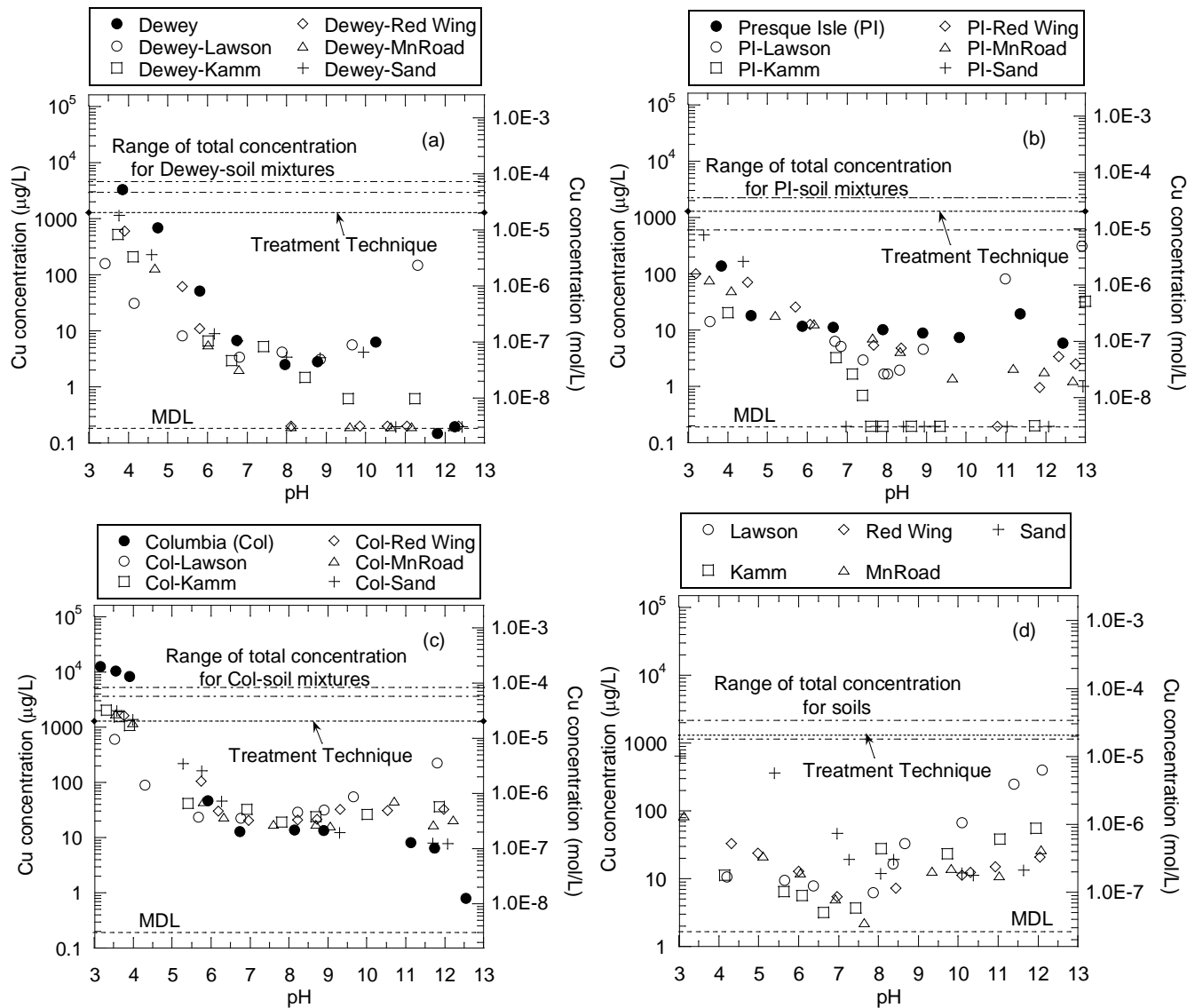
Figure 3.15.   Concentrations of Cu as a function of pH in leachates from fly ashes, soil-fly ash mixtures, and soils: (a) Dewey fly ash, (b) Presque Isle fly ash, (c) Columbia fly ash, and (d) soils. Note: MDL = method detection limit, MCL = maximum contaminant level.
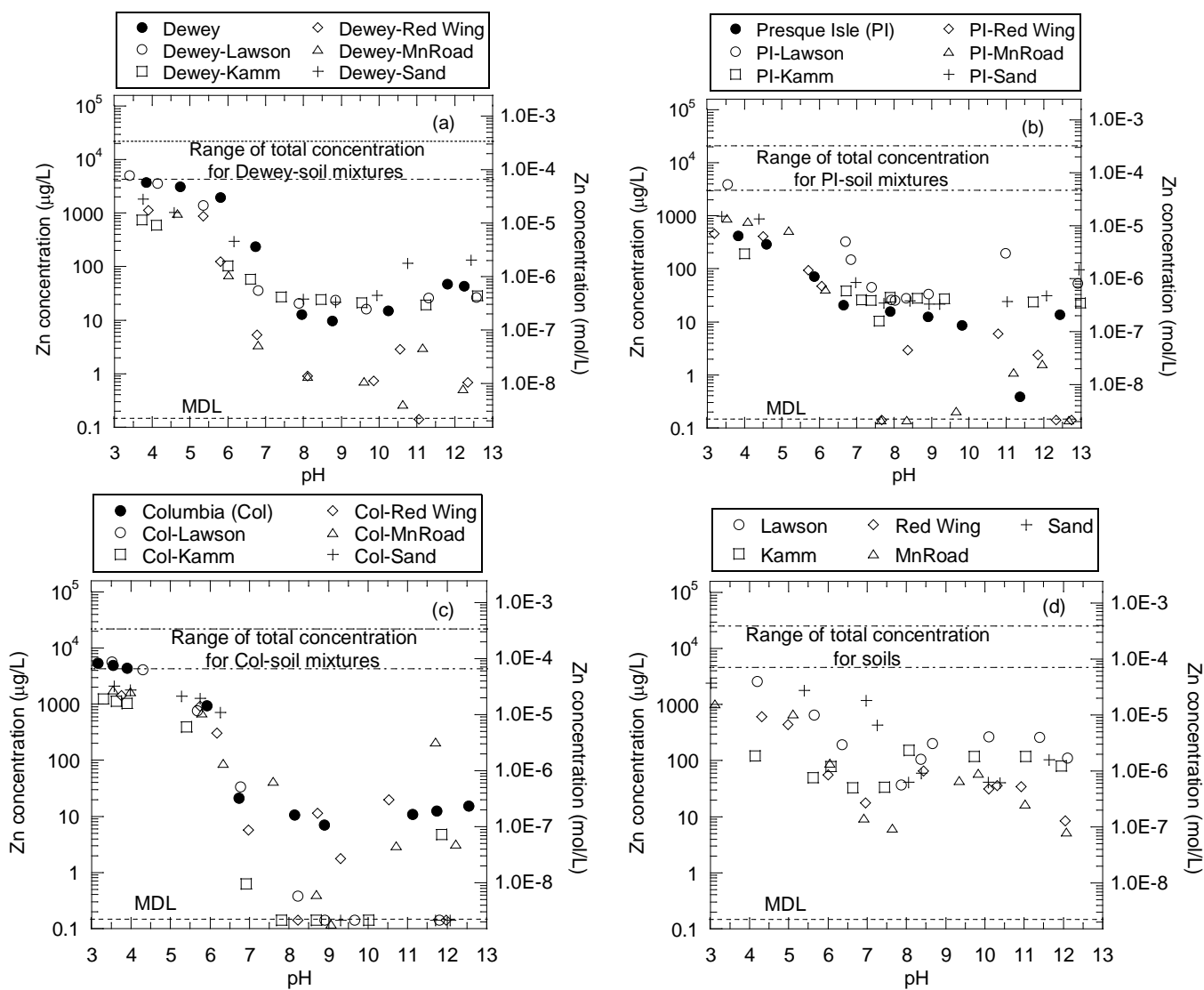
Figure 3.16. Concentrations of Zn as a function of pH in leachates from fly ashes, soil-fly ash mixtures, and soils: (a) Dewey fly ash, (b) Presque Isle fly ash, (c) Columbia fly ash, and (d) soils. Note: MDL = method detection limit.
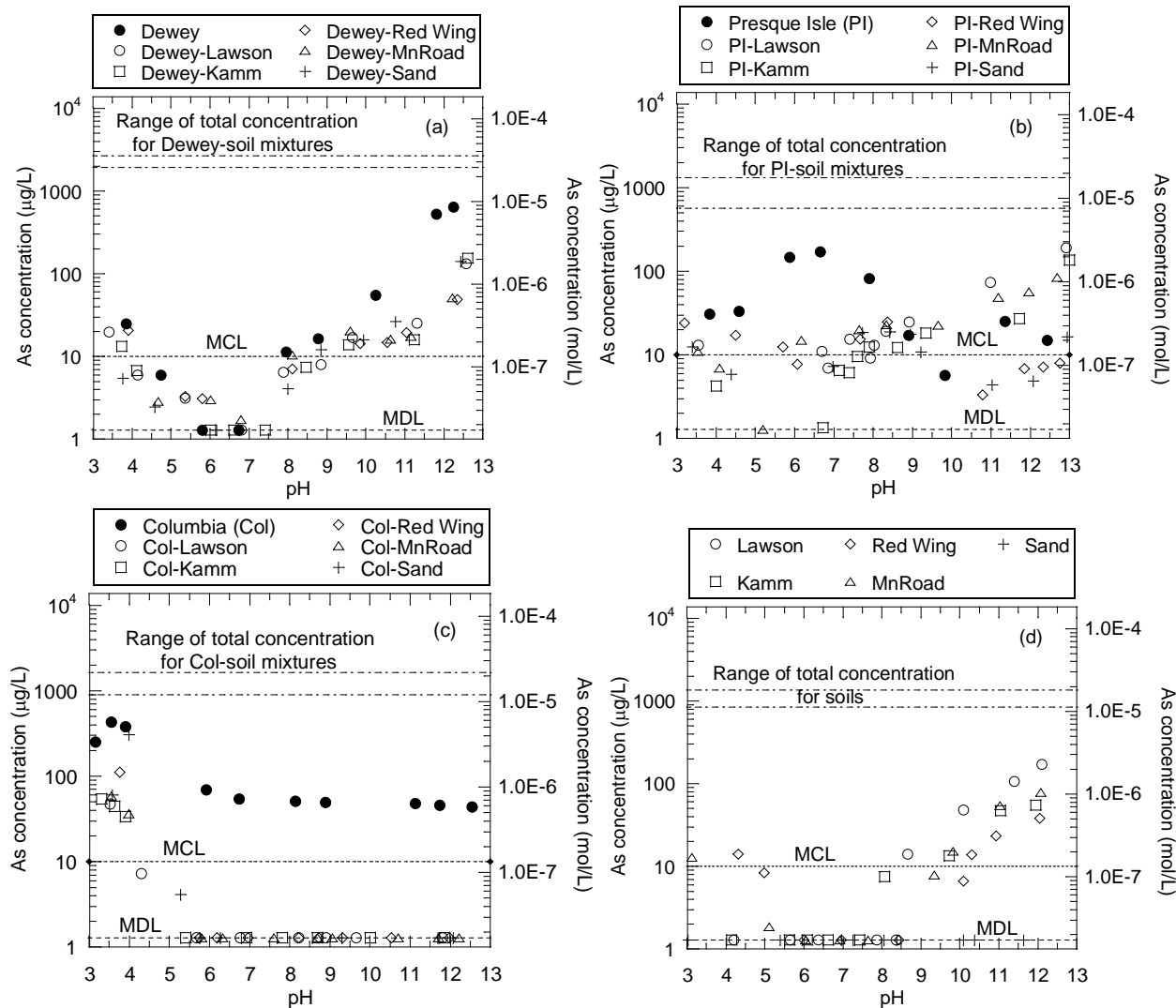
Figure 3.17. Concentrations of As as a function of pH in leachates from fly ashes, soil-fly ash mixtures, and soils: (a) Dewey fly ash, (b) Presque Isle fly ash, (c) Columbia fly ash, and (d) soils. Note: MDL = method detection limit, MCL = maximum contaminant level
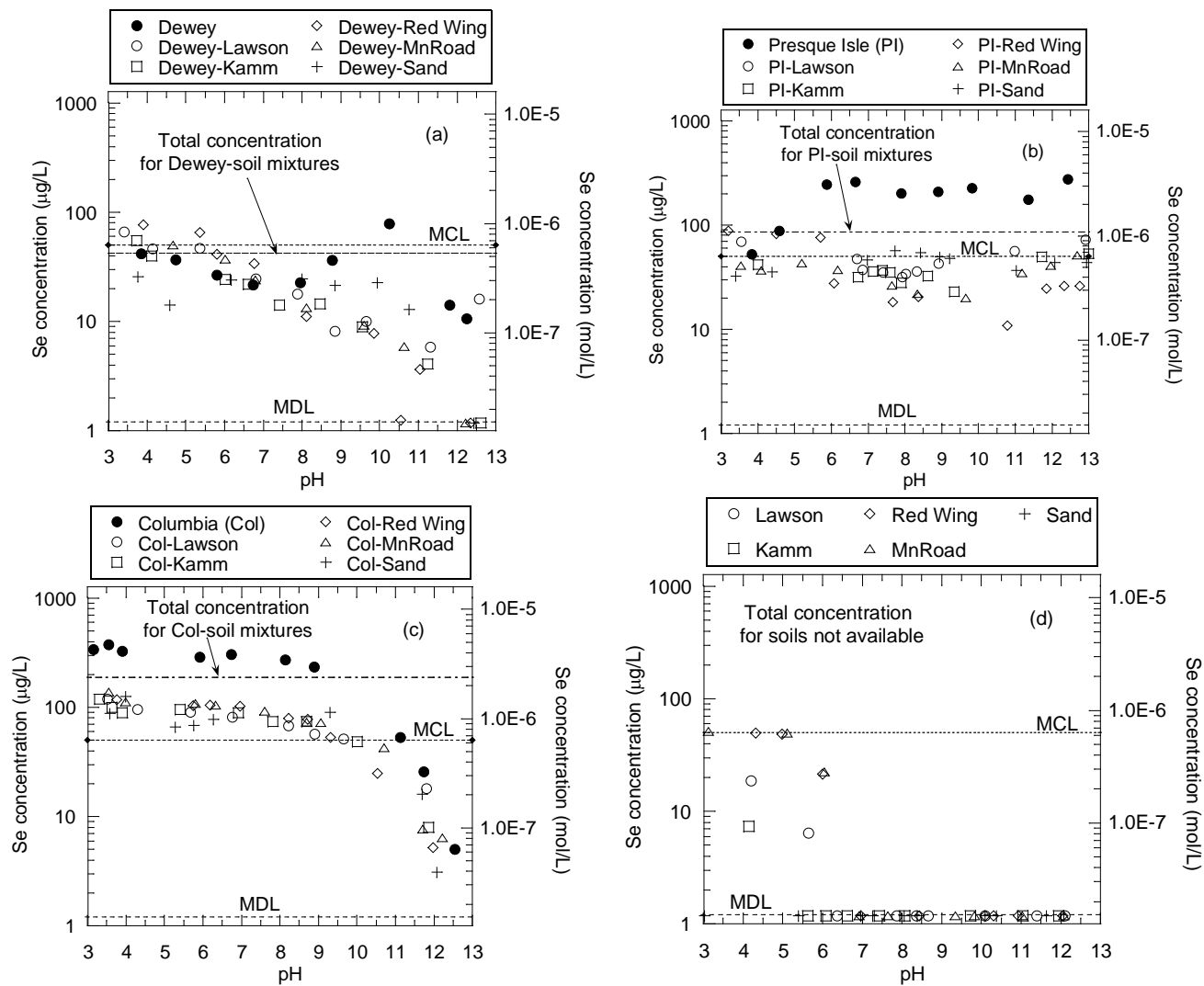
Figure 3.18. Concentrations of Se as a function of pH in leachates from fly ashes, soil-fly ash mixtures, and soils: (a) Dewey fly ash, (b) Presque Isle fly ash, (c) Columbia fly ash, and (d) soils. Note: MDL = method detection limit, MCL = maximum contaminant level.
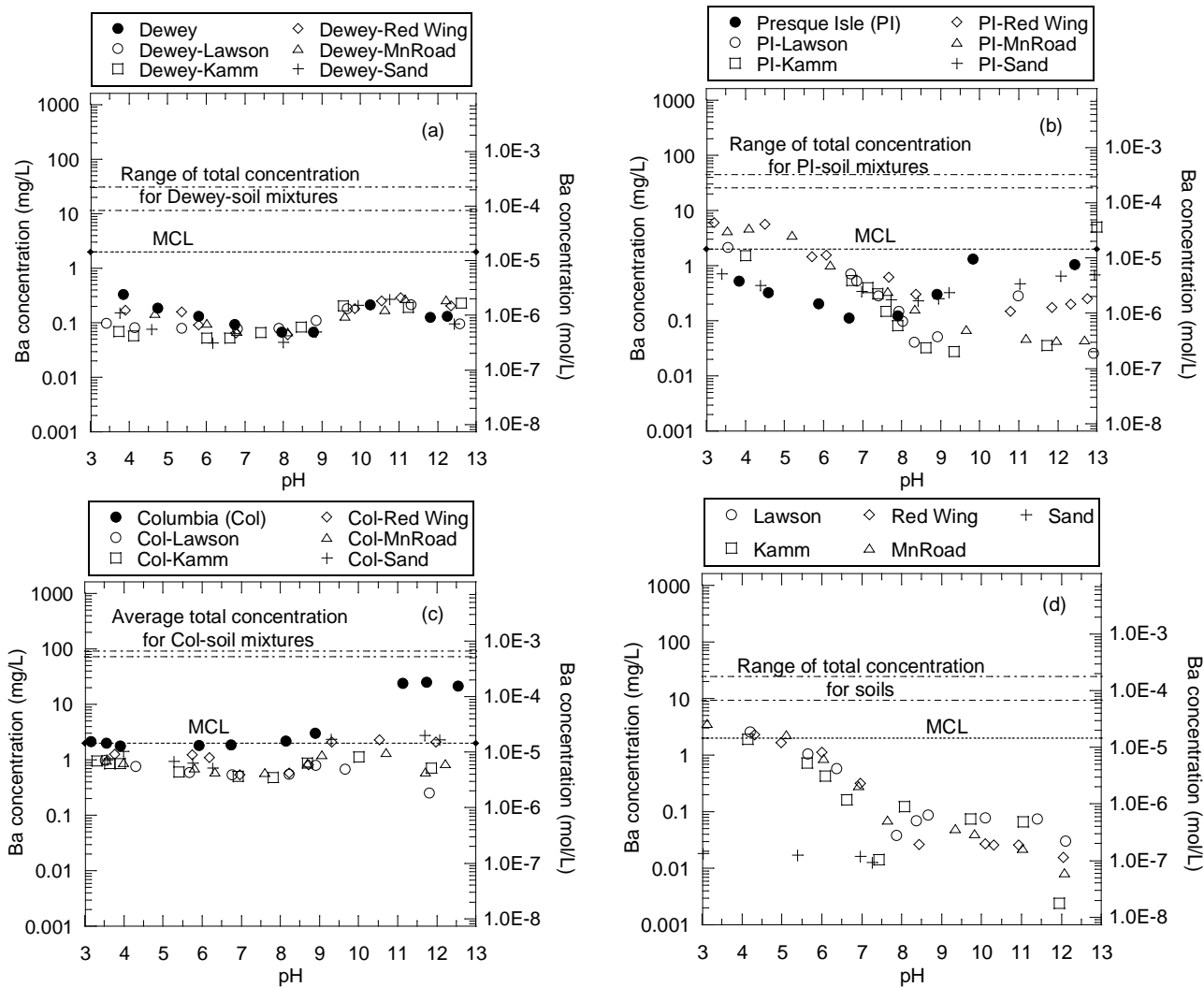
Figure 3.19. Concentrations of Ba as a function of pH in leachates from fly ashes, soil-fly ash mixtures, and soils: (a) Dewey fly ash, (b) Presque Isle fly ash, (c) Columbia fly ash, and (d) soils. Note: MCL = maximum contaminant level.
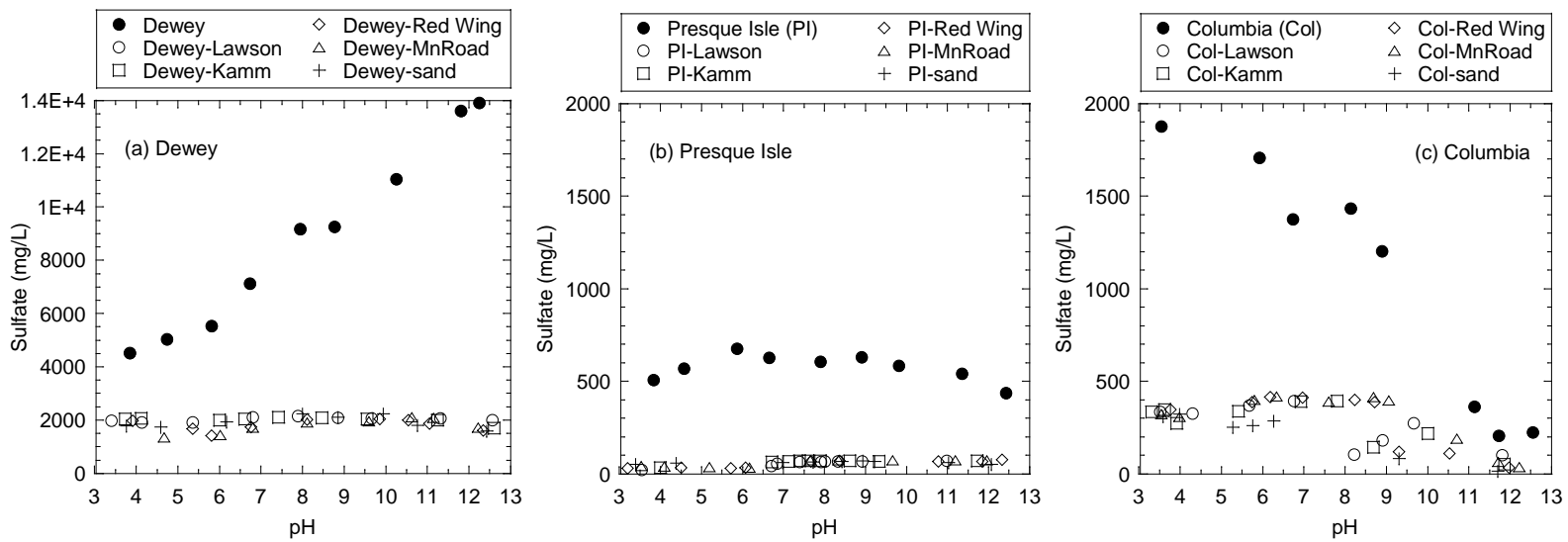
Figure 3.20. Sulfate concentrations as a function of pH in leachates from fly ashes and soil-fly ash mixtures: (a) Dewey fly ash, (b) Presque Isle fly ash, and (c) Columbia fly ash.
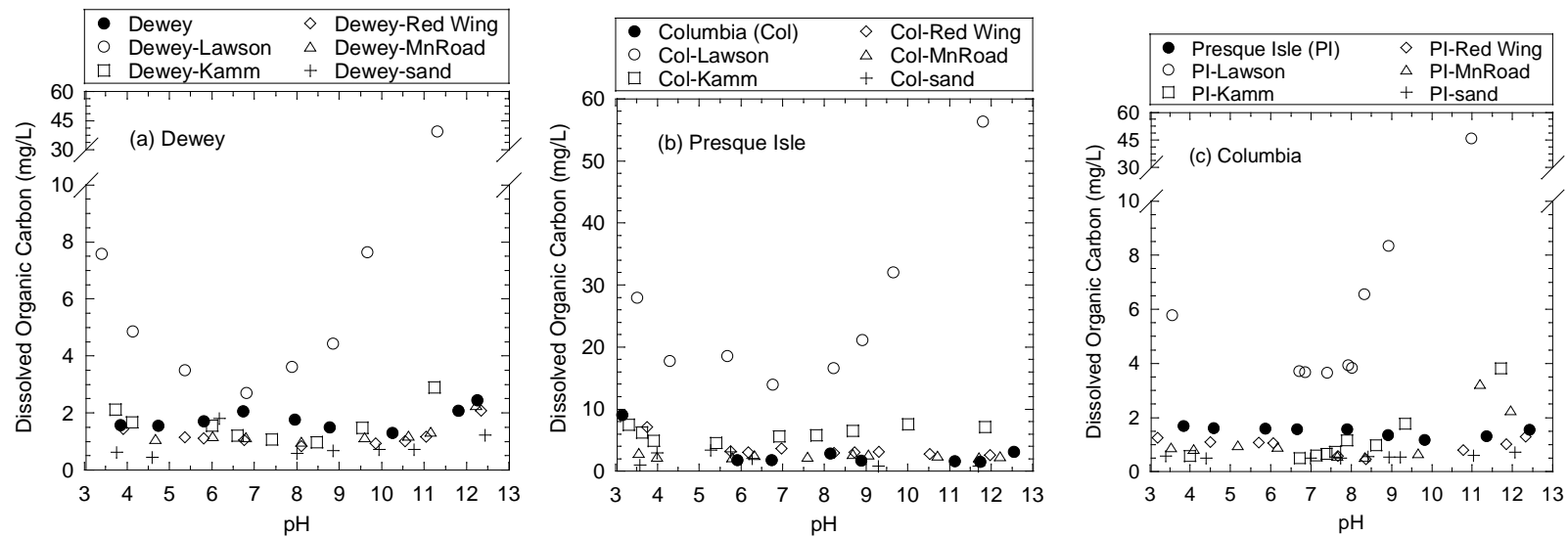
Figure 3.21. Dissolved organic carbon (DOC) concentrations as a function of pH in leachates from fly ashes and soil-fly ash mixtures: (a) Dewey fly ash, (b) Presque Isle fly ash, and (c) Columbia fly ash.
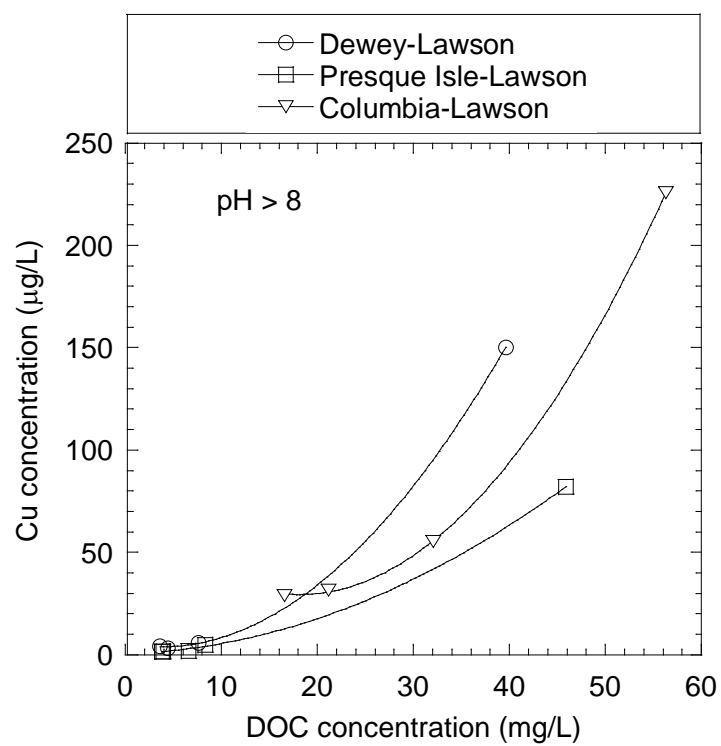
Figure 3.22.   Relationship between Cu and dissolved organic carbon (DOC) in
leachates from the mixtures of Lawson clay with Dewey, Presque Isle,
and Columbia fly ash at pH > 8.
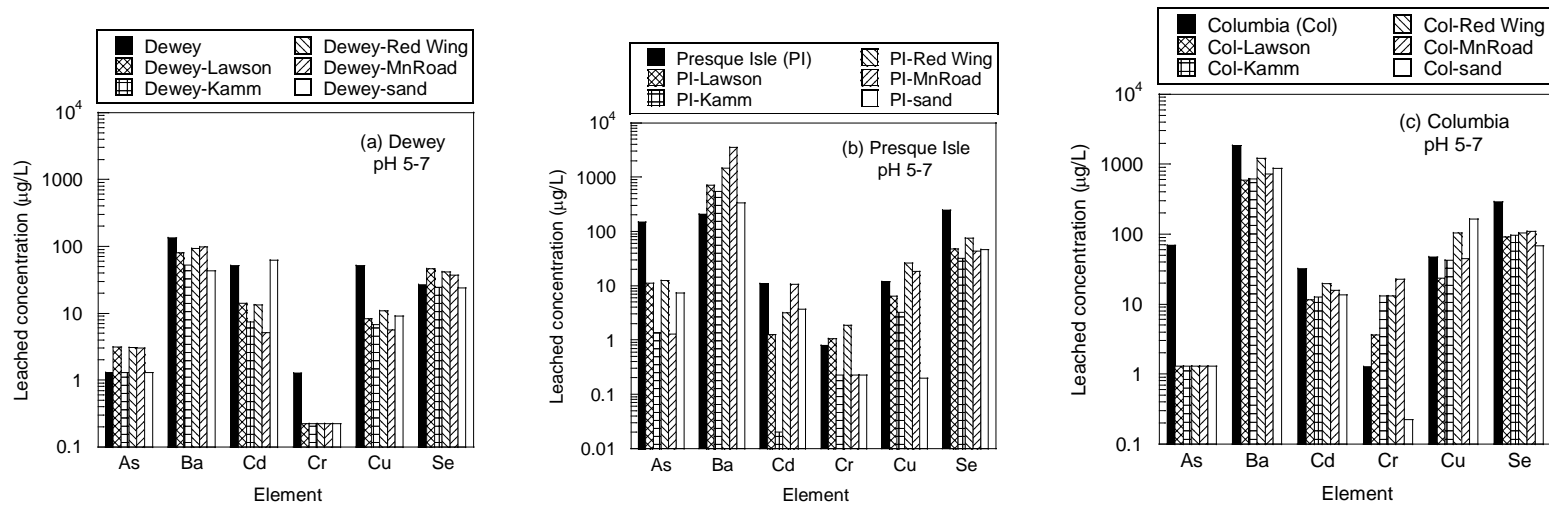
Figure 3.23. Concentrations of trace elements at pH 5-7 in leachates from fly ashes and soil-fly ash mixtures: (a) Dewey fly ash, (b) Presque Isle fly ash, and (c) Columbia fly ash.
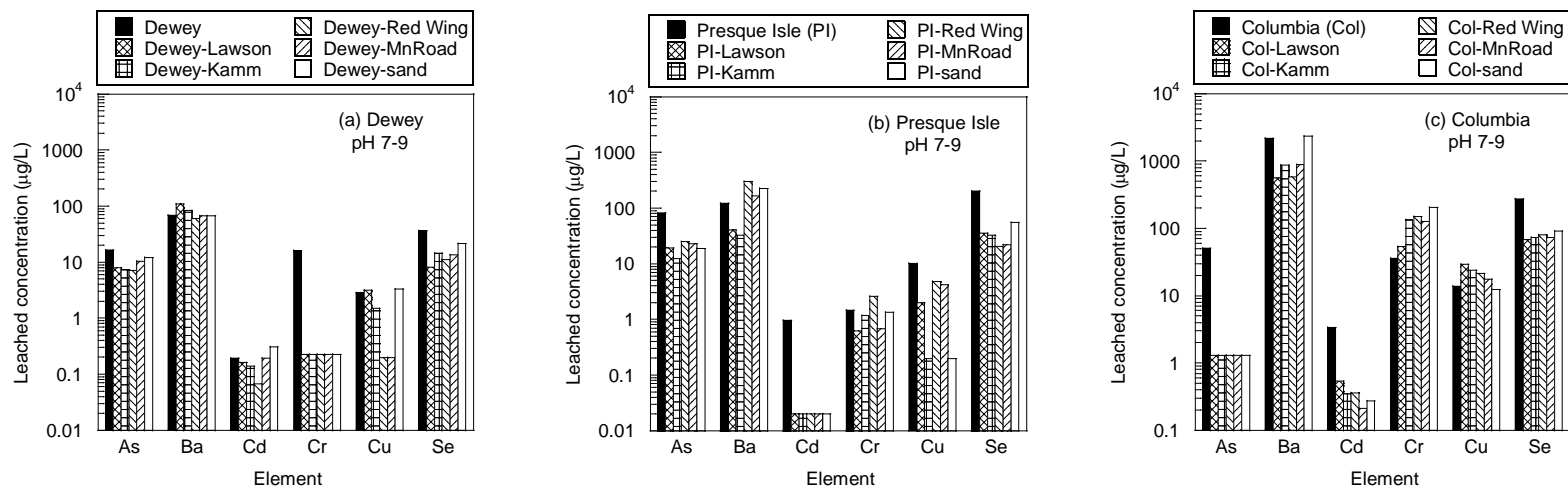
Figure 3.24. Concentrations of trace elements at pH 7-9 in leachates from fly ashes and soil-fly ash mixtures: (a) Dewey fly ash, (b) Presque Isle fly ash, and (c) Columbia fly ash.
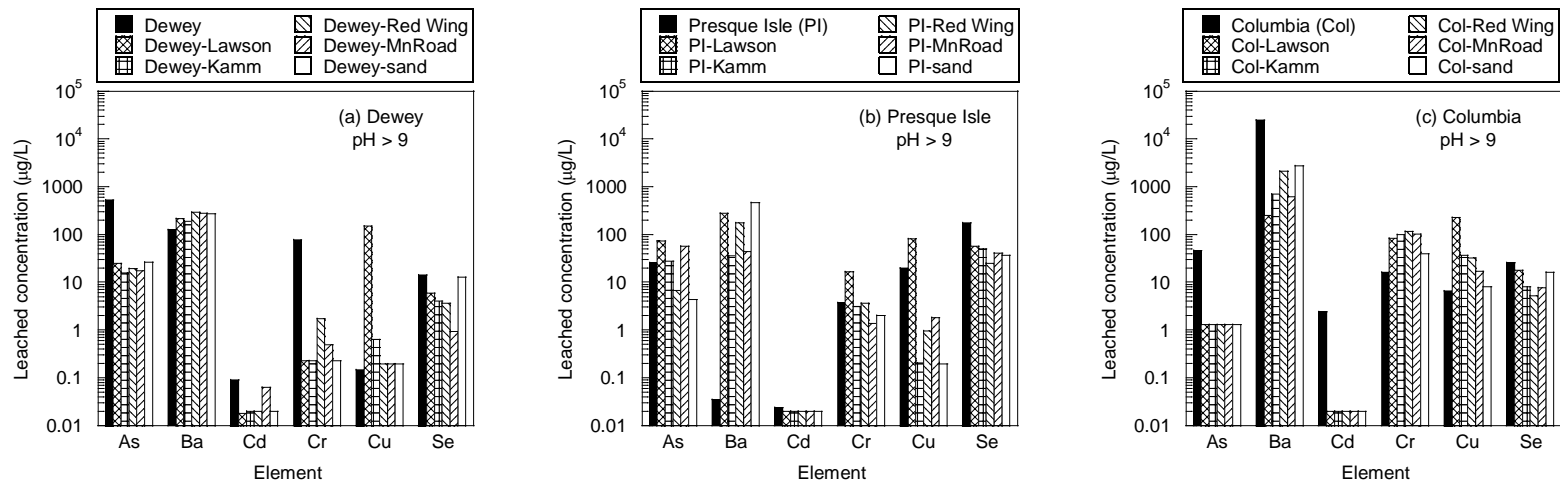
Figure 3.25. Concentrations of trace elements at pH > 9 in leachates from fly ashes and soil-fly ash mixtures: (a) Dewey fly ash, (b) Presque Isle fly ash, and (c) Columbia fly ash.

SECTION 4

GEOCHEMICAL MODELING

4.1 Introduction

Several leaching studies have identified two key equilibrium mechanisms controlling the release of constituents from combustion residues and leachate composition: solubility (dissolution-precipitation reactions) control and sorption control (Fruchter et al. 1990, Kosson et al. 1996, Dijkstra et al. 2002, Mudd et al. 2004, van der Sloot and Dijkstra 2004, Wang et al. 2004). Insight into mechanisms controlling the release of major and trace elements is needed for predicting solute concentrations in drainage from pavements employing soil stabilized with fly ash. If release is controlled by dissolution-precipitation reactions, geochemical equilibria models defined by thermodynamic data can be used to predict aqueous concentrations assuming equilibrium between the leachate and potential solubility-controlling solids (Garavaglia and Caramuscio 1994, Apul et al. 2005). However, if release of an element is limited by sorption reactions or dissolution kinetics, predicting solute concentrations requires more complex models incorporating sorption or kinetic algorithms (Eary et al. 1990, Fruchter et al. 1990, Mattigod et al. 1990, Reardon et al. 1995).

Release of elements controlled by dissolution-precipitation reactions begins as unstable mineral phases, mostly oxide anhydrous phases, dissolve when fly ash comes into contact with water (Reardon et al. 1995). Precipitation of more stable and less soluble hydrous secondary phases may also occur if the secondary phase has rapid dissolution-precipitation kinetics (Mattigod et al. 1990) and the dissolved concentration reaches saturation (Eary et al. 1990). Geochemical equilibria models are capable of

predicting the speciation of soluble species and saturation indices (SI) of minerals or solid phases for elements controlled by the precipitation-dissolution reactions defined by thermodynamic data (Allison et al. 1991). They have been used successfully to determine speciation of soluble species and to calculate saturation indices of solids and minerals phases in leachates from wastes and industrial byproducts (Fruchter et al. 1990, Garavaglia and Caramuscio 1994, van der Sloot 1996, Dijkstra et al. 2002, Mudd et al. 2004, Apul et al. 2005, Malviya and Chaudhary 2006, Cornelis et al. 2008b). However, none of the studies have investigated mechanisms controlling release of elements, especially trace elements from soil-fly ash mixtures.

The objective of this study was to examine whether leaching of elements from soil-fly ash mixtures is controlled by dissolution-precipitation reactions and to investigate how the type of soil and fly ash affect mechanisms controlling leaching. MINTEQA2 for Windows was used in this study to determine the predominant chemical species (oxidation state) of redox-sensitive elements in leachates and the state of saturation of the leachate with respect to mineral phases. Experimental data from pH-dependent leaching tests, including concentrations of cations and anions, leachate pH, and leachate E_h, were used as input. Tests were conducted on a range of soils and fly ashes used for soil stabilization in roadway construction projects in Wisconsin and Minnesota. The soils included organic clay, silt, clay, and sand. The fly ashes were cementitous Class C and off-specification high-carbon fly ashes.

4.2   Materials

Three fly ashes were used in this study: Dewey, Presque Isle, and Columbia fly ash. Table 4.1 presents information on each fly ash including type of coal and source, collection method, and type of storage and boiler used at the power plants. Dewey and Presque Isle fly ashes are referred to as 'off-specification' fly ashes because their

composition and properties do not meet the criteria for Class C or Class F ash in ASTM C 618. Columbia fly ash is classified as Class C fly ash (Table 4.2 and Table 4.3).

Four fine-grained soils (Lawson, Kamm, Red Wing, and MnRoad) and a sand (Portage) were used to represent the range of composition and properties of soils usually encountered in roadway construction in Wisconsin and Minnesota. Classifications and general properties of the soils are shown in Table 4.4. Lawson soil is highly plastic organic clay having the highest cation exchange capacity (CEC), which is consistent with the high organic matter and clay content of the soil. Kamm clay is moderately plastic clay having moderate CEC, organic matter, and clay content. Red Wing silt and MnRoad clay have low plasticity and relatively low percent clay and CEC. Portage sand is uniformly graded silica sand and has no measurable plasticity, clay fraction, or organic content.

Total elemental analysis of soils and fly ashes was conducted using US EPA Method 3050B (Table 4.5). Major elements for the soils and fly ashes include Al, Ca, Fe, K, Mg, Na, and P. The Red Wing and MnRoad soils contain greater amounts of Ca and Mg than the Lawson and Kamm soils, which is likely associated with dolomite $[Mg,Ca(CO_3)]$ and calcite $(CaCO_3)$ in these soils (Table 4.6). Columbia fly ash, a Class C fly ash, has the highest amount of Ca, which is consistent with results obtained from X-ray fluorescence spectrometry (XRF) (Table 4.3). Trace elements in the soils, including As, Cd, Co, Cr, and Zn, vary from non-detect to contents comparable to those in the fly ashes. Among the three fly ashes, Presque Isle fly ash contains the least As, Cd, Co, Cr, Cu, Mn, Mo, Sr, and Zn.

4.3   Experimental Methods

All of the fine-grained soils were prepared by air-drying followed by crushing until the soil passed the No. 10 sieve (2 mm opening). The air-dried fine-grained soils were

then ground again using a mortar and pestle until the consistency was a fine powder. The sand was air dried, but was not sieved or crushed. Soil-fly ash mixtures were prepared by mixing the air-dried and crushed soil with 20% by weight fly ash and deionized (DI) water to achieve a target gravimetric water content of 25%. A study by Taştan (2005) found that the highest level of stabilization (strength and stiffness) of organic soil can be achieved when 20% fly ash is used. Each mixture was thoroughly blended, stored in sealed plastic bags, and allowed to cure in a 100% humidity room for 7 d prior to testing.

Leaching tests were performed for pH from 3 to 13 on the soils, fly ashes, and soil-fly ash mixtures. The tests were conducted in HDPE bottles with 40 g of dry crushed material (soils, fly ashes, and soil-fly ash mixtures) having a particle size < 2 mm at a LS of 10. Deionized (DI) water was added to the bottle in combination with HNO_3 or KOH to obtain each desired endpoint pH. All samples were rotated end-over-end at 28 ± 2 rpm for 72 hr. Kinetic pH equilibrium tests showed that a 72-hr contact time was sufficient to achieve equilibrium. After rotation, the suspension was allowed to settle and the supernatant was withdrawn and filtered through a 0.45-μm membrane filter. An aliquot of unpreserved filtrate from each extraction was collected for measurement of pH and oxidation-reduction (redox) potential (E_h).

Leachates were analyzed to determine the concentration of dissolved organic carbon (DOC), sulfate, and dissolved major and minor elements, including Al, As, Ba, Ca, Cd, Cu, Cr, Fe, Mg, Na, Se, Sr, and Zn. DOC was analyzed on a Shimadzu TOC-5000 analyzer with ASI-5000 autosampler and Balston 78-30 high purity TOC gas generator. Organic carbon was converted to CO_2 by high-temperature combustion (690 ^{o}C) and quantified by a non-dispersive infrared detector. Sulfate concentration was determined by high-performance liquid chromatography (HPLC) using a Shimadzu

Liquid Chromatography Model LC-10ATvp equipped with system controller, degasser, auto-injector, column oven, and conductivity detector. Sulfate was separated from other anions on an Alltech Allsep anion column (51207 – 100 x 4.6 mm) using 4-mM p-hydroxybenzoic acid adjusted to pH 7.5 with lithium hydroxide as a mobile phase for elution. The column temperature was set at 35 ^{o}C and the flow rate was 1.0 mL/min. Elemental analysis was conducted with a Varian Vista-MPX ICP-OES using US EPA Method 6010B. Prior to ICP analysis, all samples were prepared and digested following Standard Methods 3010 and 3030 to reduce interference from organic matter and to convert metals associated with particulates to free metal forms (Clesceri et al. 1999).

Data corresponding to four pH values (Appendix D) were selected for modeling, representing slight acid conditions (pH 5-6), neutral conditions (pH 7-8), slightly alkaline conditions (pH 9-10), and highly alkaline conditions (pH >11).

4.4   Geochemical Analysis

MINTEQA2 was run in two different steps. The first step consisted of determining speciation (oxidation state) in the leachates, which was used to identify the predominant oxidation state of the redox-sensitive elements. The second step consisted of calculating aqueous concentrations of species in the leachates and the state of saturation of the leachates with respect to solids or minerals. Prior to the simulations, the MINTEQA2 database was amended with additional solubility constants of hydrolysis species, soluble complexes, and minerals of As- and Se-species (Appendix E) using the MINTEQA2 Database Editor.

4.4.1   Predominant Oxidation States

Speciation was determined by allowing redox and aqueous complexation reactions and using aqueous concentrations, pH and E_h data from the leaching tests as

input. When the equilibrium E_h and redox couple (oxidized and reduced form) are specified as equilibrium constraints, MINTEQA2 will calculate the amount of the element in each of the two oxidation states corresponding to the specified equilibrium E_h (Appendix F) (Allison et al. 1991). Once speciation of an element is known, the predominant oxidation state was determined for the following redox sensitive elements: As, Cr, Cu, Fe, and Se. Other elements observed in the leachate, including Al, Ba, Ca, Cd, Mg, Na, Sr, and Zn have low or no redox sensitivity elements and were not included in the speciation determination.

Predominant oxidation states identified from speciation results (Appendix G) are summarized in Table 4.7. The results showed that Cr and Se were mainly dominated by a reduced state [Cr(III) and Se(IV)], whereas As, Fe, and Cu existed in an oxidized state as As(V), Fe(III), and Cu(II). As, Cr, and Se are of particular of interest because they form oxyanions that can be present in a range of different species depending on the pH and redox potential. (Cornelis et al. 2008a).

Pentavalent arsenic [As(V)] was found to be a dominant oxidation state in all leachates, which is consistent with previous leaching studies on fly ash (Turner 1981, Fruchter et al. 1990, van der Hoek et al. 1996, Xu et al. 2001). Small amounts of As(III) can also co-exist with As(V) in fly ash (Shah et al. 2007). As a result, both As(V) and As(III) can be found in leachate. However, As(III) would be eventually oxidized to As(V) in the presence of oxygen (Cherry et al. 1979). Therefore, As(V) is the most likely predominant oxidation state under the leaching test conditions used in this study and was used in all subsequent analyses.

Trivalent chromium [Cr(III)] was found to be predominant for most of the leachates (82%). Rai and Szelmeczka (1990), Garavaglia and Caramuscio (1994), Reardon et al. (1995), and Cornelis et al. (2008a) also report Cr(III) as a dominant species in fly ash leachates. Solubility is an important factor determining speciation of Cr

101

in leachates because Cr(III) is less soluble than Cr(VI) (Rai and Szelmeczka 1990, Reardon et al. 1995). Concentrations of Cr in leachates from fly ashes at neutral pH were very low (1.53×10^{-8} – 3.19×10^{-7} mol/L, or 0.03%-4.68% of the available Cr for fly ash) relative to the total concentration of Cr in the solid (Table 4.5), indicating low solubility of Cr. Based on the solubility, Cr(III) is more likely a dominant state and was selected for modeling study for the entire pH range of 5-13.

Selenium (IV) was identified as the dominant Se species in all leachates (Appendix G). The presence of Se(IV) in both fly ash and fly ash leachates has been reported by Niss et al. (1993), Reardon et al. (1995), van der Hoek et al. (1996), Jackson and Miller (1999), Ariese et al. (2002), and Narukawa et al (2005). Calcium selenite [$CaSeO_3$] is believed to be a major source of the Se(IV) in fly ash (Seames and Wendt 2000). However, the aerobic conditions during leaching tests should favor the oxidized state [Se(VI)] as selenate [SeO_4^{2-}]. Mattigod et al. (1990) indicate that native Se should be oxidized to Se(IV) and Se(VI) in oxygenated environments. van der Hoek et. al (1996) also indicates that a minor amount of Se(VI) is present on the fly ash surface. Therefore, Se(VI) may also be present in fly ash leachate.

A confounding factor is the potential underestimate of E_h from the platinum (Pt) electrode used in this study. In natural waters, the redox potential measured by a Pt electrode in the presence of atmospheric oxygen can be approximately 0.4-0.5 V lower than the upper limit of water stability on E_h-pH diagram (Langmuir 1997). This means that the measured E_h is not thermodynamically accurate, and could possibly lead to an interpretation of reducing conditions by MINTEQA2 rather than oxidizing conditions [i.e., Se(IV) rather than Se(VI)].

Because speciation was not directly determined, the oxidation states can only be inferred from the measured redox potential and speciation results from MINTEQA2. No

conclusive evidence exists to define the state of Se in the system. Accordingly, Se was modeled in the reduced state [Se(IV)] and oxidized state [Se(VI)].

4.4.2   Aqueous Phase Composition and SI Calculation

Aqueous phase equilibrium composition and SI of all leachates with respect to solids or minerals were computed by allowing aqueous complexation reactions at fixed pH, as suggested by Apul et al. (2005). Input data included the leachate pH and aqueous concentration of the components. Components corresponding to the predominant oxidation states identified previously were selected for the simulations, which include Al^{3+}, As(V) as H_3AsO_4, Ba^{2+}, Ca^{2+}, Cd^{2+}, Cu^{2+}, Cr(III) as $Cr(OH)_2^+$, Fe^{3+}, Mg^{2+}, Na^+, Se(IV) as $HSeO_3^-$ or Se(VI) as SeO_4^{2-}, Sr^{2+}, Zn^{2+}, Cl^-, CO_3^{2-}, PO_4^{3-}, and SO_4^{2-}. Data for Cl^- and PO_4^{3-} concentrations were not available. Thus, the Cl^- concentration was approximated as the concentration of Na^+ (i.e., all Cl^- was from dissolution of NaCl), and all P was assumed to exist as PO_4^{3-}. The aqueous phase concentration analysis and the SI calculation were performed assuming equilibrium between the leachate and potential solubility-controlling minerals in the solid in an open system at 25 ^oC under the influence of atmospheric CO_2.

The conditions in the leaching test are assumed to be under influence of atmospheric $CO_{2(g)}$ because slurries and leachates were exposed to the atmosphere during preparation procedures before the leaching test and during sample collection and filtration after the leaching test. Atmospheric $CO_{2(g)}$ was also not precluded from a headspace of 20% of the leaching test bottle volume during the extraction. Accordingly, the system in this study is assumed to be in equilibrium with the partial pressure of atmospheric CO_2 at $10^{-3.5}$ atm (3.16 x10^{-4} atm, or 32.02 N/m^2) (Langmuir 1997, Mudd et al. 2004). Mudd et al. (2004) showed that including the effect of CO_2 is important for the

modeling study when the system is exposed to atmospheric CO_2 because CO_2 greatly affects the carbonate geochemistry in the leachate and the solubility-controlling solids.

MINTEQA2 accounts for deviations from ideality by expressing the *activity* of each species in solution rather than actual concentration. Single ion activity coefficients were computed via the Davies equation using the ionic strength of the solutions calculated from leachate concentrations (Appendix F). MINTEQA2 computes the state to which the solution is undersaturated or oversaturated with respect to various minerals and solids in the MINTEQA2 database (Appendix F) using the computed activities. Potential controlling-solids or minerals were identified based on the saturation index (i.e., $-1 \geq SI \leq +1$) and chemical composition consistent with the elements and minerals in fly ash and soil (Polettini and Pomi 2004, Dijkstra et al. 2006).

Log activity diagrams were created by graphing calculated log activities of elements of interest obtained from MINTEQA2 vs. leachate pH to discern whether the concentration of the elements of interest was controlled by mineral solubility. If release of an element is controlled by mineral solubility, calculated activities of elements of interest should consistently fall in close proximity to the stability/solubility line of the mineral or solid (Garavaglia and Caramuscio 1994). Elements that are not solubility-controlled are indicated by either significant oversaturation or undersaturation with respect to the solid/mineral stability line.

4.5   Mechanisms Controlling Leaching

Concentrations of Al, Ca, Fe, Mg, Ba, Cd, Cu, Cr, Sr, and Zn in the leachates from fly ash and soil-fly ash mixture were found to be consistent with the dissolution/precipitation of solid/minerals. Table 4.7 summarizes the dominant oxidation state and controlling-solids for each element of interest. Oxide and hydroxide minerals apparently control leaching of Al, Fe, Cr and Zn, and carbonate minerals appear to

control leaching of Mg and Cd. Leaching of Cu is likely controlled by oxides and/or carbonate minerals. Both carbonate and sulfate minerals are found to be controlling solids for Ca, Ba, and Sr depending on the leachate pH. Leaching of As and Se is not solubility-controlled and no geochemical reactions were elucidated based on the results from this study.

4.5.1   Oxide and Hydroxide Minerals

Leaching of Al, Fe, Cr, Cu, and Zn from the fly ashes and the soil-fly ash mixtures are most likely controlled by oxides and hydroxides minerals/solids (also see Section 4.4.2 for discussion on Cu). This is in good agreement with the XRF data (Table 4.3), especially Al and Fe, which show that a complex aluminosilicate comprised of Al_2O_3, Fe_2O_3, and SiO_2 was a major mineral, as has been reported in past studies (Theis and Wirth 1977a, Adriano et al. 1980). When fly ash is contacted with water, dissolution and hydrolysis of these oxides occur, and ultimately metal hydroxide precipitates are formed (Talbot et al. 1978, Khanra et al. 1998).

In the pH range of 5-13, concentrations of Al in all leachates are consistent with dissolution-precipitation of aluminum hydroxides, including amorphous $Al(OH)_3$, gibbsite [crystalline $Al(OH)_3$], and boehmite [γ-$AlO(OH)$] (Figure 4.1). Aluminosilicates, such as mullite ($Al_6Si_2O_{13}$), are believed to be a source of Al^{3+} that forms the aluminum hydroxide precipitates (Roy and Griffin 1984). Mullite could have been one of the controlling solids for Al in the fly ash and soil-fly ash leachates, but no conclusion can be made due to a lack of mineralogical data and the unavailability of mullite in the MINTEQA2 database. Fruchter et al. (1990), Mattigod et al. (1990), Murarka et al. (1992), Garavaglia and Caramuscio (1994), and Mudd et al. (2004) suggest that amorphous $Al(OH)_3$ and gibbsite control Al in fly ash leachates. Roy and Griffin (1984) found that amorphous

$Al(OH)_3$ and gibbsite control Al in acidic fly ash extracts, whereas boehmite, metastable phase of gibbsite, control Al in alkaline fly ash extracts

Iron is another major element for which the leachate concentration is controlled by a hydroxide mineral, ferrihydrite [$Fe(OH)_3$], over the pH range of 5-13 (Figure 4.2). Mattigod et al. (1990) and Garavaglia and Caramuscio (1994) also indicate that ferrihydrite is a controlling solid for Fe in fly ash leachates. Iron oxide, hematite [Fe_2O_3], can also be a controlling solid for Fe. Even though hematite is not predicted by MINTEQA2, it is found to be a primary mineral phase of Fe in the fly ashes (Table 4.3). Rai et al. (1987a) report that leaching of Fe from coal ash in short-term and long-term batch leaching experiments is controlled by solubility of both Fe oxide and hydroxide.

Amorphous $Cr(OH)_3$, crystalline $Cr(OH)_3$, and Cr_2O_3 have comparable solubilities and are identified as potential controlling oxide and hydroxide solids for Cr^{3+} (Figure 4.3). Reardon (1995) and Rai and Szelmeczka (1990) have reported that leaching of Cr^{3+} from fly ash is controlled by $Cr(OH)_3$. Chromium hydroxides are likely to be formed in the leachates, whereas Cr_2O_3 is originally present in the fly ashes (Table 4.3). The presence of Cr_2O_3 as a primary phase in fly ash was also reported by Theis et al. (1982). In materials enriched with Fe, Cr(III) can form solid solutions with amorphous iron hydroxide [$(Fe,Cr)(OH)_{3(am)}$] that are more likely to control aqueous Cr(III) concentrations rather than $Cr(OH)_3$ (Rai et al. 1987a, Rai and Szelmeczka 1990). However, data from this study could not be assessed with the formation of $(Fe,Cr)(OH)_{3(am)}$.

Zincite [ZnO] and zinc hydroxide [$Zn(OH)_2$] were identified as potential controlling solids for Zn^{2+} (Figure 4.4), although slight undersaturation with respect to these solids was observed. Zincite is a primary phase in fly ash (Theis et al. 1982) and has been reported to control leaching of Zn in fly ash leachate (Murarka et al. 1992, Garavaglia and Caramuscio 1994). Formation of $Zn(OH)_2$ could have occurred later in the leachates

after Zn leached from the solid phase. Shuman (1977) proposed that Zn may form $Zn(OH)_2$ upon sorption to hydrous Al oxide under alkaline conditions.

Undersaturation can be caused by insufficient availability of the element in the solid phase that can dissolve, incomplete dissolution due to slow kinetics, or sorption (Allison et al. 1991). To evaluate whether these factors may have contributed to the undersaturation that was observed, additional simulations were conducted over the pH range of 5-13 using "potential maximum concentrations" corresponding to complete dissolution of Zn in the solid phase.

When "potential maximum concentrations" were employed, the Zn activity increased 2-5 orders of magnitude and approached the solubility lines for zincite and zinc hydroxide throughout the pH range of 8-13 (Figure 4.4). An increase in leached concentrations implies that Zn^{2+} in the solid phases was incompletely dissolved. Undersaturation of Zn in the pH 8-13 in the leachates from fly ashes and soil-fly ash mixtures in this study may have been due to sorption processes. Sorption processes, such as surface complexation or surface precipitation, have been reported to control leaching of Zn from waste materials produced at high temperatures, such as bottom ash from municipal solid waste incinerator (MSWI) (Meima and Comans 1998, Dijkstra et al. 2006) and weathered steel slag (Apul et al. 2005). Sorption processes are reported to be responsible for undersaturation with respect to Zn-minerals in leachates from MSWI bottom ash (Polettini and Pomi 2004). In contrast, the undersaturation of Zn at pH 5-7 even with "potential maximum concentrations" is probably due to insufficient availability of Zn in the solid phase.

4.5.2 Carbonate Minerals

Carbonate minerals were found to control leaching of Mg and Cd in the pH range of 8-13. Dolomite $[Mg,Ca(CO_3)_2]$ and magnesite $[MgCO_3]$ have comparable solubilities and appear to be controlling solids for Mg (Figure 4.5). Garavaglia and Caramuscio (1994) identified dolomite as a controlling solid in fly ash leachates collected in lysimeter test cells. Apul et al. (2005) reports dolomite as a controlling solid in steel slag leachates obtained from pH stat leaching tests.

Simulations based on "potential maximum concentrations" were conducted to determine if sufficient Mg^{2+} was available to attain equilibrium with dolomite and magnesite at pH 5-7. Predictions from these simulations are shown in the lower row of Figure 4.5. Although the activities are closer to the stability lines, undersaturation is evident. This implies that undersaturation of Mg^{2+} at pH 5-7 is likely due to insufficient availability of Mg in the solid phase, which is similar to undersaturation in Zn in the same pH range.

Garavaglia and Caramuscio (1994), Apul et al. (2005), and Dijkstra et al. (2006) report brucite $[Mg(OH)_2]$ as a solid controlling Mg^{2+} in leachate at high pH. However, brucite is unlikely the controlling solid for Mg in these leachates despite the presence of periclase [MgO] in the three fly ashes. Based on the SI, all leachates are significantly undersaturated with respect to brucite (i.e. -8.84 > SI < -2.01) (Appendix H). However, formation of $Mg(OH)_2$ may have been responsible for the low or non-detectable level of Mg in some of the leachates under highly alkaline conditions (pH >11) (Warren and Dudas 1984).

Otavite $[CdCO_{3(s)}]$ was identified as potential solubility-controlling solids for Cd at pH > 8 (-2.3 > SI < -0.02) (Figure 4.6 and Appendix H). The finding is consistent with van der Sloot et al. (1996), whom reports otavite as a controlling solid for Cd in leachates

from MSWI bottom ash and from sewage amended soil at pH 6 and pH 9-10. Eary et al. (1990) also suggest that the Cd concentrations are controlled by otavite for fly ash leachate in slightly acid to alkaline pH.

Malachite $[Cu_2(OH)_2CO_3]$ and tenorite $[CuO]$ have comparable solubilities and appear to be potential controlling solids for Cu when pH > 7 (-2.0 > SI < -2.0) (Figure 4.7 and Appendix H). Fruchter et al. (1990) indicates that tenorite is the most likely solubility-controlling solid phase for Cu among other solids that may be present in near-surface geologic environments, including malachite, $Cu_4SO_4(OH)_6$, and $Cu(OH)_2$. Tenorite has also been found as a common ore mineral under oxidizing conditions (Rai et al. 1987a) similar to the extraction conditions in this study. Tenorite as a controlling solid for Cu in fly ash leachates is also identified by Eary et al. (1990), Fruchter et al. (1990), Murarka et al. (1992), and Garavaglia and Caramuscio (1994). However, malachite has been identified as a controlling solid for Cu in fly ash pond leachate by Theis and Richter (1979) and in MSWI bottom ash leachates by Dijkstra et al. (2006).

Undersaturation is evident for both Cd (Figure 4.6) and Cu (Figure 4.7), especially at pH 5-7 and for pH > 10. Even when "potential maximum concentrations" were used in the simulations, undersaturation was still pronounced (not shown). Substantial undersaturation, particularly under strongly alkaline conditions, is unanticipated when all Cd and Cu in the solid phases are assumed to dissolve.

Inspection of the species distribution of dissolved Cd and Cu complexes and their activities revealed that a majority of the dissolved Cd and Cu was present as $Cd(CO_3)_2^{2-}{}_{(aq)}$ and $Cu(CO_3)_2^{2-}{}_{(aq)}$ at concentrations several orders of magnitude higher than other dissolved Cd and Cu species. When $Cd(CO_3)_2^{2-}{}_{(aq)}$ was excluded and actual leachates concentrations were used in the simulations, the Cd^{2+} activity was close to saturation with respect to otavite for pH 8-13. With an exception in the pH range of 5-7, only slightly undersaturation was observed (Figure 4.8). Similarly, the Cu^{2+} activity became saturated

with respect to tenorite when actual leachates concentrations were used and $Cu(CO_3)_2^{2-}$ $_{(aq)}$ was excluded, except for pH 5-7 (Figure 4.9). Because simulations including the species $Cd(CO_3)_2^{2-}$$_{(aq)}$ and $Cu(CO_3)_2^{2-}$$_{(aq)}$ underestimate the activity of $Cd^{2+}$$_{(aq)}$ and $Cu^{2+}$$_{(aq)}$, undersaturation is predicted when soluble Cd and Cu concentrations are actually more than sufficient to saturation with respect to the minerals.

The significance of $Cd(CO_3)_2^{2-}$$_{(aq)}$ and $Cu(CO_3)_2^{2-}$$_{(aq)}$ is ambiguous as $Cd(CO_3)_2^{2-}$ $_{(aq)}$ has not been studied or reported as frequently as $CdCO_{3(aq)}$. Archer (1998) cites studies that report the formation constant for the double carbonate $[Cd(CO_3)_2^{2-}$$_{(aq)}]$, but only summarizes and discusses the formation constant for single carbonate $[CdCO_3^0$$_{(aq)}]$. This suggested that the significant carbonate species is $CdCO_{3(aq)}$ and that the double carbonate $Cd(CO_3)_2^{2-}$$_{(aq)}$ is less important species. Similarly, Bilinski et al. (1976) concludes that carbonate species are less significant for Cd than for other metals at concentrations representative of groundwater (i.e., $\sim10^{-6}$ M). The $Cu(CO_3)_2^{2-}$$_{(aq)}$ species is presumed insignificant like $Cd(CO_3)_2^{2-}$$_{(aq)}$. Based on the findings reported in Figure 4.8 and 4.9, simulations with $Cd(CO_3)_2^{2-}$$_{(aq)}$ and $Cu(CO_3)_2^{2-}$$_{(aq)}$ excluded are likely to provide more reasonable and reliable results than those with $Cd(CO_3)_2^{2-}$$_{(aq)}$ and $Cu(CO_3)_2^{2-}$$_{(aq)}$ included.

Simulations based on "potential maximum concentrations" with $Cd(CO_3)_2^{2-}$$_{(aq)}$ excluded predict undersaturation with otavite at pH 5-7 and oversaturation at pH > 9 (Figure 4.8). Undersaturation with respect to otavite observed at pH 5-7 is similar to those occurring for Mg^{2+} and Zn^{2+} in the same pH range, where availability in the solid phase limits dissolved concentrations. An increase of the Cd^{2+} activity relative to those obtained from leachate concentrations indicates that some of the Cd^{2+} in the samples has not dissolved, which is similar to Cu at pH 5-7 when "potential maximum concentrations" were used and $Cu(CO_3)_2^{2-}$$_{(aq)}$ was excluded in the simulations (Figure 4.9).

Undersaturation based on leachate concentrations and exclusion of double carbonate species for Cd at pH 5-13 (Figure 4.8) and for Cu at pH 5-7 (Figure 4.9) represents a system where adsorption and slow dissolution are logical explanations. If kinetic data is available and the activities plotted in the diagram based on the leachate concentrations do not change over time, perhaps slow dissolution kinetics is not the factor inducing the undersaturation observed. Then adsorption is more likely to be responsible for undersaturation of Cd and Cu in fly ash leachates, especially in neutral to alkaline pH range (Theis and Wirth 1977a). However, the conclusion of whether reaction kinetic or sorption is attributed to the undersaturation can not be made based on data from this study.

4.5.3   Carbonate and Sulfate Minerals

Carbonate and sulfate minerals were found to have a prominent role in controlling the leaching of Ca, Ba, and Sr depending on the leachate pH. Ca, Ba, and Sr follow a similar pattern as shown in Figure 4.10, 4.11, and 4.12. Sulfate minerals appear to control Ca, Ba, and Sr in the leachate at slightly acid to alkaline pH (pH 5 to 9-10), whereas carbonate minerals became more important for highly alkaline pH (pH >10).

Calcium and sulfur are among major soluble elements leached from fly ashes and soil-fly ash mixtures. Warren and Dudas (1984) found that most of the Ca leached from fly ash is associated with CaO on the surface of ash particles, and is relatively unstable compared with other major oxides present in fly ash (Elseewi et al. 1980). Sulfur leached from fly ash exists as sulfate (SO_4^{2-}) under oxidizing conditions (Fruchter et al. 1990). Sulfate concentrations in leachates from the fly ashes were found to be very high (1,411 to 13,912 mg/L), especially for the Dewey fly ash.

Gypsum [$CaSO_4$] and anhydrite [$CaSO_4.2H_2O$], which are commonly found in fly ash (Warren and Dudas 1985, Rai et al. 1987a), were identified as potential solubility-

controlling solids for Ca at slightly acid to alkaline pH (pH 5-9) (Figure 4.10). Slight undersaturation with respect to gypsum and anhydrite occurs in this pH range, which is probably due to incomplete dissolution of mineral phases or insufficient minerals in the solid phase. Under alkaline conditions, when carbonate species (CO_3^{2-}) become more important (Stumm and Morgan 1996), calcite [$CaCO_3$] and/or aragonite [$CaCO_3$] controls the Ca^{2+} activity. However, the leachates were oversaturated with respect to calcite at alkaline pH (pH>9). Kirby and Rimstidt (1994) also report oversaturation with respect to calcite in MSWI leachates.

Oversaturation with respect to calcite in the presence of gypsum is due to the common ion effect when Ca comes from sources other than dissolution of calcite (Langmuir 1997, Al-Barrak and Rowell 2006). Dissolution of gypsum that is much more soluble than calcite contributes Ca into the leachate, providing Ca as a common ion in the leachates and causing precipitation of calcite (Equation 1) (Langmuir 1997):

$$CaSO_4.2H_2O_{(s)} + 2HCO_3^- \rightarrow CaCO_3 + SO_4^{2-} + 2H_2O + CO_2 \qquad (1)$$
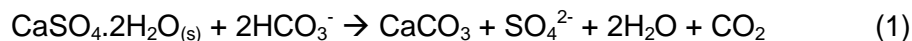
Other studies have reported that the Ca concentration in fly ash leachate is controlled by gypsum or anhydrite and calcite or aragonite. Roy and Griffin (1984) concluded that anhydrite controls leaching of Ca from fly ashes, but Ca concentrations in highly alkaline solutions in contact with atmospheric $CO_{2(g)}$ are controlled by calcite solubility. Mattigod et al. (1990) report that Ca concentrations in fly ash leachate are controlled by gypsum at acidic to neutral pH, and by calcite at alkaline pH. Both calcite and aragonite control the leaching of Ca from coal fly ash when the system is in equilibrium with atmospheric $CO_{2(g)}$ (Mudd et al. 2004). Calcite and aragonite have been identified by other studies (Warren and Dudas 1985, Kirby and Rimstidt 1994) as one of important carbonate minerals controlling Ca in combustion fly ash and MSWI leachates.

Dissolution and precipitation of gypsum and anhydrite also control sulfate concentration in fly ash leachate (Mudd et al. 2004), which reacts with Ba and Sr to form

Ba-sulfate and Sr-sulfate. Barium and Sr can also form sparingly soluble carbonate compounds (Fruchter et al. 1990). The behavior and geochemical controls of Ba and Sr are complex and related, as they can exist in pure sulfate or carbonate minerals and may also exist as Ba-Sr co-precipitates (McBride 1994).

The Ba concentration is independent of pH from pH 5 to 10 and is likely controlled by barite [$BaSO_4$], even though slight oversaturation is evident (Figure 4.11). In strongly alkaline pH (pH > 10), witherite [$BaCO_3$] is less soluble than barite (Eary et al. 1990). As a result, witherite controls Ba concentration over barite for pH > 10. Witherite controls Ba under alkaline conditions in ash leachates was also observed by Eary et al (1990) and Mudd et al.(2004).

The leaching behavior of Sr is analogous to Ca and Ba when sulfate and carbonate minerals are potential solubility controlling solid for Sr (Figure 4.12). Celestite [$SrSO_4$] was found to control leaching of Sr^{2+} at approximately pH 5-8, whereas strontianite [$SrCO_3$] was a dominant controlling mineral under alkaline conditions. Previous studies have also identified celestite as potential controlling solid for Sr in fly ash leachates at acid to slightly alkaline pH (Garavaglia and Caramuscio 1994, Reardon et al. 1995, Mudd et al. 2004). Eary et al. (1990) and Garavaglia and Caramuscio (1994) report that strontianite controls Sr at highly alkaline pH.

Some studies have reported the formation of Ba-Sr sulfate co-precipitate in fly ash leachates, yielding barite-celestite or $(Ba,Sr)SO_4$ (Eary et al. 1990, Fruchter et al. 1990, Mudd et al. 2004). In acidic to mildly alkaline pH, the leachates are approximately an order of magnitude oversaturated with respect to barite (Figure 4.11) and undersaturated with respect to celestite up to an order of magnitude (Figure 4.12). These characteristics are associated with the formation of a solid-solution of Ba-Sr sulfate (Ainsworth and Rai 1987), which has been noted by Eary et al. (1990), Fruchter et al. (1990), and Mudd et al. (2004).

Because Sr easily substitutes for Ba, substantial quantities of Sr could be removed from leachates in the form of a $(Ba,Sr)SO_4$ solid solution, the solubility of which is considerably lower than that of celestite (Reardon et al. 1995). In addition, celestite $(K_{sp} = 10^{-6.62})$ is less likely to precipitate due to its high solubility compared to barite $(K_{sp} = 10^{-9.88})$ and the lower solid phase concentration of Sr in the ashes and soils relative to Ba. As a result, undersaturation with respect to celestite and oversaturation with respect to barite were observed.

However, other studies have reported that Ba could be potentially controlled by both barite and $Ba(S,Cr)O_4$ solid solutions (Fallman 2000, Astrup et al. 2006). Therefore, the concentrations of Ba and Sr are potentially controlled by dissolution-precipitation of barite and celestite, $(Ba,Sr)SO_4$ solid solution or $Ba(S,Cr)O_4$ solid solution.

Oversaturation of the leachates with respect to carbonate minerals is again observed for witherite (Figure 4.11) and strontianite (Figure 4.12). For the case of witherite and strontianite, oversaturation of carbonate minerals observed may be due to (1) incomplete thermodynamic data for carbonate minerals and aqueous complexes in the MINTEQA2 database used in the study, (2) formation of more soluble nonstoichiometry (i.e., solid solution) and/or small (submicron) particle sizes of the carbonates in leachate rather than well-crystallized pure phases assumed in MINTEQA2, (3) different solution models used to define the mineral K_{sp} (some of the K_{sp} obtained from the literature reviews) and in the calculation of saturation index, (4) inhibition of carbonate nucleation by adsorbed substances, and (5) slow nucleation and precipitation rates that require times exceeding residence times of the water in the system of interest (Langmuir 1997). However, results acquired from this study can not evaluate the effect(s) of these factors on oversaturation conditions.

4.5.4 Non-Solubility Controlling Mechanism

No controlling solids were identified for selenium [both Se(IV) and Se(VI)] and arsenic [As(V)] for all fly ashes and soil-fly ash mixtures. The leachates were considerably undersaturated with respect to all selenite (-80.0 > SI < -1.1) and selenate solids (-72.0 > SI < -3.0) and most of the arsenate solids (-40.0 > SI < -5.5), except $Ba_3(AsO_4)_2$ (Appendix H and Appendix I). Even when "maximum potential concentrations" of As and Se were applied, equilibrium was not obtained for the solids or minerals available in MINTEQA2 database.

Cornelis et al. (2008a) report that Se can precipitate as calcium metalate compounds (e.g. $CaSeO_3.2H_2O$ for SeO_3^{2-} and $CaSeO_4.2H_2O$ for SeO_4^{2-}). However, the Se activities (both SeO_3^{2-} and SeO_4^{2-}) in all leachates were 4-20 orders of magnitude undersaturated to Ca-selenite and Ca-selenate compounds (Figure 4.13). The undersaturation is probably because Ca-selenite and Ca-selenate are highly soluble (Cornelis et al. 2008a). Smith and Martell (1976) also indicate that selenite and selenate minerals are too soluble to control leaching of Se. Significant undersaturation of SeO_3^{2-} and SeO_4^{2-} was also found with respect to the solubility of trivalent metal-selenite/selenate, such as $Fe_2(SeO_3)_3.2H_2O$ and $Fe_2(SeO_4)_3$ (Figure 4.13), and other divalent metals-selenite/selenate, such as Ba-, Mg-, and Sr-selenite/selenate (Appendix J).

These findings suggest that leaching of Se [both Se(IV) and Se(VI)] from fly ashes and soil-fly ash mixtures is not solubility-controlled. Previous studies have also reported the absence of solubility-controlling solids for Se in alkaline waste leachates (Fruchter et al. 1990, Murarka et al. 1992, Garavaglia and Caramuscio 1994). Cornelis et al. (2008a) indicate that adsorption and solid-solution formation with common minerals in alkaline waste reduces concentrations of oxyanions below saturation levels with

respect to metalate solubility. Johnston and Eagleson (1989) suggest that co-precipitation of selenate with sulfate minerals, such as gypsum and barite, can be a controlling mechanism for Se solubility. However, based on data in this study, no conclusion can be established regarding adsorption, solid-solution formation, or co-precipitation as a mechanism controlling Se leaching.

Arsenate [AsO_4^{3-}] can react with metals in solution (e.g. Al, Ca, Fe, and Mn) to form relatively insoluble metal arsenates (Yan-Chu 1994) in the same manner as Se. Arsenate is also a phosphate analogue and isomorphous replacement of phosphorus by arsenic in minerals, such as apatite [$Ca_5(PO)_4)_3(OH,F)$], is well known (Wagemann 1978). However, all leachates in this study were significantly undersaturated with respect to all arsenate minerals/solids included in the MINTEQA2 database (-40.0 > SI < -5.5), except $Ba_3(AsO_4)_2$ (Appendix H and Appendix I), indicating an absence of solubility controlling solids for As.

Bothe and Brown (1999) report that arsenate apatites, such as $Ca_5(AsO_4)_3(OH)$ and $Ca_4(OH)_2(AsO_4)_2.4H_2O$ [or $Ca_4(AsO_4)(OH).2H_2O$], are less soluble and only form when Ca activities are high. Hydrated Ca arsenates, such as $Ca_3(AsO_4)_2.xH_2O$ and $CaNaAsO_4.7.5H_2O$, have been reported by Cornelis et al. (2008a) as the most probable controlling solids for leaching of arsenate when Ca is abundant. However, all leachates were very undersaturated with respect to arsenate apatites (-40.0 > SI < -6.1) (Appendix H), suggesting that leaching of As from the fly ashes and soil-fly ash mixtures is not controlled by arsenate apatites.

Undersaturation of the leachates with respect to johnbaumite [$Ca_5(AsO_4)_3OH$], one of the arsenate apatites included in MINTEQA2 database, is illustrated in Figure 4.14. Under alkaline conditions, the calcium potential (pH-½pCa^{2+}) appears to be controlled by calcite rather than by johnbaumite. This is most likely because johnbaumite

is unstable relative to calcite in the presence of $CO_{2(g)}$, especially at pH > 8 (Nishimura et al. 1985).

Leachates were also undersaturated with respect to other arsenate minerals and solids. This is probably because arsenate salts of Al, Ca, Fe, and Mn generally are too soluble to control As(V) in leachates and in natural waters (Sadiq 1997, Hering and Kneebone 2002). Furthermore, the majority of arsenic containing minerals are slow to nucleate, and formation of some minerals requires very specific circumstances (Holm et al. 1979). For instance, johnbaumite $[Ca_5(AsO_4)_3OH]$ forms only when the calcium source is very pure, the pH is 9.5-10, and magnesium is absent (Bothe and Brown 1999), which are not the conditions encountered in this study. One or a combination of these factors could preclude formation of arsenate minerals containing major elements in this study.

Arsenate can also form sparingly soluble precipitates with trace metals, such as Ba, Cd, Cu, Mn, and Zn. Among these, barium arsenate $[Ba_3(AsO_4)_{2(s)}]$ is the least soluble As(V) solid $[Ks = 7.7x10^{-51}$, Frankenthal (1963)] and forms in natural environments (Wagemann 1978). Consequently, $Ba_3(AsO_4)_2(s)$ can be a potential controlling solid for As. In this study, $Ba_3(AsO_4)_{2(s)}$ was found as the only As-bearing solid where oversaturation was observed (Figure 4.15). Carbonate mineral (witherite $[BaCO_3]$) control the leaching of Ba under alkaline conditions, which is similarly to the case of johnbaumite. The reactions and activity ratio functions used to draw the solubility lines for SI = 0 and for $-1 \geq SI \leq 1$ in Figure 4.14 and 4.15 are summarized in Table 4.8.

As shown in Figure 4.15, arsenate is likely to precipitate as less soluble Ba-arsenate solid than more soluble Al-, Mg-, and Ca-arsenate solid/mineral. Within the experimental time frame, the leachates may not have been in equilibrium (oversaturated) with $Ba_3(AsO_4)_{2(s)}$. The system probably would have proceeded towards equilibrium through dissolution of $Ba_3(AsO_4)_{2(s)}$ had longer term tests been conducted. In this case,

trace element (i.e. Ba^{2+}) appears to be more significant than with major elements (i.e. Al, Mg, and Ca) in controlling the leaching of As fly ashes and soil-fly ash mixtures.

Other studies have reported mechanisms controlling As differently. Crecelius et al. (1986) and Frankenberger (2002) report that dissolved As concentrations in natural waters can be controlled either by the solubility of minerals containing As or by sorption or arsenic onto mineral phases. However, the absence of solubility controlling solids for leachate from fly ash has been acknowledged by Fruchter et al. (1990), Murarka et al. (1992), and Garavaglia and Caramuscio (1994). Others report that leaching of As(V) from fly ashes is associated with dissolution-precipitation of As_2O_5 from fly ash and sorption-desorption of dissolved arsenate onto Fe_2O_3 and Al_2O_3 on fly ash particles, and onto dissolved Fe- and Al-hydroxides in aqueous solutions (Xu et al. 2001). Therefore, leaching of As in this study may involve in dissolution-precipitation of arsenate solids/minerals, kinetics of dissolution-precipitation, or sorption on mineral phases.

4.6 Consistency in Leaching Mechanisms for Fly Ashes and Soil-Fly Ash Mixtures

The consistency in leaching mechanism is observed in most of the major and trace element studied regardless of whether leaching was from a fly ash alone or a soil-fly ash mixture. Similar controlling mechanisms (dissolution-precipitation or sorption), similar controlling factors (such as pH, redox conditions, ionic strength, and ionic composition of solute), and chemistry of a particular element are believed to be important factors leading to the consistency.

van der Sloot (1996) and van der Sloot et al. (1996, 2007) report the consistency in leaching behavior of elements from various types of waste (such as coal fly ash, MSWI fly ash, MSWI bottom ash, sewage sludge), stabilized wastes (such as cement-stabilized MSWI fly ash, stabilized waste construction materials), and soils. The studies

concluded that similar controlling mechanisms (e.g. solubility control or sorption control) and controlling factors (e.g. pH, redox conditions) are responsible for the consistency in leaching behaviors observed.

Even though dissolution-precipitation reactions were unable to explain the undersaturation observed at pH 5-7 in many elements, the calculated activities in all leachates are consistent and should be associated with similar controlling mechanisms, such as sorption process or kinetic or limited availability in the solid phases. As and Se were not solubility-controlled. However, the calculated activities as a function of pH in all leachates were very comparable and consistent. Similar controlling mechanisms, such as sorption, solid-solution or co-precipitation is also anticipated for As and Se.

4.7   Conclusions

Mechanisms controlling the leaching of major and trace elements from soil stabilized with fly ash were investigated using the equilibrium geochemical code MINTEQA2 and data from pH-dependent leaching tests conducted on three fly ashes (Dewey, Presque Isle, and Columbia) and mixtures of the fly ashes with five soils (Lawson, Kamm, Red Wing, MnRoad, and sand).

Speciation analysis conducted with MINTEQA2 indicated that As, Fe, and Cu exist in an oxidized state [As(V), Fe(III), and Cu(II)], whereas Cr and Se are in a reduced state [Cr(III) and Se(IV)]. However, redox potential (E_h) measured from platinum (Pt) electrode may underestimate the true redox conditions in the system. Oxidation states calculated by geochemical modeling using only measured E_h from Pt electrode should be cautiously interpreted.

Dissolution-precipitation reactions identified as the mechanisms controlling aqueous concentrations of many of the major and trace elements (Al, Ba, Ca, Cd, Cr, Cu, Fe, Mg, Sr, and Zn) leached from the fly ash and the soil-fly ash mixtures with oxide,

hydroxide, sulfate, and carbonate solids. These minerals/solids are either originally present in fly ash or form in the leachate. Oxide and hydroxide minerals apparently control leaching of Al, Fe, Cr and Zn whereas carbonate minerals predominantly control leaching of Mg and Cd. Leaching of Cu is controlled by oxide and/or carbonate minerals. Both carbonate and sulfate minerals are controlling solids for Ca, Ba, and Sr depending on pH of the leachate. Leaching of As and Se are not solubility-controlled and geochemical reactions controlling the concentration of the elements could not be identified.

The aqueous concentration as a function of pH for each element show a similar tendency and consistency in controlling mechanism regardless of whether leaching was from a fly ash alone or a soil-fly ash mixture, which is believed to be determined by similar factors, such as controlling mechanism, chemistry of a particular element, and environmental conditions (e.g. pH, redox conditions, ionic strength, and ionic composition of solute).

The presence of some species can underestimate the predicted activity of free ion in the solution. In this study, the presence of $Cd(CO_3)_2^{2-}{}_{(aq)}$ and $Cu(CO_3)_2^{2-}{}_{(aq)}$ significantly underestimate the activity of $Cd^{2+}{}_{(aq)}$ and $Cu^{2+}{}_{(aq)}$. The presence or absence of these species should be validated. Undersaturation observed in many elements (i.e., Cu, Cd, Zn, and Mg) at pH 5-7 is likely to be associated with sorption process, slow dissolution kinetic, or availability in the solid phases. Incorporation the geochemical model with sorption process or reaction kinetic or solid-solution formation should improve the prediction of elements showing undersaturation, and probably would be able to identify the mechanisms controlling As and Se.

Table 4.1.   Coal source, fly ash collection method, storage type, and boiler type of the power plants producing Dewey, Presque Isle, and Columbia fly ashes.

Information	Dewey[1]	Presque Isle[1]	Columbia[2]
Company	Alliant Energy	WE Energy	Columbia Power Station (Unit 2)
Location	Cassville, WI	Marquette, MI	Portage, WI
Type of Coal and Source	Sub-Bituminous	Bituminous	Sub-Bituminous
	80% Montana Coal with Colorado or Petroleum Coke	100% Colorado Bituminous	Wyoming Power River Basin coal with Colorado or Petroleum Coke
Collection Method	Electrostatic	Fabric Filter	Electrostatic
Storage Type	Dry Silo	Dry Silo	Dry Silo
Type of Boiler	Cyclone	Front Wall/Tangential	Pulverized
Combustion Temperature (°F)	2000[3]	3000-3200[4]	2450[3]

Source: [1]Sauer (2006); and [2]Acosta (2003), [3]Alliant Energy, and [4]WE Energy.

Table 4.2.   Properties of Dewey, Presque Isle, and Columbia fly ashes along with chemical and physical criteria for Class C and Class F fly ashes stated in ASTM C 618.

Chemical Requirements	ASTM Requirements		Dewey	Presque Isle	Columbia
	Class F	Class C			
$SiO_2 + Al_2O_3 + Fe_2O_3$ (%)	≥ 70	≥ 50	19.04[1]	59.65[1]	58.88[1]
SO_3 (%)	≤ 5	≤ 5	-	-	3.7[3]
Moisture Content (%)	≤ 3	≤ 3	0.44	0.18	0.06
Loss on Ignition (%)	≤ 6	≤ 6	49.1[1]	32.4[1]	0.98[1]
Physical Requirements	ASTM Requirements		Dewey[2]	Presque Isle[2]	Columbia[4]
	Class F	Class C			
Fineness (%)	≤ 34	≤ 34	12.7	39.2	14.4
Strength Activity @ 7 d (%)	≥ 75	≥ 75	82.7	48.5	95.8

Source: [1]X-Ray Fluorescence Spectrometry; [2]Sauer (2006); [3]Bin-Shafique et al. (2002); and [4]Acosta et al. (2003).

Table 4.3.   Chemical compositions of Dewey, Presque Isle, and Columbia fly ashes along with the composition of typical Class C and Class F fly ashes.

Chemical Species	Percent of Composition				
	Typical Class F[1]	Typical Class C[1]	Dewey[2]	Presque Isle[2]	Columbia[2]
CaO	9	24	9.43	2.99	26.86
SiO_2	55	40	9.43	36.07	33.77
Al_2O_3	26	17	7.43	19.94	19.34
Fe_2O_3	7	6	2.18	3.64	5.77
MgO	2	5	2.16	1.06	5.64
Na_2O	-	-	5.44	1.02	2.05
K_2O	-	-	0.36	0.73	0.35
Cr_2O_3	-	-	0.02	0.01	0.01
TiO_2	-	-	0.56	0.59	1.55
MnO	-	-	0.02	0.01	0.04
P_2O_5	-	-	0.156	0.56	0.814
SrO	-	-	0.38	0.19	0.38
BaO	-	-	0.7	0.23	0.68

Source: [1]ACAA(2003); and [2]X-Ray Fluorescence Spectrometry (XRF).

Table 4.4.   Sampling locations and properties of soils used in study.

Sample	Sampling Location	USCS[1] Soil Classification		Properties					
		Group Symbol	Group Name	Liquid Limit	Plastic Limit	Percent Fines (%)	Percent Clay (%)	Organic Matter Content (%)	CEC (cmol$_c$/kg)
Lawson	Hwy 11 Green County, WI	OL-OH[2]	Organic clay[2]	50[2]	19[2]	97[2]	54[2]	6.3	45
Kamm	McFarland, Dane County, WI	CL-CH[3]	Lean clay/fat clay	48[4]	30[4]	91[4]	38[4]	2.0	25
Red Wing	Red Wing, Goodhue County, Mn	ML[5]	Silt[5]	28[5]	11[5]	88[5]	6[5]	1.2	8
MnRoad	I-94 Wright County, WI	CL[5]	Lean clay[5]	26[5]	9[5]	60[5]	15[5]	1.5	19
Sand	Portage County, WI	SP[6]	Poorly graded sand[6]	Non-plastic	Non-plastic	Non-plastic	0	0.0	0

Note: [1] Unified Soil Classification System; [2] Tastan (2005); [3] Department of Natural Resources, WI; [4] Park (2007); [5] Gupta et. Al. (2006); [6] Lee and Benson (2004).

Table 4.5.   Solid-phase concentration (mg/kg) from total elemental analysis of soils and fly ashes.

Element	Solid phase concentration (mg/kg)							
	Soil					Fly Ash		
	Lawson	Kamm	Red Wing	MnRoad	Sand	Dewey	Presque Isle	Columbia
Ag	0.06	0.05	<0.00048*	0.03	<0.00048*	0.50	0.19	0.55
Al	24,770	17,510	8577	11,770	25.74	28,280	19,610	75,230
As	13.51	13.06	8.49	8.55	4.16	79.63	11.91	28.11
B	55.04	44.51	31.53	35.82	9.22	509	600	610
Ba	244	168	93.38	151	<0.00003*	575	1279	3621
Be	0.88	0.69	0.31	0.46	<0.00001*	1.70	1.91	2.64
Ca	6641	5180	43,760	28,790	135	49,740	17,770	246,300
Cd	0.89	0.36	0.37	0.41	0.01	1.26	0.61	1.51
Co	<0.00016*	<0.00016*	<0.00016*	1.01	<0.00016*	4.99	<0.00016*	5.60
Cr	33.35	26.90	16.56	21.89	0.25	34.05	12.45	60.44
Cu	20.89	21.52	11.44	12.97	0.99	145	26.20	179
Fe	19,920	18,820	11,750	13,010	144	12,790	13,240	20,270
K	3,022	1869	1788	2259	9.12	4572	1074	3111
Li	16.73	11.18	7.75	11.43	<0.00029*	28.30	27.16	29.80
Mg	5394	5375	16,840	9992	80.52	10,010	3290	24,650
Mn	929	760	401	551	1.32	150	39.27	176
Mo	0.60	<0.00052*	<0.00052*	<0.00052*	<0.00052*	177	28.65	7.22
Na	99.17	78.62	696	424	143	25,561	1,162	8,692
Ni	24.39	23.03	13.51	18.49	0.20	1001	157	44.96
P	1087	531	589	395	<0.00313*	649	2325	3357
Pb	51.35	14.08	8.03	7.39	<0.00085*	20.46	20.79	27.91
Sb	5.27	3.44	1.64	2.24	<0.00344*	<0.00344*	1.93	7.65
Se	<0.00118*	<0.00118*	<0.00118*	<0.00118*	<0.00118*	2.11	4.31	9.43
Sn	3.17	1.45	2.85	1.60	7.87	34.17	13.20	8.45
Sr	20.75	23.40	41.34	36.30	0.85	1385	968	1622
Tl	<0.00404*	<0.00404*	<0.00404*	<0.00404*	<0.00404*	<0.00404*	<0.00404*	<0.00404*
V	55.62	51.89	32.46	50.41	<0.00024*	1514	406	198
Zn	2522	74.70	46.64	61.34	29.84	97.27	34.54	94.11

Note: *concentration below method detection limit.

Table 4.6.   Mineral constituents of soils determined by X-ray diffraction (XRD).

Mineral Constituents	Chemical Formula	Weight Percent (%)			
		Lawson	Kamm	Red Wing	MnRoad
Quartz	SiO_2	52	48	46	44
Plagioclase	$(Na,Ca)AlSi_3O_8$	16	15	8	9
K-Feldspar	$KAlSi_3O_8$	7	8	5	4
Calcite	$CaCO_3$	NA	NA	2	2
Dolomite	$(Ca,Mg)CO_3$	3	2	9	6
Kaolinite	$Al_2Si_2O_5(OH)_4$	2	2	2	2
Chlorite	$(Mg,Al)_6(Si,Al)_4O_{10}(OH)_8$	0.2	0.2	1	1
Illite/Mica	$KAl_2(Si_3AlO_{10})(OH)_2$	6	6	2	3
Montmorillonite	$Na_{0.3}(Al,Mg)_2Si_4O_{10}(OH)_2 \cdot xH_2O$	15*	19*	25	29

Note: *randomly ordered mixed-layer illite/smectite with 90% smectite layer, NA = not
     applicable.

Table 4.7.   Speciation and Controlling Solids for Elements.

Element	Speciation	Solubility-Controlling Solids
Al	Al(III)	Amorphous $Al(OH)_3$, gibbsite [crystalline $Al(OH)_3$], and boehmite [γ-AlO(OH)]
As	As(V)	None
Ba	Ba(II)	Barite [$BaSO_4$] and witherite [$BaCO_3$]
Ca	Ca(II)	Gypsum [$CaSO_4$], anhydrite [$CaSO_4.2H_2O$], calcite [$CaCO_3$], and aragonite [$CaCO_3$]
Cd	Cd(II)	Otavite [$CdCO_3$]
Cu	Cu(II)	Tenorite [CuO], and malachite [$Cu_2(CO_3)(OH)_2$]
Cr	Cr(III)	Amorphous $Cr(OH)_3$, crystalline $Cr(OH)_3$, and Cr_2O_3
Fe	Fe(III)	Ferrihydrite [$Fe(OH)_3$]
Mg	Mg(II)	Dolomite [$Mg,Ca(CO_3)_2$] and magnesite [$MgCO_3$]
Se	Se(IV) or Se(VI)	None
Sr	Sr(II)	Celestite [$SrSO_4$] and strontianite [$SrCO_3$]
Zn	Zn(II)	Zincite [ZnO] and zinc hydroxide [$Zn(OH)_2$]

Table 4.8. Reactions and activity ratio functions for calcite, witherite, johnbaumite, and $Ba_3(AsO_4)_{2(s)}$ at SI = 0 and $-1 \geq SI \leq 1$.

Mineral	Reaction	Activity Ratio Function	y-Intercept for SI = 0	y-Intercept for $-1 \geq SI \leq 1$
Calcite [$CaCO_3$]	$Ca^{2+} + CO_{2(g)} + 2H_2O = CaCO_{3(s)} + 2H^+$ (K_1 = -9.67)	$(pH-\frac{1}{2}pCa^{2+}) = b_1$	b_1 = 6.56	$b_1^* = b_1$ -1 = 5.56 $b_1^{**} = b_1$+1 = 7.56
Witherite [$BaCO_3$]	$Ba^{2+} + CO_{2(g)} + 2H_2O = BaCO_{3(s)} + 2H^+$ (K_2 = -9.58)	$(pH-\frac{1}{2}pBa^{2+}) = b_2$	b_2 = 6.51	$b_2^* = b_2$ -1 = 5.51 $b_2^{**} = b_2$+1 = 7.51
Johnbaumite [$Ca_5(AsO_4)_3OH$]	$5Ca^{2+} + 3H_2AsO_4^- + OH^- = Ca_5(AsO_4)_3OH + 6H^+$ (K_3 = -15.26)	$(pH-\frac{1}{2}pCa^{2+}) = a_3(pH+pH_2AsO_4^-)+b_3$	b_3 = 2.93	$b_3^* = b_3$ -1 = 1.93 $b_3^{**} = b_3$+1 = 3.93
$Ba_3(AsO_4)_2$	$3Ba^{2+} + 2H_2AsO_4^- = Ba_3(AsO_4)_2 + 4H^+$ (K_4 = 13.39)	$(pH-\frac{1}{2}pBa^{2+}) = a_4(pH+pH_2AsO_4^-)+ b_4$	b_4 = -2.23	$b_4^* = b_4$ -1 = -3.23 $b_4^{**} = b_4$+1 = -1.23

Note: _____ stability line for SI = 0 and - - - - - stability line for $-1 \geq SI \leq 1$ in Figure 4.14 and 4.15.
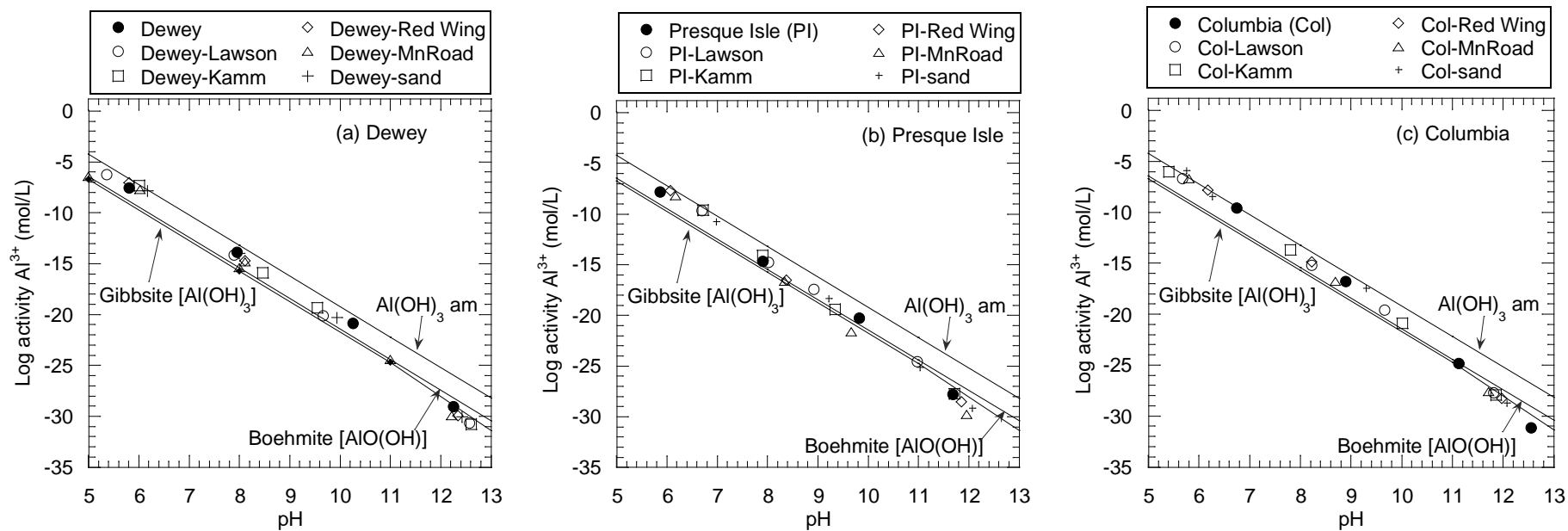
Figure 4.1.   Log activity of Al^{3+} vs. pH in leachates from fly ashes and soil-fly ash mixtures: (a) Dewey fly ash, (b) Presque Isle fly ash, and (c) Columbia fly ash.
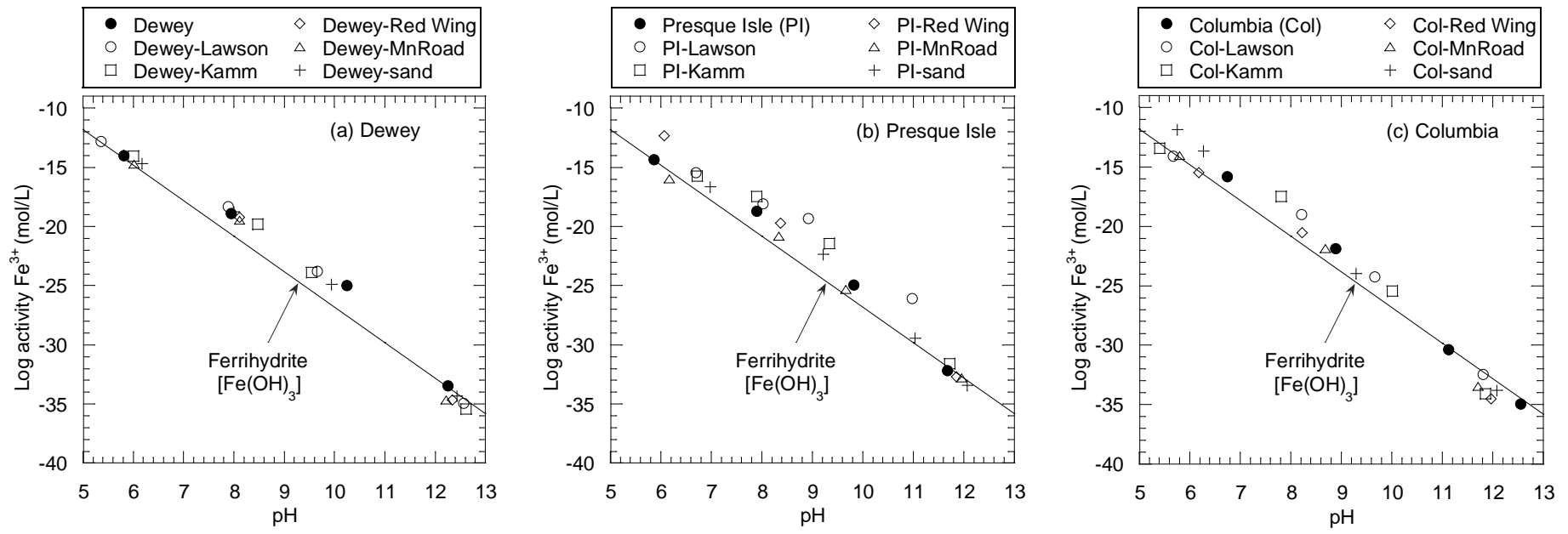
Figure 4.2.   Log activity of Fe^{3+} vs. pH in leachates from fly ashes and soil-fly ash mixtures: (a) Dewey fly ash, (b) Presque Isle fly ash, and (c) Columbia fly ash.
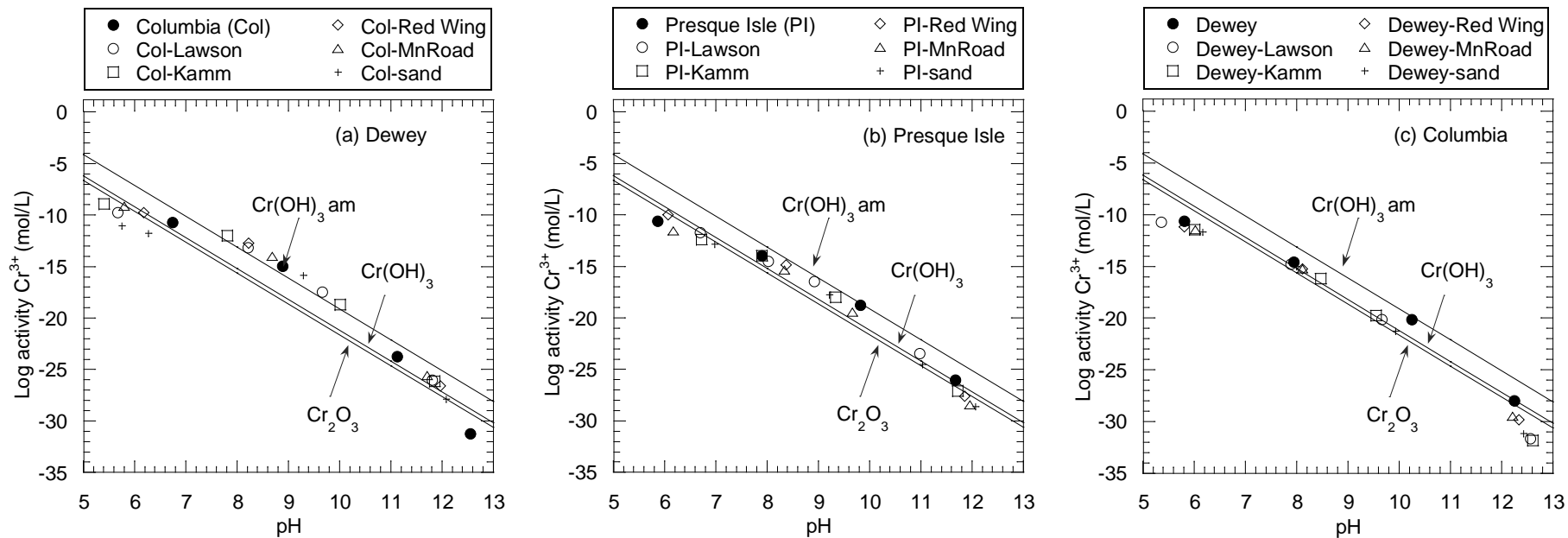
Figure 4.3. Log activity of Cr^{3+} vs. pH in leachates from fly ashes and soil-fly ash mixtures: (a) Dewey fly ash, (b) Presque Isle fly ash, and (c) Columbia fly ash.
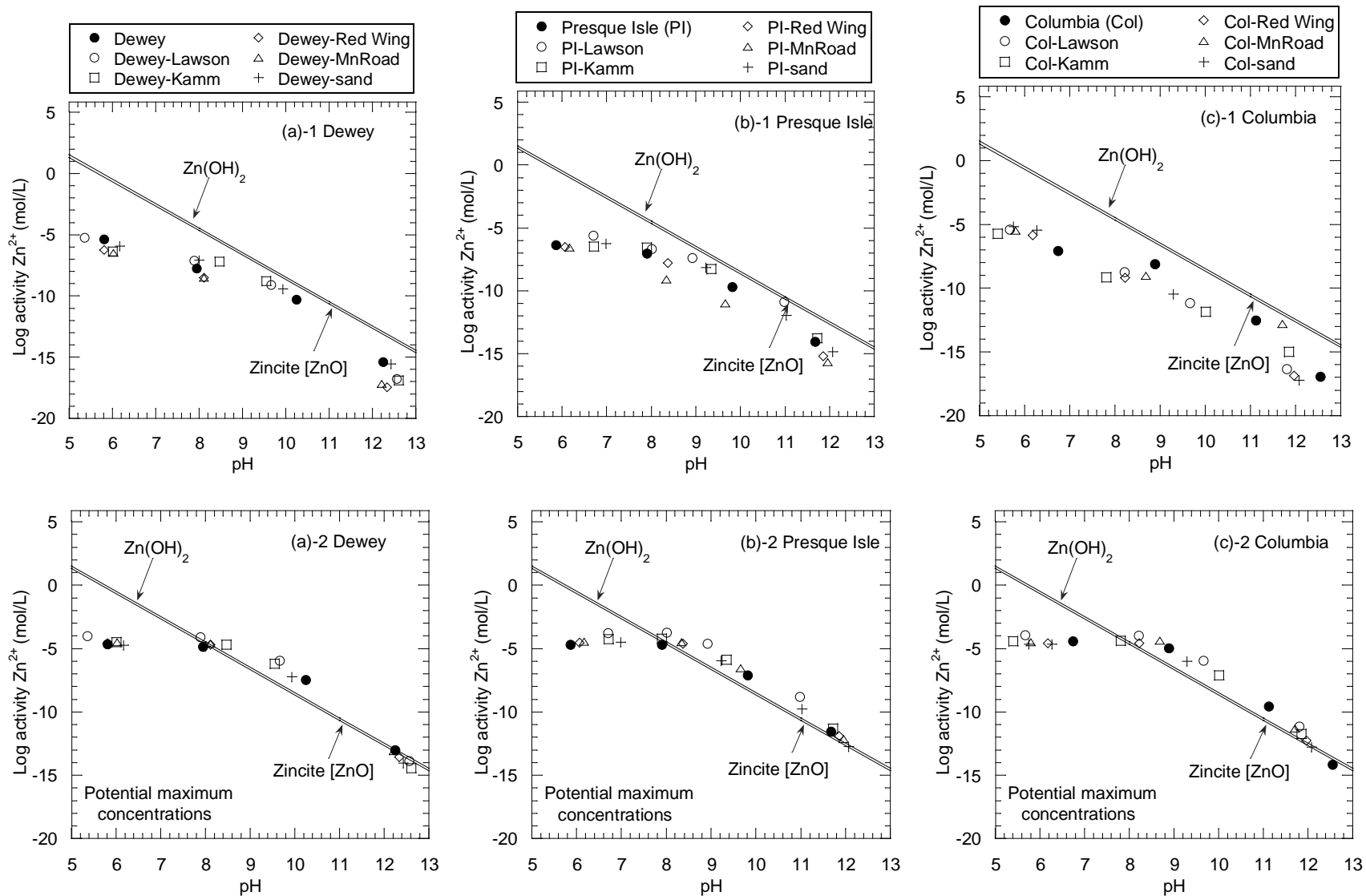
Figure 4.4.   Log activity of Zn^{2+} vs. pH in leachates from fly ashes and soil-fly ash mixtures based on measured concentration: (a)-1 Dewey fly ash, (b)-1 Presque Isle fly ash, and (c)-1 Columbia fly ash and based on "potential maximum concentration": (a)-2 Dewey fly ash, (b)-2 Presque Isle fly ash, and (c)-2 Columbia fly ash
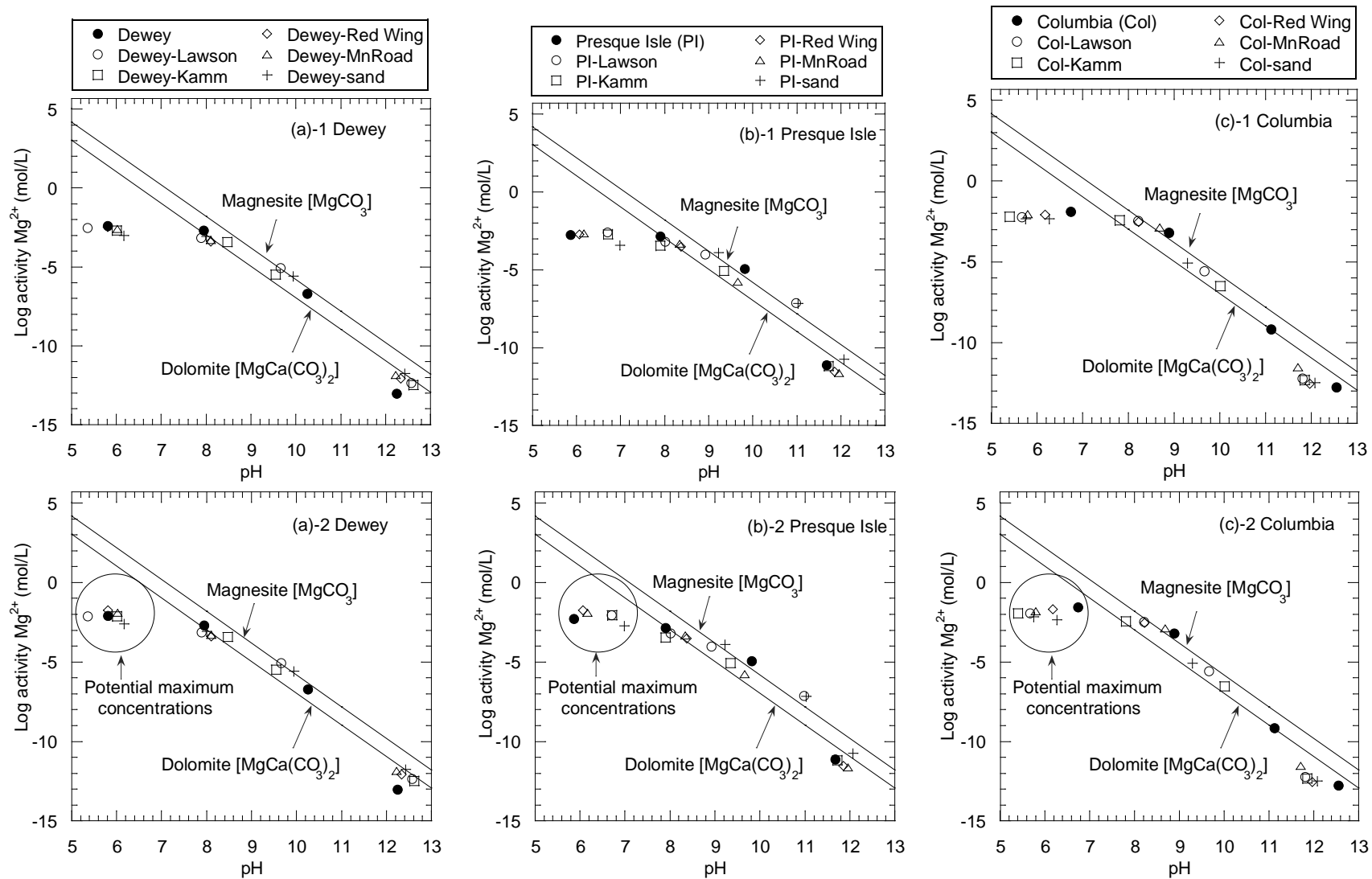
Figure 4.5.   Log activity of Mg^{2+} vs. pH in leachates from fly ashes and soil-fly ash mixtures based on measured concentration: (a)-1 Dewey fly ash, (b)-1 Presque Isle fly ash, and (c)-1 Columbia fly ash and based on "potential maximum concentration": (a)-2 Dewey fly ash, (b)-2 Presque Isle fly ash, and (c)-2 Columbia fly ash
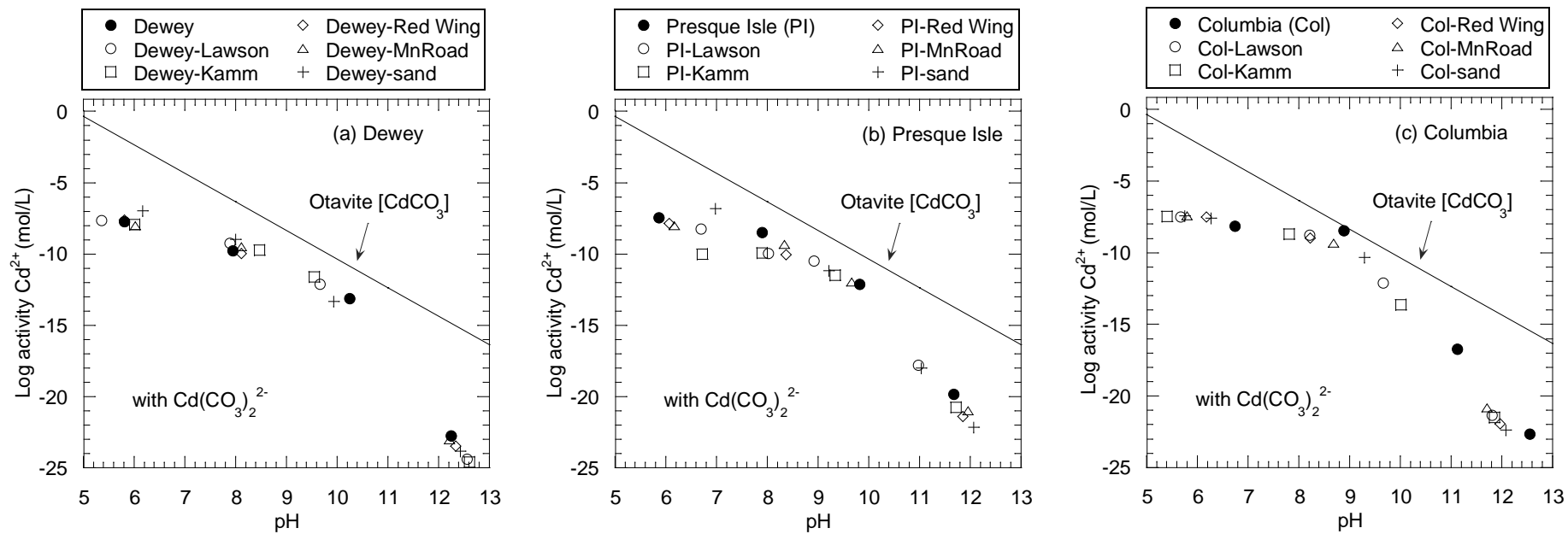
Figure 4.6. Log activity of Cd^{2+} vs. pH in leachates from fly ashes and soil-fly ash mixtures in the presence of $Cd(CO_3)_2^{2-}_{(aq)}$: (a) Dewey fly ash, (b) Presque Isle fly ash, and (c) Columbia fly ash and Columbia-soil mixtures.
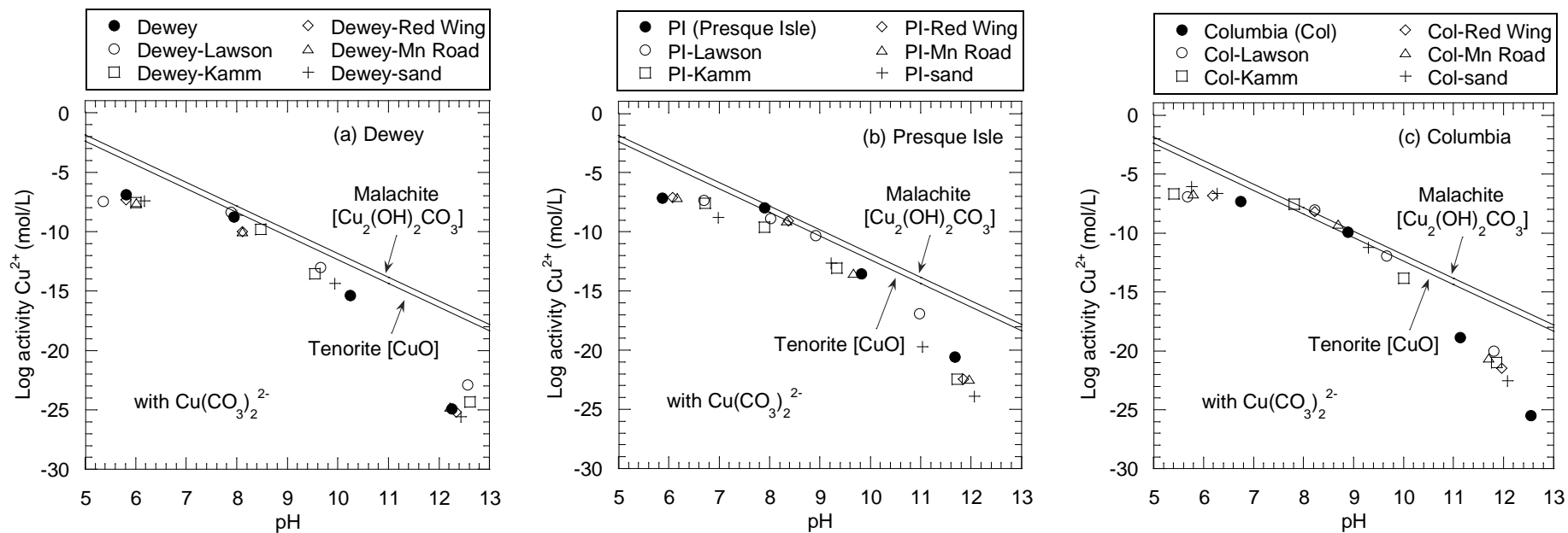
Figure 4.7. Log activity of Cu^{2+} vs. pH in leachates from fly ashes and soil-fly ash mixtures in the presence of Cu(CO$_3$)$_2^{2-}$$_{(aq)}$: (a) Dewey fly ash, (b) Presque Isle fly ash, and (c) Columbia fly ash and Columbia-soil mixtures.
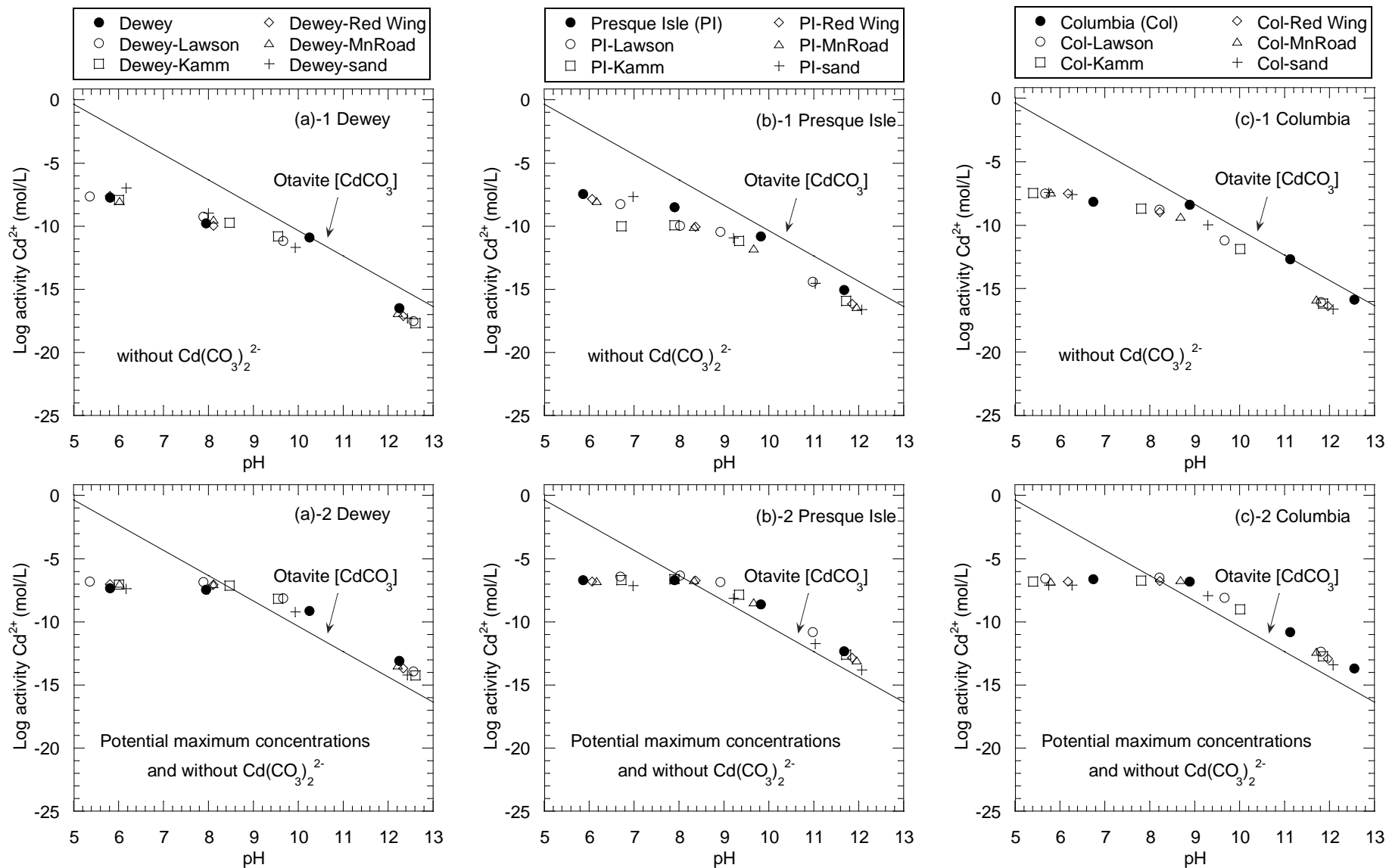
Figure 4.8. Log activity of Cd^{2+} vs. pH in leachates from fly ashes and soil-fly ash mixtures the absence of $Cd(CO_3)_2^{2-}_{(aq)}$ based on measured concentration: (a) Dewey fly, (b) Presque Isle fly ash, and (c) Columbia fly ash and based on based on "potential maximum concentration": (a)-2 Dewey fly ash, (b)-2 Presque Isle fly ash, and (c)-2 Columbia fly ash.
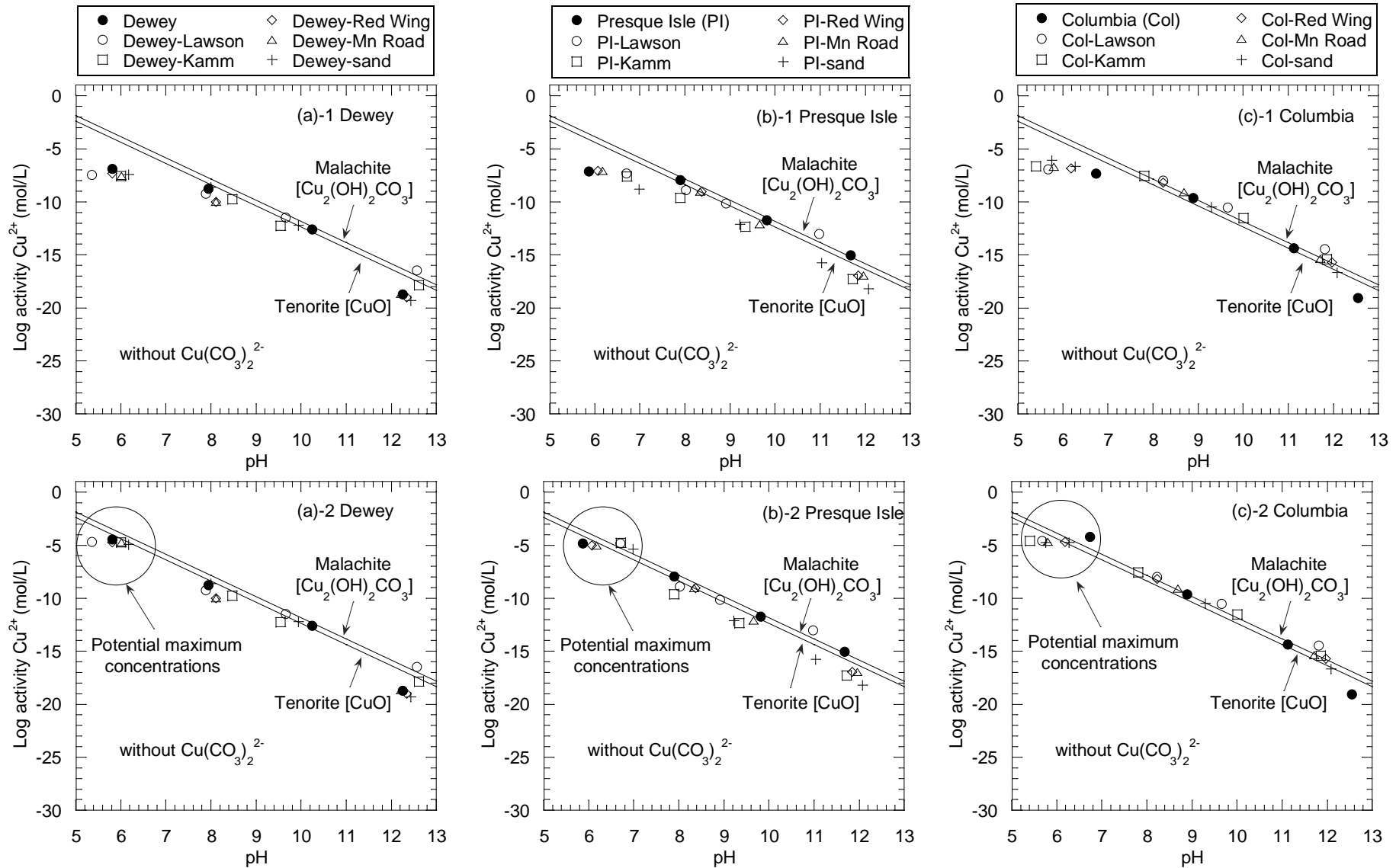
Figure 4.9.   Log activity of Cu^{2+} vs. pH in leachates from fly ashes and soil-fly ash mixtures the absence of $Cu(CO_3)_2{}^{2-}{}_{(aq)}$ based on measured concentration: (a) Dewey fly, (b) Presque Isle fly ash, and (c) Columbia fly ash and based on based on "potential maximum concentration": (a)-2 Dewey fly ash, (b)-2 Presque Isle fly ash, and (c)-2 Columbia fly ash.
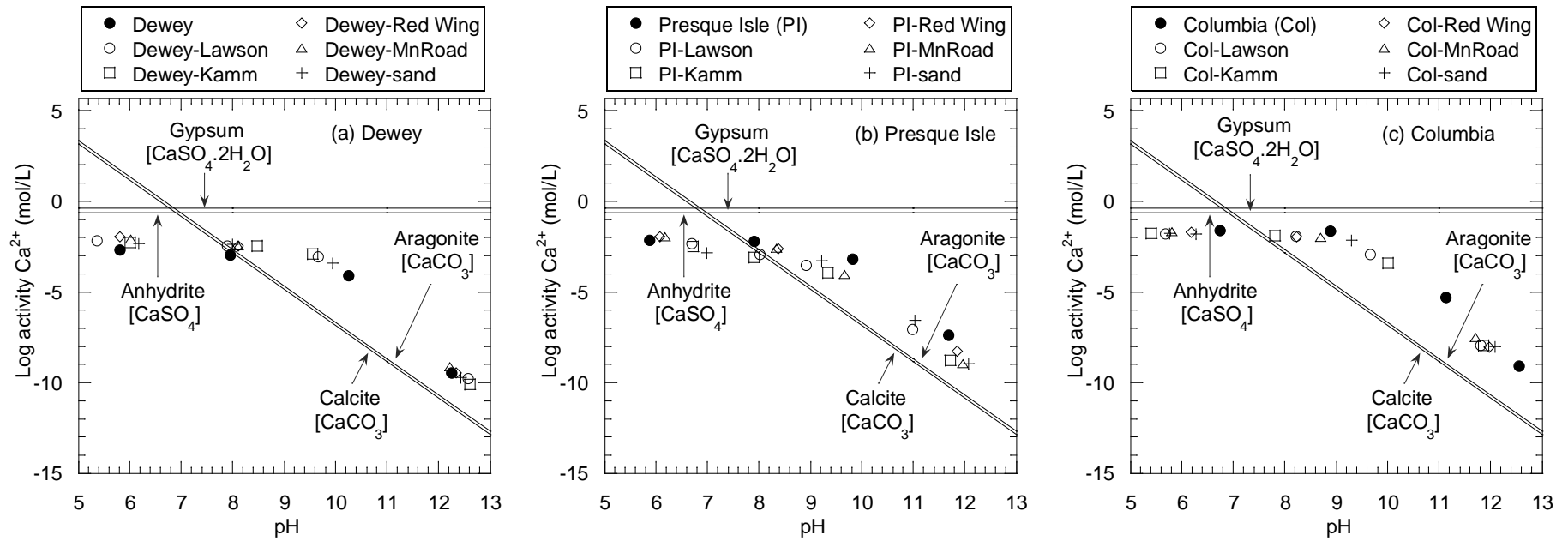
Figure 4.10. Log activity of Ca^{2+} vs. pH in leachates from fly ashes and soil-fly ash mixtures: (a) Dewey fly ash, (b) Presque Isle fly ash, and (c) Columbia fly ash.
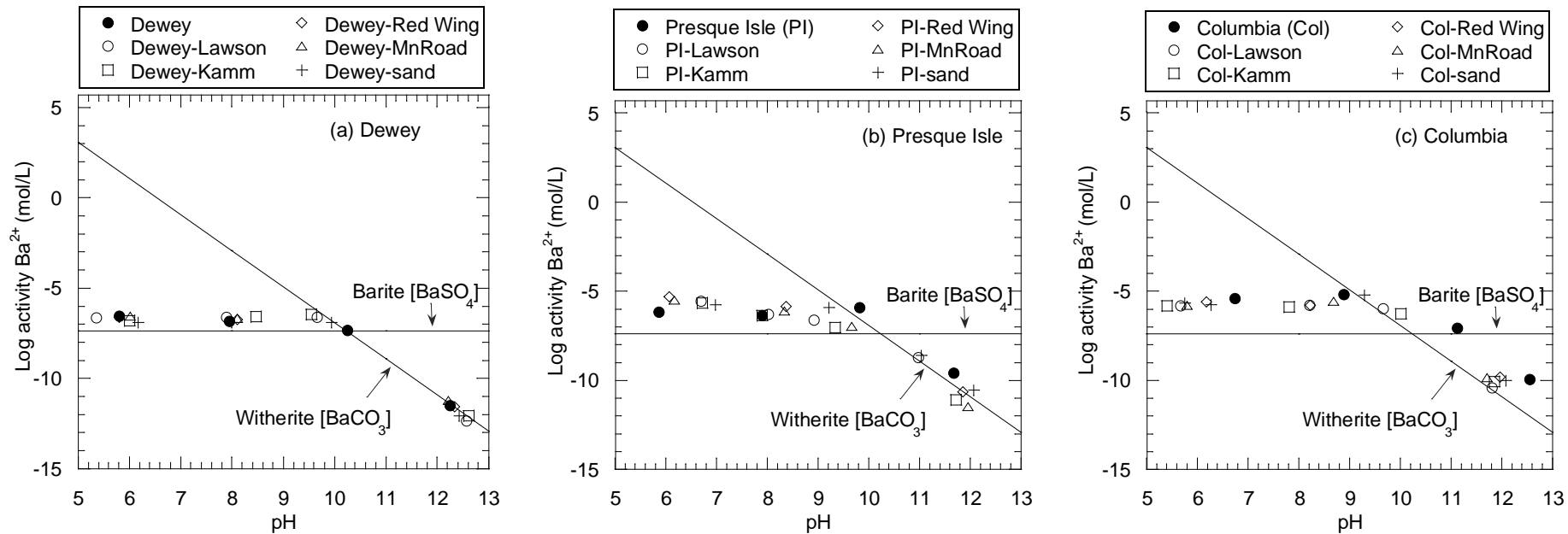
Figure 4.11. Log activity of Ba^{2+} vs. pH in leachates from fly ashes and soil-fly ash mixtures: (a) Dewey fly ash, (b) Presque Isle fly ash, and (c) Columbia fly ash.
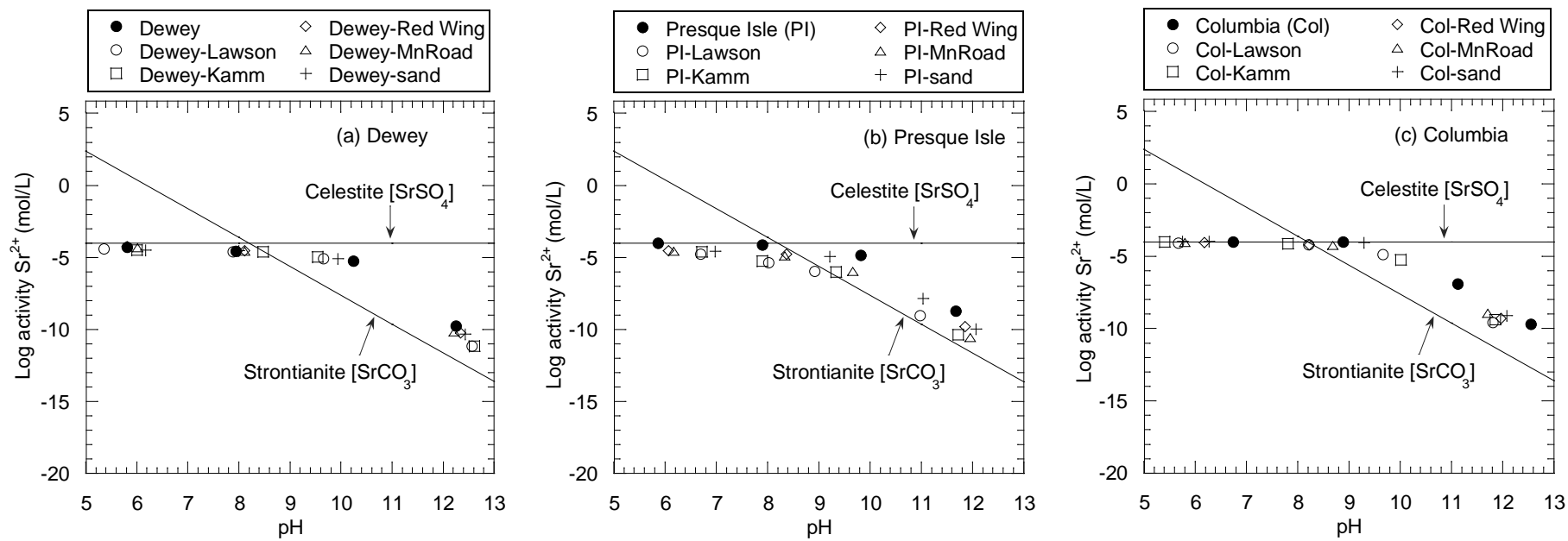
Figure 4.12. Log activity of Sr^{2+} vs. pH in leachates from fly ashes and soil-fly ash mixtures: (a) Dewey fly ash, (b) Presque Isle fly ash, and (c) Columbia fly ash.

140
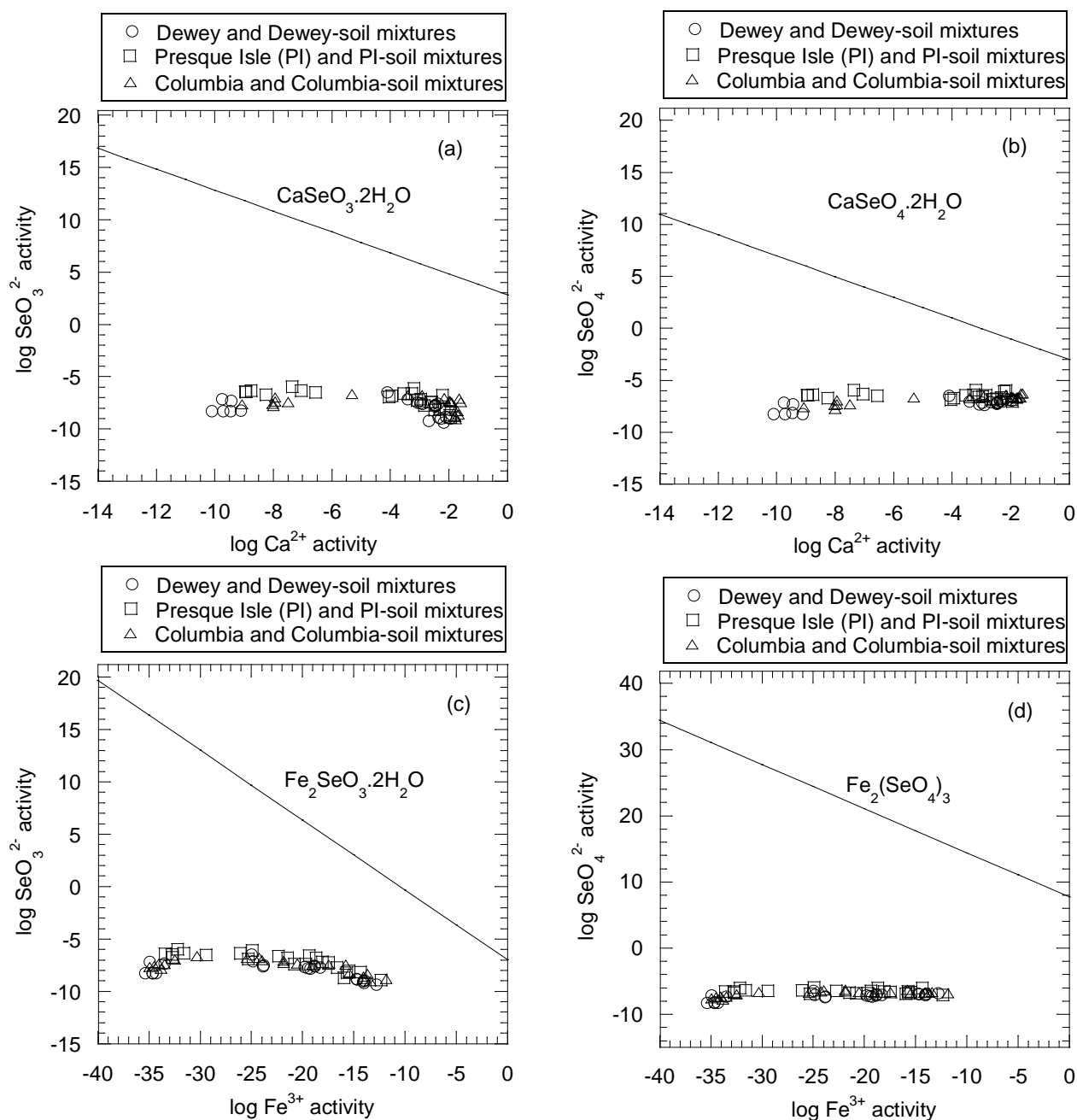
Figure 4.13. Log activity plot of: (a) selenite (SeO_3^{2-}) vs. Ca^{2+} in relation to the solubility of $CaSeO_3.2H_2O$ and (b) selenate (SeO_4^{2-}) vs. Ca^{2+} in relation to the solubility of $CaSeO_4.2H_2O$, (c) selenite (SeO_3^{2-}) vs. Fe^{3+} in relation to the solubility of $Fe_2SeO_3.2H_2O$, and (d) selenate (SeO_4^{2-}) vs. Fe^{3+} in relation to the solubility of $Fe_2(SeO_4)_3$ for Dewey, Presque Isle, and Columbia fly ashes and soil-fly ash mixtures.
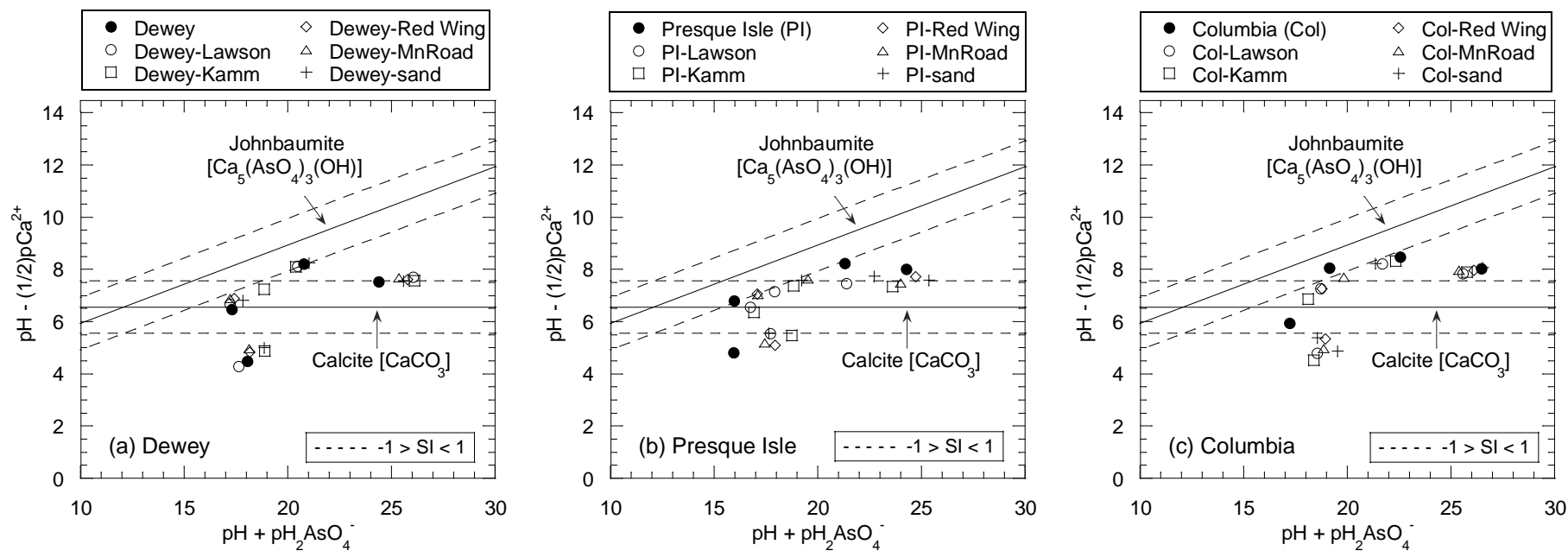
Figure 4.14. Activity ratio diagram of pH+pH$_2$AsO$_4^-$ vs. pH-(1/2) pCa^{2+} for the leachates from (a) Dewey fly ash and Dewey-soil mixtures, (b) Presque Isle (PI) fly ash and PI-soil mixtures, and (c) Columbia fly ash and Columbia-soil mixtures. (Note ——Stability line for SI = 0 and - - - - - Stability line for -1 $\geq$ SI $\leq$1).
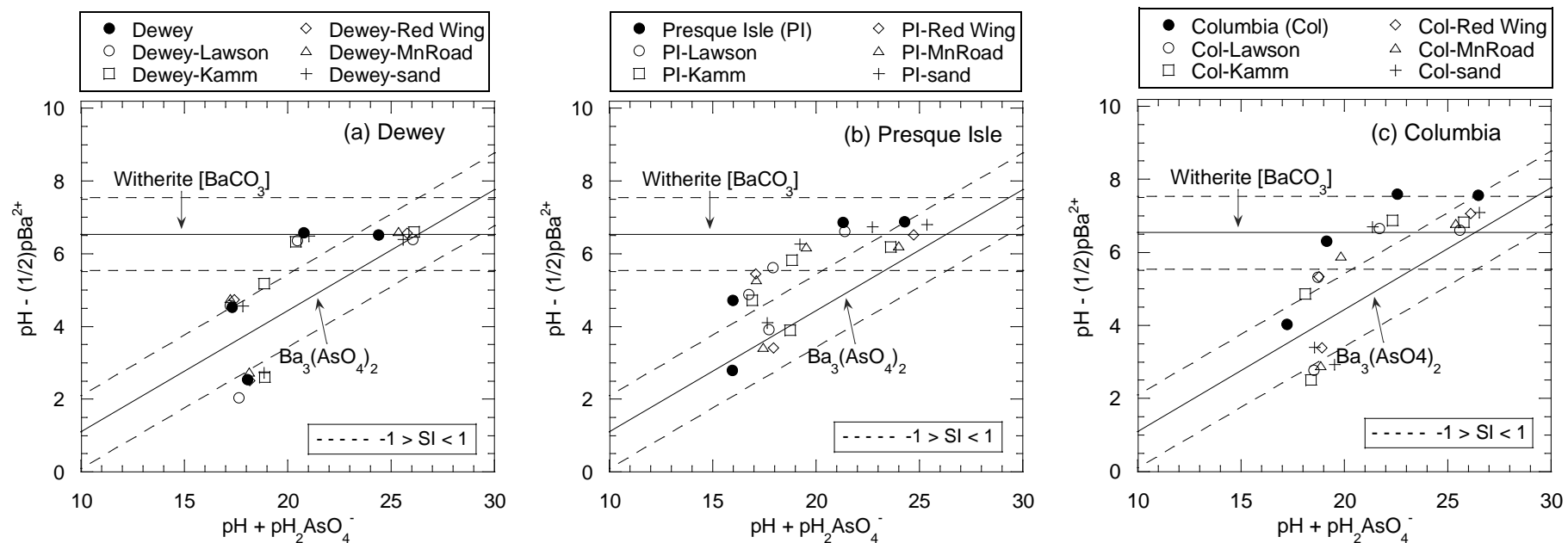
Figure 4.15. Activity ratio diagram of pH+pH$_2$AsO$_4^-$ vs. pH-(1/2) pBa^{2+} for the leachates from (a) Dewey fly ash and Dewey-soil mixtures, (b) Presque Isle (PI) fly ash and PI-soil mixtures, and (c) Columbia fly ash and Columbia-soil mixtures. (Note ——Stability line for SI = 0 and - - - - - Stability line for -1 $\geq$ SI $\leq$ 1).

SECTION 5

SUMMARY AND CONCLUSIONS

The pH-dependent leaching tests were used to investigate the leaching behaviors and leaching controlling mechanisms of soil-fly ash mixtures. The study focused on major and trace elements, including Al, As, Ba, Ca, Cd, Cu, Cr, Fe, Mg, Se, Sr, and Zn. The leaching tests were conducted on a range of soils and fly ashes used for soil stabilization in roadway construction projects in Wisconsin and Minnesota. The soils included organic clay, clay, silt, and sand, whereas the fly ashes included Class C and off-specification high-carbon fly ashes. In order to determine mechanisms controlling leaching, MINTEQA2 for Windows was used to determine the predominant chemical species (oxidation state) of redox-sensitive elements in leachates and the state of saturation of the leachate with respect to mineral phases. Experimental data from pH-dependent leaching tests, including concentrations of cations and anions, leachate pH, and leachate E_h, were used as input.

The followings are main conclusions and recommendations from this study.

1) Leaching of most of the elements studied (except As, Se and Ba) follows three well-characterized leaching patterns reported by other studies: cationic pattern, oxyanion pattern, and amphoteric pattern.

2) Dissolution-precipitation reactions are important controlling mechanisms for Ca, Cd, Cu, Cr, Fe, Mg, Sr, and Zn. The leaching of Ba might be associated with dissolution-precipitation and solid-solution formation, whereas solid-solution and sorption probably control the leaching of As and Se.

3) The similarity and consistency in leaching behavior and leaching mechanism as a function of pH for a given element (except As and Se) were observed in the leaching from soil, fly ash, and soil-fly ash mixtures. This offers the opportunity to transfer knowledge of soil and fly ash that has been extensively characterized and studied to soils stabilized with fly ash.

4) Different fly ash types show different abilities in immobilizing trace elements to some extent. Immobilization in cementitious compounds produced from self-cementing Class C Columbia fly ash is pronounced for As and Se. Chemical inclusion of As in binder hydration products (e.g. calcium silicate hydrates) is likely to be mechanism for As immobilization in stabilized soils, whereas solid solution formation with ettringite is more important for Se (and probably As) at pH > 11.5. High carbon fly ashes (Dewey and Presque Isle fly ashes) have adsorption ability for Cd, Cr, Sr, and Se. The abilities of fly ash to retain trace elements should promote the beneficial use of fly ash in soil stabilization, especially off-specification fly ash.

5) Both soil and fly ash enriched with trace elements can be a potential source for releasing trace elements into leachate from soil-fly ash mixture. Leaching of dissolved organic carbon (DOC) from organic soil (Lawson clay) enhanced leaching of some trace elements having high affinity with DOC (Cu in this case). These factors should be taken into consideration when selecting soil and fly ash used in stabilization, especially organic soil and soil or fly ash abundant in trace elements of concern.

6) Geochemical modeling is a useful tool to identify the mechanisms controlling leaching from fly ash and soil stabilized with fly ash. However, the presence of some species in the database can significantly affect the results. Aqueous metal-dicarbonate ($Cd(CO_3)_2^{2-}{}_{(aq)}$ and $Cu(CO_3)_2^{2-}{}_{(aq)}$ in this case play an

important role in determining the degree of saturation with respect to the mineral or solid of interest. The presence of suspicious species should be validated.

7) Incorporation the geochemical model with sorption process or reaction kinetic or solid-solution formation should improve the prediction of many elements showing undersaturation, and probably would be able to identify the mechanisms controlling As and Se.

SECTION 6

REFERENCES

ACAA. (2003). "Fly Ash Facts for Highway Engineers." FHWA-IF-03-019, US Department of Transportation, Federal Highway Administration, Washington, DC.

ACAA. (2008a). "2008 Coal Combustion Product (CCP) Production and Use Survey." American Coal Ash Association, Aurora, CO.

ACAA. (2008b). "Coal Combustion Products Beneficial Use and Production (1966-2007)." American Coal Ash Association, Aurora, CO.

Acosta, H. A., Edil, T. B., and Benson, C. H. (2003). "Soil stabilization and drying using fly ash." Geo Engineering Report No. 03-03, University of Wisconsin-Madison, Madison.

Adriano, D. C., Page, A. L., Elseewi, A. A., Chang, A. C., and Straughan, I. (1980). "Utilization and disposal of fly ash and other coal residues in terrestrial ecosystems: A review." *Journal of Environmental Quality*, 9(3), 333.

Ainsworth, C. C., and Rai, D. (1987). "Chemical characterization of fossil fuel wastes." EA-5321, Electric Power Research Institute, Palo Alto, CA.

Al-Barrak, K., and Rowell, D. L. (2006). "The solubility of gypsum in calcareous soils." *Geoderma*, 136(3-4), 830.

Allison, J. D., Brown, D. S., and Novo-Gradac, K. J. (1991). "MINTEQA2/PRODEFA2 A geochemical Assessment model for environmental systems: Version 3.0 User's manual." EPA/600/3-91/021, U.S. Environmental Protection Agency, Washington, D. C.

Anderson, M. A., Ferguson, J. F., and Gavis, J. (1976). "Arsenate adsorption on amorphous aluminum hydroxide." *Journal of colloid and interface science*, 54(3), 391-399.

Anderson, M. A., and Malotky, D. T. (1979). "Adsorption of protolyzable anions on hydrous oxides at the isoelectric pH." *Journal of colloid and interface science*, 72(3), 413-427.

Apul, D. S., Gardner, K. H., Eighmy, T. T., Fallman, A.-M., and Comans, R. N. J. (2005). "Simultaneous application of dissolution/precipitation and surface complexation/surface precipitation modeling to contaminant leaching." *Environmental Science and Technology*, 39(15), 5736.

Archer, D. G. (1998). "Thermodynamic properties of import to environmental processes and remediation. I. Previous thermodynamic property values for cadmium and some of its compounds." *Journal of Physical and Chemical Reference Data*, 27(5), 915-946.

Ariese, F., Swart, K., Morabito, R., Brunori, C., Balzamo, S., Slobodnik, J., Korenkova, E., Janos, P., Wildnerova, M., Hlavay, J., Polyak, K., Fodor, P., and Muntau, H. (2002). "Leaching studies of inorganic and organic compounds from fly ash." *International Journal of Environmental Analytical Chemistry*, 82(11-12), 751.

Arman, A., and Munfakh, G. A. (1970). "Stabilization of Organic Soils with Lime." Division of Engineering Research Bulletin No. 103, Department of Civil Engineering and Division of Engineering Research, Louisiana State University, Baton Rouge, Louisiana.

Ashworth, D. J., and Alloway, B. J. (2004). "Soil mobility of sewage sludge-derived dissolved organic matter, copper, nickel and zinc." *Environmental Pollution*, 127(1), 137.

Astrup, T., Dijkstra, J. J., Comans, R. N. J., Van der Sloot, H. A., and Christensen, T. H. (2006). "Geochemical modeling of leaching from MSWI air-pollution-control residues." *Environmental Science & Technology*, 40(11), 3551-3557.

Baltrus, J. P., Wells, A. W., Fauth, D. J., Diehl, J. R., and White, C. M. (2001). "Characterization of carbon concentrates from coal-combustion fly ash." *Energy and Fuels*, 15(2), 455-462.

Baur, I., and Johnson, C. A. (2003). "Sorption of selenite and selenate to cement minerals." *Environmental Science & Technology*, 37(15), 3442-3447.

Bayat, B. (2002). "Combined removal of zinc (II) and cadmium (II) from aqueous solutions by adsorption onto high-calcium Turkish fly ash." *Water Air And Soil Pollution*, 136(1-4), 69-92.

Bilinski, H., Huston, R., and Stumm, W. (1976). "Determination of stability-constants of some hydroxo and carbonato complexes of Pb(II), Cu(II), Cd(II) And Zn(II) in dilute-solutions by anodic-stripping voltammetry and differential pulse polarography." *Analytica Chimica Acta*, 84(1), 157-164.

Bin-Shafique, M. S., Benson, C. H., and Edil, T. B. (2002). "Leaching of heavy metals from fly ash stabilized soils used in highway pavements." Geo Engineering Report No. 02-14, Geo Engineering Program, University of Wisconsin-Madison, Madison, WI.

Bohn, H. L., McNeal, B. L., and O'Connor, G. A. (2001). *Soil Chemistry*, John Wiley & Sons, Inc., New York.

Bothe, J. V., and Brown, P. W. (1999). "The stabilities of calcium arsenates at 231C." *Journal of Hazardous Materials*, 69(2), 197.

Boyd, S. A., and Sommers, L. E. (1990). "Humic and fulvic acid fractions from sewage sludges and sludge amended soils." Humic substances in soils and crop sciences., C. E. Clapp, R. L. Malcolm, and P. R. Bloom, eds., American Society of Agronomy, Madison, WI, USA, 203-220.

Brunori, C., Balzamo, S., and Morabito, R. (1999). "Comparison between different leaching/extraction tests for the evaluation of metal release from fly ash." *International Journal of Environmental Analytical Chemistry*, 75(1), 19.

Camacho, L. M., and Munson-McGee, S. H. (2006). "Anomalous transient leaching behavior of metals solidified/stabilized by pozzolanic fly ash." *Journal Of Hazardous Materials*, 137(1), 144-151.

Cherry, J. A., Shaikh, A. U., Tallman, D. E., and Nicholson, R. V. (1979). "Arsenic species As an indicator of redox conditions in groundwater." *Journal Of Hydrology*, 43(1-4), 373-392.

Clesceri, L. S., Greenberg, A. E., and Eaton, A. D. (1999). *Standard Methods for the Examination of Water and Wastewater*, American Public Health Association, Washington, D. C.

Cornelis, G., Johnson, C. A., Van Gerven, T., and Vandecasteele, C. (2008a). "Leaching mechanisms of oxyanionic metalloid and metal species in alkaline solid wastes: A review." *Applied Geochemistry*, 23(5), 955-976.

Cornelis, G., Poppe, S., Van Gerven, T., Van den Broeck, E., Ceulemans, M., and Vandecasteele, C. (2008b). "Geochemical modelling of arsenic and selenium leaching in alkaline water treatment sludge from the production of non-ferrous metals." *Journal of Hazardous Materials*, 159(2-3), 271-279.

Crecelius, E. A., Bloom, N. S., Cowan, C. E., and Jenne, E. A. (1986). "Speciation of selenium and arsenic in natural waters and sediments. Volume 2: Arsenic

speciation." EPRI EA-4641, Final Report. Research Project 2020-2, Electric Power Res. Inst., Palo Alto.

Creek, D. N., and Shackelford, C. D. (1992). "Permeability and leaching characteristics of fly ash liner materials." Transportation Research Record 1345, TRB, NRC, Washington, D.C.

Davis, J. A., Kent, D. B., Rea, B. A., Maest, A. S., and Garabedian, S. P. (1993). "Influence of redox environment and aqueous speciation on metal transport in groundwater: Preliminary results of trace injection studies." Metals in groundwater, H. E. Allen, E. M. Perdue, and D. S., eds., Lewis Pubishers, Chelsea, MI, 223-273.

de Groot, G. J., van der Sloot, H. A., and Dijkstra, J. J. (1989). *Environmental aspects of stabilization and solidification of hazardous and radioactive wastes*, ASTM, Philadelphia, PA.

Dermatas, D., and Meng, X. (2003). "Utilization of fly ash for stabilization/solidification of heavy metal contaminated soils." *Engineering Geology*, 70(3-4), 377-394.

Dijkstra, J. J., Meeussen, J. C. L., and Comans, R. N. J. (2004). "Leaching of heavy metals from contaminated soils: An experimental and modeling study." *Environmental Science and Technology*, 38(16), 4390.

Dijkstra, J. J., Van der Sloot, H. A., and Comans, R. N. J. (2002). "Process identification and model development of contaminant transport in MSWI bottom ash." *Waste Management*, 22(5), 531.

Dijkstra, J. J., Van Der Sloot, H. A., and Comans, R. N. J. (2006). "The leaching of major and trace elements from MSWI bottom ash as a function of pH and time." *Applied Geochemistry*, 21(2), 335.

Drakonaki, S., Diamadopoulos, E., Vamvouka, D., and Lahaniatis, M. (1998). "Leaching behavior of lignite fly ash." *Journal of Environmental Science and Health, Part A: Toxic/Hazardous Substances & Environmental Engineering*, 33(2), 237.

Dusing, D. C., Bishop, P. L., and Keener, T. C. (1992). "Effect of redox potential on leaching from stabilized/solidified waste materials." *Journal of the Air & Waste Management Association*, 42(1), 56.

Eary, L. E., Rai, D., Mattigod, S. V., and Ainsworth, C. C. (1990). "Geochemical factors controlling the mobilization of Inorganic constituents from fossil-fuel combustion residues: II. Review of the minor elements." *Journal of Environmental Quality*, 19(2), 202-214.

Edil, T. B., Benson, C. H., Sazzad, B.-S., Tanyu, B. F., Kim, W.-H., and Senol, A. (2002). "Field evaluation of construction alternatives for roadways over soft subgrade." 1786, Transportation Research Record.

Edil, T. B., Sandstrom, L. K., and Berthouex, P. M. (1992). "Interaction of inorganic leachate with compacted pozzolanic fly ash." *Journal of Geotechnical Engineering*, 118(9), 1410-1430.

Egozy, Y. (1980). "Adsorption of cadmium and cobalt on montmorillonite as a function of solution composition." *Clays Clay Miner*, 28, 311-318.

Eighmy, T. T., Eusden, J. D., Krzanowski, J. E., Domingo, D. S., Stampfli, D., Martin, J. R., and Erickson, P. M. (1995). "Comprehensive approach toward understanding element speciation and leaching behavior in municipal solid-waste incineration electrostatic precipitator ash." *Environmental Science & Technology*, 29(3), 629-646.

Elseewi, A. A., Page, A. L., and Grimm, S. R. (1980). "Chemical characterization of fly ash aqueous systems." *Journal of Environmental Quality*, 9(3), 424.

EPRI. (1989). "Coal ash and the environment: Characteristics of fly ash." EPRI Technical Brief RP2485-8, EPRI.

Fallman, A. M. (2000). "Leaching of chromium and barium from steel slag in laboratory and field tests - a solubility controlled process?" *Waste Management*, 20(2-3), 149-154.

Fan, M., Brown, R. C., Wheelock, T. D., Cooper, A. T., Nomura, M., and Zhuang, Y. (2005). "Production of a complex coagulant from fly ash." *Chemical Engineering Journal*, 106(3), 269-277.

Fernandez-Olmo, I., Lasa, C., and Irabien, A. (2007). "Modeling of zinc solubility in stabilized/solidified electric arc furnace dust." *Journal of Hazardous Materials*, 144(3), 720-724.

Fish, W. (1993). "Sub-surface redox chemistry: A comparison of equilibrium and reaction-based approaches." Metals in groundwater, H. E. Allen, E. M. Perdue, and D. S., eds., Lewis Pubishers, Chelsea, MI, 73-101.

Fisher, G. L., and Natusch, D. F. S. (1979). "Size depence of physical and chemical properties of coal fly ash." Analytical methods for coal and coal products, C. J. Karr, ed., Academic Press, New York, 489-541.

Fleming, L. N., Abinteh, H. N., and Inyang, H. I. (1996). "Leachant pH effects on the leachability of metals from fly ash." *Journal of Soil Contamination*, 5(1), 53-59.

Frankenberger, W. T., Jr. (2002). *Environmental chemistry of arsenic*, Marcel Dekker, New York.

Frankenthal, R. P. (1963). "Equilibrium constants." Handbook of Analytical Chemistry, L. Meites, ed., McGraw-Hill, Toronto, CA, 1-13 to 1-19.

Fruchter, J. S., Ral, D., and Zachara, J. M. (1990). "Identification of solubility-controlling solid phases in a large fly ash field lysimeter." *Environmental Science and Technology*, 24(8), 1173.

Fytianos, K., Tsaniklidi, B., and Voudrias, E. (1998). "Leachability of heavy metals in Greek fly ash from coal combustion." *Environment International*, 24(4), 477-486.

Gabrisova, A., Havlica, J., and Sahu, S. (1991). "Stability of calcium sulphoaluminate hydrates in water solutions with various pH values." *Cement and Concrete Research*, 21(6), 1023.

Garavaglia, R., and Caramuscio, P. (1994). "Coal fly-ash leaching behaviour and solubility controlling solids." Maastricht, Neth, 87.

Garrabrants, A. C., Sanchez, F., and Kosson, D. S. (2004). "Changes in constituent equilibrium leaching and pore water characteristics of a Portland cement mortar as a result of carbonation." *Waste Management*, 24(1), 19-36.

Georgakopoulos, A., Filippidis, A., Kassoli-Fournaraki, A., Fernandez-Turiel, J.-L., Llorens, J.-F., and Mousty, F. (2002). "Leachability of major and trace elements of fly ash from Ptolemais power station, Northern Greece." *Energy Sources*, 24(2), 103-113.

Gimenez, J., Martinez, M., de Pablo, J., Rovira, M., and Duro, L. (2006). "Sorption of selenium(IV) and selenium(VI) onto magnetite." *Applied Surface Science*, 252(10), 3767.

Gitari, W. M., Petrik, L. F., Etchebers, O., Key, D. L., and Okujeni, C. (2008). "Utilization of fly ash for treatment of coal mines wastewater: Solubility controls on major inorganic contaminants." *Fuel*, 87(12), 2450.

Goldberg, S., and Glaubig, R. A. (1988). "Anion sorption on a calcareous, montmorillonitic soil-selenium." *Soil Science Society of America Journal*, 52(4), 954.

Goldberg, S., Lesch, S. M., Suarez, D. L., and Basta, N. T. (2005). "Predicting arsenate adsorption by soils using soil chemical parameters in the constant capacitance model." *Soil Science Society Of America Journal*, 69(5), 1389-1398.

Gorman, J. M., Sencindiver, J. C., Horvath, D. J., Singh, R. N., and Keefer, R. F. (2000). "Erodibility of fly ash used as a topsoil substitute in mineland reclamation." *Journal Of Environmental Quality*, 29(3), 805-811.

Goswami, R. K., and Mahanta, C. (2007). "Leaching characteristics of residual lateritic soils stabilised with fly ash and lime for geotechnical applications." *Waste Management*, 27(4), 466.

Gupta, S., Ranaivoson, A., Edil, T., Benson, C., and Sawangsuriya, A. (2006). "Pavement design using unsaturated soil technology." Minnesota Department of Transportation, St. Paul, MN.

Gupta, S. K., and Chen, K. Y. (1978). "Arsenic removal by adsorption." *Journal water pollution control federation*, 50(3), 493-506.

Hampton, M. B., and Edil, T. B. (1998). "Strength gain of organic ground with cement-type binders." Boston, MA, USA, 135.

Hassett, D. J., Pflughoeft-Hassett, D. F., and Heebink, L. V. (2003). "Leaching of CCB'S: over 25 years of research." *Proceedings of the International Ash Utilisation Symposium*, University of Kentucky, Kentucky.

Heebink, L. V., and Hassett, D. J. (2001). "Coal fly ash trace element mobility in soil stabilization." Proceedings of the International Ash Utilization Symposium, Center for Applied Energy Research, University of Kentucky.

Hering, J. G., and Kneebone, P. E. (2002). "Biogeochemical controls on arsenic occurence and mobility in water supplies." Environmental chemistry of arsenic, W. T. Frankenberger, Jr., ed., Marcel Dekker, New York, 391.

Hesbach, P., Beck, M., Eick, M., Daniels, W. L., Burgers, C., Greiner, A., Hassett, D. J., and Heebink, L. V. (2005). "Inter-laboratory comparison of leaching." *World of Coal Ash*, University of Kentucky.

Hingston, F. J., Quirk, J. P., and Posner, A. M. (1972). "Anion adsorption by goethite and gibbsite.1. Role of proton in determining adsorption envelopes." *Journal off soil science*, 23(2), 177-&.

Hodgson, L., Dyer, D., and Brown, D. A. (1981). "Neutralization and dissolution of high-calcium fly ash." *Journal of Environmental Quality*, 11(1), 93.

Holm, T. R., Anderson, M. A., Iverson, D. G., and Standforth, R. S. (1979). "Chemical modeling in aqueous systems: speciation, sorption, solubility, and kinetics." *The 176th meeting of the American Chemical Society*, Miami Beach, Florida.

Hwang, J. H., Sun, X., and Li, Z. (2002). "Unburned Carbon from Fly Ash for Mercury Adsorption: I. Separation and Characterization of Unburned Carbon." *Journal of Minerals & Materials Characterization & Engineering*, 1(1), 39-60.

Hyun, S., Burns, P. E., Murarka, I., and Lee, L. S. (2006). "Selenium(IV) and (VI) sorption by soils surrounding fly ash management facilities." *Vadose Zone Journal*, 5(4), 1110-1118.

Impellitteri, C. A., Allen, H. E., Yin, Y., You, S.-J., and Saxe, J. K. (2001). "Soil properties controlling metal partitioning." Heavy Metals Release in Soils, H. M. Selim and D. L. Sparks, eds., Lewis Publishers, Boca Raton, Fl, 149-165.

Iyer, R. S., Stanmore, B. R., and Pullammanappallil, P. C. (1999). "Solid-liquid mass transfer during leaching of calcium from dilute slurries of flyash." *Chemical Engineering Research and Design, Transactions of the Institute of Chemical Engineers, Part A*, 77(8), 764.

Jackson, B. P., and Miller, W. P. (1999). "Soluble arsenic and selenium species in fly ash/organic waste-amended soils using ion chromatography - inductively coupled plasma mass spectrometry." *Environmental Science and Technology*, 33(2), 270.

Jackson, B. P., Miller, W. P., Schumann, A. W., and Sumner, M. E. (1999). "Trace element solubility from land application of fly ash/organic waste mixtures." *Journal of Environmental Quality*, 28(2), 639.

Jenne, E. A. (1968). *Trace inorganics in water*, American Chemical Society, Washington, D.C.

Johnston, H. M., and Eagleson, K. E. (1989). "Chemical characteristics of Ontario hydro coal fly ash: A review." Report no. 89-155-K, Ontario Hydro Research Division, Canada.

Kenkel, J. (2003). *Analytical chemistry for technicians*, Lewis Publishers, Boca Raton, FL.

Khanra, S., Mallick, D., Dutta, S. N., and Chaudhuri, S. K. (1998). "Studies on the phase mineralogy and leaching characteristics of coal fly ash." *Water, Air and Soil Pollution*, 107(1-4), 251-275.

Kida, A., Noma, Y., and Imada, T. (1996). "Chemical speciation and leaching properties of elements in municipal incinerator ashes." *Waste Management*, 16(5-6), 527.

Kim, A. G. (2002). "Physical and chemical characteristics of CCB." *Coal Combustion By-Products and Western Coal Mines:A Technical Interactive Forum*, Golden, Colorado, 18.

Kim, A. G., and Kazonich, G. (2004). "The silicate/non-silicate distribution of metals in fly ash and its effect on solubility." *Fuel*, 83(17-18), 2285-2292.

Kinniburgh, D. G., van Riemsdijk, W. H., Koopal, L. K., Borkovec, M., Benedetti, M. F., and Avena, M. J. (1999). "Ion binding to natural organic matter: competition, heterogeneity, stoichiometry and thermodynamic consistency." *Colloids and Surfaces A: Physicochemical and Engineering Aspects*, 151(1-2), 147.

Kirby, C. S., and Rimstidt, J. D. (1994). "Interaction of municipal solid waste ash with water." *Environmental Science and Technology*, 28(3), 443-451.

Kosson, D. S., van der Sloot, H. A., and Eighmy, T. T. (1996). "An approach for estimation of contaminant release during utilization and disposal of municipal waste combustion residues." *Journal of Hazardous Materials*, 47(1-3), 43-75.

Kosson, D. S., Van Der Sloot, H. A., Sanchez, F., and Garrabrants, A. C. (2002). "An integrated framework for evaluating leaching in waste management and utilization of secondary materials." *Environmental Engineering Science*, 19(3), 159-204.

Kretzschmar, R., and Christ, I. (2001). "Proton and metal cation binding to humic substances in relation to chemical composition and molecular size." Humic substances: structures, models and functions., E. A. Ghabbour and G. Davies, eds., The Royal Society of Chemistry, Cambridge, UK.

Kumarathasan, P., McCarthy, G. J., Hassett, D. J., and Pflughoeft-Hassett, D. E. (1990). "Oxyanion substituted ettringites: synthesis and characterization, and their potential role in immobilization of As, B, Cr, Se and V." *Research Society Symposium Proceedings*, Pittsburgh, 83-104.

Langmuir, D. (1997). *Aqueous Environmental Geochemistry*, Prentice-Hall, Inc., New Jersey.

Lavkulich, L. M. (1981). "Exchangeable Cations and Total Exchange Capacity by the Ammonium Acetate Method at pH 7.0." *Soil Sampling and Methods of Analysis*, M. R. Carter, ed., Canadian Society of Soil Science, Ottawa, Ontario, Canada, 173-175.

Lee, J. S., and Nriagu, J. O. (2007). "Stability constants for metal arsenates." *Environmental Chemistry*, 4(2), 123-133.

Lee, T., and Benson, C. H. (2004). "Sorption and degradation of alachlor and metolachlor in ground water using green sands." *Journal of Environmental Quality*, 33(5), 1682.

Lim, T. T., Tay, J. H., Tan, L. C., Choa, V., and Teh, C. I. (2004). "Changes in mobility and speciation of heavy metals in clay-amended incinerator fly ash." *Environmental Geology*, 47(1), 1-10.

Lin, C. J., and Chang, J. E. (2001). "Effect of fly ash characteristics on the removal of Cu(II) from aqueous solution." *Chemosphere*, 44(5), 1185.

Lumsdon, D. G., Fraser, A. R., Russell, J. D., and Livesey, N. T. (1984). "New infrared band assignments for the arsenate ion adsorbed on synthetic goethite (α-FeOOH)." *Journal of soil science*, 35(3), 381-386.

Malviya, R., and Chaudhary, R. (2006). "Leaching behavior and immobilization of heavy metals in solidified/stabilized products." *Journal of Hazardous Materials*, 137(1), 207.

Mattigod, S. V., Rai, D., Eary, L. E., and Ainsworth, C. C. (1990). "Geochemical factors controlling the mobilization of inorganic constituents from fossil fuel combustion residues: I. Review of the major elements." *Journal of Environmental Quality*, 19, 188-201.

McBride, M. B. (1994). *Environmental Chemistry of Soils*, Oxford University Press, New York.

McCarthy, J. F., and Zachara, J. M. (1989). "Subsurface transport of contaminants." *Environmental Science and Technology*, 23(5), 496.

Meima, J. A., and Comans, R. N. J. (1997). "Geochemical modeling of weathering reactions in municipal solid waste incinerator bottom ash." *Environmental Science & Technology*, 31(5), 1269-1276.

Meima, J. A., and Comans, R. N. J. (1998). "Application of surface complexation/precipitation modeling to contaminant leaching from weathered municipal solid waste incinerator bottom ash." *Environmental Science and Technology*, 32(5), 688.

Meima, J. A., and Comans, R. N. J. (1999). "Leaching of trace elements from municipal solid waste incinerator bottom ash at different stages of weathering." *Applied Geochemistry*, 14(2), 159.

Meima, J. A., Van Zomeren, A., and Comans, R. N. J. (1999). "Complexation of Cu with dissolved organic carbon in municipal solid waste incinerator bottom ash leachates." *Environmental Science and Technology*, 33(9), 1424.

Merrill, D. T., Manzione, M. A., Peterson, J. J., Parker, D. S., Chow, W., and Hobbs, A. O. (1986). "Field-evaluation of arsenic and selenium removal by iron coprecipitation." *Journal water pollution control federation*, 58(1), 18-26.

Mizutani, S., Yoshida, T., Sakai, S.-i., and Takatsuki, H. (1996). "Release of metals from MSW I fly ash and availability in alkali condition." *Waste Management Proceedings of the 1996 Seminar on Cycle and Stabilization Technologies of Municipal Solid Waste (MSW) Incineration Residue, Mar 5-8 1996*, 16(5-6), 537-544.

Mudd, G. M., Weaver, T. R., and Kodikara, J. (2004). "Environmental geochemistry of leachate from leached brown coal ash." *Journal of Environmental Engineering-Asce*, 130(12), 1514-1526.

Murarka, I. P., Rai, D., and Ainsworth, C. C. (1992). "Geochemical basis for predicting leaching of inorganic constituents from coal-combustion residues." *Waste Testing and Quality Assurance Symposium*, Washington, DC, USA, 279-288.

Myneni, S. C. B., Traina, S. J., Logan, T. J., and Waychunas, G. A. (1997). "Oxyanion behavior in alkaline environments: Sorption and desorption of arsenate in ettringite." *Environmental Science & Technology*, 31(6), 1761-1768.

Nagataki, S., Kamada, H., and Hosada, N. (1995). "Mechanical properties of pulverized fuel ash by-product." *11th International Symposium on Management and Use of Coal Combustion Byproducts (CCBs)*, 59-1 - 59-23.

Narukawa, T., Takatsu, A., Chiba, K., Riley, K. W., and French, D. H. (2005). "Investigation on chemical species of arsenic, selenium and antimony in fly ash from coal fuel thermal power stations." *Journal Of Environmental Monitoring*, 7(12), 1342-1348.

Niss, N. D., Schabron, J. F., and Brown, T. H. (1993). "Determination of selenium species in coal fly-ash extracts." *Environmental Science & Technology*, 27(5), 827-829.

O'Donnell, J. B. (2009). "Leaching of trace elements from roadway materials stabilized with fly ash," University of Wisconsin, Madison.

Peak, D. (2006). "Adsorption mechanisms of selenium oxyanions at the aluminum oxide/water interface." *Journal Of Colloid And Interface Science*, 303(2), 337-345.

Pierce, M. L., and Moore, C. B. (1982). "Adsorption of arsenite and arsenate on amorphous iron hydroxide." *Water Research*, 16(7), 1247-1253.

Pohland, F. G., Cross, W. H., and Gould, J. P. (1993). "Metal speciation and mobility as influence by landfill disposal practices." Metals in groundwater, H. E. Allen, E. M. Perdue, and D. S., eds., Lewis Pubishers, Chelsea, MI, 411-429.

Polettini, A., and Pomi, R. (2004). "The leaching behavior of incinerator bottom ash as affected by accelerated ageing." *Journal of Hazardous Materials*, 113(1-3), 211-217.

Rai, D., Ainsworth, C. C., Eary, L. E., Mattigod, S. V., and Jackson, D. R. (1987a). "Inorganic and organic constituents in fossil fuel combustion residues. Volume 1: A critical review." EPRI-EA-5176-Vol.1, Pacific Northwest Lab., Richland, WA (USA); Electric Power Research Inst., Palo Alto, CA (USA).

Rai, D., Sass, B. M., and Moore, D. A. (1987b). "Chromium(III) hydrolysis constants and solubility of chromium(III) hydroxide." *Inorganic Chemistry*, 26(3), 345-349.

Rai, D., and Szelmeczka, R. W. (1990). "Aqueous behavior of chromium in coal fly ash." *Journal of Environmental Quality*, 19(3), 378-382.

Rao, M., Parwate, A. V., and Bhole, A. G. (2002). "Removal of Cr^{6+} and Ni^{2+} from aqueous solution using bagasse and fly ash." *Waste Management*, 22(7), 821-830.

Reardon, E. J., Czank, C. A., Warren, C. J., Dayal, R., and Johnston, H. M. (1995). "Determining controls on element concentrations in fly ash leachate." *Waste Management & Research*, 13(5), 435.

Ricou, P., Hequet, V., Lecuyer, I., and Cloirec, P. L. (1999). "Influence of operating conditions on heavy metal cation removal by fly ash in aqueous solution." *International Ash Utilization Symposium*, University of Kentucky.

Riemsdijk, W. H. v., and Hiemstra, T. (1993). "Adsorption to Heterogeneous Surfaces." Metals in groundwater, H. E. Allen, E. M. Perdue, and D. S., eds., Lewis Pubishers, Chelsea, MI, 1-36.

Rousseau, P. D. S., Przybylowicz, W. J., Scheepers, R., Prozesky, V. M., Pineda, C. A., Churms, C. L., and Ryan, C. G. (1997). "Geochemical analysis of medium sized fly ash particles using the NAC nuclear microprobe." *Nuclear Instruments & Methods in Physics Research, Section B: Beam Interactions with Materials and Atoms*, 130(1-4), 582.

Roy, W. R., and Griffin, R. A. (1984). "Illinois basin coal fly ashs. 2. Equilibria relationships and qualitative modeling of ash-water reactions." *Environmental Science and Technology*, 18(10), 739.

Sadiq, M. (1997). "Arsenic chemistry in soils: an overview of thermodynamic predictions and field observations." *Water, Air, and Soil Pollution*, 93(1-4), 117.

Sauer, J. J. (2006). "Evaluation of metals leaching from gray iron foundry and coal combustion byproducts," MS Thesis, University of Wisconsin, Madison, WI.

Sauer, J. J., Benson, C. H., and Edil, T. B. (2005). "Leaching of heavy metals from organic soils stabilized with high carbon fly ash." Geo Engineering Report No. 05-01, Geo Engineering Program, University of Wisconsin-Madison, Madison, WI.

Sauve, S., Hendershot, W., and Allen, H. E. (2000). "Solid-solution partitioning of metals in contaminated soils: dependence on pH, total metal burden, and organic matter." *Environmental Science and Technology*, 34(7), 1125.

Seames, W. S., and Wendt, J. O. L. (2000). "Partitioning of arsenic, selenium, and cadmium during the combustion of Pittsburgh and Illinois #6 coals in a self-sustained combustor." *Fuel Processing Technology*, 63(2), 179.

Seby, F., Potin-Gautier, M., Giffaut, E., Borge, G., and Donard, O. F. X. (2001). "A critical review of thermodynamic data for selenium species at 25°C." *Chemical Geology*, 171(3-4), 173-194.

Senol, A., Bin-Shafique, S., Edil, T. B., and Benson, C. H. (2002). "Use of class C fly ash for stabilization of soft subgrade." *Fifth International Congress on Advances in Civil Engineering*, Istanbul Technical University, Istanbul, Turkey, 963-97.

Shah, P., Strezov, V., Stevanov, C., and Nelson, P. F. (2007). "Speciation of arsenic and selenium in coal combustion products." *Energy and Fuels*, 21(2), 506.

Shuman, L. M. (1977). "Adsorption of Zn by Fe and Al hydrous oxides as influenced by aging and pH." *Soil Science Society of America Journal*, 41(4), 703-706.

Smith, R. M., and Martell, A. E. (1976). *Critical stability constants. Volume 4: Inorganic complexes*, Plenum Press, New York.

Stevenson, F. J. (1982). *Humus chemistry: genesis, composition, reactions*, John Wiley & Sons, New York.

Stevenson, F. J. (1994). *Humus chemistry: genesis, composition, reactions*, John Wiley & Sons, New York.

Stumm, W., and Morgan, J. J. (1996). *Aquatic Chemistry: Chemical Equilibria and Rates in Natural Waters*, John Wiley & Sons, New York.

Talbot, R. W., Anderson, M. A., and Andren, A. W. (1978). "Qualitative model of heterogeneous equilibria in a fly ash pond." *Environmental Science and Technology*, 12(9), 1056.

Taştan, E. O. (2005). "Stabilization of organic soils using fly ash," MS Thesis, University of Wisconsin, Madison, WI.

Terrel, R. L., Epps, J. A., and Associates. (1979). "Soil Stabilization in Pavement Structures: A User's Manual Volume 2." DOT-FH-11-9406, Federal Highway Administration, Department of Transportation, Washington.

Theis, T. L., Halvorson, M., Levine, A., Stankunas, A., and Unites, D. (1982). "Fly ash attenuation mechanisms." Report and technical studies on the disposal and utilization of fossil-fuel combustion by-products. Vol. II, USEPA, Washington, D. C.

Theis, T. L., and Richter, R. O. (1979). "Chemical speciation of heavy metals in power plant ash pond leachate." 13(2), 219-224.

Theis, T. L., and Wirth, J. L. (1977a). "Sorptive behavior of trace metals on fly ash in aqueous system." 11(12), 1096-1100.

Theis, T. L., and Wirth, J. L. (1977b). "Sorptive behavior of trace metals only fly ash in aqueous system." 11(12), 1096-1100.

Tiruta-Barna, L., Imyim, A., and Barna, R. (2004). "Long-term prediction of the leaching behavior of pollutants from solidified wastes." *Advances in Environmental Research*, 8(3-4), 697.

Tiruta-Barna, L., Rakotoarisoa, Z., and Mehu, J. (2006). "Assessment of the multi-scale leaching behaviour of compacted coal fly ash." *Journal of Hazardous Materials*, 137(3), 1466.

Tsiridis, V., Petala, M., Samaras, P., and Sakellaropoulos, G. P. (2004). "An integrated approach for the assessment of toxic properties of fly ash." *Second International Conference on Waste Management and the Environment, Sep 29-Oct 1 2004*, Rhodes, Greece, 559-568.

Turner, J. P. (1997). "Evaluation of western coal fly ashes for stabilization of low-volume roads." *Proceedings of the 1997 Symposium on Testing Soil Mixed with Waste or Recycled Materials*, New Orleans, LA, USA, 157.

Turner, R. R. (1981). "Oxidation-State Of Arsenic In Coal Ash Leachate." *Environmental Science & Technology*, 15(9), 1062-1066.

Ugurlu, A. (2004). "Leaching characteristics of fly ash." *Environmental Geology*, 46(6-7), 890-895.

USEPA. (1996). "Method 3050B. Acid Digestion of Sediments, Sludges, and Soils." Test Method for Evaluating Solid Waste: Physical/Chemical Methods, U.S. EPA, Washington, D. C., 3050B-1 - 3050B-12.

USEPA. (2005). "Using Coal Ash in Highway Construction: A Guide to Benefits and Impacts." EPA-530-K-05-002, US Environmental Protection Agency, Washington, D. C.

van der Hoek, E. E., Bonouvrie, P. A., and Comans, R. N. J. (1994). "Sorption of As and Se on mineral components of fly ash: Relevance for leaching processes." *Applied Geochemistry*, 9(4), 403.

van der Hoek, E. E., van Elteren, J. T., and Comans, R. N. J. (1996). "Determination of As, Sb and Se speciation in fly-ash leachates." *International Journal Of Environmental Analytical Chemistry*, 63(1), 67-79.

van der Sloot, H. A. (1990). "Leaching behaviour of waste and stabilized waste materials; characterization for environmental assessment purposes." *Waste Management & Research*, 8(3), 215-228.

van der Sloot, H. A. (1991). "Systematic leaching behaviour of trace elements from construction materials and waste materials." *Studies in Environmental Science*(48), 19.

van der Sloot, H. A. (1996). "Developments in evaluating environmental impact from utilization of bulk inert wastes using laboratory leaching tests and field evaluation." *Waste Management*, 16(1-3), 65-81.

van der Sloot, H. A. (2002). "Characterization of the leaching behaviour of concrete mortars and of cement-stabilized wastes with different waste loading for long term environmental assessment." *Waste Management*, 22(2), 181-186.

van der Sloot, H. A., Comans, R. N. J., and Hjelmar, O. (1996). "Similarities in the leaching behaviour of trace contaminants from waste, stabilized waste, construction materials and soils." *Science of the Total Environment Proceedings of the 1994 Conference on the Science of Total Environment, Jun 4 1994*, 178(1-3), 111.

van der Sloot, H. A., and Dijkstra, J. J. (2004). "Development of Horizontally Standardized Leaching Tests for Construction Materials: A Material Based or

Release Based Approach?" ECN-C--04-060, Dutch Ministry of Housing, Spatial Planning and the Enviroment.

van der Sloot, H. A., Hoede, D., and Commans, R. N. J. (1994). "The influence of reducing properties on leaching of elements from waste materials and construction materials." WASCON 1994: Environmental aspects of construction with waste materials., J. J. J. M. Goumans, H. A. v. d. Sloot, and T. G. Aalbers, eds., Elsevier, Amsterdam, 483-490.

van der Sloot, H. A., Rietra, R. P. J. J., Vroon, R. C., Scharff, H., and Woelders, J. A. (2001). "Similarities in the long term leaching behaviour of predominantly inorganic waste, MSWI bottom ash, degraded MSW and bioreactor residues." *Proceedings of the 8th Waste Management and Landfill Symposium*, Cagliari, Italy, 199–208.

van der Sloot, H. A., Seignette, P., Comans, R. N. J., Van Zomeren, A., Dijkstra, J. J., Meeussen, H., Kosson, D. S., and Hjelmar, O. (2003). "Evaluation of environmental aspects of alternative materials using an integrated approach assisted by a database/expert system." *Recycling and Reuse of Waste Materials, Proceedings of the International Symposium, Sep 9-11 2003*, Dundee, United Kingdom, 769-789.

van der Sloot, H. A., van Zomeren, A., Dijkstra, J. J., Meeussen, J. C. L., Comans, R. N. J., and Scharff, H. (2005). "Prediction of the leaching behaviour of waste mixtures by chemical speciation modelling based on a limited set of key parameters." ECN-RX-05-164, ECN, Environmental Risk Assessment, Petten, The Netherlands.

van der Sloot, H. A., van Zomeren, A., Meeussen, J. C. L., Seignette, P., and Bleijerveld, R. (2007). "Test method selection, validation against field data, and predictive modelling for impact evaluation of stabilised waste disposal." *Journal of Hazardous Materials*, 141(2), 354.

Vassilev, S. V., Menendez, R., Alvarez, D., Diaz-Somoano, M., and Martinez-Tarazona, M. R. (2003). "Phase-mineral and chemical composition of coal fly ashes as a basis for their multicomponent utilization. 1. Characterization of feed coals and fly ashes." *Fuel*, 82, 1793-1811.

Wagemann, R. (1978). "Some theoretical aspects of stability and solubility of inorganic arsenic in freshwater environment." *Water Research*, 12(3), 139-145.

Wang, J., Teng, X., Wang, H., and Ban, H. (2004). "Characterizing the metal adsorption capability of a class F coal fly ash." *Environmental Science and Technology*, 38(24), 6710-6715.

Wang, T., Wang, J., Burken, J. G., Ban, H., and Ladwig, K. (2007). "The leaching characteristics of selenium from coal fly ashes." *Journal Of Environmental Quality*, 36(6), 1784.

Warren, C. J., and Dudas, M. J. (1984). "Weathering processes in relation to leachate properties of alkaline fly ash." *Journal of Environmental Quality*, 13(4), 530.

Warren, C. J., and Dudas, M. J. (1985). "Formation of secondary minerals in artificially weathered fly ash." *Journal of Environmental Quality*, 14(3), 405-410.

Warren, C. J., and Dudas, M. J. (1986). "Mobilization and attenuation of trace elements in an artificially weathered fly ash." EPRI EA-4747, Electric Power Research Institute, Palo Alto, CA.

White, D. J., Harrington, D., and Thomas, Z. (2005). "Fly Ash Soil Stabilization for Non-Uniform Subgrade Soils, Volume I: Engineering Properties and Construction Guidelines." IHRB Project TR-461; FHWA Project 4, Center for Transportation Research and Education, Iowa State University, Ames, IA.

Whiting, K. S. (1992). "The Thermodynamics and Geochemistry of As with the Application to Subsurface Waters at the Sharon Steel Superfund Site Midvale, Utah," MSc., Colorado School of Mines.

Xu, Y.-H., Nakajima, T., and Ohki, A. (2001). "Leaching of arsenic from coal fly ashes 1. Leaching behavior of arsenic and mechanism study." *Toxicological and Environmental Chemistry*, 81(1-2), 55-68.

Yan-Chu, H. (1994). *Arsenic in the environment: Part I. Cycling and characterization*, Wiley, New York.

Zhang, M., and Reardon, E. J. (2003). "Removal of B, Cr, Mo, and Se from wastewater by incorporation into hydrocalumite and ettringite." *Environmental Science and Technology*, 37(13), 2947.

Zhou, L. X., and Wong, J. W. C. (2003). "Behavior of heavy metals in soil: Effect of dissolved organic matter." Geochemical and hydrological reactivity of heavy metals in soils, H. M. S. W. L. Kingery, ed., CRC Press LLC, Raton, Florida, 245-270.

APPENDIX A

METHOD DETECTION LIMITS FOR ANALYSES CONDUCTED WITH VARIAN VISTA-MPX INDUCTIVELY COUPLED PLASMA-OPTICAL EMISSION SPECTROMETER (ICP-OES)

Table A-1. Method detection limits for analyses conducted with Varian Vista-MPX
inductively coupled plasma-optical emission spectrophotometer (ICP-OES)

Element	Wavelength (nm)	Detection Limit (μg/L)
Ag	328.068	0.477
Al	396.152	0.892
As	188.980	1.289
B	249.772	0.200
Ba	455.403	0.035
Be	313.042	0.011
Ca	315.887	1.448
Cd	214.439	0.020
Co	238.892	0.164
Cr	267.716	0.224
Cu	327.395	0.197
Fe	238.204	0.426
K	766.491	3.262
Li	670.783	0.294
Mg	279.800	1.279
Mn	257.610	0.023
Mo	202.032	0.518
Na	568.821	3.065
Ni	231.604	0.315
P	213.618	3.134
Pb	220.353	0.848
Sb	206.834	3.445
Se	196.026	1.184
Si	251.611	1.715
Sn	189.927	2.109
Sr	407.771	0.006
Tl	190.794	4.044
V	292.401	0.238
Zn	213.857	0.142

APPENDIX B

**NEUTRALIZATION CURVES FROM TITRATION TEST FOR SOILS, FLY ASHES,
AND SOIL-FLY ASH MIXTURES**
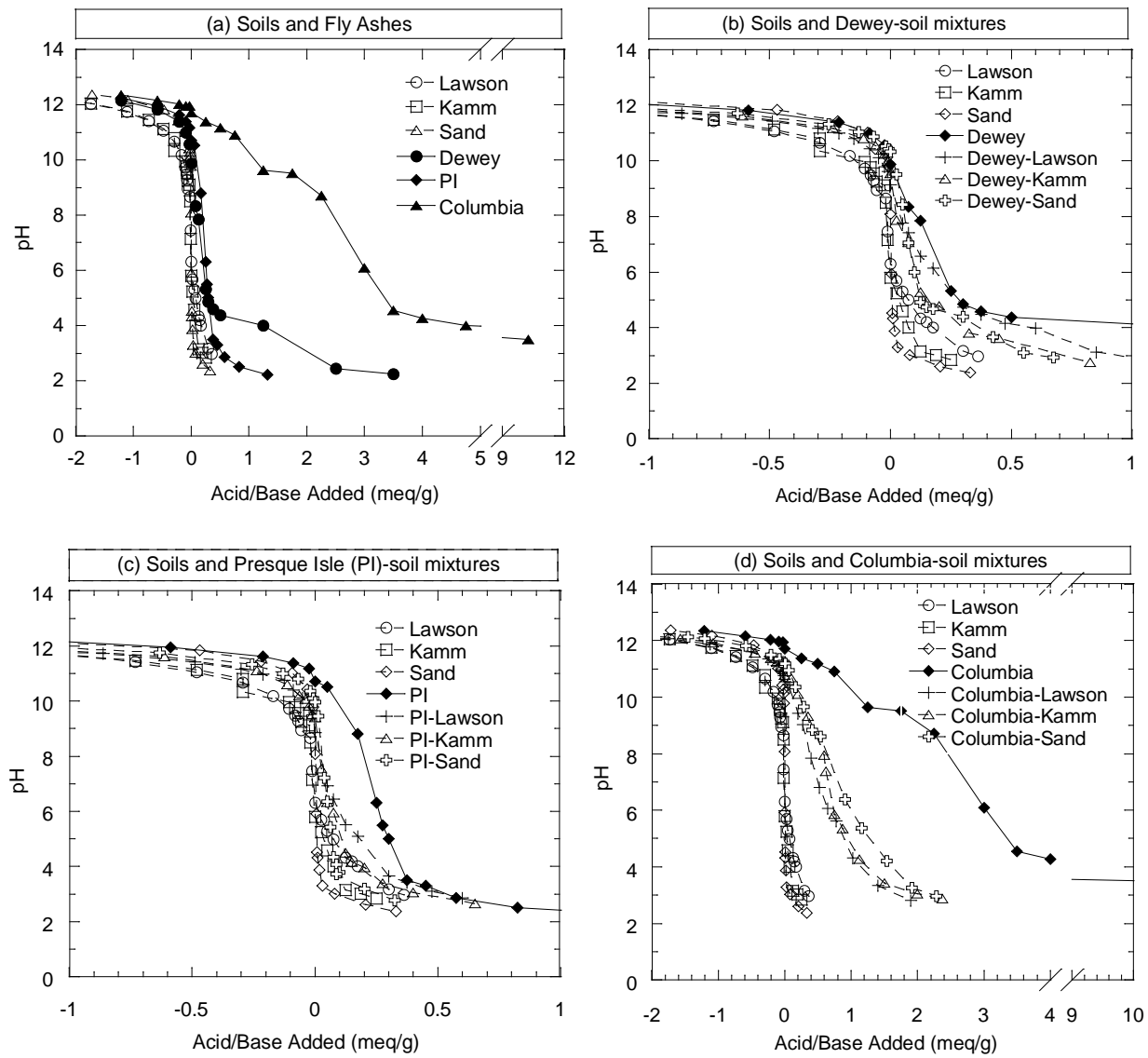
Figure B-1. Neutralization curves from titration test for soils, fly ashes, and soil-fly ash mixtures.

APPENDIX C

PH VS. TIME FROM KINETIC BATCH TESTS
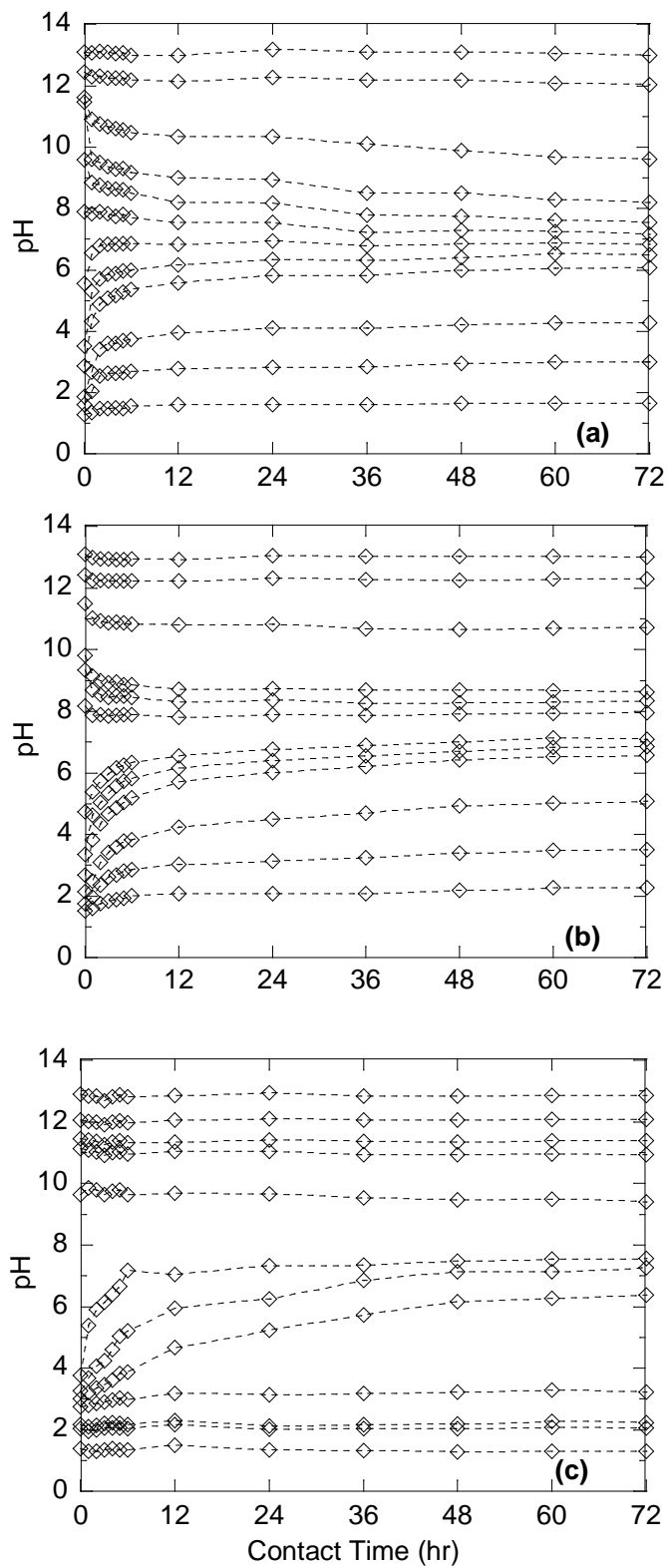
Figure C-1. pH vs. time from kinetic batch tests on (a) Lawson soil, (b) Kamm clay,   and
(c) sand.
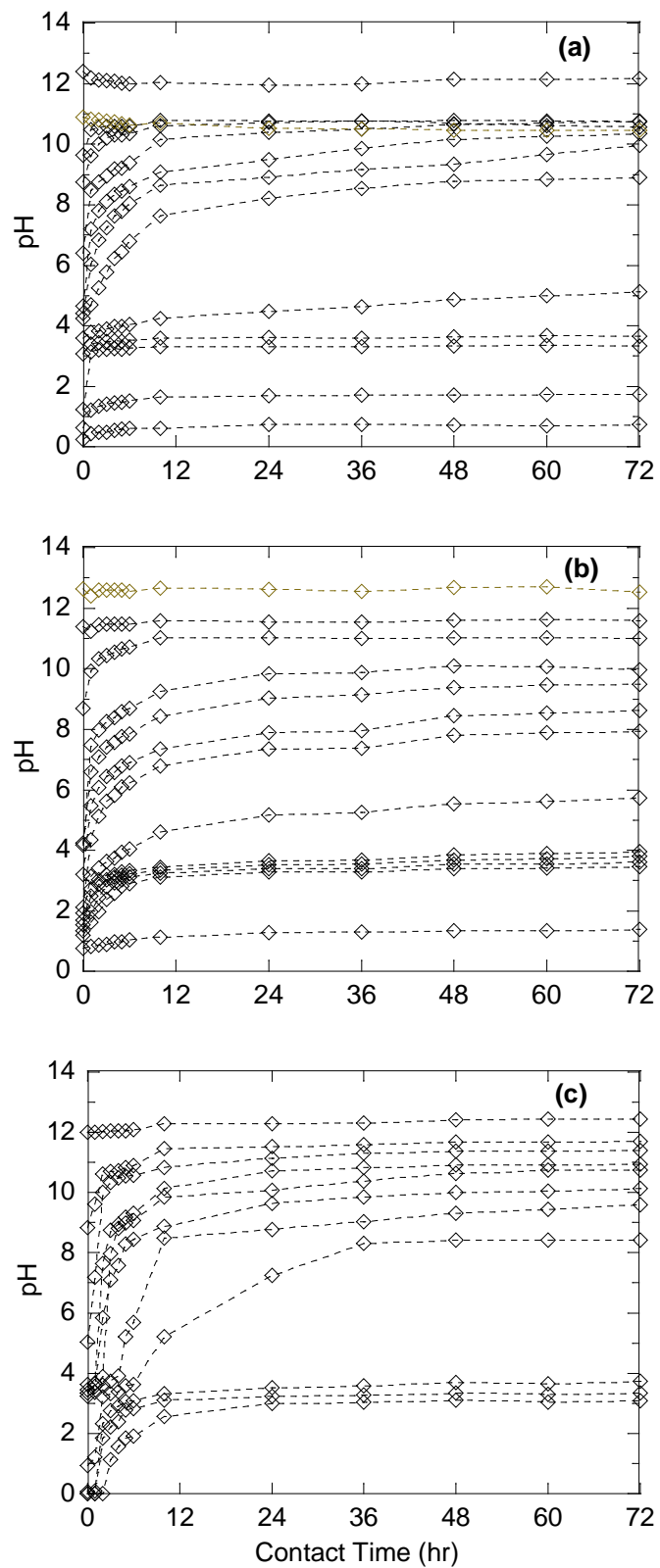
Figure C-2. pH vs. time from kinetic batch tests on (a) Dewey, (b) Presque Isle, and (c) Columbia fly ash.
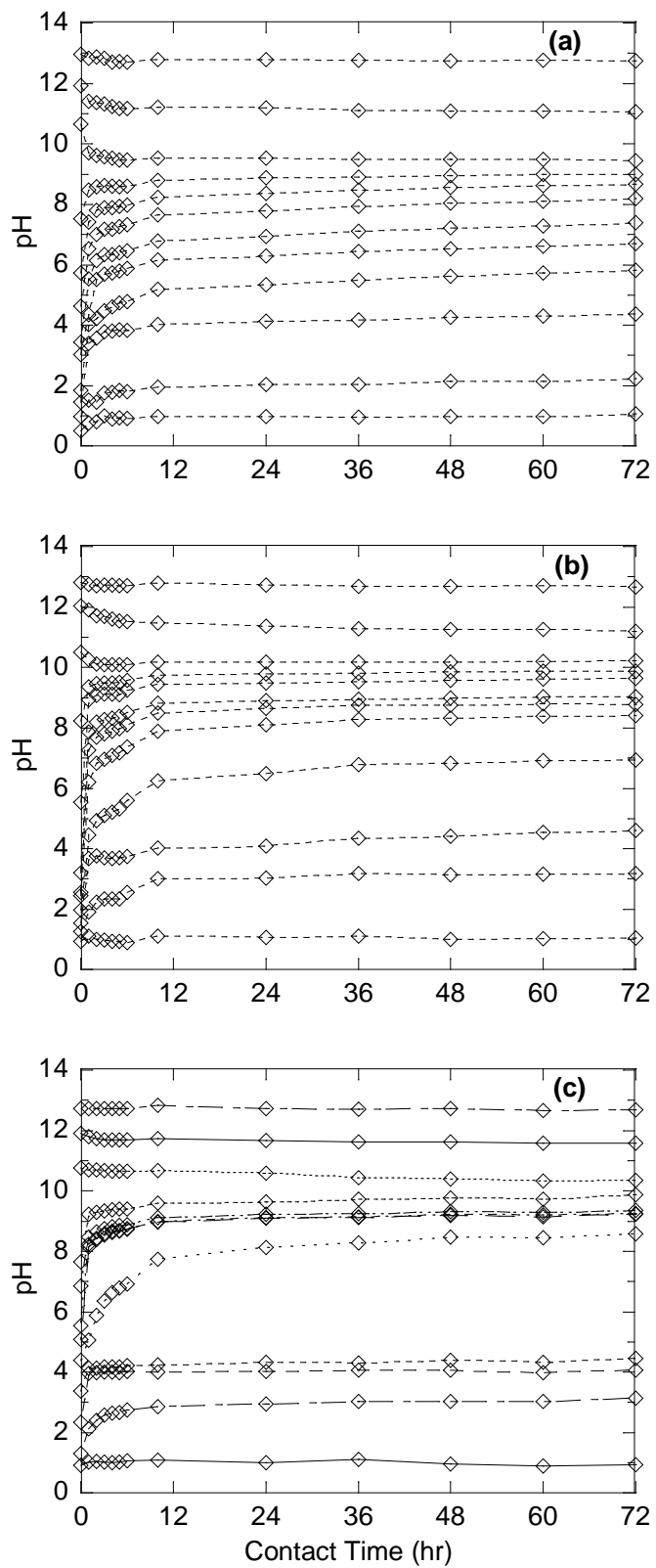
Figure C-3. pH vs. time from kinetic batch tests on (a) Dewey-Lawson, (b) Dewey-Kamm, and (c) Dewey-sand.
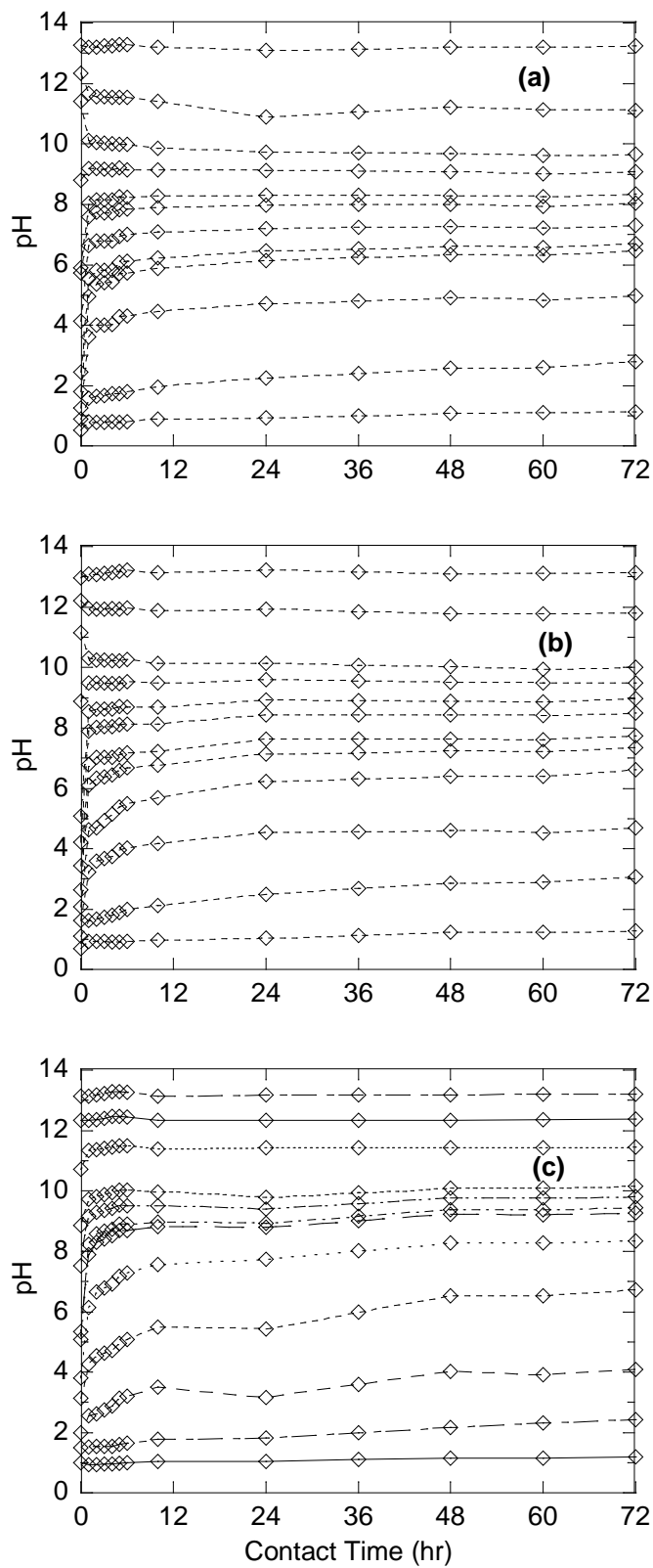
Figure C-4. pH vs. time from kinetic batch tests on (a) Presque Isle-Lawson, (b) Presque Isle-Kamm, and (c) Presque Isle-sand.
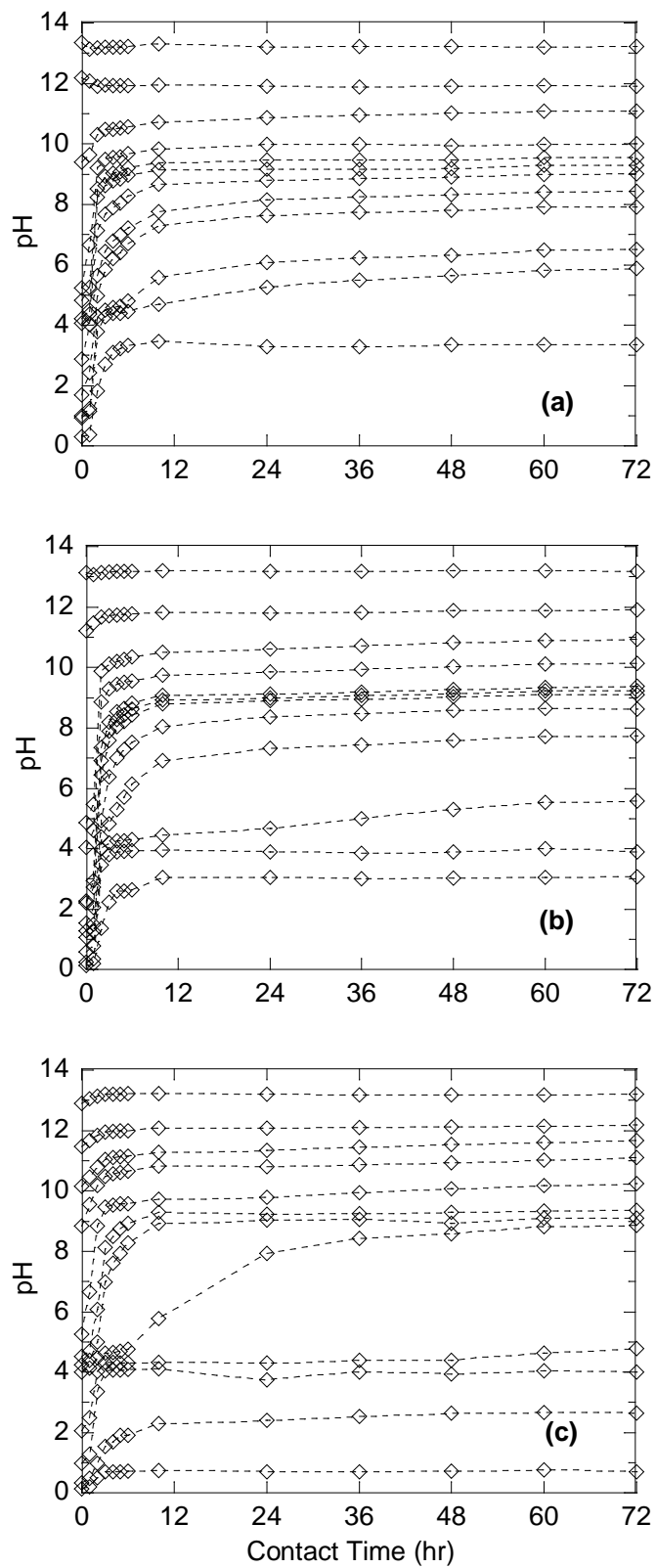
Figure C-5. pH vs. time from kinetic batch tests on (a) Columbia-Lawson, (b) Columbia-Kamm, and (c) Columbia–sand.

APPENDIX D

**EQUILIBRIUM LEACHING CONCENTRATIONS AS A FUNCTION OF PH
FOR FLY ASHES AND THE MIXTURES OF SOIL-FLY ASH
OBTAINED FROM BATCH LEACHING TESTS FOR MODELING STUDY**

Table D-1. Equilibrium leaching concentrations as a function of pH for Dewey and Dewey-soil obtained from batch leaching tests for modeling study.

Sample	pH	Eq of Acid/Base (meq/g)	Eh (mV)	DOC (mg/L)	Sulfate (mg/L)	Al (mg/L)	As (mg/L)	B (mg/L)	Ba (mg/L)	Ca (mg/L)	Cd (mg/L)	Cr (mg/L)	Cu (mg/L)	Fe (mg/L)	Mg (mg/L)	Na (mg/L)	P (mg/L)	Se (mg/L)	Sr (mg/L)	Zn (mg/L)
Dewey																				
D-1	5.81	1.95	290	1.72	5,531	0.17143	<0.00129*	19.9596	0.13363	483.789	0.05165	0.00128	0.05195	0.00766	506.458	3169.50	0.10303	0.02664	25.2840	1.98376
D-2	7.95	0.90	182	1.77	9,171	0.64606	0.01141	13.5788	0.06867	338.337	0.00061	0.00053	0.00256	0.00355	350.275	3270.74	0.04663	0.02266	16.6641	0.01277
D-3	10.25	0.32	75	1.31	11,043	94.8659	0.05524	12.2631	0.21273	293.394	0.00219	0.04443	0.00637	0.20485	0.30831	3408.56	0.10229	0.07865	24.5430	0.01498
D-4	12.25	-0.86	-31	2.45	13,912	64.9350	0.63765	2.16789	0.13317	11.9774	0.00005	0.06207	<0.0002*	0.06174	<0.00128*	3059.96	0.32498	0.01066	6.00669	0.04337
Dewey-Lawson																				
DL-1	5.36	0.58	279	3.50	1,912	0.99388	0.00311	6.22718	0.08060	940.814	0.01409	<0.00022*	0.00823	0.01504	237.471	380.889	0.13910	0.04654	12.0838	1.38702
DL-2	7.89	0.10	230	3.61	2,147	0.19299	0.00642	4.05074	0.08065	555.659	0.00039	<0.00022*	0.00424	0.00930	61.5762	353.286	0.14506	0.01778	7.63670	0.02059
DL-3	9.66	-0.05	151	7.64	2,065	2.32149	0.01695	3.40293	0.18456	377.625	0.00009	<0.00022*	0.00569	0.01482	1.80689	339.367	0.22771	0.01001	5.26505	0.01625
DL-4	12.57	-0.90	58	111.30	2,002	30.3598	0.13264	1.44863	0.09676	29.7608	0.00002	<0.00022*	0.36657	0.04239	0.02979	257.412	1.23655	0.01605	1.17605	0.02664
Dewey-Kamm																				
DK-1	6.01	0.45	350	1.56	2,012	0.29975	<0.00129*	5.70203	0.05271	777.400	0.00736	<0.00022*	0.00671	0.01747	176.163	354.100	0.09668	0.02422	10.2986	0.10346
DK-2	8.47	0.10	238	0.97	2,091	0.66116	0.00736	4.65278	0.08421	541.347	0.00014	<0.00022*	0.00148	0.01074	34.4251	346.236	0.19912	0.01453	8.10444	0.02412
DK-3	9.55	0.00	189	1.48	2,052	4.86246	0.01381	4.55510	0.20448	422.804	0.00012	<0.00022*	0.00063	0.00492	0.55039	336.993	0.08100	0.00899	6.03557	0.02116
DK-4	12.61	-0.80	70	9.86	1,701	31.5690	0.15302	1.18758	0.22764	16.4475	<0.00002*	0.00048	0.02059	0.02067	0.02806	245.345	0.22498	<0.00118*	1.45625	0.02842
Dewey-Red Wing																				
DR-1	5.81	0.87	376	1.11	1,411	0.24516	0.00307	5.56219	0.09274	1443.66	0.01338	<0.00022*	0.01089	0.00851	261.005	334.588	0.25484	0.04149	15.6574	0.12465
DR-2	8.11	0.15	240	0.83	2,022	0.35653	0.00708	3.51183	0.06006	524.069	0.00007	<0.00022*	<0.0002*	0.00380	35.3560	298.527	0.04313	0.01105	9.68379	0.00090
DR-3	10.55	-0.02	156	1.02	1,992	14.1581	0.01474	1.96828	0.25481	313.130	<0.00002*	0.00142	<0.0002*	0.10172	0.10784	306.558	0.04027	0.00125	8.35255	0.00288
DR-4	12.34	-0.42	84	2.09	1,615	17.7219	0.04896	0.66084	0.20312	20.9354	<0.00002*	0.00204	<0.0002*	0.00981	0.02103	263.365	0.17566	<0.00118*	3.50760	0.00069
Dewey-MnRoad																				
DM-1	6.02	0.87	375	1.19	1,444	0.11242	0.00300	4.99856	0.09775	1043.79	0.00516	<0.00022*	0.00565	0.00375	188.977	326.560	0.09919	0.03733	12.8786	0.07081
DM-2	8.11	0.15	270	1.00	1,916	0.28442	0.01043	4.38979	0.06785	514.387	0.00020	<0.00022*	<0.0002*	0.00225	41.8090	296.752	0.12341	0.01340	8.41276	0.00089
DM-3	10.63	-0.02	140	1.20	2,114	2.72652	0.01616	4.05967	0.17316	349.646	<0.00002*	<0.00022*	<0.0002*	0.00179	0.18550	293.479	0.18168	0.00590	6.73391	0.00027
DM-4	12.22	-0.42	78	2.27	1,728	6.31113	0.05083	1.41531	0.26418	26.8086	<0.00002*	0.00137	<0.0002*	0.00317	0.02009	233.369	0.10157	<0.00118*	2.43549	0.00052
Dewey-Sand																				
DS-1	6.17	0.20	347	1.82	1,943	0.18777	<0.00129*	4.63495	0.04284	657.421	0.06250	<0.00022*	0.00906	0.00801	82.0761	318.892	0.26622	0.02401	10.3868	0.29614
DS-2	8.00	0.15	271	0.59	2,230	0.74354	0.00409	4.30344	0.04346	655.964	0.00071	<0.00022*	0.00344	0.00581	73.3605	331.387	0.27272	0.02463	9.97690	0.02479
DS-3	9.94	0.01	180	0.72	2,225	20.3358	0.01603	2.87375	0.21207	460.056	0.00009	<0.00022*	0.00415	0.01555	1.29948	367.493	0.08693	0.02270	11.9507	0.02905
DS-4	12.43	-0.40	54	1.22	1,594	34.5289	0.14134	0.91472	0.09643	17.5031	0.00002	<0.00022*	<0.0002*	0.04622	0.06619	267.402	0.41672	<0.00118*	4.52351	0.13366

Note: * Concentration below method detection limit.

Table D-2. Equilibrium leaching concentrations as a function of pH for Presque Isle (PI) and PI-soil mixtures obtained from batch leaching tests for modeling study.

Sample	pH	Eq of Acid/Base (meq/g)	Eh (mV)	DOC (mg/L)	Sulfate (mg/L)	Al (mg/L)	As (mg/L)	B (mg/L)	Ba (mg/L)	Ca (mg/L)	Cd (mg/L)	Cr (mg/L)	Cu (mg/L)	Fe (mg/L)	Mg (mg/L)	Na (mg/L)	P (mg/L)	Se (mg/L)	Sr (mg/L)	Zn (mg/L)
Presque Isle (PI)																				
P-1	5.87	0.50	323	1.60	678	0.09895	0.14786	43.8260	0.20619	732.877	0.01081	0.00079	0.01184	0.00441	109.235	30.8129	3.80200	0.24664	21.1946	0.07189
P-2	7.90	0.35	263	1.58	605	0.07803	0.08238	39.1720	0.12246	608.845	0.00096	0.00147	0.01019	0.00396	81.0680	25.2743	0.87546	0.20209	15.3487	0.01582
P-3	9.82	0.15	174	1.18	585	7.63596	0.00568	34.4820	1.30660	453.645	0.00039	0.02330	0.00755	0.00446	3.62230	21.3120	0.06823	0.22586	12.7080	0.00870
P-4	11.68	0.00	-9	1.35	499	5.59727	0.01060	16.2623	0.91506	127.611	0.00012	0.02576	0.01293	0.00598	0.00883	7.67472	0.07487	0.18693	5.66961	0.01005
PI-Lawson																				
PL-1	6.70	0.70	263	3.72	43	0.12503	0.01107	5.89305	0.70956	375.180	0.00125	0.00106	0.00635	0.01624	122.798	9.13111	1.38438	0.04745	2.93725	0.32623
PL-2	8.02	0.05	207	3.83	68	0.12878	0.01294	4.80653	0.09882	69.4882	<0.00002*	0.00070	0.00166	0.02984	23.3246	3.60274	1.27044	0.03388	0.58020	0.02549
PL-3	8.92	-0.07	175	8.34	66	1.10308	0.02490	4.37616	0.05184	20.8449	<0.00002*	0.00205	0.00465	0.79197	3.80246	2.85663	1.60924	0.04289	0.15313	0.03366
PL-4	10.98	-0.17	49	45.89	69	14.8228	0.07322	5.13537	0.27965	10.3442	<0.00002*	0.01650	0.08210	10.9290	3.58052	2.29338	2.38984	0.05605	0.10252	0.19695
PI-Kamm																				
PK-1	6.72	0.53	259	0.51	64	0.15638	0.00134	6.31227	0.54347	235.171	<0.00002*	<0.00022*	0.00326	0.00930	82.0825	7.85181	0.61515	0.03171	3.68773	0.03861
PK-2	7.90	0.06	223	1.16	69	0.21326	0.01240	5.80507	0.08121	48.1735	<0.00002*	0.00134	<0.0002*	0.06355	11.9300	3.36441	1.10769	0.02808	0.75482	0.02921
PK-3	9.34	-0.04	175	1.77	67	0.53125	0.01837	5.53154	0.02768	15.3566	<0.00002*	0.00180	<0.0002*	0.19214	0.59433	3.05089	1.12276	0.02294	0.22238	-0.02739
PK-4	11.72	-0.09	29	3.82	71	8.57683	0.02737	5.45684	0.03576	6.11291	<0.00002*	0.00310	0.00020	0.03168	0.00948	2.98723	0.32569	0.04944	0.16232	-0.02391
PI-Red Wing																				
PR-1	6.07	0.50	213	1.06	32	0.14569	0.00778	6.48801	1.56803	1083.72	0.00374	0.00613	0.01277	1.17919	106.491	23.1557	1.92721	0.02768	6.06356	0.04758
PR-2	8.37	0.05	164	0.46	70	0.05388	0.02499	5.89120	0.30189	160.739	<0.00002*	0.00259	0.00479	0.00672	11.8322	9.75095	1.64769	0.02049	2.47953	0.00292
PR-3	10.78	-0.03	142	0.80	67	2.11178	0.00332	5.78749	0.14922	40.3899	<0.00002*	0.00372	<0.0002*	0.00120	0.01583	8.22689	0.26717	0.01080	1.02636	0.00598
PR-4	11.85	-0.10	102	1.01	67	5.00153	0.00682	5.74238	0.17401	36.1888	<0.00002*	0.00361	0.00096	0.00873	0.00753	7.99545	0.25902	0.02473	1.00685	0.00239
PI-Mn Rd																				
PM-1	6.17	0.50	380	0.93	34	0.08295	0.01508	6.37222	1.02717	1023.29	0.00267	<0.00022*	0.01288	<0.00043*	126.679	17.1266	3.50449	0.03707	5.41217	0.04109
PM-2	8.34	0.05	311	0.55	74	0.03233	0.02286	5.78245	0.16463	171.803	<0.00002*	0.00067	0.00424	<0.00043*	19.5349	5.18305	2.14850	0.02192	1.88445	<0.00014*
PM-3	9.66	-0.03	240	0.68	74	0.06484	0.02274	5.43280	0.06900	32.96530	<0.00002*	0.00106	0.00141	<0.00043*	0.28679	3.82982	0.23483	0.01995	0.52427	0.00021
PM-4	11.96	-0.20	95	2.28	75	0.72512	0.05662	5.52109	0.04384	12.00610	<0.00002*	0.00136	0.00183	0.01825	0.01021	3.51781	0.16666	0.04064	0.28513	0.00160
PI-Sand																				
PS-1	6.98	0.19	207	0.50	59	0.10265	0.00729	4.24842	0.33838	84.6344	0.00369	<0.00022*	<0.0002*	0.00374	10.7394	3.03223	0.33894	0.04648	2.84946	0.05619
PS-2	9.22	0.06	40	0.54	67	2.28869	0.01090	4.25324	0.32611	55.8590	<0.00002*	0.00118	<0.0002*	0.00851	4.27941	2.36854	0.13337	0.04801	2.08230	0.02146
PS-3	11.03	0.05	12	0.61	63	5.59404	0.00440	3.97964	0.46890	40.5761	<0.00002*	0.00204	<0.0002*	0.00764	0.13400	2.05630	0.07131	0.03668	1.94516	0.02425
PS-4	12.07	0.02	-48	0.72	52	8.11258	0.00487	3.01800	0.64890	20.1981	<0.00002*	0.00234	<0.0002*	0.01119	0.00219	2.07508	0.07276	0.04387	1.73623	0.03137

Note: * Concentration below method detection limit.

Table D-3. Equilibrium leaching concentrations as a function of pH for Columbia and Columbia-soil mixtures obtained from batch leaching tests for modeling study.

Sample	pH	Eq of Acid/Base (meq/g)	Eh (mV)	DOC (mg/L)	Sulfate (mg/L)	Al (mg/L)	As (mg/L)	B (mg/L)	Ba (mg/L)	Ca (mg/L)	Cd (mg/L)	Cr (mg/L)	Cu (mg/L)	Fe (mg/L)	Mg (mg/L)	Na (mg/L)	P (mg/L)	Se (mg/L)	Sr (mg/L)	Zn (mg/L)
Columbia																				
C-1	6.74	9.00	323	1.82	1,375	0.26042	0.05442	1.75824	1.87900	3775.75	0.00453	0.01659	0.01300	0.00952	1121.31	410.142	0.16773	0.30586	31.8000	0.02115
C-2	8.89	5.00	284	1.74	1,204	4.21670	0.04970	6.16649	3.00700	3264.59	0.00380	0.06031	0.01351	0.00202	54.8775	343.289	0.13464	0.23398	29.8640	0.00698
C-3	11.13	1.50	227	1.64	362	39.0803	0.04834	0.41676	24.1670	1109.96	0.00211	0.03707	0.00817	0.00298	0.06114	206.317	0.12920	0.05318	26.5080	0.01089
C-4	12.55	0.00	-26	3.12	225	7.94809	0.04413	1.95969	21.6480	134.403	0.00101	0.00062	0.00080	0.03536	0.01074	184.116	0.12482	0.00506	31.5220	0.01524
Columbia-Lawson																				
CL-1	5.68	1.45	357	18.52	367	0.32654	<0.00129*	5.72470	0.59448	1983.62	0.01150	0.00362	0.02362	0.00350	423.830	55.6389	0.11216	0.09057	22.1080	0.76375
CL-2	8.22	0.65	235	16.62	105	0.32580	<0.00129*	4.24972	0.55702	1194.03	0.00054	0.05311	0.02901	0.01258	206.596	37.3582	0.35737	0.06788	13.4730	0.00038
CL-3	9.66	0.15	122	32.05	274	7.22486	<0.00129*	2.30789	0.67126	447.798	0.00008	0.10323	0.05517	0.00499	0.45516	24.2800	0.33538	0.05136	6.44654	<0.00014*
CL-4	11.81	-0.10	53	56.32	101	22.8922	<0.00129*	1.03537	0.25390	59.7773	<0.00002*	0.08283	0.22583	0.01047	<0.00128*	17.4140	0.60047	0.01805	1.36934	<0.00014*
Columbia-Kamm																				
CK-1	5.41	1.53	411	4.51	337	0.78965	<0.00129*	6.03890	0.61312	2114.58	0.01268	0.01303	0.04210	0.00492	457.078	65.1146	0.20357	0.09580	25.5910	0.39597
CK-2	7.81	0.80	303	5.80	394	0.25090	<0.00129*	4.69584	0.47622	1379.30	0.00064	0.09768	0.01919	0.03980	245.821	41.5318	0.22796	0.07446	17.2563	<0.00014*
CK-3	10.01	0.22	182	7.57	217	10.6005	<0.00129*	2.82813	1.12385	582.354	0.00008	0.13925	0.02624	0.00843	0.18853	28.8102	0.24341	0.04876	9.75934	<0.00014*
CK-4	11.86	-0.50	68	7.14	51	22.6979	<0.00129*	0.93205	0.70811	77.8992	<0.00002*	0.09891	0.03610	<0.00043*	<0.00128*	20.2638	0.24776	0.00795	2.76961	0.00477
Columbia-Red Wing																				
CR-1	6.18	2.15	237	3.02	414	0.22400	<0.00129*	6.16850	1.09420	2644.43	0.01281	0.01871	0.03067	0.00154	635.180	77.7264	0.17650	0.10520	24.4970	0.30710
CR-2	8.23	0.65	187	2.97	401	0.83643	<0.00129*	4.71395	0.57942	1181.50	0.00036	0.14903	0.02121	<0.00043*	183.574	45.6236	0.16781	0.07967	14.4980	<0.00014*
CR-3	10.53	0.10	93	2.82	110	33.2744	<0.00129*	0.77367	2.27647	304.960	<0.00002*	0.14862	0.03129	0.00776	0.01631	31.8584	0.18582	0.02481	8.47177	0.01978
CR-4	11.97	-0.05	-43	2.58	33	28.8740	<0.00129*	0.63789	2.10481	104.552	<0.00002*	0.11579	0.03257	<0.00043*	<0.00128*	28.1994	0.18607	0.00521	5.28033	<0.00014*
Columbia-Mn Rd																				
CM-1	5.80	2.50	324	2.24	399	0.47827	<0.00129*	6.41241	0.71803	2830.49	0.01575	0.02285	0.04426	0.00702	704.966	80.6117	0.08117	0.10900	25.5730	0.70718
CM-2	8.69	0.50	177	2.82	414	0.69333	<0.00129*	4.15857	0.87645	1097.35	0.00021	0.12649	0.01748	<0.00043*	80.3512	38.6305	0.27063	0.07374	13.2223	0.00041
CM-3	10.71	0.15	117	2.49	189	6.32938	<0.00129*	2.18814	1.36733	438.70	<0.00002*	0.12711	0.04563	<0.00043*	0.10015	29.0837	0.11167	0.04292	8.74917	0.00300
CM-4	11.71	0.00	14	2.26	65	11.5247	<0.00129*	0.98205	0.60933	104.59	<0.00002*	0.10129	0.01692	<0.00043*	0.00410	22.0808	0.11736	0.00769	3.61359	0.21093
Columbia-Sand																				
CS-1	5.76	1.35	259	3.14	260	2.33288	<0.00129*	3.91076	0.87316	1990.43	0.01363	<0.00022*	0.16244	0.91550	339.652	73.5110	0.36588	0.06806	27.8970	1.27747
CS-2	6.27	1.28	223	2.11	285	0.08283	<0.00129*	3.43717	0.71554	1950.32	0.00978	<0.00022*	0.04587	0.14655	328.604	71.0017	0.31476	0.07757	26.9920	0.71699
CS-3	9.30	0.40	211	0.87	81	36.4952	<0.00129*	1.96274	2.34233	1005.39	0.00027	0.20458	0.01240	<0.00043*	0.66287	53.2372	0.32816	0.09039	21.6720	<0.00014*
CS-4	12.08	0.00	92	0.84	7	27.2688	<0.00129*	1.19924	2.30368	183.254	<0.00002*	0.01521	0.00775	0.00572	0.00245	44.6173	0.30050	0.00311	14.6725	<0.00014*

Note: * Concentration below method detection limit.

APPENDIX E

ADDITIONAL SOLUBILITY CONSTANTS OF ARSENIC AND SELENIUM SPECIES INCLUDED IN MINTEQA2 DATABASE

173

Expressing the Reaction in Terms of MINTEQA2 Components

All reactions in MINTEQA2 are written as formation reactions from the MINTEQA2 components. Solid and dissolved reactions obtained from literatures and their associated thermodynamic constants may need to be added or subtracted from other reactions as required to reformulate the reaction in terms of MINTEQA2 components.

The component H_3AsO_4 is used in the reactions in MINTEQA2 for arsenate and $HSeO_3^-$ for selenite. Therefore, the reactions containing other formulas of arsenate and selenite obtained from literatures are needed to reformulate.

An example is the species $CaAsO_4^-$ given in Whiting (1992) by the reaction:

$$AsO_4^{3-} + Ca^{2+} = CaAsO_4^- \qquad \log K = 6.22$$

This reaction cannot be used in MINTEQA2 because AsO_4^{3-} is not a MINTEQA2 component. To reformulate the reaction for MINTEQA2, the reaction for the formation of H_3AsO_4 from the components AsO_4^{3-} and H^+ must be added to this reaction:

$$AsO_4^{3-} + Ca^{2+} = CaAsO_4^- \qquad \log K = 6.22 \qquad (1)$$

$$H_3AsO_4 = AsO_4^{3-} + 3H^+ \qquad \log K = -20.7 \qquad (2)$$

$$\overline{Ca^{2+} + H_3AsO_4 = CaAsO_4^- \qquad \log K = -14.48 \qquad (3)}$$
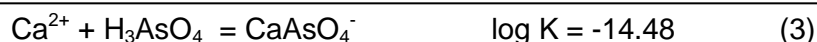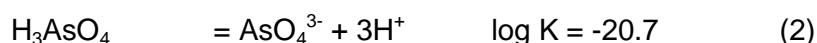
The final reaction (3) and its associated thermodynamic constants are now correctly expressed in term of MINTEQA2 components and are appropriate form for the MINTEQA2 thermodynamic database. Other formula of selenite is required to reformulate to $HSeO_3^-$ and its thermodynamic constants are needed to recalculate in the same manner as arsenate.

The following reactions and associated equilibrium constants are obtained from MINTEQA2 database and used to reformulate arsenate and selenite/selenate and their equilibrium constants obtained from literatures.

For arsenate:

$$H_3AsO_4 = AsO_4^{3-} + 3H^+ \qquad \log K = -20.7$$

$$H_3AsO_4 = HAsO_4^{2-} + 2H^+ \qquad \log K = -9.2$$

$$H_3AsO_4 = H_2AsO_4^- + H^+ \qquad \log K = -2.24$$

For selenite:

$$HSeO_3^- = SeO_3^{2-} + H^+ \qquad \log K = -8.4$$

For selenate:

$$SeO_4^{2-} + H^+ = HSeO_4^- \qquad \log K = 1.7$$

.
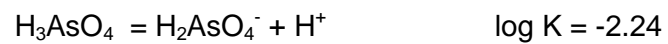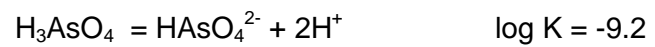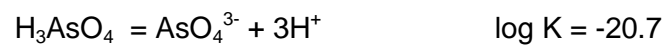
Table E-1 Reaction and equilibrium constant (log K) for arsenate obtained from
literatures.

Element Species	Reaction	log K	Source
As(V) as arsenate (soluble)			
$CaAsO_4^-$	$Ca^{2+} + AsO_4^{3-} = CaAsO_4^-$	6.22	Whiting (1992)[1]
$CaHAsO_4^0$	$Ca^{2+} + HAsO_4^{2-} = CaHAsO_4^0$	2.69	Whiting (1992)[1]
$CaH_2AsO_4^+$	$Ca^{2+} + H_2AsO_4^- = CaH_2AsO_4^+$	1.06	Whiting (1992)[1]
$FeAsO_4^0$	$Fe^{3+} + AsO_4^{3-} = FeAsO_4^0$	18.9	Whiting (1992)[1]
$FeHAsO_4^+$	$Fe^{3+} + HAsO_4^{2-} = FeHAsO_4^+$	6.45	Whiting (1992)[1]
$FeH_2AsO_4^{2+}$	$Fe^{3+} + H_2AsO_4^- = FeH_2AsO_4^{2+}$	4.04	Whiting (1992)[1]
$AlAsO_4^0$	$Al^{3+} + AsO_4^{3-} = AlAsO_4^0$	18.9	Whiting (1992)[1]
$AlHAsO_4^+$	$Al^{3+} + HAsO_4^{2-} = AlHAsO_4^+$	6.45	Whiting (1992)[1]
$AlH_2AsO_4^{2+}$	$Al^{3+} + H_2AsO4^- = AlH_2AsO_4^{2+}$	4.04	Whiting (1992)[1]
$MgAsO_4-$	$Mg^{2+} + AsO_4^{3-} = MgAsO_4^-$	6.34	Whiting (1992)[1]
$MgHAsO_4^0$	$Mg^{2+} + HAsO_4^{2-} = MgHAsO_4^0$	2.86	Whiting (1992)[1]
$MgH_2AsO_4^+$	$Mg^{2+} + H_2AsO_4^- = MgH_2AsO_4^+$	1.52	Whiting (1992)[1]
As(V) as arsenate (solid)			
$CaNaAsO_4.7.5H_2O$	$Ca^{2+}+Na^++AsO_4^{3-}+7.5H_2O =CaNaAsO_4.7.5H_2O$	9.08	Raposo et al. (2004)[2]
$Ca_5 (AsO4)_3(OH)$	$5Ca^{2+} + 3AsO_4^{3-} + OH^- = Ca_5(AsO_4)_3(OH)$	40.12	Zhu et al. (2005)[2]
$Ca_4(OH)_2(AsO_4)_2.4H_2O$	$4Ca^{2+}+ 2AsO_4^{3-} +2OH^-+ 4H_2O =$ $Ca_4(OH)_2(AsO_4)_2.4H_2O$	27.49	Zhu et al. (2005)[2]
$Mg_3(AsO_4)_2$	$3Mg^{2+} + 2AsO_4^{3-} = Mg_3(AsO_4)_2$	21.09	Lee and Nriagu (2007)
$FeAsO_4$	$Fe^{3+} + AsO_4^{3-} = FeAsO_4$	20.46	Lee and Nriagu (2007)
$Cd_3(AsO4)_2$	$3Cd^{2+} + 2AsO_4^{3-} = Cd_3(AsO_4)_2$	33.29	Lee and Nriagu (2007)
$Cu_3(AsO4)_2$	$3Cu^{2+} + 2AsO_4^{3-} = Cu_3(AsO_4)_2$	35.63	Lee and Nriagu (2007)

Note: 1cited in Cornelis et al. (2008b), 2cited in Cornelis et al. (2008a), 3cited in Se'by et al. (2001).

Table E-2 Reaction and equilibrium constant (log K) for arsenate corrected for
MINTEQA2 database.

Element Species	Reaction	log K	Based on Source
As(V) as arsenate (soluble)			
$CaAsO_4^-$	$Ca^{2+} + H_3AsO_4 = CaAsO_4^- + 3H^+$	-14.48	Whiting (1992)[1]
$CaHAsO_4^0$	$Ca^{2+} + H_3AsO_4 = CaHAsO_4^0 + 2H^+$	-6.51	Whiting (1992)[1]
$CaH_2AsO_4^+$	$Ca^{2+} + H_3AsO_4 = CaH_2AsO_4^+ + H^+$	-1.18	Whiting (1992)[1]
$FeAsO_4^0$	$Fe^{3+} + H_3AsO_4 = FeAsO_4^0 + 3H^+$	-1.80	Whiting (1992)[1]
$FeHAsO_4^+$	$Fe^{3+} + H_3AsO_4 = FeHAsO_4^+ + 2H^+$	-2.75	Whiting (1992)[1]
$FeH_2AsO_4^{2+}$	$Fe^{3+} + H_3AsO_4 = FeH_2AsO_4^{2+} + H^+$	1.80	Whiting (1992)[1]
$AlAsO_4^0$	$Al^{3+} + H_3AsO_4 = AlAsO_4^0 + 3H^+$	-1.80	Whiting (1992)[1]
$AlHAsO_4^+$	$Al^{3+} + H_3AsO_4 = AlHAsO_4^+ + 2H^+$	-2.75	Whiting (1992)[1]
$AlH_2AsO_4^{2+}$	$Al^{3+} + H_3AsO_4 = AlH_2AsO_4^{2+} + H^+$	1.80	Whiting (1992)[1]
$MgAsO_4-$	$Mg^{2+} + H_3AsO_4 = MgAsO_4^- + 3H^+$	-14.36	Whiting (1992)[1]
$MgHAsO_4^0$	$Mg^{2+} + H_3AsO_4 = MgHAsO_4^0 + 2H^+$	-6.34	Whiting (1992)[1]
$MgH_2AsO_4^+$	$Mg^{2+} + H_3AsO_4 = MgH_2AsO_4^+ + H^+$	-0.72	Whiting (1992)[1]
As(V) as arsenate (solid)			
$CaNaAsO_4.7.5H_2O$	$Ca^{2+}+Na^+ + H_3AsO_4 +7.5H_2O = CaNaAsO_4.7.5H_2O + 3H^+$	-11.62	Raposo et al. (2004)[2]
$Ca_5 (AsO4)_3(OH)$	$5Ca^{2+} + 3H_3AsO_4 + H_2O = Ca_5(AsO_4)_3(OH)+10H^+$	-35.98	Zhu et al. (2005)[2]
$Ca_4(OH)_2(AsO_4)_2.4H_2O$	$4Ca^{2+}+ 2H_3AsO_4 + 6H_2O = Ca_4(OH)_2(AsO_4)_2.4H_2O + 8H^+$	-41.90	Zhu et al. (2005)[2]
$Mg_3(AsO_4)_2$	$3Mg^{2+} + 2H_3AsO_4 = Mg_3(AsO_4)_2 + 6H^+$	-20.31	Lee and Nriagu (2007)
$FeAsO_4$	$Fe^{3+} + H_3AsO_4 = FeAsO_4 + 3H^+$	-0.24	Lee and Nriagu (2007)
$Cd_3(AsO4)_2$	$3Cd^{2+} + 2H_3AsO_4 = Cd_3(AsO_4)_2 + 6H^+$	-8.11	Lee and Nriagu (2007)
$Cu_3(AsO4)_2$	$3Cu^{2+} + 2H_3AsO_4 = Cu_3(AsO_4)_2 + 6H^+$	-5.77	Lee and Nriagu (2007)

Note: [1]cited in Cornelis et al. (2008b), [2]cited in Cornelis et al. (2008a), [3]cited in Se'by et al. (2001).

Table E-3 Reaction and equilibrium constant (log K) for selenite and selenate obtained from literatures.

Element Species	Reaction	log K	Source
SeIV as selenite (soluble)			
$CaSeO_3^0$	$Ca^{2+} + SeO_3^{2-} = CaSeO_3^0$	3.17	Liu and Narasimhan (1994)[3]
$CdSeO_3^0$	$Cd^{2+} + SeO_3^{2-} = CdSeO_3^0$	-0.08	Elrashidi et al. (1987)[3]
$CuSeO_3^0$	$Cu^{2+} + SeO_3^{2-} = CuSeO_3^0$	-0.02	Elrashidi et al. (1987)[3]
$FeSeO_3^+$	$Fe^{3+} + SeO_3^{2-} = FeSeO_3^+$	11.15	Rai et al. (1995)[3]
$MgSeO_3^0$	$Mg^{2+} + SeO_3^{2-} = MgSeO_3^0$	2.87	Liu and Narasimhan (1994)[3]
$Na_2SeO_3^0$	$2Na^+ + SeO_3^{2-} = Na_2SeO_3^0$	0.02	Elrashidi et al. (1987)[3]
$ZnSeO_3^0$	$Zn^{2+} + SeO_3^{2-} = ZnSeO_3^0$	-0.06	Elrashidi et al. (1987)[3]
SeIV as selenite (solid)			
$Al_2(SeO_3)_3$	$2Al^{3+} + 3SeO_3^{2-} = Al_2(SeO_3)_3$	32.47	Essington (1988)[3]
$CaSeO_3$	$Ca^{2+} + SeO_3^{2-} = CaSeO_3$	7.65	Essington (1988)[3]
$CaSeO_3.H_2O$	$Ca^{2+} + SeO_3^{2-} + H_2O = CaSeO_3.H_2O$	6.84	Baur and Johnson (2003)[2]
$CdSeO_3$	$Cd^{2+} + SeO_3^{2-} = CdSeO_3$	8.84	Elrashidi et al. (1987)[3]
$CuSeO_3$	$Cu^{2+} + SeO_3^{2-} = CuSeO_3$	8.42	Feroci et al. (1997)[3]
$Fe_2(SeO_3)_3$	$2Fe^{3+} + 3SeO_3^{2-} = Fe_2SeO_3$	41.58	Rai et al. (1995)[3]
$Fe_2(SeO_3)_3.6H_2O$	$2Fe^{3+} + 3SeO_3^{2-} + 6H_2O = Fe_2(SeO_3)_3.6H_2O$	13.90	Elrashidi et al. (1987)[3]
$MgSeO_3$	$Mg^{2+} + SeO_3^{2-} = MgSeO_3$	7.56	Sharmasarkar et al. (1996)[3]
Na_2SeO_3	$2Na^+ + SeO_3^{2-} = Na_2SeO_3$	3.51	Essington (1988)[3]
$ZnSeO_3$	$Zn^{2+} + SeO_3^{2-} = ZnSeO_3$	10.26	Essington (1988)[3]
$ZnSeO_3.H_2O$	$Zn^{2+} + SeO_3^{2-} + H_2O = ZnSeO_3.H_2O$	7.70	Sharmasarkar et al. (1996)[3]
SeVI as selenate (soluble)			
H_2SeO_4	$HSeO_4^- + H^+ = H_2SeO_4$	-2.01	Se´by et al. (2001)
$CaSeO_4^0$	$Ca^{2+} + SeO_4^{2-} = CaSeO_4^0$	2.00	Parker et al. (1997)[3]
$MgSeO_4^0$	$Mg^{2+} + SeO_4^{2-} = MgSeO_4^0$	2.20	Parker et al. (1997)[3]
$Na_2SeO_4^0$	$2Na^+ + SeO_4^{2-} = Na_2SeO_4^0$	0.02	Elrashidi et al. (1987)[3]
$NaHSeO_4^0$	$Na^+ + HSeO_4^- = NaHSeO_4^0$	0.01	Elrashidi et al. (1987)[3]
SeVI as selenate (solid)			
$Al_2(SeO_4)_3$	$2Al^{3+} + 3SeO_4^{2-} = Al_2(SeO_4)_3$	21.46	Essington (1988)[3]
$CaSeO_4$	$Ca^{2+} + SeO_4^{2-} = CaSeO_4$	4.77	Essington (1988)[3]
$CuSeO_4$	$Cu^{2+} + SeO_4^{2-} = CuSeO_4$	7.05	Essington (1988)[3]
$Fe_2(SeO_4)_3$	$2Fe^{3+} + 3SeO_4^{2-} = Fe_2(SeO_4)_3$	23.19	Essington (1988)[3]
$MgSeO_4$	$Mg^{2+} + SeO_4^{2-} = MgSeO_4$	5.78	Essington (1988)[3]
$ZnSeO_4$	$Zn^{2+} + SeO_4^{2-} = ZnSeO_4$	6.73	Essington (1988)[3]

Note: [1]cited in Cornelis et al. (2008b), [2]cited in Cornelis et al. (2008a), [3]cited in Se'by et al. (2001).

Table E-4 Reaction and equilibrium constant (log K) for selenite and selenate corrected for MINTEQA2 database.

Element Species	Reaction	log K	Based on Source
SeIV as selenite (soluble)			
$CaSeO_3^0$	$Ca^{2+} + HSeO_3^- = CaSeO_3^0 + H^+$	-5.23	Liu and Narasimhan (1994)[3]
$CdSeO_3^0$	$Cd^{2+} + HSeO_3^- = CdSeO_3^0 + H^+$	-8.48	Elrashidi et al. (1987)[3]
$CuSeO_3^0$	$Cu^{2+} + HSeO_3^- = CuSeO_3^0 + H^+$	-8.42	Elrashidi et al. (1987)[3]
$FeSeO_3^+$	$Fe^{3+} + HSeO_3^- = FeSeO_3^+ + H^+$	2.75	Rai et al. (1995)[3]
$MgSeO_3^0$	$Mg^{2+} + HSeO_3^- = MgSeO_3^0 + H^+$	-5.53	Liu and Narasimhan (1994)[3]
$Na_2SeO_3^0$	$2Na^+ + HSeO_3^- = Na_2SeO_3^0 + H^+$	-8.38	Elrashidi et al. (1987)[3]
$ZnSeO_3^0$	$Zn^{2+} + HSeO_3^- = ZnSeO_3^0 + H^+$	-8.46	Elrashidi et al. (1987)[3]
SeIV as selenite (solid)			
$Al_2(SeO_3)_3$	$2Al^{3+} + 3HSeO_3^- = Al_2(SeO_3)_3 + 3H^+$	7.27	Essington (1988)[3]
$CaSeO_3$	$Ca^{2+} + HSeO_3^- = CaSeO_3 + H^+$	-0.75	Essington (1988)[3]
$CaSeO_3.H_2O$	$Ca^{2+} + HSeO_3^- + H_2O = CaSeO_3.H_2O + H^+$	-1.56	Baur and Johnson (2003)[2]
$CdSeO_3$	$Cd^{2+} + HSeO_3^- = CdSeO_3 + H^+$	0.44	Elrashidi et al. (1987)[3]
$CuSeO_3$	$Cu^{2+} + HSeO_3^- = CuSeO_3 + H^+$	0.02	Feroci et al. (1997)[3]
$Fe_2(SeO_3)_3$	$2Fe^{3+} + 3HSeO_3^- = Fe_2SeO_3 + 3H^+$	16.38	Rai et al. (1995)[3]
$Fe_2(SeO_3)_3.6H_2O$	$2Fe^{3+} + 3HSeO_3^- + 6H_2O = Fe_2(SeO_3)_3.6H_2O + 3H^+$	-11.30	Elrashidi et al. (1987)[3]
$MgSeO_3$	$Mg^{2+} + HSeO_3^- = MgSeO_3 + H^+$	-0.84	Sharmasarkar et al. (1996)[3]
Na_2SeO_3	$2Na^+ + HSeO_3^- = Na_2SeO_3 + H^+$	-4.89	Essington (1988)[3]
$ZnSeO_3$	$Zn^{2+} + HSeO_3^- = ZnSeO_3 + H^+$	1.86	Essington (1988)[3]
$ZnSeO_3.H_2O$	$Zn^{2+} + HSeO_3^- + H_2O = ZnSeO_3.H_2O + H^+$	-0.70	Sharmasarkar et al. (1996)[3]
SeVI as selenate (soluble)			
H_2SeO_4	$HSeO_4^- + H^+ = H_2SeO_4 + H^+$	-2.01	Se´by et al. (2001)
$CaSeO_4^0$	$Ca^{2+} + SeO_4^{2-} = CaSeO_4^0 + H^+$	2.00	Parker et al. (1997)[3]
$MgSeO_4^0$	$Mg^{2+} + SeO_4^{2-} = MgSeO_4^0 + H^+$	2.20	Parker et al. (1997)[3]
$Na_2SeO_4^0$	$2Na^+ + SeO_4^{2-} = Na_2SeO_4^0 + H^+$	0.02	Elrashidi et al. (1987)[3]
$NaHSeO_4^0$	$Na^+ + SeO_4^{2-} = NaHSeO_4^0 + H^+$	1.71	Elrashidi et al. (1987)[3]
SeVI as selenate (solid)			
$Al_2(SeO_4)_3$	$2Al^{3+} + 3SeO_4^{2-} = Al_2(SeO_4)_3 + H^+$	21.46	Essington (1988)[3]
$CaSeO_4$	$Ca^{2+} + SeO_4^{2-} = CaSeO_4 + H^+$	4.77	Essington (1988)[3]
$CuSeO_4$	$Cu^{2+} + SeO_4^{2-} = CuSeO_4 + H^+$	7.05	Essington (1988)[3]
$Fe_2(SeO_4)_3$	$2Fe^{3+} + 3SeO_4^{2-} = Fe_2(SeO_4)_3 + H^+$	23.19	Essington (1988)[3]
$MgSeO_4$	$Mg^{2+} + SeO_4^{2-} = MgSeO_4 + H^+$	5.78	Essington (1988)[3]
$ZnSeO_4$	$Zn^{2+} + SeO_4^{2-} = ZnSeO_4 + H^+$	6.73	Essington (1988)[3]

Note: [1]cited in Cornelis et al. (2008b), [2]cited in Cornelis et al. (2008a), [3]cited in Se'by et al. (2001).

179

APPENDIX F

CALCULATIONS AND EQUATIONS USED IN MINTEQA2 TO DETERMINE SPECIATION AND SATURATION INDEX

Element Speciation Calculation

When the equilibrium E_h and redox couple are specified as equilibrium constraints, mass is shifted from one member of the redox couple to the other in such a way as to cause their activity ratio to honor the Nernst equation at equilibrium (Allison et al. 1991).

$$E_h(\text{volt}) = E^o + \frac{2.303RT}{nF} \log \left[\frac{a_{Ox}}{a_{\text{Re}\,d}} \right]$$

where R = 0.001987 kcal/mol; T is absolute temperature; F, the Faraday constant, is 23.061 kcal/volt g eq, a_{Ox} is chemical activity of oxidized state, and a_{Red} is chemical activity reduced state for the half-reaction written as a reduction reaction:

$$A + B + ne^- \quad = \quad C + D$$
$$\text{oxidized state} \qquad \text{reduced state}$$
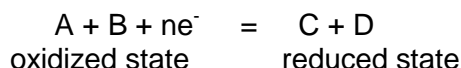
At 25^oC, the term 2.303RT/F is 0.05916 volts, which is known as the Nernst factor.

For example, if Fe^{2+} and Fe^{3+} are selected as components, the E_h is specified, and the redox couple $Fe^{3+} + e^- = Fe^{2+}$ is specified as an equilibrium constraint. MINTEQA2 will calculate the amount or iron in each of the two oxidation states corresponding to the specified equilibrium E_h.

Chemical Activity Calculation

In this study, the Davies equation was selected to estimate activity coefficient for ionic species to take account for non-ideal effects in solution. The Davies equation as implemented in MINTEQA2 is:

$$\log \gamma_i = -Az_i^2 \frac{\left(\sqrt{I} - 0.24I \right)}{1 + \sqrt{I}}$$

where γ_i = activity coefficient, A = constant, zi = charge on each species i, I = solution ionic strength.

The ionic strength (I) is calculated from

$$I_{i=1}^{m} = \frac{1}{2}\sum z_i^2 C_i$$

where C_i = concentration of ion species I, m = number of charged species present in the solution, and z_i = charge on species i.

For any particular species *I*, the concentration of species *I*, [S_i], is related to the activity {S_i} by the activity coefficient, γ_I:

$$\{S_i\} = \gamma [S_i]$$

Saturation Index calculation

The saturation index for a mineral is defined as

$$SI = \log\frac{(IAP)}{K_{sp}}$$

where K_{sp} is solubility product for mineral (calculated from theoretical thermodynamic data) and IAP is ion activity product (calculated from the activities dissolved mineral constituents).

If the saturation index is positive, the solution is supersaturated/ oversaturated with respect to that mineral, and precipitation of the mineral is likely to occur. If the saturation index is negative, the solution is undersaturated with respect to the mineral, and dissolution of the mineral is likely to occur. The solution is in equilibrium with the mineral when the saturation index is zero (IAP = K_{sp}) (Allison et al. 1991).

APPENDIX G

**SPECIATION OF ARSENIC, CHROMIUM, COPPER, IRON, AND SENENIUM
CALCULATED USING MINTEQA2**

Table G-1.   Speciation of As, Cr, Cu, Fe and Se calculated using MINTEQA2: Dewey.

Species in Solution	Concentration (mol/L)			
	D-1	D-2	D-3	D-4
	pH 5.81, Eh 290	pH 7.95, Eh 182	pH 10.25, Eh 75	pH 12.25, Eh -31
H^+	1.55E-06	1.12E-08	5.69E-11	6.24E-13
H_3AsO_4	4.31E-12	2.74E-14	3.33E-18	2.70E-22
H_3AsO_3	1.28E-14	1.91E-17	2.42E-22	7.54E-27
$Cr(OH)_2^+$	1.07E-08	7.43E-09	7.66E-10	1.13E-13
CrO_4^{2-}	1.67E-26	2.68E-19	6.71E-12	5.49E-09
Cu^+	4.86E-09	3.47E-09	9.43E-11	5.61E-16
Cu^{2+}	7.97E-07	8.49E-09	3.69E-12	4.67E-19
Fe^{2+}	1.27E-07	1.36E-09	8.06E-14	2.11E-20
Fe^{3+}	9.50E-16	1.52E-19	1.47E-25	9.81E-34
$HSeO_3^-$	3.36E-07	2.12E-07	1.34E-08	1.40E-11
SeO_4^{2-}	2.85E-16	1.06E-13	1.32E-11	4.72E-12
$HCrO_4^-$	8.33E-26	9.69E-21	1.18E-15	7.33E-15
$H_2CrO_4 (aq)$	1.04E-31	8.80E-29	5.32E-26	3.01E-27
$Cr_2O_7^{2-}$	0.00E+00	3.26E-39	4.95E-29	2.29E-27
$FeAsO_4$	1.72E-11	4.61E-11	3.94E-14	9.33E-21
$FeHAsO_4^+$	2.99E-18	5.80E-20	2.51E-25	6.54E-34
$FeH_2AsO_4^{2+}$	1.65E-19	2.32E-23	5.19E-31	1.78E-41
$CuSeO_3$	6.51E-16	6.05E-16	3.16E-18	2.63E-26
$FeSeO_3^+$	1.14E-13	1.59E-15	1.78E-20	5.42E-30
Cr^{3+}	9.69E-11	3.50E-15	9.83E-21	3.02E-28
OH^-	6.51E-09	8.99E-07	1.81E-04	1.99E-02
$CuOH^+$	1.63E-08	2.40E-08	2.02E-09	1.94E-14
$Cu(OH)_2 (aq)$	2.11E-11	4.29E-09	7.13E-08	6.24E-11
$Cu(OH)_3^-$	2.82E-16	7.91E-12	2.65E-08	2.55E-09
$Cu(OH)_4^{2-}$	1.45E-23	5.61E-17	3.87E-11	4.90E-10
$Cu_2(OH)_2^{2+}$	1.15E-11	2.49E-11	1.80E-13	2.00E-23
$FeOH^+$	3.27E-11	4.84E-11	5.55E-13	1.10E-17
$Fe(OH)_2 (aq)$	1.68E-16	3.44E-14	7.81E-14	1.41E-16
$Fe(OH)_3^-$	3.47E-19	9.78E-15	4.47E-12	8.87E-13
$FeOH^{2+}$	3.95E-12	8.73E-14	1.61E-17	6.77E-24
$Fe(OH)_2^+$	9.93E-09	3.04E-08	1.08E-09	3.46E-14
$Fe(OH)_3 (aq)$	6.92E-11	2.92E-08	2.05E-07	5.99E-10
$Fe(OH)_4^-$	4.20E-14	2.45E-09	3.46E-06	1.11E-06
$Fe2(OH)_2^{4+}$	5.25E-22	2.55E-25	9.34E-33	2.80E-45
$Fe3(OH)_4^{5+}$	7.66E-29	1.13E-31	1.60E-40	0.00E+00
$Cr(OH)^{2+}$	1.37E-08	6.83E-11	3.64E-14	7.07E-20
$Cr(OH)_3 (aq)$	2.62E-11	2.50E-09	5.09E-08	6.84E-10
$Cr(OH)_4^-$	6.78E-15	8.95E-11	3.67E-07	5.42E-07
CrO_2^-	8.04E-15	1.06E-10	4.35E-07	6.42E-07
SeO_3^{2-}	8.69E-10	7.54E-08	9.83E-07	1.35E-07
$H_2SeO_3 (aq)$	2.22E-10	1.01E-12	3.18E-16	3.02E-21
$FeHSeO_3^{2+}$	8.34E-19	8.42E-23	4.86E-30	1.95E-41
$HSeO_4^-$	2.20E-20	5.91E-20	3.59E-20	9.77E-23
AsO_3^{3-}	6.34E-32	2.47E-28	2.72E-26	1.94E-24
$HAsO_3^{2-}$	2.52E-24	7.14E-23	3.75E-23	1.69E-23
$H_2AsO_3^-$	4.26E-18	8.75E-19	2.24E-21	7.65E-24
$H_4AsO_3^+$	9.87E-21	1.06E-25	6.83E-33	2.34E-39
AsO_4^{3-}	2.36E-15	3.91E-11	4.14E-08	7.69E-06
$HAsO_4^{2-}$	1.14E-09	1.38E-07	6.95E-07	8.16E-07
$H_2AsO_4^-$	1.60E-08	1.41E-08	3.45E-10	3.07E-12

Table G-2.   Speciation of As, Cr, Cu, Fe and Se calculated using MINTEQA2: Dewey-
Lawson.

Species in Solution	Concentration (mol/L)			
	DL-1	DL-2	DL-3	DL-4
	pH 5.36, Eh 279	pH 7.89, Eh 230	pH 9.66, Eh 151	pH 12.57, Eh 58
H^+	4.37E-06	1.29E-08	2.20E-10	3.11E-13
H_3AsO_4	3.06E-11	2.01E-14	1.65E-17	4.56E-24
H_3AsO_3	1.71E-12	4.41E-19	4.89E-23	2.86E-32
$Cr(OH)_2^+$	9.23E-10	3.25E-09	4.92E-11	2.90E-20
CrO_4^{2-}	7.94E-31	1.38E-17	8.76E-13	4.30E-09
Cu^+	1.20E-09	1.08E-09	7.66E-11	2.98E-15
Cu^{2+}	1.28E-07	1.70E-08	5.69E-11	8.94E-17
Fe^{2+}	2.67E-07	7.92E-10	5.83E-14	2.67E-23
Fe^{3+}	1.31E-15	5.71E-19	1.99E-24	4.85E-35
$HSeO_3^-$	5.87E-07	1.72E-07	6.51E-09	7.73E-12
SeO_4^{2-}	9.46E-18	2.37E-12	3.97E-11	2.73E-08
$HCrO_4^-$	1.12E-29	5.75E-19	6.09E-16	2.44E-15
$H_2CrO_4 (aq)$	3.94E-35	6.00E-27	1.07E-25	4.59E-28
$Cr_2O_7^{2-}$	0.00E+00	1.15E-35	1.30E-29	2.74E-28
$FeAsO_4$	7.47E-12	8.42E-11	4.71E-14	4.95E-23
$FeHAsO_4^+$	3.66E-18	1.22E-19	1.16E-24	1.73E-36
$FeH_2AsO_4^{2+}$	5.71E-19	5.58E-23	9.19E-30	2.52E-44
$CuSeO_3$	6.47E-17	8.58E-16	6.25E-18	4.75E-24
$FeSeO_3^+$	9.69E-14	4.24E-15	3.16E-20	2.16E-31
Cr^{3+}	6.63E-11	2.02E-15	9.13E-21	2.45E-35
OH^-	2.31E-09	7.83E-07	4.63E-05	4.32E-02
$CuOH^+$	9.27E-10	4.19E-08	8.13E-09	6.88E-12
$Cu(OH)_2 (aq)$	4.26E-13	6.53E-09	7.43E-08	4.43E-08
$Cu(OH)_3^-$	2.02E-18	1.05E-11	7.05E-09	3.94E-06
$Cu(OH)_4^{2-}$	3.69E-26	6.47E-17	2.60E-12	1.78E-06
$Cu_2(OH)_2^{2+}$	3.72E-14	7.60E-11	2.89E-12	2.72E-18
$FeOH^+$	2.44E-11	2.46E-11	1.05E-13	2.59E-20
$Fe(OH)_2 (aq)$	4.46E-17	1.52E-14	3.82E-15	6.64E-19
$Fe(OH)_3^-$	3.26E-20	3.77E-15	5.58E-14	9.10E-15
$FeOH^{2+}$	1.92E-12	2.87E-13	5.75E-17	5.72E-25
$Fe(OH)_2^+$	1.71E-09	8.69E-08	1.01E-09	5.42E-15
$Fe(OH)_3 (aq)$	4.24E-12	7.29E-08	4.97E-08	1.88E-10
$Fe(OH)_4^-$	9.12E-16	5.31E-09	2.14E-07	7.59E-07
$Fe2(OH)_2^{4+}$	1.25E-22	2.75E-24	1.15E-31	0.00E+00
$Fe3(OH)_4^{5+}$	3.14E-30	3.48E-30	1.75E-39	0.00E+00
$Cr(OH)^{2+}$	3.31E-09	3.43E-11	8.94E-15	9.80E-27
$Cr(OH)_3 (aq)$	7.98E-13	9.53E-10	8.46E-10	3.52E-16
$Cr(OH)_4^-$	7.35E-17	2.97E-11	1.56E-09	6.08E-13
CrO_2^-	8.70E-17	3.52E-11	1.85E-09	7.20E-13
SeO_3^{2-}	5.39E-10	5.33E-08	1.21E-07	1.76E-07
$H_2SeO_3 (aq)$	1.09E-09	9.43E-13	6.04E-16	7.66E-22
$FeHSeO_3^{2+}$	2.00E-18	2.58E-22	3.31E-29	4.19E-43
$HSeO_4^-$	2.06E-21	1.52E-18	4.28E-19	2.40E-19
AsO_3^{3-}	3.77E-31	3.76E-30	8.86E-29	9.64E-29
$HAsO_3^{2-}$	4.22E-23	1.25E-24	4.89E-25	3.29E-28
$H_2AsO_3^-$	2.01E-16	1.76E-20	1.15E-22	6.33E-29
$H_4AsO_3^+$	3.70E-18	2.82E-27	5.33E-33	4.20E-45
AsO_4^{3-}	7.49E-16	1.89E-11	3.31E-09	1.70E-06
$HAsO_4^{2-}$	1.02E-09	7.66E-08	2.22E-07	7.07E-08
$H_2AsO_4^-$	4.04E-08	8.97E-09	4.36E-10	1.13E-13

Table G-3.   Speciation of As, Cr, Cu, Fe and Se calculated using MINTEQA2: Dewey-Kamm**.**

Species in Solution	Concentration (mol/L)			
	DK-1	DK-2	DK-3	DK-4
	pH 6.01, Eh 350	pH 8.47, Eh 238	pH 9.55, Eh189	pH 12.61, Eh 70
H^+	9.79E-07	3.39E-09	2.83E-10	2.85E-13
H_3AsO_4	2.57E-12	3.01E-16	2.24E-17	3.80E-24
H_3AsO_3	2.84E-17	2.46E-22	5.73E-24	7.79E-33
$Cr(OH)_2^+$	2.38E-09	1.79E-09	7.63E-11	8.59E-21
CrO_4^{2-}	6.50E-23	5.85E-14	2.50E-11	9.14E-09
Cu^+	6.06E-11	6.74E-11	3.16E-12	7.70E-17
Cu^{2+}	1.03E-07	1.46E-09	1.03E-11	3.74E-18
Fe^{2+}	1.02E-07	1.75E-11	1.15E-14	5.74E-24
Fe^{3+}	7.89E-15	1.73E-20	1.72E-24	1.71E-35
$HSeO_3^-$	3.06E-07	8.43E-08	7.41E-09	4.01E-13
SeO_4^{2-}	1.10E-13	1.19E-10	4.06E-10	4.84E-09
$HCrO_4^-$	2.05E-22	6.39E-16	2.25E-14	4.65E-15
H_2CrO_4 (aq)	1.62E-28	1.75E-24	5.10E-24	7.92E-28
$Cr_2O_7^{2-}$	1.46E-42	1.42E-29	1.77E-26	1.01E-27
$FeAsO_4$	3.40E-10	2.09E-12	2.60E-14	1.83E-23
$FeHAsO_4^+$	3.74E-17	7.97E-22	8.26E-25	5.86E-37
$FeH_2AsO_4^{2+}$	1.30E-18	9.63E-26	8.38E-30	8.41E-45
$CuSeO_3$	1.21E-16	1.37E-16	9.98E-19	1.10E-26
$FeSeO_3^+$	1.37E-12	2.39E-16	2.42E-20	4.12E-33
Cr^{3+}	8.50E-12	7.70E-17	2.34E-20	6.31E-36
OH^-	1.03E-08	2.98E-06	3.59E-05	4.76E-02
$CuOH^+$	3.33E-09	1.36E-08	1.14E-09	3.11E-13
$Cu(OH)_2$ (aq)	6.84E-12	8.07E-09	8.09E-09	2.18E-09
$Cu(OH)_3^-$	1.45E-16	4.93E-11	5.96E-10	2.14E-07
$Cu(OH)_4^{2-}$	1.18E-23	1.16E-15	1.70E-13	1.08E-07
$Cu_2(OH)_2^{2+}$	4.80E-13	8.05E-12	5.67E-14	5.61E-21
$FeOH^+$	4.17E-11	2.06E-12	1.61E-14	6.00E-21
$Fe(OH)_2$ (aq)	3.41E-16	4.86E-15	4.55E-16	1.68E-19
$Fe(OH)_3^-$	1.11E-18	4.57E-15	5.16E-15	2.54E-15
$FeOH^{2+}$	5.21E-11	3.29E-14	3.86E-17	2.15E-25
$Fe(OH)_2^+$	2.08E-07	3.79E-08	5.28E-10	2.20E-15
$Fe(OH)_3$ (aq)	2.30E-09	1.21E-07	2.02E-08	8.30E-11
$Fe(OH)_4^-$	2.21E-12	3.34E-08	6.74E-08	3.70E-07
$Fe2(OH)_2^{4+}$	9.09E-20	3.63E-26	5.13E-32	0.00E+00
$Fe3(OH)_4^{5+}$	2.76E-25	2.01E-32	4.08E-40	0.00E+00
$Cr(OH)^{2+}$	1.90E-09	4.97E-12	1.78E-14	2.69E-27
$Cr(OH)_3$ (aq)	9.19E-12	1.99E-09	1.02E-09	1.13E-16
$Cr(OH)_4^-$	3.78E-15	2.36E-10	1.46E-09	2.16E-13
CrO_2^-	4.47E-15	2.80E-10	1.73E-09	2.56E-13
SeO_3^{2-}	1.25E-09	9.96E-08	1.06E-07	1.02E-08
H_2SeO_3 (aq)	1.27E-10	1.22E-13	8.86E-16	3.60E-23
$FeHSeO_3^{2+}$	6.32E-18	3.82E-24	3.26E-29	7.01E-45
$HSeO_4^-$	5.39E-18	2.01E-17	5.64E-18	3.81E-20
AsO_3^{3-}	5.56E-34	1.16E-31	4.83E-30	3.65E-29
$HAsO_3^{2-}$	1.40E-26	1.01E-26	3.44E-26	1.10E-28
$H_2AsO_3^-$	1.49E-20	3.73E-23	1.05E-23	1.90E-29
$H_4AsO_3^+$	1.38E-23	4.14E-31	8.04E-34	1.40E-45
AsO_4^{3-}	5.56E-15	1.57E-11	2.09E-09	1.97E-06
$HAsO_4^{2-}$	1.71E-09	1.67E-08	1.82E-07	7.26E-08
$H_2AsO_4^-$	1.52E-08	5.13E-10	4.59E-10	1.04E-13

Table G-4. Speciation of As, Cr, Cu, Fe and Se calculated using MINTEQA2: Dewey-Red Wing.

Species in Solution	Concentration (mol/L)			
	DR-1	DR-2	DR-3	DR-4
	pH 5.81, Eh 376	pH 8.11, Eh 240	pH 10.55, Eh 156	pH 12.34, Eh 84
H^+	1.55E-06	7.77E-09	2.86E-11	5.12E-13
H_3AsO_4	1.02E-11	8.39E-15	2.08E-19	1.04E-23
H_3AsO_3	3.74E-17	3.07E-20	6.94E-27	2.48E-32
$Cr(OH)_2^+$	1.89E-09	2.78E-09	2.38E-12	3.33E-19
CrO_4^{2-}	6.75E-23	7.95E-16	1.71E-08	3.93E-08
Cu^+	3.60E-11	2.14E-11	2.51E-14	3.30E-18
Cu^{2+}	1.68E-07	5.01E-10	2.33E-14	2.49E-19
Fe^{2+}	4.67E-08	5.95E-11	1.12E-16	1.71E-23
Fe^{3+}	9.92E-15	6.34E-20	4.89E-27	7.36E-35
$HSeO_3^-$	5.23E-07	9.24E-08	1.03E-10	8.70E-13
SeO_4^{2-}	3.59E-13	1.27E-11	4.46E-10	4.36E-09
$HCrO_4^-$	3.37E-22	1.99E-17	1.48E-12	4.14E-14
H_2CrO_4 (aq)	4.22E-28	1.25E-25	3.34E-23	1.37E-26
$Cr_2O_7^{2-}$	3.95E-42	1.38E-32	7.88E-23	7.45E-26
$FeAsO_4$	4.24E-10	1.78E-11	6.25E-16	4.58E-23
$FeHAsO_4^+$	7.38E-17	1.55E-20	2.01E-27	2.64E-36
$FeH_2AsO_4^{2+}$	4.07E-18	4.29E-24	2.11E-33	6.03E-44
$CuSeO_3$	2.14E-16	2.25E-17	2.99E-22	1.02E-27
$FeSeO_3^+$	1.86E-12	4.20E-16	8.74E-24	2.84E-32
Cr^{3+}	1.70E-11	6.26E-16	7.94E-24	6.38E-34
OH^-	6.51E-09	1.30E-06	3.63E-04	2.47E-02
$CuOH^+$	3.43E-09	2.05E-09	2.51E-11	1.24E-14
$Cu(OH)_2$ (aq)	4.44E-12	5.29E-10	1.76E-09	4.84E-11
$Cu(OH)_3^-$	5.93E-17	1.41E-12	1.31E-09	2.45E-09
$Cu(OH)_4^{2-}$	3.05E-24	1.44E-17	3.86E-12	5.98E-10
$Cu_2(OH)_2^{2+}$	5.09E-13	1.81E-13	2.80E-17	8.26E-24
$FeOH^+$	1.20E-11	3.06E-12	1.53E-15	1.07E-20
$Fe(OH)_2$ (aq)	6.21E-17	3.15E-15	4.26E-16	1.66E-19
$Fe(OH)_3^-$	1.28E-19	1.29E-15	4.89E-14	1.30E-15
$FeOH^{2+}$	4.13E-11	5.28E-14	1.04E-18	5.94E-25
$Fe(OH)_2^+$	1.04E-07	2.65E-08	1.39E-10	3.63E-15
$Fe(OH)_3$ (aq)	7.26E-10	3.69E-08	5.23E-08	7.64E-11
$Fe(OH)_4^-$	4.40E-13	4.47E-09	1.77E-06	1.76E-07
$Fe2(OH)_2^{4+}$	5.73E-20	9.31E-26	4.09E-35	0.00E+00
$Fe3(OH)_4^{5+}$	8.72E-26	3.60E-32	9.25E-44	0.00E+00
$Cr(OH)^{2+}$	2.39E-09	1.77E-11	5.74E-17	1.75E-25
$Cr(OH)_3$ (aq)	4.60E-12	1.35E-09	3.14E-10	2.46E-15
$Cr(OH)_4^-$	1.19E-15	6.99E-11	4.54E-09	2.42E-12
CrO_2^-	1.41E-15	8.28E-11	5.38E-09	2.87E-12
SeO_3^{2-}	1.35E-09	4.76E-08	1.53E-08	1.06E-08
H_2SeO_3 (aq)	3.45E-10	3.06E-13	1.22E-18	1.51E-22
$FeHSeO_3^{2+}$	1.36E-17	1.54E-23	1.21E-33	8.55E-44
$HSeO_4^-$	2.77E-17	4.92E-18	6.01E-19	7.10E-20
AsO_3^{3-}	1.84E-34	1.20E-30	6.44E-30	1.30E-29
$HAsO_3^{2-}$	7.33E-27	2.40E-25	4.35E-27	8.77E-29
$H_2AsO_3^-$	1.24E-20	2.03E-21	1.28E-25	3.13E-29
$H_4AsO_3^+$	2.87E-23	1.18E-28	9.85E-38	7.01E-45
AsO_4^{3-}	5.53E-15	3.62E-11	2.13E-08	6.04E-07
$HAsO_4^{2-}$	2.69E-09	8.82E-08	1.76E-07	4.95E-08
$H_2AsO_4^-$	3.78E-08	6.22E-09	4.31E-11	1.47E-13

Table G-5.   Speciation of As, Cr, Cu, Fe and Se calculated using MINTEQA2: Dewey-
MnRoad.

Species in Solution	Concentration (mol/L)			
	DM-1	DM-2	DM-3	DM-4
	pH 6.02, Eh 375	pH 8.11, Eh 270	pH 10.63, Eh 140	pH 12.22, Eh 78
H^+	9.56E-07	7.77E-09	2.39E-11	6.66E-13
H_3AsO_4	5.91E-12	1.23E-14	1.53E-19	2.71E-23
H_3AsO_3	8.95E-18	4.38E-21	1.23E-26	1.79E-31
$Cr(OH)_2^+$	2.40E-09	2.78E-09	4.50E-13	2.45E-18
CrO_4^{2-}	1.39E-21	2.64E-14	1.52E-09	2.63E-08
Cu^+	1.93E-11	6.70E-12	2.98E-14	1.00E-17
Cu^{2+}	8.61E-08	5.03E-10	1.49E-14	5.75E-19
Fe^{2+}	9.99E-09	1.10E-11	1.78E-18	2.02E-23
Fe^{3+}	2.04E-15	3.76E-20	4.20E-29	6.43E-35
$HSeO_3^-$	4.71E-07	1.12E-07	8.25E-11	1.47E-12
SeO_4^{2-}	1.27E-12	1.59E-10	1.80E-10	1.93E-09
$HCrO_4^-$	4.28E-21	6.60E-16	1.09E-13	3.80E-14
$H_2CrO_4 (aq)$	3.31E-27	4.15E-24	2.04E-24	1.68E-26
$Cr_2O_7^{2-}$	6.38E-40	1.52E-29	4.28E-25	6.11E-26
$FeAsO_4$	2.17E-10	1.55E-11	6.79E-18	5.13E-23
$FeHAsO_4^+$	2.33E-17	1.36E-20	1.82E-29	3.84E-36
$FeH_2AsO_4^{2+}$	7.91E-19	3.75E-24	1.59E-35	1.11E-43
$CuSeO_3$	1.61E-16	2.75E-17	1.83E-22	3.22E-27
$FeSeO_3^+$	5.59E-13	3.02E-16	7.12E-26	3.58E-32
Cr^{3+}	8.20E-12	6.26E-16	1.05E-24	7.32E-33
OH^-	1.06E-08	1.30E-06	4.37E-04	1.85E-02
$CuOH^+$	2.86E-09	2.06E-09	1.93E-11	2.25E-14
$Cu(OH)_2 (aq)$	6.01E-12	5.32E-10	1.62E-09	6.78E-11
$Cu(OH)_3^-$	1.30E-16	1.42E-12	1.45E-09	2.58E-09
$Cu(OH)_4^{2-}$	1.08E-23	1.45E-17	5.17E-12	4.57E-10
$Cu_2(OH)_2^{2+}$	3.54E-13	1.83E-13	1.66E-17	2.68E-23
$FeOH^+$	4.18E-12	5.65E-13	2.90E-17	9.94E-21
$Fe(OH)_2 (aq)$	3.49E-17	5.81E-16	9.72E-18	1.19E-19
$Fe(OH)_3^-$	1.17E-19	2.39E-16	1.34E-15	6.97E-16
$FeOH^{2+}$	1.38E-11	3.13E-14	1.07E-20	4.21E-25
$Fe(OH)_2^+$	5.63E-08	1.57E-08	1.70E-12	2.03E-15
$Fe(OH)_3 (aq)$	6.37E-10	2.19E-08	7.70E-10	3.29E-11
$Fe(OH)_4^-$	6.26E-13	2.65E-09	3.13E-08	5.67E-08
$Fe2(OH)_2^{4+}$	6.35E-21	3.27E-26	4.34E-39	0.00E+00
$Fe3(OH)_4^{5+}$	5.22E-27	7.52E-33	0.00E+00	0.00E+00
$Cr(OH)^{2+}$	1.88E-09	1.77E-11	9.06E-18	1.62E-24
$Cr(OH)_3 (aq)$	9.51E-12	1.35E-09	7.14E-11	1.39E-14
$Cr(OH)_4^-$	4.00E-15	6.99E-11	1.24E-09	1.02E-11
CrO_2^-	4.73E-15	8.28E-11	1.47E-09	1.21E-11
SeO_3^{2-}	1.97E-09	5.77E-08	1.47E-08	1.31E-08
$H_2SeO_3 (aq)$	1.92E-10	3.71E-13	8.11E-19	3.40E-22
$FeHSeO_3^{2+}$	2.52E-18	1.11E-23	8.26E-36	1.37E-43
$HSeO_4^-$	6.07E-17	6.16E-17	2.01E-19	4.33E-20
AsO_3^{3-}	1.87E-34	1.71E-31	2.00E-29	3.63E-29
$HAsO_3^{2-}$	4.61E-27	3.41E-26	1.12E-26	3.44E-28
$H_2AsO_3^-$	4.81E-21	2.90E-22	2.73E-25	1.69E-28
$H_4AsO_3^+$	4.24E-24	1.69E-29	1.45E-37	5.89E-44
AsO_4^{3-}	1.37E-14	5.32E-11	2.77E-08	6.08E-07
$HAsO_4^{2-}$	4.11E-09	1.30E-07	1.88E-07	7.03E-08
$H_2AsO_4^-$	3.57E-08	9.15E-09	3.83E-11	2.86E-13

Table G-6. Speciation of As, Cr, Cu, Fe and Se calculated using MINTEQA2: Dewey-sand**.**

Species in Solution	Concentration (mol/L)			
	DS-1	DS-2	DS-3	DS-4
	pH 6.17, Eh 347	pH 8.00, Eh 271	pH 9.94, Eh 180	pH 12.43, Eh 54
H^+	6.77E-07	1.00E-08	1.16E-10	4.21E-13
H_3AsO_4	1.72E-12	7.88E-15	4.21E-18	1.49E-23
H_3AsO_3	1.15E-17	4.29E-21	3.60E-25	2.43E-31
$Cr(OH)_2^+$	2.76E-09	3.03E-09	1.39E-11	3.37E-19
CrO_4^{2-}	4.83E-22	7.08E-15	3.51E-10	4.29E-09
Cu^+	9.07E-11	1.43E-10	4.86E-12	5.43E-18
Cu^{2+}	1.37E-07	1.12E-08	1.12E-11	1.32E-19
Fe^{2+}	2.94E-08	5.30E-11	1.67E-15	1.17E-22
Fe^{3+}	2.02E-15	1.89E-19	1.78E-25	1.65E-34
$HSeO_3^-$	3.02E-07	2.23E-07	7.78E-09	9.10E-13
SeO_4^{2-}	2.60E-13	1.60E-10	3.16E-09	8.49E-10
$HCrO_4^-$	1.05E-21	2.28E-16	1.27E-13	3.55E-15
H_2CrO_4 (aq)	5.76E-28	1.85E-24	1.18E-23	9.42E-28
$Cr_2O_7^{2-}$	3.85E-41	1.81E-30	5.70E-25	5.62E-28
$FeAsO_4$	1.76E-10	2.33E-11	7.31E-15	2.48E-22
$FeHAsO_4^+$	1.34E-17	2.62E-20	9.49E-26	1.18E-35
$FeH_2AsO_4^{2+}$	3.22E-19	9.33E-24	3.96E-31	2.24E-43
$CuSeO_3$	2.31E-16	9.43E-16	2.78E-18	6.57E-28
$FeSeO_3^+$	5.03E-13	2.34E-15	6.32E-21	7.43E-32
Cr^{3+}	4.71E-12	1.13E-15	7.21E-22	4.66E-34
OH^-	1.49E-08	1.01E-06	8.84E-05	3.07E-02
$CuOH^+$	6.41E-09	3.55E-08	3.04E-09	7.78E-15
$Cu(OH)_2$ (aq)	1.90E-11	7.13E-09	5.28E-08	3.70E-11
$Cu(OH)_3^-$	5.82E-16	1.47E-11	9.57E-09	2.34E-09
$Cu(OH)_4^{2-}$	6.84E-23	1.17E-16	6.76E-12	7.24E-10
$Cu_2(OH)_2^{2+}$	1.78E-12	5.46E-11	4.05E-13	3.35E-24
$FeOH^+$	1.74E-11	2.12E-12	5.69E-15	8.67E-20
$Fe(OH)_2$ (aq)	2.06E-16	1.69E-15	3.93E-16	1.64E-18
$Fe(OH)_3^-$	9.69E-19	5.39E-16	1.10E-14	1.60E-14
$FeOH^{2+}$	1.93E-11	1.22E-13	9.70E-18	1.55E-24
$Fe(OH)_2^+$	1.12E-07	4.76E-08	3.23E-10	1.13E-14
$Fe(OH)_3$ (aq)	1.78E-09	5.15E-08	3.02E-08	2.89E-10
$Fe(OH)_4^-$	2.48E-12	4.83E-09	2.49E-07	8.28E-07
$Fe2(OH)_2^{4+}$	1.25E-20	4.98E-25	3.31E-33	0.00E+00
$Fe3(OH)_4^{5+}$	2.03E-26	3.46E-31	1.65E-41	0.00E+00
$Cr(OH)^{2+}$	1.53E-09	2.48E-11	1.33E-15	1.48E-25
$Cr(OH)_3$ (aq)	1.54E-11	1.15E-09	4.53E-10	3.02E-15
$Cr(OH)_4^-$	9.14E-15	4.60E-11	1.59E-09	3.70E-12
CrO_2^-	1.08E-14	5.44E-11	1.89E-09	4.39E-12
SeO_3^{2-}	1.79E-09	8.90E-08	2.76E-07	1.42E-08
H_2SeO_3 (aq)	8.70E-11	9.49E-13	3.78E-16	1.27E-22
$FeHSeO_3^{2+}$	1.60E-18	1.10E-22	3.49E-30	1.88E-43
$HSeO_4^-$	8.79E-18	7.98E-17	1.77E-17	1.09E-20
AsO_3^{3-}	6.78E-34	7.81E-32	4.60E-30	2.62E-28
$HAsO_3^{2-}$	1.18E-26	2.02E-26	1.32E-26	1.36E-27
$H_2AsO_3^-$	8.74E-21	2.20E-22	1.62E-24	3.80E-28
$H_4AsO_3^+$	3.86E-24	2.13E-29	2.06E-35	5.05E-44
AsO_4^{3-}	1.12E-14	1.59E-11	5.95E-09	1.78E-06
$HAsO_4^{2-}$	2.38E-09	4.99E-08	2.08E-07	1.12E-07
$H_2AsO_4^-$	1.46E-08	4.54E-09	2.13E-10	2.62E-13

Table G-7.   Speciation of As, Cr, Cu, Fe and Se calculated using MINTEQA2: Presque Isle.

Species in Solution	Concentration (mol/L)			
	P-1	P-2	P-3	P-4
	pH 5.87, Eh 323	pH 7.90, Eh 263	pH 9.82, Eh 174	pH 11.68, Eh -9
H^+	1.35E-06	1.26E-08	1.53E-10	2.21E-12
H_3AsO_4	4.25E-10	2.45E-13	2.61E-18	2.60E-22
H_3AsO_3	7.35E-14	3.94E-19	6.21E-25	1.81E-26
$Cr(OH)_2^+$	7.22E-09	2.13E-08	2.59E-09	6.51E-13
CrO_4^{2-}	1.22E-24	4.93E-15	6.17E-09	1.36E-10
Cu^+	3.06E-10	7.05E-10	1.98E-11	8.54E-13
Cu^{2+}	1.81E-07	4.05E-08	3.62E-11	1.45E-15
Fe^{2+}	5.45E-08	8.84E-11	1.76E-15	1.42E-19
Fe^{3+}	1.48E-15	2.32E-19	1.48E-25	1.23E-32
$HSeO_3^-$	3.11E-06	1.94E-06	1.02E-07	1.05E-09
SeO_4^{2-}	5.22E-14	3.76E-10	1.13E-08	3.33E-11
$HCrO_4^-$	5.28E-24	1.99E-16	2.96E-12	7.79E-16
$H_2CrO_4 (aq)$	5.76E-30	2.03E-24	3.60E-22	1.25E-27
$Cr_2O_7^{2-}$	1.40E-45	1.39E-30	3.08E-22	2.35E-29
$FeAsO_4$	3.97E-09	4.43E-10	1.65E-15	3.37E-21
$FeHAsO_4^+$	6.02E-16	6.27E-19	2.83E-26	8.35E-34
$FeH_2AsO_4^{2+}$	2.90E-17	2.82E-22	1.55E-31	7.32E-41
$CuSeO_3$	1.57E-15	2.34E-14	8.94E-17	2.10E-21
$FeSeO_3^+$	1.87E-12	1.97E-14	5.26E-20	2.11E-27
Cr^{3+}	4.96E-11	1.28E-14	2.33E-19	1.64E-26
OH^-	7.48E-09	8.02E-07	6.70E-05	5.10E-03
$CuOH^+$	4.25E-09	1.02E-07	7.44E-09	1.87E-11
$Cu(OH)_2 (aq)$	6.32E-12	1.62E-08	9.80E-08	1.70E-08
$Cu(OH)_3^-$	9.70E-17	2.66E-11	1.35E-08	1.78E-07
$Cu(OH)_4^{2-}$	5.74E-24	1.69E-16	7.21E-12	7.98E-09
$Cu_2(OH)_2^{2+}$	7.84E-13	4.49E-10	2.42E-12	1.69E-17
$FeOH^+$	1.61E-11	2.79E-12	4.56E-15	2.31E-17
$Fe(OH)_2 (aq)$	9.51E-17	1.77E-15	2.39E-16	8.36E-17
$Fe(OH)_3^-$	2.25E-19	4.49E-16	5.07E-15	1.35E-13
$FeOH^{2+}$	7.03E-12	1.19E-13	6.13E-18	2.90E-23
$Fe(OH)_2^+$	2.03E-08	3.66E-08	1.55E-10	4.60E-14
$Fe(OH)_3 (aq)$	1.62E-10	3.13E-08	1.10E-08	2.25E-10
$Fe(OH)_4^-$	1.13E-13	2.34E-09	6.86E-08	1.07E-07
$Fe2(OH)_2^{4+}$	1.67E-21	4.74E-25	1.32E-33	4.34E-44
$Fe3(OH)_4^{5+}$	4.98E-28	2.56E-31	3.13E-42	0.00E+00
$Cr(OH)^{2+}$	8.01E-09	2.20E-10	3.27E-13	1.31E-18
$Cr(OH)_3 (aq)$	2.02E-11	6.37E-09	6.43E-08	1.11E-09
$Cr(OH)_4^-$	6.02E-15	2.03E-10	1.72E-07	2.26E-07
CrO_2^-	7.13E-15	2.41E-10	2.03E-07	2.68E-07
SeO_3^{2-}	9.24E-09	6.19E-07	2.75E-06	2.37E-06
$H_2SeO_3 (aq)$	1.79E-09	1.04E-11	6.55E-15	8.86E-19
$FeHSeO_3^{2+}$	1.20E-17	1.17E-21	3.82E-29	2.45E-38
$HSeO_4^-$	3.50E-18	2.36E-16	8.38E-17	2.95E-21
AsO_3^{3-}	5.51E-31	3.65E-30	3.45E-30	5.90E-26
$HAsO_3^{2-}$	1.91E-23	1.18E-24	1.31E-26	2.42E-24
$H_2AsO_3^-$	2.80E-17	1.61E-20	2.12E-24	4.70E-24
$H_4AsO_3^+$	4.92E-20	2.47E-27	4.69E-35	1.98E-38
AsO_4^{3-}	3.53E-13	2.51E-10	1.61E-09	9.40E-08
$HAsO_4^{2-}$	1.49E-07	9.87E-07	7.41E-08	4.70E-08
$H_2AsO_4^-$	1.82E-06	1.12E-07	1.00E-10	7.58E-13

Table G-8. Speciation of As, Cr, Cu, Fe and Se calculated using MINTEQA2: Presque Isle-Lawson

Species in Solution	Concentration (mol/L)			
	PL-1	PL-2	PL-3	PL-4
	pH 6.70, Eh 263	pH 8.02, Eh 207	pH 8.92, Eh 175	pH 10.98, Eh 49
H^+	2.00E-07	9.56E-09	1.21E-09	1.08E-11
H_3AsO_4	3.26E-12	2.28E-14	7.39E-16	1.13E-19
H_3AsO_3	1.32E-15	1.65E-18	1.03E-20	2.16E-24
$Cr(OH)_2^+$	1.73E-08	9.31E-09	6.13E-09	1.04E-11
CrO_4^{2-}	2.53E-22	1.63E-17	6.46E-14	1.10E-10
Cu^+	1.48E-09	7.79E-10	5.41E-10	5.43E-11
Cu^{2+}	8.48E-08	5.04E-09	1.01E-09	8.10E-13
Fe^{2+}	1.05E-07	2.90E-09	5.69E-10	1.57E-14
Fe^{3+}	2.75E-16	8.57E-19	4.88E-20	1.13E-26
$HSeO_3^-$	5.89E-07	3.02E-07	1.25E-07	1.71E-09
SeO_4^{2-}	2.86E-14	1.71E-12	2.95E-11	3.62E-11
$HCrO_4^-$	1.63E-22	5.01E-19	2.49E-16	3.42E-15
$H_2CrO_4 (aq)$	2.63E-29	3.87E-27	2.41E-25	2.82E-26
$Cr_2O_7^{2-}$	9.18E-43	8.73E-36	2.16E-30	4.28E-28
$FeAsO_4$	1.77E-09	3.52E-10	3.19E-10	1.37E-14
$FeHAsO_4^+$	3.97E-17	3.77E-19	4.32E-20	1.65E-26
$FeH_2AsO_4^{2+}$	2.82E-19	1.28E-22	1.86E-24	6.67E-33
$CuSeO_3$	9.46E-16	6.03E-16	3.93E-16	4.39E-19
$FeSeO_3^+$	4.52E-13	1.51E-14	2.76E-15	8.08E-22
Cr^{3+}	2.58E-12	3.18E-15	3.38E-17	5.26E-24
OH^-	5.05E-08	1.06E-06	8.41E-06	9.89E-04
$CuOH^+$	1.35E-08	1.67E-08	2.65E-08	2.27E-09
$Cu(OH)_2 (aq)$	1.36E-10	3.52E-09	4.42E-08	4.23E-07
$Cu(OH)_3^-$	1.41E-14	7.61E-12	7.62E-10	8.58E-07
$Cu(OH)_4^{2-}$	5.60E-21	6.35E-17	5.08E-14	7.06E-09
$Cu_2(OH)_2^{2+}$	7.86E-12	1.21E-11	3.06E-11	2.34E-13
$FeOH^+$	2.11E-10	1.21E-10	1.88E-10	5.53E-13
$Fe(OH)_2 (aq)$	8.44E-15	1.02E-13	1.24E-12	4.11E-13
$Fe(OH)_3^-$	1.35E-16	3.39E-14	3.31E-12	1.28E-10
$FeOH^{2+}$	8.91E-12	5.79E-13	2.59E-13	6.09E-18
$Fe(OH)_2^+$	1.74E-07	2.37E-07	8.36E-07	2.10E-09
$Fe(OH)_3 (aq)$	9.43E-09	2.68E-07	7.50E-06	2.11E-06
$Fe(OH)_4^-$	4.44E-11	2.63E-08	5.87E-06	1.94E-04
$Fe2(OH)_2^{4+}$	2.65E-21	1.12E-23	2.29E-24	1.54E-33
$Fe3(OH)_4^{5+}$	6.74E-27	3.89E-29	2.85E-29	5.81E-41
$Cr(OH)^{2+}$	2.83E-09	7.29E-11	6.08E-12	9.63E-17
$Cr(OH)_3 (aq)$	3.28E-10	3.68E-09	1.92E-08	3.64E-09
$Cr(OH)_4^-$	6.60E-13	1.55E-10	6.43E-09	1.43E-07
CrO_2^-	7.82E-13	1.83E-10	7.62E-09	1.70E-07
SeO_3^{2-}	1.18E-08	1.27E-07	4.18E-07	7.08E-07
$H_2SeO_3 (aq)$	5.01E-11	1.23E-12	6.38E-14	7.44E-18
$FeHSeO_3^{2+}$	4.25E-19	6.79E-22	1.58E-23	4.32E-32
$HSeO_4^-$	2.85E-19	8.14E-19	1.76E-18	1.75E-20
AsO_3^{3-}	3.02E-30	3.47E-29	1.10E-28	4.35E-26
$HAsO_3^{2-}$	1.56E-23	8.53E-24	3.36E-24	1.03E-23
$H_2AsO_3^-$	3.39E-18	8.89E-20	4.39E-21	1.09E-22
$H_4AsO_3^+$	1.30E-22	7.84E-27	6.13E-30	1.15E-35
AsO_4^{3-}	8.29E-13	5.30E-11	8.76E-10	2.52E-07
$HAsO_4^{2-}$	5.20E-08	1.59E-07	3.27E-07	7.25E-07
$H_2AsO_4^-$	9.42E-08	1.38E-08	3.55E-09	6.37E-11

Table G-9.   Speciation of As, Cr, Cu, Fe and Se calculated using MINTEQA2: Presque Isle-Kamm.

Species in Solution	Concentration (mol/L)			
	PK-1	PK-2	PK-3	PK-4
	pH 6.72, Eh 259	pH 7.90, Eh 223	pH 9.34, Eh 175	pH 11.72, Eh 29
H^+	1.91E-07	1.26E-08	4.59E-10	2.02E-12
H_3AsO_4	3.73E-13	3.67E-14	7.89E-17	5.17E-22
H_3AsO_3	1.88E-16	1.33E-18	1.58E-22	1.55E-27
$Cr(OH)_2^+$	3.66E-09	1.94E-08	1.38E-09	6.32E-14
CrO_4^{2-}	4.39E-23	4.20E-17	4.82E-12	1.95E-09
Cu^+	8.83E-10	6.41E-11	4.29E-12	2.33E-15
Cu^{2+}	4.32E-08	7.74E-10	8.05E-12	1.75E-17
Fe^{2+}	6.32E-08	6.73E-09	4.64E-12	1.20E-19
Fe^{3+}	1.41E-16	3.71E-18	4.00E-22	4.60E-32
$HSeO_3^-$	3.94E-07	2.70E-07	2.96E-08	2.52E-10
SeO_4^{2-}	1.60E-14	2.32E-12	1.27E-10	2.03E-10
$HCrO_4^-$	2.70E-23	1.70E-18	7.04E-15	1.01E-14
$H_2CrO_4 (aq)$	4.16E-30	1.74E-26	2.60E-24	1.47E-26
$Cr_2O_7^{2-}$	2.52E-44	1.01E-34	1.73E-27	3.98E-27
$FeAsO_4$	1.19E-10	1.07E-09	5.03E-12	3.23E-20
$FeHAsO_4^+$	2.55E-18	1.51E-18	2.59E-22	7.32E-33
$FeH_2AsO_4^{2+}$	1.73E-20	6.78E-22	4.26E-27	5.89E-40
$CuSeO_3$	3.37E-16	6.27E-17	1.94E-18	6.56E-24
$FeSeO_3^+$	1.62E-13	4.42E-14	1.40E-17	2.02E-27
Cr^{3+}	4.96E-13	1.15E-14	1.10E-18	1.35E-27
OH^-	5.29E-08	8.01E-07	2.21E-05	5.60E-03
$CuOH^+$	7.19E-09	1.95E-09	5.54E-10	2.46E-13
$Cu(OH)_2 (aq)$	7.57E-11	3.11E-10	2.42E-09	2.44E-10
$Cu(OH)_3^-$	8.22E-15	5.11E-13	1.10E-10	2.81E-09
$Cu(OH)_4^{2-}$	3.43E-21	3.23E-18	1.93E-14	1.39E-10
$Cu_2(OH)_2^{2+}$	2.24E-12	1.65E-13	1.34E-14	2.92E-21
$FeOH^+$	1.33E-10	2.13E-10	4.02E-12	2.12E-17
$Fe(OH)_2 (aq)$	5.56E-15	1.35E-13	7.00E-14	8.38E-17
$Fe(OH)_3^-$	9.30E-17	3.43E-14	4.90E-13	1.49E-13
$FeOH^{2+}$	4.78E-12	1.90E-12	5.56E-15	1.17E-22
$Fe(OH)_2^+$	9.80E-08	5.89E-07	4.71E-08	2.03E-13
$Fe(OH)_3 (aq)$	5.56E-09	5.05E-07	1.11E-06	1.08E-09
$Fe(OH)_4^-$	2.74E-11	3.77E-08	2.28E-06	5.66E-07
$Fe2(OH)_2^{4+}$	7.62E-22	1.21E-22	1.06E-27	7.26E-43
$Fe3(OH)_4^{5+}$	1.09E-27	1.04E-27	7.46E-34	0.00E+00
$Cr(OH)^{2+}$	5.70E-10	2.00E-10	5.21E-13	1.17E-19
$Cr(OH)_3 (aq)$	7.25E-11	5.82E-09	1.14E-08	1.18E-10
$Cr(OH)_4^-$	1.53E-13	1.85E-10	1.00E-08	2.64E-08
CrO_2^-	1.81E-13	2.20E-10	1.19E-08	3.13E-08
SeO_3^{2-}	8.25E-09	8.58E-08	2.61E-07	6.26E-07
$H_2SeO_3 (aq)$	3.20E-11	1.45E-12	5.75E-15	1.93E-19
$FeHSeO_3^{2+}$	1.46E-19	2.62E-21	3.05E-26	2.16E-38
$HSeO_4^-$	1.53E-19	1.46E-18	2.88E-18	1.63E-20
AsO_3^{3-}	4.94E-31	1.22E-29	3.10E-29	6.84E-27
$HAsO_3^{2-}$	2.43E-24	3.94E-24	3.60E-25	2.53E-25
$H_2AsO_3^-$	5.06E-19	5.42E-20	1.78E-22	4.43E-25
$H_4AsO_3^+$	1.78E-23	8.29E-27	3.60E-32	1.56E-39
AsO_4^{3-}	1.09E-13	3.72E-11	1.71E-09	2.52E-07
$HAsO_4^{2-}$	6.51E-09	1.47E-07	2.42E-07	1.13E-07
$H_2AsO_4^-$	1.13E-08	1.68E-08	9.97E-10	1.66E-12

Table G-10. Speciation of As, Cr, Cu, Fe and Se calculated using MINTEQA2: Presque Isle-Red Wing.

Species in Solution	Concentration (mol/L)			
	PR-1	PR-2	PR-3	PR-4
	pH 6.07, Eh 213	pH 8.37, Eh 164	pH 10.78, Eh 142	pH 11.85, Eh 102
H^+	8.58E-07	4.27E-09	1.69E-11	1.51E-12
H_3AsO_4	1.32E-11	9.20E-15	1.47E-20	5.32E-23
H_3AsO_3	4.73E-12	3.78E-18	5.08E-28	2.99E-31
$Cr(OH)_2^+$	6.87E-08	2.41E-08	1.55E-12	7.20E-17
CrO_4^{2-}	4.94E-28	3.50E-17	5.25E-08	6.93E-08
Cu^+	2.09E-08	4.86E-09	1.16E-14	2.61E-16
Cu^{2+}	1.74E-07	5.90E-09	6.33E-15	3.46E-17
Fe^{2+}	2.08E-05	3.82E-10	2.81E-19	5.97E-22
Fe^{3+}	8.02E-15	2.12E-20	7.27E-30	4.11E-33
$HSeO_3^-$	3.49E-07	1.34E-07	5.21E-10	7.74E-11
SeO_4^{2-}	4.54E-18	2.99E-13	3.76E-09	4.63E-08
$HCrO_4^-$	1.33E-27	4.80E-19	2.65E-12	2.59E-13
H_2CrO_4 (aq)	9.11E-34	1.66E-27	3.49E-23	2.77E-25
$Cr_2O_7^{2-}$	0.00E+00	8.01E-36	2.54E-22	2.66E-24
$FeAsO_4$	2.53E-09	3.92E-11	3.09E-19	6.72E-22
$FeHAsO_4^+$	2.44E-16	1.88E-20	5.88E-31	1.14E-34
$FeH_2AsO_4^{2+}$	7.53E-18	2.86E-24	3.68E-37	6.99E-42
$CuSeO_3$	2.61E-16	6.99E-16	6.83E-22	5.14E-24
$FeSeO_3^+$	1.73E-12	3.69E-16	1.07E-25	6.92E-29
Cr^{3+}	1.96E-10	1.64E-15	1.86E-24	9.10E-31
OH^-	1.19E-08	2.37E-06	6.19E-04	7.62E-03
$CuOH^+$	6.35E-09	4.38E-08	1.14E-11	6.37E-13
$Cu(OH)_2$ (aq)	1.49E-11	2.06E-08	1.36E-09	8.46E-10
$Cu(OH)_3^-$	3.64E-16	9.99E-11	1.72E-09	1.32E-08
$Cu(OH)_4^{2-}$	3.47E-23	1.87E-15	8.74E-12	9.09E-10
$Cu_2(OH)_2^{2+}$	1.77E-12	8.31E-11	5.88E-18	2.00E-20
$FeOH^+$	9.58E-09	3.57E-11	6.40E-18	1.39E-19
$Fe(OH)_2$ (aq)	8.94E-14	6.69E-14	3.02E-18	7.33E-19
$Fe(OH)_3^-$	3.37E-16	5.00E-14	5.92E-16	1.77E-15
$FeOH^{2+}$	5.90E-11	3.20E-14	2.57E-21	1.35E-23
$Fe(OH)_2^+$	2.65E-07	2.92E-08	5.71E-13	3.07E-14
$Fe(OH)_3$ (aq)	3.34E-09	7.40E-08	3.65E-10	2.19E-10
$Fe(OH)_4^-$	3.71E-12	1.63E-08	2.10E-08	1.56E-07
$Fe2(OH)_2^{4+}$	1.22E-19	3.44E-26	2.58E-40	9.81E-45
$Fe3(OH)_4^{5+}$	4.98E-25	1.48E-32	0.00E+00	0.00E+00
$Cr(OH)^{2+}$	4.88E-08	8.42E-11	2.23E-17	1.02E-22
$Cr(OH)_3$ (aq)	3.03E-10	2.13E-08	3.45E-10	1.80E-13
$Cr(OH)_4^-$	1.44E-13	2.00E-09	8.51E-09	5.47E-11
CrO_2^-	1.70E-13	2.37E-09	1.01E-08	6.48E-11
SeO_3^{2-}	1.67E-09	1.26E-07	1.33E-07	2.67E-07
H_2SeO_3 (aq)	1.26E-10	2.44E-13	3.61E-18	4.36E-20
$FeHSeO_3^{2+}$	7.07E-18	7.43E-24	8.85E-36	5.61E-40
$HSeO_4^-$	1.89E-22	6.36E-20	2.94E-18	2.68E-18
AsO_3^{3-}	1.48E-28	8.93E-28	2.41E-30	3.51E-30
$HAsO_3^{2-}$	3.15E-21	9.79E-23	9.36E-28	9.18E-29
$H_2AsO_3^-$	2.87E-15	4.56E-19	1.60E-26	1.16E-28
$H_4AsO_3^+$	2.01E-18	8.01E-27	4.27E-39	2.24E-43
AsO_4^{3-}	4.56E-14	2.40E-10	7.71E-09	6.90E-08
$HAsO_4^{2-}$	1.18E-08	3.21E-07	3.66E-08	2.20E-08
$H_2AsO_4^-$	8.96E-08	1.24E-08	5.21E-12	2.32E-13

Table G-11. Speciation of As, Cr, Cu, Fe and Se calculated using MINTEQA2: Presque Isle-MnRoad**.

Species in Solution	Concentration (mol/L)			
	PM-1	PM-2	PM-3	PM-4
	pH 6.17, Eh 380	pH 8.34, Eh 311	pH 9.66, Eh 240	pH 11.96, Eh 95
H^+	6.77E-07	4.58E-09	2.20E-10	1.18E-12
H_3AsO_4	2.03E-11	9.63E-15	2.22E-17	2.04E-22
H_3AsO_3	1.04E-17	4.87E-23	6.45E-26	1.19E-30
$Cr(OH)_2^+$	2.75E-09	6.40E-09	3.05E-11	1.31E-17
CrO_4^{2-}	2.28E-20	1.75E-10	1.76E-08	2.61E-08
Cu^+	3.56E-11	1.64E-11	5.95E-13	3.06E-16
Cu^{2+}	1.94E-07	6.07E-09	1.41E-11	3.16E-17
Fe^{2+}	5.04E-10	9.75E-14	5.26E-17	6.12E-22
Fe^{3+}	1.25E-16	1.65E-21	5.74E-26	3.35E-33
$HSeO_3^-$	4.66E-07	1.36E-07	9.83E-09	9.68E-11
SeO_4^{2-}	5.25E-12	2.30E-08	6.11E-08	7.39E-08
$HCrO_4^-$	4.97E-20	2.58E-12	1.23E-11	7.37E-14
$H_2CrO_4 (aq)$	2.72E-26	9.53E-21	2.16E-21	6.07E-26
$Cr_2O_7^{2-}$	8.57E-38	2.31E-22	5.28E-21	2.19E-25
$FeAsO_4$	1.29E-10	2.60E-12	1.83E-15	4.16E-21
$FeHAsO_4^+$	9.76E-18	1.33E-21	4.51E-26	5.53E-34
$FeH_2AsO_4^{2+}$	2.35E-19	2.18E-25	3.56E-31	2.70E-41
$CuSeO_3$	5.05E-16	6.80E-16	2.34E-18	7.27E-24
$FeSeO_3^+$	4.79E-14	2.72E-17	1.38E-21	8.42E-29
Cr^{3+}	4.71E-12	5.02E-16	5.66E-21	1.06E-31
OH^-	1.49E-08	2.21E-06	4.63E-05	9.91E-03
$CuOH^+$	9.10E-09	4.20E-08	2.02E-09	7.32E-13
$Cu(OH)_2 (aq)$	2.70E-11	1.85E-08	1.84E-08	1.24E-09
$Cu(OH)_3^-$	8.26E-16	8.35E-11	1.75E-09	2.53E-08
$Cu(OH)_4^{2-}$	9.72E-23	1.46E-15	6.45E-13	2.29E-09
$Cu_2(OH)_2^{2+}$	3.58E-12	7.65E-11	1.78E-13	2.69E-20
$FeOH^+$	2.98E-13	8.51E-15	9.48E-17	1.78E-19
$Fe(OH)_2 (aq)$	3.52E-18	1.49E-17	3.45E-18	1.20E-18
$Fe(OH)_3^-$	1.66E-20	1.04E-17	5.05E-17	3.78E-15
$FeOH^{2+}$	1.20E-12	2.33E-15	1.66E-18	1.36E-23
$Fe(OH)_2^+$	6.90E-09	1.99E-09	2.92E-11	3.87E-14
$Fe(OH)_3 (aq)$	1.10E-10	4.69E-09	1.43E-09	3.54E-10
$Fe(OH)_4^-$	1.53E-13	9.63E-10	6.18E-09	3.27E-07
$Fe2(OH)_2^{4+}$	4.77E-23	1.82E-28	9.52E-35	1.12E-44
$Fe3(OH)_4^{5+}$	4.81E-30	5.29E-36	4.20E-44	0.00E+00
$Cr(OH)^{2+}$	1.53E-09	2.40E-11	5.53E-15	1.47E-23
$Cr(OH)_3 (aq)$	1.54E-11	5.29E-09	5.24E-10	4.17E-14
$Cr(OH)_4^-$	9.14E-15	4.64E-10	9.65E-10	1.65E-11
CrO_2^-	1.08E-14	5.50E-10	1.14E-09	1.95E-11
SeO_3^{2-}	2.76E-09	1.19E-07	1.82E-07	4.41E-07
$H_2SeO_3 (aq)$	1.34E-10	2.65E-13	9.12E-16	4.19E-20
$FeHSeO_3^{2+}$	1.53E-19	5.87E-25	1.44E-30	5.44E-40
$HSeO_4^-$	1.77E-16	5.24E-15	6.59E-16	3.24E-18
AsO_3^{3-}	6.13E-34	9.33E-33	1.17E-31	3.22E-29
$HAsO_3^{2-}$	1.07E-26	1.10E-27	6.45E-28	6.28E-28
$H_2AsO_3^-$	7.90E-21	5.47E-24	1.52E-25	6.02E-28
$H_4AsO_3^+$	3.49E-24	1.10E-31	7.03E-36	6.99E-43
AsO_4^{3-}	1.32E-13	2.04E-10	4.45E-09	6.11E-07
$HAsO_4^{2-}$	2.81E-08	2.93E-07	2.99E-07	1.45E-07
$H_2AsO_4^-$	1.73E-07	1.21E-08	5.86E-10	1.16E-12

Table G-12. Speciation of As, Cr, Cu, Fe and Se calculated using MINTEQA2: Presque
Isle-sand.

Species in Solution	Concentration (mol/L)			
	PS-1	PS-2	PS-3	PS-4
	pH 6.98, Eh 207	pH 9.22, Eh 40	pH 11.03, Eh 12	pH 12.07, Eh -48
H^+	1.05E-07	6.05E-10	9.59E-12	9.27E-13
H_3AsO_4	8.62E-13	8.13E-17	5.24E-21	7.92E-24
H_3AsO_3	7.51E-15	1.04E-17	1.42E-24	1.90E-27
$Cr(OH)_2^+$	3.83E-09	1.39E-09	1.02E-12	9.81E-15
CrO_4^{2-}	3.85E-24	1.31E-19	2.86E-13	5.17E-12
Cu^+	3.28E-10	9.45E-10	4.03E-13	3.96E-15
Cu^{2+}	2.12E-09	9.25E-12	1.42E-15	1.61E-18
Fe^{2+}	3.81E-08	1.06E-10	2.91E-17	3.65E-20
Fe^{3+}	1.12E-17	4.76E-23	4.94E-30	8.03E-34
$HSeO_3^-$	5.67E-07	7.92E-08	1.00E-09	9.21E-11
SeO_4^{2-}	2.43E-15	4.05E-15	1.68E-12	2.27E-12
$HCrO_4^-$	1.30E-24	2.53E-22	7.97E-18	1.10E-17
H_2CrO_4 (aq)	1.10E-31	1.23E-31	5.87E-29	6.98E-30
$Cr_2O_7^{2-}$	0.00E+00	2.24E-42	2.33E-33	5.00E-33
$FeAsO_4$	1.32E-10	2.72E-13	3.97E-19	7.59E-23
$FeHAsO_4^+$	1.56E-18	1.84E-23	4.27E-31	7.90E-36
$FeH_2AsO_4^{2+}$	5.80E-21	3.98E-28	1.53E-37	3.08E-43
$CuSeO_3$	4.34E-17	4.54E-18	5.09E-22	4.33E-25
$FeSeO_3^+$	3.39E-14	3.40E-18	2.35E-25	2.27E-29
Cr^{3+}	1.57E-13	1.92E-18	4.08E-25	5.20E-29
OH^-	9.63E-08	1.68E-05	1.11E-03	1.29E-02
$CuOH^+$	6.42E-10	4.84E-10	4.48E-12	4.67E-14
$Cu(OH)_2$ (aq)	1.23E-11	1.61E-09	9.39E-10	1.01E-10
$Cu(OH)_3^-$	2.43E-15	5.53E-11	2.14E-09	2.68E-09
$Cu(OH)_4^{2-}$	1.84E-21	7.35E-15	1.97E-11	3.22E-10
$Cu_2(OH)_2^{2+}$	1.78E-14	1.02E-14	9.15E-19	1.12E-22
$FeOH^+$	1.46E-10	6.98E-11	1.16E-15	1.33E-17
$Fe(OH)_2$ (aq)	1.11E-14	9.24E-13	9.63E-16	1.15E-16
$Fe(OH)_3^-$	3.38E-16	4.90E-12	3.38E-13	4.69E-13
$FeOH^{2+}$	6.94E-13	5.04E-16	3.01E-21	4.01E-24
$Fe(OH)_2^+$	2.59E-08	3.24E-09	1.17E-12	1.43E-14
$Fe(OH)_3$ (aq)	2.67E-09	5.80E-08	1.32E-09	1.66E-10
$Fe(OH)_4^-$	2.39E-11	9.06E-08	1.36E-07	2.00E-07
$Fe2(OH)_2^{4+}$	1.61E-23	8.68E-30	3.72E-40	1.40E-45
$Fe3(OH)_4^{5+}$	6.06E-30	4.19E-37	0.00E+00	0.00E+00
$Cr(OH)^{2+}$	3.28E-10	6.89E-13	8.42E-18	8.80E-21
$Cr(OH)_3$ (aq)	1.38E-10	8.67E-09	4.02E-10	4.00E-11
$Cr(OH)_4^-$	5.30E-13	5.79E-09	1.78E-08	2.05E-08
CrO_2^-	6.28E-13	6.86E-09	2.10E-08	2.43E-08
SeO_3^{2-}	2.16E-08	5.29E-07	4.64E-07	5.56E-07
H_2SeO_3 (aq)	2.53E-11	2.03E-14	3.89E-18	3.07E-20
$FeHSeO_3^{2+}$	1.67E-20	9.74E-27	1.12E-35	1.17E-40
$HSeO_4^-$	1.27E-20	1.21E-22	7.24E-22	7.48E-23
AsO_3^{3-}	1.19E-28	8.85E-25	4.01E-26	1.20E-25
$HAsO_3^{2-}$	3.21E-22	1.36E-20	8.48E-24	1.73E-24
$H_2AsO_3^-$	3.68E-17	8.87E-18	8.00E-23	1.25E-24
$H_4AsO_3^+$	3.90E-22	3.11E-27	6.74E-36	8.73E-40
AsO_4^{3-}	1.51E-12	7.67E-10	1.64E-08	5.52E-08
$HAsO_4^{2-}$	4.98E-08	1.44E-07	4.23E-08	9.71E-09
$H_2AsO_4^-$	4.74E-08	7.80E-10	3.32E-12	5.84E-14

Table G-13. Speciation of As, Cr, Cu, Fe and Se calculated using MINTEQA2:
Columbia.

Species in Solution	Concentration (mol/L)			
	C-1	C-2	C-3	C-4
	pH 6.74, Eh 323	pH 8.89, Eh 284	pH 11.13, Eh 227	pH 12.55, Eh -26
H^+	1.82E-07	1.29E-09	7.64E-12	3.24E-13
H_3AsO_4	1.41E-11	1.69E-15	3.33E-20	1.78E-24
H_3AsO_3	4.44E-17	5.55E-24	3.06E-31	8.49E-30
$Cr(OH)_2^+$	2.73E-07	1.40E-07	7.92E-18	2.49E-16
CrO_4^{2-}	7.63E-18	3.30E-07	7.13E-07	1.52E-09
Cu^+	2.94E-10	2.54E-11	2.08E-15	1.98E-16
Cu^{2+}	1.74E-07	3.32E-09	3.20E-14	2.24E-19
Fe^{2+}	7.18E-09	2.63E-14	1.06E-21	6.98E-22
Fe^{3+}	1.95E-16	1.57E-22	7.89E-31	4.75E-35
$HSeO_3^-$	3.79E-06	5.85E-07	1.07E-11	2.97E-12
SeO_4^{2-}	2.59E-11	5.45E-07	6.67E-07	1.31E-11
$HCrO_4^-$	4.46E-18	1.36E-09	1.56E-11	9.12E-16
H_2CrO_4 (aq)	6.57E-25	1.41E-18	9.11E-23	1.80E-28
$Cr_2O_7^{2-}$	6.93E-34	6.45E-17	8.99E-21	3.81E-29
$FeAsO_4$	7.08E-09	1.91E-12	7.79E-19	1.70E-23
$FeHAsO_4^+$	1.45E-16	2.77E-22	6.67E-31	6.20E-37
$FeH_2AsO_4^{2+}$	9.42E-19	1.28E-26	1.92E-37	9.81E-45
$CuSeO_3$	1.36E-14	5.62E-15	1.51E-22	4.44E-27
$FeSeO_3^+$	2.23E-12	3.88E-17	4.87E-28	7.98E-32
Cr^{3+}	3.40E-11	8.88E-16	2.05E-30	2.25E-31
OH^-	5.55E-08	7.85E-06	1.40E-03	4.11E-02
$CuOH^+$	3.03E-08	8.11E-08	1.26E-10	1.66E-14
$Cu(OH)_2$ (aq)	3.33E-10	1.26E-07	3.30E-08	1.03E-10
$Cu(OH)_3^-$	3.79E-14	2.03E-09	9.48E-08	8.68E-09
$Cu(OH)_4^{2-}$	1.66E-20	1.26E-13	1.11E-09	3.72E-09
$Cu_2(OH)_2^{2+}$	3.97E-11	2.86E-10	7.22E-16	1.58E-23
$FeOH^+$	1.57E-11	8.08E-15	5.25E-20	6.52E-19
$Fe(OH)_2$ (aq)	6.89E-16	4.99E-17	5.50E-20	1.60E-17
$Fe(OH)_3^-$	1.21E-17	1.24E-16	2.43E-17	2.09E-13
$FeOH^{2+}$	6.87E-12	7.79E-16	5.95E-22	5.43E-25
$Fe(OH)_2^+$	1.47E-07	2.34E-09	2.87E-13	4.96E-15
$Fe(OH)_3$ (aq)	8.71E-09	1.96E-08	4.07E-10	1.65E-10
$Fe(OH)_4^-$	4.50E-11	1.43E-08	5.30E-08	6.33E-07
$Fe2(OH)_2^{4+}$	1.59E-21	2.07E-29	1.49E-41	0.00E+00
$Fe3(OH)_4^{5+}$	3.44E-27	7.23E-37	0.00E+00	0.00E+00
$Cr(OH)^{2+}$	4.08E-08	1.49E-10	5.25E-23	8.72E-23
$Cr(OH)_3$ (aq)	5.65E-09	4.09E-07	3.92E-15	2.89E-12
$Cr(OH)_4^-$	1.25E-11	1.28E-07	2.19E-13	4.75E-09
CrO_2^-	1.48E-11	1.52E-07	2.59E-13	5.63E-09
SeO_3^{2-}	8.34E-08	1.83E-06	6.28E-09	6.40E-08
H_2SeO_3 (aq)	2.93E-10	3.20E-13	3.28E-20	3.09E-22
$FeHSeO_3^{2+}$	1.92E-18	2.38E-25	1.86E-38	1.61E-43
$HSeO_4^-$	2.35E-16	3.48E-14	2.26E-16	1.22E-22
AsO_3^{3-}	1.36E-31	4.85E-32	1.78E-32	2.43E-26
$HAsO_3^{2-}$	6.33E-25	1.59E-27	2.94E-30	8.81E-26
$H_2AsO_3^-$	1.26E-19	2.22E-24	2.18E-29	1.79E-26
$H_4AsO_3^+$	4.02E-24	3.56E-33	1.16E-42	1.37E-42
AsO_4^{3-}	4.77E-12	1.64E-09	2.14E-07	5.64E-07
$HAsO_4^{2-}$	2.71E-07	6.54E-07	4.31E-07	2.49E-08
$H_2AsO_4^-$	4.48E-07	7.59E-09	2.66E-11	4.21E-14

Table G-14. Speciation of As, Cr, Cu, Fe and Se calculated using MINTEQA2:
Columbia-Lawson.

Species in Solution	Concentration (mol/L)			
	CL-1	CL-2	CL-3	CL-4
	pH 5.68, Eh 357	pH 8.22, Eh 235	pH 9.66, Eh 122	pH 11.81, Eh 53
H^+	2.09E-06	6.04E-09	2.20E-10	1.65E-12
H_3AsO_4	5.91E-12	9.31E-16	1.25E-18	1.33E-23
H_3AsO_3	1.74E-16	3.03E-21	3.57E-23	4.06E-30
$Cr(OH)_2^+$	2.55E-08	5.92E-07	2.28E-08	4.99E-13
CrO_4^{2-}	1.65E-23	4.34E-13	1.37E-11	8.99E-07
Cu^+	1.65E-10	2.89E-09	2.29E-09	5.49E-13
Cu^{2+}	3.66E-07	5.58E-08	5.50E-10	1.07E-14
Fe^{2+}	3.95E-08	1.20E-10	6.09E-14	6.94E-21
Fe^{3+}	4.01E-15	1.06E-19	6.72E-25	6.99E-33
$HSeO_3^-$	1.15E-06	5.17E-07	3.33E-08	7.32E-11
SeO_4^{2-}	7.31E-14	1.03E-10	2.12E-11	7.28E-10
$HCrO_4^-$	1.11E-22	8.42E-15	9.49E-15	3.72E-12
$H_2CrO_4 (aq)$	1.88E-28	4.11E-23	1.67E-24	4.37E-24
$Cr_2O_7^{2-}$	4.29E-43	2.47E-27	3.16E-27	5.45E-22
$FeAsO_4$	4.05E-11	7.03E-12	1.21E-15	2.22E-22
$FeHAsO_4^+$	9.51E-18	4.76E-21	2.98E-26	4.11E-35
$FeH_2AsO_4^{2+}$	7.09E-19	1.02E-24	2.36E-31	2.74E-42
$CuSeO_3$	7.57E-16	1.80E-14	3.09E-16	1.39E-21
$FeSeO_3^+$	1.22E-12	5.02E-15	5.45E-20	1.04E-28
Cr^{3+}	4.19E-10	8.08E-14	4.23E-18	7.42E-27
OH^-	4.83E-09	1.67E-06	4.63E-05	6.93E-03
$CuOH^+$	5.55E-09	2.93E-07	7.86E-08	1.81E-10
$Cu(OH)_2 (aq)$	5.33E-12	9.75E-08	7.18E-07	2.20E-07
$Cu(OH)_3^-$	5.28E-17	3.35E-10	6.82E-08	3.14E-06
$Cu(OH)_4^{2-}$	2.01E-24	4.43E-15	2.51E-11	1.95E-07
$Cu_2(OH)_2^{2+}$	1.34E-12	3.72E-09	2.70E-10	1.61E-15
$FeOH^+$	7.53E-12	7.96E-12	1.10E-13	1.48E-18
$Fe(OH)_2 (aq)$	2.88E-17	1.05E-14	3.98E-15	7.17E-18
$Fe(OH)_3^-$	4.39E-20	5.58E-15	5.83E-14	1.57E-14
$FeOH^{2+}$	1.24E-11	1.13E-13	1.94E-17	2.13E-23
$Fe(OH)_2^+$	2.31E-08	7.32E-08	3.41E-10	4.44E-14
$Fe(OH)_3 (aq)$	1.19E-10	1.31E-07	1.68E-08	2.91E-10
$Fe(OH)_4^-$	5.36E-14	2.05E-08	7.22E-08	1.88E-07
$Fe2(OH)_2^{4+}$	5.14E-21	4.31E-25	1.30E-32	2.52E-44
$Fe3(OH)_4^{5+}$	1.74E-27	4.63E-31	6.73E-41	0.00E+00
$Cr(OH)^{2+}$	4.37E-08	2.93E-09	4.14E-12	7.65E-19
$Cr(OH)_3 (aq)$	4.61E-11	3.71E-07	3.91E-07	1.14E-09
$Cr(OH)_4^-$	8.86E-15	2.47E-08	7.21E-07	3.16E-07
CrO_2^-	1.05E-14	2.93E-08	8.55E-07	3.74E-07
SeO_3^{2-}	2.20E-09	3.43E-07	6.17E-07	2.28E-07
$H_2SeO_3 (aq)$	1.02E-09	1.33E-12	3.09E-15	4.53E-20
$FeHSeO_3^{2+}$	1.20E-17	1.43E-22	5.70E-29	9.20E-40
$HSeO_4^-$	7.61E-18	3.10E-17	2.28E-19	4.66E-20
AsO_3^{3-}	3.49E-34	2.54E-31	6.47E-29	3.51E-29
$HAsO_3^{2-}$	1.87E-26	3.93E-26	3.57E-25	1.02E-27
$H_2AsO_3^-$	4.27E-20	2.58E-22	8.41E-23	1.43E-27
$H_4AsO_3^+$	1.80E-22	9.05E-30	3.89E-33	3.32E-42
AsO_4^{3-}	1.31E-15	8.63E-12	2.52E-10	1.27E-08
$HAsO_4^{2-}$	8.60E-10	1.63E-08	1.69E-08	4.51E-09
$H_2AsO_4^-$	1.63E-08	8.91E-10	3.32E-11	5.25E-14

Table G-15. Speciation of As, Cr, Cu, Fe and Se calculated using MINTEQA2: Columbia-Kamm.

Species in Solution	Concentration (mol/L)			
	CK-1	CK-2	CK-3	CK-4
	pH 5.41, Eh 411	pH 7.81, Eh 303	pH 10.01, Eh 182	pH 11.86, Eh 68
H^+	3.90E-06	1.55E-08	9.86E-11	1.48E-12
H_3AsO_4	1.12E-11	5.66E-15	2.43E-19	9.39E-24
H_3AsO_3	1.71E-17	6.12E-22	1.29E-26	7.09E-31
$Cr(OH)_2^+$	5.90E-08	1.48E-06	5.69E-09	8.35E-14
CrO_4^{2-}	5.03E-22	1.05E-11	4.81E-07	1.76E-06
Cu^+	3.60E-11	3.32E-10	2.02E-11	3.46E-14
Cu^{2+}	6.58E-07	9.03E-08	5.06E-11	1.22E-15
Fe^{2+}	3.69E-08	3.15E-10	4.47E-16	1.00E-22
Fe^{3+}	3.08E-14	3.92E-18	5.18E-26	1.85E-34
$HSeO_3^-$	1.21E-06	7.48E-07	1.42E-08	2.82E-11
SeO_4^{2-}	8.00E-13	1.75E-09	1.09E-08	1.29E-09
$HCrO_4^-$	6.29E-21	5.25E-13	1.48E-10	6.39E-12
$H_2CrO_4 (aq)$	1.98E-26	6.58E-21	1.16E-20	6.68E-24
$Cr_2O_7^{2-}$	1.38E-39	9.60E-24	7.73E-19	1.62E-21
$FeAsO_4$	9.09E-11	9.30E-11	1.98E-16	5.67E-24
$FeHAsO_4^+$	3.98E-17	1.62E-19	2.19E-27	9.40E-37
$FeH_2AsO_4^{2+}$	5.53E-18	8.95E-23	7.78E-33	5.61E-44
$CuSeO_3$	7.66E-16	1.64E-14	2.67E-17	6.76E-23
$FeSeO_3^+$	5.25E-12	1.05E-13	3.91E-21	1.15E-30
Cr^{3+}	3.37E-09	1.34E-12	2.16E-19	1.02E-27
OH^-	2.60E-09	6.51E-07	1.04E-04	7.81E-03
$CuOH^+$	5.34E-09	1.85E-07	1.61E-08	2.30E-11
$Cu(OH)_2 (aq)$	2.75E-12	2.39E-08	3.27E-07	3.13E-08
$Cu(OH)_3^-$	1.47E-17	3.19E-11	6.97E-08	5.01E-07
$Cu(OH)_4^{2-}$	3.01E-25	1.64E-16	5.80E-11	3.53E-08
$Cu_2(OH)_2^{2+}$	1.24E-12	1.48E-09	1.13E-11	2.62E-17
$FeOH^+$	3.78E-12	8.12E-12	1.79E-15	2.37E-20
$Fe(OH)_2 (aq)$	7.74E-18	4.19E-15	1.45E-16	1.28E-19
$Fe(OH)_3^-$	6.35E-21	8.62E-16	4.76E-15	3.17E-16
$FeOH^{2+}$	5.08E-11	1.63E-12	3.30E-18	6.19E-25
$Fe(OH)_2^+$	5.08E-08	4.10E-07	1.29E-10	1.43E-15
$Fe(OH)_3 (aq)$	1.41E-10	2.86E-07	1.41E-08	1.05E-11
$Fe(OH)_4^-$	3.40E-14	1.73E-08	1.37E-07	7.63E-09
$Fe2(OH)_2^{4+}$	8.73E-20	8.91E-23	3.86E-34	0.00E+00
$Fe3(OH)_4^{5+}$	6.53E-26	5.36E-28	7.69E-43	0.00E+00
$Cr(OH)^{2+}$	1.89E-07	1.88E-08	4.66E-13	1.15E-19
$Cr(OH)_3 (aq)$	5.72E-11	3.61E-07	2.19E-07	2.14E-10
$Cr(OH)_4^-$	5.91E-15	9.36E-09	9.04E-07	6.65E-08
CrO_2^-	7.00E-15	1.11E-08	1.07E-06	7.87E-08
SeO_3^{2-}	1.24E-09	1.93E-07	5.93E-07	9.97E-08
$H_2SeO_3 (aq)$	2.00E-09	4.93E-12	5.86E-16	1.55E-20
$FeHSeO_3^{2+}$	9.68E-17	7.66E-21	1.84E-30	9.16E-42
$HSeO_4^-$	1.55E-16	1.35E-15	5.22E-17	7.28E-20
AsO_3^{3-}	5.34E-36	3.02E-33	2.69E-31	8.95E-30
$HAsO_3^{2-}$	5.32E-28	1.20E-27	6.53E-28	2.28E-28
$H_2AsO_3^-$	2.25E-21	2.03E-23	6.82E-26	2.82E-28
$H_4AsO_3^+$	3.29E-23	4.71E-30	6.29E-37	5.19E-43
AsO_4^{3-}	3.89E-16	3.09E-12	5.62E-10	1.31E-08
$HAsO_4^{2-}$	4.72E-10	1.50E-08	1.66E-08	4.08E-09
$H_2AsO_4^-$	1.66E-08	2.11E-09	1.44E-11	4.19E-14

Table G-16. Speciation of As, Cr, Cu, Fe and Se calculated using MINTEQA2:
Columbia-Red Wing**.**

Species in Solution	Concentration (mol/L)			
	CR-1	CR-2	CR-3	CR-4
	pH 6.18, Eh 237	pH 8.23, Eh 187	pH 10.53, Eh 93	pH 11.97, Eh -43
H^+	6.62E-07	5.90E-09	3.00E-11	1.16E-12
H_3AsO_4	1.69E-12	8.89E-16	2.00E-20	4.33E-24
H_3AsO_3	5.67E-14	1.16E-19	9.89E-26	1.12E-27
$Cr(OH)_2^+$	2.32E-07	1.65E-06	7.27E-10	7.72E-13
CrO_4^{2-}	1.23E-25	5.09E-15	2.52E-09	1.78E-10
Cu^+	2.12E-08	1.30E-08	5.17E-11	1.09E-12
Cu^{2+}	4.41E-07	3.86E-08	4.12E-12	5.27E-16
Fe^{2+}	2.60E-08	2.48E-11	1.20E-16	2.81E-21
Fe^{3+}	2.47E-17	3.37E-21	4.48E-28	7.18E-35
$HSeO_3^-$	1.32E-06	6.01E-07	2.21E-09	1.41E-11
SeO_4^{2-}	2.33E-16	3.06E-12	6.16E-11	2.50E-13
$HCrO_4^-$	2.62E-25	9.64E-17	2.30E-13	4.90E-16
H_2CrO_4 (aq)	1.40E-31	4.59E-25	5.42E-24	3.94E-28
$Cr_2O_7^{2-}$	0.00E+00	3.23E-31	1.89E-24	9.72E-30
$FeAsO_4$	2.26E-12	2.29E-13	4.81E-18	2.01E-24
$FeHAsO_4^+$	1.68E-19	1.51E-22	1.62E-29	2.61E-37
$FeH_2AsO_4^{2+}$	3.96E-21	3.18E-26	1.77E-35	1.26E-44
$CuSeO_3$	3.32E-15	1.48E-14	1.09E-18	1.80E-23
$FeSeO_3^+$	2.74E-14	1.90E-16	1.64E-23	2.68E-31
Cr^{3+}	3.81E-10	2.15E-13	2.65E-21	6.05E-27
OH^-	1.53E-08	1.71E-06	3.47E-04	1.01E-02
$CuOH^+$	2.11E-08	2.08E-07	4.25E-09	1.24E-11
$Cu(OH)_2$ (aq)	6.41E-11	7.07E-08	2.85E-07	2.16E-08
$Cu(OH)_3^-$	2.01E-15	2.49E-10	2.02E-07	4.50E-07
$Cu(OH)_4^{2-}$	2.42E-22	3.37E-15	5.69E-10	4.18E-08
$Cu_2(OH)_2^{2+}$	1.93E-11	1.87E-09	8.03E-13	7.78E-18
$FeOH^+$	1.57E-11	1.68E-12	1.55E-15	8.37E-19
$Fe(OH)_2$ (aq)	1.90E-16	2.27E-15	4.14E-16	5.78E-18
$Fe(OH)_3^-$	9.17E-19	1.23E-15	4.54E-14	1.86E-14
$FeOH^{2+}$	2.41E-13	3.69E-15	9.13E-20	2.97E-25
$Fe(OH)_2^+$	1.42E-09	2.44E-09	1.16E-11	8.64E-16
$Fe(OH)_3$ (aq)	2.33E-11	4.47E-09	4.18E-09	8.07E-12
$Fe(OH)_4^-$	3.31E-14	7.12E-10	1.35E-07	7.63E-09
$Fe2(OH)_2^{4+}$	1.96E-24	4.57E-28	3.12E-37	0.00E+00
$Fe3(OH)_4^{5+}$	4.08E-32	1.64E-35	0.00E+00	0.00E+00
$Cr(OH)^{2+}$	1.26E-07	7.97E-09	1.83E-14	8.49E-19
$Cr(OH)_3$ (aq)	1.33E-09	1.06E-06	9.18E-08	2.52E-09
$Cr(OH)_4^-$	8.07E-13	7.21E-08	1.27E-06	1.02E-06
CrO_2^-	9.56E-13	8.54E-08	1.50E-06	1.21E-06
SeO_3^{2-}	8.01E-09	4.09E-07	3.12E-07	6.60E-08
H_2SeO_3 (aq)	3.72E-10	1.51E-12	2.74E-17	5.97E-21
$FeHSeO_3^{2+}$	8.55E-20	5.29E-24	2.38E-33	1.69E-42
$HSeO_4^-$	7.68E-21	8.97E-19	8.71E-20	1.07E-23
AsO_3^{3-}	3.60E-30	1.05E-29	7.96E-29	3.26E-26
$HAsO_3^{2-}$	6.12E-23	1.58E-24	5.65E-26	6.18E-25
$H_2AsO_3^-$	4.41E-17	1.01E-20	1.75E-24	5.78E-25
$H_4AsO_3^+$	1.86E-20	3.40E-28	1.47E-36	6.41E-40
AsO_4^{3-}	1.19E-14	8.86E-12	1.78E-09	1.40E-08
$HAsO_4^{2-}$	2.46E-09	1.63E-08	1.54E-08	3.23E-09
$H_2AsO_4^-$	1.47E-08	8.71E-10	3.96E-12	2.51E-14

Table G-17. Speciation of As, Cr, Cu, Fe and Se calculated using MINTEQA2: Columbia-MnRoad.

Species in Solution	Concentration (mol/L)			
	CM-1	CM-2	CM-3	CM-4
	pH 5.80, Eh 324	pH 8.69, Eh 177	pH 10.71, Eh 117	pH 11.71, Eh 14
H^+	1.59E-06	2.05E-09	1.99E-11	2.07E-12
H_3AsO_4	4.41E-12	1.10E-16	8.16E-21	2.60E-23
H_3AsO_3	9.73E-16	3.77E-21	2.71E-27	2.63E-28
$Cr(OH)_2^+$	1.90E-07	6.67E-07	2.54E-10	2.22E-12
CrO_4^{2-}	1.37E-23	3.69E-13	1.77E-07	1.04E-08
Cu^+	1.11E-09	4.19E-09	1.07E-11	3.72E-13
Cu^{2+}	6.82E-07	8.46E-09	2.20E-12	1.56E-15
Fe^{2+}	9.82E-08	1.59E-12	5.02E-19	3.16E-21
Fe^{3+}	2.77E-15	1.46E-22	4.87E-30	6.76E-34
$HSeO_3^-$	1.38E-06	3.15E-07	2.50E-09	4.01E-11
SeO_4^{2-}	1.54E-14	1.77E-11	1.59E-09	9.43E-12
$HCrO_4^-$	6.97E-23	2.42E-15	1.06E-11	5.52E-14
H_2CrO_4 (aq)	8.93E-29	4.00E-24	1.64E-22	8.23E-26
$Cr_2O_7^{2-}$	1.70E-43	2.04E-28	4.00E-21	1.18E-25
$FeAsO_4$	4.75E-11	2.94E-14	7.17E-20	2.24E-23
$FeHAsO_4^+$	8.47E-18	6.75E-24	1.60E-31	5.20E-36
$FeH_2AsO_4^{2+}$	4.80E-19	4.93E-28	1.17E-37	4.27E-43
$CuSeO_3$	2.23E-15	4.90E-15	9.75E-19	9.14E-23
$FeSeO_3^+$	1.32E-12	1.24E-17	2.97E-25	4.66E-30
Cr^{3+}	1.80E-09	1.05E-14	4.16E-22	4.96E-26
OH^-	6.37E-09	4.94E-06	5.26E-04	5.47E-03
$CuOH^+$	1.36E-08	1.31E-07	3.39E-09	2.14E-11
$Cu(OH)_2$ (aq)	1.72E-11	1.29E-07	3.43E-07	2.08E-08
$Cu(OH)_3^-$	2.25E-16	1.30E-09	3.70E-07	2.34E-07
$Cu(OH)_4^{2-}$	1.13E-23	5.10E-14	1.59E-09	1.13E-08
$Cu_2(OH)_2^{2+}$	8.04E-12	7.44E-10	5.15E-13	2.22E-17
$FeOH^+$	2.47E-11	3.09E-13	9.76E-18	5.47E-19
$Fe(OH)_2$ (aq)	1.24E-16	1.21E-15	3.93E-18	2.12E-18
$Fe(OH)_3^-$	2.50E-19	1.89E-15	6.54E-16	3.67E-15
$FeOH^{2+}$	1.12E-11	4.60E-16	1.48E-21	1.69E-24
$Fe(OH)_2^+$	2.76E-08	8.76E-10	2.81E-13	2.86E-15
$Fe(OH)_3$ (aq)	1.88E-10	4.63E-09	1.53E-10	1.50E-11
$Fe(OH)_4^-$	1.11E-13	2.13E-09	7.49E-09	7.63E-09
$Fe2(OH)_2^{4+}$	4.25E-21	7.16E-30	8.41E-41	0.00E+00
$Fe3(OH)_4^{5+}$	1.72E-27	9.25E-38	0.00E+00	0.00E+00
$Cr(OH)^{2+}$	2.47E-07	1.12E-09	4.28E-15	4.20E-18
$Cr(OH)_3$ (aq)	4.52E-10	1.23E-06	4.84E-08	4.07E-09
$Cr(OH)_4^-$	1.15E-13	2.43E-07	1.01E-06	8.86E-07
CrO_2^-	1.36E-13	2.87E-07	1.20E-06	1.05E-06
SeO_3^{2-}	3.48E-09	6.19E-07	5.40E-07	9.74E-08
H_2SeO_3 (aq)	9.28E-10	2.74E-13	2.04E-17	3.15E-20
$FeHSeO_3^{2+}$	9.92E-18	1.20E-25	2.87E-35	5.08E-41
$HSeO_4^-$	1.22E-18	1.80E-18	1.47E-18	7.75E-22
AsO_3^{3-}	4.50E-33	8.17E-30	7.82E-30	1.07E-27
$HAsO_3^{2-}$	1.83E-25	4.28E-25	3.60E-27	4.07E-26
$H_2AsO_3^-$	3.16E-19	9.50E-22	7.27E-26	7.32E-26
$H_4AsO_3^+$	7.66E-22	3.83E-30	2.67E-38	2.69E-40
AsO_4^{3-}	2.25E-15	2.65E-11	2.60E-09	1.18E-08
$HAsO_4^{2-}$	1.12E-09	1.69E-08	1.46E-08	5.44E-09
$H_2AsO_4^-$	1.60E-08	3.12E-10	2.45E-12	8.14E-14

200

Table G-18. Speciation of As, Cr, Cu, Fe and Se calculated using MINTEQA2:
Columbia-sand.

Species in Solution	Concentration (mol/L)			
	CS-1	CS-2	CS-3	CS-4
	pH 5.76, Eh 259	pH 6.27, Eh 223	pH 9.30, Eh 211	pH 12.08, Eh 92
H^+	1.75E-06	5.39E-07	5.03E-10	9.07E-13
H_3AsO_4	4.70E-12	1.31E-12	6.66E-18	1.95E-24
H_3AsO_3	1.97E-13	8.63E-14	9.71E-25	8.28E-33
$Cr(OH)_2^+$	1.75E-09	2.96E-09	1.80E-07	3.84E-17
CrO_4^{2-}	3.71E-29	1.07E-27	2.43E-08	2.92E-07
Cu^+	4.95E-08	5.21E-08	7.87E-11	6.25E-16
Cu^{2+}	2.47E-06	6.33E-07	6.01E-10	5.93E-17
Fe^{2+}	1.61E-05	2.50E-06	3.54E-15	7.33E-23
Fe^{3+}	3.70E-14	1.39E-15	1.24E-24	3.76E-34
$HSeO_3^-$	8.59E-07	9.75E-07	1.25E-07	5.16E-12
SeO_4^{2-}	4.70E-17	1.08E-16	6.75E-09	7.35E-09
$HCrO_4^-$	2.04E-28	1.85E-27	3.89E-11	6.07E-13
$H_2CrO_4 (aq)$	2.86E-34	8.01E-34	1.57E-20	3.75E-25
$Cr_2O_7^{2-}$	0.00E+00	0.00E+00	5.30E-20	1.52E-23
$FeAsO_4$	4.93E-10	1.81E-10	1.00E-15	9.31E-24
$FeHAsO_4^+$	9.68E-17	1.10E-17	5.65E-26	9.48E-37
$FeH_2AsO_4^{2+}$	6.10E-18	2.11E-19	1.02E-30	3.64E-44
$CuSeO_3$	4.47E-15	4.30E-15	5.58E-16	9.07E-25
$FeSeO_3^+$	9.65E-12	1.38E-12	1.68E-19	6.04E-31
Cr^{3+}	2.07E-11	3.25E-12	1.73E-16	1.96E-31
OH^-	5.84E-09	1.88E-08	2.02E-05	1.32E-02
$CuOH^+$	4.42E-08	3.72E-08	3.77E-08	1.75E-12
$Cu(OH)_2 (aq)$	5.08E-11	1.39E-10	1.50E-07	3.88E-09
$Cu(OH)_3^-$	6.08E-16	5.35E-15	6.22E-09	1.05E-07
$Cu(OH)_4^{2-}$	2.83E-23	7.96E-22	9.97E-13	1.30E-08
$Cu_2(OH)_2^{2+}$	8.56E-11	5.99E-11	6.17E-11	1.58E-19
$FeOH^+$	3.63E-09	1.85E-09	2.80E-15	2.73E-20
$Fe(OH)_2 (aq)$	1.66E-14	2.74E-14	4.45E-17	2.41E-19
$Fe(OH)_3^-$	3.06E-17	1.63E-16	2.84E-16	1.01E-15
$FeOH^{2+}$	1.34E-10	1.65E-11	1.58E-17	1.91E-24
$Fe(OH)_2^+$	2.95E-07	1.19E-07	1.22E-10	6.95E-15
$Fe(OH)_3 (aq)$	1.82E-09	2.40E-09	2.61E-09	8.28E-11
$Fe(OH)_4^-$	9.89E-13	4.20E-12	4.91E-09	1.02E-07
$Fe2(OH)_2^{4+}$	6.26E-19	9.28E-21	8.51E-33	0.00E+00
$Fe3(OH)_4^{5+}$	2.83E-24	1.64E-26	1.55E-41	0.00E+00
$Cr(OH)^{2+}$	2.53E-09	1.31E-09	7.46E-11	3.37E-23
$Cr(OH)_3 (aq)$	3.77E-12	2.08E-11	1.35E-06	1.60E-13
$Cr(OH)_4^-$	8.76E-16	1.56E-14	1.09E-06	8.41E-11
CrO_2^-	1.04E-15	1.85E-14	1.29E-06	9.96E-11
SeO_3^{2-}	2.01E-09	7.29E-09	1.01E-06	3.19E-08
$H_2SeO_3 (aq)$	6.32E-10	2.23E-10	2.67E-14	1.68E-21
$FeHSeO_3^{2+}$	8.05E-17	3.51E-18	4.00E-28	3.06E-42
$HSeO_4^-$	4.00E-21	2.89E-21	1.67E-16	2.37E-19
AsO_3^{3-}	7.23E-31	1.03E-29	1.45E-31	5.64E-31
$HAsO_3^{2-}$	3.14E-23	1.42E-22	1.84E-27	7.91E-30
$H_2AsO_3^-$	5.86E-17	8.27E-17	9.98E-25	5.57E-30
$H_4AsO_3^+$	1.71E-19	2.30E-20	2.42E-34	4.20E-45
AsO_4^{3-}	1.91E-15	1.74E-14	1.10E-10	1.47E-08
$HAsO_4^{2-}$	1.01E-09	2.91E-09	1.70E-08	2.51E-09
$H_2AsO_4^-$	1.57E-08	1.41E-08	7.68E-11	1.47E-14

APPENDIX H

SATURATION INDICES FOR ALL MINERALS CALCULATED USING MINTEQA2

Table H-1. Saturation indices for all minerals calculated using MINTEQA2: Dewey

Solid/Mineral	Saturation Index				Solid/Mineral	Saturation Index			
	D-1	D-2	D-3	D-4		D-1	D-2	D-3	D-4
	pH 5.81	pH 7.95	pH 10.25	pH 12.25		pH 5.81	pH 7.95	pH 10.25	pH 12.25
CaNaAsO$_4$.7.5H$_2$O	-13.732	-6.867	-4.903	-11.611	AZURITE	-12.139	-4.918	-2.610	-9.035
Ca$_5$(AsO$_4$)$_3$OH	-38.749	-16.549	-9.674	-27.249	ARTINITE	-12.832	-4.825	-3.689	-8.311
Ca$_4$(OH)$_2$(AsO$_4$)$_2$:4H$_2$O	-37.801	-20.34	-13.453	-26.06	HYDROMAGNESITE	-31.771	-11.752	-8.913	-20.467
Mg$_3$(AsO4)$_2$	-24.315	-10.815	-16.047	-30.212	MAGNESITE	-4.974	-0.970	-0.402	-2.713
FeAsO$_4$	-12.655	-10.344	-13.009	-19.126	NESQUEHONITE	-7.772	-3.769	-3.201	-5.512
Cd$_3$(AsO$_4$)$_2$	-28.088	-19.838	-16.319	-28.292	ARAGONITE	-4.372	-0.379	3.077	1.745
Cu$_3$(AsO$_4$)$_2$	-23.163	-14.453	-19.081	-32.739	CALCITE	-4.233	-0.240	3.216	1.884
Al$_2$(SeO$_3$)$_3$	-10.222	-17.914	-28.725	-47.572	DOLOMITE (ordered)	-8.052	-0.055	3.969	0.326
CaSeO$_3$	-4.230	-2.868	-2.943	-9.117	DOLOMITE (disordered)	-8.602	-0.605	3.419	-0.224
CaSeO$_3$:H$_2$O	-5.043	-3.681	-3.756	-9.930	HUNTITE	-20.042	-4.037	1.123	-7.142
CdSeO$_3$	-8.090	-8.468	-8.514	-14.935	STRONTIANITE	-5.036	-1.060	2.883	2.382
CuSeO$_3$	-7.649	-7.873	-10.635	-17.618	WITHERITE	-8.001	-4.022	0.079	-0.068
Fe$_2$(SeO$_3$)$_3$	-14.064	-18.823	-27.811	-47.336	THERMONATRITE	-12.704	-8.445	-4.492	-8.010
Fe$_2$(SeO$_3$)$_3$.6H$_2$O	-41.760	-46.520	-55.510	-75.034	AlOHSO$_4$	-0.463	-4.381	-8.845	-14.850
MgSeO$_3$	-4.046	-2.673	-5.637	-12.789	Al$_4$(OH)$_{10}$SO$_4$	3.245	-0.373	-5.162	-17.653
Na$_2$SeO$_3$	-7.727	-6.098	-5.676	-14.036	Zn$_2$(OH)$_2$SO$_4$	-8.549	-8.819	-9.039	-15.023
ZnSeO$_3$	-4.295	-5.052	-6.516	-12.427	Zn$_4$(OH)$_6$SO$_4$	-16.927	-13.448	-9.533	-17.658
ZnSeO$_3$.H$_2$O	-6.858	-7.615	-9.079	-14.990	Zn$_3$O(SO$_4$)$_2$	-27.271	-29.684	-32.192	-43.090
SeO$_2$	-12.544	-15.175	-18.707	-23.548	ZINCOSITE	-11.240	-13.384	-15.672	-20.586
Al(OH)$_3$ (am)	-0.921	-0.821	-0.929	-3.091	ZnSO$_4$.H$_2$O	-6.675	-8.820	-11.108	-16.021
BOEHMITE	1.304	1.404	1.296	-0.866	BIANCHITE	-5.562	-7.708	-9.996	-14.910
DIASPORE	3.009	3.109	3.001	0.839	GOSLARITE	-5.319	-7.464	-9.753	-14.667
GIBBSITE	1.588	1.688	1.580	-0.582	Cd$_3$(OH)$_4$SO$_4$	-24.473	-21.731	-15.631	-24.215
Zn(OH)$_2$ (am)	-6.213	-4.338	-2.271	-3.341	Cd$_3$OH$_2$(SO$_4$)$_2$	-22.195	-23.471	-21.727	-34.154
Zn(OH)$_2$	-5.939	-4.064	-1.997	-3.067	Cd$_4$(OH)$_6$SO$_4$	-26.427	-21.431	-11.846	-22.010
Zn(OH)$_2$ (beta)	-5.493	-3.618	-1.551	-2.621	CdSO$_4$	-9.514	-11.278	-12.149	-17.572
Zn(OH)$_2$ (gamma)	-5.473	-3.598	-1.531	-2.601	CdSO$_4$.H$_2$O	-7.962	-9.727	-10.598	-16.021
Zn(OH)$_2$ (epsilon)	-5.273	-3.398	-1.331	-2.401	CdSO$_4$.2.67H$_2$O	-7.820	-9.585	-10.456	-15.880
ZnO (active)	-4.924	-3.050	-0.982	-2.052	ANTLERITE	-8.116	-4.914	-6.961	-17.230
ZINCITE	-5.070	-3.195	-1.128	-2.198	BROCHANTITE	-9.802	-4.193	-5.471	-17.882
Cd(OH)$_2$ (am)	-9.844	-7.590	-4.105	-5.685	LANGITE	-12.071	-6.463	-7.741	-20.151
Cd(OH)$_2$	-9.758	-7.504	-4.019	-5.599	CuOCuSO$_4$	-14.377	-13.581	-16.397	-24.525
MONTEPONITE	-11.214	-8.961	-5.475	-7.055	CuSO$_4$	-11.764	-13.375	-16.961	-22.946
Cu(OH)$_2$	-3.926	-1.519	-0.750	-2.892	CHALCANTHITE	-6.198	-7.810	-11.397	-17.382
TENORITE	-2.893	-0.486	0.283	-1.859	Fe$_2$(SO$_4$)$_3$	-30.176	-39.097	-50.558	-67.089
FERRIHYDRITE	0.212	1.779	2.582	0.081	H-JAROSITE	-4.840	-8.177	-14.480	-29.668
GOETHITE	2.915	4.482	5.285	2.784	Na-JAROSITE	-0.945	-2.151	-6.477	-23.425
Cr(OH)$_3$ (am)	-2.020	0.454	1.777	-0.059	EPSOMITE	-2.254	-2.271	-6.059	-12.213
Cr(OH)$_3$	-4.106	-1.632	-0.309	-2.145	ANHYDRITE	-0.275	-0.301	-1.200	-6.376
BRUCITE	-7.633	-3.630	-3.062	-5.373	GYPSUM	-0.031	-0.057	-0.956	-6.132
PERICLASE	-12.371	-8.367	-7.799	-10.110	CELESTITE	0.387	0.344	-0.069	-4.413
Mg(OH)$_2$ (active)	-9.583	-5.580	-5.012	-7.323	BARITE	1.482	1.442	1.187	-2.803
LIME	-23.760	-19.767	-16.310	-17.643	MIRABILITE	-2.905	-2.667	-3.071	-10.432
PORTLANDITE	-13.867	-9.874	-6.418	-7.751	THENARDITE	-4.314	-4.073	-4.475	-11.837
Ba(OH)$_2$.8H$_2$O	-19.342	-15.366	-11.266	-11.412	CuSeO$_3$.2H$_2$O	-8.186	-8.410	-11.172	-18.155
As$_2$O$_5$	-38.351	-36.862	-43.799	-51.032	Fe$_2$(SeO$_3$)$_3$.2H$_2$O	-9.823	-14.582	-23.571	-43.096
Al$_2$O$_3$	0.114	0.315	0.099	-4.225	Fe$_2$(OH)$_4$SeO$_3$	-7.164	-6.662	-8.587	-18.430
HEMATITE	8.233	11.367	12.973	7.971	MgSeO$_3$.6H$_2$O	-6.278	-4.906	-7.871	-15.022
MAGHEMITE	0.429	3.563	5.169	0.167	CaSeO$_3$.2H$_2$O	-6.299	-4.938	-5.013	-11.187
LEPIDOCROCITE	2.035	3.602	4.405	1.904	SrSeO$_3$	-7.378	-6.033	-5.622	-10.964
Cr$_2$O$_3$	-3.174	1.774	4.420	0.748	BaSeO$_3$	-9.173	-7.825	-7.256	-12.243
SPINEL	-7.867	-3.663	-3.311	-9.946	Na$_2$SeO$_3$.5H$_2$O	-13.151	-11.523	-11.102	-19.462
MAGNESIOFERRITE	-0.832	6.306	8.480	1.168	Zn$_3$(PO$_4$)$_2$.4H$_2$O	-8.119	-10.063	-12.224	-22.953
NATRON	-10.781	-6.524	-2.572	-6.090	Cd$_3$(PO$_4$)$_2$	-18.053	-18.858	-16.766	-29.025
CUPRIC FERRITE	5.577	11.118	13.494	6.351	Cu$_3$(PO$_4$)$_2$	-11.219	-11.563	-17.618	-31.562
MgCr$_2$O$_4$	-12.519	-3.567	-0.353	-6.336	Cu$_3$(PO$_4$)$_2$.3H$_2$O	-12.957	-13.302	-19.358	-33.301
ZnCl2	-14.388	-16.774	-19.233	-24.391	STRENGITE	-1.358	-3.575	-6.954	-13.214
Zn$_2$(OH)$_3$Cl	-9.468	-7.849	-5.978	-10.162	Mg$_3$(PO$_4$)$_2$	-11.401	-6.955	-13.615	-28.065
Zn$_5$(OH)$_8$Cl$_2$	-20.792	-15.681	-9.870	-19.310	MgHPO$_4$.3H$_2$O	-3.782	-3.562	-7.176	-13.246
CdCl$_2$	-9.054	-11.061	-12.103	-17.771	HYDROXYLAPATITE	-4.453	4.165	8.900	-9.040
CdCl$_2$.H$_2$O	-8.022	-10.029	-11.071	-16.739	CaHPO$_4$.2H$_2$O	-3.233	-3.023	-3.749	-8.841
CdCl$_2$.2.5H$_2$O	-7.807	-9.814	-10.856	-16.524	CaHPO$_4$	-2.947	-2.737	-3.463	-8.555
CdOHCl	-6.451	-6.327	-5.106	-8.730	Ca$_3$(PO$_4$)$_2$ (beta)	-6.583	-2.169	-0.164	-11.680
MELANOTHALLITE	-15.109	-16.962	-20.719	-26.949	Ca$_4$H(PO$_4$)$_3$.3H$_2$O	-10.653	-6.030	-4.751	-21.358
ATACAMITE	-4.695	-2.011	-2.736	-9.063	SrHPO$_4$	-4.525	-4.333	-4.572	-8.832
Fe(OH)$_{2.7}$Cl$_{0.3}$	4.403	5.331	5.455	2.341	BaHPO$_4$	-6.310	-6.115	-6.196	-10.101
CrCl$_3$	-38.283	-42.200	-47.668	-55.635	AlAsO$_4$.2H$_2$O	-10.745	-9.900	-13.477	-19.255
HALITE	-3.612	-3.613	-3.900	-7.703	Zn$_3$(AsO$_4$)$_2$.2.5H$_2$O	-26.510	-19.398	-20.132	-30.575
SMITHSONITE	-5.383	-3.509	-1.441	-2.511	Cu$_3$(AsO$_4$)$_2$.2H$_2$O	-23.498	-14.789	-19.417	-33.075
ZnCO$_3$.H$_2$O	-5.126	-3.252	-1.184	-2.254	FeAsO$_4$.2H$_2$O	-12.821	-10.510	-13.175	-19.292
OTAVITE	-5.758	-3.504	-0.019	-1.599	Ca$_3$(AsO$_4$)$_2$.4H$_2$O	-27.138	-13.670	-10.239	-21.469
CuCO$_3$	-5.397	-2.990	-2.220	-4.362	Ba$_3$(AsO$_4$)$_2$	-7.506	5.920	11.285	3.614
MALACHITE	-6.843	-2.029	-0.490	-4.774					

Table H-2. Saturation indices for all minerals calculated using MINTEQA2: Dewey-Lawson

Solid/Mineral	Saturation Index				Solid/Mineral	Saturation Index			
	DL-1	DL-2	DL-3	DL-4		DL-1	DL-2	DL-3	DL-4
	pH 5.36	pH 7.89	pH 9.66	pH 12.57		pH 5.36	pH 7.89	pH 9.66	pH 12.57
CaNaAsO$_4$.7.5H$_2$O	-15.031	-7.306	-5.944	-14.338	AZURITE	-16.551	-4.128	-2.948	-0.349
Ca$_5$(AsO$_4$)$_3$OH	-39.513	-14.259	-9.449	-30.573	ARTINITE	-14.881	-5.992	-2.747	-5.705
Ca$_4$(OH)$_2$(AsO$_4$)$_2$:4H$_2$O	-38.566	-18.535	-13.386	-28.046	HYDROMAGNESITE	-36.905	-14.682	-6.570	-13.966
Mg$_3$(AsO4)$_2$	-26.584	-12.390	-14.027	-29.662	MAGNESITE	-6.003	-1.559	0.064	-1.416
FeAsO$_4$	-12.375	-9.850	-13.302	-21.293	NESQUEHONITE	-8.795	-4.350	-2.728	-4.207
Cd$_3$(AsO$_4$)$_2$	-29.677	-18.416	-20.063	-32.936	ARAGONITE	-4.771	0.022	2.935	2.069
Cu$_3$(AsO$_4$)$_2$	-26.758	-13.474	-18.799	-27.398	CALCITE	-4.632	0.161	3.074	2.208
Al$_2$(SeO$_3$)$_3$	-8.143	-18.964	-30.261	-50.336	DOLOMITE (ordered)	-9.480	-0.243	4.293	1.947
CaSeO$_3$	-3.907	-2.529	-2.918	-9.275	DOLOMITE (disordered)	-10.030	-0.793	3.743	1.397
CaSeO$_3$:H$_2$O	-4.718	-3.339	-3.729	-10.085	HUNTITE	-23.528	-5.402	2.378	-2.926
CdSeO$_3$	-8.171	-8.119	-9.803	-15.851	STRONTIANITE	-6.052	-1.225	1.845	1.601
CuSeO$_3$	-8.399	-7.672	-10.581	-15.205	WITHERITE	-9.003	-3.911	-0.355	-0.278
Fe$_2$(SeO$_3$)$_3$	-12.156	-18.211	-28.519	-49.772	THERMONATRITE	-15.352	-10.351	-6.949	-10.808
Fe$_2$(SeO$_3$)$_3$.6H$_2$O	-39.840	-45.894	-56.202	-77.454	AlOHSO$_4$	-0.023	-5.183	-9.368	-17.009
MgSeO$_3$	-4.354	-3.323	-5.004	-11.973	Al$_4$(OH)$_{10}$SO$_4$	3.564	-2.462	-8.730	-21.779
Na$_2$SeO$_3$	-9.655	-8.068	-7.969	-17.317	Zn$_2$(OH)$_2$SO$_4$	-9.623	-8.171	-8.534	-18.054
ZnSeO$_3$	-4.353	-4.605	-6.344	-13.675	Zn$_4$(OH)$_6$SO$_4$	-19.553	-11.778	-9.015	-22.215
ZnSeO$_3$.H$_2$O	-6.913	-7.166	-8.905	-16.235	Zn$_3$O(SO$_4$)$_2$	-28.643	-28.901	-31.192	-48.390
SeO$_2$	-11.822	-15.237	-18.539	-24.029	ZINCOSITE	-11.537	-13.247	-15.174	-22.853
Al(OH)$_3$ (am)	-0.961	-1.250	-1.944	-3.747	ZnSO$_4$.H$_2$O	-6.970	-8.680	-10.607	-18.285
BOEHMITE	1.262	0.973	0.279	-1.524	BIANCHITE	-5.846	-7.555	-9.482	-17.160
DIASPORE	2.967	2.678	1.984	0.181	GOSLARITE	-5.601	-7.310	-9.236	-16.914
GIBBSITE	1.548	1.259	0.565	-1.238	Cd$_3$(OH)$_4$SO$_4$	-26.394	-20.866	-19.499	-27.012
Zn(OH)$_2$ (am)	-6.989	-3.828	-2.264	-4.105	Cd$_3$OH$_2$(SO$_4$)$_2$	-23.637	-22.979	-25.103	-38.455
Zn(OH)$_2$	-6.715	-3.554	-1.990	-3.831	Cd$_4$(OH)$_6$SO$_4$	-29.149	-20.153	-17.167	-25.239
Zn(OH)$_2$ (beta)	-6.269	-3.108	-1.544	-3.385	CdSO$_4$	-9.834	-11.239	-13.110	-19.507
Zn(OH)$_2$ (gamma)	-6.249	-3.088	-1.524	-3.365	CdSO$_4$.H$_2$O	-8.281	-9.685	-11.557	-17.953
Zn(OH)$_2$ (epsilon)	-6.049	-2.888	-1.324	-3.165	CdSO$_4$.2.67H$_2$O	-8.135	-9.539	-11.411	-17.807
ZnO (active)	-5.703	-2.541	-0.978	-2.819	ANTLERITE	-12.044	-4.492	-6.803	-10.042
ZINCITE	-5.849	-2.687	-1.124	-2.964	BROCHANTITE	-15.199	-3.506	-5.424	-7.796
Cd(OH)$_2$ (am)	-10.644	-7.177	-5.558	-6.117	LANGITE	-17.467	-5.773	-7.691	-10.063
Cd(OH)$_2$	-10.558	-7.091	-5.472	-6.031	CuOCuSO$_4$	-16.837	-13.426	-16.131	-20.236
MONTEPONITE	-12.017	-8.550	-6.931	-7.490	CuSO$_4$	-12.753	-13.483	-16.580	-21.552
Cu(OH)$_2$	-5.395	-1.254	-0.861	0.006	CHALCANTHITE	-7.177	-7.906	-11.003	-15.974
TENORITE	-4.365	-0.224	0.170	1.036	Fe$_2$(SO$_4$)$_3$	-28.987	-39.413	-50.284	-72.582
FERRIHYDRITE	0.087	2.181	1.981	-0.411	H-JAROSITE	-4.253	-7.712	-15.294	-34.144
GOETHITE	2.787	4.881	4.681	2.290	Na-JAROSITE	-1.685	-2.645	-8.525	-29.305
Cr(OH)$_3$ (am)	-3.449	0.069	0.015	-2.825	EPSOMITE	-2.786	-3.212	-5.080	-12.397
Cr(OH)$_3$	-5.534	-2.017	-2.070	-4.910	ANHYDRITE	-0.192	-0.271	-0.848	-7.553
BRUCITE	-8.660	-4.216	-2.593	-4.073	GYPSUM	0.057	-0.022	-0.599	-7.303
PERICLASE	-13.400	-8.955	-7.333	-8.812	CELESTITE	-0.148	-0.192	-0.613	-6.694
Mg(OH)$_2$ (active)	-10.610	-6.166	-4.543	-6.023	BARITE	0.961	1.183	1.248	-4.513
LIME	-24.159	-19.366	-16.453	-17.319	MIRABILITE	-5.052	-4.921	-5.010	-14.705
PORTLANDITE	-14.264	-9.471	-6.558	-7.424	THENARDITE	-6.481	-6.352	-6.441	-16.137
Ba(OH)$_2$.8H$_2$O	-20.326	-15.232	-11.676	-11.597	CuSeO$_3$.2H$_2$O	-8.931	-8.204	-11.114	-15.737
As$_2$O$_5$	-37.533	-36.672	-43.176	-54.373	Fe$_2$(SeO$_3$)$_3$.2H$_2$O	-7.911	-13.966	-24.274	-45.526
Al$_2$O$_3$	0.028	-0.550	-1.939	-5.545	Fe$_2$(OH)$_4$SeO$_3$	-6.696	-5.922	-9.625	-19.897
HEMATITE	7.975	12.163	11.763	6.980	MgSeO$_3$.6H$_2$O	-6.573	-5.542	-7.222	-14.190
MAGHEMITE	0.171	4.359	3.959	-0.824	CaSeO$_3$.2H$_2$O	-5.972	-4.594	-4.983	-11.339
LEPIDOCROCITE	1.907	4.001	3.801	1.410	SrSeO$_3$	-7.673	-6.260	-6.493	-12.226
Cr$_2$O$_3$	-6.038	0.997	0.890	-4.791	BaSeO$_3$	-9.454	-7.775	-7.522	-12.935
SPINEL	-8.983	-5.117	-4.883	-9.968	Na$_2$SeO$_3$.5H$_2$O	-15.068	-13.481	-13.381	-22.729
MAGNESIOFERRITE	-2.118	6.514	7.736	1.474	Zn$_3$(PO$_4$)$_2$.4H$_2$O	-9.171	-7.064	-9.539	-25.947
NATRON	-13.410	-8.407	-5.005	-8.863	Cd$_3$(PO$_4$)$_2$	-19.185	-16.163	-18.471	-31.033
CUPRIC FERRITE	3.848	12.178	12.170	8.254	Cu$_3$(PO$_4$)$_2$	-14.356	-9.311	-15.297	-23.585
MgCr$_2$O$_4$	-16.412	-4.933	-3.418	-10.578	Cu$_3$(PO$_4$)$_2$.3H$_2$O	-16.088	-11.043	-17.028	-25.316
ZnCl2	-16.051	-17.998	-20.032	-27.958	STRENGITE	-0.845	-2.440	-6.222	-14.057
Zn$_2$(OH)$_3$Cl	-11.464	-7.695	-6.367	-13.091	Mg$_3$(PO$_4$)$_2$	-13.211	-7.257	-9.555	-24.879
Zn$_5$(OH)$_8$Cl$_2$	-25.562	-14.862	-10.643	-25.930	MgHPO$_4$.3H$_2$O	-4.165	-3.409	-5.369	-12.292
CdCl$_2$	-10.741	-12.383	-14.362	-21.005	HYDROXYLAPATITE	-4.530	8.365	12.184	-8.479
CdCl$_2$.H$_2$O	-9.707	-11.349	-13.328	-19.971	CaHPO$_4$.2H$_2$O	-2.988	-1.884	-2.553	-8.863
CdCl$_2$.2.5H$_2$O	-9.488	-11.130	-13.108	-19.752	CaHPO$_4$	-2.707	-1.603	-2.273	-8.582
CdOHCl	-7.694	-6.782	-6.962	-10.562	Ca$_3$(PO$_4$)$_2$ (beta)	-6.502	0.497	2.072	-11.414
MELANOTHALLITE	-17.464	-18.432	-21.636	-26.855	Ca$_4$H(PO$_4$)$_3$.3H$_2$O	-10.325	-2.223	-1.317	-21.113
ATACAMITE	-8.076	-2.348	-3.361	-4.670	SrHPO$_4$	-4.902	-3.764	-4.277	-9.964
Fe(OH)$_{2.7}$Cl$_{0.3}$	4.145	5.473	4.733	1.429	BaHPO$_4$	-6.674	-5.270	-5.297	-10.663
CrCl$_3$	-41.041	-45.187	-50.637	-62.605	AlAsO$_4$.2H$_2$O	-10.374	-10.233	-14.179	-21.580
HALITE	-5.379	-5.433	-5.531	-10.503	Zn$_3$(AsO$_4$)$_2$.2.5H$_2$O	-28.022	-17.676	-19.490	-36.209
SMITHSONITE	-6.162	-3.000	-1.437	-3.278	Cu$_3$(AsO$_4$)$_2$.2H$_2$O	-27.090	-13.805	-19.130	-27.728
ZnCO$_3$.H$_2$O	-5.903	-2.741	-1.177	-3.018	FeAsO$_4$.2H$_2$O	-12.536	-10.011	-13.463	-21.453
OTAVITE	-6.561	-3.094	-1.475	-2.034	Ca$_3$(AsO$_4$)$_2$.4H$_2$O	-27.507	-12.268	-10.032	-23.829
CuCO$_3$	-6.868	-2.727	-2.334	-1.467	Ba$_3$(AsO$_4$)$_2$	-9.695	6.444	10.608	-0.358
MALACHITE	-9.783	-1.501	-0.715	1.018					

Table H-3. Saturation indices for all minerals calculated using MINTEQA2: Dewey-Kamm

Solid/Mineral	Saturation Index				Solid/Mineral	Saturation Index			
	DK-1	DK-2	DK-3	DK-4		DK-1	DK-2	DK-3	DK-4
	pH 6.01	pH 8.47	pH 9.55	pH 12.61		pH 6.01	pH 8.47	pH 9.55	pH 12.61
CaNaAsO$_4$.7.5H$_2$O	-14.449	-7.223	-6.003	-14.698	AZURITE	-12.961	-4.858	-5.831	-4.243
Ca$_5$(AsO$_4$)$_3$OH	-37.215	-13.438	-9.444	-32.009	ARTINITE	-12.554	-4.179	-4.004	-5.765
Ca$_4$(OH)$_2$(AsO$_4$)$_2$:4H$_2$O	-36.23	-17.225	-13.415	-29.175	HYDROMAGNESITE	-31.087	-10.149	-9.713	-14.116
Mg$_3$(AsO4)$_2$	-25.580	-12.935	-15.745	-29.839	MAGNESITE	-4.839	-0.652	-0.565	-1.446
FeAsO$_4$	-12.901	-11.247	-13.603	-21.687	NESQUEHONITE	-7.631	-3.443	-3.356	-4.236
Cd$_3$(AsO$_4$)$_2$	-29.112	-19.660	-19.565	-33.195	ARAGONITE	-3.565	1.166	2.886	1.810
Cu$_3$(AsO$_4$)$_2$	-25.655	-17.470	-21.515	-31.379	CALCITE	-3.426	1.305	3.025	1.949
Al$_2$(SeO$_3$)$_3$	-9.245	-22.354	-29.024	-53.998	DOLOMITE (ordered)	-7.110	1.808	3.615	1.658
CaSeO$_3$	-3.642	-2.490	-2.845	-10.739	DOLOMITE (disordered)	-7.660	1.258	3.065	1.108
CaSeO$_3$:H$_2$O	-4.452	-3.300	-3.656	-11.549	HUNTITE	-18.831	-1.538	0.444	-3.275
CdSeO$_3$	-8.095	-8.550	-9.570	-17.113	STRONTIANITE	-4.829	-0.042	1.772	1.693
CuSeO$_3$	-8.142	-9.020	-11.420	-17.708	WITHERITE	-7.872	-2.732	-0.427	0.094
Fe$_2$(SeO$_3$)$_3$	-13.543	-21.053	-28.922	-54.088	THERMONATRITE	-14.113	-9.207	-7.137	-10.924
Fe$_2$(SeO$_3$)$_3$.6H$_2$O	-41.226	-48.736	-56.605	-81.770	AlOHSO$_4$	-0.388	-6.379	-8.712	-17.177
MgSeO$_3$	-4.131	-3.522	-5.510	-13.208	Al$_4$(OH)$_{10}$SO$_4$	5.780	-3.771	-6.767	-22.017
Na$_2$SeO$_3$	-9.356	-8.029	-8.035	-18.639	Zn$_2$(OH)$_2$SO$_4$	-10.529	-7.140	-8.095	-18.272
ZnSeO$_3$	-5.134	-4.616	-6.113	-14.916	Zn$_4$(OH)$_6$SO$_4$	-20.142	-8.559	-8.357	-22.506
ZnSeO$_3$.H$_2$O	-7.695	-7.176	-8.674	-17.477	Zn$_3$O(SO$_4$)$_2$	-30.616	-27.933	-30.422	-48.789
SeO$_2$	-12.763	-16.341	-18.417	-25.234	ZINCOSITE	-12.603	-13.310	-14.844	-23.034
Al(OH)$_3$ (am)	-0.101	-1.288	-1.508	-3.770	ZnSO$_4$.H$_2$O	-8.036	-8.743	-10.277	-18.467
BOEHMITE	2.122	0.935	0.714	-1.548	BIANCHITE	-6.912	-7.618	-9.152	-17.341
DIASPORE	3.827	2.640	2.419	0.157	GOSLARITE	-6.666	-7.373	-8.906	-17.095
GIBBSITE	2.408	1.221	1.001	-1.261	Cd$_3$(OH)$_4$SO$_4$	-24.567	-20.001	-18.947	-27.329
Zn(OH)$_2$ (am)	-6.830	-2.733	-2.155	-4.141	Cd$_3$OH$_2$(SO$_4$)$_2$	-23.034	-23.272	-24.331	-38.917
Zn(OH)$_2$	-6.556	-2.459	-1.881	-3.867	Cd$_4$(OH)$_6$SO$_4$	-26.304	-18.614	-16.505	-25.613
Zn(OH)$_2$ (beta)	-6.110	-2.013	-1.435	-3.421	CdSO$_4$	-10.042	-11.722	-12.779	-19.709
Zn(OH)$_2$ (gamma)	-6.090	-1.993	-1.415	-3.401	CdSO$_4$.H$_2$O	-8.488	-10.169	-11.226	-18.156
Zn(OH)$_2$ (epsilon)	-5.890	-1.793	-1.215	-3.201	CdSO$_4$.2.67H$_2$O	-8.342	-10.023	-11.080	-18.009
ZnO (active)	-5.544	-1.447	-0.869	-2.855	ANTLERITE	-9.678	-6.379	-9.465	-14.081
ZINCITE	-5.690	-1.593	-1.014	-3.001	BROCHANTITE	-11.637	-5.637	-9.046	-13.133
Cd(OH)$_2$ (am)	-9.627	-6.503	-5.448	-6.174	LANGITE	-13.904	-7.904	-11.313	-15.400
Cd(OH)$_2$	-9.541	-6.417	-5.362	-6.088	CuOCuSO$_4$	-15.669	-15.071	-17.832	-22.977
MONTEPONITE	-11.000	-7.876	-6.821	-7.547	CuSO$_4$	-12.781	-14.884	-17.321	-22.995
Cu(OH)$_2$	-4.198	-1.497	-1.822	-1.292	CHALCANTHITE	-7.204	-9.307	-11.743	-17.417
TENORITE	-3.168	-0.467	-0.791	-0.262	Fe$_2$(SO$_4$)$_3$	-31.226	-42.412	-50.390	-73.718
FERRIHYDRITE	0.804	2.417	1.597	-0.761	H-JAROSITE	-4.549	-9.318	-16.005	-35.486
GOETHITE	3.505	5.118	4.297	1.939	Na-JAROSITE	-1.362	-3.678	-9.330	-30.705
Cr(OH)$_3$ (am)	-2.238	0.420	0.106	-2.536	EPSOMITE	-2.847	-3.463	-5.488	-12.572
Cr(OH)$_3$	-4.324	-1.665	-1.979	-4.621	ANHYDRITE	-0.211	-0.284	-0.676	-7.957
BRUCITE	-7.497	-3.309	-3.222	-4.103	GYPSUM	0.038	-0.035	-0.427	-7.707
PERICLASE	-12.236	-8.049	-7.962	-8.842	CELESTITE	-0.149	-0.166	-0.464	-6.747
Mg(OH)$_2$ (active)	-9.447	-5.259	-5.172	-6.053	BARITE	0.868	1.204	1.397	-4.287
LIME	-22.953	-18.222	-16.502	-17.578	MIRABILITE	-5.037	-4.934	-4.977	-14.966
PORTLANDITE	-13.058	-8.327	-6.607	-7.683	THENARDITE	-6.467	-6.365	-6.408	-16.399
Ba(OH)$_2$.8H$_2$O	-19.194	-14.053	-11.748	-11.226	CuSeO$_3$.2H$_2$O	-8.675	-9.552	-11.953	-18.240
As$_2$O$_5$	-40.020	-39.938	-43.009	-54.460	Fe$_2$(SeO$_3$)$_3$.2H$_2$O	-9.298	-16.807	-24.677	-49.842
Al$_2$O$_3$	1.748	-0.626	-1.068	-5.592	Fe$_2$(OH)$_4$SeO$_3$	-6.201	-6.554	-10.271	-21.803
HEMATITE	9.410	12.636	10.995	6.279	MgSeO$_3$.6H$_2$O	-6.349	-5.740	-7.728	-15.425
MAGHEMITE	1.606	4.832	3.191	-1.525	CaSeO$_3$.2H$_2$O	-5.707	-4.554	-4.910	-12.803
LEPIDOCROCITE	2.625	4.238	3.417	1.059	SrSeO$_3$	-7.390	-6.181	-6.443	-13.339
Cr$_2$O$_3$	-3.618	1.699	1.071	-4.213	BaSeO$_3$	-9.263	-7.702	-7.472	-13.769
SPINEL	-6.099	-4.286	-4.640	-10.045	Na$_2$SeO$_3$.5H$_2$O	-14.769	-13.441	-13.447	-24.051
MAGNESIOFERRITE	0.481	7.894	6.339	0.743	Zn$_3$(PO$_4$)$_2$.4H$_2$O	-10.407	-5.923	-9.747	-27.739
NATRON	-12.170	-7.263	-5.193	-8.979	Cd$_3$(PO$_4$)$_2$	-17.846	-16.283	-18.677	-32.888
CUPRIC FERRITE	6.480	12.407	10.441	6.254	Cu$_3$(PO$_4$)$_2$	-12.479	-12.184	-18.716	-29.162
MgCr$_2$O$_4$	-12.828	-3.324	-3.864	-10.030	Cu$_3$(PO$_4$)$_2$.3H$_2$O	-14.211	-13.915	-20.447	-30.892
ZnCl2	-17.249	-18.079	-19.699	-28.111	STRENGITE	-0.984	-3.274	-6.875	-15.249
Zn$_2$(OH)$_3$Cl	-11.825	-6.095	-6.037	-13.222	Mg$_3$(PO$_4$)$_2$	-11.434	-6.679	-11.977	-26.652
Zn$_5$(OH)$_8$Cl$_2$	-26.124	-10.566	-9.873	-26.229	MgHPO$_4$.3H$_2$O	-3.858	-3.574	-6.266	-13.163
CdCl$_2$	-11.081	-12.884	-14.028	-21.179	HYDROXYLAPATITE	-1.071	10.872	11.134	-12.298
CdCl$_2$.H$_2$O	-10.047	-11.850	-12.994	-20.145	CaHPO$_4$.2H$_2$O	-2.639	-1.811	-2.871	-9.963
CdCl$_2$.2.5H$_2$O	-9.828	-11.631	-12.775	-19.925	CaHPO$_4$	-2.358	-1.530	-2.590	-9.683
CdOHCl	-7.356	-6.695	-6.740	-10.678	Ca$_3$(PO$_4$)$_2$ (beta)	-4.598	1.787	1.388	-13.874
MELANOTHALLITE	-17.625	-19.850	-22.373	-28.269	Ca$_4$H(PO$_4$)$_3$.3H$_2$O	-8.072	-0.860	-2.318	-24.673
ATACAMITE	-6.361	-3.423	-5.171	-7.325	SrHPO$_4$	-4.536	-3.652	-4.618	-10.713
Fe(OH)$_{2.7}$Cl$_{0.3}$	4.659	5.533	4.382	1.061	BaHPO$_4$	-6.399	-5.162	-5.637	-11.133
CrCl$_3$	-41.868	-46.599	-50.211	-62.491	AlAsO$_4$.2H$_2$O	-10.758	-11.904	-13.660	-21.647
HALITE	-5.438	-5.449	-5.513	-10.619	Zn$_3$(AsO$_4$)$_2$.2.5H$_2$O	-30.032	-17.659	-18.995	-36.405
SMITHSONITE	-6.003	-1.906	-1.328	-3.314	Cu$_3$(AsO$_4$)$_2$.2H$_2$O	-25.987	-17.801	-21.845	-31.709
ZnCO$_3$.H$_2$O	-5.743	-1.647	-1.068	-3.054	FeAsO$_4$.2H$_2$O	-13.062	-11.408	-13.764	-21.847
OTAVITE	-5.544	-2.420	-1.365	-2.091	Ca$_3$(AsO$_4$)$_2$.4H$_2$O	-26.376	-12.101	-10.012	-24.692
CuCO$_3$	-5.671	-2.970	-3.295	-2.765	Ba$_3$(AsO$_4$)$_2$	-8.788	6.714	10.559	0.668
MALACHITE	-7.390	-1.988	-2.636	-1.578					

Table H-4. Saturation indices for all minerals calculated using MINTEQA2: Dewey-Red Wing.

Solid/Mineral	Saturation Index				Solid/Mineral	Saturation Index			
	DR-1	DR-2	DR-3	DR-4		DR-1	DR-2	DR-3	DR-4
	pH 5.81	pH 8.11	pH 10.55	pH 12.34		pH 5.81	pH 8.11	pH 10.55	pH 12.34
$CaNaAsO_4.7.5H_2O$	-14.051	-6.933		-13.968	AZURITE	-13.408	-7.758		-9.364
$Ca_5(AsO_4)_3OH$	-35.519	-12.743		-30.497	ARTINITE	-12.959	-5.578		-6.014
$Ca_4(OH)_2(AsO_4)_2:4H_2O$	-35.16	-17.242		-28.098	HYDROMAGNESITE	-32.100	-13.649		-14.738
$Mg_3(AsO4)_2$	-24.758	-12.166		-29.567	MAGNESITE	-5.042	-1.352		-1.570
$FeAsO_4$	-12.708	-10.334		-21.415	NESQUEHONITE	-7.834	-4.143		-4.361
$Cd_3(AsO_4)_2$	-27.957	-19.708		-32.550	ARAGONITE	-3.654	0.444		1.914
$Cu_3(AsO_4)_2$	-24.673	-17.501		-35.853	CALCITE	-3.516	0.583		2.053
$Al_2(SeO_3)_3$	-8.651	-20.551		-52.315	DOLOMITE (ordered)	-7.402	0.386		1.638
$CaSeO_3$	-3.310	-2.671		-10.088	DOLOMITE (disordered)	-7.952	-0.164		1.088
$CaSeO_3:H_2O$	-4.120	-3.481		-10.898	HUNTITE	-19.528	-4.360		-3.544
$CdSeO_3$	-7.764	-8.981		-16.567	STRONTIANITE	-5.014	-0.672		2.075
$CuSeO_3$	-7.870	-9.446		-18.868	WITHERITE	-8.067	-3.588		0.043
$Fe_2(SeO_3)_3$	-13.322	-20.474		-52.550	THERMONATRITE	-14.568	-10.052		-10.318
$Fe_2(SeO_3)_3.6H_2O$	-41.006	-48.157		-80.232	$AlOHSO_4$	-0.626	-5.575		-16.632
$MgSeO_3$	-3.911	-3.681		-12.786	$Al_4(OH)_{10}SO_4$	4.534	-2.696		-21.409
Na_2SeO_3	-9.389	-8.333		-17.486	$Zn_2(OH)_2SO_4$	-10.970	-10.481		-20.043
$ZnSeO_3$	-4.981	-6.102		-15.518	$Zn_4(OH)_6SO_4$	-21.120	-15.954		-26.573
$ZnSeO_3.H_2O$	-7.542	-8.663		-18.078	$Zn_3O(SO_4)_2$	-31.227	-32.589		-51.185
SeO_2	-12.341	-15.801		-24.687	ZINCOSITE	-12.774	-14.625		-23.658
$Al(OH)_3$ (am)	-0.437	-1.197		-3.749	$ZnSO_4.H_2O$	-8.207	-10.057		-19.091
BOEHMITE	1.786	1.026		-1.527	BIANCHITE	-7.084	-8.933		-17.965
DIASPORE	3.491	2.731		0.178	GOSLARITE	-6.838	-8.687		-17.719
GIBBSITE	2.072	1.312		-1.240	$Cd_3(OH)_4SO_4$	-24.744	-22.206		-26.805
$Zn(OH)_2$ (am)	-7.099	-4.760		-5.289	$Cd_3OH_2(SO_4)_2$	-23.114	-24.764		-37.869
$Zn(OH)_2$	-6.825	-4.486		-5.015	$Cd_4(OH)_6SO_4$	-26.573	-21.791		-25.089
$Zn(OH)_2$ (beta)	-6.379	-4.040		-4.569	$CdSO_4$	-10.036	-11.982		-19.185
$Zn(OH)_2$ (gamma)	-6.359	-4.020		-4.549	$CdSO_4.H_2O$	-8.482	-10.428		-17.632
$Zn(OH)_2$ (epsilon)	-6.159	-3.820		-4.349	$CdSO_4.2.67H_2O$	-8.337	-10.282		-17.485
ZnO (active)	-5.813	-3.474		-4.003	ANTLERITE	-10.028	-8.567		-18.667
ZINCITE	-5.958	-3.620		-4.149	BROCHANTITE	-12.136	-8.791		-19.436
$Cd(OH)_2$ (am)	-9.718	-7.476		-6.174	LANGITE	-14.403	-11.058		-21.703
$Cd(OH)_2$	-9.632	-7.390		-6.088	$CuOCuSO_4$	-15.869	-16.291		-25.867
MONTEPONITE	-11.091	-8.849		-7.547	$CuSO_4$	-12.833	-15.138		-24.178
$Cu(OH)_2$	-4.348	-2.464		-2.999	CHALCANTHITE	-7.257	-9.561		-18.600
TENORITE	-3.317	-1.434		-1.969	$Fe_2(SO_4)_3$	-31.978	-41.318		-72.248
FERRIHYDRITE	0.282	1.895		-0.812	H-JAROSITE	-5.921	-9.459		-34.591
GOETHITE	2.983	4.596		1.888	Na-JAROSITE	-2.962	-4.241		-29.507
$Cr(OH)_3$ (am)	-2.559	0.236		-1.631	EPSOMITE	-2.953	-3.450		-12.172
$Cr(OH)_3$	-4.645	-1.850		-3.716	ANHYDRITE	-0.203	-0.293		-7.328
BRUCITE	-7.699	-4.009		-4.227	GYPSUM	0.045	-0.044		-7.079
PERICLASE	-12.439	-8.749		-8.967	CELESTITE	-0.237	-0.083		-5.842
$Mg(OH)_2$ (active)	-9.649	-5.959		-6.177	BARITE	0.771	1.061		-3.813
LIME	-23.042	-18.944		-17.474	MIRABILITE	-5.395	-5.066		-13.836
PORTLANDITE	-13.148	-9.049		-7.579	THENARDITE	-6.824	-6.498		-15.269
$Ba(OH)_2.8H_2O$	-19.389	-14.909		-11.277	$CuSeO_3.2H_2O$	-8.403	-9.978		-19.400
As_2O_5	-38.590	-37.068		-53.815	$Fe_2(SeO_3)_3.2H_2O$	-9.077	-16.229		-48.304
Al_2O_3	1.076	-0.445		-5.549	$Fe_2(OH)_4SeO_3$	-6.824	-7.057		-21.359
HEMATITE	8.366	11.592		6.177	$MgSeO_3.6H_2O$	-6.131	-5.899		-15.003
MAGHEMITE	0.562	3.788		-1.627	$CaSeO_3.2H_2O$	-5.375	-4.735		-12.152
LEPIDOCROCITE	2.103	3.716		1.008	$SrSeO_3$	-7.154	-6.271		-12.411
Cr_2O_3	-4.259	1.330		-2.403	$BaSeO_3$	-9.036	-8.017		-13.273
SPINEL	-6.974	-4.804		-10.127	$Na_2SeO_3.5H_2O$	-14.803	-13.745		-22.898
MAGNESIOFERRITE	-0.766	6.150		0.516	$Zn_3(PO_4)_2.4H_2O$	-10.079	-11.764		-29.844
NATRON	-12.626	-8.108		-8.373	$Cd_3(PO_4)_2$	-16.986	-18.959		-31.550
CUPRIC FERRITE	5.287	10.396		4.446	$Cu_3(PO_4)_2$	-11.792	-14.843		-32.944
$MgCr_2O_4$	-13.672	-4.393		-8.344	$Cu_3(PO_4)_2.3H_2O$	-13.524	-16.574		-34.674
ZnCl2	-17.184	-19.512		-28.653	STRENGITE	-0.939	-3.676		-14.631
$Zn_2(OH)_3Cl$	-12.195	-9.852		-15.215	$Mg_3(PO_4)_2$	-10.907	-8.538		-25.687
$Zn_5(OH)_8Cl_2$	-27.134	-20.108		-31.363	$MgHPO_4.3H_2O$	-3.494	-4.153		-12.618
$CdCl_2$	-10.838	-13.263		-20.573	HYDROXYLAPATITE	0.182	7.625		-9.770
$CdCl_2.H_2O$	-9.805	-12.229		-19.539	$CaHPO_4.2H_2O$	-2.161	-2.412		-9.190
$CdCl_2.2.5H_2O$	-9.586	-12.010		-19.319	$CaHPO_4$	-1.880	-2.131		-8.909
CdOHCl	-7.280	-7.371		-10.375	$Ca_3(PO_4)_2$ (beta)	-3.733	-0.137		-12.223
MELANOTHALLITE	-17.440	-20.223		-29.370	$Ca_4H(PO_4)_3.3H_2O$	-6.730	-3.385		-22.249
ATACAMITE	-6.493	-5.059		-10.435	$SrHPO_4$	-4.154	-4.162		-9.663
$Fe(OH)_{2.7}Cl_{0.3}$	4.187	5.100		1.101	$BaHPO_4$	-6.026	-5.898		-10.514
$CrCl_3$	-41.687	-45.892		-60.677	$AlAsO_4.2H_2O$	-10.379	-10.378		-21.303
HALITE	-5.499	-5.574		-10.013	$Zn_3(AsO_4)_2.2.5H_2O$	-29.409	-20.872		-39.203
SMITHSONITE	-6.272	-3.933		-4.462	$Cu_3(AsO_4)_2.2H_2O$	-25.004	-17.832		-36.184
$ZnCO_3.H_2O$	-6.012	-3.674		-4.202	$FeAsO_4.2H_2O$	-12.869	-10.495		-21.576
OTAVITE	-5.635	-3.393		-2.091	$Ca_3(AsO_4)_2.4H_2O$	-25.216	-11.398		-23.734
$CuCO_3$	-5.820	-3.937		-4.472	$Ba_3(AsO_4)_2$	-7.942	7.016		1.162
MALACHITE	-7.688	-3.921		-4.991					

Table H-5. Saturation indices for all minerals calculated using MINTEQA2: Dewey-MnRoad.

Solid/Mineral	Saturation Index			
	DM-1	DM-2	DM-3	DM-4
	pH 6.02	pH 8.11	pH 10.63	pH 12.22
CaNaAsO4.7.5H2O	-13.527	-6.730		-13.365
Ca5(AsO4)3OH	-33.989	-12.13		-28.858
Ca4(OH)2(AsO4)2:4H2O	-33.948	-16.833		-26.933
Mg3(AsO4)2	-23.814	-11.508		-28.785
FeAsO4	-12.813	-10.358		-21.358
Cd3(AsO4)2	-27.853	-17.900		-31.709
Cu3(AsO4)2	-24.182	-17.091		-34.643
Al2(SeO3)3	-9.498	-20.503		-52.169
CaSeO3	-3.276	-2.588		-9.718
CaSeO3:H2O	-4.086	-3.398		-10.529
CdSeO3	-8.004	-8.432		-16.305
CuSeO3	-7.980	-9.362		-18.483
Fe2(SeO3)3	-14.355	-20.682		-52.490
Fe2(SeO3)3.6H2O	-42.039	-48.364		-80.172
MgSeO3	-3.871	-3.515		-12.543
Na2SeO3	-9.233	-8.255		-17.075
ZnSeO3	-5.054	-6.012		-15.172
ZnSeO3.H2O	-7.615	-8.573		-17.733
SeO2	-12.593	-15.719		-24.424
Al(OH)3 (am)	-0.481	-1.296		-4.071
BOEHMITE	1.741	0.926		-1.849
DIASPORE	3.446	2.631		-0.144
GIBBSITE	2.028	1.213		-1.562
Zn(OH)2 (am)	-6.920	-4.753		-5.208
Zn(OH)2	-6.646	-4.479		-4.934
Zn(OH)2 (beta)	-6.200	-4.033		-4.488
Zn(OH)2 (gamma)	-6.180	-4.013		-4.468
Zn(OH)2 (epsilon)	-5.980	-3.813		-4.268
ZnO (active)	-5.634	-3.467		-3.922
ZINCITE	-5.779	-3.612		-4.067
Cd(OH)2 (am)	-9.705	-7.009		-6.176
Cd(OH)2	-9.619	-6.923		-6.090
MONTEPONITE	-11.078	-8.382		-7.549
Cu(OH)2	-4.206	-2.463		-2.878
TENORITE	-3.175	-1.432		-1.848
FERRIHYDRITE	0.144	1.668		-1.178
GOETHITE	2.844	4.369		1.522
Cr(OH)3 (am)	-2.186	0.236		-1.679
Cr(OH)3	-4.271	-1.849		-3.765
BRUCITE	-7.407	-3.925		-4.249
PERICLASE	-12.146	-8.665		-8.989
Mg(OH)2 (active)	-9.357	-5.875		-6.199
LIME	-22.756	-18.943		-17.369
PORTLANDITE	-12.861	-9.048		-7.474
Ba(OH)2.8H2O	-18.915	-14.852		-11.166
As2O5	-38.524	-36.662		-52.968
Al2O3	0.986	-0.643		-6.194
HEMATITE	8.090	11.138		5.445
MAGHEMITE	0.286	3.334		-2.359
LEPIDOCROCITE	1.964	3.489		0.642
Cr2O3	-3.512	1.332		-2.500
SPINEL	-6.771	-4.920		-10.794
MAGNESIOFERRITE	-0.750	5.780		-0.238
NATRON	-12.216	-8.111		-8.225
CUPRIC FERRITE	5.152	9.944		3.835
MgCr2O4	-12.633	-4.308		-8.463
ZnCl2	-17.434	-19.509		-28.424
Zn2(OH)3Cl	-12.052	-9.839		-14.978
Zn5(OH)8Cl2	-26.668	-20.074		-30.809
CdCl2	-11.255	-12.801		-20.427
CdCl2.H2O	-10.221	-11.767		-19.393
CdCl2.2.5H2O	-10.002	-11.547		-19.174
CdOHCl	-7.482	-6.906		-10.303
MELANOTHALLITE	-17.727	-20.227		-29.101
ATACAMITE	-6.424	-5.059		-10.119
Fe(OH)2.7Cl0.3	3.984	4.872		0.757
CrCl3	-41.957	-45.899		-60.504
HALITE	-5.509	-5.578		-9.866
SMITHSONITE	-6.093	-3.926		-4.381
ZnCO3.H2O	-5.833	-3.666		-4.121
OTAVITE	-5.622	-2.925		-2.093
CuCO3	-5.679	-3.936		-4.351
MALACHITE	-7.404	-3.918		-4.749

Solid/Mineral	Saturation Index			
	DM-1	DM-2	DM-3	DM-4
	pH 6.02	pH 8.11	pH 10.63	pH 12.22
AZURITE	-12.983	-7.754		-9.000
ARTINITE	-12.374	-5.411		-6.057
HYDROMAGNESITE	-30.636	-13.230		-14.847
MAGNESITE	-4.749	-1.268		-1.592
NESQUEHONITE	-7.541	-4.060		-4.383
ARAGONITE	-3.368	0.445		2.019
CALCITE	-3.229	0.584		2.158
DOLOMITE (ordered)	-6.824	0.471		1.722
DOLOMITE (disordered)	-7.374	-0.079		1.172
HUNTITE	-18.364	-4.108		-3.504
STRONTIANITE	-4.670	-0.725		1.914
WITHERITE	-7.593	-3.531		0.154
THERMONATRITE	-14.159	-10.055		-10.170
AlOHSO4	-1.003	-5.698		-16.661
Al4(OH)10SO4	4.022	-3.116		-22.405
Zn2(OH)2SO4	-10.944	-10.489		-19.587
Zn4(OH)6SO4	-20.736	-15.946		-25.954
Zn3O(SO4)2	-31.355	-32.612		-50.353
ZINCOSITE	-12.928	-14.640		-23.283
ZnSO4.H2O	-8.360	-10.073		-18.715
BIANCHITE	-7.236	-8.948		-17.590
GOSLARITE	-6.991	-8.702		-17.344
Cd3(OH)4SO4	-25.038	-20.827		-26.518
Cd3OH2(SO4)2	-23.740	-23.409		-37.287
Cd4(OH)6SO4	-26.854	-19.946		-24.804
CdSO4	-10.355	-11.538		-18.893
CdSO4.H2O	-8.802	-9.984		-17.340
CdSO4.2.67H2O	-8.656	-9.838		-17.193
ANTLERITE	-9.935	-8.586		-18.019
BROCHANTITE	-11.901	-8.809		-18.657
LANGITE	-14.168	-11.076		-20.924
CuOCuSO4	-15.918	-16.312		-25.330
CuSO4	-13.023	-15.160		-23.763
CHALCANTHITE	-7.447	-9.582		-18.185
Fe2(SO4)3	-33.251	-41.841		-72.098
H-JAROSITE	-7.000	-10.185		-35.101
Na-JAROSITE	-3.836	-4.970		-29.943
EPSOMITE	-2.992	-3.389		-11.900
ANHYDRITE	-0.249	-0.316		-6.929
GYPSUM	0.000	-0.067		-6.680
CELESTITE	-0.225	-0.159		-5.708
BARITE	0.912	1.094		-3.409
MIRABILITE	-5.318	-5.093		-13.395
THENARDITE	-6.748	-6.524		-14.827
CuSeO3.2H2O	-8.513	-9.895		-19.015
Fe2(SeO3)3.2H2O	-10.110	-16.436		-48.245
Fe2(OH)4SeO3	-7.352	-7.428		-21.827
MgSeO3.6H2O	-6.090	-5.733		-14.761
CaSeO3.2H2O	-5.341	-4.653		-11.783
SrSeO3	-7.061	-6.242		-12.307
BaSeO3	-8.814	-7.878		-12.898
Na2SeO3.5H2O	-14.646	-13.667		-22.486
Zn3(PO4)2.4H2O	-10.765	-10.833		-29.325
Cd3(PO4)2	-18.171	-16.651		-31.281
Cu3(PO4)2	-12.590	-13.931		-32.305
Cu3(PO4)2.3H2O	-14.322	-15.663		-34.036
STRENGITE	-1.688	-3.449		-14.859
Mg3(PO4)2	-11.252	-7.379		-25.477
MgHPO4.3H2O	-3.812	-3.616		-12.502
HYDROXYLAPATITE	-0.221	8.989		-8.830
CaHPO4.2H2O	-2.486	-1.958		-8.947
CaHPO4	-2.205	-1.677		-8.666
Ca3(PO4)2 (beta)	-4.097	0.772		-11.632
Ca4H(PO4)3.3H2O	-7.419	-2.021		-21.414
SrHPO4	-4.421	-3.761		-9.685
BaHPO4	-6.164	-5.388		-10.266
AlAsO4.2H2O	-10.391	-10.274		-21.202
Zn3(AsO4)2.2.5H2O	-28.806	-20.442		-38.113
Cu3(AsO4)2.2H2O	-24.513	-17.422		-34.973
FeAsO4.2H2O	-12.974	-10.519		-21.518
Ca3(AsO4)2.4H2O	-24.291	-10.989		-22.571
Ba3(AsO4)2	-6.455	7.592		2.341

Table H-6. Saturation indices for all minerals calculated using MINTEQA2: Dewey-sand.

Solid/Mineral	Saturation Index				Solid/Mineral	Saturation Index			
	DS-1	DS-2	DS-3	DS-4		DS-1	DS-2	DS-3	DS-4
	pH 6.17	pH 8.00	pH 9.94	pH 12.43		pH 6.17	pH 8.00	pH 9.94	pH 12.43
CaNaAsO$_4$.7.5H$_2$O	-14.042	-7.562	-6.067	-13.926	AZURITE	-11.616	-4.193	-3.331	-9.644
Ca$_5$(AsO$_4$)$_3$OH	-35.861	-14.684	-9.972	-30.398	ARTINITE	-12.570	-5.401	-2.663	-5.020
Ca$_4$(OH)$_2$(AsO$_4$)$_2$:4H$_2$O	-35.163	-18.624	-13.575	-28.083	HYDROMAGNESITE	-31.128	-13.205	-6.360	-12.253
Mg$_3$(AsO4)$_2$	-25.527	-12.757	-15.047	-27.666	MAGNESITE	-4.848	-1.263	0.106	-1.073
FeAsO$_4$	-13.039	-10.625	-14.117	-20.627	NESQUEHONITE	-7.639	-4.055	-2.686	-3.864
Cd$_3$(AsO$_4$)$_2$	-25.258	-18.213	-21.143	-32.093	ARAGONITE	-3.317	0.313	3.174	1.836
Cu$_3$(AsO$_4$)$_2$	-24.232	-14.793	-20.328	-35.724	CALCITE	-3.179	0.452	3.313	1.975
Al$_2$(SeO$_3$)$_3$	-9.812	-18.257	-29.551	-52.440	DOLOMITE (ordered)	-6.871	0.344	4.574	2.057
CaSeO$_3$	-3.557	-2.321	-2.871	-10.341	DOLOMITE (disordered)	-7.421	-0.206	4.024	1.507
CaSeO$_3$:H$_2$O	-4.367	-3.132	-3.681	-11.151	HUNTITE	-18.608	-4.224	2.744	-2.131
CdSeO$_3$	-6.998	-7.717	-9.972	-16.726	STRONTIANITE	-4.503	-0.890	2.432	2.185
CuSeO$_3$	-7.856	-7.777	-10.901	-19.137	WITHERITE	-7.622	-3.965	-0.094	-0.282
Fe$_2$(SeO$_3$)$_3$	-14.384	-18.759	-29.578	-51.909	THERMONATRITE	-13.874	-10.191	-6.526	-10.488
Fe$_2$(SeO$_3$)$_3$.6H$_2$O	-42.067	-46.442	-57.261	-79.591	AlOHSO$_4$	-0.709	-4.932	-9.315	-16.612
MgSeO$_3$	-4.301	-3.112	-5.153	-12.464	Al$_4$(OH)$_{10}$SO$_4$	5.339	-0.774	-6.750	-20.786
Na$_2$SeO$_3$	-9.280	-7.992	-7.738	-17.832	Zn$_2$(OH)$_2$SO$_4$	-9.257	-7.817	-8.610	-15.946
ZnSeO$_3$	-4.520	-4.398	-6.279	-13.554	Zn$_4$(OH)$_6$SO$_4$	-17.316	-10.842	-8.577	-18.198
ZnSeO$_3$.H$_2$O	-7.080	-6.958	-8.840	-16.114	Zn$_3$O(SO$_4$)$_2$	-28.848	-28.483	-31.600	-45.129
SeO$_2$	-12.925	-15.320	-18.731	-24.863	ZINCOSITE	-12.107	-13.184	-15.507	-21.700
Al(OH)$_3$ (am)	-0.141	-0.771	-1.302	-3.548	ZnSO$_4$.H$_2$O	-7.540	-8.616	-10.939	-17.132
BOEHMITE	2.082	1.452	0.921	-1.326	BIANCHITE	-6.416	-7.492	-9.815	-16.007
DIASPORE	3.787	3.157	2.626	0.379	GOSLARITE	-6.170	-7.246	-9.569	-15.761
GIBBSITE	2.368	1.738	1.207	-1.039	Cd$_3$(OH)$_4$SO$_4$	-21.071	-19.637	-20.022	-26.938
Zn(OH)$_2$ (am)	-6.053	-3.537	-2.007	-3.150	Cd$_3$OH$_2$(SO$_4$)$_2$	-19.819	-21.978	-26.215	-38.182
Zn(OH)$_2$	-5.779	-3.263	-1.733	-2.876	Cd$_4$(OH)$_6$SO$_4$	-21.549	-18.438	-17.668	-25.206
Zn(OH)$_2$ (beta)	-5.333	-2.817	-1.287	-2.430	CdSO$_4$	-9.064	-10.981	-13.677	-19.350
Zn(OH)$_2$ (gamma)	-5.313	-2.797	-1.267	-2.410	CdSO$_4$.H$_2$O	-7.510	-9.428	-12.124	-17.796
Zn(OH)$_2$ (epsilon)	-5.113	-2.597	-1.067	-2.210	CdSO$_4$.2.67H$_2$O	-7.364	-9.282	-11.978	-17.650
ZnO (active)	-4.767	-2.250	-0.721	-1.864	ANTLERITE	-8.614	-4.785	-7.775	-19.138
ZINCITE	-4.913	-2.396	-0.867	-2.010	BROCHANTITE	-10.124	-3.821	-6.523	-19.990
Cd(OH)$_2$ (am)	-8.368	-6.692	-5.536	-6.158	LANGITE	-12.391	-6.088	-8.790	-22.257
Cd(OH)$_2$	-8.282	-6.606	-5.450	-6.072	CuOCuSO$_4$	-15.053	-13.698	-16.975	-26.234
MONTEPONITE	-9.741	-8.065	-6.909	-7.531	CuSO$_4$	-12.614	-13.733	-17.297	-24.452
Cu(OH)$_2$	-3.750	-1.276	-0.988	-3.093	CHALCANTHITE	-7.037	-8.156	-11.720	-18.874
TENORITE	-2.719	-0.245	0.042	-2.062	Fe$_2$(SO$_4$)$_3$	-32.423	-40.393	-52.536	-71.622
FERRIHYDRITE	0.628	2.033	1.739	-0.228	H-JAROSITE	-5.642	-8.613	-17.198	-33.201
GOETHITE	3.328	4.733	4.439	2.472	Na-JAROSITE	-2.336	-3.466	-10.218	-28.202
Cr(OH)$_3$ (am)	-1.968	0.154	-0.245	-2.681	EPSOMITE	-3.136	-3.145	-5.628	-11.855
Cr(OH)$_3$	-4.054	-1.931	-2.330	-4.766	ANHYDRITE	-0.245	-0.207	-1.198	-7.587
BRUCITE	-7.505	-3.920	-2.551	-3.730	GYPSUM	0.004	0.041	-0.949	-7.337
PERICLASE	-12.244	-8.660	-7.291	-8.470	CELESTITE	-0.104	-0.084	-0.614	-5.912
Mg(OH)$_2$ (active)	-9.455	-5.870	-4.501	-5.680	BARITE	0.836	0.900	0.919	-4.318
LIME	-22.705	-19.075	-16.213	-17.552	MIRABILITE	-5.079	-4.990	-5.176	-14.187
PORTLANDITE	-12.811	-9.180	-6.319	-7.657	THENARDITE	-6.510	-6.420	-6.607	-15.620
Ba(OH)$_2$.8H$_2$O	-18.944	-15.287	-11.415	-11.601	CuSeO$_3$.2H$_2$O	-8.389	-8.310	-11.433	-19.669
As$_2$O$_5$	-39.942	-37.925	-44.322	-53.405	Fe$_2$(SeO$_3$)$_3$.2H$_2$O	-10.139	-14.514	-25.333	-47.663
Al$_2$O$_3$	1.668	0.408	-0.654	-5.148	Fe$_2$(OH)$_4$SeO$_3$	-6.717	-6.302	-10.300	-20.367
HEMATITE	9.057	11.867	11.279	7.344	MgSeO$_3$.6H$_2$O	-6.520	-5.330	-7.372	-14.681
MAGHEMITE	1.253	4.063	3.475	-0.460	CaSeO$_3$.2H$_2$O	-5.622	-4.386	-4.936	-12.405
LEPIDOCROCITE	2.448	3.853	3.559	1.592	SrSeO$_3$	-7.227	-6.008	-6.097	-12.476
Cr$_2$O$_3$	-3.077	1.167	0.370	-4.503	BaSeO$_3$	-9.176	-7.914	-7.453	-13.772
SPINEL	-6.188	-3.863	-3.556	-9.229	Na$_2$SeO$_3$.5H$_2$O	-14.693	-13.405	-13.150	-23.243
MAGNESIOFERRITE	0.118	6.513	7.294	2.181	Zn$_3$(PO$_4$)$_2$.4H$_2$O	-7.501	-6.168	-10.733	-23.158
NATRON	-11.930	-8.248	-4.583	-8.543	Cd$_3$(PO$_4$)$_2$	-13.493	-14.683	-20.369	-31.233
CUPRIC FERRITE	6.575	11.859	11.559	5.520	Cu$_3$(PO$_4$)$_2$	-10.558	-9.354	-17.644	-32.955
MgCr$_2$O$_4$	-12.296	-4.467	-3.895	-9.946	Cu$_3$(PO$_4$)$_2$.3H$_2$O	-12.290	-11.085	-19.376	-34.686
ZnCl2	-16.872	-17.988	-20.309	-26.684	STRENGITE	-0.873	-2.577	-7.447	-13.913
Zn$_2$(OH)$_3$Cl	-10.471	-7.254	-6.121	-11.022	Mg$_3$(PO$_4$)$_2$	-10.883	-6.347	-11.393	-23.927
Zn$_5$(OH)$_8$Cl$_2$	-22.639	-13.688	-9.893	-20.838	MgHPO$_4$.3H$_2$O	-3.578	-3.102	-6.310	-11.987
CdCl$_2$	-10.221	-12.178	-14.873	-20.727	HYDROXYLAPATITE	1.030	9.856	10.434	-9.754
CdCl$_2$.H$_2$O	-9.187	-11.144	-13.839	-19.693	CaHPO$_4$.2H$_2$O	-2.103	-1.582	-3.297	-9.133
CdCl$_2$.2.5H$_2$O	-8.968	-10.925	-13.620	-19.474	CaHPO$_4$	-1.822	-1.301	-3.016	-8.853
CdOHCl	-6.296	-6.437	-7.206	-10.444	Ca$_3$(PO$_4$)$_2$ (beta)	-3.280	1.394	0.825	-12.187
MELANOTHALLITE	-17.576	-18.734	-22.297	-29.634	Ca$_4$H(PO$_4$)$_3$.3H$_2$O	-6.219	-1.023	-3.307	-22.156
ATACAMITE	-5.664	-2.532	-3.883	-10.707	SrHPO$_4$	-3.922	-3.417	-4.672	-9.418
Fe(OH)$_{2.7}$Cl$_{0.3}$	4.422	5.282	4.411	1.659	BaHPO$_4$	-5.861	-5.313	-6.018	-10.704
CrCl$_3$	-42.196	-45.523	-51.697	-61.982	AlAsO$_4$.2H$_2$O	-10.759	-10.380	-14.110	-20.898
HALITE	-5.518	-5.494	-5.586	-10.183	Zn$_3$(AsO$_4$)$_2$.2.5H$_2$O	-27.624	-18.057	-19.866	-32.377
SMITHSONITE	-5.226	-2.709	-1.180	-2.323	Cu$_3$(AsO$_4$)$_2$.2H$_2$O	-24.563	-15.124	-20.659	-36.055
ZnCO$_3$.H$_2$O	-4.967	-2.450	-0.921	-2.063	FeAsO$_4$.2H$_2$O	-13.200	-10.786	-14.278	-20.787
OTAVITE	-4.285	-2.609	-1.453	-2.075	Ca$_3$(AsO$_4$)$_2$.4H$_2$O	-25.556	-12.648	-10.461	-23.558
CuCO$_3$	-5.223	-2.749	-2.461	-4.566	Ba$_3$(AsO$_4$)$_2$	-7.961	5.027	10.244	0.598
MALACHITE	-6.493	-1.545	-0.970	-5.178					

Table H-7. Saturation indices for all minerals calculated using MINTEQA2: Presque Isle.

Solid/Mineral	Saturation Index			
	P-1	P-2	P-3	P-4
	pH 5.87	pH 7.90	pH 9.82	pH 11.68
CaNaAsO$_4$.7.5H$_2$O	-12.836	-6.916	-7.636	-12.534
Ca$_5$(AsO$_4$)$_3$OH	-29.16	-9.254	-10.912	-22.283
Ca$_4$(OH)$_2$(AsO$_4$)$_2$:4H$_2$O	-30.962	-15.025	-14.219	-22.102
Mg$_3$(AsO4)$_2$	-20.754	-8.961	-14.326	-27.716
FeAsO$_4$	-10.682	-8.967	-14.799	-19.439
Cd$_3$(AsO$_4$)$_2$	-22.677	-13.661	-19.757	-27.207
Cu$_3$(AsO$_4$)$_2$	-19.416	-9.703	-20.111	-25.974
Al$_2$(SeO$_3$)$_3$	-7.527	-17.096	-26.314	-41.017
CaSeO$_3$	-2.633	-1.354	-1.632	-5.670
CaSeO$_3$:H$_2$O	-3.443	-2.164	-2.442	-6.481
CdSeO$_3$	-6.747	-6.443	-8.065	-12.147
CuSeO$_3$	-6.860	-6.323	-9.384	-12.936
Fe$_2$(SeO$_3$)$_3$	-11.499	-16.170	-26.607	-40.682
Fe$_2$(SeO$_3$)$_3$.6H$_2$O	-39.180	-43.851	-54.288	-68.362
MgSeO$_3$	-3.320	-2.089	-3.469	-9.530
Na$_2$SeO$_3$	-10.548	-9.367	-9.026	-15.540
ZnSeO$_3$	-4.243	-3.574	-5.539	-9.765
ZnSeO$_3$.H$_2$O	-6.803	-6.134	-8.099	-12.325
SeO$_2$	-11.599	-14.319	-17.464	-21.047
Al(OH)$_3$ (am)	-0.986	-1.692	-1.583	-3.560
BOEHMITE	1.236	0.530	0.639	-1.338
DIASPORE	2.941	2.235	2.344	0.367
GIBBSITE	1.523	0.817	0.926	-1.051
Zn(OH)$_2$ (am)	-7.102	-3.714	-2.534	-3.177
Zn(OH)$_2$	-6.828	-3.440	-2.260	-2.903
Zn(OH)$_2$ (beta)	-6.382	-2.994	-1.814	-2.457
Zn(OH)$_2$ (gamma)	-6.362	-2.974	-1.794	-2.437
Zn(OH)$_2$ (epsilon)	-6.162	-2.774	-1.594	-2.237
ZnO (active)	-5.817	-2.429	-1.248	-1.891
ZINCITE	-5.962	-2.574	-1.394	-2.037
Cd(OH)$_2$ (am)	-9.443	-6.419	-4.896	-5.395
Cd(OH)$_2$	-9.357	-6.333	-4.810	-5.309
MONTEPONITE	-10.816	-7.792	-6.270	-6.768
Cu(OH)$_2$	-4.080	-0.823	-0.739	-0.708
TENORITE	-3.050	0.207	0.292	0.322
FERRIHYDRITE	0.081	1.825	1.324	-0.339
GOETHITE	2.782	4.525	4.024	2.362
Cr(OH)$_3$ (am)	-1.812	0.912	1.901	0.159
Cr(OH)$_3$	-3.897	-1.174	-0.185	-1.926
BRUCITE	-7.849	-3.899	-2.134	-4.612
PERICLASE	-12.589	-8.639	-6.873	-9.352
Mg(OH)$_2$ (active)	-9.799	-5.849	-4.084	-6.562
LIME	-23.107	-19.109	-16.242	-16.698
PORTLANDITE	-13.212	-9.214	-6.347	-6.802
Ba(OH)$_2$.8H$_2$O	-18.819	-14.963	-10.676	-10.630
As$_2$O$_5$	-34.135	-34.192	-44.854	-50.808
Al$_2$O$_3$	-0.025	-1.436	-1.218	-5.173
HEMATITE	7.963	11.450	10.449	7.123
MAGHEMITE	0.159	3.646	2.645	-0.681
LEPIDOCROCITE	1.902	3.645	3.144	1.482
Cr$_2$O$_3$	-2.765	2.682	4.660	1.176
SPINEL	-8.225	-5.686	-3.703	-10.136
MAGNESIOFERRITE	-1.319	6.118	6.882	1.077
NATRON	-14.522	-10.622	-7.135	-10.065
CUPRIC FERRITE	5.152	11.895	10.978	7.683
MgCr$_2$O$_4$	-12.329	-2.931	0.812	-5.150
ZnCl2	-19.333	-20.165	-23.022	-28.234
Zn$_2$(OH)$_3$Cl	-13.275	-8.609	-8.267	-11.837
Zn$_5$(OH)$_8$Cl$_2$	-29.297	-16.576	-14.711	-22.495
CdCl$_2$	-12.708	-13.905	-16.419	-21.487
CdCl$_2$.H$_2$O	-11.674	-12.871	-15.385	-20.453
CdCl$_2$.2.5H$_2$O	-11.455	-12.651	-15.166	-20.233
CdOHCl	-8.077	-7.163	-7.660	-10.443
MELANOTHALLITE	-19.317	-20.281	-24.234	-28.772
ATACAMITE	-7.030	-2.627	-4.476	-6.699
Fe(OH)$_{2.7}$Cl$_{0.3}$	3.664	4.775	3.668	1.320
CrCl$_3$	-44.158	-47.765	-52.831	-61.426
HALITE	-7.521	-7.682	-7.957	-11.707
SMITHSONITE	-6.275	-2.887	-1.707	-2.350
ZnCO$_3$.H$_2$O	-6.016	-2.628	-1.447	-2.090
OTAVITE	-5.360	-2.336	-0.814	-1.312
CuCO$_3$	-5.553	-2.296	-2.212	-2.181
MALACHITE	-7.153	-0.639	-0.470	-0.409

Solid/Mineral	Saturation Index			
	P-1	P-2	P-3	D-4
	pH 5.87	pH 7.90	pH 9.82	pH 11.68
AZURITE	-12.606	-2.836	-2.582	-2.490
ARTINITE	-13.258	-5.358	-1.827	-6.784
HYDROMAGNESITE	-32.848	-13.099	-4.271	-16.664
MAGNESITE	-5.192	-1.242	0.523	-1.955
NESQUEHONITE	-7.983	-4.033	-2.267	-4.746
ARAGONITE	-3.719	0.279	3.146	2.690
CALCITE	-3.580	0.418	3.285	2.829
DOLOMITE (ordered)	-7.617	0.331	4.964	2.029
DOLOMITE (disordered)	-8.167	-0.219	4.414	1.479
HUNTITE	-20.043	-4.196	3.968	-3.923
STRONTIANITE	-4.655	-0.717	2.429	2.275
WITHERITE	-7.500	-3.644	0.642	0.688
THERMONATRITE	-16.468	-12.568	-9.081	-12.013
AlOHSO$_4$	-1.462	-6.236	-9.846	-15.511
Al$_4$(OH)$_{10}$SO$_4$	2.049	-4.842	-8.125	-19.722
Zn$_2$(OH)$_2$SO$_4$	-11.262	-8.554	-9.912	-14.887
Zn$_4$(OH)$_6$SO$_4$	-21.419	-11.935	-10.932	-17.192
Zn$_3$O(SO$_4$)$_2$	-31.810	-29.781	-33.678	-42.984
ZINCOSITE	-13.064	-13.744	-16.282	-20.613
ZnSO$_4$.H$_2$O	-8.496	-9.176	-11.714	-16.046
BIANCHITE	-7.370	-8.050	-10.588	-14.919
GOSLARITE	-7.124	-7.804	-10.342	-14.673
Cd$_3$(OH)$_4$SO$_4$	-24.204	-19.200	-18.352	-23.536
Cd$_3$OH$_2$(SO$_4$)$_2$	-22.859	-21.923	-24.794	-33.667
Cd$_4$(OH)$_6$SO$_4$	-25.756	-17.728	-15.358	-21.041
CdSO$_4$	-10.046	-11.090	-13.287	-17.474
CdSO$_4$.H$_2$O	-8.492	-9.536	-11.733	-15.920
CdSO$_4$.2.67H$_2$O	-8.346	-9.390	-11.586	-15.773
ANTLERITE	-9.511	-3.809	-7.274	-10.871
BROCHANTITE	-11.351	-2.392	-5.772	-9.339
LANGITE	-13.618	-4.659	-8.039	-11.605
CuOCuSO$_4$	-15.620	-13.175	-16.725	-20.352
CuSO$_4$	-12.851	-13.662	-17.296	-20.954
CHALCANTHITE	-7.273	-8.084	-11.718	-15.375
Fe$_2$(SO$_4$)$_3$	-33.238	-41.955	-54.113	-68.503
H-JAROSITE	-7.095	-10.000	-18.940	-31.304
Na-JAROSITE	-5.086	-6.041	-13.238	-27.068
EPSOMITE	-3.386	-3.504	-5.456	-11.623
ANHYDRITE	-0.554	-0.623	-1.475	-5.619
GYPSUM	-0.304	-0.374	-1.225	-5.369
CELESTITE	-0.163	-0.293	-0.867	-4.709
BARITE	1.052	0.839	1.407	-2.236
MIRABILITE	-7.577	-7.745	-7.977	-14.596
THENARDITE	-9.011	-9.179	-9.411	-16.031
CuSeO$_3$.2H$_2$O	-7.392	-6.855	-9.915	-13.468
Fe$_2$(SeO$_3$)$_3$.2H$_2$O	-7.253	-11.924	-22.361	-36.436
Fe$_2$(OH)$_4$SeO$_3$	-6.484	-5.716	-9.863	-16.771
MgSeO$_3$.6H$_2$O	-5.536	-4.306	-5.685	-11.746
CaSeO$_3$.2H$_2$O	-4.697	-3.418	-3.696	-7.734
SrSeO$_3$	-6.052	-4.834	-4.833	-8.570
BaSeO$_3$	-7.727	-6.591	-5.449	-8.987
Na$_2$SeO$_3$.5H$_2$O	-15.959	-14.778	-14.437	-20.951
Zn$_3$(PO$_4$)$_2$.4H$_2$O	-7.693	-5.410	-12.071	-20.444
Cd$_3$(PO$_4$)$_2$	-13.765	-12.574	-18.210	-26.150
Cu$_3$(PO$_4$)$_2$	-8.594	-6.705	-16.655	-23.007
Cu$_3$(PO$_4$)$_2$.3H$_2$O	-10.325	-8.436	-18.385	-24.737
STRENGITE	0.058	-2.138	-7.741	-12.625
Mg$_3$(PO$_4$)$_2$	-8.962	-4.993	-9.900	-23.779
MgHPO$_4$.3H$_2$O	-2.444	-2.435	-5.771	-11.471
HYDROXYLAPATITE	3.452	11.622	10.653	-1.290
CaHPO$_4$.2H$_2$O	-1.027	-0.969	-3.204	-6.881
CaHPO$_4$	-0.747	-0.689	-2.923	-6.601
Ca$_3$(PO$_4$)$_2$ (beta)	-1.531	2.583	0.981	-6.829
Ca$_4$H(PO$_4$)$_3$.3H$_2$O	-3.393	0.778	-3.058	-14.545
SrHPO$_4$	-2.596	-2.599	-4.555	-7.930
BaHPO$_4$	-4.261	-4.346	-5.161	-8.337
AlAsO$_4$.2H$_2$O	-8.701	-9.435	-14.657	-19.611
Zn$_3$(AsO$_4$)$_2$.2.5H$_2$O	-24.965	-14.857	-21.978	-29.861
Cu$_3$(AsO$_4$)$_2$.2H$_2$O	-19.747	-10.033	-20.442	-26.304
FeAsO$_4$.2H$_2$O	-10.842	-9.127	-14.959	-19.599
Ca$_3$(AsO$_4$)$_2$.4H$_2$O	-20.954	-9.015	-11.076	-18.397
Ba$_3$(AsO$_4$)$_2$	-1.787	9.723	11.921	6.103

Table H-8. Saturation indices for all minerals calculated using MINTEQA2:Presque Isle-Lawson.

Solid/Mineral	Saturation Index				Solid/Mineral	Saturation Index			
	PL-1	PL-2	PL-3	PL-4		PL-1	PL-2	PL-3	PL-4
	pH 6.70	pH 8.02	pH 8.92	pH 10.98		pH 6.70	pH 8.02	pH 8.92	pH 10.98
$CaNaAsO_4.7.5H_2O$	-12.794	-8.866	-8.017	-10.540	AZURITE	-8.196	-4.948	-3.266	0.390
$Ca_5(AsO_4)_3OH$	-27.014	-14.054	-11.485	-18.943	ARTINITE	-9.616	-5.558	-3.625	-1.579
$Ca_4(OH)_2(AsO_4)_2:4H_2O$	-28.537	-18.554	-16.035	-20.607	HYDROMAGNESITE	-23.744	-13.599	-8.768	-3.652
$Mg_3(AsO4)_2$	-18.830	-10.812	-10.234	-14.129	MAGNESITE	-3.371	-1.343	-0.376	0.647
$FeAsO_4$	-11.056	-8.786	-8.499	-12.552	NESQUEHONITE	-6.162	-4.133	-3.166	-2.143
$Cd_3(AsO_4)_2$	-23.631	-18.864	-17.310	-23.796	ARAGONITE	-2.228	-0.216	0.994	1.594
$Cu_3(AsO_4)_2$	-18.545	-13.366	-14.005	-17.314	CALCITE	-2.090	-0.077	1.133	1.733
$Al_2(SeO_3)_3$	-11.012	-18.531	-22.174	-35.628	DOLOMITE (ordered)	-4.306	-0.264	1.912	3.535
$CaSeO_3$	-2.732	-2.453	-2.490	-5.744	DOLOMITE (disordered)	-4.856	-0.814	1.362	2.985
$CaSeO_3:H_2O$	-3.542	-3.263	-3.300	-6.554	HUNTITE	-13.090	-4.991	-0.882	2.787
$CdSeO_3$	-7.476	-8.264	-8.220	-11.914	STRONTIANITE	-3.740	-1.694	-0.508	0.526
$CuSeO_3$	-6.981	-7.631	-8.318	-10.953	WITHERITE	-5.245	-3.333	-1.832	0.168
$Fe_2(SeO_3)_3$	-13.479	-16.071	-16.917	-29.621	THERMONATRITE	-15.828	-13.930	-12.331	-11.614
$Fe_2(SeO_3)_3.6H_2O$	-41.160	-43.752	-44.597	-57.301	$AlOHSO_4$	-3.602	-6.914	-8.586	-13.662
$MgSeO_3$	-3.089	-2.794	-3.074	-5.905	$Al_4(OH)_{10}SO_4$	1.838	-4.953	-6.478	-14.392
Na_2SeO_3	-11.499	-11.334	-10.982	-14.119	$Zn_2(OH)_2SO_4$	-9.171	-8.186	-7.761	-10.583
$ZnSeO_3$	-3.396	-3.561	-3.735	-6.934	$Zn_4(OH)_6SO_4$	-14.454	-10.331	-7.760	-9.273
$ZnSeO_3.H_2O$	-5.956	-6.121	-6.295	-9.494	$Zn_3O(SO_4)_2$	-30.065	-29.664	-29.885	-36.184
SeO_2	-13.190	-14.923	-16.170	-20.024	ZINCOSITE	-13.410	-13.994	-14.641	-18.117
$Al(OH)_3$ (am)	-0.343	-1.503	-1.454	-2.400	$ZnSO_4.H_2O$	-8.842	-9.426	-10.073	-13.550
BOEHMITE	1.879	0.719	0.768	-0.178	BIANCHITE	-7.716	-8.299	-8.946	-12.423
DIASPORE	3.584	2.424	2.473	1.527	GOSLARITE	-7.470	-8.053	-8.700	-12.176
GIBBSITE	2.166	1.006	1.055	0.109	$Cd_3(OH)_4SO_4$	-24.403	-23.718	-21.564	-25.216
$Zn(OH)_2$ (am)	-4.665	-3.096	-2.024	-1.369	$Cd_3OH_2(SO_4)_2$	-25.841	-27.310	-26.876	-34.659
$Zn(OH)_2$	-4.391	-2.822	-1.750	-1.095	$Cd_4(OH)_6SO_4$	-25.094	-23.464	-20.018	-23.511
$Zn(OH)_2$ (beta)	-3.945	-2.376	-1.304	-0.649	$CdSO_4$	-11.968	-13.175	-13.603	-17.575
$Zn(OH)_2$ (gamma)	-3.925	-2.356	-1.284	-0.629	$CdSO_4.H_2O$	-10.414	-11.621	-12.050	-16.021
$Zn(OH)_2$ (epsilon)	-3.725	-2.156	-1.084	-0.429	$CdSO_4.2.67H_2O$	-10.267	-11.474	-11.903	-15.874
ZnO (active)	-3.380	-1.811	-0.738	-0.084	ANTLERITE	-7.885	-6.789	-6.827	-7.302
ZINCITE	-3.525	-1.956	-0.884	-0.229	BROCHANTITE	-8.255	-6.076	-5.554	-4.810
$Cd(OH)_2$ (am)	-8.581	-7.636	-6.344	-6.185	LANGITE	-10.521	-8.342	-7.820	-7.077
$Cd(OH)_2$	-8.495	-7.550	-6.258	-6.099	$CuOCuSO_4$	-15.464	-15.451	-16.050	-17.743
MONTEPONITE	-9.955	-9.009	-7.718	-7.558	$CuSO_4$	-14.164	-15.234	-16.393	-19.306
$Cu(OH)_2$	-2.610	-1.527	-0.967	0.252	CHALCANTHITE	-8.585	-9.655	-10.814	-13.726
TENORITE	-1.580	-0.497	0.063	1.282	$Fe_2(SO_4)_3$	-38.796	-42.647	-44.910	-58.446
FERRIHYDRITE	1.477	2.781	4.229	3.658	H-JAROSITE	-8.474	-8.867	-7.964	-17.939
GOETHITE	4.177	5.481	6.929	6.358	Na-JAROSITE	-6.145	-5.590	-3.887	-13.504
$Cr(OH)_3$ (am)	-0.418	0.710	1.439	0.699	EPSOMITE	-4.347	-4.470	-5.224	-8.332
$Cr(OH)_3$	-2.503	-1.375	-0.646	-1.387	ANHYDRITE	-1.846	-1.986	-2.496	-6.027
BRUCITE	-6.028	-3.999	-3.033	-2.010	GYPSUM	-1.596	-1.736	-2.246	-5.777
PERICLASE	-10.768	-8.739	-7.773	-6.750	CELESTITE	-2.031	-2.139	-2.672	-5.769
$Mg(OH)_2$ (active)	-7.978	-5.949	-4.983	-3.960	BARITE	0.524	0.283	0.064	-2.067
LIME	-21.616	-19.604	-18.394	-17.794	MIRABILITE	-9.720	-9.973	-10.095	-13.508
PORTLANDITE	-11.721	-9.708	-8.498	-7.898	THENARDITE	-11.154	-11.409	-11.530	-14.944
$Ba(OH)_2.8H_2O$	-16.563	-14.649	-13.149	-11.149	$CuSeO_3.2H_2O$	-7.513	-8.163	-8.850	-11.485
As_2O_5	-37.674	-35.743	-38.064	-45.028	$Fe_2(SeO_3)_3.2H_2O$	-9.233	-11.825	-12.670	-25.375
Al_2O_3	1.261	-1.058	-0.961	-2.852	$Fe_2(OH)_4SeO_3$	-5.283	-4.408	-2.760	-7.756
HEMATITE	10.754	13.362	16.258	15.115	$MgSeO_3.6H_2O$	-5.305	-5.009	-5.290	-8.121
MAGHEMITE	2.950	5.558	8.454	7.311	$CaSeO_3.2H_2O$	-4.796	-4.517	-4.554	-7.808
LEPIDOCROCITE	3.297	4.601	6.049	5.478	$SrSeO_3$	-6.727	-6.416	-6.476	-9.296
Cr_2O_3	0.023	2.279	3.736	2.255	$BaSeO_3$	-7.063	-6.884	-6.630	-8.484
SPINEL	-5.118	-5.408	-4.345	-5.213	$Na_2SeO_3.5H_2O$	-16.909	-16.744	-16.392	-19.529
MAGNESIOFERRITE	3.292	7.929	11.791	11.672	$Zn_3(PO_4)_2.4H_2O$	-3.432	-2.904	-2.783	-8.604
NATRON	-13.881	-11.982	-10.383	-9.666	$Cd_3(PO_4)_2$	-14.232	-15.574	-14.797	-22.103
CUPRIC FERRITE	9.412	13.103	16.559	16.635	$Cu_3(PO_4)_2$	-7.236	-8.166	-9.582	-13.711
$MgCr_2O_4$	-7.720	-3.435	-1.011	-1.469	$Cu_3(PO_4)_2.3H_2O$	-8.966	-9.896	-11.312	-15.441
ZnCl2	-19.584	-21.395	-22.320	-26.002	STRENGITE	-0.071	-0.857	-0.958	-5.421
$Zn_2(OH)_3Cl$	-9.745	-8.297	-7.150	-8.010	$Mg_3(PO_4)_2$	-6.550	-4.643	-4.841	-9.556
$Zn_5(OH)_8Cl_2$	-19.800	-15.335	-11.968	-13.032	$MgHPO_4.3H_2O$	-2.149	-2.209	-2.791	-5.660
$CdCl_2$	-14.535	-16.970	-17.676	-21.852	HYDROXYLAPATITE	6.330	10.126	11.529	2.853
$CdCl_2.H_2O$	-13.501	-15.936	-16.641	-20.818	$CaHPO_4.2H_2O$	-1.062	-1.138	-1.477	-4.769
$CdCl_2.2.5H_2O$	-13.281	-15.716	-16.421	-20.598	$CaHPO_4$	-0.781	-0.858	-1.197	-4.489
CdOHCl	-8.560	-9.304	-9.012	-11.020	$Ca_3(PO_4)_2$ (beta)	-0.110	1.750	2.282	-3.702
MELANOTHALLITE	-20.536	-22.833	-24.270	-27.388	$Ca_4H(PO_4)_3.3H_2O$	-2.006	-0.223	-0.030	-9.306
ATACAMITE	-5.434	-4.959	-4.836	-4.567	$SrHPO_4$	-3.207	-3.251	-3.613	-6.471
$Fe(OH)_{2.7}Cl_{0.3}$	4.657	5.453	6.602	5.380	$BaHPO_4$	-3.532	-3.709	-3.757	-5.649
$CrCl_3$	-46.796	-50.739	-53.005	-60.251	$AlAsO_4.2H_2O$	-9.827	-10.021	-11.133	-15.561
HALITE	-8.546	-9.287	-9.486	-11.296	$Zn_3(AsO_4)_2.2.5H_2O$	-21.192	-14.554	-13.656	-18.657
SMITHSONITE	-3.839	-2.270	-1.197	-0.542	$Cu_3(AsO_4)_2.2H_2O$	-18.875	-13.696	-14.335	-17.644
$ZnCO_3.H_2O$	-3.579	-2.010	-0.937	-0.282	$FeAsO_4.2H_2O$	-11.216	-8.947	-8.659	-12.712
OTAVITE	-4.499	-3.553	-2.262	-2.102	$Ca_3(AsO_4)_2.4H_2O$	-20.019	-12.050	-10.741	-15.905
$CuCO_3$	-4.083	-3.000	-2.440	-1.221	$Ba_3(AsO_4)_2$	1.439	9.108	11.288	10.324
MALACHITE	-4.213	-2.047	-0.926	1.511					

Table H-9. Saturation indices for all minerals calculated using MINTEQA2: Presque Isle-Kamm.

Solid/Mineral	Saturation Index				Solid/Mineral	Saturation Index			
	PK-1	PK-2	PK-3	PK-4		PK-1	PK-2	PK-3	PK-4
	pH 6.72	pH 7.90	pH 9.34	pH 11.72		pH 6.72	pH 7.90	pH 9.34	pH 11.72
CaNaAsO$_4$.7.5H$_2$O	-13.978	-9.562	-8.079	-13.601	AZURITE	-8.849	-7.853	-7.359	-7.898
Ca$_5$(AsO$_4$)$_3$OH	-30.716	-16.467	-12.095	-26.755	ARTINITE	-9.806	-6.585	-4.008	-6.729
Ca$_4$(OH)$_2$(AsO$_4$)$_2$:4H$_2$O	-31.088	-20.418	-16.154	-25.965	HYDROMAGNESITE	-24.220	-16.166	-9.726	-16.527
Mg$_3$(AsO4)$_2$	-21.167	-12.687	-12.653	-26.317	MAGNESITE	-3.467	-1.856	-0.568	-1.928
FeAsO$_4$	-12.293	-8.677	-10.267	-18.051	NESQUEHONITE	-6.257	-4.646	-3.358	-4.718
Cd$_3$(AsO$_4$)$_2$	-30.820	-19.850	-18.772	-28.260	ARAGONITE	-2.353	-0.598	1.425	1.369
Cu$_3$(AsO$_4$)$_2$	-21.250	-16.606	-19.942	-30.064	CALCITE	-2.215	-0.459	1.564	1.508
Al$_2$(SeO$_3$)$_3$	-11.304	-17.373	-26.787	-42.069	DOLOMITE (ordered)	-4.526	-1.160	2.152	0.735
CaSeO$_3$	-3.026	-2.678	-3.096	-7.471	DOLOMITE (disordered)	-5.076	-1.710	1.602	0.185
CaSeO$_3$:H$_2$O	-3.836	-3.488	-3.906	-8.281	HUNTITE	-13.501	-6.913	-1.026	-5.164
CdSeO$_3$	-9.358	-8.325	-9.129	-13.416	STRONTIANITE	-3.562	-1.803	0.306	0.727
CuSeO$_3$	-7.368	-8.443	-10.719	-15.217	WITHERITE	-5.277	-3.636	-1.436	-0.725
Fe$_2$(SeO$_3$)$_3$	-14.409	-15.048	-21.719	-40.659	THERMONATRITE	-15.896	-14.223	-11.475	-12.822
Fe$_2$(SeO$_3$)$_3$.6H$_2$O	-42.090	-42.728	-49.399	-68.339	AlOHSO$_4$	-3.278	-6.275	-10.206	-16.067
MgSeO$_3$	-3.353	-3.151	-4.303	-9.981	Al$_4$(OH)$_{10}$SO$_4$	2.484	-3.281	-10.351	-19.703
Na$_2$SeO$_3$	-11.736	-11.470	-11.163	-16.828	Zn$_2$(OH)$_2$SO$_4$	-10.653	-8.173	-8.677	-14.839
ZnSeO$_3$	-4.414	-3.546	-4.795	-9.846	Zn$_4$(OH)$_6$SO$_4$	-17.634	-10.601	-8.722	-16.350
ZnSeO$_3$.H$_2$O	-6.974	-6.106	-7.355	-12.406	Zn$_3$O(SO$_4$)$_2$	-32.179	-29.496	-31.694	-43.286
SeO$_2$	-13.359	-14.767	-17.207	-21.525	ZINCOSITE	-14.042	-13.839	-15.534	-20.963
Al(OH)$_3$ (am)	-0.236	-1.159	-2.205	-3.369	ZnSO$_4$.H$_2$O	-9.475	-9.272	-10.966	-16.395
BOEHMITE	1.986	1.063	0.017	-1.147	BIANCHITE	-8.348	-8.145	-9.839	-15.269
DIASPORE	3.691	2.768	1.722	0.558	GOSLARITE	-8.102	-7.899	-9.593	-15.022
GIBBSITE	2.273	1.350	0.304	-0.860	Cd$_3$(OH)$_4$SO$_4$	-29.323	-24.074	-22.052	-26.653
Zn(OH)$_2$ (am)	-5.514	-3.238	-2.047	-2.780	Cd$_3$OH$_2$(SO$_4$)$_2$	-30.545	-27.370	-28.233	-37.531
Zn(OH)$_2$	-5.240	-2.964	-1.773	-2.506	Cd$_4$(OH)$_6$SO$_4$	-31.727	-24.037	-20.379	-24.948
Zn(OH)$_2$ (beta)	-4.794	-2.518	-1.327	-2.060	CdSO$_4$	-13.464	-13.097	-14.346	-19.011
Zn(OH)$_2$ (gamma)	-4.774	-2.498	-1.307	-2.040	CdSO$_4$.H$_2$O	-11.910	-11.543	-12.792	-17.457
Zn(OH)$_2$ (epsilon)	-4.574	-2.298	-1.107	-1.840	CdSO$_4$.2.67H$_2$O	-11.763	-11.396	-12.645	-17.310
ZnO (active)	-4.229	-1.952	-0.761	-1.494	ANTLERITE	-8.321	-9.398	-11.790	-17.025
ZINCITE	-4.374	-2.098	-0.907	-1.640	BROCHANTITE	-8.908	-9.654	-11.881	-17.295
Cd(OH)$_2$ (am)	-10.294	-7.853	-6.217	-6.185	LANGITE	-11.175	-11.920	-14.148	-19.562
Cd(OH)$_2$	-10.208	-7.767	-6.131	-6.099	CuOCuSO$_4$	-15.682	-17.092	-19.648	-24.704
MONTEPONITE	-11.667	-9.226	-7.590	-7.558	CuSO$_4$	-14.165	-15.907	-18.628	-23.504
Cu(OH)$_2$	-2.828	-2.495	-2.331	-2.510	CHALCANTHITE	-8.586	-10.327	-13.048	-17.924
TENORITE	-1.798	-1.465	-1.301	-1.480	Fe$_2$(SO$_4$)$_3$	-38.570	-41.206	-49.212	-69.286
FERRIHYDRITE	1.265	3.058	3.383	0.391	H-JAROSITE	-8.676	-7.445	-12.241	-30.611
GOETHITE	3.965	5.758	6.083	3.091	Na-JAROSITE	-6.381	-4.314	-7.736	-26.780
Cr(OH)$_3$ (am)	-1.056	0.911	1.197	-0.754	EPSOMITE	-4.226	-4.688	-6.286	-12.342
Cr(OH)$_3$	-3.142	-1.175	-0.888	-2.840	ANHYDRITE	-1.754	-2.072	-2.935	-7.688
BRUCITE	-6.123	-4.513	-3.225	-4.585	GYPSUM	-1.505	-1.823	-2.685	-7.438
PERICLASE	-10.863	-9.253	-7.965	-9.325	CELESTITE	-1.637	-1.952	-2.728	-7.003
Mg(OH)$_2$ (active)	-8.073	-6.463	-5.175	-6.535	BARITE	0.708	0.275	-0.410	-4.395
LIME	-21.741	-19.986	-17.962	-18.019	MIRABILITE	-9.571	-9.970	-10.108	-16.152
PORTLANDITE	-11.846	-10.091	-8.067	-8.124	THENARDITE	-11.006	-11.406	-11.544	-17.587
Ba(OH)$_2$.8H$_2$O	-16.594	-14.953	-12.753	-12.041	CuSeO$_3$.2H$_2$O	-7.899	-8.975	-11.251	-15.749
As$_2$O$_5$	-39.725	-36.078	-39.908	-49.491	Fe$_2$(SeO$_3$)$_3$.2H$_2$O	-10.163	-10.802	-17.473	-36.413
Al$_2$O$_3$	1.476	-0.370	-2.462	-4.790	Fe$_2$(OH)$_4$SeO$_3$	-5.875	-3.698	-5.488	-15.791
HEMATITE	10.331	13.916	14.566	8.581	MgSeO$_3$.6H$_2$O	-5.569	-5.366	-6.518	-12.197
MAGHEMITE	2.527	6.112	6.762	0.777	CaSeO$_3$.2H$_2$O	-5.090	-4.742	-5.159	-9.534
LEPIDOCROCITE	3.085	4.878	5.203	2.211	SrSeO$_3$	-6.719	-6.368	-6.699	-10.596
Cr$_2$O$_3$	-1.254	2.680	3.252	-0.651	BaSeO$_3$	-7.264	-7.031	-7.271	-10.878
SPINEL	-4.998	-5.234	-6.038	-9.726	Na$_2$SeO$_3$.5H$_2$O	-17.146	-16.880	-16.573	-22.238
MAGNESIOFERRITE	2.774	7.970	9.908	2.563	Zn$_3$(PO$_4$)$_2$.4H$_2$O	-6.590	-2.816	-4.872	-17.658
NATRON	-13.949	-12.275	-9.527	-10.874	Cd$_3$(PO$_4$)$_2$	-19.979	-15.713	-16.434	-26.927
CUPRIC FERRITE	8.771	12.688	13.503	7.339	Cu$_3$(PO$_4$)$_2$	-8.499	-10.559	-15.694	-26.821
MgCr$_2$O$_4$	-9.092	-3.547	-1.687	-6.950	Cu$_3$(PO$_4$)$_2$.3H$_2$O	-10.229	-12.289	-17.424	-28.551
ZnCl2	-20.581	-21.349	-23.149	-28.646	STRENGITE	-0.588	-0.323	-2.813	-11.099
Zn$_2$(OH)$_3$Cl	-11.517	-8.486	-7.600	-11.448	Mg$_3$(PO$_4$)$_2$	-7.447	-5.670	-7.435	-22.104
Zn$_5$(OH)$_8$Cl$_2$	-24.192	-15.854	-12.890	-21.319	MgHPO$_4$.3H$_2$O	-2.549	-2.466	-3.992	-10.647
CdCl$_2$	-16.395	-17.000	-18.355	-23.087	HYDROXYLAPATITE	4.789	8.984	10.657	-5.509
CdCl$_2$.H$_2$O	-15.361	-15.965	-17.320	-22.053	CaHPO$_4$.2H$_2$O	-1.492	-1.264	-2.055	-7.406
CdCl$_2$.2.5H$_2$O	-15.141	-15.746	-17.100	-21.833	CaHPO$_4$	-1.212	-0.984	-1.775	-7.126
CdOHCl	-10.346	-9.428	-9.287	-11.638	Ca$_3$(PO$_4$)$_2$ (beta)	-1.095	1.116	1.557	-9.201
MELANOTHALLITE	-20.901	-23.614	-26.441	-31.384	Ca$_4$H(PO$_4$)$_3$.3H$_2$O	-3.422	-0.983	-1.333	-17.442
ATACAMITE	-5.943	-6.802	-7.968	-10.709	SrHPO$_4$	-3.334	-3.103	-3.809	-8.681
Fe(OH)$_{2.7}$Cl$_{0.3}$	4.423	5.759	5.635	1.928	BaHPO$_4$	-3.869	-3.756	-4.370	-8.953
CrCl$_3$	-47.656	-50.257	-54.457	-63.555	AlAsO$_4$.2H$_2$O	-10.745	-9.845	-12.806	-18.761
HALITE	-8.654	-9.340	-9.461	-12.517	Zn$_3$(AsO$_4$)$_2$.2.5H$_2$O	-25.790	-15.313	-15.570	-27.352
SMITHSONITE	-4.688	-2.411	-1.220	-1.953	Cu$_3$(AsO$_4$)$_2$.2H$_2$O	-21.580	-16.936	-20.272	-30.394
ZnCO$_3$.H$_2$O	-4.428	-2.151	-0.960	-1.693	FeAsO$_4$.2H$_2$O	-12.453	-8.837	-10.427	-18.211
OTAVITE	-6.211	-3.770	-2.134	-2.102	Ca$_3$(AsO$_4$)$_2$.4H$_2$O	-22.446	-13.531	-11.291	-21.045
CuCO$_3$	-4.301	-3.969	-3.804	-3.984	Ba$_3$(AsO$_4$)$_2$	-0.708	7.862	10.633	3.183
MALACHITE	-4.648	-3.984	-3.655	-4.014					

Table H-10. Saturation indices for all minerals calculated using MINTEQA2: Presque Isle-Red Wing.

Solid/Mineral	Saturation Index				Solid/Mineral	Saturation Index			
	PR-1	PR-2	DR-3	DR-4		PR-1	PR-2	PR-3	PR-4
	pH 6.07	pH 8.37	pH 10.78	pH 11.85		pH 6.07	pH 8.37	pH 10.78	pH 11.85
CaNaAsO$_4$.7.5H$_2$O	-14.163	-7.407		-13.646	AZURITE	-11.214	-3.344		-6.074
Ca$_5$(AsO$_4$)$_3$OH	-32.153	-9.934		-26.186	ARTINITE	-12.437	-4.815		-6.926
Ca$_4$(OH)$_2$(AsO$_4$)$_2$:4H$_2$O	-32.555	-15.121		-25.071	HYDROMAGNESITE	-30.797	-11.743		-17.021
Mg$_3$(AsO4)$_2$	-23.528	-10.386		-28.808	MAGNESITE	-4.782	-0.971		-2.027
FeAsO$_4$	-10.067	-9.689		-19.855	NESQUEHONITE	-7.573	-3.761		-4.817
Cd$_3$(AsO$_4$)$_2$	-26.737	-17.725		-30.452	ARAGONITE	-3.116	0.815		2.141
Cu$_3$(AsO$_4$)$_2$	-22.030	-12.450		-30.434	CALCITE	-2.977	0.954		2.280
Al$_2$(SeO$_3$)$_3$	-9.599	-22.810		-44.721	DOLOMITE (ordered)	-6.604	1.138		1.408
CaSeO$_3$	-3.205	-2.364		-7.327	DOLOMITE (disordered)	-7.154	0.588		0.858
CaSeO$_3$:H$_2$O	-4.015	-3.174		-8.138	HUNTITE	-18.209	-2.847		-4.688
CdSeO$_3$	-7.941	-8.597		-14.044	STRONTIANITE	-4.773	-0.398		1.522
CuSeO$_3$	-7.572	-8.038		-15.238	WITHERITE	-6.254	-2.184		-0.035
Fe$_2$(SeO$_3$)$_3$	-9.789	-20.012		-43.960	THERMONATRITE	-16.323	-12.384		-12.260
Fe$_2$(SeO$_3$)$_3$.6H$_2$O	-37.471	-47.693		-71.640	AlOHSO$_4$	-2.572	-8.408		-16.801
MgSeO$_3$	-4.084	-3.364		-10.709	Al$_4$(OH)$_{10}$SO$_4$	3.118	-8.628		-21.584
Na$_2$SeO$_3$	-11.578	-10.730		-16.895	Zn$_2$(OH)$_2$SO$_4$	-12.592	-9.795		-17.516
ZnSeO$_3$	-5.164	-4.924		-11.637	Zn$_4$(OH)$_6$SO$_4$	-22.241	-12.782		-21.352
ZnSeO$_3$.H$_2$O	-7.725	-7.484		-14.198	Zn$_3$O(SO$_4$)$_2$	-34.723	-32.460		-47.477
SeO$_2$	-12.775	-15.865		-22.154	ZINCOSITE	-14.647	-15.181		-22.478
Al(OH)$_3$ (am)	-0.260	-2.230		-3.751	ZnSO$_4$.H$_2$O	-10.080	-10.614		-17.910
BOEHMITE	1.962	-0.008		-1.529	BIANCHITE	-8.954	-9.487		-16.783
DIASPORE	3.667	1.697		0.176	GOSLARITE	-8.708	-9.241		-16.537
GIBBSITE	2.249	0.279		-1.242	Cd$_3$(OH)$_4$SO$_4$	-26.096	-22.658		-27.002
Zn(OH)$_2$ (am)	-6.849	-3.518		-3.942	Cd$_3$OH$_2$(SO$_4$)$_2$	-26.589	-27.016		-38.232
Zn(OH)$_2$	-6.575	-3.244		-3.668	Cd$_4$(OH)$_6$SO$_4$	-27.667	-21.795		-25.297
Zn(OH)$_2$ (beta)	-6.129	-2.798		-3.222	CdSO$_4$	-11.902	-13.332		-19.362
Zn(OH)$_2$ (gamma)	-6.109	-2.778		-3.202	CdSO$_4$.H$_2$O	-10.348	-11.779		-17.808
Zn(OH)$_2$ (epsilon)	-5.909	-2.578		-3.002	CdSO$_4$.2.67H$_2$O	-10.201	-11.632		-17.661
ZnO (active)	-5.563	-2.232		-2.656	ANTLERITE	-9.957	-5.951		-15.553
ZINCITE	-5.708	-2.378		-2.802	BROCHANTITE	-11.333	-4.703		-15.215
Cd(OH)$_2$ (am)	-9.461	-7.027		-6.184	LANGITE	-13.600	-6.970		-17.482
Cd(OH)$_2$	-9.375	-6.941		-6.098	CuOCuSO$_4$	-16.530	-15.148		-23.840
MONTEPONITE	-10.834	-8.400		-7.558	CuSO$_4$	-14.224	-15.466		-23.248
Cu(OH)$_2$	-3.616	-0.992		-1.902	CHALCANTHITE	-8.646	-9.887		-17.668
TENORITE	-2.586	0.038		-0.872	Fe$_2$(SO$_4$)$_3$	-33.513	-46.062		-71.757
FERRIHYDRITE	2.699	2.223		-0.317	H-JAROSITE	-2.916	-12.075		-33.437
GOETHITE	5.399	4.923		2.383	Na-JAROSITE	-0.835	-8.025		-29.325
Cr(OH)$_3$ (am)	-0.573	1.474		-0.836	EPSOMITE	-4.813	-4.866		-12.793
Cr(OH)$_3$	-2.658	-0.612		-2.921	ANHYDRITE	-1.788	-1.722		-7.268
BRUCITE	-7.439	-3.628		-4.684	GYPSUM	-1.538	-1.472		-7.018
PERICLASE	-12.179	-8.368		-9.424	CELESTITE	-2.119	-1.608		-6.561
Mg(OH)$_2$ (active)	-9.389	-5.578		-6.634	BARITE	0.461	0.665		-4.057
LIME	-22.504	-18.573		-17.247	MIRABILITE	-9.270	-9.194		-15.942
PORTLANDITE	-12.609	-8.678		-7.352	THENARDITE	-10.703	-10.630		-17.377
Ba(OH)$_2$.8H$_2$O	-17.573	-13.502		-11.352	CuSeO$_3$.2H$_2$O	-8.104	-8.570		-15.770
As$_2$O$_5$	-38.140	-36.431		-51.685	Fe$_2$(SeO$_3$)$_3$.2H$_2$O	-5.543	-15.766		-39.714
Al$_2$O$_3$	1.429	-2.512		-5.554	Fe$_2$(OH)$_4$SeO$_3$	-2.424	-6.466		-17.835
HEMATITE	13.199	12.246		7.167	MgSeO$_3$.6H$_2$O	-6.301	-5.579		-12.925
MAGHEMITE	5.395	4.442		-0.637	CaSeO$_3$.2H$_2$O	-5.269	-4.428		-9.391
LEPIDOCROCITE	4.519	4.043		1.503	SrSeO$_3$	-7.346	-6.060		-10.430
Cr$_2$O$_3$	-0.287	3.806		-0.814	BaSeO$_3$	-7.656	-6.677		-10.817
SPINEL	-6.361	-6.491		-10.589	Na$_2$SeO$_3$.5H$_2$O	-16.990	-16.140		-22.305
MAGNESIOFERRITE	4.327	7.184		1.049	Zn$_3$(PO$_4$)$_2$.4H$_2$O	-8.130	-5.623		-22.133
NATRON	-14.377	-10.437		-10.312	Cd$_3$(PO$_4$)$_2$	-15.018	-15.202		-27.912
CUPRIC FERRITE	10.851	12.521		6.532	Cu$_3$(PO$_4$)$_2$	-8.401	-8.017		-25.985
MgCr$_2$O$_4$	-9.440	-1.537		-7.212	Cu$_3$(PO$_4$)$_2$.3H$_2$O	-10.132	-9.747		-27.715
ZnCl2	-19.742	-21.671		-29.247	STRENGITE	2.077	-2.142		-12.300
Zn$_2$(OH)$_3$Cl	-13.099	-9.067		-13.492	Mg$_3$(PO$_4$)$_2$	-8.929	-4.983		-23.388
Zn$_5$(OH)$_8$Cl$_2$	-28.691	-17.295		-26.569	MgHPO$_4$.3H$_2$O	-2.633	-2.565		-11.239
CdCl$_2$	-13.390	-16.215		-22.525	HYDROXYLAPATITE	4.671	13.095		-3.131
CdCl$_2$.H$_2$O	-12.356	-15.181		-21.490	CaHPO$_4$.2H$_2$O	-1.023	-0.835		-7.128
CdCl$_2$.2.5H$_2$O	-12.136	-14.961		-21.271	CaHPO$_4$	-0.743	-0.555		-6.848
CdOHCl	-8.427	-8.623		-11.356	Ca$_3$(PO$_4$)$_2$ (beta)	-0.920	3.386		-7.873
MELANOTHALLITE	-19.517	-22.153		-30.215	Ca$_4$H(PO$_4$)$_3$.3H$_2$O	-2.778	1.716		-15.836
ATACAMITE	-6.434	-3.816		-9.212	SrHPO$_4$	-3.313	-2.681		-8.380
Fe(OH)$_{2.7}$Cl$_{0.3}$	6.182	4.917		1.305	BaHPO$_4$	-3.614	-3.288		-8.757
CrCl$_3$	-43.914	-49.757		-62.794	AlAsO$_4$.2H$_2$O	-9.977	-11.093		-20.241
HALITE	-7.781	-8.441		-11.955	Zn$_3$(AsO$_4$)$_2$.2.5H$_2$O	-28.208	-16.506		-33.033
SMITHSONITE	-6.022	-2.691		-3.115	Cu$_3$(AsO$_4$)$_2$.2H$_2$O	-22.360	-12.780		-30.764
ZnCO$_3$.H$_2$O	-5.762	-2.431		-2.855	FeAsO$_4$.2H$_2$O	-10.227	-9.849		-20.015
OTAVITE	-5.378	-2.944		-2.101	Ca$_3$(AsO$_4$)$_2$.4H$_2$O	-23.150	-9.647		-20.923
CuCO$_3$	-5.089	-2.466		-3.376	Ba$_3$(AsO$_4$)$_2$	-2.053	11.864		3.058
MALACHITE	-6.225	-0.978		-2.798					

Table H-11. Saturation indices for all minerals calculated using MINTEQA2: Presque Isle-MnRoad.

Solid/Mineral	Saturation Index				Solid/Mineral	Saturation Index			
	PM-1	PM-2	PM-3	PM-4		PM-1	PM-2	PM-3	PM-4
	pH 6.17	pH 8.34	pH 9.66	pH 11.96		pH 6.17	pH 8.34	pH 9.66	pH 11.96
$CaNaAsO_4.7.5H_2O$	-13.521	-7.755	-7.887	-13.864	AZURITE	-10.599	-3.515	-4.784	-5.374
$Ca_5(AsO_4)_3OH$	-29.777	-10.134	-11.517	-26.496	ARTINITE	-11.881	-4.513	-4.131	-6.664
$Ca_4(OH)_2(AsO_4)_2:4H_2O$	-30.852	-15.279	-15.406	-25.597	HYDROMAGNESITE	-29.407	-10.986	-10.034	-16.365
$Mg_3(AsO4)_2$	-21.703	-9.942	-14.266	-26.985	MAGNESITE	-4.504	-0.82	-0.629	-1.896
$FeAsO_4$	-12.913	-10.894	-13.897	-18.916	NESQUEHONITE	-7.294	-3.61	-3.419	-4.686
$Cd_3(AsO_4)_2$	-25.567	-17.892	-20.128	-29.025	ARAGONITE	-2.938	0.778	1.969	1.661
$Cu_3(AsO_4)_2$	-20.424	-12.631	-18.794	-28.306	CALCITE	-2.799	0.917	2.108	1.8
$Al_2(SeO_3)_3$	-9.958	-23.016	-31.628	-46.446	DOLOMITE (ordered)	-6.148	1.252	2.634	1.06
$CaSeO_3$	-3.007	-2.341	-3.325	-7.759	DOLOMITE (disordered)	-6.698	0.702	2.084	0.51
$CaSeO_3:H_2O$	-3.817	-3.151	-4.135	-8.569	HUNTITE	-17.197	-2.43	-0.667	-4.773
$CdSeO_3$	-7.861	-8.589	-9.878	-13.997	STRONTIANITE	-4.619	-0.583	0.979	0.973
$CuSeO_3$	-7.347	-8.035	-10.634	-14.957	WITHERITE	-6.233	-2.514	-0.722	-0.636
$Fe_2(SeO_3)_3$	-16.412	-22.233	-29.871	-43.368	THERMONATRITE	-16.386	-12.998	-10.75	-13.168
$Fe_2(SeO_3)_3.6H_2O$	-44.094	-49.913	-57.551	-71.048	$AlOHSO_4$	-2.95	-8.536	-12.171	-17.857
$MgSeO_3$	-3.786	-3.152	-5.137	-10.530	$Al_4(OH)_{10}SO_4$	2.113	-9.337	-16.099	-25.444
Na_2SeO_3	-11.621	-11.283	-11.211	-17.755	$Zn_2(OH)_2SO_4$	-12.482	-12.442	-13.599	-18.197
$ZnSeO_3$	-5.006	-6.220	-7.678	-11.870	$Zn_4(OH)_6SO_4$	-21.853	-18.143	-17.864	-22.593
$ZnSeO_3.H_2O$	-7.566	-8.780	-10.238	-14.430	$Zn_3O(SO_4)_2$	-34.641	-36.398	-39.43	-48.56
SeO_2	-12.755	-15.804	-17.980	-22.106	ZINCOSITE	-14.676	-16.472	-18.347	-22.879
$Al(OH)_3$ (am)	-0.469	-2.424	-3.466	-4.686	$ZnSO_4.H_2O$	-10.108	-11.904	-13.779	-18.311
BOEHMITE	1.753	-0.202	-1.244	-2.464	BIANCHITE	-8.983	-10.777	-12.652	-17.184
DIASPORE	3.458	1.503	0.461	-0.759	GOSLARITE	-8.737	-10.531	-12.406	-16.938
GIBBSITE	2.040	0.085	-0.957	-2.177	$Cd_3(OH)_4SO_4$	-26.084	-22.749	-22.683	-27.126
$Zn(OH)_2$ (am)	-6.710	-4.874	-4.156	-4.222	$Cd_3OH_2(SO_4)_2$	-26.745	-27.041	-29.568	-38.478
$Zn(OH)_2$	-6.436	-4.600	-3.882	-3.948	$Cd_4(OH)_6SO_4$	-27.596	-21.938	-20.986	-25.421
$Zn(OH)_2$ (beta)	-5.990	-4.154	-3.436	-3.502	$CdSO_4$	-12.01	-13.319	-15.026	-19.484
$Zn(OH)_2$ (gamma)	-5.970	-4.134	-3.416	-3.482	$CdSO_4.H_2O$	-10.456	-11.765	-13.472	-17.93
$Zn(OH)_2$ (epsilon)	-5.770	-3.934	-3.216	-3.282	$CdSO_4.2.67H_2O$	-10.309	-11.618	-13.325	-17.783
ZnO (active)	-5.424	-3.589	-2.871	-2.936	ANTLERITE	-9.509	-6.056	-9.918	-14.975
ZINCITE	-5.570	-3.734	-3.016	-3.082	BROCHANTITE	-10.681	-4.865	-9.15	-14.404
$Cd(OH)_2$ (am)	-9.401	-7.079	-6.193	-6.185	LANGITE	-12.947	-7.132	-11.417	-16.671
$Cd(OH)_2$	-9.315	-6.993	-6.107	-6.099	$CuOCuSO_4$	-16.287	-15.196	-18.635	-23.495
MONTEPONITE	-10.775	-8.452	-7.566	-7.558	$CuSO_4$	-14.187	-15.457	-18.473	-23.136
$Cu(OH)_2$	-3.411	-1.049	-1.472	-1.669	CHALCANTHITE	-8.609	-9.877	-12.893	-17.557
TENORITE	-2.381	-0.019	-0.442	-0.639	$Fe_2(SO_4)_3$	-40.7	-48.265	-57.155	-71.672
FERRIHYDRITE	-0.643	1.022	0.467	-0.092	H-JAROSITE	-13.276	-15.545	-22.396	-33.006
GOETHITE	2.058	3.722	3.167	2.608	Na-JAROSITE	-11.226	-11.801	-17.529	-29.348
$Cr(OH)_3$ (am)	-1.855	0.873	0.716	-1.357	EPSOMITE	-4.702	-4.648	-7.051	-12.783
$Cr(OH)_3$	-3.940	-1.212	-1.370	-3.443	ANHYDRITE	-1.778	-1.693	-3.094	-7.869
BRUCITE	-7.161	-3.477	-3.286	-4.552	GYPSUM	-1.528	-1.443	-2.844	-7.619
PERICLASE	-11.901	-8.217	-8.026	-9.292	CELESTITE	-2.132	-1.728	-2.758	-7.232
$Mg(OH)_2$ (active)	-9.111	-5.427	-5.236	-6.502	BARITE	0.313	0.402	-0.399	-4.78
LIME	-22.326	-18.610	-17.418	-17.727	MIRABILITE	-9.5	-9.742	-10.087	-16.971
PORTLANDITE	-12.431	-8.715	-7.523	-7.831	THENARDITE	-10.933	-11.177	-11.522	-18.407
$Ba(OH)_2.8H_2O$	-17.552	-13.831	-12.038	-11.952	$CuSeO_3.2H_2O$	-7.879	-8.567	-11.165	-15.489
As_2O_5	-37.150	-36.441	-41.336	-50.256	$Fe_2(SeO_3)_3.2H_2O$	-12.167	-17.986	-25.624	-39.121
Al_2O_3	1.010	-2.900	-4.984	-7.424	$Fe_2(OH)_4SeO_3$	-9.087	-8.807	-12.094	-17.338
HEMATITE	6.516	9.844	8.734	7.616	$MgSeO_3.6H_2O$	-6.003	-5.368	-7.353	-12.745
MAGHEMITE	-1.288	2.040	0.930	-0.188	$CaSeO_3.2H_2O$	-5.071	-4.405	-5.388	-9.823
LEPIDOCROCITE	1.178	2.842	2.287	1.728	$SrSeO_3$	-7.172	-6.185	-6.799	-10.932
Cr_2O_3	-2.851	2.604	2.289	-1.857	$BaSeO_3$	-7.616	-6.946	-7.33	-11.37
SPINEL	-6.502	-6.728	-8.622	-12.327	$Na_2SeO_3.5H_2O$	-17.032	-16.693	-16.621	-23.165
MAGNESIOFERRITE	-2.078	4.934	4.014	1.629	$Zn_3(PO_4)_2.4H_2O$	-7.454	-9.387	-14.101	-23.726
NATRON	-14.440	-11.050	-8.802	-11.220	$Cd_3(PO_4)_2$	-14.58	-15.054	-19.262	-28.667
CUPRIC FERRITE	4.373	10.063	8.529	7.214	$Cu_3(PO_4)_2$	-7.527	-7.882	-16.019	-26.038
$MgCr_2O_4$	-11.725	-2.587	-2.712	-8.124	$Cu_3(PO_4)_2.3H_2O$	-9.258	-9.612	-17.749	-27.768
ZnCl2	-20.066	-23.521	-25.755	-30.435	STRENGITE	-1.135	-3.19	-7.179	-12.452
$Zn_2(OH)_3Cl$	-13.053	-12.027	-12.067	-14.506	$Mg_3(PO_4)_2$	-7.836	-4.224	-10.52	-23.747
$Zn_5(OH)_8Cl_2$	-28.459	-24.572	-23.934	-28.877	$MgHPO_4.3H_2O$	-2.226	-2.261	-5.504	-11.484
$CdCl_2$	-13.793	-16.761	-18.827	-23.434	HYDROXYLAPATITE	5.948	13.369	9.026	-6.656
$CdCl_2.H_2O$	-12.759	-15.727	-17.792	-22.399	$CaHPO_4.2H_2O$	-0.716	-0.719	-2.961	-7.983
$CdCl_2.2.5H_2O$	-12.539	-15.507	-17.573	-22.179	$CaHPO_4$	-0.435	-0.439	-2.681	-7.703
CdOHCl	-8.599	-8.922	-9.512	-11.811	$Ca_3(PO_4)_2$ (beta)	-0.128	3.581	0.289	-10.064
MELANOTHALLITE	-19.774	-22.704	-26.078	-30.890	$Ca_4H(PO_4)_3.3H_2O$	-1.679	2.027	-3.508	-18.882
ATACAMITE	-6.255	-4.177	-6.499	-9.200	$SrHPO_4$	-3.03	-2.714	-4.585	-9.306
$Fe(OH)_{2.7}Cl_{0.3}$	2.771	3.642	2.644	1.393	$BaHPO_4$	-3.465	-3.465	-5.106	-9.734
$CrCl_3$	-45.889	-51.098	-55.683	-64.678	$AlAsO_4.2H_2O$	-9.691	-11.291	-14.781	-20.461
HALITE	-8.043	-8.995	-9.347	-12.863	$Zn_3(AsO_4)_2.2.5H_2O$	-26.801	-20.585	-23.326	-32.444
SMITHSONITE	-5.883	-4.047	-3.330	-3.395	$Cu_3(AsO_4)_2.2H_2O$	-20.754	-12.961	-19.124	-28.636
$ZnCO_3.H_2O$	-5.623	-3.787	-3.070	-3.135	$FeAsO_4.2H_2O$	-13.073	-11.054	-14.057	-19.076
OTAVITE	-5.318	-2.996	-2.110	-2.102	$Ca_3(AsO_4)_2.4H_2O$	-21.625	-9.768	-11.087	-20.932
$CuCO_3$	-4.884	-2.523	-2.946	-3.143	$Ba_3(AsO_4)_2$	-1.002	10.866	11.348	2.686
MALACHITE	-5.815	-1.092	-1.938	-2.332					

Table H-12. Saturation indices for all minerals calculated using MINTEQA2: Presque Isle-sand.

Solid/Mineral	Saturation Index				Solid/Mineral	Saturation Index			
	PS-1	PS-2	PS-3	PS-4		PS-1	PS-2	PS-3	PS-4
	pH 6.98	pH 9.22	pH 11.03	pH 12.07		pH 6.98	pH 9.22	pH 11.03	pH 12.07
$CaNaAsO_4.7.5H_2O$	-12.844	-8.251	-11.373	-15.337	AZURITE	-10.893	-7.364	-7.482	-8.473
$Ca_5(AsO_4)_3OH$	-26.607	-11.069	-19.963	-29.396	ARTINITE	-10.364	-2.591	-4.431	-8.003
$Ca_4(OH)_2(AsO_4)_2:4H_2O$	-28.243	-15.18	-20.891	-27.381	HYDROMAGNESITE	-25.615	-6.184	-10.782	-19.713
$Mg_3(AsO4)_2$	-19.791	-11.295	-21.075	-31.717	MAGNESITE	-3.746	0.141	-0.779	-2.565
$FeAsO_4$	-11.319	-11.927	-17.088	-20.599	NESQUEHONITE	-6.536	-2.649	-3.569	-5.355
$Cd_3(AsO_4)_2$	-20.007	-19.598	-26.464	-31.749	ARAGONITE	-2.195	1.861	2.188	1.887
$Cu_3(AsO_4)_2$	-21.080	-20.714	-27.853	-34.127	CALCITE	-2.057	2.000	2.327	2.026
$Al_2(SeO_3)_3$	-12.244	-24.000	-37.385	-45.100	DOLOMITE (ordered)	-4.647	3.295	2.703	0.615
$CaSeO_3$	-2.933	-2.236	-5.422	-7.712	DOLOMITE (disordered)	-5.197	2.745	2.153	0.065
$CaSeO_3:H_2O$	-3.743	-3.046	-6.232	-8.522	HUNTITE	-14.180	1.535	-0.897	-6.557
$CdSeO_3$	-6.556	-8.725	-12.186	-14.175	STRONTIANITE	-3.071	1.111	1.805	1.757
$CuSeO_3$	-8.114	-10.297	-13.849	-16.168	WITHERITE	-4.870	-0.542	0.391	0.535
$Fe_2(SeO_3)_3$	-14.868	-22.999	-36.841	-44.545	THERMONATRITE	-16.157	-11.922	-11.799	-13.841
$Fe_2(SeO_3)_3.6H_2O$	-42.549	-50.679	-64.521	-72.225	$AlOHSO_4$	-3.996	-9.228	-14.266	-17.287
$MgSeO_3$	-3.697	-3.170	-7.603	-11.378	$Al_4(OH)_{10}SO_4$	0.648	-7.102	-16.407	-22.051
Na_2SeO_3	-12.061	-11.186	-14.576	-18.607	$Zn_2(OH)_2SO_4$	-9.472	-8.689	-12.573	-16.244
$ZnSeO_3$	-3.716	-4.487	-8.135	-10.886	$Zn_4(OH)_6SO_4$	-14.926	-8.968	-13.121	-18.316
$ZnSeO_3.H_2O$	-6.276	-7.048	-10.695	-13.446	$Zn_3O(SO_4)_2$	-30.580	-31.602	-39.236	-45.816
SeO_2	-13.424	-16.783	-20.296	-22.285	ZINCOSITE	-13.625	-15.430	-19.179	-22.088
$Al(OH)_3$ (am)	-0.608	-1.448	-2.871	-3.745	$ZnSO_4.H_2O$	-9.057	-10.862	-14.611	-17.520
BOEHMITE	1.614	0.774	-0.648	-1.523	BIANCHITE	-7.930	-9.735	-13.484	-16.394
DIASPORE	3.319	2.479	1.057	0.182	GOSLARITE	-7.684	-9.489	-13.238	-16.147
GIBBSITE	1.901	1.061	-0.362	-1.236	$Cd_3(OH)_4SO_4$	-21.068	-21.890	-25.350	-27.498
$Zn(OH)_2$ (am)	-4.751	-2.163	-2.298	-3.060	$Cd_3OH_2(SO_4)_2$	-22.636	-27.850	-34.925	-39.221
$Zn(OH)_2$	-4.477	-1.889	-2.024	-2.786	$Cd_4(OH)_6SO_4$	-20.605	-20.236	-23.644	-25.793
$Zn(OH)_2$ (beta)	-4.031	-1.443	-1.578	-2.340	$CdSO_4$	-10.943	-14.145	-17.708	-19.856
$Zn(OH)_2$ (gamma)	-4.011	-1.423	-1.558	-2.320	$CdSO_4.H_2O$	-9.389	-12.591	-16.154	-18.302
$Zn(OH)_2$ (epsilon)	-3.811	-1.223	-1.358	-2.120	$CdSO_4.2.67H_2O$	-9.242	-12.444	-16.007	-18.155
ZnO (active)	-3.465	-0.878	-1.012	-1.774	ANTLERITE	-10.710	-11.574	-15.307	-18.445
ZINCITE	-3.611	-1.023	-1.158	-1.920	BROCHANTITE	-11.979	-11.666	-15.439	-18.907
$Cd(OH)_2$ (am)	-7.427	-6.236	-6.185	-6.185	LANGITE	-14.245	-13.933	-17.705	-21.173
$Cd(OH)_2$	-7.341	-6.150	-6.099	-6.099	$CuOCuSO_4$	-17.391	-19.430	-23.124	-25.932
MONTEPONITE	-8.800	-7.610	-7.558	-7.559	$CuSO_4$	-15.192	-18.408	-22.063	-24.540
$Cu(OH)_2$	-3.509	-2.332	-2.372	-2.702	CHALCANTHITE	-9.613	-12.829	-16.483	-18.961
TENORITE	-2.479	-1.302	-1.342	-1.672	$Fe_2(SO_4)_3$	-39.871	-51.102	-65.248	-73.429
FERRIHYDRITE	1.133	2.106	0.455	-0.414	H-JAROSITE	-9.763	-15.629	-27.811	-34.713
GOETHITE	3.833	4.806	3.155	2.286	Na-JAROSITE	-7.599	-11.348	-23.468	-31.392
$Cr(OH)_3$ (am)	-0.733	1.084	-0.256	-1.230	EPSOMITE	-4.850	-5.356	-9.890	-13.824
$Cr(OH)_3$	-2.819	-1.002	-2.341	-3.315	ANHYDRITE	-1.942	-2.278	-5.566	-8.015
BRUCITE	-6.402	-2.516	-3.436	-5.222	GYPSUM	-1.692	-2.028	-5.316	-7.765
PERICLASE	-11.142	-7.256	-8.176	-9.962	CELESTITE	-1.491	-1.702	-4.623	-6.818
$Mg(OH)_2$ (active)	-8.352	-4.466	-5.386	-7.172	BARITE	0.769	0.704	-1.976	-3.981
LIME	-21.583	-17.527	-17.200	-17.501	MIRABILITE	-10.177	-10.335	-13.825	-18.016
PORTLANDITE	-11.688	-7.632	-7.305	-7.606	THENARDITE	-11.612	-11.770	-15.261	-19.452
$Ba(OH)_2.8H_2O$	-16.187	-11.859	-10.925	-10.782	$CuSeO_3.2H_2O$	-8.645	-10.828	-14.381	-16.700
As_2O_5	-37.512	-40.675	-47.696	-52.980	$Fe_2(SeO_3)_3.2H_2O$	-10.622	-18.753	-32.595	-40.299
Al_2O_3	0.731	-0.948	-3.793	-5.542	$Fe_2(OH)_4SeO_3$	-6.204	-7.617	-14.433	-18.159
HEMATITE	10.067	12.013	8.711	6.973	$MgSeO_3.6H_2O$	-5.913	-5.386	-9.819	-13.593
MAGHEMITE	2.263	4.209	0.907	-0.831	$CaSeO_3.2H_2O$	-4.997	-4.300	-7.486	-9.776
LEPIDOCROCITE	2.953	3.926	2.275	1.406	$SrSeO_3$	-6.293	-5.470	-8.290	-10.326
Cr_2O_3	-0.608	3.025	0.347	-1.602	$BaSeO_3$	-6.922	-5.953	-8.533	-10.378
SPINEL	-6.023	-3.816	-7.580	-11.115	$Na_2SeO_3.5H_2O$	-17.472	-16.596	-19.986	-24.017
MAGNESIOFERRITE	2.231	8.063	3.841	0.317	$Zn_3(PO_4)_2.4H_2O$	-5.240	-6.970	-14.639	-21.465
NATRON	-14.209	-9.975	-9.851	-11.894	$Cd_3(PO_4)_2$	-12.320	-18.241	-25.351	-29.893
CUPRIC FERRITE	7.826	10.948	7.607	5.539	$Cu_3(PO_4)_2$	-11.483	-17.447	-24.831	-30.362
$MgCr_2O_4$	-8.725	-1.205	-4.803	-8.538	$Cu_3(PO_4)_2.3H_2O$	-13.213	-19.177	-26.561	-32.092
ZnCl2	-21.118	-23.242	-27.120	-29.947	STRENGITE	-1.190	-4.963	-10.247	-13.386
$Zn_2(OH)_3Cl$	-10.640	-7.821	-9.962	-12.518	$Mg_3(PO_4)_2$	-9.224	-7.058	-17.082	-26.981
$Zn_5(OH)_8Cl_2$	-21.675	-13.450	-17.866	-23.740	$MgHPO_4.3H_2O$	-3.298	-4.158	-8.710	-12.767
$CdCl_2$	-14.829	-18.350	-22.042	-24.108	HYDROXYLAPATITE	4.168	10.211	0.949	-7.369
$CdCl_2.H_2O$	-13.794	-17.316	-21.008	-23.073	$CaHPO_4.2H_2O$	-1.804	-2.494	-5.799	-8.371
$CdCl_2.2.5H_2O$	-13.575	-17.096	-20.788	-22.853	$CaHPO_4$	-1.524	-2.214	-5.519	-8.091
CdOHCl	-8.129	-9.295	-11.115	-12.148	$Ca_3(PO_4)_2$ (beta)	-1.562	1.114	-5.169	-10.614
MELANOTHALLITE	-22.883	-26.418	-30.201	-32.596	$Ca_4H(PO_4)_3.3H_2O$	-4.201	-2.215	-11.804	-19.820
ATACAMITE	-7.956	-7.959	-9.910	-11.603	$SrHPO_4$	-3.313	-3.878	-6.817	-9.134
$Fe(OH)_{2.7}Cl_{0.3}$	4.096	4.362	2.149	0.971	$BaHPO_4$	-3.933	-4.351	-7.050	-9.177
$CrCl_3$	-49.283	-54.535	-61.489	-65.561	$AlAsO_4.2H_2O$	-10.012	-12.432	-17.365	-20.881
HALITE	-9.434	-9.673	-11.483	-13.537	$Zn_3(AsO_4)_2.2.5H_2O$	-21.287	-16.687	-24.112	-31.681
SMITHSONITE	-3.924	-1.337	-1.471	-2.233	$Cu_3(AsO_4)_2.2H_2O$	-21.410	-21.044	-28.183	-34.457
$ZnCO_3.H_2O$	-3.664	-1.077	-1.211	-1.973	$FeAsO_4.2H_2O$	-11.479	-12.087	-17.248	-20.759
OTAVITE	-3.344	-2.154	-2.102	-2.102	$Ca_3(AsO_4)_2.4H_2O$	-19.759	-10.752	-16.792	-22.980
$CuCO_3$	-4.982	-3.806	-3.845	-4.175	$Ba_3(AsO_4)_2$	2.725	12.546	8.327	3.472
MALACHITE	-6.011	-3.658	-3.737	-4.397					

Table H-13. Saturation indices for all minerals calculated using MINTEQA2: Columbia.

Solid/Mineral	Saturation Index			
	C-1	C-2	C-3	C-4
	pH 6.74	pH 8.89	pH 11.13	pH 12.55
CaNaAsO$_4$.7.5H$_2$O	-9.882	-5.467	-7.921	-14.215
Ca$_5$(AsO$_4$)$_3$OH	-21.524	-6.053	-12.453	-28.532
Ca$_4$(OH)$_2$(AsO$_4$)$_2$:4H$_2$O	-24.35	-11.206	-14.909	-26.249
Mg$_3$(AsO4)$_2$	-15.546	-10.363	-21.727	-31.813
FeAsO$_4$	-10.812	-12.338	-17.496	-21.759
Cd$_3$(AsO$_4$)$_2$	-22.053	-13.747	-20.042	-28.825
Cu$_3$(AsO$_4$)$_2$	-17.185	-15.020	-22.692	-36.127
Al$_2$(SeO$_3$)$_3$	-8.971	-22.363	-36.987	-52.831
CaSeO$_3$	-1.398	-1.084	-4.291	-9.078
CaSeO$_3$:H$_2$O	-2.210	-1.894	-5.101	-9.888
CdSeO$_3$	-6.748	-6.631	-10.477	-14.665
CuSeO$_3$	-6.325	-8.255	-12.560	-18.299
Fe$_2$(SeO$_3$)$_3$	-12.384	-23.390	-38.949	-51.258
Fe$_2$(SeO$_3$)$_3$.6H$_2$O	-40.072	-51.076	-66.632	-78.939
MgSeO$_3$	-1.792	-2.716	-8.251	-12.875
Na$_2$SeO$_3$	-7.715	-7.479	-11.222	-18.023
ZnSeO$_3$	-4.258	-4.917	-8.885	-14.335
ZnSeO$_3$.H$_2$O	-6.819	-7.478	-11.445	-16.895
SeO$_2$	-12.655	-16.582	-20.614	-24.486
Al(OH)$_3$ (am)	-0.127	-0.931	-2.194	-4.309
BOEHMITE	2.096	1.291	0.028	-2.087
DIASPORE	3.801	2.996	1.733	-0.382
GIBBSITE	2.382	1.578	0.315	-1.800
Zn(OH)$_2$ (am)	-6.063	-2.794	-2.730	-4.308
Zn(OH)$_2$	-5.789	-2.520	-2.456	-4.034
Zn(OH)$_2$ (beta)	-5.343	-2.074	-2.010	-3.588
Zn(OH)$_2$ (gamma)	-5.323	-2.054	-1.990	-3.568
Zn(OH)$_2$ (epsilon)	-5.123	-1.854	-1.790	-3.368
ZnO (active)	-4.776	-1.508	-1.444	-3.022
ZINCITE	-4.922	-1.653	-1.589	-3.168
Cd(OH)$_2$ (am)	-8.389	-4.344	-4.157	-4.474
Cd(OH)$_2$	-8.303	-4.258	-4.071	-4.388
MONTEPONITE	-9.761	-5.717	-5.530	-5.847
Cu(OH)$_2$	-2.490	-0.492	-0.765	-2.632
TENORITE	-1.459	0.539	0.266	-1.602
FERRIHYDRITE	1.220	1.609	-0.122	-0.468
GOETHITE	3.922	4.310	2.579	2.232
Cr(OH)$_3$ (am)	0.705	2.871	0.836	-2.362
Cr(OH)$_3$	-1.381	0.786	-1.250	-4.447
BRUCITE	-5.267	-2.263	-3.766	-4.518
PERICLASE	-10.006	-7.002	-8.506	-9.257
Mg(OH)$_2$ (active)	-7.217	-4.213	-5.716	-6.468
LIME	-20.817	-16.575	-15.751	-16.666
PORTLANDITE	-10.923	-6.681	-5.856	-6.771
Ba(OH)$_2$.8H$_2$O	-16.329	-11.791	-9.204	-9.246
As$_2$O$_5$	-36.677	-40.504	-47.358	-55.190
Al$_2$O$_3$	1.697	0.088	-2.440	-6.670
HEMATITE	10.245	11.020	7.558	6.864
MAGHEMITE	2.441	3.216	-0.246	-0.940
LEPIDOCROCITE	3.042	3.430	1.699	1.352
Cr$_2$O$_3$	2.271	6.603	2.531	-3.865
SPINEL	-3.920	-2.526	-6.557	-11.538
MAGNESIOFERRITE	3.545	7.324	2.358	0.913
NATRON	-10.646	-6.477	-6.182	-9.110
CUPRIC FERRITE	9.024	11.797	8.061	5.500
MgCr$_2$O$_4$	-4.709	2.627	-2.949	-10.097
ZnCl2	-17.884	-19.048	-23.888	-28.410
Zn$_2$(OH)$_3$Cl	-10.992	-6.671	-8.993	-13.623
Zn$_5$(OH)$_8$Cl$_2$	-23.691	-11.780	-16.360	-27.197
CdCl$_2$	-11.245	-11.634	-16.350	-19.611
CdCl$_2$.H$_2$O	-10.212	-10.600	-15.316	-18.577
CdCl$_2$.2.5H$_2$O	-9.994	-10.382	-15.097	-18.358
CdOHCl	-6.819	-4.991	-7.256	-9.044
MELANOTHALLITE	-17.318	-19.754	-24.930	-29.741
ATACAMITE	-3.646	-1.867	-4.863	-10.070
Fe(OH)$_{2.7}$Cl$_{0.3}$	4.864	4.588	2.122	1.334
CrCl$_3$	-41.027	-45.510	-54.901	-62.515
HALITE	-5.373	-5.508	-7.815	-10.752
SMITHSONITE	-5.235	-1.967	-1.903	-3.481
ZnCO$_3$.H$_2$O	-4.977	-1.708	-1.643	-3.222
OTAVITE	-4.305	-0.261	-0.074	-0.391
CuCO$_3$	-3.962	-1.965	-2.238	-4.105
MALACHITE	-3.972	0.023	-0.522	-4.257

Solid/Mineral	Saturation Index			
	C-1	C-2	C-3	C-4
	pH 6.74	pH 8.89	pH 11.13	pH 12.55
AZURITE	-7.834	-1.842	-2.660	-8.262
ARTINITE	-8.096	-2.088	-5.092	-6.595
HYDROMAGNESITE	-19.939	-4.920	-12.434	-16.191
MAGNESITE	-2.609	0.394	-1.109	-1.861
NESQUEHONITE	-5.403	-2.398	-3.900	-4.651
ARAGONITE	-1.429	2.813	3.637	2.722
CALCITE	-1.290	2.952	3.776	2.861
DOLOMITE (ordered)	-2.744	4.501	3.822	2.156
DOLOMITE (disordered)	-3.294	3.951	3.272	1.606
HUNTITE	-10.004	3.248	-0.438	-3.608
STRONTIANITE	-2.905	1.382	2.951	3.030
WITHERITE	-4.999	-0.466	2.116	2.072
THERMONATRITE	-12.581	-8.417	-8.127	-11.056
AlOHSO$_4$	-2.465	-7.496	-13.301	-18.484
Al$_4$(OH)$_{10}$SO$_4$	3.623	-3.820	-13.414	-24.941
Zn$_2$(OH)$_2$SO$_4$	-11.047	-8.735	-13.148	-19.374
Zn$_4$(OH)$_6$SO$_4$	-19.125	-10.276	-14.559	-23.942
Zn$_3$O(SO$_4$)$_2$	-32.416	-31.063	-39.953	-50.827
ZINCOSITE	-13.887	-14.845	-19.322	-23.969
ZnSO$_4$.H$_2$O	-9.321	-10.278	-14.754	-19.402
BIANCHITE	-8.201	-9.156	-13.629	-18.276
GOSLARITE	-7.956	-8.910	-13.383	-18.030
Cd$_3$(OH)$_4$SO$_4$	-22.905	-14.997	-18.978	-22.998
Cd$_3$OH$_2$(SO$_4$)$_2$	-23.423	-19.742	-28.265	-35.353
Cd$_4$(OH)$_6$SO$_4$	-23.404	-11.452	-15.246	-19.582
CdSO$_4$	-10.855	-11.037	-15.391	-18.777
CdSO$_4$.H$_2$O	-9.302	-9.484	-13.838	-17.224
CdSO$_4$.2.67H$_2$O	-9.158	-9.338	-13.692	-17.077
ANTLERITE	-6.605	-4.838	-10.196	-18.867
BROCHANTITE	-6.855	-3.090	-8.721	-19.259
LANGITE	-9.123	-5.358	-10.988	-21.526
CuOCuSO$_4$	-14.302	-14.534	-19.621	-26.425
CuSO$_4$	-13.124	-15.353	-20.167	-25.103
CHALCANTHITE	-7.551	-9.778	-14.589	-19.524
Fe$_2$(SO$_4$)$_3$	-36.548	-48.450	-65.536	-75.437
H-JAROSITE	-7.406	-14.692	-28.966	-36.144
Na-JAROSITE	-3.451	-8.656	-22.786	-31.429
EPSOMITE	-2.675	-3.894	-9.935	-13.754
ANHYDRITE	-0.128	-0.112	-3.828	-7.812
GYPSUM	0.120	0.137	-3.579	-7.563
CELESTITE	-0.278	-0.216	-3.188	-6.179
BARITE	1.688	1.996	0.036	-3.076
MIRABILITE	-5.565	-5.622	-9.869	-15.865
THENARDITE	-6.986	-7.049	-11.301	-17.299
CuSeO$_3$.2H$_2$O	-6.859	-8.788	-13.092	-18.831
Fe$_2$(SeO$_3$)$_3$.2H$_2$O	-8.141	-19.146	-34.704	-47.012
Fe$_2$(OH)$_4$SeO$_3$	-5.260	-8.411	-15.905	-20.470
MgSeO$_3$.6H$_2$O	-4.016	-4.937	-10.469	-15.091
CaSeO$_3$.2H$_2$O	-3.465	-3.149	-6.356	-11.142
SrSeO$_3$	-5.358	-4.998	-7.461	-11.254
BaSeO$_3$	-6.282	-5.676	-7.127	-11.042
Na$_2$SeO$_3$.5H$_2$O	-13.132	-12.894	-16.634	-23.434
Zn$_3$(PO$_4$)$_2$.4H$_2$O	-10.560	-9.802	-16.685	-28.415
Cd$_3$(PO$_4$)$_2$	-16.584	-13.500	-20.019	-27.964
Cu$_3$(PO$_4$)$_2$	-9.806	-12.863	-20.759	-33.356
Cu$_3$(PO$_4$)$_2$.3H$_2$O	-11.540	-14.596	-22.490	-35.086
STRENGITE	-1.795	-5.931	-11.200	-15.044
Mg$_3$(PO$_4$)$_2$	-7.196	-7.236	-18.823	-28.073
MgHPO$_4$.3H$_2$O	-2.857	-4.377	-9.417	-13.665
HYDROXYLAPATITE	5.925	13.562	7.070	-7.999
CaHPO$_4$.2H$_2$O	-1.732	-2.014	-4.726	-9.138
CaHPO$_4$	-1.449	-1.732	-4.445	-8.858
Ca$_3$(PO$_4$)$_2$ (beta)	-0.645	3.032	-1.571	-11.312
Ca$_4$H(PO$_4$)$_3$.3H$_2$O	-3.214	0.182	-7.133	-21.286
SrHPO$_4$	-3.839	-4.076	-6.046	-9.464
BaHPO$_4$	-4.753	-4.745	-5.701	-9.242
AlAsO$_4$.2H$_2$O	-9.113	-11.831	-16.520	-22.551
Zn$_3$(AsO$_4$)$_2$.2.5H$_2$O	-24.388	-18.408	-25.068	-37.636
Cu$_3$(AsO$_4$)$_2$.2H$_2$O	-17.518	-15.352	-23.023	-36.457
FeAsO$_4$.2H$_2$O	-10.975	-12.499	-17.657	-21.919
Ca$_3$(AsO$_4$)$_2$.4H$_2$O	-16.631	-7.729	-12.107	-22.684
Ba$_3$(AsO$_4$)$_2$	3.173	12.946	13.837	5.875

Table H-14. Saturation indices for all minerals calculated using MINTEQA2: Columbia-Lawson.

Solid/Mineral	Saturation Index				Solid/Mineral	Saturation Index			
	CL-1	CL-2	CL-3	CL-4		CL-1	CL-2	CL-3	CL-4
	pH 5.68	pH 8.22	pH 9.66	pH 11.81		pH 5.68	pH 8.22	pH 9.66	pH 11.81
CaNaAsO$_4$.7.5H$_2$O	-15.419	-8.279	-8.123	-13.953	AZURITE	-13.057	-1.104	-0.004	1.059
Ca$_5$(AsO$_4$)$_3$OH	-37.056	-12.924	-12.362	-27.71	ARTINITE	-13.008	-3.326	-3.769	-8.460
Ca$_4$(OH)$_2$(AsO$_4$)$_2$:4H$_2$O	-36.241	-16.863	-15.224	-25.94	HYDROMAGNESITE	-32.222	-8.018	-9.127	-20.854
Mg$_3$(AsO4)$_2$	-25.572	-11.405	-18.016	-32.856	MAGNESITE	-5.067	-0.226	-0.448	-2.793
FeAsO$_4$	-13.599	-11.091	-14.983	-20.641	NESQUEHONITE	-7.858	-3.017	-3.238	-5.584
Cd$_3$(AsO$_4$)$_2$	-29.176	-18.103	-22.667	-32.188	ARAGONITE	-3.740	1.193	3.089	2.362
Cu$_3$(AsO$_4$)$_2$	-25.062	-13.464	-18.309	-25.050	CALCITE	-3.601	1.332	3.228	2.501
Al$_2$(SeO$_3$)$_3$	-7.271	-20.269	-27.100	-43.938	DOLOMITE (ordered)	-7.512	2.261	3.935	0.863
CaSeO$_3$	-2.933	-1.725	-2.056	-7.291	DOLOMITE (disordered)	-8.062	1.711	3.385	0.313
CaSeO$_3$:H$_2$O	-3.744	-2.536	-2.866	-8.101	HUNTITE	-19.688	-0.233	0.997	-6.766
CdSeO$_3$	-7.462	-7.378	-9.144	-14.225	STRONTIANITE	-5.097	-0.159	2.045	1.658
CuSeO$_3$	-7.290	-7.031	-8.891	-13.045	WITHERITE	-7.548	-2.430	0.252	0.132
Fe$_2$(SeO$_3$)$_3$	-12.978	-18.782	-27.299	-44.337	THERMONATRITE	-16.393	-11.627	-9.165	-11.570
Fe$_2$(SeO$_3$)$_3$.6H$_2$O	-40.661	-46.464	-54.980	-72.018	AlOHSO$_4$	-1.069	-7.476	-9.638	-15.985
MgSeO$_3$	-3.474	-2.358	-4.806	-11.661	Al$_4$(OH)$_{10}$SO$_4$	4.081	-5.057	-7.447	-18.761
Na$_2$SeO$_3$	-10.753	-9.712	-9.477	-16.390	Zn$_2$(OH)$_2$SO$_4$	-10.272	-12.262	-13.438	-19.837
ZnSeO$_3$	-3.950	-5.922	-7.694	-13.056	Zn$_4$(OH)$_6$SO$_4$	-19.283	-17.768	-18.034	-26.140
ZnSeO$_3$.H$_2$O	-6.510	-8.483	-10.254	-15.616	Zn$_3$O(SO$_4$)$_2$	-30.400	-36.134	-38.941	-50.885
SeO$_2$	-11.879	-15.604	-17.830	-22.339	ZINCOSITE	-12.645	-16.389	-18.019	-23.564
Al(OH)$_3$ (am)	-0.440	-1.350	-1.426	-3.082	ZnSO$_4$.H$_2$O	-8.078	-11.821	-13.452	-18.997
BOEHMITE	1.783	0.872	0.796	-0.860	BIANCHITE	-6.954	-10.696	-12.325	-17.870
DIASPORE	3.488	2.577	2.501	0.845	GOSLARITE	-6.708	-10.450	-12.079	-17.624
GIBBSITE	2.069	1.159	1.083	-0.573	Cd$_3$(OH)$_4$SO$_4$	-25.663	-19.731	-20.435	-26.844
Zn(OH)$_2$ (am)	-6.530	-4.777	-4.322	-5.176	Cd$_3$OH$_2$(SO$_4$)$_2$	-24.473	-24.037	-26.827	-37.927
Zn(OH)$_2$	-6.256	-4.503	-4.048	-4.902	Cd$_4$(OH)$_6$SO$_4$	-27.651	-17.909	-18.153	-25.135
Zn(OH)$_2$ (beta)	-5.810	-4.057	-3.602	-4.456	CdSO$_4$	-10.635	-12.322	-13.947	-19.211
Zn(OH)$_2$ (gamma)	-5.790	-4.037	-3.582	-4.436	CdSO$_4$.H$_2$O	-9.082	-10.769	-12.393	-17.657
Zn(OH)$_2$ (epsilon)	-5.590	-3.837	-3.382	-4.236	CdSO$_4$.2.67H$_2$O	-8.936	-10.622	-12.247	-17.510
ZnO (active)	-5.244	-3.491	-3.037	-3.890	ANTLERITE	-10.117	-3.660	-4.645	-8.273
ZINCITE	-5.389	-3.637	-3.182	-4.036	BROCHANTITE	-12.108	-1.666	-2.284	-5.558
Cd(OH)$_2$ (am)	-9.878	-6.068	-5.608	-6.180	LANGITE	-14.375	-3.933	-4.551	-7.825
Cd(OH)$_2$	-9.792	-5.982	-5.522	-6.094	CuOCuSO$_4$	-16.075	-13.603	-14.955	-18.938
MONTEPONITE	-11.251	-7.441	-6.981	-7.554	CuSO$_4$	-13.156	-14.668	-16.386	-20.723
Cu(OH)$_2$	-4.231	-0.246	0.121	0.475	CHALCANTHITE	-7.579	-9.090	-10.807	-15.144
TENORITE	-3.200	0.784	1.151	1.505	Fe$_2$(SO$_4$)$_3$	-34.341	-45.458	-53.553	-71.138
FERRIHYDRITE	-0.239	2.447	1.528	-0.228	H-JAROSITE	-8.365	-11.298	-18.227	-32.877
GOETHITE	2.461	5.148	4.228	2.472	Na-JAROSITE	-6.318	-6.869	-12.567	-28.419
Cr(OH)$_3$ (am)	-1.554	2.677	2.700	0.532	EPSOMITE	-3.417	-4.071	-6.377	-13.413
Cr(OH)$_3$	-3.640	0.591	0.615	-1.553	ANHYDRITE	-0.729	-1.292	-1.481	-6.900
BRUCITE	-7.724	-2.883	-3.105	-5.450	GYPSUM	-0.480	-1.043	-1.232	-6.650
PERICLASE	-12.463	-7.623	-7.845	-10.190	CELESTITE	-0.760	-1.318	-1.199	-6.277
Mg(OH)$_2$ (active)	-9.674	-4.833	-5.055	-7.400	BARITE	0.849	0.471	1.068	-3.743
LIME	-23.128	-18.195	-16.299	-17.026	MIRABILITE	-7.660	-8.388	-8.010	-15.105
PORTLANDITE	-13.233	-8.300	-6.404	-7.131	THENARDITE	-9.090	-9.820	-9.444	-16.540
Ba(OH)$_2$.8H$_2$O	-18.869	-13.750	-11.066	-11.185	CuSeO$_3$.2H$_2$O	-7.823	-7.564	-9.423	-13.577
As$_2$O$_5$	-39.330	-39.685	-45.630	-53.433	Fe$_2$(SeO$_3$)$_3$.2H$_2$O	-8.733	-14.536	-23.053	-40.091
Al$_2$O$_3$	1.070	-0.752	-0.905	-4.217	Fe$_2$(OH)$_4$SeO$_3$	-7.404	-5.757	-9.822	-17.842
HEMATITE	7.323	12.695	10.856	7.344	MgSeO$_3$.6H$_2$O	-5.693	-4.576	-7.023	-13.876
MAGHEMITE	-0.481	4.891	3.052	-0.460	CaSeO$_3$.2H$_2$O	-4.998	-3.790	-4.120	-9.355
LEPIDOCROCITE	1.581	4.268	3.348	1.592	SrSeO$_3$	-6.774	-5.561	-5.584	-10.479
Cr$_2$O$_3$	-2.249	6.212	6.258	1.922	BaSeO$_3$	-8.055	-6.662	-6.206	-10.835
SPINEL	-7.005	-3.986	-4.361	-10.018	Na$_2$SeO$_3$.5H$_2$O	-16.166	-15.123	-14.887	-21.800
MAGNESIOFERRITE	-1.834	8.379	6.317	0.460	Zn$_3$(PO$_4$)$_2$.4H$_2$O	-8.954	-11.221	-15.515	-25.299
NATRON	-14.450	-9.681	-7.218	-9.622	Cd$_3$(PO$_4$)$_2$	-18.047	-14.146	-18.424	-27.365
CUPRIC FERRITE	4.361	13.718	12.244	9.087	Cu$_3$(PO$_4$)$_2$	-12.024	-7.597	-12.155	-18.316
MgCr$_2$O$_4$	-11.686	1.615	1.439	-5.243	Cu$_3$(PO$_4$)$_2$.3H$_2$O	-13.755	-9.328	-13.886	-20.046
ZnCl2	-17.930	-21.573	-24.333	-29.791	STRENGITE	-1.751	-2.828	-6.576	-11.944
Zn$_2$(OH)$_3$Cl	-11.715	-10.907	-11.605	-15.614	Mg$_3$(PO$_4$)$_2$	-11.564	-4.568	-10.892	-25.152
Zn$_5$(OH)$_8$Cl$_2$	-25.604	-22.235	-23.176	-32.048	MgHPO$_4$.3H$_2$O	-3.809	-2.731	-5.781	-11.738
CdCl$_2$	-12.313	-13.899	-16.654	-21.831	HYDROXYLAPATITE	-1.118	12.257	13.248	-1.221
CdCl$_2$.H$_2$O	-11.280	-12.865	-15.619	-20.796	CaHPO$_4$.2H$_2$O	-2.538	-1.367	-2.300	-6.639
CdCl$_2$.2.5H$_2$O	-11.061	-12.646	-15.400	-20.576	CaHPO$_4$	-2.257	-1.087	-2.020	-6.359
CdOHCl	-8.097	-6.985	-8.133	-11.007	Ca$_3$(PO$_4$)$_2$ (beta)	-4.571	2.701	2.730	-6.674
MELANOTHALLITE	-18.638	-20.049	-22.897	-27.147	Ca$_4$H(PO$_4$)$_3$.3H$_2$O	-7.945	0.499	-0.405	-14.148
ATACAMITE	-6.916	-1.645	-2.519	-4.112	SrHPO$_4$	-4.528	-3.353	-3.978	-7.976
Fe(OH)$_{2.7}$Cl$_{0.3}$	3.468	5.345	3.944	1.497	BaHPO$_4$	-5.799	-4.444	-4.591	-8.322
CrCl$_3$	-42.655	-46.517	-51.316	-60.391	AlAsO$_4$.2H$_2$O	-10.752	-11.840	-14.888	-20.446
HALITE	-7.069	-7.384	-7.760	-11.265	Zn$_3$(AsO$_4$)$_2$.2.5H$_2$O	-28.442	-23.538	-28.118	-38.483
SMITHSONITE	-5.703	-3.950	-3.495	-4.349	Cu$_3$(AsO$_4$)$_2$.2H$_2$O	-25.393	-13.795	-18.639	-25.380
ZnCO$_3$.H$_2$O	-5.443	-3.690	-3.236	-4.089	FeAsO$_4$.2H$_2$O	-13.760	-11.251	-15.143	-20.801
OTAVITE	-5.794	-1.985	-1.525	-2.098	Ca$_3$(AsO$_4$)$_2$.4H$_2$O	-26.212	-11.767	-12.024	-22.007
CuCO$_3$	-5.703	-1.719	-1.352	-0.998	Ba$_3$(AsO$_4$)$_2$	-7.125	7.873	9.975	1.812
MALACHITE	-7.454	0.515	1.248	1.957					

Table H-15. Saturation indices for all minerals calculated using MINTEQA2: Columbia-Kamm.

Solid/Mineral	Saturation Index CK-1 pH 5.41	CK-2 pH 7.81	CK-3 pH 10.01	CK-4 pH 11.86
$CaNaAsO_4.7.5H_2O$	-15.980	-8.840	-8.281	-14.012
$Ca_5(AsO_4)_3OH$	-39.161	-15.086	-13.155	-27.558
$Ca_4(OH)_2(AsO_4)_2:4H_2O$	-37.99	-18.832	-15.604	-25.762
$Mg_3(AsO4)_2$	-26.787	-12.536	-20.007	-33.223
$FeAsO_4$	-13.562	-10.179	-15.740	-22.272
$Cd_3(AsO_4)_2$	-30.371	-19.186	-23.872	-32.556
$Cu_3(AsO_4)_2$	-25.620	-13.394	-20.513	-27.893
$Al_2(SeO_3)_3$	-6.699	-17.342	-29.664	-45.483
$CaSeO_3$	-3.153	-1.732	-2.535	-7.652
$CaSeO_3:H_2O$	-3.964	-2.542	-3.345	-8.462
$CdSeO_3$	-7.670	-7.352	-9.823	-14.700
$CuSeO_3$	-7.286	-6.622	-9.904	-14.345
$Fe_2(SeO_3)_3$	-12.333	-15.799	-29.648	-48.657
$Fe_2(SeO_3)_3.6H_2O$	-40.017	-43.482	-57.329	-76.338
$MgSeO_3$	-3.689	-2.349	-5.749	-12.136
Na_2SeO_3	-10.863	-9.663	-9.668	-16.844
$ZnSeO_3$	-4.484	-6.345	-8.395	-12.073
$ZnSeO_3.H_2O$	-7.044	-8.906	-10.956	-14.633
SeO_2	-11.581	-14.821	-18.533	-22.815
$Al(OH)_3$ (am)	-0.601	-1.062	-1.654	-3.141
BOEHMITE	1.622	1.160	0.568	-0.919
DIASPORE	3.327	2.865	2.273	0.786
GIBBSITE	1.908	1.447	0.855	-0.632
$Zn(OH)_2$ (am)	-7.362	-5.983	-4.321	-3.717
$Zn(OH)_2$	-7.088	-5.709	-4.047	-3.443
$Zn(OH)_2$ (beta)	-6.642	-5.263	-3.601	-2.997
$Zn(OH)_2$ (gamma)	-6.622	-5.243	-3.581	-2.977
$Zn(OH)_2$ (epsilon)	-6.422	-5.043	-3.381	-2.777
ZnO (active)	-6.076	-4.697	-3.035	-2.431
ZINCITE	-6.221	-4.843	-3.181	-2.577
$Cd(OH)_2$ (am)	-10.384	-6.827	-5.585	-6.179
$Cd(OH)_2$	-10.298	-6.741	-5.499	-6.093
MONTEPONITE	-11.757	-8.200	-6.958	-7.553
$Cu(OH)_2$	-4.525	-0.620	-0.189	-0.349
TENORITE	-3.494	0.410	0.841	0.681
FERRIHYDRITE	-0.364	2.763	1.408	-1.674
GOETHITE	2.337	5.463	4.108	1.026
$Cr(OH)_3$ (am)	-1.515	2.640	2.487	0.554
$Cr(OH)_3$	-3.600	0.554	0.402	-1.531
BRUCITE	-8.237	-3.658	-3.344	-5.449
PERICLASE	-12.976	-8.397	-8.084	-10.189
$Mg(OH)_2$ (active)	-10.187	-5.608	-5.294	-7.399
LIME	-23.646	-18.985	-16.076	-16.910
PORTLANDITE	-13.751	-9.090	-6.180	-7.015
$Ba(OH)_2.8H_2O$	-19.405	-14.655	-10.650	-10.738
As_2O_5	-39.006	-38.493	-46.904	-53.804
Al_2O_3	0.748	-0.176	-1.360	-4.334
HEMATITE	7.074	13.327	10.617	4.452
MAGHEMITE	-0.730	5.523	2.813	-3.352
LEPIDOCROCITE	1.457	4.583	3.228	0.146
Cr_2O_3	-2.171	6.139	5.832	1.966
SPINEL	-7.840	-4.184	-5.054	-10.134
MAGNESIOFERRITE	-2.596	8.236	5.839	-2.431
NATRON	-14.859	-10.417	-6.707	-9.600
CUPRIC FERRITE	3.818	13.975	11.695	5.371
$MgCr_2O_4$	-12.121	0.767	0.774	-5.197
ZnCl2	-18.091	-21.872	-24.975	-28.310
$Zn_2(OH)_3Cl$	-13.043	-12.866	-11.924	-12.685
$Zn_5(OH)_8Cl_2$	-29.093	-27.359	-23.812	-24.731
$CdCl_2$	-12.148	-13.750	-17.274	-21.808
$CdCl_2.H_2O$	-11.114	-12.716	-16.240	-20.774
$CdCl_2.2.5H_2O$	-10.895	-12.497	-16.021	-20.554
CdOHCl	-8.268	-7.290	-8.431	-10.995
MELANOTHALLITE	-18.260	-19.515	-23.851	-27.950
ATACAMITE	-7.168	-1.939	-3.461	-5.750
$Fe(OH)_{2.7}Cl_{0.3}$	3.444	5.797	3.727	0.054
$CrCl_3$	-41.608	-45.193	-52.495	-60.336
HALITE	-6.937	-7.297	-7.826	-11.243
SMITHSONITE	-6.535	-5.156	-3.494	-2.890
$ZnCO_3.H_2O$	-6.275	-4.897	-3.234	-2.630
OTAVITE	-6.301	-2.744	-1.502	-2.097
$CuCO_3$	-5.997	-2.093	-1.662	-1.822
MALACHITE	-8.042	-0.233	0.628	0.309

Solid/Mineral	Saturation Index CK-1 pH 5.41	CK-2 pH 7.81	CK-3 pH 10.01	CK-4 pH 11.86
AZURITE	-13.939	-2.226	-0.934	-1.414
ARTINITE	-14.034	-4.875	-4.247	-8.458
HYDROMAGNESITE	-34.788	-11.891	-10.322	-20.849
MAGNESITE	-5.580	-1.000	-0.687	-2.792
NESQUEHONITE	-8.371	-3.792	-3.477	-5.583
ARAGONITE	-4.258	0.403	3.312	2.478
CALCITE	-4.119	0.542	3.451	2.616
DOLOMITE (ordered)	-8.544	0.696	3.919	0.979
DOLOMITE (disordered)	-9.094	0.146	3.369	0.429
HUNTITE	-21.745	-3.346	0.503	-6.648
STRONTIANITE	-5.579	-0.902	2.410	1.966
WITHERITE	-8.083	-3.335	0.668	0.579
THERMONATRITE	-16.801	-12.361	-8.654	-11.548
$AlOHSO_4$	-0.743	-5.823	-10.800	-16.507
$Al_4(OH)_{10}SO_4$	3.925	-2.539	-9.291	-19.459
$Zn_2(OH)_2SO_4$	-11.449	-13.309	-14.369	-17.381
$Zn_4(OH)_6SO_4$	-22.125	-21.228	-18.963	-20.767
$Zn_3O(SO_4)_2$	-31.922	-37.022	-40.805	-47.433
ZINCOSITE	-12.990	-16.230	-18.952	-22.568
$ZnSO_4.H_2O$	-8.423	-11.662	-14.385	-18.001
BIANCHITE	-7.299	-10.537	-13.258	-16.874
GOSLARITE	-7.054	-10.291	-13.012	-16.628
$Cd_3(OH)_4SO_4$	-26.695	-20.640	-21.300	-27.304
$Cd_3OH_2(SO_4)_2$	-25.018	-23.581	-28.626	-38.850
$Cd_4(OH)_6SO_4$	-29.189	-19.577	-18.995	-25.594
$CdSO_4$	-10.655	-11.715	-14.858	-19.673
$CdSO_4.H_2O$	-9.101	-10.161	-13.304	-18.119
$CdSO_4.2.67H_2O$	-8.955	-10.015	-13.158	-17.972
ANTLERITE	-10.512	-3.416	-6.510	-11.209
BROCHANTITE	-12.797	-1.796	-4.459	-9.318
LANGITE	-15.064	-4.063	-6.726	-11.585
$CuOCuSO_4$	-16.176	-12.985	-16.509	-21.049
$CuSO_4$	-12.963	-13.676	-17.631	-22.010
CHALCANTHITE	-7.386	-8.098	-12.052	-16.431
$Fe_2(SO_4)_3$	-33.129	-40.729	-56.594	-75.419
H-JAROSITE	-7.765	-7.620	-20.454	-38.141
Na-JAROSITE	-5.922	-3.557	-14.538	-33.673
EPSOMITE	-3.443	-3.480	-7.550	-13.875
ANHYDRITE	-0.760	-0.717	-2.192	-7.247
GYPSUM	-0.511	-0.467	-1.942	-6.997
CELESTITE	-0.755	-0.696	-1.769	-6.433
BARITE	0.801	0.932	0.549	-3.760
MIRABILITE	-7.582	-7.757	-8.433	-15.546
THENARDITE	-9.011	-9.189	-9.867	-16.981
$CuSeO_3.2H_2O$	-7.819	-7.154	-10.436	-14.877
$Fe_2(SeO_3)_3.2H_2O$	-8.088	-11.554	-25.402	-44.411
$Fe_2(OH)_4SeO_3$	-7.355	-4.342	-10.764	-21.210
$MgSeO_3.6H_2O$	-5.908	-4.567	-7.965	-14.351
$CaSeO_3.2H_2O$	-5.218	-3.797	-4.599	-9.716
$SrSeO_3$	-6.959	-5.521	-5.922	-10.647
$BaSeO_3$	-8.292	-6.783	-6.494	-10.864
$Na_2SeO_3.5H_2O$	-16.276	-15.075	-15.079	-22.254
$Zn_3(PO_4)_2.4H_2O$	-10.350	-13.537	-17.131	-22.001
$Cd_3(PO_4)_2$	-18.465	-15.117	-19.974	-28.441
$Cu_3(PO_4)_2$	-11.805	-7.415	-14.706	-21.867
$Cu_3(PO_4)_2.3H_2O$	-13.537	-9.146	-16.436	-23.598
STRENGITE	-1.326	-1.860	-7.506	-13.929
$Mg_3(PO_4)_2$	-12.002	-5.587	-13.229	-26.228
$MgHPO_4.3H_2O$	-3.772	-2.853	-6.830	-12.276
HYDROXYLAPATITE	-2.058	10.262	11.936	-2.261
$CaHPO_4.2H_2O$	-2.506	-1.506	-2.887	-7.062
$CaHPO_4$	-2.224	-1.225	-2.607	-6.782
$Ca_3(PO_4)_2$ (beta)	-5.025	1.635	1.781	-7.406
$Ca_4H(PO_4)_3.3H_2O$	-8.366	-0.706	-1.941	-15.303
$SrHPO_4$	-4.460	-3.444	-4.423	-8.208
$BaHPO_4$	-5.784	-4.696	-4.985	-8.415
$AlAsO_4.2H_2O$	-10.751	-10.956	-15.753	-20.690
$Zn_3(AsO_4)_2.2.5H_2O$	-30.614	-25.965	-29.388	-34.476
$Cu_3(AsO_4)_2.2H_2O$	-25.951	-13.724	-20.844	-28.223
$FeAsO_4.2H_2O$	-13.723	-10.340	-15.900	-22.432
$Ca_3(AsO_4)_2.4H_2O$	-27.443	-12.946	-12.627	-22.031
$Ba_3(AsO_4)_2$	-8.408	6.351	9.948	2.780

Table H-16. Saturation indices for all minerals calculated using MINTEQA2: Columbia-Red Wing.

Solid/Mineral	Saturation Index				Solid/Mineral	Saturation Index			
	CR-1	CR-2	CR-3	CR-4		CR-1	CR-2	CR-3	CR-4
	pH 6.18	pH 8.23	pH 10.53	pH 11.97		pH 6.18	pH 8.23	pH 10.53	pH 11.97
$CaNaAsO_4.7.5H_2O$	-14.077	-8.231		-14.182	AZURITE	-9.835	-1.507		-1.743
$Ca_5(AsO_4)_3OH$	-32.752	-13.074		-28.1	ARTINITE	-10.724	-3.415		-8.457
$Ca_4(OH)_2(AsO_4)_2:4H_2O$	-32.645	-16.964		-26.037	HYDROMAGNESITE	-26.512	-8.241		-20.847
$Mg_3(AsO4)_2$	-22.915	-11.633		-33.887	MAGNESITE	-3.924	-0.271		-2.792
$FeAsO_4$	-13.854	-12.604		-22.716	NESQUEHONITE	-6.716	-3.062		-5.582
$Cd_3(AsO_4)_2$	-26.927	-18.727		-33.220	ARAGONITE	-2.648	1.191		2.607
$Cu_3(AsO_4)_2$	-22.610	-13.962		-28.886	CALCITE	-2.509	1.330		2.746
$Al_2(SeO_3)_3$	-7.974	-19.251		-46.733	DOLOMITE (ordered)	-5.278	2.215		1.109
$CaSeO_3$	-2.335	-1.654		-7.934	DOLOMITE (disordered)	-5.828	1.665		0.559
$CaSeO_3:H_2O$	-3.146	-2.465		-8.744	HUNTITE	-15.169	-0.368		-6.517
$CdSeO_3$	-6.950	-7.482		-15.112	STRONTIANITE	-4.085	-0.124		2.247
$CuSeO_3$	-6.711	-7.093		-14.867	WITHERITE	-6.318	-2.389		1.051
$Fe_2(SeO_3)_3$	-14.200	-21.496		-50.117	THERMONATRITE	-15.121	-11.433		-11.482
$Fe_2(SeO_3)_3.6H_2O$	-41.884	-49.178		-77.797	$AlOHSO_4$	-1.701	-6.497		-16.963
$MgSeO_3$	-2.825	-2.330		-12.547	$Al_4(OH)_{10}SO_4$	4.619	-2.879		-19.937
Na_2SeO_3	-9.975	-9.445		-17.190	$Zn_2(OH)_2SO_4$	-10.153	-12.527		-21.167
$ZnSeO_3$	-3.874	-6.272		-14.153	$Zn_4(OH)_6SO_4$	-18.025	-18.878		-27.889
$ZnSeO_3.H_2O$	-6.435	-8.832		-16.714	$Zn_3O(SO_4)_2$	-30.732	-36.243		-53.336
SeO_2	-12.373	-15.532		-23.227	ZINCOSITE	-13.096	-16.232		-24.686
$Al(OH)_3$ (am)	-0.050	-0.951		-3.148	$ZnSO_4.H_2O$	-8.529	-11.664		-20.118
BOEHMITE	2.173	1.272		-0.926	BIANCHITE	-7.406	-10.539		-18.991
DIASPORE	3.878	2.977		0.779	GOSLARITE	-7.161	-10.293		-18.745
GIBBSITE	2.459	1.558		-0.639	$Cd_3(OH)_4SO_4$	-23.666	-19.682		-27.752
$Zn(OH)_2$ (am)	-5.960	-5.199		-5.385	$Cd_3OH_2(SO_4)_2$	-23.497	-23.408		-39.747
$Zn(OH)_2$	-5.686	-4.925		-5.111	$Cd_4(OH)_6SO_4$	-24.648	-18.037		-26.041
$Zn(OH)_2$ (beta)	-5.240	-4.479		-4.665	$CdSO_4$	-10.650	-11.919		-20.122
$Zn(OH)_2$ (gamma)	-5.220	-4.459		-4.645	$CdSO_4.H_2O$	-9.097	-10.366		-18.568
$Zn(OH)_2$ (epsilon)	-5.020	-4.259		-4.445	$CdSO_4.2.67H_2O$	-8.951	-10.219		-18.421
ZnO (active)	-4.674	-3.914		-4.099	ANTLERITE	-7.917	-3.484		-11.987
ZINCITE	-4.819	-4.059		-4.245	BROCHANTITE	-8.834	-1.624		-10.205
$Cd(OH)_2$ (am)	-8.872	-6.245		-6.179	LANGITE	-11.101	-3.891		-12.472
$Cd(OH)_2$	-8.786	-6.159		-6.093	$CuOCuSO_4$	-14.948	-13.292		-21.717
MONTEPONITE	-10.245	-7.618		-7.553	$CuSO_4$	-13.103	-14.222		-22.569
$Cu(OH)_2$	-3.157	-0.380		-0.459	CHALCANTHITE	-7.527	-8.645		-16.990
TENORITE	-2.126	0.650		0.571	$Fe_2(SO_4)_3$	-37.143	-46.651		-76.989
FERRIHYDRITE	-0.109	0.981		-1.786	H-JAROSITE	-10.017	-14.537		-39.374
GOETHITE	2.592	3.681		0.914	Na-JAROSITE	-7.333	-10.011		-34.872
$Cr(OH)_3$ (am)	-0.011	3.133		0.512	EPSOMITE	-3.297	-3.536		-14.323
$Cr(OH)_3$	-2.097	1.047		-1.573	ANHYDRITE	-0.658	-0.714		-7.567
BRUCITE	-6.582	-2.928		-5.449	GYPSUM	-0.410	-0.465		-7.317
PERICLASE	-11.321	-7.667		-10.189	CELESTITE	-0.769	-0.703		-6.601
$Mg(OH)_2$ (active)	-8.532	-4.878		-7.399	BARITE	1.058	1.091		-3.736
LIME	-22.036	-18.197		-16.781	MIRABILITE	-7.411	-7.614		-15.928
PORTLANDITE	-12.142	-8.302		-6.886	THENARDITE	-8.839	-9.047		-17.364
$Ba(OH)_2.8H_2O$	-17.642	-13.709		-10.266	$CuSeO_3.2H_2O$	-7.244	-7.625		-15.399
As_2O_5	-40.100	-39.779		-54.469	$Fe_2(SeO_3)_3.2H_2O$	-9.955	-17.250		-45.870
Al_2O_3	1.850	0.047		-4.348	$Fe_2(OH)_4SeO_3$	-7.638	-8.616		-21.846
HEMATITE	7.584	9.763		4.229	$MgSeO_3.6H_2O$	-5.045	-4.548		-14.763
MAGHEMITE	-0.220	1.959		-3.575	$CaSeO_3.2H_2O$	-4.401	-3.719		-9.998
LEPIDOCROCITE	1.712	2.801		0.034	$SrSeO_3$	-6.256	-5.453		-10.778
Cr_2O_3	0.838	7.124		1.882	$BaSeO_3$	-7.319	-6.549		-10.804
SPINEL	-5.083	-3.231		-10.148	$Na_2SeO_3.5H_2O$	-15.388	-14.857		-22.600
MAGNESIOFERRITE	-0.430	5.402		-2.654	$Zn_3(PO_4)_2.4H_2O$	-8.252	-13.137		-27.829
NATRON	-13.180	-9.488		-9.534	$Cd_3(PO_4)_2$	-16.037	-15.324		-29.263
CUPRIC FERRITE	5.696	10.651		5.038	$Cu_3(PO_4)_2$	-9.809	-8.649		-23.020
$MgCr_2O_4$	-7.457	2.482		-5.281	$Cu_3(PO_4)_2.3H_2O$	-11.541	-10.380		-24.750
ZnCl2	-18.087	-21.839		-29.912	STRENGITE	-2.125	-4.618		-14.453
$Zn_2(OH)_3Cl$	-10.939	-11.674		-15.989	$Mg_3(PO_4)_2$	-9.144	-5.350		-27.050
$Zn_5(OH)_8Cl_2$	-23.482	-24.191		-33.007	$MgHPO_4.3H_2O$	-3.171	-3.100		-12.688
$CdCl_2$	-12.035	-13.920		-21.741	HYDROXYLAPATITE	2.829	11.275		-2.850
$CdCl_2.H_2O$	-11.001	-12.885		-20.707	$CaHPO_4.2H_2O$	-1.950	-1.693		-7.345
$CdCl_2.2.5H_2O$	-10.782	-12.666		-20.487	$CaHPO_4$	-1.669	-1.413		-7.065
CdOHCl	-7.455	-7.084		-10.962	$Ca_3(PO_4)_2$ (beta)	-2.304	2.048		-7.841
MELANOTHALLITE	-18.291	-20.027		-27.993	$Ca_4H(PO_4)_3.3H_2O$	-5.090	-0.481		-16.021
ATACAMITE	-5.132	-1.836		-5.936	$SrHPO_4$	-4.019	-3.642		-8.339
$Fe(OH)_{2.7}Cl_{0.3}$	3.489	3.903		-0.047	$BaHPO_4$	-5.073	-4.727		-8.354
$CrCl_3$	-42.203	-45.827		-60.279	$AlAsO_4.2H_2O$	-10.747	-11.487		-21.029
HALITE	-6.797	-7.208		-11.177	$Zn_3(AsO_4)_2.2.5H_2O$	-27.502	-24.899		-40.146
SMITHSONITE	-5.133	-4.372		-4.558	$Cu_3(AsO_4)_2.2H_2O$	-22.941	-14.292		-29.217
$ZnCO_3.H_2O$	-4.873	-4.113		-4.298	$FeAsO_4.2H_2O$	-14.015	-12.765		-22.876
OTAVITE	-4.788	-2.162		-2.096	$Ca_3(AsO_4)_2.4H_2O$	-23.707	-11.867		-22.308
$CuCO_3$	-4.629	-1.853		-1.932	$Ba_3(AsO_4)_2$	-4.206	7.901		3.533
MALACHITE	-5.306	0.246		0.089					

Table H-17. Saturation indices for all minerals calculated using MINTEQA2: Columbia-MnRoad.

Solid/Mineral	Saturation Index				Solid/Mineral	Saturation Index			
	CM-1	CM-2	CM-3	CM-4		CM-1	CM-2	CM-3	CM-4
	pH 5.80	pH 8.69	pH 10.71	pH 11.71		pH 5.80	pH 8.69	pH 10.71	pH 11.71
$CaNaAsO_4.7.5H_2O$	-15.120	-8.022		-13.299	AZURITE	-11.641	-1.567		-2.189
$Ca_5(AsO_4)_3OH$	-36.256	-11.848		-25.832	ARTINITE	-12.166	-2.276		-7.443
$Ca_4(OH)_2(AsO_4)_2:4H_2O$	-35.472	-15.552		-24.525	HYDROMAGNESITE	-30.117	-5.392		-18.312
$Mg_3(AsO4)_2$	-24.955	-12.078		-30.901	MAGNESITE	-4.645	0.299		-2.285
$FeAsO_4$	-13.511	-13.663		-21.725	NESQUEHONITE	-7.438	-2.492		-5.075
$Cd_3(AsO_4)_2$	-28.840	-19.193		-31.754	ARAGONITE	-3.385	2.083		2.607
$Cu_3(AsO_4)_2$	-24.294	-16.176		-27.868	CALCITE	-3.247	2.222		2.746
$Al_2(SeO_3)_3$	-6.800	-22.963		-44.963	DOLOMITE (ordered)	-6.737	3.676		1.616
$CaSeO_3$	-2.642	-1.644		-7.250	DOLOMITE (disordered)	-7.287	3.126		1.066
$CaSeO_3:H_2O$	-3.453	-2.454		-8.060	HUNTITE	-18.069	2.232		-4.996
$CdSeO_3$	-7.197	-7.800		-14.427	STRONTIANITE	-4.833	0.767		2.081
$CuSeO_3$	-6.882	-7.994		-14.332	WITHERITE	-7.269	-1.273		0.514
$Fe_2(SeO_3)_3$	-12.343	-24.101		-47.549	THERMONATRITE	-15.852	-10.645		-11.180
$Fe_2(SeO_3)_3.6H_2O$	-40.028	-51.783		-75.229	AlOHSO_4	-1.030	-7.894		-16.220
$MgSeO_3$	-3.116	-2.641		-11.356	$Al_4(OH)_{10}SO_4$	5.111	-5.879		-19.615
Na_2SeO_3	-10.275	-9.539		-16.205	$Zn_2(OH)_2SO_4$	-10.232	-11.244		-13.324
$ZnSeO_3$	-3.848	-6.080		-9.990	$Zn_4(OH)_6SO_4$	-18.915	-15.450		-13.086
$ZnSeO_3.H_2O$	-6.409	-8.641		-12.550	$Zn_3O(SO_4)_2$	-30.486	-34.749		-41.131
SeO_2	-11.942	-16.413		-22.543	ZINCOSITE	-12.771	-16.021		-20.323
$Al(OH)_3$ (am)	-0.110	-1.485		-3.288	$ZnSO_4.H_2O$	-8.204	-11.454		-15.755
BOEHMITE	2.113	0.737		-1.066	BIANCHITE	-7.081	-10.328		-14.628
DIASPORE	3.818	2.442		0.639	GOSLARITE	-6.836	-10.082		-14.382
GIBBSITE	2.399	1.024		-0.779	$Cd_3(OH)_4SO_4$	-24.970	-18.854		-26.868
$Zn(OH)_2$ (am)	-6.365	-4.127		-1.905	$Cd_3OH_2(SO_4)_2$	-24.070	-23.443		-37.980
$Zn(OH)_2$	-6.091	-3.853		-1.631	$Cd_4(OH)_6SO_4$	-26.630	-16.646		-25.157
$Zn(OH)_2$ (beta)	-5.645	-3.407		-1.185	$CdSO_4$	-10.598	-12.219		-19.239
$Zn(OH)_2$ (gamma)	-5.625	-3.387		-1.165	$CdSO_4.H_2O$	-9.045	-10.665		-17.685
$Zn(OH)_2$ (epsilon)	-5.425	-3.187		-0.965	$CdSO_4.2.67H_2O$	-8.899	-10.519		-17.538
ZnO (active)	-5.079	-2.841		-0.619	ANTLERITE	-8.992	-4.406		-11.550
ZINCITE	-5.224	-2.986		-0.765	BROCHANTITE	-10.511	-2.566		-9.918
$Cd(OH)_2$ (am)	-9.550	-5.682		-6.179	LANGITE	-12.779	-4.833		-12.184
$Cd(OH)_2$	-9.464	-5.596		-6.093	$CuOCuSO_4$	-15.422	-14.194		-21.132
MONTEPONITE	-10.923	-7.055		-7.552	$CuSO_4$	-12.974	-15.105		-21.835
$Cu(OH)_2$	-3.759	-0.400		-0.607	CHALCANTHITE	-7.399	-9.527		-16.256
TENORITE	-2.728	0.630		0.423	$Fe_2(SO_4)_3$	-34.388	-49.201		-73.825
FERRIHYDRITE	0.173	1.000		-1.527	H-JAROSITE	-7.710	-16.206		-36.833
GOETHITE	2.874	3.700		1.173	Na-JAROSITE	-5.392	-11.286		-32.181
$Cr(OH)_3$ (am)	-0.572	3.218		0.712	EPSOMITE	-3.288	-3.828		-12.934
$Cr(OH)_3$	-2.658	1.132		-1.373	ANHYDRITE	-0.665	-0.685		-6.684
BRUCITE	-7.303	-2.358		-4.942	GYPSUM	-0.416	-0.435		-6.434
PERICLASE	-12.042	-7.098		-9.682	CELESTITE	-0.786	-0.675		-5.883
$Mg(OH)_2$ (active)	-9.253	-4.308		-6.892	BARITE	0.838	1.345		-3.391
LIME	-22.773	-17.305		-16.781	MIRABILITE	-7.412	-7.689		-14.745
PORTLANDITE	-12.879	-7.410		-6.886	THENARDITE	-8.839	-9.122		-16.180
$Ba(OH)_2.8H_2O$	-18.593	-12.592		-10.803	$CuSeO_3.2H_2O$	-7.415	-8.526		-14.864
As_2O_5	-39.978	-41.934		-53.004	$Fe_2(SeO_3)_3.2H_2O$	-8.099	-19.856		-43.303
Al_2O_3	1.731	-1.021		-4.629	$Fe_2(OH)_4SeO_3$	-6.643	-9.460		-20.645
HEMATITE	8.148	9.801		4.745	$MgSeO_3.6H_2O$	-5.336	-4.859		-13.572
MAGHEMITE	0.344	1.997		-3.059	$CaSeO_3.2H_2O$	-4.707	-3.708		-9.314
LEPIDOCROCITE	1.994	2.820		0.293	$SrSeO_3$	-6.574	-5.444		-10.260
Cr_2O_3	-0.284	7.294		2.282	$BaSeO_3$	-7.839	-6.314		-10.657
SPINEL	-5.923	-3.730		-9.922	$Na_2SeO_3.5H_2O$	-15.689	-14.950		-21.615
MAGNESIOFERRITE	-0.588	6.009		-1.630	$Zn_3(PO_4)_2.4H_2O$	-9.188	-11.547		-16.525
NATRON	-13.911	-8.700		-9.233	$Cd_3(PO_4)_2$	-17.791	-15.263		-28.398
CUPRIC FERRITE	5.658	10.668		5.406	$Cu_3(PO_4)_2$	-11.335	-10.336		-22.602
$MgCr_2O_4$	-9.300	3.222		-4.374	$Cu_3(PO_4)_2.3H_2O$	-13.068	-12.067		-24.332
ZnCl2	-17.704	-21.817		-26.130	STRENGITE	-1.703	-5.413		-13.762
$Zn_2(OH)_3Cl$	-11.355	-10.053		-8.878	$Mg_3(PO_4)_2$	-11.027	-5.269		-24.665
$Zn_5(OH)_8Cl_2$	-24.718	-19.878		-15.305	$MgHPO_4.3H_2O$	-3.752	-3.344		-11.749
$CdCl_2$	-11.924	-14.407		-21.439	HYDROXYLAPATITE	-0.438	13.292		-1.553
$CdCl_2.H_2O$	-10.890	-13.373		-20.405	$CaHPO_4.2H_2O$	-2.548	-1.616		-6.913
$CdCl_2.2.5H_2O$	-10.672	-13.154		-20.185	$CaHPO_4$	-2.266	-1.335		-6.633
CdOHCl	-7.739	-7.046		-10.811	$Ca_3(PO_4)_2$ (beta)	-4.236	3.094		-6.977
MELANOTHALLITE	-18.104	-21.097		-27.840	$Ca_4H(PO_4)_3.3H_2O$	-7.619	0.643		-14.725
ATACAMITE	-5.942	-2.401		-6.082	$SrHPO_4$	-4.628	-3.566		-8.072
$Fe(OH)_{2.7}Cl_{0.3}$	3.889	3.764		0.256	$BaHPO_4$	-5.884	-4.425		-8.460
$CrCl_3$	-41.580	-47.318		-59.626	$AlAsO_4.2H_2O$	-10.746	-13.099		-20.437
HALITE	-6.768	-7.340		-10.875	$Zn_3(AsO_4)_2.2.5H_2O$	-28.595	-23.836		-28.241
SMITHSONITE	-5.538	-3.300		-1.078	$Cu_3(AsO_4)_2.2H_2O$	-24.625	-16.506		-28.198
$ZnCO_3.H_2O$	-5.278	-3.040		-0.818	$FeAsO_4.2H_2O$	-13.673	-13.823		-21.885
OTAVITE	-5.467	-1.599		-2.096	$Ca_3(AsO_4)_2.4H_2O$	-25.797	-11.346		-20.843
$CuCO_3$	-5.231	-1.873		-2.081	$Ba_3(AsO_4)_2$	-6.936	9.094		3.386
MALACHITE	-6.510	0.206		-0.208					

Table H-18. Saturation indices for all minerals calculated using MINTEQA2: Columbia-sand.

Solid/Mineral	Saturation Index				Solid/Mineral	Saturation Index			
	CS-1	CS-2	CS-3	CS-4		CS-1	CS-2	CS-3	CS-4
	pH 5.76	pH 6.27	pH 9.30	pH 12.08		pH 5.76	pH 6.27	pH 9.30	pH 12.08
$CaNaAsO_4.7.5H_2O$	-16.044	-13.541	-7.742	-14.264	AZURITE	-10.041	-8.650	-1.957	-3.864
$Ca_5(AsO_4)_3OH$	-39.199	-31.15	-11.165	-28.017	ARTINITE	-12.861	-10.849	-4.174	-7.885
$Ca_4(OH)_2(AsO_4)_2:4H_2O$	-37.556	-31.515	-14.394	-25.818	HYDROMAGNESITE	-31.856	-26.825	-10.139	-19.418
$Mg_3(AsO4)_2$	-27.348	-22.340	-17.983	-33.840	MAGNESITE	-4.993	-3.987	-0.650	-2.506
$FeAsO_4$	-12.099	-11.394	-15.458	-22.116	NESQUEHONITE	-7.785	-6.779	-3.441	-5.296
$Cd_3(AsO_4)_2$	-30.475	-25.846	-20.519	-34.023	ARAGONITE	-3.569	-2.557	3.136	2.853
$Cu_3(AsO_4)_2$	-24.042	-20.661	-19.622	-31.818	CALCITE	-3.431	-2.418	3.275	2.992
$Al_2(SeO_3)_3$	-5.899	-9.384	-23.587	-48.477	DOLOMITE (ordered)	-7.269	-5.250	3.780	1.641
$CaSeO_3$	-2.970	-2.455	-1.546	-8.173	DOLOMITE (disordered)	-7.819	-5.800	3.230	1.091
$CaSeO_3:H_2O$	-3.781	-3.266	-2.356	-8.983	HUNTITE	-19.297	-15.266	0.438	-5.414
$CdSeO_3$	-7.437	-7.055	-8.178	-15.594	STRONTIANITE	-4.828	-3.820	2.148	2.692
$CuSeO_3$	-6.493	-6.527	-9.079	-16.059	WITHERITE	-7.216	-6.280	0.325	1.094
$Fe_2(SeO_3)_3$	-8.605	-10.678	-27.502	-49.559	THERMONATRITE	-15.988	-14.997	-9.137	-11.325
$Fe_2(SeO_3)_3.6H_2O$	-36.288	-38.361	-55.183	-77.240	$AlOHSO_4$	-0.374	-2.337	-8.605	-17.844
$MgSeO_3$	-3.608	-3.100	-4.547	-12.746	$Al_4(OH)_{10}SO_4$	7.770	2.821	-3.226	-21.254
Na_2SeO_3	-10.555	-10.062	-8.986	-17.518	$Zn_2(OH)_2SO_4$	-9.794	-9.216	-13.502	-22.247
$ZnSeO_3$	-3.768	-3.493	-7.248	-14.810	$Zn_4(OH)_6SO_4$	-18.026	-15.902	-18.132	-29.312
$ZnSeO_3.H_2O$	-6.328	-6.053	-9.809	-17.370	$Zn_3O(SO_4)_2$	-29.835	-29.451	-39.052	-55.325
SeO_2	-12.087	-12.585	-17.368	-23.712	ZINCOSITE	-12.558	-12.752	-18.066	-25.594
$Al(OH)_3$ (am)	0.558	-0.437	-0.364	-3.293	$ZnSO_4.H_2O$	-7.991	-8.185	-13.499	-21.026
BOEHMITE	2.781	1.785	1.859	-1.071	BIANCHITE	-6.866	-7.061	-12.373	-19.900
DIASPORE	4.486	3.490	3.564	0.634	GOSLARITE	-6.621	-6.815	-12.127	-19.654
GIBBSITE	3.067	2.072	2.145	-0.784	$Cd_3(OH)_4SO_4$	-25.268	-23.597	-18.957	-28.482
$Zn(OH)_2$ (am)	-6.140	-5.367	-4.339	-5.557	$Cd_3OH_2(SO_4)_2$	-24.381	-23.677	-25.378	-41.213
$Zn(OH)_2$	-5.866	-5.093	-4.065	-5.283	$Cd_4(OH)_6SO_4$	-27.024	-24.473	-16.172	-26.769
$Zn(OH)_2$ (beta)	-5.420	-4.647	-3.619	-4.837	$CdSO_4$	-10.705	-10.793	-13.474	-20.856
$Zn(OH)_2$ (gamma)	-5.400	-4.627	-3.599	-4.817	$CdSO_4.H_2O$	-9.152	-9.240	-11.921	-19.302
$Zn(OH)_2$ (epsilon)	-5.200	-4.427	-3.399	-4.617	$CdSO_4.2.67H_2O$	-9.006	-9.094	-11.774	-19.155
ZnO (active)	-4.854	-4.081	-3.053	-4.271	ANTLERITE	-7.403	-6.980	-6.628	-14.845
ZINCITE	-4.999	-4.227	-3.199	-4.417	BROCHANTITE	-8.388	-7.502	-4.918	-13.770
$Cd(OH)_2$ (am)	-9.645	-8.766	-5.105	-6.177	LANGITE	-10.656	-9.769	-7.185	-16.037
$Cd(OH)_2$	-9.559	-8.680	-5.019	-6.091	$CuOCuSO_4$	-14.367	-14.407	-16.287	-23.868
MONTEPONITE	-11.018	-10.139	-6.478	-7.550	$CuSO_4$	-12.453	-12.957	-17.067	-24.013
$Cu(OH)_2$	-3.225	-2.762	-0.530	-1.166	CHALCANTHITE	-6.876	-7.380	-11.489	-18.434
TENORITE	-2.194	-1.731	0.500	-0.136	$Fe_2(SO_4)_3$	-30.252	-33.734	-55.232	-77.188
FERRIHYDRITE	2.259	1.969	0.733	-0.780	H-JAROSITE	-1.475	-4.279	-20.672	-37.830
GOETHITE	4.960	4.670	3.433	1.920	Na-JAROSITE	0.774	-1.534	-14.998	-33.251
$Cr(OH)_3$ (am)	-2.611	-1.766	3.253	-0.491	EPSOMITE	-3.646	-3.607	-6.610	-14.774
$Cr(OH)_3$	-4.697	-3.852	1.168	-2.576	ANHYDRITE	-0.861	-0.815	-1.464	-8.058
BRUCITE	-7.650	-6.644	-3.307	-5.163	GYPSUM	-0.612	-0.567	-1.214	-7.808
PERICLASE	-12.390	-11.384	-8.047	-9.903	CELESTITE	-0.793	-0.753	-1.127	-6.892
$Mg(OH)_2$ (active)	-9.600	-8.594	-5.257	-7.113	BARITE	0.878	0.847	1.110	-4.430
LIME	-22.957	-21.945	-16.251	-16.535	MIRABILITE	-7.557	-7.533	-8.013	-16.509
PORTLANDITE	-13.063	-12.050	-6.356	-6.640	THENARDITE	-8.987	-8.964	-9.446	-17.944
$Ba(OH)_2.8H_2O$	-18.538	-17.601	-10.994	-10.223	$CuSeO_3.2H_2O$	-7.026	-7.060	-9.611	-16.591
As_2O_5	-41.327	-39.336	-44.990	-55.279	$Fe_2(SeO_3)_3.2H_2O$	-4.360	-6.433	-23.256	-45.313
Al_2O_3	3.065	1.074	1.221	-4.638	$Fe_2(OH)_4SeO_3$	-2.615	-3.693	-10.949	-20.319
HEMATITE	12.320	11.740	9.267	6.240	$MgSeO_3.6H_2O$	-5.827	-5.319	-6.763	-14.962
MAGHEMITE	4.516	3.936	1.463	-1.564	$CaSeO_3.2H_2O$	-5.035	-4.520	-3.610	-10.237
LEPIDOCROCITE	4.080	3.790	2.553	1.040	$SrSeO_3$	-6.713	-6.203	-5.018	-10.818
Cr_2O_3	-4.363	-2.673	7.365	-0.123	$BaSeO_3$	-7.931	-7.493	-5.671	-11.245
SPINEL	-4.936	-5.921	-2.437	-10.152	$Na_2SeO_3.5H_2O$	-15.968	-15.475	-14.397	-22.929
MAGNESIOFERRITE	3.237	3.663	4.526	-0.356	$Zn_3(PO_4)_2.4H_2O$	-6.920	-6.043	-14.906	-28.635
NATRON	-14.045	-13.054	-7.191	-9.378	$Cd_3(PO_4)_2$	-16.487	-15.289	-16.255	-29.547
CUPRIC FERRITE	10.363	10.247	10.005	6.342	$Cu_3(PO_4)_2$	-8.144	-8.194	-13.448	-25.431
$MgCr_2O_4$	-13.727	-11.032	2.343	-7.000	$Cu_3(PO_4)_2.3H_2O$	-9.875	-9.926	-15.179	-27.162
ZnCl2	-17.455	-17.732	-22.948	-29.928	STRENGITE	1.179	0.169	-7.041	-13.592
$Zn_2(OH)_3Cl$	-10.892	-9.871	-10.938	-16.254	$Mg_3(PO_4)_2$	-10.480	-8.903	-10.840	-26.483
$Zn_5(OH)_8Cl_2$	-23.569	-20.754	-21.858	-33.709	$MgHPO_4.3H_2O$	-3.304	-3.018	-5.654	-12.547
$CdCl_2$	-11.996	-12.166	-14.749	-21.583	HYDROXYLAPATITE	1.029	3.931	14.476	-2.057
$CdCl_2.H_2O$	-10.962	-11.132	-13.715	-20.549	$CaHPO_4.2H_2O$	-1.936	-1.643	-1.923	-7.244
$CdCl_2.2.5H_2O$	-10.743	-10.913	-13.495	-20.329	$CaHPO_4$	-1.655	-1.362	-1.643	-6.964
CdOHCl	-7.822	-7.467	-6.929	-10.882	$Ca_3(PO_4)_2$ (beta)	-3.197	-1.599	3.533	-7.394
MELANOTHALLITE	-17.548	-18.133	-22.146	-28.544	$Ca_4H(PO_4)_3.3H_2O$	-5.968	-4.078	0.775	-15.474
ATACAMITE	-4.863	-4.460	-3.120	-7.272	$SrHPO_4$	-3.827	-3.539	-3.545	-8.039
$Fe(OH)_{2.7}Cl_{0.3}$	5.979	5.532	3.359	0.982	$BaHPO_4$	-5.036	-4.819	-4.188	-8.456
$CrCl_3$	-43.585	-44.314	-48.660	-61.048	$AlAsO_4.2H_2O$	-10.753	-10.753	-13.506	-21.580
HALITE	-6.824	-6.853	-7.045	-11.021	$Zn_3(AsO_4)_2.2.5H_2O$	-29.268	-24.959	-27.530	-41.471
SMITHSONITE	-5.313	-4.540	-3.512	-4.730	$Cu_3(AsO_4)_2.2H_2O$	-24.373	-20.992	-19.953	-32.148
$ZnCO_3.H_2O$	-5.053	-4.280	-3.252	-4.470	$FeAsO_4.2H_2O$	-12.260	-11.555	-15.618	-22.276
OTAVITE	-5.562	-4.683	-1.022	-2.094	$Ca_3(AsO_4)_2.4H_2O$	-27.697	-22.669	-11.242	-22.382
$CuCO_3$	-4.698	-4.234	-2.003	-2.639	$Ba_3(AsO_4)_2$	-8.128	-3.328	10.832	2.852
MALACHITE	-5.443	-4.516	-0.053	-1.325					

APPENDIX I

SATURATION INDICES FOR SELENATE MINERLS CALCULATED USING MINTEQA2

Table I-1. Saturation Indices for selenate minerals calculated Using MINTEQA2: Dewey and Dewey-soil mixtures.

Dewey

Solid/Mineral	Saturation Index			
	D-1	D-2	D-3	D-4
	pH 5.81	pH 7.95	pH 10.25	pH 12.25
$Al_2(SeO_4)_3$	-14.905	-27.658	-39.688	-58.593
$CaSeO_4$	-5.001	-5.326	-5.808	-12.001
$CuSeO_4$	-6.910	-8.821	-11.989	-18.992
$Fe_2(SeO_4)_3$	-26.127	-35.947	-46.154	-65.737
$MgSeO_4$	-3.717	-4.031	-7.401	-14.573
$ZnSeO_4$	-5.717	-8.160	-10.030	-15.962
$ZnSeO_4:6H_2O$	-10.943	-13.388	-15.259	-21.191
$CdSeO_4:2H_2O$	-12.977	-15.042	-15.495	-21.935
$CuSeO_4:5H_2O$	-11.534	-13.446	-16.615	-23.617
$MgSeO_4:6H_2O$	-8.314	-8.629	-12.000	-19.171
$CaSeO_4:2H_2O$	-6.757	-7.082	-7.564	-13.757
$SrSeO_4$	-6.969	-7.311	-7.306	-12.668
$BaSeO_4$	-6.174	-6.513	-6.350	-11.357
Na_2SeO_4	-10.408	-10.466	-10.451	-18.831

Dewey-Lawson

Solid/Mineral	Saturation Index			
	DL-1	DL-2	DL-3	DL-4
	pH 5.36	pH 7.89	pH 9.66	pH 12.57
$Al_2(SeO_4)_3$	-11.412	-28.091	-40.795	-61.312
$CaSeO_4$	-4.207	-4.781	-5.640	-12.146
$CuSeO_4$	-7.188	-8.414	-11.793	-16.560
$Fe_2(SeO_4)_3$	-22.805	-34.718	-46.434	-68.127
$MgSeO_4$	-3.553	-4.476	-6.625	-13.744
$ZnSeO_4$	-5.302	-7.507	-9.716	-17.187
$ZnSeO_4:6H_2O$	-10.516	-12.721	-14.929	-22.399
$CdSeO_4:2H_2O$	-12.582	-14.482	-16.635	-22.833
$CuSeO_4:5H_2O$	-11.801	-13.027	-16.405	-21.172
$MgSeO_4:6H_2O$	-8.137	-9.059	-11.208	-18.326
$CaSeO_4:2H_2O$	-5.958	-6.532	-7.391	-13.897
$SrSeO_4$	-6.792	-7.332	-8.034	-13.917
$BaSeO_4$	-5.983	-6.258	-6.474	-12.036
Na_2SeO_4	-11.864	-12.230	-12.601	-22.093

Dewey-Kamm

Solid/Mineral	Saturation Index			
	DK-1	DK-2	DK-3	DK-4
	pH 6.01	pH 8.47	pH 9.55	pH 12.61
$Al_2(SeO_4)_3$	-14.315	-31.872	-39.369	-64.958
$CaSeO_4$	-4.542	-4.872	-5.504	-13.606
$CuSeO_4$	-7.532	-9.892	-12.568	-19.056
$Fe_2(SeO_4)_3$	-25.993	-37.950	-46.647	-72.428
$MgSeO_4$	-3.931	-4.804	-7.069	-14.975
$ZnSeO_4$	-6.684	-7.648	-9.422	-18.420
$ZnSeO_4:6H_2O$	-11.898	-12.861	-14.634	-23.632
$CdSeO_4:2H_2O$	-13.106	-15.043	-16.340	-24.091
$CuSeO_4:5H_2O$	-12.145	-14.505	-17.181	-23.668
$MgSeO_4:6H_2O$	-8.514	-9.387	-11.651	-19.557
$CaSeO_4:2H_2O$	-6.293	-6.623	-7.255	-15.356
$SrSeO_4$	-7.110	-7.384	-7.922	-15.026
$BaSeO_4$	-6.393	-6.314	-6.361	-12.866
Na_2SeO_4	-12.167	-12.321	-12.603	-23.408

Dewey-Red Wing

Solid/Mineral	Saturation Index			
	DR-1	DR-2	DR-3	DR-4
	pH 5.81	pH 8.11	pH 10.55	pH 12.34
$Al_2(SeO_4)_3$	-13.417	-29.867		-62.911
$CaSeO_4$	-4.108	-4.986		-12.857
$CuSeO_4$	-7.158	-10.251		-20.080
$Fe_2(SeO_4)_3$	-25.467	-37.170		-70.526
$MgSeO_4$	-3.610	-4.896		-14.455
$ZnSeO_4$	-6.429	-9.068		-18.845
$ZnSeO_4:6H_2O$	-11.643	-14.280		-24.057
$CdSeO_4:2H_2O$	-12.674	-15.408		-23.447
$CuSeO_4:5H_2O$	-11.771	-14.863		-24.692
$MgSeO_4:6H_2O$	-8.194	-9.479		-19.037
$CaSeO_4:2H_2O$	-5.860	-6.737		-14.608
$SrSeO_4$	-6.772	-7.406		-14.000
$BaSeO_4$	-6.064	-6.562		-12.272
Na_2SeO_4	-12.098	-12.559		-22.099

Dewey-Mn Road

Solid/Mineral	Saturation Index			
	DM-1	DM-2	DM-3	DM-4
	pH 6.02	pH 8.11	pH 10.63	pH 12.22
$Al_2(SeO_4)_3$	-14.710	-29.811		-63.208
$CaSeO_4$	-4.223	-4.901		-12.606
$CuSeO_4$	-7.418	-10.165		-19.863
$Fe_2(SeO_4)_3$	-26.948	-37.370		-70.909
$MgSeO_4$	-3.718	-4.728		-14.331
$ZnSeO_4$	-6.652	-8.975		-18.716
$ZnSeO_4:6H_2O$	-11.865	-14.188		-23.928
$CdSeO_4:2H_2O$	-13.062	-14.856		-23.303
$CuSeO_4:5H_2O$	-12.030	-14.777		-24.475
$MgSeO_4:6H_2O$	-8.302	-9.310		-18.913
$CaSeO_4:2H_2O$	-5.974	-6.651		-14.356
$SrSeO_4$	-6.829	-7.374		-14.015
$BaSeO_4$	-5.992	-6.421		-12.016
Na_2SeO_4	-12.090	-12.477		-21.877

Dewey-Sand

Solid/Mineral	Saturation Index			
	DS-1	DS-2	DS-3	DS-4
	pH 6.17	pH 8.00	pH 9.94	pH 12.43
$Al_2(SeO_4)_3$	-15.218	-27.417	-40.352	-63.415
$CaSeO_4$	-4.569	-4.585	-5.681	-13.212
$CuSeO_4$	-7.358	-8.531	-12.201	-20.493
$Fe_2(SeO_4)_3$	-27.169	-35.299	-47.759	-70.264
$MgSeO_4$	-4.213	-4.275	-6.864	-14.235
$ZnSeO_4$	-6.182	-7.311	-9.740	-17.066
$ZnSeO_4:6H_2O$	-11.395	-12.524	-14.953	-22.278
$CdSeO_4:2H_2O$	-12.121	-14.091	-16.893	-23.708
$CuSeO_4:5H_2O$	-11.971	-13.143	-16.813	-25.104
$MgSeO_4:6H_2O$	-8.796	-8.858	-11.447	-18.817
$CaSeO_4:2H_2O$	-6.320	-6.336	-7.432	-14.962
$SrSeO_4$	-7.058	-7.091	-7.727	-14.167
$BaSeO_4$	-6.418	-6.407	-6.493	-12.873
Na_2SeO_4	-12.202	-12.166	-12.458	-22.607

Table I-2. Saturation Indices for selenate minerals calculated Using MINTEQA2: Presque Isle and Presque Isle-soil mixtures.

Presque Isle (PI)

Solid/Mineral	Saturation Index			
	P-1	P-2	P-3	P-4
	pH 5.87	pH 7.90	pH 9.82	pH 11.68
$Al_2(SeO_4)_3$	-12.150	-25.886	-36.927	-51.974
$CaSeO_4$	-3.384	-3.494	-4.379	-8.536
$CuSeO_4$	-6.102	-6.953	-10.621	-14.290
$Fe_2(SeO_4)_3$	-23.503	-32.340	-44.600	-59.018
$MgSeO_4$	-2.971	-3.129	-5.116	-11.296
$ZnSeO_4$	-5.644	-6.364	-8.937	-13.275
$ZnSeO_4:6H_2O$	-10.856	-11.576	-14.148	-18.485
$CdSeO_4:2H_2O$	-11.609	-12.693	-14.924	-19.123
$CuSeO_4:5H_2O$	-10.713	-11.564	-15.232	-18.900
$MgSeO_4:6H_2O$	-7.552	-7.710	-9.697	-15.876
$CaSeO_4:2H_2O$	-5.134	-5.244	-6.130	-10.286
$SrSeO_4$	-5.624	-5.794	-6.401	-10.255
$BaSeO_4$	-4.708	-4.961	-4.427	-8.083
Na_2SeO_4	-13.209	-13.418	-13.684	-20.308

PI-Lawson

Solid/Mineral	Saturation Index			
	PL-1	PL-2	PL-3	PL-4
	pH 6.70	pH 8.02	pH 8.92	pH 10.98
$Al_2(SeO_4)_3$	-17.831	-27.802	-32.608	-46.645
$CaSeO_4$	-4.215	-4.753	-5.177	-8.626
$CuSeO_4$	-6.954	-8.422	-9.496	-12.325
$Fe_2(SeO_4)_3$	-27.678	-32.723	-34.730	-48.018
$MgSeO_4$	-3.472	-3.994	-4.662	-7.687
$ZnSeO_4$	-5.529	-6.511	-7.073	-10.467
$ZnSeO_4:6H_2O$	-10.740	-11.721	-12.283	-15.677
$CdSeO_4:2H_2O$	-13.070	-14.675	-15.017	-18.906
$CuSeO_4:5H_2O$	-11.565	-13.032	-14.106	-16.935
$MgSeO_4:6H_2O$	-8.053	-8.574	-9.242	-12.267
$CaSeO_4:2H_2O$	-5.965	-6.503	-6.927	-10.376
$SrSeO_4$	-7.030	-7.536	-7.984	-10.998
$BaSeO_4$	-4.776	-5.414	-5.548	-7.596
Na_2SeO_4	-14.892	-15.544	-15.580	-18.912

PI-Kamm

Solid/Mineral	Saturation Index			
	PK-1	PK-2	PK-3	PK-4
	pH 6.72	pH 7.90	pH 9.34	pH 11.72
$Al_2(SeO_4)_3$	-18.035	-26.515	-37.574	-53.070
$CaSeO_4$	-4.480	-4.936	-5.901	-10.348
$CuSeO_4$	-7.311	-9.191	-12.015	-16.584
$Fe_2(SeO_4)_3$	-28.521	-31.570	-39.887	-59.039
$MgSeO_4$	-3.707	-4.308	-6.009	-11.759
$ZnSeO_4$	-6.518	-6.453	-8.251	-13.373
$ZnSeO_4:6H_2O$	-11.729	-11.663	-13.461	-18.583
$CdSeO_4:2H_2O$	-14.922	-14.692	-16.045	-20.403
$CuSeO_4:5H_2O$	-11.922	-13.801	-16.625	-21.194
$MgSeO_4:6H_2O$	-8.288	-8.888	-10.589	-16.339
$CaSeO_4:2H_2O$	-6.230	-6.686	-7.651	-12.098
$SrSeO_4$	-6.993	-7.445	-8.325	-12.293
$BaSeO_4$	-4.947	-5.518	-6.307	-9.985
Na_2SeO_4	-15.100	-15.638	-15.879	-21.614

PI-Red Wing

Solid/Mineral	Saturation Index			
	PR-1	PR-2	DR-3	DR-4
	pH 6.07	pH 8.37	pH 10.78	pH 11.85
$Al_2(SeO_4)_3$	-14.971	-32.154		-55.645
$CaSeO_4$	-4.205	-4.689		-10.183
$CuSeO_4$	-7.062	-8.853		-16.580
$Fe_2(SeO_4)_3$	-22.541	-36.737		-62.265
$MgSeO_4$	-3.985	-4.589		-12.465
$ZnSeO_4$	-6.815	-7.898		-15.133
$ZnSeO_4:6H_2O$	-12.027	-13.109		-20.343
$CdSeO_4:2H_2O$	-13.052	-15.032		-21.010
$CuSeO_4:5H_2O$	-11.674	-13.463		-21.190
$MgSeO_4:6H_2O$	-8.567	-9.169		-17.045
$CaSeO_4:2H_2O$	-5.956	-6.439		-11.934
$SrSeO_4$	-7.166	-7.205		-12.106
$BaSeO_4$	-4.887	-5.232		-9.903
Na_2SeO_4	-14.489	-14.965		-21.649

PI-Mn Road

Solid/Mineral	Saturation Index			
	PM-1	PM-2	PM-3	PM-4
	pH 6.17	pH 8.34	pH 9.66	pH 11.96
$Al_2(SeO_4)_3$	-15.607	-32.321	-42.519	-57.389
$CaSeO_4$	-4.100	-4.652	-6.165	-10.620
$CuSeO_4$	-6.930	-8.837	-11.964	-16.305
$Fe_2(SeO_4)_3$	-29.441	-38.918	-48.141	-61.690
$MgSeO_4$	-3.779	-4.364	-6.878	-12.291
$ZnSeO_4$	-6.748	-9.181	-11.168	-15.372
$ZnSeO_4:6H_2O$	-11.960	-14.392	-16.378	-20.582
$CdSeO_4:2H_2O$	-13.065	-15.010	-16.828	-20.968
$CuSeO_4:5H_2O$	-11.541	-13.447	-16.574	-20.915
$MgSeO_4:6H_2O$	-8.361	-8.944	-11.458	-16.871
$CaSeO_4:2H_2O$	-5.850	-6.402	-7.915	-12.370
$SrSeO_4$	-7.085	-7.317	-8.459	-12.613
$BaSeO_4$	-4.939	-5.488	-6.400	-10.461
Na_2SeO_4	-14.624	-15.505	-15.961	-22.516

PI-Sand

Solid/Mineral	Saturation Index			
	PS-1	PS-2	PS-3	PS-4
	pH 6.98	pH 9.22	pH 11.03	pH 12.07
$Al_2(SeO_4)_3$	-19.325	-34.391	-48.379	-56.093
$CaSeO_4$	-4.503	-4.909	-8.298	-10.587
$CuSeO_4$	-8.174	-11.460	-15.215	-17.532
$Fe_2(SeO_4)_3$	-29.329	-40.770	-55.215	-62.918
$MgSeO_4$	-4.168	-4.744	-9.378	-13.153
$ZnSeO_4$	-5.936	-7.811	-11.660	-14.409
$ZnSeO_4:6H_2O$	-11.146	-13.021	-16.870	-19.619
$CdSeO_4:2H_2O$	-12.236	-15.508	-19.172	-21.160
$CuSeO_4:5H_2O$	-12.784	-16.070	-19.825	-22.142
$MgSeO_4:6H_2O$	-8.748	-9.324	-13.959	-17.733
$CaSeO_4:2H_2O$	-6.254	-6.660	-10.048	-12.337
$SrSeO_4$	-6.683	-6.964	-9.985	-12.021
$BaSeO_4$	-4.722	-4.857	-7.638	-9.483
Na_2SeO_4	-15.542	-15.770	-19.359	-23.390

Table I-3. Saturation Indices for selenate minerals calculated Using MINTEQA2: Columbia and Columbia-soil mixtures.

Columbia

Solid/Mineral	Saturation Index			
	C-1	C-2	C-3	C-4
	pH 6.74	pH 8.89	pH 11.13	pH 12.55
$Al_2(SeO_4)_3$	-16.519	-30.905	-48.046	-63.661
$CaSeO_4$	-3.124	-3.141	-7.183	-11.911
$CuSeO_4$	-6.541	-8.802	-13.943	-19.594
$Fe_2(SeO_4)_3$	-27.312	-39.312	-57.389	-69.469
$MgSeO_4$	-2.418	-3.673	-10.044	-14.608
$ZnSeO_4$	-6.634	-7.624	-12.431	-17.773
$ZnSeO_4:6H_2O$	-11.853	-12.840	-17.643	-22.984
$CdSeO_4:2H_2O$	-12.587	-12.800	-17.480	-21.609
$CuSeO_4:5H_2O$	-11.158	-13.417	-18.555	-24.205
$MgSeO_4:6H_2O$	-7.006	-8.259	-14.626	-19.189
$CaSeO_4:2H_2O$	-4.877	-4.893	-8.934	-13.661
$SrSeO_4$	-5.904	-5.875	-9.174	-12.907
$BaSeO_4$	-4.238	-3.964	-6.249	-10.105
Na_2SeO_4	-11.351	-11.446	-16.033	-22.736

Columbia-Lawson

Solid/Mineral	Saturation Index			
	CL-1	CL-2	CL-3	CL-4
	pH 5.68	pH 8.22	pH 9.66	pH 11.81
$Al_2(SeO_4)_3$	-11.910	-29.013	-37.376	-54.786
$CaSeO_4$	-3.689	-3.850	-4.691	-10.127
$CuSeO_4$	-6.537	-7.646	-10.016	-14.363
$Fe_2(SeO_4)_3$	-24.996	-34.906	-44.955	-62.565
$MgSeO_4$	-3.130	-3.383	-6.342	-13.396
$ZnSeO_4$	-5.356	-8.697	-10.979	-16.521
$ZnSeO_4:6H_2O$	-10.569	-13.909	-16.190	-21.731
$CdSeO_4:2H_2O$	-12.329	-13.613	-15.889	-21.170
$CuSeO_4:5H_2O$	-11.149	-12.258	-14.627	-18.974
$MgSeO_4:6H_2O$	-7.713	-7.965	-10.923	-17.976
$CaSeO_4:2H_2O$	-5.440	-5.601	-6.441	-11.877
$SrSeO_4$	-6.350	-6.506	-7.039	-12.134
$BaSeO_4$	-5.041	-5.017	-5.072	-9.900
Na_2SeO_4	-13.419	-13.746	-14.022	-21.111

Columbia-Kamm

Solid/Mineral	Saturation Index			
	CK-1	CK-2	CK-3	CK-4
	pH 5.41	pH 7.81	pH 10.01	pH 11.86
$Al_2(SeO_4)_3$	-10.590	-25.929	-40.465	-56.308
$CaSeO_4$	-3.660	-3.804	-5.346	-10.481
$CuSeO_4$	-6.283	-7.184	-11.204	-15.655
$Fe_2(SeO_4)_3$	-23.604	-31.767	-47.829	-66.862
$MgSeO_4$	-3.096	-3.322	-7.459	-13.865
$ZnSeO_4$	-5.641	-9.068	-11.856	-15.527
$ZnSeO_4:6H_2O$	-10.854	-14.280	-17.067	-20.737
$CdSeO_4:2H_2O$	-12.288	-13.536	-16.744	-21.639
$CuSeO_4:5H_2O$	-10.896	-11.796	-15.815	-20.266
$MgSeO_4:6H_2O$	-7.679	-7.904	-12.040	-18.445
$CaSeO_4:2H_2O$	-5.411	-5.555	-7.096	-12.231
$SrSeO_4$	-6.286	-6.414	-7.552	-12.297
$BaSeO_4$	-5.029	-5.086	-5.534	-9.924
Na_2SeO_4	-13.280	-13.645	-14.388	-21.555

Columbia-Red Wing

Solid/Mineral	Saturation Index			
	CR-1	CR-2	CR-3	CR-4
	pH 6.18	pH 8.23	pH 10.53	pH 11.97
$Al_2(SeO_4)_3$	-14.146	-28.016		-57.088
$CaSeO_4$	-3.603	-3.786		-10.633
$CuSeO_4$	-6.468	-7.715		-16.019
$Fe_2(SeO_4)_3$	-27.752	-37.641		-67.851
$MgSeO_4$	-2.993	-3.362		-14.145
$ZnSeO_4$	-5.791	-9.054		-17.405
$ZnSeO_4:6H_2O$	-11.006	-14.266		-22.616
$CdSeO_4:2H_2O$	-12.329	-13.724		-21.920
$CuSeO_4:5H_2O$	-11.082	-12.326		-20.629
$MgSeO_4:6H_2O$	-7.578	-7.944		-18.726
$CaSeO_4:2H_2O$	-5.354	-5.537		-12.383
$SrSeO_4$	-6.344	-6.405		-12.297
$BaSeO_4$	-4.817	-4.910		-9.732
Na_2SeO_4	-13.152	-13.487		-21.699

Columbia-Mn Road

Solid/Mineral	Saturation Index			
	CM-1	CM-2	CM-3	CM-4
	pH 5.80	pH 8.69	pH 10.71	pH 11.71
$Al_2(SeO_4)_3$	-11.990	-31.793		-55.775
$CaSeO_4$	-3.582	-3.797		-10.077
$CuSeO_4$	-6.312	-8.637		-15.641
$Fe_2(SeO_4)_3$	-24.913	-40.312		-65.742
$MgSeO_4$	-2.956	-3.695		-13.083
$ZnSeO_4$	-5.438	-8.884		-13.442
$ZnSeO_4:6H_2O$	-10.653	-14.096		-18.653
$CdSeO_4:2H_2O$	-12.249	-14.064		-21.364
$CuSeO_4:5H_2O$	-10.926	-13.249		-20.251
$MgSeO_4:6H_2O$	-7.541	-8.277		-17.663
$CaSeO_4:2H_2O$	-5.334	-5.548		-11.827
$SrSeO_4$	-6.334	-6.418		-11.906
$BaSeO_4$	-5.009	-4.697		-9.714
Na_2SeO_4	-13.125	-13.602		-20.910

Columbia-Sand

Solid/Mineral	Saturation Index			
	CS-1	CS-2	CS-3	CS-4
	pH 5.76	pH 6.27	pH 9.30	pH 12.08
$Al_2(SeO_4)_3$	-10.734	-15.597	-32.650	-59.312
$CaSeO_4$	-3.792	-3.737	-3.777	-11.006
$CuSeO_4$	-5.804	-6.298	-9.800	-17.368
$Fe_2(SeO_4)_3$	-20.819	-24.272	-43.945	-67.774
$MgSeO_4$	-3.330	-3.281	-5.678	-14.479
$ZnSeO_4$	-5.239	-5.424	-10.129	-18.261
$ZnSeO_4:6H_2O$	-10.452	-10.637	-15.341	-23.471
$CdSeO_4:2H_2O$	-12.370	-12.448	-14.520	-22.537
$CuSeO_4:5H_2O$	-10.417	-10.911	-14.412	-21.979
$MgSeO_4:6H_2O$	-7.913	-7.864	-10.259	-19.059
$CaSeO_4:2H_2O$	-5.543	-5.488	-5.527	-12.756
$SrSeO_4$	-6.354	-6.304	-6.069	-12.471
$BaSeO_4$	-4.983	-5.004	-4.133	-10.308
Na_2SeO_4	-13.287	-13.253	-13.127	-22.233

APPENDIX J

LOG ACTIVITY VS. PH PLOT OF SELENITE AND SELENATE
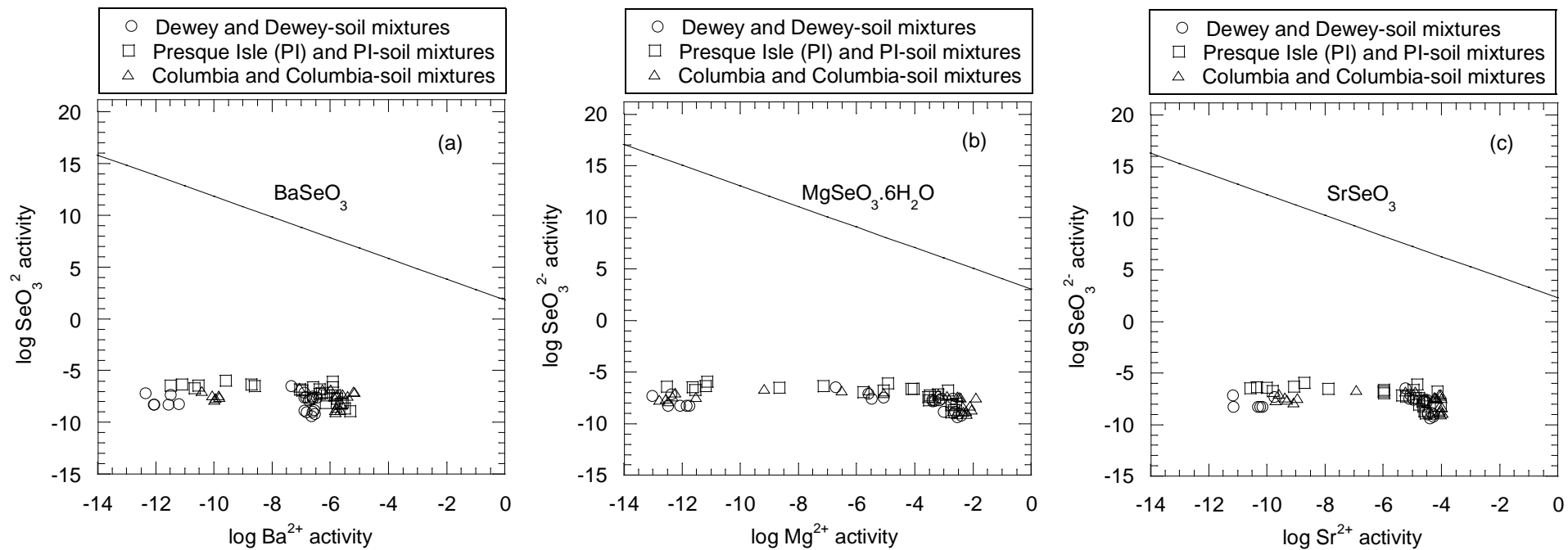**FOR Ba^{2+}, Mg^{2+}, AND Sr^{2+}**

Figure J-1. Log activity plot of selenite vs. (a) Ba^{2+}, (b) Mg^{2+}, and (c) Sr^{2+}.
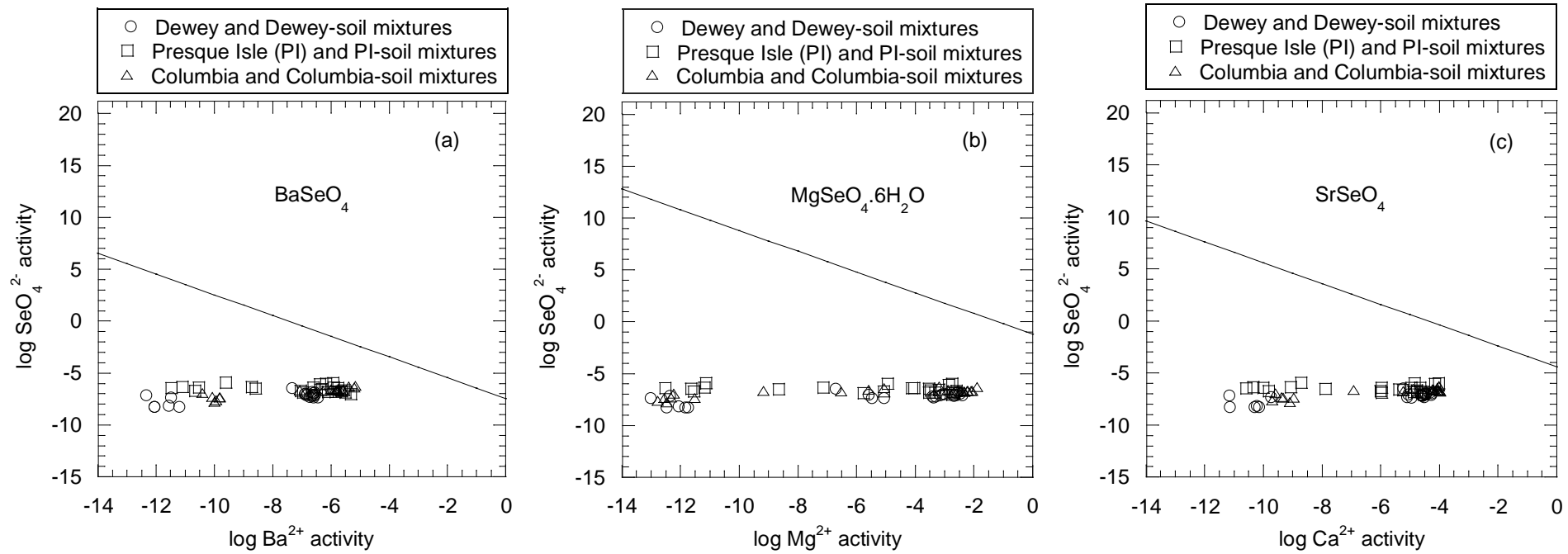
Figure J-2. Log activity plot of selenate vs. (a) Ba^{2+}, (b) Mg^{2+}, and (c) Sr^{2+}